SPAWAR
Systems Center
San Diego

TECHNICAL REPORT 1716
ADDENDUM
February 1999

Environmental Analysis of U.S. Navy Shipboard Solid Waste Discharges: Addendum to the Report of Findings

S. L. Curtis
C. N. Katz
D. B. Chadwick

Approved for public release;
distribution is unlimited.

SSC San Diego

19990506 018

SSC SAN DIEGO
San Diego, California 92152–5001

H. A. Williams, CAPT, USN
Commanding Officer

R. C. Kolb
Executive Director

ADMINISTRATIVE INFORMATION

The work detailed in this report was performed for Naval Sea Systems Command by the Marine Environmental Quality Branch, Code D362, SSC San Diego.

Released by
J. G. Grovhoug, Head
Marine Environmental Quality
Branch

Under authority of
R. H. Moore, Head
Environmental Sciences
Division

ACKNOWLEDGMENTS

The following individuals contributed to this report: D. B. Chadwick, C. N. Katz, S. L. Curtis, J. J. Rohr, D. Ladd, J. Allen, and A. Patterson, Marine Sciences Division, SSC San Diego; W. Glad, Engineering Services Division, SSC San Diego; M. A. Moran, W. Ye, and B. Binder, Department of Marine Sciences, University of Georgia; R. Vetter, L. Robertson, and C. A. Kimbrell, Genetics and Physiology Group, Southwest Fisheries Science Center, National Oceanic and Atmospheric Administration; M. Hyman, Naval Coastal System Station; S. Jenkins, Scripps Institute of Oceanography; D. Ondercin, Applied Physics Laboratory, John Hopkins University; Merkel and Associates, Inc.; A. Valkirs, Computer Sciences Corporation.

EXECUTIVE SUMMARY

This Addendum provides follow-on findings to a report published in January 1996 (Chadwick et al., 1996) detailing a study of the fate and effects of U.S. Navy shipboard solid waste discharges. The study was requested as part of the Navy's effort to evaluate solid waste discharge compliance alternatives. The objective of the study was to determine to what extent, if any, Navy solid waste discharges lead to adverse marine environmental effects. Along with the original findings, the final results presented in this Addendum suggest that there will be no significant adverse environmental impact from the discharges studied.

The Naval Command, Control and Ocean Surveillance Center (NCCOSC) RDT&E Division (currently SPAWAR Systems Center San Diego (SSC SD)) Code D362 was tasked by the Naval Sea Systems Command (NAVSEA 03R16) to perform the environmental analysis. The environmental analysis was conducted as part of the Navy's overall effort to respond to U.S. legislation requiring compliance with Annex V of the International Convention for the Prevention of Pollution from Ships, 1973, as modified by the Protocol of 1978 (MARPOL 73/78). MARPOL 73/78 Annex V prohibits the discharge of non-food solid wastes into sensitive oceanographic and ecological areas throughout the world, known as Special Areas. The eight existing and proposed Special Areas include: the Baltic Sea, the North Sea, the Mediterranean Sea, the Wider Caribbean Region, the Antarctic area, the Black Sea, the Red Sea, and the "Gulfs" area.

The Navy researched alternatives for ways to comply with the MARPOL restrictions and developed a compliance plan for the U.S. Congress. Subsequently, the law was changed to allow for the use of the preferred alternative. This alternative consists of an equipment suite comprised of a plastics processor to handle plastic waste, pulpers for food, paper, and cardboard products, and a shredder for metal and glass waste. Plastic wastes must be retained on board and food waste discharges are not restricted, therefore the environmental analysis was conducted only on the paper, cardboard, metal, and glass waste streams generated by pulpers and shredders.

The initial shipboard solid waste discharge study involved a review of pertinent literature, characterization of the waste stream, fate modeling, and field tests. The literature review focused on the regulatory framework and environmental characteristics of Special Areas, characteristics of the bulk waste stream constituents, general ocean discharge issues, and Navy vessel operational parameters. The waste stream characterization included physical, chemical, and biological assays, as well as degradation and corrosion studies. Dispersion and fate studies included scaling analysis, ship wake dilution modeling, and ambient dilution modeling for the pulped material. Field tests were conducted to validate the fate modeling.

This Addendum presents information not finalized for publication at the time of the original report. This includes a review of characteristics of three Special Areas; follow-on biological interaction studies of sardine filter feeding and microbial degradation; chemical characterization of the inorganic components of the pulped material; and a study of ocean bottom transport with regard to shredded cans. A general review of sensitive species and habitats was conducted, with particular emphasis on coral reefs, and endangered and threatened species. Results of a full-scale field test are detailed along with a comparison to wake dispersion modeling results. Ambient modeling results are also finalized for a range of conditions in each of the Special Areas. Finally, the findings of these follow-on studies are interpreted within the framework and context of the original report.

Follow-on Key Findings for the Pulped Paper and Cardboard Waste Stream

- The inorganic portion of pulped paper and cardboard waste stream was comprised primarily of calcium, chlorine, titanium, silicon, and aluminum with smaller amounts of sodium, magnesium, potassium and iron, and a trace of sulfur. These components are likely found in the form of oxides and carbonates and in total, make up about 3% of the pulp material. The percentages are comparable to those found in typical marine sediments. Therefore the inorganic fraction of the pulp material should pose no ecological risk to benthic organisms. The results here corroborate the original findings that the pulped material is primarily (>95%) composed of organic cellulose.

- Microbial degradation rates of the pulped material varied between $0.04\%\cdot d^{-1}$ to $0.4\%\cdot d^{-1}$ over a broad range of nutrient and temperature regimes, with temperature the dominant factor. This corresponds to half-lives of approximately 1773 to 173 days respectively. Thus, the long term fate of the pulp material will be controlled by natural degradation over a time period of 1 to 5 years.

- Initial dilution of the pulped material in the wake of a moving ship was successfully characterized during full-scale field tests using a Navy frigate. Independent measurements of pulped paper and of dye, a surrogate of the liquid phase of the discharge, were used to define the average and minimum dilution levels throughout the wake. These results were used successfully to validate model predictions, with differences less than 20% at the end of wake mixing. The excellent agreement between model and field results indicates that the model can be used successfully to predict the short-term fate of solid wastes discharged from ships under a variety of conditions, a critical component to determining potential ecological impacts.

- Ambient modeling simulations were run for a variety of conditions in all Special Areas to estimate the long term fate of pulped material. Dilution levels range from about 10^5 to 10^8 with the depth of water being the major control on the dilution. In shallow seas, wind induced mixing is the dominant process for dilution while current induced mixing dominates dilution in deep seas. At the end of ambient dilution, particle concentrations just above the sea floor were predicted to range from 0.056 $mg\cdot L^{-1}$ to 0.0000081 $mg\cdot L^{-1}$ considering all of the Special Areas. These results indicate that exposure levels at the seafloor would be reduced below those found in the wake by factors of about 3 to 1000.

- The long-term (30 day) feeding interference study on sardines indicated that pulped material affected weight gain at the minimum practical laboratory test concentration of 0.01 $mg\cdot L^{-1}$, and that pulp accumulated in stomachs at higher test concentrations of 0.1 and 1 $mg\cdot L^{-1}$. The expected exposures in the water column 30 days after discharge would be approximately 0.000033 $mg\cdot L^{-1}$. Therefore, it is unlikely that these effects would be found given the actual exposures in the field.

- An analysis of historical ship operations and identification of known coral reefs in Special Areas indicated that there is limited overlap between ship operations and coral reef locations. Potential exposure and effects are futher limited by the high initial dilution of the waste stream and the non-toxic nature of the pulp material. The estimated maximum suspended particle loads following discharge and long-term sedimentation rates were found to be well below reported background and effects levels. These findings indicate that the discharge of pulped waste is unlikely to cause environmental impacts to coral reefs.

Follow-on Key Findings for the Shredded Metal and Glass Waste Stream

- The results of five water-tunnel tests indicate that current flows exceeding the critical value (50 to 230 $cm \cdot s^{-1}$) needed to move shredded metal cans on the seafloor rarely occur in nature. It is expected that these flows occur only in localized, high-energy environments, or during episodic high-energy events. Thus, the redistribution of metal cans on the sea floor from their initial deposition location is unlikely.

- A review of historical ship operations and identification of known coral reefs in Special Areas indicated that ships will come within 1 nmi of coral reefs less than 3 times a year. It was also determined that the sinking characteristics of shredder bags minimizes their lateral transport away from the point of discharge to less than 350 m. Hence, a shredder bag would land on a coral reef, only if a ship transited and discharged while almost directly above it. These findings indicate that the discharge of shredder bags is unlikely to cause environmental impacts to coral reefs.

- A study of endangered and threatened species indicated that five species of turtle and gray whales have feeding behaviors that would potentially place them at risk for ingestion of bagged wastes. A review of feeding habitats indicated that their potential overlap with wastes discharged from navy ships is exceptionally low. Further, the low density of bag wastes on the seafloor would serve to minimize the likelihood of these species encountering the wastes. It was therefore concluded that there is an extremely low likelihood that bagged wastes will have an environmental impact to endangered and threatened species.

CONTENTS

EXECUTIVE SUMMARY i

FIGURES v

TABLES ix

ACRONYMS xi

1. INTRODUCTION 1

2. ADDITIONAL SPECIAL AREA CHARACTERISTICS 5

2.1 Black Sea 5
2.2 Red Sea 13
2.3 Gulfs Area 22
2.4 Updated Antarctic Tables 30

3. FOLLOW-ON STUDIES OF PULPER AND SHREDDER WASTE STREAM CHARACTERIZATION 31

3.1 Biological Interactions 31
3.1.1 Effects of Dispersed Paper Waste on the Filter-Feeding Capacity, Ingestion of Paper, and Growth of Pacific Sardine, *Sardinops Sagax* 31
3.1.2 Bacterial Degradation Of Cellulosic Wastes At Sea 48
3.2 Chemical Analysis of Inorganic Pulper Material 64
3.3 Ocean Bottom Transport of Shredded Cans: Laboratory Study 66

4. ADDITIONAL STUDIES FOR THE ENVIRONMENTAL IMPACT STATEMENT (EIS) U.S. NAVY SHIPBOARD SOLID WASTE DISPOSAL 80

4.1 Sensitive Species and Habitat Ecological Assessment 80
4.2 Endangered and Threatened Species Study 231
4.3 Analysis Of Potential Effects Of U.S. Navy Shipboard Solid Waste Discharges On Coral Reefs 253

5. FULL-SCALE FIELD TEST AND MODEL VALIDATION 277

5.1 Field Measurements and Modeling of Dilution in the Wake of a U.S. Navy Frigate 277
5.2 Far Field Dispersion of Paper Particulates from Surface Vessel Discharges in Marginal Seas, Part II 316

6. ANALYSIS 329

6.1 Fate and Effects of the Pulped Waste Stream 329
6.2 Fate and Effects of the Shredded Waste Stream 343

7. CONCLUSIONS 347

FIGURES

2.1-1 General area map of the Black Sea 6
2.2-1 General area map of the Red Sea 13
2.3-1 General area map of the Gulfs Area 22
3.1.1-1 Filtering efficiency experiments 39
3.1.1-2 High DPW filtering efficiency experiments. Accumulation of DPW at end of 15-day experimental period. 40
3.1.1-3 High DPW filtering efficiency experiments. Percent mortality over 15 days for sardine exposed to 30, 15, 3, and 0 $mg \cdot L^{-1}$ dry weight DPW 40
3.1.1-4 Gastric evacuation experiment. Amount of DPW consumed and rate of elimination over 12 days after a single 8-hour feeding of *Artemia* in DPW. 41
3.1.1-5 Gastric evacuation experiment. Photographs of dissected gastrointestinal (GI) tracts from esophagus (left) to anus (right). 42
3.1.1-6 Chronic exposure experiment. Percent weight change after 30-day exposure to *Artemia* only, starvation, or DPW (0.01, 0.1 and 1.0 $mg \cdot L^{-1}$) plus *Artemia* 43
3.1.2-1 Results of particle size study #2 53
3.1.2-2 Results of long-term decomposition experiment 55
3.1.2-3 Rates of degradation of mixed paper cellulose slurry by bacterial populations from oceanic and coastal sites 57
3.1.2-4 Comparison of degradation rates in two types of incubation systems: glass BOD bottles and 15-liter polyethylene/mylar bags 61
3.2-1 Pulped paper x-ray spectrum before extensive washing 64
3.2-2 Pulped paper x-ray spectrum after washing 65
3.3-1 Basic features of the SSC San Diego recirculating water tunnel 68
3.3-2 Streamwise dimensions of the flat plate on which the test samples were placed 69
4.1-1 Geographic distribution of MARPOL Special Areas 80
4.1-2 Relationship of respiratory strategy and foraging ecology of an organism to its potential susceptibility to impacts of pulped waste discharges 96
4.1-3 Generalized relationship of organism body size to potential susceptibility to impacts of shredded and pulped waste toxicity and particulate waste impacts ... 97
4.1-4 Relationship of biomass and waste stream concentration to depth in deep ocean environments 97
4.1-5 Relationship of biomass and waste stream concentration to depth in shallow sea environments 98
4.1-6 Major geographical, physical, and political features of the Antarctic region 101
4.1-7 Diagram of major water masses of the Antarctic 102
4.1-8 Distribution of krill in the Antarctic region 108
4.1-9 Pelagic food web of the Antarctic region 110
4.1-10 Antarctic benthic zonation 112
4.1-11 Benthic food web of the Antarctic region 114
4.1-12 Baltic Sea region 118
4.1-13 Schematic representation of the volume and salinity of water exchanged between the Baltic Sea and the North Sea 120
4.1-14 Salinity gradient and species richness of the Baltic Sea 121
4.1-15 The Baltic Sea trophic web 126
4.1-16 North Sea region 131
4.1-17 The North Sea trophic web 140
4.1-18 The Black Sea region 143
4.1-19 The Black Sea trophic web 149
4.1-20 The Mediterranean Sea 153

4.1-21 The Mediterranean Sea trophic web 161
4.1-22 The Red Sea and Gulf of Aden 166
4.1-23 Winter (a) and summer (b) water flow through the entrance into the Red Sea ... 168
4.1-24 Pelagic trophic web of the Red Sea 176
4.1-25 Benthic food web of the Red Sea 177
4.1-26 Wider Caribbean region 180
4.1-27 Pelagic trophic web of the Caribbean Sea 188
4.1-28 Interrelationship of shallow benthic Caribbean communities 189
4.1-29 Benthic food web of the Caribbean Sea 190
4.1-30 The Gulfs region 195
4.1-31 Pelagic trophic web of the Gulf region 204
4.1-32 Benthic food web of the Gulfs region 205
4.3-1 The distribution of coral reefs in the Red Sea and Gulf Region 255
4.3-2 Distribution of coral reefs in the Wider Caribbean Basin 256
4.3-3 Average yearly port visits by Navy ships 257
4.3-4 Average yearly post visits by various classes of Navy ships to Roosevelt Roads in the Caribbean based on a ten year average (1984-1993) 258
4.3-5 Estimated sedimentation rates for various Navy ship classes 259
4.3-6 Estimated long-term sedimentation rates at ports in MARPOL Special Areas 260
4.3-7 Estimated annual percentage of bottom beneath the ship track covered by shredder bags 261
4.3-8 Ship traffic and reef positions in the Gulfs Area 262
4.3-9 Ship traffic and reef positions in the Wider Caribbean Basin 263
4.3-10 Ship traffic and reef positions in the Red Sea 263
4.3-11 Overlap of ships and coral reefs within a 3 nmi range in the Gulfs Area 264
4.3-12 Overlap of ships and coral reefs within a 3 nmi range in the Wider Caribbean Basin 265
4.3-13 Overlap of ships and coral reefs within a 3 nmi range in the Red Sea 265
4.3-14 Overlap of ships and coral reefs within a 1 nmi range in the Gulfs Area 266
4.3-15 Overlap of ships and coral reefs within a 1 nmi range in the Wider Caribbean Basin 267
4.3-16 Overlap of ships and coral reefs within a 1 nmi range in the Red Sea 267
4.3-17 Effects of pulped paper on light transmission 273
4.3-18 Shoreward transport of shredder bags under varying conditions of shoreward current speed and discharge depth 274
5.1-1 Field measurement test area of San Diego, California 279
5.1-2 Relative fluorescence signal versus pulped paper concentration (APL, 1996.) .. 282
5.1-3 Relative dye fluorescence versus fluorescein dye concentration for five *in situ* sensors (APL, 1996) 284
5.1-4 Relative fluorescence signal as a function of fluorescein dye concentration for three flow-through fluorometers. 285
5.1-5 Density and light transmission as a function of depth for two vertical profiles made during the field experiments 291
5.1-6 Plan view dye concentration ($ug \cdot L^{-1}$) for Serpentine Run 1 (8 kts) at 2.7, 4.5, and 6.5 m depths as a function of distance behind the frigate 296
5.1-7a Cross-sectional views (looking toward frigate from behind) of dye concentration ($ug \cdot L^{-1}$) for Serpentine Run 1 (8 kts) for first 12 full-wake crossings. Concentrations were measured by the in situ fluorometer array 297

5.1-7b Cross-sectional views (looking toward frigate from behind) of dye concentration (ug·L-1) for Serpentine Run 1 (8 kts) for last 10 full-wake crossings. Concentrations were measured by the in situ fluorometer array 298
5.1-7 Plan view dye concentration (ug·L^{-1}) for Serpentine Run 4 (15 kts) at 2.7, 4.5, and 6.5 m depths as a function of distance behind the frigate 299
5.1-9 Cross-sectional views (looking toward frigate from behind) of dye concentration (ug·L^{-1}) for Serpentine Run 4 (15 kts) for first 12 (of 13) full-wake crossings. 300
5.1-10 Maximum dye concentration as a function of distance behind the frigate for both 8-kt and 15-kt runs measured at each wake crossing 301
5.1-11 Minimum dye dilution for 8-kt and 15-kt data based on 2 g·L^{-1} discharge concentration 302
5.1-12 Minimum dye dilution for 8-kt and 15-kt data based on 2 g·L^{-1} discharge concentration 302
5.1-13 Model results for pulped material concentration as a function of distance behind the frigate 303
5.1-14 Plan view of modeled dye concentration (ug·L^{-1}) at 2.5 m depth, as a function of distance behind the frigate at 8-kts 304
5.1-15 Cross-sectional views (looking toward frigate from behind) of model dye concentration (ug·L^{-1}) at selected distances behind the frigate for the 8-kt case 305
5.1-16 Model results for maximum dye concentration (ug·L^{-1}) as a function of distance behind frigate 306
5.1-17 Minimum dilution for model dye results as a function of distance behind frigate .306
5.1-18 Plan view of modeled dye concentration (ug·L^{-1}) at 1 m depth, as a function of distance behind the frigate at 15-kts 306
5.1-19 Cross-sectional views (looking toward frigate from behind) of model dye concentration (ug·L^{-1}) at selected distances behind the frigate for the 15-kt case. 307
5.1-20 Modeled and measured pulp concentrations as a function of distance behind frigate 308
5.1-21 Modeled and measured dilution values as a function of distance behind frigate. 309
5.1-22 Modeled and measured minimum and average dilution values as a function of distance behind frigate for the 8-kt case 310
5.1-23 Modeled and measured minimum and average dilution values as a function of distance behind frigate for the 15-kt case 310
5.1-24 Wake width as a function of distance behind the frigate for both 8-kt and 15-kt data 311
5.1-25a Mass balance of dye as a function of distance behind the frigate for the 8-kt case 312
5.1-25b Mass balance of dye as a function of distance behind the frigate for the 15-kt case 313
5.2-1 Size distribution of paper particulate discharge based upon fraction of the total mass distributed among 9 size bins 318
5.2-2 Size distribution of paper particulate discharge based upon particle numbers in each of 9 size bins 319
5.2-3 Settling velocity of paper particulate based upon laboratory observations (NRaD) 321
5.2-4 Dilution history of total discharge during the first 200 hours, western Mediterranean Sea (fall) 324
5.2-5 Dilution history of total discharge over complete residence time, western Mediterranean Sea (fall) 325
6.1-1 Degradation rate of pulped paper waste as a function of water temperature 330

6.1-2 Settling time of pulper effluent for each of the Special Areas assuming no degradation 332
6.1-3 Estimated water column exposure limits based on model results compared to measured biological response levels for the pulped paper particle phase 335
6.1-4 Predicted concentration of paper pulp in sediment as a function of time based on estimated rates of vertical mixing, burial, and degradation 337
6.1-5 Fraction of pulped paper remaining in sediment over time based on estimated removal rates due to biodegradation 338

TABLES

2.1-1 Representative oceanographic characteristics of the Black Sea 10
2.2-1 Representative oceanographic characteristics of the Red Sea 19
2.3-1 Representative oceanographic characteristics of the Persian Gulf 27
2.3-2 Representative oceanographic characteristics of the Gulf of Oman 28
2.4-1 Representative oceanographic characteristics of the Antarctic area 30
3.1.1-1 Mean standard length (SL), mean wet weight, and N of sardines used in the filtering efficiency experiment and exponential regression equations of prey density (nauplii/L/fish) as a function of time (h) 38
3.1.1-2 N, mean and standard deviation of standard length, wet weight, and dry weight of gut contents of sardines used in the chronic exposure treatments, and the mean and standard deviation of wet weight change from beginning to end of exposure 44
3.1.1-3 P-values of ANOVA of wet weight changes (upper matrix) and dry weight of gut contents (lower matrix) 44
3.1.2-1 Elemental analysis of white paper and mixed paper slurries 50
3.1.2-2 Water samples collected for bacterial community source studies 56
3.1.2-3 Rates of degradation of mixed paper slurry by bacterial populations from oceanic and coastal sites 58
3.1.2-4 Results of temperature/nutrient matrix studies presented as percent decomposition of paper slurry in 30 d 60
3.1.2-5 Results of temperature/nutrient matrix studies presented as the decomposition constant (k) assuming first order degradation kinetics 60
3.2-1 ICP results (in weight percentage) of dried pulp 65
3.3-1 Summary of water tunnel experiments 67
3.3-2 Oceanic extrapolations via equations 1a and 1b 71
3.3-3 Oceanic extrapolations via equations 2a and 2b (beginning of turbulent velocity profile, y = 0) 73
3.3-4 Oceanic extrapolations via equations 2a and 2b (beginning of turbulent velocity profile, y = 30 k0) 74
3.3-5 Oceanic extrapolations via equations 3a and 3b (beginning of turbulent velocity profile, y = d0 76
4.1-1 Summary of Unique Species and Ecological Considerations for each MARPOL Designated Special Area 208
4.1-2 Sensitive Biological Communities Associated with Pulped Paper Waste Discharge within MARPOL Special Areas 212
4.1-3 Sensitive Biological Communities Associated with Shredded Waste Discharge within MARPOL Special Areas 215
4.2-1 Listed U.S. and foreign threatened and endangered species in the world oceans 234
4.2-2 Listed U.S. and foreign threatened and endangered species found within MARPOL Special Areas 235
4.2-3 Summary table of species feeding behavior 243
4.2-4 Annual U.S. Navy shredded metal and glass discharges in MARPOL Special Areas 244
4.2-5 Known endangered and threatened species worldwide 247
4.3-1 Number of visits within a 3 nmi range in each Special Area 264
4.3-2 Number of visits within a 1 nmi range in each Special Area 266
4.3-3 Comparison of effects on overlap of ships and coral reefs from 3 nmi and 12 nmi discharge limits 268

4.3-4 Comparison of using port visit data versus more precise ship transit data 269
4.3-5 Background sedimentation and suspended sediment loads near coral reefs 270
4.3-6 Effects levels for sedimentation and suspended sediment loads on coral reefs .. 271
4.3-7 Comparison of pulper discharge levels to background and effects levels 272
5.1-1 Personnel involved in the field tests 280
5.1-2 Chronology of field tests performed 287
5.1-3 Pulped paper sample collection summary 288
5.1-4 Fluorescein dye sampling summary 288
5.1-5 Pulped paper characteristics used as model inputs 290
5.1-6 Sample filtration efficiency as determined both fluorometrically and gravimetrically 291
5.1-7 Average pulped paper concentrations as a function of distance behind frigate ... 292
5.1-8 Average pulped paper concentrations as a function of distance behind frigate ... 292
5.1-9 Average dilution levels of pulped paper based on a discharge concentration of 9.6 $g \cdot L^{-1}$ 293
5.1-10 Comparison of the average in situ pulped paper concentrations measured at two discharge rates: 109 and 45 $kg \cdot hr^{-1}$ for samples collected 630 m aft of the frigate 293
5.1-11 Average dye concentrations and calculated dilution based on flow-through fluorometer measurements made during continuous dye discharge periods for FTL runs 294
5.1-12 Mass ratio of pulped paper to dye measured during FTL runs at 8 kts 314
5.2-1 Particle size in the far field initial data plane at 20 knots 319
5.2-2 Particle size dependent dynamic parameters 320
5.2-3 Boundary conditions and input forcing for shallow sea cases 322
5.2-4 Boundary conditions and input forcing for deep sea cases 322
5.2-5 Summary of residence time, dilution and seabed particle accumulation, northern Persian Gulf and southern North Sea. 325
5.2-6 Summary of residence time, dilution and seabed particle accumulation, northern central Baltic Sea and southern Red Sea 325
5.2-7 Summary of residence time, dilution and seabed particle accumulation, northern south central Black Sea and Caribbean Sea 326
5.2-8 Summary of residence time, dilution and seabed particle accumulation, northern Red Sea and western Mediterranean Sea 326
5.2-9 Summary of residence time, dilution and seabed particle accumulation, western Mediterranean Sea 326
6.1-1 Estimated fate of a typical one day discharge of pulped paper from a CVN 68 class ship under a range of conditions representing all MARPOL Special Areas 333
6.1-2 Estimated steady-state exposure levels and fate in four MARPOL Special Areas from the combined pulped paper discharge of one BG and one ARG within 10000 nmi2 (32400 km2) operational area 340
6.1-3 Annual basin-wide constituent loading from U.S. Navy ships into eight MARPOL Special Areas based on estimated pulped paper discharges and results from chemical analysis 341
6.1-4 Comparison of basin-wide constituent loading from Navy ships 342
6.2-1 Annual mass loading estimates of the shredded metal/glass waste stream and Fe and Sn components into Special Areas by U.S. Navy ships 344
6.2-2 Estimate of oxygen utilization for the complete corrosion of the annual shredded metal waste stream in to each Special Area 345
6.2-3 Steady-state loading estimates of Fe and Sn in Special Areas 346

ACRONYMS

ARG	Amphibious Ready Group
BG	Battle Group
BOD	Biochemical Oxygen Demand
CNO	Chief of Naval Operations
C:N:P	Carbon:Nitrogen:Phosphorous Ratio
COD	Chemical Oxygen Demand
DOC	Dissolved Organic Carbon
DOM	Dissolved Organic Material
DPW	Dispersed Paper Waste
EIS	Environmental Impact Statement
EMPSKD	Employment Schedule Data
FAO	Food and Agriculture Organization of the United Nations
GI	Gastrointestinal
HUFA	Highly Unsaturated Fatty Acids
ICP	Inductively Coupled Plasma
IMO	International Maritime Organization
KFUPM	King Fahd University of Petroleum and Minerals
MARPOL	International Convention for the Prevention of Pollution from Ships
MESEDA	Metalliferous Sediment Atlantis II Deep
MMPA	Marine Mammal Protection Act
MPPRCA	Marine Plastic Pollution Research and Control Act
mpy	mil per year
NAVSEA	Naval Sea Systems Command
NCCOSC	Naval Command, Control and Ocean Surveillance Center
NMFS	National Marine Fisheries Service
PERSGA	Environmental Programme for the Red Sea and the Gulf of Aden
POC	Particulate Organic Carbon
PPMT	Pre-Pilot Mining Tests
ppt	parts per thousand
psu	Practical Salinity Units
SEM	Scanning Electron Microscopy
SPAWARSYSCEN	Space and Naval Warfare Systems Center
SWFSC	Southwest Fisheries Science Center
TCA	Trichloroacetic Acid
TDU	Trash Disposal Unit
TOC	Total Organic Carbon
TSS	Total Suspended Solids
UAE	United Arab Emirates
UNEP	United Nations Environmental Programme
USFWS	United States Fish and Wildlife Service

1. INTRODUCTION

This Addendum is the final component of a comprehensive report, NRaD TR 1716, published in January 1996 (Chadwick et al., 1996) detailing the fate and effects of U.S. Navy shipboard solid waste discharges. The study was requested as part of the Navy's effort to evaluate solid waste discharge compliance alternatives. The objective of the study was to determine to what extent, if any, Navy solid waste discharges lead to adverse marine environmental effects. At the time the original report was published, there were ongoing studies and characterizations that were not possible to include in the published report. This Addendum contains the findings from all of the remaining studies and integrates the information into a final analysis of environmental impacts.

The Naval Command, Control and Ocean Surveillance Center (NCCOSC) RDT&E Division (currently SPAWAR Systems Center San Diego (SSC San Diego)) Code D362 was tasked by the Naval Sea Systems Command (NAVSEA 03R16) to perform an environmental analysis. The environmental analysis was conducted as part of the Navy's overall effort to respond to U.S. legislation requiring compliance with Annex V of the International Convention for the Prevention of Pollution from Ships, 1973, as modified by the Protocol of 1978 (MARPOL 73/78). MARPOL 73/78 Annex V prohibits the discharge of non-food solid wastes into sensitive oceanographic and ecological areas throughout the world, known as Special Areas. There are currently eight existing and proposed Special Areas: the Baltic Sea, the North Sea, the Mediterranean Sea, the Wider Caribbean Region (including the Gulf of Mexico and the Caribbean Sea), the Antarctic area, the Black Sea, the Red Sea, and the "Gulfs" area (including the Persian Gulf).

The Navy researched alternatives for ways to comply with the MARPOL restrictions and developed a compliance plan for the U.S. Congress. Subsequently, the law was changed to allow for the use of the preferred alternative. This alternative consists of an equipment suite comprised of a plastics processor to handle plastics waste, pulpers for food and paper/cardboard products, and a shredder for metal and glass waste. This suite will be installed on all commissioned ships, with the exception of a few vessels whose waste generation rates would allow for temporary storage onboard. The equipment suite will be used not only in Special Areas, but also in the open ocean as an improvement to current solid waste discharge practices. The environmental analysis was conducted on the pulper and shredder waste streams, including paper, cardboard, metal and glass. Plastic wastes must be retained on board and food wastes are not restricted, therefore, neither were focused on in the environmental analysis. A related study focused on the submarine solid waste which is discharged through trash disposal unit (TDU) cans and reported on in NRaD TR 1738 dated May 1997 (Katz et al., 1997).

The initial shipboard study involved a review of pertinent literature, characterization of the waste stream, model simulations, and field tests. The literature review focused on the regulatory framework of Special Areas, their environmental characteristics, the bulk waste stream constituents, general ocean discharge issues, and Navy vessel operational parameters. The waste stream characterization included physical, chemical, and biological assays as well as degradation and corrosion studies. Dispersion and fate studies entailed scaling analysis, ship wake dilution modeling, and ambient dilution modeling for the pulped material only. Small-scale field tests were conducted to develop test methodologies and to begin to validate the model simulations.

The study was approached primarily from a theoretical standpoint because few ships are installed with pulpers and shredders. A conceptual framework similar to that of an environmental risk assessment was used in which the material discharged was characterized with regards to its potential for biological impacts and in which the operational and receiving environments were characterized to determine the likely exposures. The analysis was approached for three spatial and temporal scales, including: a local scale, or single ship daily discharge case; a regional scale, using an operational scenario that involves a

battle group (BG) and an amphibious ready group (ARG) for a duration of 6 months; and a basin-wide, longer term assessment that considered Special Areas as a whole. Water column and sea floor processes were addressed in all cases.

The findings of the original study suggested that the discharge of paper and cardboard, and metal and glass waste streams as proposed will have no significant environmental consequences on a local, regional, or basin-wide scale in Special Areas. Furthermore, the findings supported a conclusion that the discharge of these waste streams using pulpers and shredders is superior to current discharge practice utilized in open ocean environments. The assessment was based on measurements, model simulations, and extrapolations to real-world conditions expected in Special Areas. The following key findings from the original report are presented here for review:

PREVIOUS KEY FINDINGS OF THE PULPED PAPER AND CARDBOARD WASTE STREAM

- The pulped paper and cardboard is an organic material that is composed mostly of refractory cellulose. The pulped material was measured to be approximately 0.3% solids by weight of which approximately 92% is organic matter, and is low in nutrients compared to background organic matter. All of this indicates that the material will not be a significant source of nutrients in the water column or the benthos and will most likely be avoided as a food source. Productivity should not be significantly enhanced and eutrophication should not be a major factor, however, microbial degradation may be hindered in nutrient limited ocean areas.
- The material contains no significant amounts of toxic chemicals. A 126 priority pollutant scan showed no pollutants at levels which would be expected to produce impacts and only trace amounts of zinc (6 $mg \cdot kg^{-1}$), acetone (2 $mg \cdot kg^{-1}$), and aliphatic hydrocarbons (6 $mg \cdot kg^{-1}$), which are well below threshold levels of concern for standard sediment criteria.
- On a mass basis, the waste stream is made up of predominantly large particles and most of the pulped material should settle to the sea floor where it will degrade through natural processes. Approximately 85% of the material is expected to sink within 1 to 10 days at average depths found in Special Areas with measured average sink rates of 0.5 $m \cdot min^{-1}$ for particles greater than 1000 μm. Another 12% will probably sink within 10 to 100 days while approximately 3% may remain in suspension, subject to microbial degradation and other processes in the water column. The measured degradation rate under optimal nutrient and temperature conditions was approximately 0.6% per day, however, the rate could be as low as 0.01% per day in cold, nutrient limited waters. The paper density was measured to be approximately 1.5 $g \cdot cm^{-3}$, indicating that density variations in the water column will not significantly affect sinking of particles greater than 200 μm in size. Approximately 95% of the material will eventually be deposited on the sea floor. Therefore, exposure in the water column will be limited and the sea floor processes are assumed to be the dominant ones. No harmful effects have been seen in either regime given the expected waste concentrations.
- Discharge into the wake is the most critical factor in the dilution and dispersion of the pulped material. Modeling indicates that maximum concentrations of pulped paper following dilution in the wake will be approximately 0.2 $mg \cdot L^{-1}$, a dilution factor of 100,000 fold in a matter of minutes. Field measurements and modeling results support subsequent ambient dilution estimates up to 1,000,000 fold in approximately 1 hour. These levels are a fraction of background levels found in many ocean areas and are well below any concentration found to have toxicity in laboratory bioassays.
- The potential impacts on water column and benthic biota tested occur only at concentrations significantly greater than would be found after discharge. Biological interactions tested with a large range of organisms from bacteria to small fish showed that the most sensitive response occurred in filter-feeding sardines causing a temporary feeding interference effect at concentrations from 1 to

3 $mg \cdot L^{-1}$, or 5 to 15 times higher than found in the wake dilution. No biological effects were observed in any organism tested at concentration levels expected in the water column with wake dilution based on both particle and water phase testing. No biological effects were observed in two benthic organisms tested at concentration levels that would be expected in the sediments after 1000 ships had passed over the same location.

- Mass loading on an annual basis from regional and basin-wide Naval operations is a miniscule fraction of other coastal inputs in Special Areas. Based on an operational scenario with an ARG and a BG deployed for 6 months in a 10,000 nm^2 area, the accumulated concentrations are well below those causing biological effects.

PREVIOUS KEY FINDINGS FOR THE SHREDDED METAL AND GLASS WASTE STREAM

- The shredded material is mostly composed of tin-coated steel cans (71% by weight) and glass (13% by weight). Minor components include aluminum cans, burlap bags, food waste, and paper labels. The elemental constituents of the metal and glass are not unlike those found in naturally occurring materials in the marine environment. Of these, only iron and tin are significantly enhanced in the waste stream relative to the concentrations found in typical marine sediments.
- The shredded material, discharged in burlap bags, sinks rapidly through the water column. This result indicates that the waste will have minimal impact in the water column and that its dominant fate and effects will occur on the sea floor. The proposed discharge method also appears to be an improvement over previous methods such as compacting that sometimes led to floating wastes. Based on the measured sink rates and estimates of shoreward transport in Special Areas, it is unlikely that the material will be a source of coastal litter if the bags are discharged outside the regulatory limits of 12 nmi or even 3 nmi.
- The ultimate fate of the shredded material is deposition, corrosion, and burial on the sea floor. Corrosion of the metal is likely to occur over a period of several years, although the rates can be highly variable. Corrosion is a process that will lead to a change in the aesthetic nature of the waste stream from a component of litter to a component more typical of sedimentary materials. The time scales for burial and redistribution of metal and glass waste on the sea floor can be relatively long, ranging to hundreds of years for complete burial and degradation.
- Seawater leaching of the metal/glass was shown to cause some effects under laboratory conditions. However, the biological effects were shown to occur at concentrations that are estimated to occur within a few centimeters of the bag. Colonization of the metal and glass components in San Diego Bay over a year showed a highly diverse array of organisms, suggesting that many organisms are not negatively affected by the material.
- The effect of operating a large number of ships in a limited region as described above does not load the sea floor with bags at a significantly higher per unit area rate than already described for a single swath discharge. Any biological effects could therefore still be related to any that would be found within or near a single bag. These results could be altered if operational practices acted to concentrate the discharges in particular areas that are significantly smaller than an operational area. This suggests that operational discharge practices should be minimized in areas that are constantly traveled such as before and after leaving Navy ports.
- The annual input of the shredded metal/glass waste stream from U.S. Navy ships operating in Special Areas constitutes a tiny fraction of basin-wide inputs. It is estimated that it would take hundreds to billions of years of U.S. Navy discharges to match a single year discharge from other basin sources such as rivers or industrial discharges. The amount of material discharged annually by U.S. Navy ships would cover only a tiny fraction (billionths) of the sea floor.

- From a basin-wide perspective, there is at least a billion times more oxygen available in Special Areas than is needed to completely oxidize the annual discharge of metal components of the waste stream implying that it is improbable that the discharges will have any impact on the oxygen budget of any of the seas.
- Based on a steady-state analysis of the inputs and corrosion rates, the amount accumulated on the sea floor as a litter component would be roughly equivalent to about three years of discharges.

This Addendum addresses only the work that was ongoing at the time the original report was published. The reports generated from the individual studies are presented in chapter form, with an analysis chapter that integrates the new information with the original findings for a final assessment. The following studies were conducted and reported on in the following chapters:

1. Researching the oceanographic and ecological characteristics for the remaining Special Areas that were not published in the January report, the Black Sea, the Red Sea, and the Gulfs Area, and updating the summary tables for the Antarctic area--Chapter 2.
2. Performing long-term monitoring of paper particle ingestion on sardines--Chapter 3
3. Expanding cellulose degradation studies to cover a wider range of seawater conditions and actual sea water samples--Chapter 3.
4. Performing chemical analysis on the inorganic component of the pulped paper--Chapter 3.
5. Conducting a small scale experiment to measure forces required to transport shredded material on the ocean bottom--Chapter 3.
6. Compiling a review of sensitive species and habitats--Chapter 4.
7. Researching potential effects of solid waste to endangered and threatened species--Chapter 4.
8. Evaluating potential effects of solid waste to coral reef environments based on a 3 nmi discharge limit for the pulped material and a 12 nmi discharge limit for the shredded material--Chapter 4.
9. Performing a full-scale field test to validate the modeling results and preliminary estimates of dilution in the wake of a ship--Chapter 5.
10. Expanding the ambient modeling conditions to include the remaining Special Areas--Chapter 5.
11. Incorporating an analysis of long-term, steady-state loadings from the pulped paper waste stream--Chapter 6.
12. Revising the initial analysis to include the results of the ongoing work--Chapter 6.

REFERENCES

Chadwick, D.B, C.N. Katz, S.L. Curtis, J.Rohr, M. Caballero, A. Valkirs, and A. Patterson 1996. *Environmental Analysis of U.S. Navy Shipboard Solid Waste Discharges: Report of Findings*, Naval Command, Control, and Ocean Surveillance Center Technical Report, 1716, January 1996, 268 pp.

Katz, C.N., S.L Curtis, and D.B. Chadwick, 1997. *Environmental Analysis of U.S. Navy Submarine Solid Waste Discharges, Report of Findings* Naval Command, Control, and Ocean Surveillance Center Technical Report, 1738, May 1997, 158 pp.

2. ADDITIONAL SPECIAL AREA CHARACTERISTICS

by Aldis Valkirs and Charles N. Katz

This section of the report is a review of the oceanographic setting of the remaining three MARPOL Special Areas: Black Sea, Red Sea, and the Gulfs Area. These three Special Areas are included in the revision to Technical Report 1716, however, they are included here as well for those who are using the original report dated January 1996. As with the original report, the reviews were performed to obtain background on the special oceanographic, ecological, pollution, and vessel traffic conditions in these areas. Much of the information gathered forms the basis for their inclusion as MARPOL Special Areas. For each area, an attempt was made to tabulate quantitative data of pertinent physical, chemical, and biological parameters that could be used as guides for comparing navy ship solid wastes to background conditions or other inputs to Special Areas. It was not possible to obtain numbers for all parameters in all areas. Furthermore, because there is a high degree of variability even within a single Special Area, a "typical" or average number was used, even though its meaning is somewhat limited. The tabulations for the Black Sea, Red Sea, and the Gulfs Area are included at the end of each review, and an updated tabulation is included for the Antarctic area.

2.1 BLACK SEA

General Description. The Black Sea is an enclosed basin in Eastern Europe (see Figure 2.1-1). It is surrounded by Romania, Bulgaria, Turkey, Georgia, Russia, and Ukraine. The only connection to the Mediterranean Sea is through the Bosphorous Strait. The Black Sea is the largest anoxic basin in the world, consisting of a shelf region, basin slope, basin apron, and the abyssal plain. It is roughly elliptical with an area of 423,000 km^2 and a volume of 534,000 km^3 (Egon and Ross, 1974). The shelf, basin slope, basin apron, and abyssal plain regions occupy 29.9, 27.3, 30.6, and 12.2% of the total area, respectively. A maximum depth of 2,206 m has been recorded in the Euxine Abyssal Plain in the center of the Black Sea (Egon and Ross, 1974). The average depth is 1,240 m (Balkas et al., 1990). The surface water is a relatively thin layer of oxygenated water about 150-200 m deep. Below this layer the oxygen content decreases abruptly to zero. Under this layer hydrogen sulfide is present to the bottom (Ostlund, 1974). Approximately 90% of the total water volume is anoxic (Deuser, 1972). The two-layered system is maintained by the influx of fresh river water at the surface, and saline water from the Bosphorous Strait which, due to its higher density, sinks to depths below the surface layer.

Physical/Chemical Oceanography. Since the Black Sea is located in a semi-arid climate, evaporation (332-392 $km^3 \cdot yr^{-1}$) exceeds rainfall (225-300 $km^3 \cdot yr^{-1}$). However, runoff (350 $km^3 \cdot yr^{-1}$) primarily from the humid area to the north leads to an excess of net freshwater inflow. Surface seawater is, therefore, diluted. Average surface water salinity ranges from 18-18.5 psu in winter to 17.25-17.50 psu in the summer. Much lower summer values may be seen in the north- northeast shelf regions in the summer ranging from 14-16 psu due to river runoff. In the central Black Sea salinity is about 18.5 psu. A notable permanent halocline is seen at depths between 100-200 m. The mean salinity of deep waters ranges from 22.2-22.4 psu (Balkas et al., 1990).

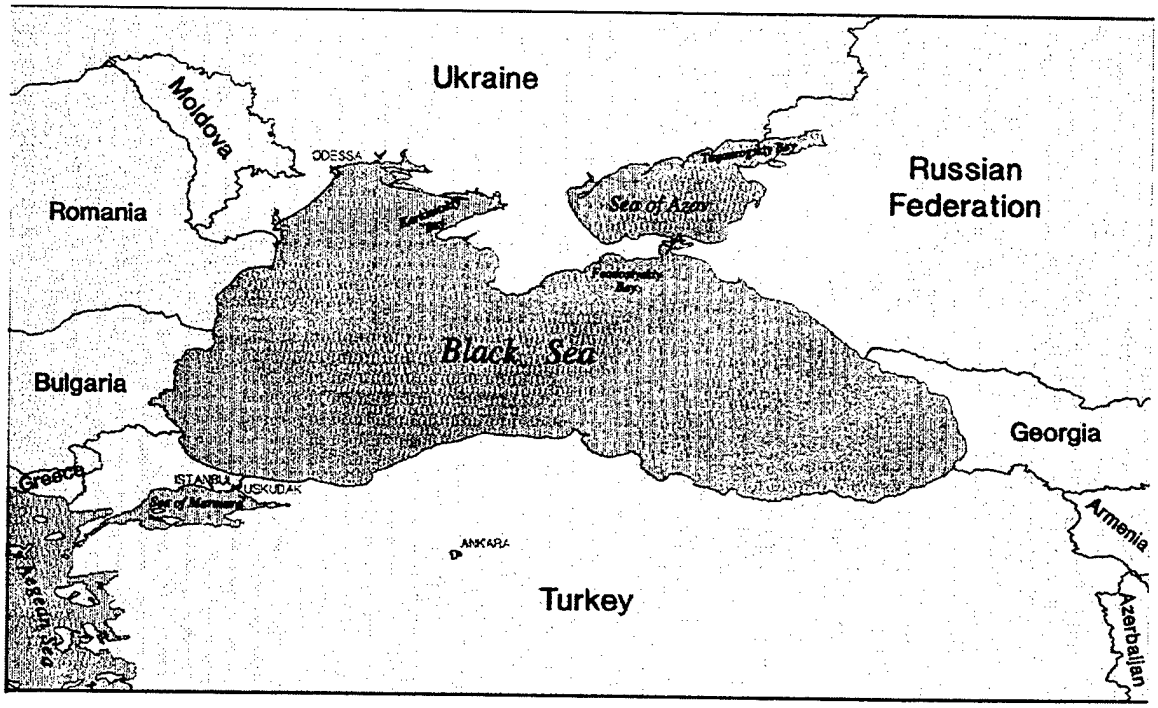

Figure 2.1-1. General area map of the Black Sea.

Surface water temperature varies seasonally as well as regionally. The mean annual surface temperature varies from 16°C in the southern Black Sea to 13°C in the northeastern Black Sea. The mean temperature in the northwest is coolest at 11°C. Winter temperatures are considerably lower in surface waters, ranging from 7-8°C in the central and southern basin, to 3-4°C in the north. The northwest coast and shelf areas may experience surface water temperatures as cold as 0°C. Summer temperatures in surface waters can reach 24-25°C in the western half of the Black Sea. Below the 50-70 m surface layer, the temperature of deeper waters remains relatively constant throughout the year at approximately 9°C at 1000 m. Small temperature changes occur from geothermal heat flux from the bottom, resulting in an increase of 0.1°C per 1000 m (Balkas et al., 1990). Surface water temperatures vary in response to seasonal changes in air temperatures that may range from below 0°C in winter to summertime averages of 24°C.

Essentially three different driving mechanisms are linked with circulation in the Black Sea; wind and thermohaline forces at the sea surface and source-sink forcing through the Bosphorus Strait. Thermohaline forcing may generate surface currents comparable to wind-generated currents. The principal features of the quasi-steady circulation are governed by the curl of wind stress distribution (Oguz et al., 1989). The dominant direction is north-northwest in the western half of the Black Sea. The eastern half is dominated by southerly winds. The highest average wind speed is about 16 knots in January and February. More stable summer conditions are typical with wind speeds not exceeding 10 knots in the central Black Sea (Balkas et al., 1990). Circulation in the Black Sea predominantly consists of a cyclonic boundary current essentially running parallel to the basin's periphery, two cyclonic gyres which nearly divide the basin in two, and several cyclonic and anticyclonic mesoscale eddies which are apparently products of the larger scale currents. The boundary current speed may be 40 $cm \cdot s^{-1}$ in some areas, while velocities in the central sea are lower ranging from 5-20 $cm \cdot s^{-1}$ (Balkas et al., 1990).

Oxygen depletion of the deep water is gradually increasing as the supply of carbon exceeds the supply of oxygen brought in by Mediterranean Sea water through the Bosphorus Strait. Based on the oxidation of a gram-atom of carbon from plankton which requires 1.3 moles of oxygen, the supply of carbon to the deep water exceeds the supply of oxygen by a factor of about 3000. This is based on a carbon productivity level of approximately 100 $g \cdot m^{-2} \cdot yr^{-1}$, and the assumption that only 5% of the primary production of organic matter passes through the O_2-H_2S interface ($1.7 \cdot 10^{11}$ gram-atoms). It is also estimated that the supply of oxygen brought in by the Mediterranean water is approximately $7 \cdot 10^7$ moles per year. The Mediterranean water being more saline sinks to the deep parts of the Black Sea basin and greatly limits vertical circulation. The dissolved oxygen supplied to the deep basin water is limited to that brought in by the Mediterranean water (Deuser, 1972). The oxygen depletion is a self-decelerating process. Once the bottom water is anoxic, more of the organic matter becomes fossilized. At low oxygen concentrations the redox potential decreases drastically resulting in a reduced rate of oxidation. A half-life of 1800 years has been estimated for the dissolved oxygen reservoir in the basin below the Bosphorus sill depth (Deuser, 1972).

Regarding the degree of organic matter preservation in benthic sediments, recent findings suggest that organic carbon burial rates in Black Sea deep water sediments may be similar to those in oxic open ocean sediments at similar depths and sedimentation rates. This is based on estimating the degree of preservation of organic carbon in sediments by comparison of accumulation rates with primary production rates in the overlying water column (Calvert et al., 1991). Primary production may have been underestimated by half its actual value previously due to under sampling of seasonal production maxima.

Water at depths of 300-700 m spends an average of 935 years in the Black Sea. In the very deepest areas at about 2000 m, the water is yet older (Ostlund, 1974). Particulate loading to Black Sea sediments may occur at a mean sinking rate of 1000 m per year, thus 2 years may be necessary for particles to reach the deepest bottom waters. Other sources (Hay, 1987) have estimated winter sinking rates of 125 $m \cdot day^{-1}$, while larger fecal pellets may rapidly sink at velocities of several hundred meters per day (Izdar et al., 1984). A sediment accumulation rate of 100 $g \cdot m^{-2} \cdot yr^{-1}$ has been estimated (Brewer and Spencer, 1974). Calvert et al. (1991) have reported sedimentation rates of 15.8-17.0 cm per 1000 yr. Bottom currents are generally absent. A "fluff" layer exists above the bottom sediment varying in thickness between 2 and 20 cm (Hay, 1987). The bottom sediment fraction larger than 500 μm is mainly composed of planktonic fecal pellets. These pellets typically settle through the fluff layer and become incorporated into the bottom sediments. This is unique in that in oxic benthic boundary layers planktonic fecal pellets are rapidly remineralized by micro- and macro-fauna (Pilskaln, 1988).

River runoff input from approximately half of Europe and part of Asia is discharged into the Black Sea, with approximately 55% of the suspended sediment load coming from the Danube River and approximately 29% from Caucasian rivers (Hay, 1987). The solid discharge to the Azov-Black Sea Basin in the north has been estimated at 14,945 mt per year (Balkas et al., 1990). How much of the pollutants discharged into the rivers loading into the Black Sea actually reach the Black Sea is generally not known. Even heavy metals, cyanides, ammonia and phenols are discharged without treatment from such sources as wastewater outfalls and coal and ore mines (Balkas et al., 1990).

Ecology. A brief summary of fauna and flora inhabiting the Black Sea is provided by Cihangir and Tirasin in Izdar and Murray (1989). Only a zone from the surface to 80-160 m depth is inhabited by plant and animal species due to the hydrogen sulfide layer beneath which only anaerobic bacteria are found. Sulfur metabolizing bacteria are numerous in the boundary layer between the oxygenated and hydrogen sulfide zones, and at depths near the bottom. Microflora are also abundant in the benthic mud. In the aerobic upper layer bacterial plankton form a large productive biomass, and are utilized as food by the zooplankton. Primary production estimates range from 150-200 gC $m^{-2} \cdot yr^{-1}$ to 250 gC $m^{-2} \cdot yr^{-1}$. Highest concentrations are recorded in coastal regions reflecting the influence of the general cyclonic

circulation and the doming of the hydrogen sulfide zone in the central basin where the anoxic layer is closest to the surface (Balkas et al., 1990). Phytoplankton distribution reaches its lower limit at the upper limit of the hydrogen sulfide zone. The average annual phytoplankton production has been estimated at $1200 \cdot 10^6$ mt. The most productive area is the relatively shallow northwest area where vertical mixing and high nutrient loading from rivers contribute to high productivity (Balkas et al., 1990).

Zooplankton are also restricted to existence above the hydrogen sulfide zone. The zooplankton may be grouped as cold, warm and eurytherm groups. The medusa *Aurelia aurelia* is one of the most abundant macrozooplankton species, having commercial potential as well (Cihangir and Tirasin, 1989).

Seaweeds (represented mostly by green, some brown, and red algae) are generally found at depths between 0 and 20 m. The most common and commercially important genera are *Phyllophora*, *Cystoseira* and *Ulva*. Annual macrophytobenthos production has been calculated as $17.6 \cdot 10^6$ mt (Cihangir and Tirasin, 1989).

Two molluscan species (*Raphana thomasiana* and *Mytilus galloprovincialis*) and 15 fish species are commercially important. The anchovy, sprat and horse mackerel are the three most important pelagic species accounting for approximately 90% of the total annual catch. In order of abundance, the anchovy (*Engraulis encrasicholus*) and the horse mackerel (*Trachurus mediterraneus ponticus*) occupy the first and second positions, respectively. The anchovy feeds primarily on zooplankton, aggregating in large shoals in the warmer parts of the Black Sea along the Anatolian and Crimean coasts during winter. The horse mackerel exists on a diet of zooplankton and small fish, and also winters in the warmer parts of the Black Sea. Among demersal species, the turbot (*Psetta maxima maeotica*) is the most important commercial species feeding on small fish, crustaceans, and bivalves. This species has been heavily exploited. At the top of the food chain are three dolphin species. Of these three, *Delphinus delphis* is the most abundant (Cihangir and Tirasin, 1989).

Impacts on the Marine Environment. Catastrophic ecological damage has occurred in the Black Sea due to land-based pollution, reductions in the discharges of several large rivers, and over fishing. These factors collectively have resulted in eutrophication, the undesirable dominant alteration of the ecosystem first by the jelly fish *Aurelia aurita*, and then by the population explosion of the predatory ctenophore *Mnemiopsis leidyi*, and a loss or drastic reduction in commercially important fish species (Mee, 1992; Caddy, 1994; Shushkina and Vinogradov, 1991). Eutrophic conditions resulted in the removal of the biofiltering mussel beds (*Mytilus spp.*) and oxygen-producing macroalgae (*Phyllophora spp.*) producing hypoxic conditions in as much as 95% of the Ukrainian N.W. Black Sea shelf (Mee, 1992; Sorokin, 1993). The benthic biota have been further stressed or eliminated by dumping of dredge spoils. Sixteen official dump sites exist in the western Black Sea, mostly on the continental shelf (Mee, 1992). Overwhelming evidence indicates that a major part of the Black Sea (particularly the northwestern shelf) is critically eutrophic. The Danube River alone deposits 60,000 mt of total phosphorous (about the same as the total river input to the North Sea) and 340,000 mt of total inorganic nitrogen per year (less than half the input to the North Sea) into the Black Sea. In the past 25 years the increase in nutrient load is likely a consequence of widespread use of phosphate detergents and agricultural intensification (Mee, 1992).

It has been recently reported that the Danube River annually discharges 1000 mt of chromium, 900 mt of copper, up to 60 mt of mercury, 4500 mt of lead, 6000 mt of zinc and 50,000 mt of oil into the Black Sea. These figures considerably exceed the entire river loading to the North Sea (Mee, 1992).

Significant amounts of oil from countries bordering the Black Sea are transported in the Black Sea and Bosphorous Straits (Balkas et al., 1990). This traffic has inherent ecological dangers and is also not likely to diminish in the future. Extremely high hydrocarbon levels have been found in the navigation

route from the Danube to the Bosphorous. Concentrations found in the Gulf were lower by an order of magnitude or more than those found in the shipping lane (Mee, 1992).

The near-future outlook for the Black Sea is not an optimistic one. Reduction of nutrient loading from the Danube basin and other rivers is essential to assisting the Black Sea in recovery. This, however, will not be easy or immediately possible. Reducing phosphate loading to the Rhine River has taken 15 years by countries with strong economies and political commitment. It is likely that the cleanup of the Black Sea Basin may take decades since the countries bordering the Black Sea have struggling economies and a population five times that of the Rhine basin (Mee, 1992). Commitments will also be necessary from bordering countries to cooperate in limiting fishing catches since many species are already stressed or are no longer present in commercially exploitable numbers. The need is urgent and either the fishery must be reduced to an agreed minimum, or halted entirely for a period of 3-5 years to allow for stock recovery (Caddy, 1994). The fishery has fallen to a level where of 26 species of commercial fish in the 1960s, only six remain in commercially exploitable quantities (Mee, 1992).

Table 2.1-1. Representative oceanographic characteristics of the Black Sea.

Parameter	Value	Reference(s)
Current Velocities ($cm \cdot s^{-1}$)	5-20	Balkas et al., 1990
Current Velocities ($cm \cdot s^{-1}$) Deep (700m)	10-15	Hay, 1987
Salinity (psu) surface	18.5	Balkas et al., 1990
Salinity (psu) deep water	22.2-22.4	Balkas et al., 1990
Temperature (°C) surface	13-16	Balkas et al., 1990
Temperature (°C) Deep water	9	Balkas et al., 1990
Density (sigma-t) Surface	12	Balkas et al., 1990
Density (sigma-t) Deep Water	14	Balkas et al., 1990
Sfc Layer Thickness (m)	70	Balkas et al., 1990
Permanent Halocline (m)	100-200	Balkas et al., 1990
TSS Nearshore Inputs ($kg \cdot yr^{-1}$)	$2 \cdot 10^5$	Balkas et al., 1990
Si O_2-Si ($\mu g\text{-}at \cdot L^{-1}$) Surface Water	50	Sorokin, 1993
Si O_2-Si ($\mu g\text{-}at \cdot L^{-1}$) Deep Water	300	Sorokin, 1993
PO_4-P ($\mu g\text{-}at \cdot L^{-1}$) Surface Water	0.4	Sorokin, 1993
PO_4-P ($\mu g\text{-}at \cdot L^{-1}$) Deep Water	8.4	Sorokin, 1993
NO_3 -N ($\mu g\text{-}at \cdot L^{-1}$) Surface Water	0.8	Sorokin, 1993
NO_3 -N ($\mu g\text{-}at \cdot L^{-1}$) Deep Water	0	Sorokin, 1993
NH_4 ($\mu g\text{-}at \cdot L^{-1}$) Surface Water	2.8	Sorokin, 1993
NH_4 ($\mu g\text{-}at \cdot L^{-1}$) Deep Water	96.0	Sorokin, 1993
P Nearshore Inputs ($kg \cdot yr^{-1}$) Danube River	$6 \cdot 10^7$	Mee, 1992
N Nearshore Input ($kg \cdot yr^{-1}$) Danube River	$3.4 \cdot 10^8$	Mee, 1992
P Nearshore Inputs ($kg \cdot yr^{-1}$)	$9.1 \cdot 10^7$	Estimated*
N Nearshore Input ($kg \cdot yr^{-1}$)	$5.2 \cdot 10^8$	Estimated*
POC ($mg \cdot L^{-1}$) Surface waters	0.2-0.3	Sorokin, 1993
DOC ($mg \cdot L^{-1}$) Surface waters	3-4	Sorokin, 1993
DOC ($mg \cdot L^{-1}$) Deep waters	2.2-2.6	Sorokin, 1993
Particulate Flux ($mg \cdot m^2 \cdot day^{-1}$)	200	Hay, 1987
Particulate Settling (m·day)	65-125	Hay, 1987
Sedimentation Rate (cm·1000yrs)	30	Hay, 1987
Organic Carbon Deposition ($g \cdot m^2 \cdot yr^{-1}$)	~4	Vaynshteyn et al., 1985
Surface O_2 Background ($mg \cdot L^{-1}$)	6.7	Yesin et al., 1993
Deep(below 200m) O_2 Background ($mL \cdot L^{-1}$)	anoxic	Ostlund, 1974
Residence Time (yrs)	935-2250	Ostlund, 1974; Sorokin, 1993
Vertical Water Exchange ($cm \cdot sec^{-1}$)	$0.4 \cdot 10^{-4}$	Vaklovskii and Katrich, 1984
Primary Production ($g\ C \cdot m^{-2} \cdot yr^{-1}$)	150-250	Balkas et al., 1990
Phytoplankton Biomass ($g \cdot m^2$)	8.8	Caddy, 1994
Zooplankton Biomass ($g \cdot m^2$)	8.33	Caddy, 1994
Macrophytobenthos annual production (mt)	$17.6 \cdot 10^6$	Cihangir and Tirasin, 1989
Surface Area (km^2)	$4.23 \cdot 10^5$	Egon and Ross, 1974
Average depth (m)	1,240	Balkas et al., 1990
Max Depth (m)	2206	Egon and Ross, 1974
Volume (km^3)	$5.34 \cdot 10^5$	Egon and Ross, 1974
Secchi Disk light depth (m)	35	Mee, 1992
Sediment Accumulation ($g \cdot m^{-2} \cdot yr^{-1}$)	100	Brewer and Spencer, 1974

* Estimates based on Danube River input alone, which is 2/3 of total river input to the Black Sea

REFERENCES

Balkas, T., 1990. *State of the Marine Environment in the Black Sea Region.* UNEP Regional Seas Reports and Studies, N124, pp 40.

Brewer, P. G. and D.W. Spencer, 1974. *Distribution of Some Trace Elements in the Black Sea and The Flux Between Dissolved and Particulate Phases*, in E.T. Degens and D. A. Ross, eds., *The Black Sea-Geology, Chemistry, and Biology*, The American Association of Petroleum Geologists, Tulsa, OK, 137-143.

Caddy, J. F., 1994. *A Perspective on Recent Fishery Related Events in The Black Sea.* Update of The Fishery Situation in The Black Sea, and Revision of the Conclusions of the 1990 GFCM Studies and Reviews N63, Report of the Second Technical Consultation on Stock Assessment in The Black Sea. Ankara, Turkey, 15-19 February 1993. Rome (Italy), FAO, pp. 168-190; FAO fish. rep./FAO rapp. peches 1020-1475, N495.

Calvert, S.E., R.E. Karlin, L.J. Toolin, D.J. Donahue, J.R. Southon, J.S. Vogel, 1991 *Low Organic Carbon Accumulation Rates In Black Sea Sediments.* Nature, 350, 692-695.

Cihangir, B., and E.M.Tirasin, 1989. In: *Black Sea Oceanography*, E. Izdar and J.W. Murray, eds. NATO ASI Series C: Mathematical and Physical Sciences, Kluwer Academic Publishers, V351, pp 487.

Deuser, W. G., 1972. *Organic-carbon budget of the Black Sea,* Woods Hole Oceanographic Institution Reference ; 72-77.

Egon, T, and D.A. Ross eds., 1974. *The Black Sea - Geology, Chemistry, and Biology*, American Association of Petroleum Geologists, Publisher. Memoir 20. pp 633.

Hay, B. J., 1987. *Particle Flux n The Western Black Sea in the Present and Over The Last 5,000 Years: Temporal Variability, Sources, Transport Mechanisms.* Technical Report Woods Hole Oceanographically Institute WHO I-87-44.

Izdar E. and J.W. Murray, eds., 1989. *Black Sea Oceanography*, NATO ASI Series C: Mathematical and Physical Sciences, Kluwer Academic Publishers, V351, pp 487.

Izdar, E., T. Konuk, S. Honjo, V. Asper, S. Manganini, E.T. Degens, V. Ittekkot, S.Kempe, 1984. *First Data On Sediment Trap Experiment In Black Sea Deep Water.* Naturwissenschaften, V71, N9, pp.478-479.

Mee, L. D., 1992. *The Black Sea In Crisis: A Need For Concerted International Action.* Ambio Aquatic Pollution and Environmental Quality. Section: Q508503 Characteristics, Behavior and Fate. V21, N4, pp. 278-286.

Oguz, T., M.A. Latif, H.I. Sur, E. Ozsoy, U., Unluata, 1989. *On The Dynamics Of The Southern Black Sea. In: Black Sea Oceanography.* Eds. E. Izdar, J. W. Murray, NATO ASI Series C: Mathematical and Physical Sciences V351. Kluwer Academic Publishers, pp 487.

Ostlund, H.G., 1974. Expedition Odysseus 65: Radiocarbon Age of Black Sea Water, In: *The Black Sea - Geology, Chemistry, and Biology*, T. Egon, and D.A. Ross (eds.), .American Association of Petroleum Geologists, Publisher. Memoir 20. pp 633.

Pilskaln, C.H., V. D., 1988. Composition of Surface Sediment. Ed. S. Honjo, Woods Hole Oceanographic Series 88-35, V88, N35-40.

Report of The Second Technical Consultation on Stock Assessment in The Black Sea, 1993. Ankara, Turkey, 15-19 February 1993. Rome (Italy), FAO, 1994; FAO fish. rep./FAO rapp. peches 1020-1475, N495.

Shushkina, E.A., M.Y. Vinogradov, 1991. *Marine Biology; Long-Term Changes In The Biomass of Plankton In Open Areas of The Black Sea.* Oceanology, V31, N6, Shirshov Institute of Oceanography, USSR Academy of Sciences, Moscow.

Sorokin, Y., 1993. *Essay on Ecological Situation in the Black Sea.* General Fisheries Council for the Mediterranean, Report of the Second Technical Consultation on Stock Assessment in the Black Sea. Food and Agriculture Organization of the United Nations, Ankara, Turkey, 15-19 February, 1993.

Vakulovskii, S. M., and I.Yu. Katrich, 1984. *Rate of Vertical Water Exchange in the Black Sea. Soviet Meteorology and Hydrology,* 101-104.

Vaynshteyn, M.B., V.G. Tokarev, V.A. Shakola, A. Yu. Lein, and M.V. Ivanov, 1985. *The Geochemical Activity of Sulfate-Reducing Bacteria in Sediments in the Western Part of the Black Sea.* Geochem. Int., V. 23, No.1, 110-122.

2.2 RED SEA

General Description. The Red Sea is a semi-enclosed basin surrounded by Egypt, Israel, Jordan, Saudi Arabia, Sudan, Yemen, Eritrea, and Djibouti (see Figure 2.2-1). The sea is 1932 km long and has an average width of 280 km; its widest dimension is 354 km. The total surface area of the Red Sea is estimated to be between 438 and 450 thousand km^2. Volume is estimated to be between 215 and 251 thousand km^3. In comparison to the average depth of the world's oceans (3700 m), the Red Sea is quite shallow with an estimated average depth of 491 m. Its maximum depth, however, is 2850 m (Head, 1987). From the peripheral coral reef zone, the sea bottom increases in depth quickly in a series of stepped cliffs to the main axial trough at about 500 m. This central trough deepens to about 1500 m near the central axis. Yet deeper pits or "Deeps" are found in the axial trough, which may reach over 2500 m in depth. The "Deeps" are a unique feature of the Red Sea containing hot brine pools which have highly enriched metal bearing sediments (Head, 1987). At the southern end, the Red Sea is essentially separated from the Gulf of Aden by a 100-130 m deep sill approximately 140 km north of the Straits of Bab al-Mandeb (Head, 1987). A wide and shallow shelf area exceeding 100 km at the Farasan Bank is found at the southern end of the Red Sea.

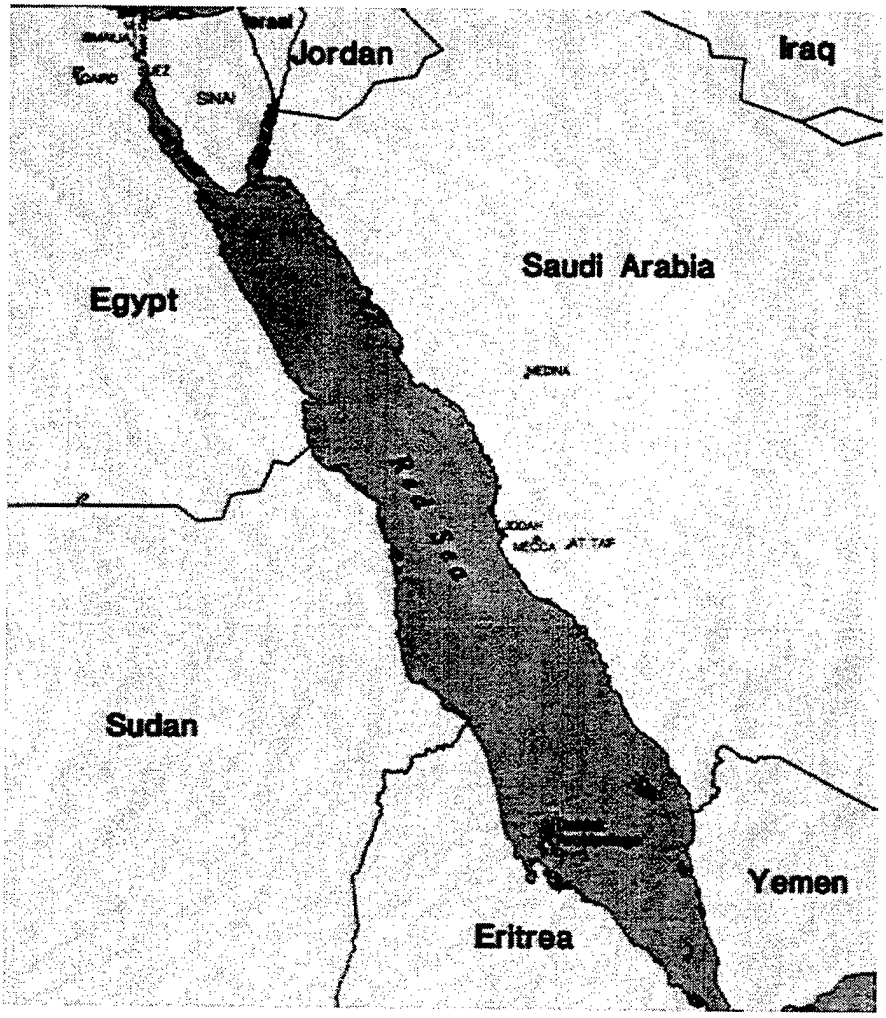

Figure 2.2-1. General area map of the Red Sea.

Two narrow gulfs (the Gulf of Suez and the Gulf of Aqaba) form at the northern end of the Red Sea. These gulfs contrast greatly in their bathymetry. To the south the Red Sea opens to the Gulf of Aden through the Strait of Bab al-Mandeb. The Gulf of Aqaba can be characterized as very steep-sided and deep, reaching maximum depths of over 1800 m near its east coast. The Gulf itself is only 30 km wide with a sill approximately 250-300 m deep separating it from the rest of the Red Sea. By contrast, the Gulf of Suez is a shallow flat-bottomed basin with typical depths between 55 and 73 m (Head, 1987). At its northern end the Suez Canal links the Red Sea with the Mediterranean Sea.

Physical/Chemical Oceanography. Surface water circulation in the Red Sea is driven by a density gradient which is established by heating and evaporation, exacerbated by temperature-induced winds. Water entering the Red Sea from the Gulf of Aden drifts northward. As it moves north, winds and high air temperatures evaporate as much as 1-2 $m \cdot yr^{-1}$ causing a rise in salinity from about 38 psu to as much as 42 psu in the Gulf of Suez. Winter cooling in the north increases seawater density further causing sinking under the northward flow returning southward at depth. This condition termed the Suez Overfall, is the main feature of circulation in the Red Sea, accomplishing water exchange all the way to the Indian Ocean (Behairy et al., 1992). Surface currents are generally strong (20-100 $cm \cdot s^{-1}$) and generally directed northeast to east. Below 400 m the currents are slow with an average speed of 8 $cm \cdot s^{-1}$ decreasing to 3 $cm \cdot s^{-1}$ near the bottom (Lange, 1980).

Red Sea surface water temperatures vary seasonally with summer temperatures exceeding 31°C and winter temperatures varying from 24°C to 26.5°C. In the Gulf of Suez winter temperatures commonly fall below 20°C (Behairy et al., 1992). In the central Red Sea, surface water temperature decreases steadily with depth from approximately 26°C at the surface to about 21.7°C at 200 m. Below 200 m, water temperature is nearly constant at about 21.7 - 21.9°C (Lange,1980). Vertical profiles of salinity show increases from surface layer values of 38.5 psu, to 40.5 psu at 200 m. Below 200 m, salinity increases only 0.15 psu to a maximum of 40.65 psu in the deep water lying above the brine pools (Lange, 1980).

Nutrients such as phosphate and nitrate are supplied to the surface layers of the pelagic environment through the Strait of Bab al-Mandeb, and by exchange with deeper layers via regeneration and advection. River input and rainfall are less important as routes of supply to the pelagic zone (Lange, 1980). A phosphate and nitrate maximum zone (1.2 and 30.4 $\mu g\text{-at} \cdot L^{-1}$, respectively) is found between 300 and 500 m depths which is likely caused by release from decaying organic matter. Silicate exhibits only a small maximum (12.6 $\mu g\text{-at} \cdot L^{-1}$) at intermediate depths due to sinking of diatom and radiolarian skeletons. Dissolved silicate is present mainly from dissolution of silica and clay particles deposited by sandstorms. An oxygen minimum zone exists between 300 and 450 m corresponding to the nutrient maximum zone. This oxygen minimum zone is likely due to maximum oxygen consumption resulting from the decay of organic matter by bacterial oxidation (Lange, 1980).

Benthic sediments are characteristically composed of carbonate components from small shells of pelagic species such as pteropods, heteropods, and foramnifera. Boring fungi or ascomycetes heavily infest many of the shells found in the sediments. The organic content of deep Red Sea sediments is <1%, although values are generally higher nearer to the coast (Thiel, 1987). Alluvial deposits create extensive soft-substrate biotopes in the intertidal zones (Price et al., 1988).

Climate. Prevailing air flow in summer is down the length of the Red Sea as part of an anti-cyclonic or counter-clockwise circulation based over Arabia. In winter, two airflow's exist, one flowing down the Red Sea axis from the Mediterranean, while the other flows up from the Arabian Sea. Both wind conditions are capable of bringing rain, although annual totals average only about 50 mm. It is important

to consider that the total annual rainfall may be deposited within a few hours resulting in floods and enormous terrestrial run-off (Behairy et al., 1992). Temperature-induced sea breezes in summer can build considerable strength, driving high energy wave conditions. These winds are the strongest in the Red Sea with the exception of occasional storms. In the central part along unprotected outer edges of the barrier reef, these winds can induce a median wave height of approximately 0.6 m (Behairy et al., 1992).

Ecology. The Red Sea exhibits all major tropical marine communities with the exception of estuaries. The lack of permanent river input prevents estuarine formation. All other systems are present, including sandy beaches, rocky intertidal zones, lagoons, mangrove communities, and coral reefs. The open sea is composed of three pelagic zones. The epipelagic zone extends from the surface to 100 m depth and represents the well-lit region of primary productivity (Head, 1987). Productivity in the Red Sea is, however, low due to the extreme stability of the water column and lack of nutrients from either fresh water run off or from inflow through the Straits of Bab al-Mandeb (Angel, 1984). The mesopelagic zone extends from 100 to about 800 m depth. Light, temperature, and food supplies decrease in this zone. The bathypelagic zone exists below 800 m and extends to the bottom. This last pelagic realm is sparsely populated and exhibits a very low biomass due to limited food supply and high metabolic rates in the high ambient temperatures (Head, 1987). This loss of energy due to high respiration rates in relatively high benthic zone temperatures leads to little available energy for biomass production (Thiel, 1987). Furthermore, food supply to the deep water is limited due to a lack of vertical transport of particulate matter. This results from a lack of fecal pellet production by zooplankton which are virtually absent in this realm. Hence, gravitational sinking of particles provides the only mechanism of food transport to the great depths. Because of high temperatures, bacterial decomposition of the sinking organic matter removes substantial amounts before it reaches deep water (Thiel, et al., 1994; Thiel, 1984).

The richest communities are found in the coral reef zones which border most of the coastal areas and islands in the shallow Red Sea (Head, 1987). The greatest abundance of reefs is found along the central and northern coasts, along the Sudanese, Saudi Arabian, and Egyptian coasts. The basic reef type is the fringing reef which may be penetrated by narrow channels called *marsas* or *sharms*. These channels may connect to seasonal rivers (Head, 1987). The main critical habitats of the Red Sea are the coral reefs, seagrass beds, mangrove stands, creeks, shallow bays and offshore islands. All have high productivity and serve as important nurseries and breeding grounds for invertebrates, fish, seabirds and turtles. Additionally, the majority of fish stocks exploited in the Red Sea are dependent on one or more of these critical habitats (Ormond, 1987).

Seagrass beds exist behind coastal or offshore reefs in sandy shallow (70 m to intertidal) lagoons. These beds serve to stabilize sediment and are areas of high productivity (Head, 1987). The intertidal zone shoreward of the seagrass beds is especially harsh considering exposure to heat and desiccation. In spite of the harsh conditions, the intertidal fauna is characterized by a diversity of Crustacea in the upper intertidal zone, with a diversity of worms, molluscs, and echinoderms in the lower zones. Mangroves are established in Red Sea intertidal areas, although they are not as abundant as in other tropical areas due to the extreme conditions and lack of estuarine environment. Collectively, the reef, seagrass and mangrove environments act together in an interactive fashion to protect and preserve the environment by controlling nutrient and sediment movement, and as protection from wave action. This may be thought of as a triangular dependence of each component on the other (Head, 1987).

Fish are extremely abundant and occupy diverse habitats in the Red Sea. In shallow waters, fish are the most conspicuous animals present after corals (Head, 1987). The Narrow-barred Spanish mackerel (*Scomberomorus commerson*) is the most important commercial species. The gray mullet (Mugilidae) is also commercially important in sandy lagoon and marsa (creek embayment) environments. The snapper

family (*Lutjanidae*) occupies reef habitats and deep water habitats, and are yet another commercially important group. Collectively, the jacks and horsemackerel represent another very important group, feeding on herrings, silversides and small reef fishes (Ormond and Edwards, 1987). Fishing in the Red Sea has been done by traditional methods with little modernization until the decade of the eighties. Thus it is unlikely that significant over fishing has occurred, with the exception of localized areas near towns and fishing villages. The Gulf of Suez has also been commercially fished (Ormond, 1987). The fishing yield is unlikely to ever be high, however, as the area of shallow shelf is small throughout the Red Sea, and because the overall productivity of the Red Sea is low (Head, 1987).

There are few species among those that may be considered endangered in the Red Sea. Those that could be considered endangered are turtles and the dugong (Ormond, 1987). The dugong (*Dugong dugong*) is a marine mammal belonging to the order *Sirenia*, a relative of the tropical manatee. The same environmental pressures caused by pollution and human activities that are detrimental to turtles are also detrimental to dugongs. These include oil pollution, underwater explosions (used in oil exploration) and human predation. These factors coupled with a low reproduction rate serve to threaten the dugongs already rare in numbers. Although knowledge of cetaceans (whales, dolphins) in the Red Sea is fragmentary, various human activities serve to threaten small cetaceans. Among these are small whale fisheries, incidental capture in fishing nets, chemical pollutants, disturbance, and habitat modification (Frazier et al., 1987).

Impacts on the Marine Environment. The Red Sea is unique in that it is a navigational channel with a long history, and has yet to be severely deteriorated environmentally. Pollution and developmental stress are just now becoming evident. The Red Sea's near complete enclosure by land makes it highly vulnerable to pollution and qualifies its status as a key environment (Head, 1987). Stress on the environment of the Red Sea comes from impacts associated with coastal development and associated forms of pollution, oil pollution, and mining of deep benthic sediments enriched with metals.

Development. Intense commercial and industrial development of many coastal areas has occurred since the late 1960s when possibly as much as 98% of the Red Sea coast was in pristine condition. The nature of this coastal development tends to occur in a strip-like fashion along the coastline near major cities. Coastal environmental deterioration accompanies large scale development of such facilities as ports, power plants, and waste disposal plants. Areas such as Jiddah, Yanbu al Bahr, Port Sudan and Aqaba are experiencing such development (Ormond, 1987). Sewage input is a particularly important urban pollution source affecting the near-coastal areas. Sewage disposal from shipping and offshore platforms, although more widespread is probably an insignificant problem. Garbage (mostly plastics) from shipping, offshore platforms, and urban and recreational areas is widely distributed along the shore of Saudi Arabia where onshore winds prevail (Dicks, 1987).

Such activities as loading of crushed phosphate and its transport have resulted in localized pollution (Hawkins et al., 1991; Hashwa, 1980). During loading on to ships approximately 0.5% of the phosphate rock may be lost to the immediate marine environment. Some of the detrimental effects noted include high turbidity, formation of an insoluble bottom layer, and increased phosphate concentrations in seawater and sediments enhancing eutrophication, particularly in the Gulf of Aqaba (Hashwa, 1980).

Oil Pollution. Oil pollution in the Red Sea is both widespread and has serious impacts. Oil input from all sources in the Red Sea is 14.61 $kg \cdot km^{-2} \cdot yr^{-1}$, while input to the rest of the world's oceans is only 9.17 $kg \cdot km^{-2} \cdot yr^{-1}$. The input of oil from refineries in the Red Sea is about 13 times the amount received by the world's oceans (Awad, 1989). The Gulf of Suez region is considered one of the world's largest offshore production areas, as well as one of the most oil-polluted (Dicks, 1987; Hanna, 1983). Approximately

20% of the world's shipping tonnage has passed through the Suez Canal (Aleem, 1984). Some reasons for oil pollution in the Gulf of Suez and the Red Sea are the opening of the Suez Canal in 1975, increases in offshore production, modification of oil transport lines following the Iran-Iraq war since 1980, the near total land-locked nature of the Red Sea which acts to confine oil pollution, and seasonal water circulation and propagation towards the south (Awad, 1989).

Another damaging aspect of offshore oil drilling operations relates to sediment brought up by the well drilling process. These cuttings are discharged as coarse particles immediately to the surrounding deep waters. A single offshore platform may produce on the order of 10,000 m^3 of cuttings. The biological effects of such cuttings include direct toxicity and simple smothering of nearby organisms (Dicks, 1987).

When oil-polluted and unpolluted reefs were studied in the Gulf of Aqaba following unusually low tides in 1970, a significant difference was seen in the ability to recolonize. The oil-polluted reef did not recolonize normally as did the relatively unpolluted reef. It is thought that oil may damage coral reproductive systems, interfere with larval production or viability, and inhibit normal settling. Reproductive effects of oil on corals have been confirmed in laboratory studies (Dicks, 1987). Repeated oil spills may damage corals in several ways. Toxicity of various oil components, limited oxygen exchange by oil film, and inhibition of photosynthesis by shading are additional damaging effects of oil pollution. It has been observed that reefs affected by natural disasters may recolonize quickly, while those affected by pollution from human activities may not return to their former states (Mergner, 1984). Mangrove communities are also very susceptible to oil pollution (Dicks, 1984, 1986). Variation in the sediments and drainage conditions under which mangroves exist determines the extent of damage by oil pollution.

The pollution issues described above have prompted the establishment of regional environmental programs such as the Environmental Programme for the Red Sea and the Gulf of Aden (PERSGA) established under the auspices of the Arab League Educational, Cultural and Scientific Organization. On a national level, Egypt, Israel, Jordan, Sudan, North Yemen, and Saudi Arabia have, or are planning to implement protected marine areas to preserve at least some of their most diverse and sensitive coastal resources (Ormond, 1987).

Mining. The discovery of metal deposits in the metalliferous mud, found beneath the brine pools along the greatest depths of the Red Sea, uncovered commercially marketable metals. This discovery prompted numerous investigations during the 1970s and 1980s. Along with estimations of the commercial value and practicality of the operations, ecological concerns were addressed as well. Due to Saudi Arabian economics and priorities, the world's metal market conditions, and international legal uncertainties, mining of metals from deep Red Sea brine pools has not yet become a commercial reality, and may not become a reality for another 20 years, possibly longer (Amann, 1989; Thiel, 1991). Much has been learned regarding potential ecological impacts from mining activity from pre-pilot mining (PPMT) tests conducted in the Red Sea under the authority of the Red Sea Commission. These findings and the further questions they have created will be summarized below.

The program metalliferous sediment Atlantis II Deep (MESEDA) conducted during the 1970s and 1980s employed a PPMT approach to begin estimates of environmental impact from deep sea mining activity. During this testing phase, a total of 12,000 m^3 of mine tailings were dumped containing 225 mt of dry particulates. The resultant particle plume was traced to 1100 m depth. Its initial lateral extent was 700 to 900 m, expanded to 5000 m after 10 days. Particulate matter concentration was between 80 and 220 $\mu g \cdot L^{-1}$. Under commercial scale conditions, 100,000 mt of sediment would be mined daily releasing 400,000 m^3 of tailings and creating a plume initially containing 25 $g \cdot L^{-1}$ dry particulate. This daily production of

tailings was predicted to release 30-180 mt of zinc, 20-50 mt of copper, 50-700 kg of cadmium, and 4-200 kg of mercury. Toxicity testing indicated that the tailings were toxic. Such a magnitude of discharge of metals is comparable to the daily discharge from the Rhine River into the North Sea. It was estimated that over a period of 15-25 years of mining activity, $44\text{-}54 \cdot 10^6$ mt of mining tailings would be discharged back into the Red Sea (Thiel, 1991).

The tailings are slurries derived from the mined sediments, brine, and seawater. After injection into seawater, the slurry grain size changes by flocculation. Only 14% of the original slurry remains in the < 2 um fraction, while more than 50% has a grain size > 6 μ. The maximum initial size of particles is 30 um (Lange, 1980). The slurry pH is approximately 6.0, its solid content ranges from 18-25 $g \cdot L^{-1}$, salt content ranges from 100-200 $g \cdot L^{-1}$, density ranges from 1.06-1.16 $g \cdot cm^{-3}$, and the dry solids density ranges from 2.5-3.9 $g \cdot m^{-3}$ (Lange, 1980).

In order to avoid possible effects in the epipelagic and mesopelagic zones such as limited light penetration, flocculation of particles and plankton entrapment, toxicity, and accumulation of toxicants, as well as limit spread of the plume, it was felt that disposal of the tailings below a depth of 1000-1100 m would be required (Karbe, 1987; Adu Gideiri, 1984; Nawab, 1984). This would result in dispersion of tailings over an area of approximately 1500 m^2. Within this area, sedimentation of as much as, or possibly more than 4 cm per year might occur. Benthic fauna would likely be eliminated in the area of greatest sedimentation as a result of the blanketing effect and toxicity from leaching (Karbe, 1987; Adu Gideiri, 1984). Disposal of the tailings was not expected to influence dissolved oxygen or salinity in the water column. Modeling studies showed the discharge depth to be of critical importance to the dispersion of the material. The overall conclusion drawn by the PPMT studies was that mining of the metalliferous muds and their return to a confined area in the axial trough presented acceptable environmental risks (Karbe, 1987).

Table 2.2-1. Representative oceanographic characteristics of the Red Sea.

Parameter	Value	Value	Reference(s)
	Surface Layer	Deep Layers	
Current Velocities ($cm \cdot s^{-1}$)	20-100	3-8	Lange, 1980
Salinity (psu)	38.5	40.5	Lange, 1980
Temperature (°C)	30	22	Wyrtki et al., 1971
Density (sigma-t)	26	29	Wyrtki et al., 1971
Evaporation ($m \cdot yr^{-1}$)	1-2		Head, 1987
Layer Thickness (m)	100	>800	Head, 1987
Surface O_2 Background ($mL \cdot L^{-1}$)	4.3	2	Lange, 1980 Wong and Degens, 1980
Si O_4-Si ($\mu g\text{-at} \cdot L^{-1}$)	0.52	10	Lange, 1980
PO_4-P ($\mu g\text{-at} \cdot L^{-1}$)	0.4	0.8	Lange, 1980
NO_3 -N ($\mu g\text{-at} \cdot L^{-1}$)	1.0	22	Lange, 1980; Wyrtki et al., 1971
Primary Production (mg $C \cdot m^{-2} \cdot day^{-1}$)	100		Weikert 1987, Thiel, 1984
Reef Productivity (g $C \cdot m^{-2} \cdot yr^{-1}$)	500-2500		Lewis, 1977
Phytoplankton Biomass (mg Chl $a \cdot m^{-2}$)	14		Thiel, 1984
Zooplankton Biomass ($mg \cdot m^{-3}$ wet wt.)	48-81		Kimor, 1973
Surface Area (km^2)	438-450		Head, 1987
Average depth (m)	491		Head, 1987
Max Depth (m)	2850		Head, 1987
Volume (km^3)	215-251		Head, 1987
1% light attenuation (per m)	0.7	0.67	Lange, 1980
Benthic Sediment % organic carbon	<1		Thiel, 1987

REFERENCES

Aleem, A.A. 1984. *The Suez Canal As A Habitat And Pathway For Marine Algae And Seagrasses.* Deep-Sea Res., 31A, pp. 901-918.

Amann, H. 1989. *The Red Sea Pilot Project: Lessons For Future Ocean Mining.* Mar. Min., 8, 1-22.

Angel, M.V. 1984. *Deep-Water Biological Processes In The Northwest Region Of The Indian Ocean.* Deep-Sea Res., 31A, 935-950.

Awad, H. 1989. *Oil Contamination In The Red Sea Environment.* Water Air Soil Pollut., 45, 235-242.

Behairy, A.K.A, C.R.C. Sheppard, and M.K. El-Sayed. 1992. *A Review Of The Geology Of Coral Reefs In The Red Sea.* UNEP Regional Seas Reports and Studies No. 152. 36 pp.

Dicks, B. 1984. *Oil Pollution In The Red Sea - Environmental Monitoring Of An Oilfield In A Coral Area, Gulf Of Suez.* Deep-Sea Res., 31A, 833-854.

Dicks, B. 1986. *Oil And The Black Mangrove, Avicennia Marina In The Northern Red Sea.* Mar. Pollut. Bull., 17, 500-503.

Dicks, B. 1987. *Pollution.* Chapter 18 pp. 383-404. In: Key Environments. Red Sea. A.J. Edwards and S.M. Head, Eds. 1987. Pergamon Press. Oxford.

Frazier, J., G.C. Bertram, and P.G.H. Evans. 1987. *Turtles And Marine Mammals.* Chapter 14 pp. 288-314. In: Key Environments. Red Sea. A.J. Edwards and S.M. Head, Eds. 1987. Pergamon Press. Oxford.

Gideiri, Y.B.A. 1984. *Impacts Of Mining On Central Red Sea Environment.* Deep-Sea Res., 31A, 823-828.

Hanna, R.G.M. 1983. *Oil Pollution On The Egyptian Red Sea Coast.* Mar. Pollut. Bull., 14, 268-271.

Hashwa, F. 1980. *The Phosphate Pollution In The Gulf Of Aqaba.* In: Proceedings of the Symposium on The Coastal and Marine Environment of the Red Sea, Gulf of Aden and Tropical Western Indian Ocean. Vol. II. pp. 109-124. 9-14 January 1980, Khartoum. The Red Sea and Gulf of Aden Environmental Programme Jeddah (ALECSO) Pub.

Hawkins, J.P., C.M. Roberts, and T. Adamson. 1991. *Effects Of A Phosphate Ship Grounding On A Red Sea Coral Reef.* Mar. Pollut. Bull., 22, 538-542.

Head, S.M. 1987. *Introduction.* Chapter 1 pp. 1-21. In: Key Environments. Red Sea. A.J. Edwards and S.M. Head, Eds. 1987. Pergamon Press. Oxford.

Karbe, L. 1987. *Hot Brines and the Deep Sea Environment.* Chapter 4 pp. 70-89. In: Key Environments. Red Sea. A.J. Edwards and S.M. Head, Eds. 1987. Pergamon Press. Oxford.

Kimor, B. 1973. *Plankton Relations of the Red Sea, Persian Gulf and Arabian Sea.* In: Ecological Studies 3: The Biology of the Indian Ocean. Zeitzschel, B. (Ed.) Springer-Verlag. New York, Heidelberg, Berlin. pp. 221-232

Lange, J., H. Baecker, J. Post, and H. Weber. 1980. *Plans And Tests For A Metal Concentration And Tailing Disposal At Sea.* In: Proceedings of the Symposium on The Coastal and Marine Environment of the Red Sea, Gulf of Aden and Tropical Western Indian Ocean, Vol. III, pp. 65-126. 9-14 January 1980, Khartoum. The Red Sea and Gulf of Aden Environmental Programme Jeddah (ALECSO) Pub.

Lewis, J.B. 1977. Processes Of Organic Production On Coral Reefs. Biol Rev. 52, 305-347.

Mergner, H. 1984. *The Ecological Research On Coral Reefs Of The Red Sea.* Deep-Sea Res., 31A, 855-884.

Nawab, Z.A. 1984. *Red Sea Mining: A New Era.* Deep-Sea Res., 31A, 813-822.

Ormond, R. 1987. *Conservation And Management.* Chapter 19 pp. 405-423. In: Key Environments. Red Sea. A.J. Edwards and S.M. Head, Eds. 1987. Pergamon Press. Oxford.

Ormond, R., and A. Edwards. 1987. *Red Sea Fishes.* Chapter 13 pp. 251-287. In: Key Environments. Red Sea. A.J. Edwards and S.M. Head, Eds. 1987. Pergamon Press. Oxford.

Price, A.R.G., C.J. Crossland, A.R. Dawson Shepard, R.J. McDowall, P.A.H. Medley, M.G. Stafford Smith, R.F.G. Ormond, and T.J. Wrathall. 1988. *Aspects Of Seagrass Ecology Along The Eastern Coast Of The Red Sea.* Botanica Marina, 31, 83-92.

Thiel, H. 1987. *Benthos Of The Deep Red Sea.* Chapter 6 pp. 112-127. In: Key Environments. Red Sea. A.J. Edwards and S.M. Head, Eds. 1987. Pergamon Press. Oxford.

Thiel, H. 1991. *From MESEDA to DISCOL: A new approach to deep-sea mining risk assessments.* Mar. Min., 10, 369-386.

Thiel, H. and H. Weikert. 1984. *Biological Oceanography Of The Red Sea Oceanic System.* Deep-Sea Res., 31A, 829-831.

Thiel, H., H. Weikert, and L. Karbe. 1986. *Risk Assessment For Mining Metalliferous Mud's In The Deep Red Sea.* Ambio, 15, 34-41.

Wong, H.K. and E.T. Degens. 1980. *The Red Sea and Gulf of Aden, A Geological and Geophysical Review.* In: Proceedings of the Symposium on The Coastal and Marine Environment of the Red Sea, Gulf of Aden and Tropical Western Indian Ocean, Vol. III, pp. 215-266. 9-14 January 1980, Khartoum. The Red Sea and Gulf of Aden Environmental Programme Jeddah (ALECSO) Pub.

Wyrtki, K., E.B. Bennett, and D.J. Rochford. 1971. *Oceanographic Atlas Of The International Indian Ocean Expedition.* Washington, D.C. : National Science Foundation

2.3 GULFS AREA

General Description. The Gulfs Area includes the Persian Gulf and Gulf of Oman (see Figure 2.3-1). These gulfs are surrounded by Iran, Iraq, United Arab Emirates, Oman, Saudi Arabia, Kuwait, and Qatar. The Persian Gulf (Arabian Gulf) is a relatively shallow water body separated from the Gulf of Oman to the south by the Strait of Hormuz. The Gulf's maximum width is 338 km and its maximum length is approximately 1000 km. The surface area is approximately $2.39 \cdot 10^5$ km^2 with a mean depth of 36 m. These dimensions give an approximate volume of $8.63 \cdot 10^3$ km^3. At the Strait of Hormuz the depth increases to more than 100 m. Along the Iranian coast a deep trough extends 100 km north from the Strait of Hormuz. The Persian Gulf along the United Arab Emirates is shallow over a wide area with many small islands and lagoons (Reynolds, 1993). Its semi-enclosed nature, shallow depth and location within a very arid setting are all important factors regarding marine pollution. Due to its narrow single connection to the Gulf of Oman via the Strait of Hormuz, water exchange is limited and water residence time has been reported to range from 2-5.5 years (Reynolds, 1993; Sheppard, 1993; Al-Rabeh et al., 1992).

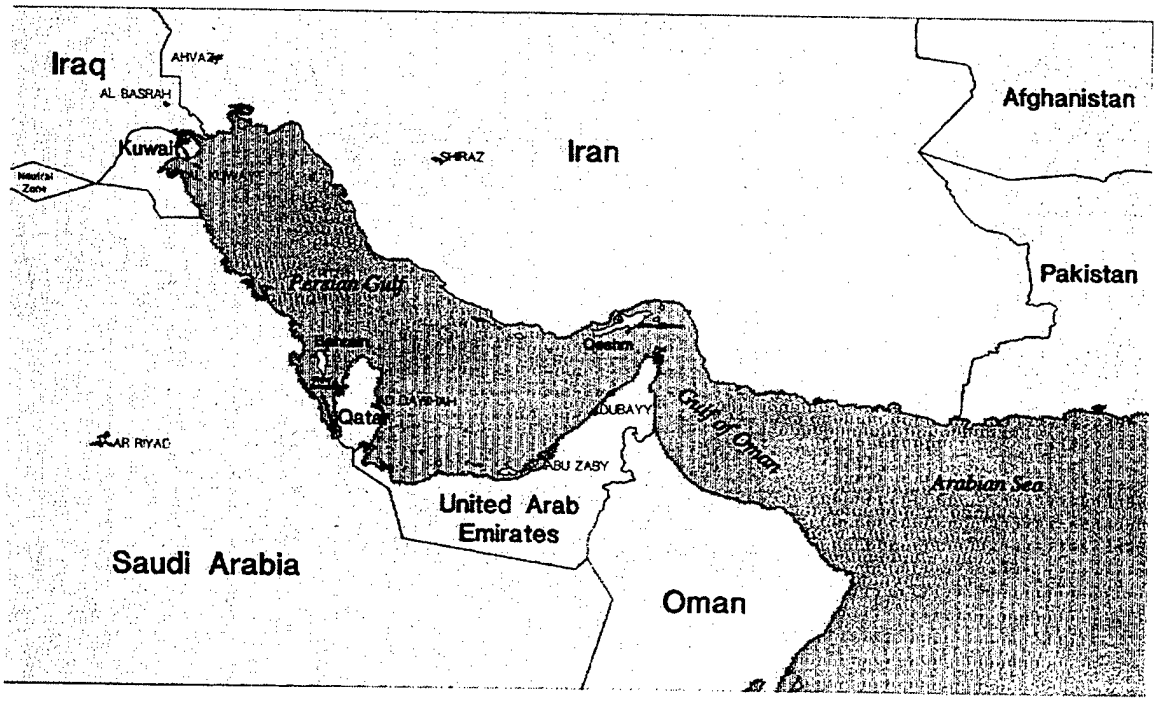

Figure 2.3-1. General area map of the Gulfs Area.

The Gulf of Oman is an approximate triangular water body approximately 600 km on its western side and 500 km long on its eastern side. At its union with the Arabian Sea it is approximately 300 km across from the Oman coastline to the Iranian coastline creating a surface area of approximately $8 \cdot 10^4$ km^2. Approximately 20% of the Gulf of Oman's coastal zone is 200 m deep or less. Approximately 50% of the Gulf of Oman is 1000 m deep or less, with maximum depths reaching 3000 m (Ross and Stoffers, 1978).

Climate. The Persian Gulf is located between latitudes 24-30°N and surrounded by deserts. The climate is more fiercely tropical in the summer, and more temperate in the winter than most seas of equivalent latitude (Sheppard, 1993). The climate is quite dry, resulting in evaporation (140-500 cm$\cdot$yr^{-1})

exceeding river runoff (10-46 $cm \cdot yr^{-1}$) by approximately a factor of 10. There is little rainfall ranging from 3-8 $cm \cdot yr^{-1}$. A northwest wind (*Shamal*) occurs year-round. In winter, the *Shamal* winds may bring the highest seas of the season. In addition, a strong sea breeze is found along the entire coastline generated by the intense thermal difference between land and sea surfaces. The direction of the sea breeze circulation is landward, hence surface pollutants are driven to coastlines more rapidly than might otherwise occur (Reynolds, 1993). Wind action also transports particulates into the Gulf waters. In the northern Gulf, dust fallout from southern Iraq has been measured at 6.9 $g \cdot m^{-2} \cdot yr^{-1}$ (Sheppard, 1993). The Persian Gulf and the Gulf of Oman weather systems are somewhat separated by the Strait of Hormuz (Reynolds, 1993). The Gulf of Oman is at the northern edge of tropical weather systems in the Arabian Sea and Indian Ocean and is subject to a monsoon circulation with southerly winds in summer, and strong northerly winds in winter.

Physical/Chemical Oceanography. The main circulation in the Persian Gulf typically follows a counterclockwise rotation, driven mainly by density gradients (Sheppard, 1993). Among the factors dominating circulation in the Persian Gulf are salinity water exchange in the Strait of Hormuz; density dominated circulation in the central and southern regions; wind-dominated circulation in the northwest region; and evaporation-induced bottom flow similar to the Mediterranean. Circulation in the southern Gulf is dominated by water exchange with the Gulf of Oman. Along the Iranian coast, southerly coastal currents flow against incoming water through the Strait of Hormuz to form a secondary current system. Freshwater flow from the Tigris, Euphrates and Karun rivers combine to form a nexus at the Shatt Al-Arab. The total average outflow of the Shatt Al-Arab is 1456 $m^3 \cdot s^{-1}$, nearly half the total river runoff into the Gulf (Reynolds, 1993).

Bottom water created in far northern areas, flows southward under the thermocline, resulting in a southerly flow of bottom water over the entire Gulf. The Gulf's vertical structure in the winter north of Qatar is very well-mixed. In the summer the northern end of the Gulf becomes a two-layered system consisting of well-mixed surface and bottom layers. In the extreme northern end of the Gulf, surface and bottom mixing can stir the water column over its entire depth due to the shallow depths in this region. The southern end of the Gulf is characterized by a year-round two-layer system of fresher upper layer water from the Gulf of Oman replacing evaporation loss, and lower more saline water exiting through the Strait of Hormuz (Reynolds, 1993).

Water entering the Persian Gulf through the Strait of Hormuz has a salinity of 36.5-37 psu. Surface salinities generally average to 37 to 40 psu (Sheppard, 1993). However, in the shallow southern embayments, salinities as high as 70 psu have been measured. Near-shore water temperatures range from 10-39°C annually, while offshore surface water temperatures range from 18-33°C (Price and Sheppard, 1991). A thermocline is found through the Gulf occurring at about 40 m near the Strait of Hormuz and rising to near 20 m to the northwest. The thermocline is most well-defined during the summer rising from the end of the Gulf (Ross and Stoffers, 1978).

Circulation in the Gulf of Oman makes a transition from estuarine to deep-ocean circulation. It is characterized by outflow of bottom water through the Strait of Hormuz into the Gulf of Oman with a return of water at the surface. The bottom water entering the Gulf of Oman from the Strait of Hormuz spreads out across the basin at a depth of approximately 200 m (Reynolds, 1993). Counter-rotating gyres create a cold-water upwelling action along the coast of Iran. A clockwise gyre has been indicated in the western Gulf of Oman by drifter buoy studies, while in the eastern Gulf a counterclockwise gyre was indicated (Reynolds, 1993). Current velocities may attain 75 $cm \cdot s^{-1}$, but usually do not exceed 50 $cm \cdot s^{-1}$ (Defense Mapping Agency, 1988). At its eastern end, the Gulf of Oman is in unrestricted contact with the northern Indian Ocean and, thus, is hydrographically similar (Ross and Stoffers, 1978).

Nutrients in the Persian Gulf are lower than in the Gulf of Oman, which are high due to monsoonal upwelling. Phosphate values rapidly decrease by mixing and biological stripping as water from the Gulf of Oman moves north through the Strait of Hormuz. Phosphate concentrations of 0.1 $\mu M \cdot kg^{-1}$ were measured in the northern end of the Persian Gulf, while values of 0.3-0.4 $\mu M \cdot kg^{-1}$ were reported at the southern end of the Gulf (Brewer et al., 1978). Phosphate concentrations continue to increase to 1 $\mu M \cdot kg^{-1}$ into the Gulf of Oman. Nitrate concentrations of 8.9 $\mu M \cdot kg^{-1}$ have also been measured in the Gulf of Oman as well. A strong oxygen minimum zone and lowered nutrient levels are present between approximately 100-400 m depth due to high productivity (Brewer et al., 1978).

The Gulf sediments have higher total organic carbon levels than natural background levels of similar seas. The sediments of the northeastern region contain 0.83-1.51% organic carbon, while levels in the northwestern region are lower. The Gulf sediments generally range from 0.5-1.0% organically bound carbon (levels as high as 2.8% were found). The distribution of total organic carbon in The Gulf sediments showed good agreement with the general water circulation pattern (Al-Ghadban, et al., 1994).

Ecology. The Persian Gulf pelagic zone is more productive than that of the central and northern Red Sea, but is 1 to 2 orders of magnitude less productive than the Arabian Sea. Chlorophyll *a* values of 0.2 to 0.86 $mg \cdot m^{-3}$ have been reported (Sheppard, 1993). Zooplankton biomass was reported to range from 0.11-2.00 $mL \cdot m^{-3}$, with highest values occurring in the central Gulf (Grice and Gibson, 1978). Biological productivity in the Gulf of Oman is relatively high with a carbon assimilation rate >1 $g \cdot cm^{-2} d^{-1}$ (Ross and Stoffers, 1978). Zooplankton biomass has been reported to range from 0.52-2.27 $mL \cdot m^{-3}$ (Grice and Gibson, 1978).

Generally, the Gulf as a whole is dominated by shallow water (10 to 12 m) soft substrate ecosystems which contain several critical marine habitats. These are typified by high biological productivity, provision for nutrients, feeding, breeding, or nesting areas for marine and other animals, areas of high species diversity such as coral reefs, and areas important for sustaining species populations in critical life stages such as seagrass and mangrove habitats (Price et al., 1993; Price and Sheppard, 1991). The distribution of coral reefs and mangroves is less extensive than those found in the Red Sea. Coral reefs are generally limited in their occurrence, with the best developed reefs found offshore. These provide nesting sites for birds and turtles. Mangroves are also found in limited numbers, mostly along the western coastline (Price and Sheppard, 1991).

Seagrass beds occupy a particularly important position in the Gulfs ecosystem. Estimates of seagrass productivity in Tarut Bay suggest that $2 \cdot 10^6$ kg of fish production could be supported annually (or the same quantity of shrimp) with a U.S. dollar value of 12 million. Seagrass beds also provide both a direct food source (turtles, dugongs, urchins and some fish), and an indirect food source (fish and crustaceans) for numerous species. Faunal richness and abundance in seagrass beds in the Gulf are higher than in the Red Sea (Price et al., 1993). Species considered vulnerable or of conservational importance include the green and hawksbill turtle (endangered), dugongs (sea cows), seasnakes, whales, and dolphins. Pearl oysters (*Pinctada radiata* and *P. margaritifera*) are commercially important, with *P. margaritifera*, regarded as commercially threatened (Price and Sheppard, 1991).

The allied war with Iraq following the attempted annexation of Kuwait in 1991 resulted in the largest oil spill in history with as much as $6 \cdot 10^6$ barrels of oil released into the Persian Gulf (Al-Rabeh et al., 1992). While this action clearly impacted many aspects of the Gulf's ecology, the immediate and long-term effects were not always possible to distinguish from other contemporary pollution sources. In the following sections important ecological components such as fisheries will be discussed, and any apparent

effects of the Gulf War oil spill will be discussed. Where possible, pre-war conditions will be described, and post oil spill recovery assessed.

Fisheries. More than 500 fish species are supported in the Persian Gulf, mostly in pelagic or soft substrate demersal habitats. Species diversity decreases moving northward and southward where environmental conditions become more extreme (Price et al., 1993). Data collected in the late 1970s indicated that the biomass of all commercially valuable demersal fish species in the Persian Gulf was approximately 500,000 mt. Estimates of yearly maximum potential yield for the Persian Gulf were 142,500 mt. For the northwestern Gulf the average pelagic species biomass was 259,000 mt, while 558,000 mt were estimated in the southwestern Gulf. The estimated yearly potential yields in the northwestern and southwestern Persian Gulf ranged from 104,000-130,000 and 223,000-279,000 mt, respectively (Venema, 1984). In 1986, the total landing (including shellfish) was 335,500 mt (Price et al., 1993). Surveys along the Saudi Arabian coast conducted in 1992 indicated that the most dominant fish species collected were the slipmouth (*Leiognathus fasciatus*), the pigface bream (*Lethrinus kallopterus*), and the therapon (*Therapon puta*). The bream is of high importance in the region composing approximately 19% of the total production of marine resources in Saudi Arabia (Hashim, 1993).

By 1992 the Saudi Arabian prawn landings had experienced disastrous decreases. The spawning biomass level had fallen to approximately 1.8% of the pre-war level leading to the possibility of a recruitment collapse. The total biomass had also declined to less than 1.5% of mean pre-war levels. A reduction in landings from 4000 mt in 1989 to 25 mt in the first half of 1992 was experienced. At this point the prawn fishery was suspended with losses in the 1991-1992 period estimated at 41 million U.S. dollars (Mathews, et al., 1993). Possible causes included massive mortality of 1991 egg, larval, and postlarval prawns due to oiling of spawning and nursery grounds in the spring of 1991. This lowered the spawning biomass. Due to the absence of immature prawns, there was a very low abundance of adult prawns in 1992. Heavy fishing of adults in early 1991 and of juveniles in late 1991 also acted to reduce the spawning biomass in spring 1992. The fishery shows no signs of recovery and will require careful management to sustain even the current low levels (Mathews, et al., 1993).

In addition to documenting significant decreases in Panaeid shrimp abundance along the Saudi Arabian coast in 1992 compared to data collected in the 1970s, another study also found significant decreases in zooplankton abundances in 1992 (Mathews, et al., 1993). Unrelated pre-war environmental changes due to coastal development pressures such as infilling and dredging, which occurred on a large scale along the Saudi Arabian coastline in relatively shallow waters used by shrimp for spawning, may also have contributed to the drastic reductions in the shrimp fishery (Mathews, et al., 1993).

Data collected in the late 1970s in the Gulf of Oman indicated that the biomass of all commercially valuable demersal fish species was approximately 100,000 mt. Estimates of yearly maximum potential yield were 36,500 mt for the Gulf of Oman. The average biomass of pelagic species in the Gulf of Oman was estimated to be 33,000 mt with estimated potential yields ranging from 13 to 17,000 mt (Venema, 1984).

Impacts on the Marine Environment. Collectively, the oceanic region represented by the Persian Gulf, the Strait of Hormuz, and the Gulf of Oman is one of the most important and frequently traveled waterways in the world. A ship passes through the Strait of Hormuz every 6 minutes. Approximately 60% of the world's marine transport of oil occurs in this region (Reynolds, 1993). Among the topics discussed below are coastal development and associated forms of pollution, and oil pollution.

Development. Domestic, urban, and industrial pollutants are a problem in several parts of the Persian Gulf although effects on ecosystem structure and function are generally not known. Coastal habitats have been lost or degraded by landfilling, dredging and sedimentation. More than 40% of the Saudi Arabian coastline has been developed. Domestic and urban sources have contributed daily inputs of raw sewage into the Gulf of as much as 40,000 m^3. This has resulted in solids and grease mats, local eutrophication, increases in BOD, and algal blooms. Industrial pollutants include desalination effluents, wastewater from fertilizer plants, and refinery effluents containing heavy metals (Price, 1993). Major gaps in knowledge exist, however, and it is not clear if increases in algal blooms and jellyfish are indicators of widespread pollution, or simply part of natural cycles.

There is a widespread co-occurrence of trash with new development along the coast. Solid waste was found at 87% of 53 sites inspected (Price, 1993). It has been estimated that $13.5 \cdot 10^6$ man-made items are stranded along 800 km of the Arabian Gulf and the Gulf of Oman shorelines. Of the items found, plastics accounted for 27.1%, while fishing floats and netting represented 16.9%. Debris pollution was much higher along the western coast of the Arabian Gulf than along the east coast of the Gulf of Oman resulting from the land-locked nature of the Arabian Gulf and its counterclockwise circulation (Khordagui and Abu-Hilal, 1994). Most of the litter is thought to be related to fishing activities, off shore oil field workers, and boat, ship and tanker traffic.

Oil Pollution. Although the Gulf War oil spill was a catastrophic single event, oil pollution in the Persian Gulf occurs routinely, and was present on a widespread basis before the war. When the Persian Gulf oil inputs to the marine environment are compared to the rest of the world as percentages of the total estimated input, the scope and nature of oil pollution in the Gulf becomes apparent. Notably, ship and tanker traffic spills and routine discharges (oily ballast) accounted for 86 spills and 58% of the total estimated input to the Gulf in 1977 and 1980, compared to 23% (1978) for the rest of the world (Dicks, 1987). In 1986, this input was estimated to range from 400,000 to 750,000 mt in the Persian Gulf. Inputs in the rest of the world's seas originate principally from refining, industrial and urban sources rather than from tanker traffic (Price, 1993).

Considering the degree of oil spillage, the levels of petroleum hydrocarbons in water, sediments and biota are not as high as might be expected. Elevated concentrations of petroleum hydrocarbons in sediments (3950 $\mu g \cdot g^{-1}$ dry wt.) and bivalve tissues (>500 $\mu g \cdot g^{-1}$ dry wt) have been reported near industrial areas. High seawater concentrations (546 $\mu g \cdot L^{-1}$) have also been reported in industrial areas (Price, 1993). In the offshore environment, petroleum hydrocarbon levels are generally low due to rapid breakdown from solar radiation and high summer temperatures. High levels of bacteria which degrade petroleum hydrocarbons have also been found in seawater samples. These factors as well as circulation patterns and wind influences act to minimize petroleum hydrocarbon contamination in offshore sediments which typically contain lower values (0.07-5.0 $\mu g \cdot g^{-1}$ dry wt.). The results of offshore sediment measurements suggest that most of the residue from oil spills in the Gulf ultimately reaches the shoreline without serious contamination of offshore benthic areas (Coles and McCain, 1990).

Beach oil is widespread, and often present in high concentrations throughout the Gulf. A recent survey of the Gulf indicated that tar balls were present in 77% of 53 coastal sites. Moderate amounts of tar balls were present in most sites, with tar concentrations of 1-10 kg m^{-1} frequently found and concentrations exceeding 10 $kg \cdot m^{-1}$ also common. Tar levels have been reported to be 100 times the maximum levels reported in other world regions (Price, 1993).

Broad-scale changes in the Persian Gulf coastal environment as a result of the Persian Gulf War were assessed with pre-war data from 1986 and post-war data from 1991 to 1992. The mean magnitude of oil

pollution was significantly greater in 1991 than in 1986. However, the mean magnitude of oil pollution decreased in 1992 to a level not significantly different from that in 1986, suggesting some recovery of surface substrata. Some species abundances (algae, birds, and fish) were significantly greater in 1991 than those noted in 1986. It was concluded that the ecosystem abundance patterns could be attributed as much to seasonal variability, background human impacts, and the semi-quantitative nature of the survey method, as to war-related consequences. The apparent increase in some faunal and floral elements would seem to indicate that the Gulf War had not caused a complete environmental collapse (Price et al., 1993c).

Table 2.3-1. Representative oceanographic characteristics of the Persian Gulf.

Parameter	Value	Reference(s)
Current Velocities ($cm \cdot s^{-1}$)	36	Defense Mapping Agency, 1988
Salinity (psu)	39	Wyrtki et al., 1971
Temperature (°C)	25	Wyrtki et al., 1971
Density (sigma-t)	28	Brewer et al., 1978
Evaporation ($cm \cdot yr^{-1}$)	200	Reynolds, 1993
Sfc Layer Thickness (m)	20	Reynolds, 1993
Wind deposited particulate ($g \cdot m^{-2} \cdot yr^{-1}$)	6.9	Sheppard, 1993
Si O_4-Si (μg at L^{-1})	3	Wyrtki et al., 1971
PO_4-P (μg at L^{-1})	0.6	Wyrtki et al., 1971
Residence Time (yrs)	2-5	Reynolds, 1993
Zooplankton Biomass ($cc \cdot m^3$)	0.11-2.00	Grice and Gibson, 1978
Primary Production (mg Chl $a \cdot m^{-3}$)	0.2-0.86	Sheppard, 1993
Surface Area (km^2)	$2.39 \cdot 10^5$	Reynolds, 1993
Average depth (m)	36	Reynolds, 1993
Max Depth (m)	100	Reynolds, 1993
Volume (km^3)	$8.63 \cdot 10^3$	Reynolds, 1993
Surface O_2 Background ($mL \cdot L^{-1}$)	5.0	Wyrtki et al., 1971
TOC (%) Bottom Sediments	0.46-2.8	Al-Ghadban et al., 1994

Table 2.3-2. Representative oceanographic characteristics of the Gulf of Oman.

Parameters	Value	Reference(s)
Current Velocities ($cm \cdot s^{-1}$)	50	Defense Mapping Agency, 1988
Salinity (psu)	36.5	Wyrtki et al., 1971
Temperature (°C)	30	Defense Mapping Agency, 1988
Density (sigma-t)	24	Defense Mapping Agency, 1988
Evaporation ($cm \cdot yr^{-1}$)	140-500	Sheppard, 1993
SiO_4-Si ($\mu g\text{-}at \cdot L^{-1}$)	5	Wyrtki et al., 1971
PO_4-P ($\mu M \cdot kg^{-1}$)	1	Brewer et al., 1978
NO_3-N ($\mu M \cdot kg^{-1}$)	8.9	Brockmann et al., 1990
Biological Productivity ($g \cdot Cm^{-2}\ yr^{-1}$)	>365	Ross and Stoffers, 1978
Zooplankton Biomass ($cc \cdot m^{-3}$)	0.52-2.27	Grice and Gibson, 1978
Dissolved Oxygen Surface ($mL \cdot L^{-1}$)	5.0	Wyrtki et al., 1971
Dissolved Oxygen 300m ($mL \cdot L^{-1}$)	0.5	Wyrtki et al., 1971
Surface Area (km^2)	$8 \cdot 10^4$	Estimated
Max Depth (m)	>3000	Ross, 1978
Average depth (m)	1000 m	Estimated
TOC (%) Bottom Sediments	1-6	Ross, 1978

REFERENCES

Al-Ghadban, A.N., P.G. Jacob, and F. Abdali. 1994. *Total Organic Carbon In The Sediments Of The Arabian Gulf And Need For Biological Productivity Investigations.* Mar. Pollut. Bull., 28, 356-374.

Al-Rabeh, A.H., H.M. Cekirge, and N. Gunay. 1992. *Modeling The Fate And Transport Of Al-Ahmadi Oil Spill.* Water, Air, and Soil Pollut., 65, 257-279.

Brewer, P.G., A.P. Fleer, S. Kadar, D.K. Shafer, and C.L. Smith. 1978. *Chemical Oceanographic Data From The Persian Gulf And Gulf Of Oman.* WHOI-78-37, Report A, 14 pp.

Coles, S.L., and J.C. McCain. 1990. *Environmental Factors Affecting Benthic Infaunal Communities Of The Western Arabian Gulf.* Mar. Environ. Res., 29, 289-315.

Defense Mapping Agency, Hydrographic/Topographic Center. 1988. *Sailing Directions (Planning Guide) For The Indian Ocean.* Third Edition. Pub. 170, 463 pp.

Dicks, B. 1987. Pollution. Chapter 18 pp. 383-404. In: Key Environments. Red Sea. A.J. Edwards and S.M. Head, Eds. 1987. Pergamon Press. Oxford.

Grice, G.D., and V. R. Gibson. 1978. *General Biological Oceanographic Data From The Persian Gulf And Gulf Of Oman.* WHOI-78-38, Report B, 34 pp.

Hashim, O.A. 1993. *Fisheries Study In The Gulf.* Mar. Pollut. Bull., 27, 279-284.

Khordagui, H.K., and A.H. Abu-Hilal. 1994. *Man-Made Litter On The Shores Of The United Arab Emirates On The Arabian Gulf And The Gulf Of Oman*. Water, Air, and Soil Pollut., 76, 343-352.

Mathews, C.P., S. Kedidi, N.I. Fita, A. Al-Yahya, and K. Al-Rasheed. 1993. *Preliminary Assessment Of The Effects Of The 1991 Gulf War On Saudi Arabian Prawn Stocks*. Mar. Pollut. Bull., 27, 251-271.

Price, A.R.G. 1993. *The Gulf: Human Impacts And Management Initiatives*. Mar. Pollut. Bull., 27, 17-27.

Price, A.R.G., and C.R.C. Sheppard, 1991. *The Gulf: Past, Present And Possible Future States*. Mar. Pollut. Bull., 22, 222-227.

Price, A.R.G., C.R.C. Sheppard, and C.M. Roberts. 1993a. *The Gulf: Its Biological Setting*. Mar. Pollut. Bull., 27, 9-15.

Price, A.R.G., C.P. Mathews, R.W. Ingle, and K. Al-Rasheed. 1993b. *Abundance Of Zooplankton And Penaeid Shrimp Larvae In The Western Gulf: Analysis Of Pre-War (1991) And Post-War Data*. Mar. Pollut. Bull., 27, 273-278.

Price, A.R.G., T.J. Wrathall, P.A.H. Medley, and A.H. Al-Moamen. 1993c. *Broadscale Changes In Coastal Ecosystems Of The Western Gulf Following The 1991 Gulf War*. Mar. Pollut. Bull., 27, 143-147.

Reynolds, R.M. 1993. *Physical Oceanography Of The Gulf, Strait Of Hormuz, And The Gulf Of Oman - Results From The Mt. Mitchell Expedition*. Mar. Pollut. Bull., 27, 35-59.

Ross, D. A., and P. Stoffers. 1978. *General Data On Bottom Sediments Including Concentration Of Various Elements And Hydrocarbons In The Persian Gulf And Gulf Of Oman*. WHOI-78-39, Report C, 74 pp.

Sheppard, C.R.C. 1993. *Physical Environment Of The Gulf Relevant To Marine Pollution: An Overview*. Mar. Pollut. Bull., 27, 3-8.

Venema, S.C. 1984. *Fishery Resources In The North Arabian Sea And Adjacent Waters*. Deep-Sea Research, 31A, 1001-1018.

2.4 UPDATED TABLE FOR THE ANTARCTIC AREA

Table 2.4-1 has been updated and the review section can be found in the original report (TR 1716).

Table 2.4-1. Representative oceanographic characteristics of the Antarctic area.

Parameter	Value	Reference(s)
Surface Current Velocity ($cm \cdot s^{-1}$)	50	Defense Mapping Agency, 1992
Deep Current Velocity ($cm \cdot s^{-1}$)	50	Defense Mapping Agency, 1992
Surface Salinity (psu) Summer	34	Defense Mapping Agency, 1992
Deep Salinity (psu)	34	Fabiano, 1993
Surface Temperature (°C) Summer	2.8-5.0	Defense Mapping Agency, 1992
Surface Temperature (°C) Winter	1.1-2.2	Defense Mapping Agency, 1992
Deep Temperature (°C)	-1	Fabiano, 1993
Density (sigma-t)	27	Defense Mapping Agency, 1992
Sfc Layer Thickness (m)	50->100 m	Nelson and Smith, 1991
Total Suspended Matter ($mg \cdot L^{-1}$)	1.3	Fabiano, 1993
POC ($\mu g \cdot L^{-1}$)	58.9	Fabiano, 1993
PO_4-P (μM)	1	Verlencar and Dhargalkar 1992
Surface NO_3-N (μM)	10	Verlencar and Dhargalkar 1992
Surface O_2 Background ($mL \cdot L^{-1}$)	8.0	Wyrtki et al., 1971
Deep O_2 Background ($mL \cdot L^{-1}$)	4.5	Wyrtki et al., 1971
Primary Production ($gC \cdot m^{-2} \cdot day^{-1}$)	0.341	Defense Mapping Agency, 1992
Chlorophyll Conc. ($\mu g \cdot L^{-1}$)	~1	Nelson and Smith, 1991
Phytoplankton Biomass (μg Chl$\cdot L^{-1}$)	0.21	Kristiansen et al., 1992.
Zooplankton (krill) Biomass ($mt \cdot 10^6$)	250	Defense Mapping Agency, 1992
Surface Area (km^2)	$3.6 \cdot 10^7$	Defense Mapping Agency, 1992
Average depth (m)	4000	Defense Mapping Agency, 1992
Max Depth (m)	5000	Defense Mapping Agency, 1992

3. FOLLOW-ON STUDIES OF PULPER AND SHREDDER WASTE STREAM CHARACTERIZATION

Several studies were on-going at the time of the original report publication. Therefore, the final reports from the individual researchers are included in this Addendum in their entirety without modification or interpretation. The Analysis section will discuss the findings in relation to U.S. Navy shipboard solid waste discharges, taking into account discharge conditions and quantities. The first two studies in this section, "Effects of Dispersed Paper Waste on the Filter-Feeding Capacity, Ingestion of Paper, and Growth of Pacific Sardine, *Sardinops Sagax*" (section 3.1.1) and "Bacterial Degradation of Cellulosic Wastes at Sea" (section 3.1.2) are comprehensive studies on potential biological interactions resulting from the pulped paper waste stream. The next two studies, sections 3.2 and 3.3, were sub-efforts undertaken by SPAWARSYSCEN San Diego to answer specific questions with regard to the pulped and shredded waste streams, respectively.

3.1 BIOLOGICAL INTERACTIONS

3.1.1 Effects of Dispersed Paper Waste on the Filter-Feeding Capacity, Ingestion of Paper, and Growth of Pacific Sardine, *Sardinops Sagax*

by Dr. Russ Vetter, Larry Robertson, and Carol A. Kimbrell

OVERVIEW

This study examined the potential impact of the release of dispersed paper waste (DPW) from ships at sea on the feeding capacity, growth, and health of Pacific sardine, *Sardinops sagax*. The DPW consisted of finely pulped paper and cardboard waste in a water slurry. A high concentration range of DPW (30,15 and 3 mg·L^{-1} dry wt DPW) was used to bracket the anticipated concentration at the point of discharge from ships. A lower concentration range (1.0,0.1,0.01 mg·L^{-1} dry wt DPW) was used to approximate anticipated concentrations at later times when mixing from the ship's wake is replaced by the natural dispersal processes of water movement and particle settlement. The high and low concentration ranges of DPW were used to test for acute and chronic effects of DPW on: filter-feeding rates, gastric accumulation of paper, growth rate, and survival. In 8 hour exposures repeated every other day for 15 days, concentrations of DPW of 1mg·L^{-1} and above had acute effects on filter-feeding rates by Pacific sardine feeding on *Artemia* nauplii. At these concentrations, stomachs became distended with paper. Increased mortality also occurred at 3.0 mg·L^{-1} and above. After a single 8 hrs feeding at either 3 or 1 mg·L^{-1} DPW plus *Artemia*, the ingested paper required more than 12 days to pass through the gastro-intestinal tract. There was no evidence of digestion or breakdown of the paper in fecal pellets. In 30-day continuous low-level exposures (1, 0.1 and 0.01 mg·L^{-1} dry wt DPW plus *Artemia*), Pacific sardine lost weight in proportion to the amounts of DPW present. Controls fed the same *Artemia* concentrations without DPW gained weight. The 1 and 0.1 mg·L^{-1} exposures contained significant accumulations of DPW in the stomach. In summary, the effects of DPW appeared to be due to mechanical disruptions caused by the paper fibers, rather than toxic effects. The impact of release of DPW from ships on sardine populations will depend on the volume of the release and the residence time in the water column.

INTRODUCTION

Small, pelagic, clupeoid fishes (e.g. sardine, anchovy, herring, and menhaden species) are an important link in most coastal pelagic ecosystems. These organisms harvest the carbon found in phytoplankton and zooplankton and convert it to a large standing stock of small, pelagic, schooling fishes. In turn, these species are the forage base for larger predacious fishes (e.g. tuna, salmon, rockfish), seabirds (pelicans, gulls, terns), and marine mammals (whales, dolphins, seals, sea lions). On a weight basis, clupeoid fisheries are the most important fisheries worldwide, constituting about one third of world catch (Blaxter and Hunter 1982). Off the west coast of North America, northern anchovy (*Engraulis mordax*) and Pacific sardine (*Sardinops sagax*) vary in abundance during different climate regimes (Baumgartner et al., 1992) but together represent the major stocks of clupeoid fishes. Presently, the sardine biomass is increasing and is estimated to be about 510,000 tons (Barnes et al., 1992, 1997).

Fish such as Pacific sardine and northern anchovy can reach such high biomass because they feed lower on the food chain than larger predacious fishes. They typically subsist on a diet of phytoplankton and zooplankton (Loukashkin, 1970; Koslow, 1981). Clupeoids can feed by two different methods. If the prey organisms are large enough, they will strike at and ingest individual particles. If the prey organisms are smaller but abundant, they may filter-feed (reviewed by Blaxter and Hunter, 1982). The initiation and cessation of filter-feeding is regulated by particle concentration, and chemical cues (Hunter and Dorr, 1982, Hunter personal communication).The fish use cartilaginous extensions of their gill rakers to filter water as it passes through the gills and collect the particles trapped on the gill rakers. The size of the particles trapped depends on the size of the sieve created by the gill rakers. This varies with species, and the size of the individual fish (Blaxter and Hunter 1982). After particles are entrained on the gill rakers it is thought that they are concentrated in epibranchial organs at the roof of the mouth (Nelson, 1967), and finally a more concentrated bolus of food from the epibranchial organ is passed down the esophagus. The extent to which food particles may be sorted from other debris prior to ingestion is unknown.

The International Convention for the Prevention of Pollution from Ships, 1973, as modified by the Protocol of 1978 (Annex V of MARPOL 73/78 1987) seeks to regulate pollution from ships in international waters. Reductions in the disposal of paper waste at sea is one area addressed in this convention. With the aim of meeting its commitments to this agreement, the United States Navy has been examining various alternative methods of paper waste disposal including incineration, storage at sea with eventual shore-based disposal, or discharge of a waste stream containing finely ground paper particles in a water slurry (dispersed paper waste).

We evaluated the potential effects of the third alternative, dispersed paper waste (DPW), on the feeding biology of Pacific sardine, a clupeoid fish likely to encounter this effluent. We investigated acute and chronic exposures to DPW. First, we examined the effect of DPW on filtering efficiency by determining the rate of disappearance of food particles in the presence and absence of DPW. This was done at a high range of DPW simulating conditions at the point of release, and at a low range of concentrations simulating dispersal of the DPW by the ship's wake. Second, we measured the rates of ingestion and of gastric evacuation of DPW inadvertently consumed during normal filter-feeding. Finally, we measured chronic effects on growth in fish exposed continuously to low levels of DPW for 4 weeks. The results provide an initial description of potential effects of the release of DPW on filter-feeding pelagic fishes.

METHODS AND MATERIALS

Collection and Maintenance of Sardines. Around 1500 sardines were captured by commercial purse seine in February 1995 and again in August 1995. The sardines were held at the Southwest Fisheries Science Center (SWFSC) aquarium in 4.6 m diameter, 0.7 m water depth ,vinyl-lined tanks, under flow-through, ambient-temperature, seawater. Sardines were fed a diet of Oregon Moist[1] pellets supplemented by weekly feedings of *Artemia* nauplii. The fish were not reproductively active during the holding and experimental periods. Fish were held up to 4 months in the holding tanks for these experiments. They continued to grow in captivity and showed no ill effects of holding. Sardines are routinely held for longer periods for spawning purposes. Exact records of holding conditions were maintained (data not shown).

Typically groups of about 60 fish were used for each experimental treatment. Fish used in a treatment were selected in the following manner. A group of fish was dipped from the holding tanks and slightly anesthetized with tricaine methansulfonate (30 $mg \cdot L^{-1}$). Fish were rapidly weighed and measured for standard length. They were immediately placed in a treatment group and allowed to recover. Assignment of a fish to a treatment was random in the beginning but as the numbers approached 60, the length compositions of the treatment groups were examined and assignments of the remaining fish were done to assure that each treatment group contained the same size distribution of individuals. This was done to equalize feeding pressure between treatments. The sardines were acclimated in the exposure trial tanks, without food, for at least 2 days prior to beginning a trial.

Exposure Tanks. Round, fiberglass tanks (1.9 m diameter, 0.61 m side depth, bottom sloping 6.4 cm to a center drain covered with a perforated cap) were filled with 1700 L each of fresh, filtered, seawater with depth determined by an external standpipe adjacent to a tank. Water flow through the in-line filter to each tank was four $L \cdot min^{-1}$ and the filter was changed every other day.

A flow-through system was used during non-exposure periods. A closed but recirculating system was used during experimental periods. A submersible bottom pump (1890 $L \cdot hrs^{-1}$) and a central airlift were used to circulate water, to resuspend paper waste, and to provide aeration. Before and after DPW exposure trials, each tank was flushed with seawater to ensure that no leftover paper or food remained. The chronic exposure tanks were kept in recirculating mode for the duration of that experiment with water changed twice daily.

Oxygen concentrations were ≥ 9.0 $mg \cdot L^{-1}$ and ammonia concentrations were ≤ 0.4 $mg \cdot L^{-1}$. The tank temperatures ranged from 15.2 to 19.2 °C over the course of the trials. Daily records of water quality were maintained (unpublished data).

Preparation, Addition, and Calculation of Artemia Concentrations. In general, fish were fed 24-48 hour old, HUFA[2]- enriched *Artemia* nauplii (Great Salt Lake, Utah cysts) every day. However, the concentration and method of feeding varied between the filter-feeding experiments, the gastric evacuation experiments, and the chronic effects on growth experiments.

---

1 Reference to trade names does not imply endorsement by the National Marine Fisheries Service, NOAA.

2 Highly Unsaturated Fatty Acids

Filter-Feeding Experiments. Anchovies consume 1.7% to 5.1% of their body wt per day (Leong and O'Connell, 1969). We assumed the same food ration for sardine. A 12-cm sardine filters 270 liters per day (Yoneda and Yoshida, 1955) and weighs about 21 g (Kondo et al., 1976). A newly hatched *Artemia* was assumed to weigh $4.17 \cdot 10^{-5}$ g wet weight. Given an exposure tank volume of 1700 L, 60 sardines/tank, mean wet weight of 16 g/fish, feeding period of 8 hours, and food consumption of 1.7% of body weight, we calculated the number of *Artemia* nauplii ($4.0 \cdot 10^{5}$) added to the high DPW exposure filtering efficiency tanks. The calculation of the number of *Artemia* nauplii ($1.5 \cdot 10^{6}$) fed to the 20-g sardines used in the low DPW exposure filtering efficiency tanks was made using 5.1% of body weight food consumption. *Artemia* concentration was increased from 1.7% to 5.1% after the high DPW exposures to spread out the time between initial introduction of food and exhaustion of food and cessation of filter-feeding. The entire quantity of *Artemia* was added at the beginning of each trial, 10 to 15 min after the addition of paper waste, by pouring from buckets evenly onto the water surface of each tank.

Gastric Evacuation Experiments. The density of Artemia nauplii used for the gastric evacuation control and DPW exposure tanks ($2700\ L^{-1}$) was an arbitrary number of nauplii meant to trigger filter-feeding behavior which would assure paper consumption along with *Artemia*. The addition of nauplii to the trial tanks was done continuously, over the 8-hour exposure to DPW.

Chronic Effects on Growth Experiments. The ration of *Artemia* nauplii given to the chronic paper exposure sardines ($18 \cdot 10^{6}$/24 hrs) was calculated on the basis of 60 fish/tank, mean wet weight of 59 g/fish, and food consumption of 5.1% of body weight per 24 hours. This ration was expected to result in positive weight gain. The sardines used for the chronic exposure trials were fed half the *Artemia* nauplii ($9 \cdot 10^{6}$) over a period of 8 hours, then the exposure tank was flushed, and the other half of the ration was fed over the following 16 hours.

Preparation, Addition, and Calculation of Paper Concentrations. All exposure trials used the same shipment of DPW slurry with a wet weight to dry weight ratio of 6.3. Frozen paper waste was weighed and thawed 24 hours prior to each trial day. Seawater was added to make a mixture which was stirred until the paper was well dispersed. The DPW mixture was added to each treatment and mixed for 10 to 15 min before adding *Artemia* at time 0. The tanks were monitored to confirm that the DPW remained suspended throughout the exposure period (data not shown). Pumps were monitored and cleared of paper as necessary throughout exposure periods, ensuring that effluent remained suspended.

Measuring the Paper and Artemia Concentrations in Tanks. DPW and *Artemia* concentrations were measured only during the filter-feeding experiments. At each sampling time four 250-mL water samples were collected from the center of each quadrant 3 inches below the surface of each tank and pooled (1000 m, total volume). Water samples were passed through labeled, dried, pre-weighed filters. The number of nauplii collected on each filter was recorded. The filter was dried to constant weight at 60°C for a minimum of 48 hours and reweighed to determine the weight of paper waste plus brine shrimp in a 1000-mL sample.

Sampling and Measurement of Fish. At the end of each experiment fish were anaesthetized and rapidly frozen to retain stomach contents. Fish were weighed and measured while frozen, and subsamples of 20 fish from each trial were thawed and the gastro-intestinal (GI) tracts weighed, dissected, examined for stomach contents, and stomach contents preserved. The amount of paper in the stomach and intestine was noted. Dead fish were weighed and measured and frozen for future examination.

EXPERIMENTAL DESIGN

Filter-feeding Experiments. Two filter-feeding experiments were done; a high concentration experiment and a low concentration experiment. Each experiment lasted 15 days with measurements taken every other day to compare the rate of disappearance of *Artemia* nauplii in the presence and absence of DPW.

High concentration experiments were done at 30, 15, and 3 mg dry wt DPW·L^{-1} plus a control tank receiving only *Artemia* nauplii. On sample days (every other day), the fish in the trial tanks were exposed to both DPW and *Artemia* for an 8 hour period. Water samples were taken at 1, 2, 3, 4, 6, and 8 hours elapsed time from the introduction of *Artemia* (time 0) during the 8-hour duration of each exposure to DPW. A visual assessment of feeding behavior was recorded at the time of each sample. After the 8 hrs exposure, the tanks were returned to flow-through seawater. On the days that the tanks received no DPW, *Artemia* was added to all tanks at the same concentration used for trials.

The low concentration experiments were done at 1, 0.1, and 0.01 mg dry wt DPW·L^{-1} plus a control tank receiving only *Artemia* nauplii. Based on the observed filtering rates at 3 mg·L^{-1} and controls, we decided to sample more frequently in the low concentration experiment. The *Artemia* and DPW were added to exposure tanks for an 8-hour period as above but DPW and *Artemia* were added every day. Water samples were taken every 15 min after initial addition of *Artemia* nauplii, and DPW and continued every 15 min until no *Artemia* were recorded in two consecutive samples.

After sampling every other day for six trials, half the fish were sacrificed on day 11. No more paper was introduced on the following days, but we continued to add *Artemia*. We used half the ration of *Artemia* because there were half as many fish. We continued to sample to determine the rate of recovery from DPW.

Gastric Evacuation Experiments. The gastric evacuation experiments were designed to measure the amount of DPW ingestion and the rate of clearance from a single exposure to *Artemia* plus DPW. The gastric evacuation fish were exposed to either none (control), 1 or 3 mg dry wt DPW·L^{-1} plus *Artemia* nauplii. Just prior to DPW exposure, a 5-fish sample was taken from each tank of 80 fish and GI tracts removed, dried and weighed to establish an empty gut baseline. At the end of the 8-hour exposure period, the tanks were flushed with clean seawater, switched from recirculating to flow-through mode and a 10-fish sample was taken from each tank. The GI tracts were removed, photographed and fixed in formalin. The carcass was frozen for future analyses. A second 10-fish sample was taken in similar fashion 24 hours later with each remaining sample taken 48 hours apart until there were no fish left to sample. Preserved GI tract wet weights were measured, and gut contents (wet and dry weights) were determined.

The control tank with 75 fish was fed *Artemia* for an 8-hour period, then switched to flow-through seawater. A 15-fish sample was removed from the tank and GI tracts were removed, examined and preserved in formalin. Subsequent 15-fish samples were taken at the above time intervals.

Chronic Exposure and Growth Experiments. The chronic exposure tanks were maintained as closed systems with recirculating seawater for a period of 4weeks except for two daily periods of flushing (30 min). In these experiments the calculated daily ration was dripped in slowly over the course of the day (above). The treatments were: fed control, starved control, and fed plus 0.01, 0.1 or 1 mg dry wt DPW·L^{-1}. The daily ration was dripped in over two periods, an 8-hour period from 0800 to 1600, followed by flushing and replenishment of DPW and a 16-hour period during the night followed by

flushing at the beginning of the work day. The ration was dripped in half as slowly during the second period. At the end of the 4 weeks all fish were anaesthetized, their wet weights and standard lengths measured, and the carcass frozen in liquid nitrogen. Later, GI tracts were removed and stomach contents removed, dried and weighed.

RESULTS

FILTER-FEEDING EXPERIMENTS

In the filter-feeding experiments we tried to determine if DPW affected filtering efficiency, if DPW was ingested along with food, and if there was higher mortality in the presence of DPW. The high DPW experiment (30, 15, and 3 mg dry wt·L^{-1}) bracketed expected conditions at the point of discharge, and the low DPW experiment (1, 0.1, 0.01 mg dry wt·L^{-1}) bracketed expected concentrations when the dispersal effect of the ship's wake ceased.

HIGH DPW FILTERING EXPERIMENT

Behavior and Appearance in Filter-Feeding Experiments. There is an obvious difference in the way the gills are flared during normal breathing and when filter-feeding. We used three subjective criteria to assess visual signs of filtering behavior: 1) little or no feeding 2) passively filtering (occasional gulping), and 3) actively filtering. At the two highest paper concentrations, the filtering activity, was a 3 when the food was first introduced in the first hour, but dropped to a 2 in the second hour and then 1 for the remainder of the 8 hrs even though abundant prey was still available. In the control tank feeding was always active (3) until the prey were gone. At the two highest paper concentrations, fish did not maintain tight schooling behavior. Occasionally an individual would display lethargic or disoriented swimming behavior.

At all three paper concentrations there were fish with lumpy abdomens. At the end of experiment when fish with this outward appearance were dissected, there were lumps of accumulated paper in the intestine that corresponded to the protrusions on the skin.

Filtering Efficiency. Results for the eight feeding trials at high DPW are presented in Table 3.1.1-1 and Figure 3.1.1-1. All three DPW concentrations had a readily observable negative effect on the ability of Pacific sardine to filter-feed on *Artemia* nauplii. There was a dose-dependent effect on filtering success with the highest concentration (30 mg dry wt·L^{-1}) almost completely inhibiting successful feeding on *Artemia* nauplii.

Ingestion of DPW. All treatments ingested the paper along with the prey, Figure 3.1.1-2. The highest ingestion rate was in the group receiving the lowest level of DPW (3 mg dry wt·L^{-1}).

Growth and Mortality. All groups lost weight during the experiment (Table 3.1.1-1). The average initial weights for the four groups were 16.19, 16.32, 16.10, and 16.12 g. At the conclusion of the experiment the average weights were respectively 14.0, 14.4, 14.3, and 13.9 g. There were no significant differences between the four groups. There were differences in mortality. All three treatment groups had higher mortality rates than did the control (Table 3.1.1-1, Figure 3.1.1-3).

LOW DPW FILTERING EXPERIMENT

Since all groups in the first experiment lost weight, we increased the starting concentration of *Artemia* from 235 nauplii·L^{-1} (1.7% of body weight) to 863 nauplii·L^{-1} (5.1% of body weight). We sampled more frequently at the beginning to measure more precisely the initial period of *Artemia* filtering, and we included two measurements of recovery during the four days following the end of the 14-day exposure period. At the highest DPW concentration (1.0 mg dry wt·L^{-1}) there was a significant effect on filtering efficiency (Figure 3.1.1-1b, Table 3.1.1-1). The other two concentrations (0.1 and 0.01 mg dry wt·L^{-1}) were the same as the control, (Figure 3.1.1-1B, Table 3.1.1-1). Therefore, the no effect level is between 1.0 and 0.1 mg dry wt·L^{-1}. At the end of 14 days half of the fish were sacrificed to determine the ending weight and stomach contents. The remaining fish were tested to see if the 14 d exposure to paper had a lasting effect on filtering efficiency. When tested on the two days following the end of the 14 d paper exposure there was no difference between the filtering rates of any of the three paper treatments and the control (Fig 3.1.1-1C). All fish actively filtered at the different concentrations and DPW was observed in the guts. There was low and evenly distributed mortality in the four treatments (Table 3.1.1-1).

GASTRIC EVACUATION EXPERIMENT

DPW was rapidly ingested and remained in the stomach and intestine beyond the 12 days of the sampling period (Figure 3.1.1-4). The amount of DPW ingested was proportional to the exposure concentration. As in the filter-feeding experiments lumps appeared on the abdomen. The lumps were caused by the distention of the stomachs filled with DPW (Figure 3.1.1-5). Both treatments exhibited this condition. Fecal pellets consisting of paper fibers were readily observed in the intestines of animals and on the bottom of the tanks.

CHRONIC EXPOSURE AND GROWTH RATE EXPERIMENTS

The effects of chronic exposure to dispersed paper were tested by exposing fish continuously to the three lower concentrations of DPW for 4 weeks. The fed controls experienced a 1.06% weight gain during the experiment while starved controls lost 8.36% (Figure 3.1.1-6, Table 3.1.1-2). All paper treatments showed a significant decrease in weight relative to the fed controls (Figure 3.1.1-6, Tables 3.1.1-2, 3.1.1-3). Both the 1.0 and 0.1 mg dry wt DPW·L^{-1} exposures retained paper in the gut and had gut contents significantly greater than the fed controls (Tables 3.1.1-2, 3.1.1-3).

None of the groups suffered high mortality, including the starved controls (Table 3.1.1-2). There were also no visually apparent signs of poor condition (such as skin lesions, scale loss, or disorientation) and there were no signs of abrasion or clogging of gill rakers.

TABLE 3.1.1-1

Mean standard length (SL), mean wet weight, and N of sardines used in the filtering efficiency experiment and exponential regression equations of prey density (nauplii/L/fish) as a function of time, (hrs).

Treatment	Paper Concentration ($mg \cdot L^{-1}$)	N			Percent Mortality (%)	SL Begin (mm)	Wet weight				f(x)=a*exp(b*x)		
		Trials	Begin	End			Begin (g)	End (g)	N	Change (g)	a	b	R^2
High DPW	30	8	60	40	33.3	120	16.2	14.5	37	-1.6	4.451	-0.092	0.985
1.7% Artemia ration	15	8	60	43	28.3	121	16.3	14.3	42	-2.0	4.110	-0.161	0.964
	3	8	60	40	33.3	121	16.1	14.8	39	-1.3	3.166	-1.530	0.973
	0	8	60	53	11.7	120	16.1	14.8	52	-1.3	4.320	-6.819	1.000
Low DPW	1	6	60	60	0.0	126	20.1	20.1	30	0.0	15.680	-6.582	0.992
5.1% Artemia ration	0.1	6	60	60	0.0	128	20.1	20.1	30	0.0	16.201	-13.276	0.999
	0.01	6	60	59	1.7	126	20.1	20.2	30	0.1	18.221	-14.679	0.994
	0	6	60	60	0.0	126	20.1	20.2	30	0.2	16.796	-14.662	0.998
Low DPW recovery	1	2									16.040	-10.057	0.999
5.1% Artemia ration	0.1	2									15.267	-8.514	1.000
	0.01	2									15.267	-8.740	1.000
	0	2									15.267	-9.801	1.000

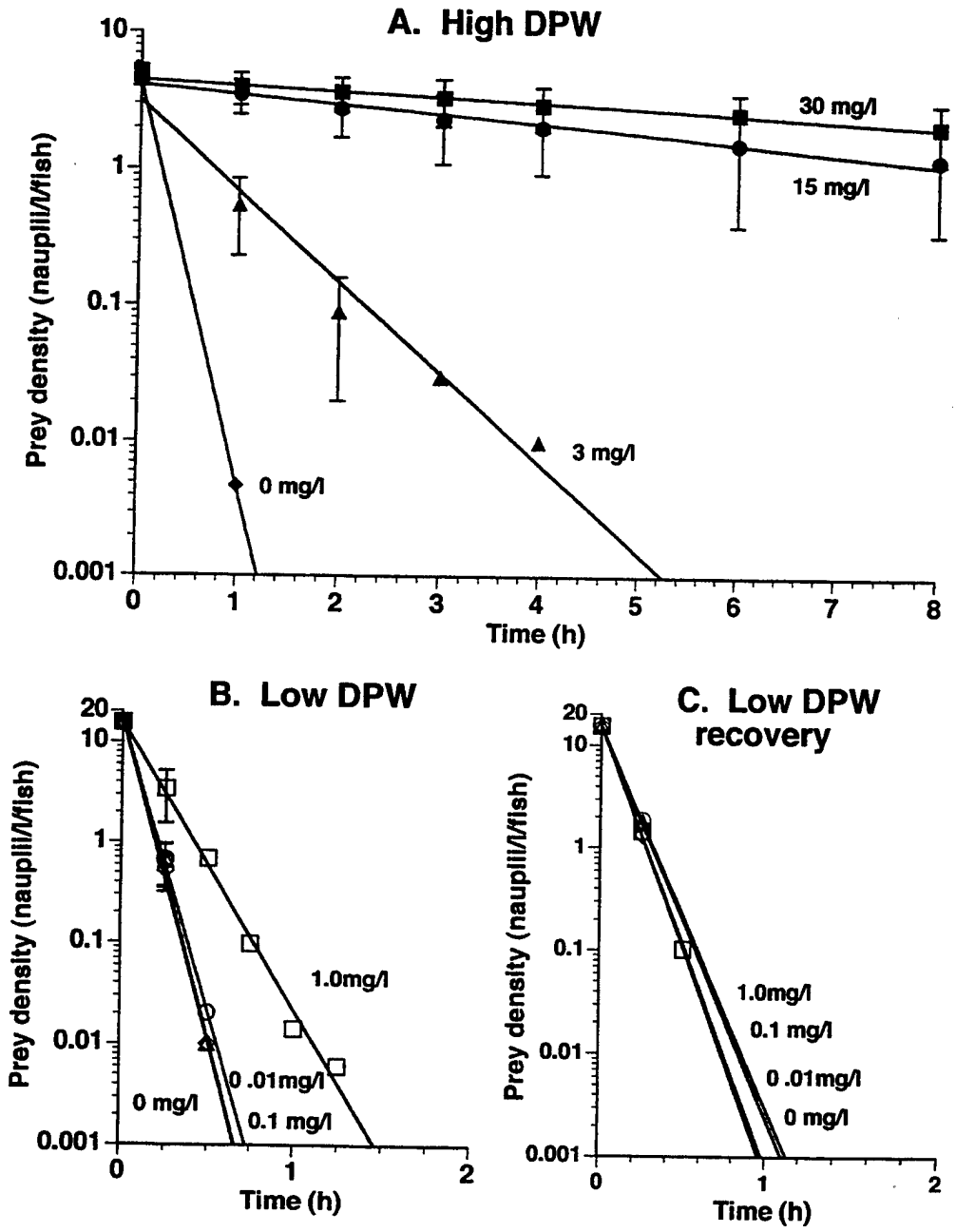

Figure 3.1.1-1. Filtering efficiency experiments. Mean rates for eight trials measuring filtering rates in the presence or absence of DPW. Prey density (nauplii/L/fish) as a function of elapsed time, (h). A. High DPW exposure. Filled squares, circles, triangles, and diamonds are 30, 15, 3, and 0 mg·L^{-1} DPW, respectively. B. Low DPW exposure. Open squares, circles, triangles, and diamonds are 1.0, 0.1, 0.01, and 0 mg·L^{-1} DPW, respectively. C. Recovery from low DPW exposure.

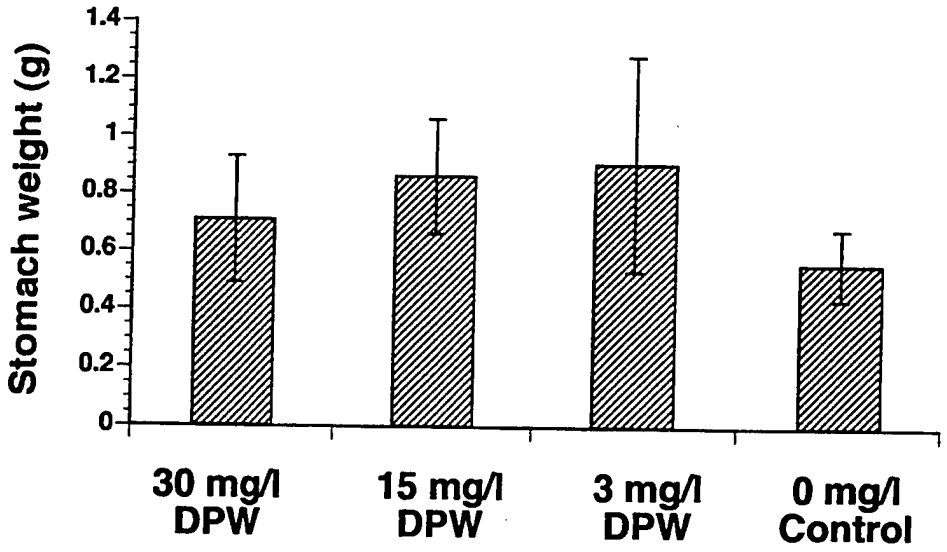

Figure 3.1.1-2. High DPW filtering efficiency experiments. Accumulation of DPW at end of 15-day experimental period. Stomach weights ±1 SD for 30, 15, 3, and 0 mg·L^{-1} dry weight DPW.

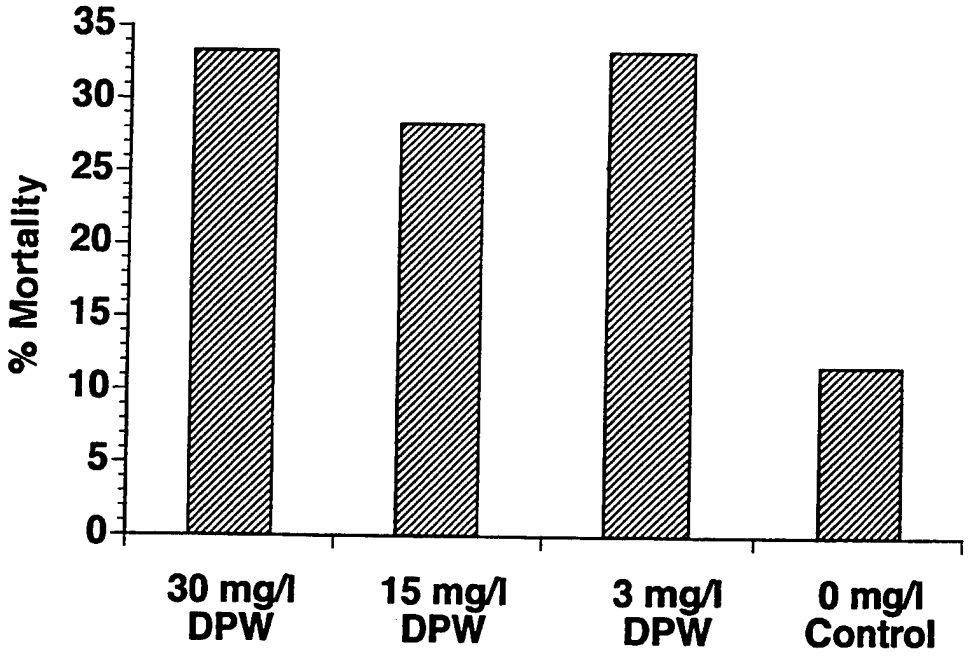

Figure 3.1.1-3. High DPW filtering efficiency experiments. Percent mortality over 15 days for sardine exposed to 30, 15, 3, and 0 mg·L^{-1} dry weight DPW.

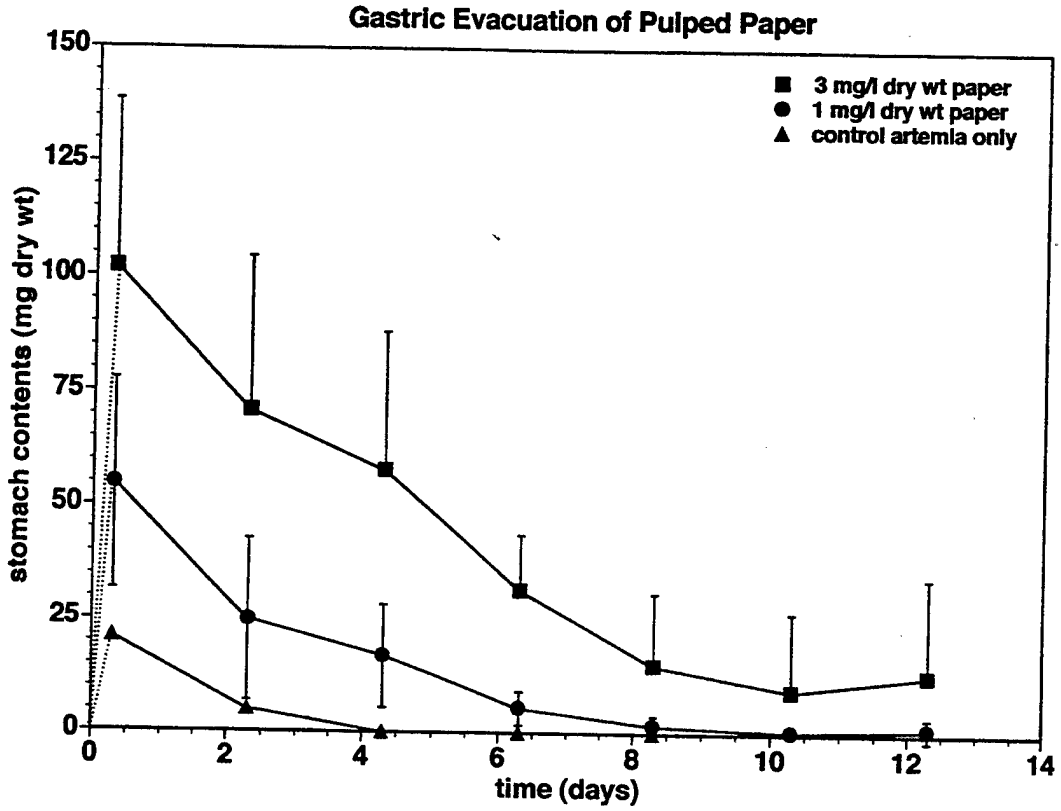

Figure 3.1.1-4. Gastric evacuation experiment. Amount of DPW consumed and rate of elimination over 12 days after a single 8-hour feeding of *Artemia* in DPW. Filled squares, circles, and triangles are 3, 1, and 0 $mg \cdot L^{-1}$ dry weight DPW, respectively.

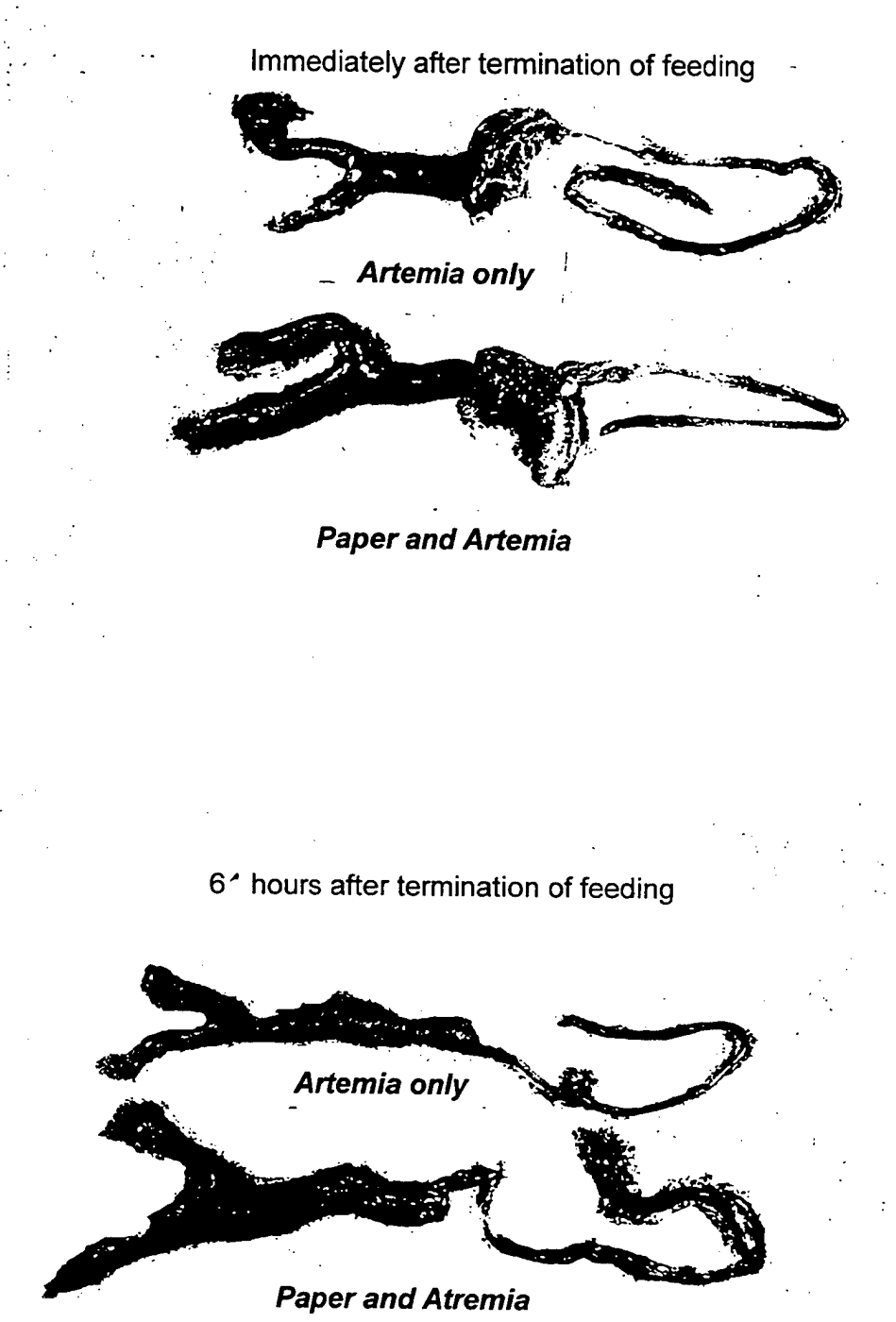

Figure 3.1.1-5. Gastric evacuation experiment. Photographs of dissected gastrointestinal (GI) tracts from esophagus (left) to anus (right). A. GI tracts immediately after feeding: upper, *Artemia* only; lower 3 $mg \cdot L^{-1}$ DPW plus *Artemia*. B. GI tracts 64 hours after termination of feeding: upper, *Artemia* only gut is empty; lower, DPW plus *Artemia* gut is filled with paper.

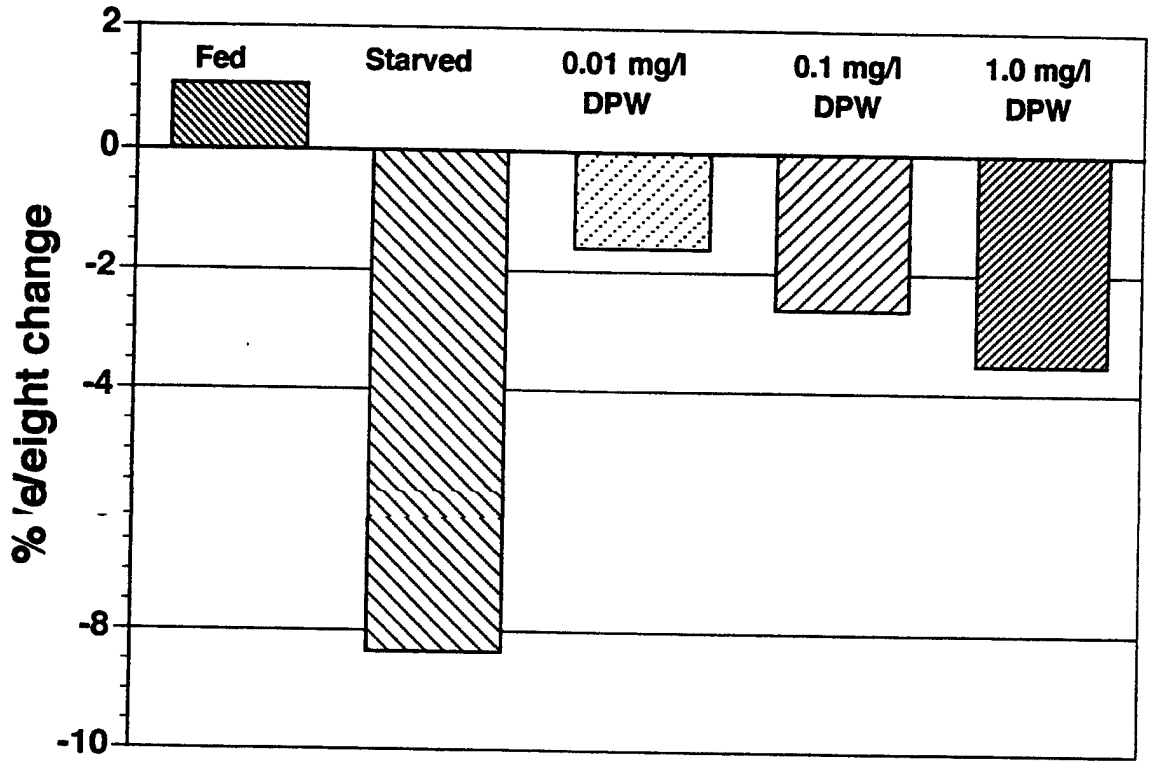

Figure 3.1.1-6. Chronic exposure experiment. Percent weight change after 30-day exposure to *Artemia* only, starvation, or DPW (0.01, 0.1 and 1.0 mg·L^{-1}) plus *Artemia*.

TABLE 3.1.1-2. N, mean and standard deviation (SD) of standard length (SL), wet weight, and dry weight of gut contents of sardines used in the chronic exposure treatments, and the mean and SD of wet weight change from beginning to end of exposure.

		Begin treatment			End treatment				Wet weight change	
			SL	Wet weight		SL	Wet weight	Dry weight gut contents		
Treatment	Paper concentration ($mg \cdot L^{-1}$)	N	Mean ± SD (mm)	Mean ± SD (g)	N	Mean ± SD (mm)	Mean ± SD (g)	Mean ± SD (g)	Mean ± SD (g)	% change
Fed control	0	60	170.2 ± 9.5	59.7 ± 11.0	56	170.2 ± 8.8	60.3 ± 9.7	0.024 ± 0.009	0.6 ± 1.9	1.06
Starved control	0	60	172.6 ± 7.4	60.7 ± 9.5	59	170.8 ± 7.8	55.6 ± 8.8	-	-5.1 ± 1.4	-8.36
Low DPW	0.01	60	171.2 ± 8.1	59.5 ± 11.3	57	170.5 ± 7.3	58.5 ± 10.6	0.021 ± 0.006	-1.0 ± 1.5	-1.61
Medium DPW	0.1	60	169.0 ± 12.0	59.0 ± 12.9	56	168.9 ± 11.5	57.5 ± 11.4	0.060 ± 0.013	-1.5 ± 2.5	-2.62
High DPW	1	60	170.4 ± 8.8	58.7 ± 10.5	58	169.7 ± 7.9	56.7 ± 9.6	0.070 ± 0.019	-2.1 ± 1.4	-3.52

TABLE 3.1.1-3. P-values of ANOVA of wet weight changes (upper matrix) and dry weight of gut content (lower matrix).

Treatment	Fed control	Starved control	Low DPW	Medium DPW	High DPW
Fed control	-	<0.001	<0.001	<0.001	<0.001
Starved control	-	-	<0.001	<0.001	<0.001
Low DPW	0.081	-	-		<0.001
Medium DPW	<0.001	-	<0.001	-	0.184
High DPW	<0.001	-	<0.001	<0.001	-

DISCUSSION

To assess the probable effects of DPW on Pacific sardine it was necessary to examine two scenarios: acute exposures to the higher doses that might be encountered if a school of sardines directly encountered a waste stream behind a ship, and chronic exposures to the lower doses that might be associated with areas with high amounts of ship traffic and associated discharges. Under both these conditions DPW had a greater effect on filter-feeding in Pacific sardine than we originally anticipated. At high DPW concentrations, 30, 15, 3, and 1 $mg \cdot L^{-1}$, there was an obvious inhibition of filtering efficiency (Figure 3.1.1-1A). Only when concentrations of DPW dropped below 1 $mg \cdot L^{-1}$ did this effect abate (Figure 3.1.1-1B). The cause of decreased filter-feeding capacity appeared to be two-fold. At the two highest concentrations (30 and 15 $mg \cdot L^{-1}$), the sardines stopped attempting to filter feed. At the next two lower concentrations (3 and 1 $mg \cdot L^{-1}$), filtering appeared normal and we can conclude that the problem was clogging and reduced efficiency of the filtering mechanism because the *Artemia* were mixed with DPW. The source of mortality in the different treatments was unknown and did not show a dose effect. All treatment groups had similar but elevated mortality when compared to controls (Table 3.1.1-1, Figure 3.1.1-3).

If exposure to higher concentrations of DPW is expected to be periodic, then the ecological significance of impaired filter-feeding rests not so much on the immediate event (the loss of food for a brief time period), but on the rate of recovery from the DPW. Recovery probably depends on the capacity for unclogging the gill raker sieves, and for clearance of ingested DPW from the gut. In the filter-feeding experiments the exposures to DPW were periodic (an 8-hour exposure every 48 hours), with feeding in the absence of paper on alternate days. Although recovery was not explicitly measured after each trial within the 15-day experiments, there was not a long-term decline in filtering efficiency among the 8 sequential trials that would suggest a cumulative effect on the gill rakers and filtering efficiency. In the low DPW experiments (Figure 3.1.1-1B) recovery was explicitly tested at the end of the 14-day experiment. At 1.0 $mg \cdot L^{-1}$ DPW, the only concentration that inhibited feeding, there was no lasting effects of paper treatment on filtering efficiency when tested on the two days following the 14-day paper trials (Figure 3.1.1-1C).

Although it was not the immediate purpose of the high DPW experiments, we did observe the accumulation of paper in the gut (Figure 3.1.1-2). This led us to examine this aspect of DPW recovery in more detail. The amount of paper ingested was dependent upon the DPW concentration in the water (Figure 3.1.1-4). The initial disappearance of stomach contents from the DPW plus *Artemia* treatments represents a combination of digestion of *Artemia* (Figure 3.1.1-4, control) and the movement of paper into the intestine. Subsequently, the reduction of paper in the stomach represents movement of paper into the intestine. Based on a microscopic examination of fecal pellets we feel that there was little to no digestion of the DPW. This is consistent with the apparent lack of cellulose digesting capabilities in most fishes.

The slow clearance of paper from the gut is a matter of concern. We would expect Pacific sardine to have a fairly rapid gut clearance rate similar to most animals that filter-feed as a means of feeding (Hunter and Kimbrell, 1980; Blaxter and Hunter, 1982). This was true for the *Artemia* fed control but not for the DPW treatments. For the 3 $mg \cdot L^{-1}$ treatment, paper was readily detectable in the stomach after 12 days. Although most of the paper in the 1 $mg \cdot L^{-1}$ treatment had left the gut, we still encountered paper in the intestine (data not shown). The results from the gastric evacuation portion of the study were surprising, because they suggest that there is very little post-entrainment sorting of *Artemia* from DPW trapped on the gill rakers. The extent to which this would inhibit future filter-feeding, ingestion and digestion of normal prey was not investigated but needs to be studied in greater detail.

Chronic effects of low levels of DPW were examined to determine long-term effects on growth, mortality and aspects of physical condition. In the chronic experiment, fish were exposed continuously to DPW except for two 30 min periods of tank flushing and cleaning each day. Controls were subjected to the same regime. The turbidity from DPW was barely visible at these concentrations and all groups behaved similarly. Fish in all treatments appeared healthy with few sores, lost scales, or other signs of stress. Mortality was low, similar between treatments, and spread over the course of the 30-day experiment (Table 2). Fed controls grew in length and gained weight over the course of the 30-day experiment, registering a 1.6% weight gain on average. In contrast the starved group lost 8.36% of its initial weight. The three groups exposed to DPW along with food lost weight, and they lost weight in proportion to the amount of DPW present (Figure 3.1.1-6, Table 3.1.1-2). Fish exposed to the two highest concentrations had significant amounts of paper in the stomach relative to controls (Tables 3.1.1-2, 3.1.1-3). Unlike the filter-feeding experiments, fish were offered food continuously in the chronic experiments; this allowed subtle differences in feeding success to be manifested over a long period of time (30 days). At the highest of the three exposures, we had previously demonstrated a slight effect on filter-feeding efficiency (Figure 3.1.1-1B), and it might be expected that fish exposed to this concentration of DPW would not grow as well as the control group. At the middle concentration (0.1 $mg \cdot L^{-1}$), we did not find inhibition of filter-feeding (Figure 3.1.1-1b), but we did find significant accumulations of paper in the gut (Table 3.1.1-2). This might have inhibited assimilation or digestion. At the lowest concentration, there was no clear explanation for why the fish did not gain weight, but the result was significant when compared to the control group (Figure 3.1.1-6, Tables 3.1.1-2, 3.1.1-3). The differences in weight gain between the three treatments and the control is quite interesting and suggests that even small amounts of DPW can have a chronic effect. These weight change differences were not apparent in the filtering efficiency experiments because of the nature of the experimental design. In the filtering experiments the DPW groups may have filtered less efficiently but the system was closed so all groups ultimately consumed the same ration as long as they ate it within 8 hrs before the tanks were flushed. In the chronic experiments we tried to simulate natural conditions where prey density is constant (*Artemia* dripped in constantly), and the rate of capture does matter (controls consume more food per hour than DPW treatments) and this shows up as differences in weight gain.

The results of this study show that DPW does have an effect on the filter-feeding capacity of Pacific sardine, one of the most abundant and ecologically important species of the California Current ecosystem. The effect appears to be caused by mechanical problems associated with the DPW fibers rather than chemical toxicity (Chadwick et al., 1996). We stress that this is a conjecture and has not been proven in our experiments. We also note that these experiments were done in filtered seawater. Pacific sardine may face similar filter-feeding problems when coastal waters are filled with natural detrital particles from disturbed sediments or fresh-water runoff.

In summary, the extent to which Pacific sardine are impacted will depend on the frequency of acute exposures, and the degree to which they are exposed to chronic low levels of DPW. They would most likely be affected in harbors and coastal areas when ship traffic is high. There are many other filter-feeding clupeoid fishes that are abundant, and are economically and ecologically important in most coastal waters of the world. These include herring, anchovy, and menhaden species. We would expect that effects on these fishes might be similar but it would most likely depend on the size and nature of the gill filtration sieves.

Funding for this study was provided by the SPAWAR Systems Center, San Diego via the Office of Naval Research. We wish to thank Everingham Brothers Bait Company for providing the live sardine for this study. Additional laboratory assistance was provided by Eric Lynn. We thank P. Smith and E. Logerwell for review and comments on the manuscript.

REFERENCES

Annex V of MARPOL 73/78. (1987). *Fundamental Restrictions Laid Out By The International Maritime Organization (IMO) In Annex V Of The International Convention For The Prevention Of Pollution From Ships (1973) And Its 1978 Protocol, Together Known As MARPOL 73/78.* The U.S. Congress ratified Annex in 1987.

Barnes, J. T., Jacobson, L. D., MacCall, A. D. and Wolf, P. (1992). *Recent Population Trends And Abundance Estimates For The Pacific Sardine (Sardinops sagax).* Calif. Coop. Oceanic Fish. Invest. Rep. 33, 60-75.

Barnes, T. J. Yaremko, M., Jacobson, L., Lo, N.C.H. and Stehly, J. (1997). *Status Of The Pacific Sardine. NOAA* Tech. Mem. NOAA-TM-NMFS-SWFSC-237. 17Pp.

Baumgartner, T., Soutar, A. and Ferreira-Bartrina, V. (1992). *Reconstruction Of The History Of Pacific Sardine And Northern Anchovy Populations Over The Past Two Millennia From Sediments Of The Santa Barbara Basin, California. Calif. Coop.* Oceanic Fish. Invest. Rep. 33, 24-40.

Blaxter, J. H. S. and Hunter, J. R. (1982) *The Biology Of The Clupeoid Fishes.* Adv. Mar. Biol., 20, 1-223.

Chadwick, D. B., Katz, C. N., Curtis, S. L., Rohr, J., Caballero, M., Valkirs, A., and Patterson, A. (1996). *Environmental Analysis Of U. S. Navy Shipboard Solid Waste Discharges.* Appendix A. Chemical analysis report. NRAD Tech. Rep. 1716.

Hunter, J. R. and Dorr, H. (1982). *Thresholds For Filter-Feeding In Northern Anchovy, Engraulis mordax.* Calif. Coop. Oceanic Fish. Invest. Rep.., 23, 198-204.

Hunter, J. R. and Kimbrell, C. A. (1980). *Egg Cannibalism In The Northern Anchovy, Engraulis mordax. Fish. Bull., U. S.* 78, 811-816.

Kondo, K., Hori, Y. and Hiramoto, K. (1976). *Life Pattern Of The Japanese Sardine, Sardinops Melanosticta (Temminck Et Schlegel), And Its Practical Procedure Of Marine Researches Of The Stock.* Suisan-Kenkyu-Sosho no. 30, 68 pp.

Koslow, J. A. (1981). *Feeding Selectivity Of Schools Of Northern Anchovy, Engraulis Mordax, In The Southern California Bight.* Fish. Bull., U.S., 79, 131-142.

Leong, R. J. H. and O'Connell, C. P. (1969). A Laboratory Study Of Particulate And Filter-Feeding Of The Northern Anchovy (*Engraulis mordax*). J. Fish. Res. Bd. Canada 26, 557-582.

Loukashkin, A. S. (1970). On The Diet And Feeding Behaviour Of The Northern Anchovy *Engraulis mordax* (Girard). Proc. Cal. Acad. Sci. 37, 419-458.

Nelson, G. J. (1967). Epibranchial Organs In Lower Teleostean Fishes. J. Zool., London 153,71-89.

Yoneda, Y. and Yoshida, Y. (1955). The Relation Between The Sardine And The Food Plankton - I. On The Food Intake By *Sardinops melanosticta.* Bulletin of the Japanese Society of Scientific Fisheries 21, No. 2.

3.1.2 BACTERIAL DEGRADATION OF CELLULOSIC WASTES AT SEA. FINAL REPORT FOR GRANT # N00014-95-0570, JANUARY 1997

by Dr. Mary Ann Moran, Wenying Ye, and Brian Binder

INTRODUCTION AND BACKGROUND

Concern over potential environmental degradation of marine habitats by anthropogenic wastes prompted an evaluation by the U.S. Navy of their waste disposal practice of releasing cellulosic wastes (shredded office paper and other paper products) from ships into open ocean waters. One of the important factors determining the ecological consequences of releasing cellulosic wastes into open ocean water is the rate of bacterial decomposition of the material within the water column and on the sea floor. Relatively little is currently known about the biological fate of cellulosic material in the open ocean or the cellulolytic abilities of natural oceanic bacterial assemblages, primarily because cellulose is not naturally abundant in such environments. Such information is critical, however, to understanding the fate of cellulosic particles released into the ocean, to determining where in the environment the bulk of decomposition is likely to occur, to understanding the potential local impacts of releases on marine food webs, and to predicting the time frame necessary for complete decomposition. This report describes studies designed to measure rates and kinetics of bacterial decomposition in seawater and determine the importance of various environmental factors (temperature and nutrient concentrations) in controlling the activity of cellulolytic bacteria in the marine pelagic environment.

Cellulose is a natural and abundant component of coastal marine environments, and previous research in these systems provide a framework for designing studies and interpreting research results. It has been found that rates of mineralization of plant polysaccharides (cellulose and hemicellulose from wood and grasses) range from 0.2 to 2.0% d^{-1} (for particles < 500 μm in diameter under aerobic conditions) in tropical and subtropical coastal marshes and mangrove swamps (Benner et al., 1984; 1985, Benner and Hodson, 1984). Temperature is an extremely important environmental determinant of polysaccharide decomposition rates in these coastal marine systems, with Q_{10} values of 3-4 for a temperature increase from 10 to 20°C (Benner et al., 1986). Furthermore, decomposition kinetics of plant polysaccharides can be complex, and mass loss does not always follow a simple negative exponential (first order) model. Instead, the specific rate of decomposition may continually decrease, so that no single decomposition parameter (k) is appropriate for describing the entire degradation process (Moran et al., 1989a).

The degradation of cellulosic waste materials at sea will be influenced by factors not operating in the shallow coastal systems that have served as the focus for previous studies. First, temperatures in the bulk of the ocean are lower than those in temperate and subtropical coastal systems, and particles spend significant amounts of time at temperatures less than 10°C. Second, particle sinking rate influences the temperature, pressure, and redox conditions experienced by the attached bacterial community. For example, larger particles (> 500 μm diameter) sinking at a rate of 50 to 100 $m \cdot d^{-1}$ are likely to move out of the upper mixed layer in less than one day and reach the sea floor (with 1-2 °C temperatures and ~ 500 atm pressure) in 40 to 80 days. By contrast, smaller particles (< 50 μm in diameter) sinking at rates of approximately 1 $m \cdot d^{-1}$ may stay in the warmer surface waters for several weeks. Third, because the background abundance of cellulolytic organisms is likely to be low in oceanic waters, bacterial community composition may constrain the rate of degradation, at least initially and perhaps overall.

The general mechanism by which organic particles are degraded in seawater is still poorly understood and much debated (Smith et al., 1992). Observations of naturally occurring particles in the ocean surface waters have shown that most particles in the sea are heavily colonized by bacteria (Alldredge and Gotschalk, 1990). However, measurements of bacterial growth rates using radiotracer techniques indicate that the attached bacteria are growing very slowly (Ducklow et al., 1982; Simon et al., 1990). If bacterial growth and respiration were the only sinks of particulate carbon, then such slow rates would suggest that it takes months to years for complete degradation of the particles and, therefore, that much of the particulate material in the upper ocean sinks to the sea floor undegraded. On the other hand, it has recently been hypothesized that attached bacterial communities have intense hydrolytic activities, even though they are not growing rapidly (Smith et al., 1992). According to this hypothesis, the bacteria are solubilizing particles at much faster rates than predicted from growth rates alone and, thus, much of the particulate material is being released as partially degraded soluble material before the particle sinks to the sea floor. If so, the hydrolytic activity of attached bacteria would result in more of the particle being degraded before it reaches the sea floor. This controversy over the decomposition of natural particles is extremely relevant to understanding the fate of cellulosic wastes at sea, particularly with regard to the rate at which the cellulosic particles decompose and the amount of particulate material that survives passage through the water column to be deposited on the sea floor.

In the studies described herein, degradation of cellulosic particles by marine bacterioplankton was studied over a range of environmental conditions typical of various locations and depths in the ocean. Direct measure of particle mass, measures of bacterial production, and measures of bacterial respiration were used to estimate rates and kinetics of bacterial degradation of cellulosic wastes under a number of nutrient and temperature regimes. Studies were also designed to examine the effect of particle size and bacterial community composition (inoculum source) on rates of decomposition. Ancillary studies were also conducted to characterize the chemical composition of the cellulose slurries.

EXPERIMENTAL DESIGN AND RESULTS

Preliminary Studies

Chemical Composition of the Cellulosic Particles. Although the paper slurries contain cellulose as the primary solid constituent, inorganic fillers added to pulped wood during the paper-making process will also be a component of the particulate matrix. Clays, calcium carbonate, and titanium dioxide are among the most commonly used fillers and are usually added to improve the whiteness and the printing properties of the paper. In most paper-making processes, fillers account for 15% or less of the total weight of the finished paper.

White paper and mixed paper slurries were analyzed for inorganic content by filtering slurry subsamples through a Whatman GF/F glass fiber filter, rinsing thoroughly with distilled water, drying at 110°C, and weighing. The filters were then combusted at 550°C for 4 hours to remove all organic materials, and the weight of the remaining inorganic fraction was determined. The elemental composition of the paper slurries (carbon, hydrogen, and nitrogen content) was determined on a Perkin-Elmer 240C CHN analyzer.

Chemical analysis revealed that the white paper and mixed paper particles were 92% organic matter by weight (Table 3.1.2-1). Thus, the biologically non-reactive inorganic fillers used in the paper-making process can only make up a small percentage (<8%) of the particle weight. CHN analysis indicated that nitrogen content of the particles is extremely low (below detectable levels) for the white paper slurry and only 0.02% of the mixed paper by weight (Table 3.1.2-1). The weight ratio of carbon to nitrogen (C:N ratio) is, therefore, >1000, a value far from the optimal C:N ratio for a bacterial substrate (C:N of 15 or

less). These data suggest that inorganic nitrogen availability in seawater may be a critical factor in determining rates of particle degradation in the ocean.

Sugar Analysis of Mixed Paper Slurry. Two replicate samples of mixed paper slurry were analyzed at the University of Georgia Complex Carbohydrate Research Center. The purpose of the analysis was to obtain detailed information about the sugar composition of the paper slurry material. HPLC analysis of acid-treated mixed paper slurry indicated that glucose was the major component of the paper material, making up 80% of the total sugar components. Minor constituents included xylose (14%) and mannose (6%). About half of the mixed paper was insoluble in strong sulfuric acid, however, and thus could not be analyzed for carbohydrate content by standard methods.

In consultation with Dr. Russ Carlson of the Complex Carbohydrate Research Center, we conducted an additional sugar analysis on the mixed paper slurry which involved a stronger hydrolysis step than in the HPLC method described above. In this approach, the paper sample was pretreated with a phenol/concentrated sulfuric acid solution at 100°C for 40 minutes, and then analyzed for total sugar spectrophotometrically based on absorbance at 490 nm (relative to a glucose standard). Although this method destroyed many of the side groups that can be used to identify individual sugar components, it successfully hydrolyzed all of the slurry material so that an accurate measure of total sugar could be obtained. Results of analysis of six replicate samples of mixed paper indicated that sugars accounted for 98±4 % of the paper slurry weight. We previously measured ash content of the slurry to be 6 to 8% of the total dry weight; thus all important components of the slurry have been identified (Table 3.1.2-1).

Table 3.1.2-1. Elemental analysis of white paper and mixed paper slurries.

Sample	Percent C	Percent N	C:N (weight ratio)	Percent Inorganic Matter	Percent Organic Matter	Percent Sugar
White paper	38.5	below detectable levels	NC	3.8	96.2	ND
Mixed Paper	38.2	0.02	1908	8	92	98 ± 4

NC---not calculated ND---not determined

Nutrient-free Seawater. In order to measure decomposition rates as a function of temperature and nutrients, it was necessary to identify a nutrient-free artificial seawater matrix in which to suspend the paper slurry; this would allow careful control of the concentration of nutrients available to bacterial degraders. A commercial artificial seawater source (Sigma Sea Salts, St. Louis, MO) was found to contain ammonium at concentrations > 4 μM and phosphate at concentrations > 2.5 μM. Another artificial seawater made in our laboratory according to the method of Lyman and Flemings (1940) contained even higher inorganic nutrient concentrations, and further testing of stock solutions made from individual salts indicated measurable ammonium present in even high-purity preparations of many sea salt chemicals. The relatively high nutrient levels in coastal seawater also precluded our use of this natural seawater source for low-nutrient experiments.

A low-nutrient artificial seawater source was therefore prepared in our laboratory using chemicals that were baked overnight at temperatures just below their melting point and then dissolved in low-organic deionized water (Harrison et al., 1980). The artificial seawater concentrate (2.5 X) was boiled for 2 hr to drive off any residual ammonium immediately before dilution to standard seawater salinity. With this method, we produced artificial seawater containing only trace levels of inorganic N and P (typically 0.06 μM ammonium and 0.015 μM phosphate).

Decomposition Method Comparisons. Three methods were tested to determine the best approach to measuring bacterial degradation of cellulosic particles: 1) gravimetric, 2) bacterial protein production, 3) bacterial respiration. These methods were tested with two types of cellulose slurry (white paper only and mixed paper/cardboard) to compare relative rates of decomposition.

Gravimetric measurements involved determining the weight of the cellulosic material at the beginning and end of a given decomposition period. Both white and mixed paper slurries were added to Pyrex flasks and suspended in natural seawater freshly collected from the Georgia nearshore at concentrations of 1 mg (dry weight) mL^{-1}. The seawater was amended with 5 μM N (as nitrate and ammonium) and 1 μM P (as PO_4). Flasks were incubated at 28°C while shaking at 200 rpm. All analyses were conducted in triplicate. After a 1 month degradation period, flask contents were filtered through an 8 μm pore-size Nuclepore filter. Filters were washed to remove salt and dried at 60 °C overnight before determination of the weight of the remaining cellulose.

Bacterial protein production measurements track increases in bacterial cell biomass by giving instantaneous measurements of the rate of incorporation of radiolabeled leucine into protein. For these experiments, ^{3}H-leucine was added to the medium in low concentrations; bacteria assimilated this amino acid and incorporated it into the bacterial proteins being synthesized within the cell. Rates of ^{3}H-leucine incorporation were, thus, proportional to rates of growth, and could be converted to carbon equivalents (e.g., amount of bacterial carbon production) by a standard conversion factor that accounts for internal isotope dilution of the leucine and the percent leucine typically found in bacterial protein (Simon and Azam, 1989). To conduct the assay, subsamples (1.7 mL) were removed from incubation flasks at daily-to-weekly intervals and pipetted into 2-mL microcentrifuge tubes. ^{3}H-leucine was added at a final concentration of 20 nM, and cells were allowed to incorporate the leucine for a 1-hour period. After the incubation period, cells were killed and proteins precipitated by the addition of trichloroacetic acid (TCA). Following a series of washes to remove unincorporated ^{3}H-leucine, bacterial cell components were pelleted by centrifugation and radioactivity in bacterial protein was determined by scintillation counting. Typically, three replicate samples and 1 control (killed sample) were analyzed from each flask at each time point.

Bacterial respiration rates were determined by cumulative measures of oxygen consumption. The microbial consumption of oxygen was tracked by measuring oxygen concentration at various intervals during the incubations with automated precision Winkler titrations.

For this method, incubations were set up in replicate 60 mL glass BOD bottles and placed in temperature controlled incubators or water baths. At the beginning of the experiment and at intervals of 2 days to several weeks, five replicate BOD bottles were sacrificed for determination of dissolved oxygen concentration. Oxygen concentrations were measured using an automated precision Winkler method. Oxygen was first chemically fixed in each bottle by the addition of both manganese chloride and sodium hydroxide-sodium iodide solutions. A brown precipitate indicated that oxygen was present and had reacted with the manganous hydroxide, forming manganic basic oxide. Upon the addition of sulfuric acid, this precipitate was dissolved and at the same time, iodine was liberated. The quantity of iodine

was determined by titrating a portion of the solution with a standard solution of sodium thiosulfate using a Mettler DL21 automatic titrator.

Results of the methods comparison. Based on gravimetric measurements, rates of decomposition of mixed paper particles averaged 15.9% (±4.8%) over a 32-day period; based on ^{3}H-leucine incorporation, rates of decomposition averaged 11.2%; based on bacterial respiration, rates of decomposition averaged 11.26%. Assuming that bacterial decomposition of cellulosic particles occurs via first-order kinetics, the measured rates translate into a decay constant, (k), of approximately -0.005 d^{-1}. Thus, the organic matter in mixed paper has a minimum half-life of approximately 140 d (4.3 months) in the ocean under temperature and nutrient conditions similar to those used in this experiment. The half-life would be longer if environmental conditions are suboptimal for some or all of the decomposition period. During the 32-day time period, bacterial numbers varied from 7.8×10^{6} mL^{-1} to 4.0×10^{7} mL^{-1}. These numbers are significantly higher than numbers commonly found in coastal seawater (approximately 2×10^{6} mL^{-1}) and reflect the additional substrate added to the seawater in the form of cellulosic particles. Microscopic examination of the flask contents reveals that most of the bacteria are attached to the particle surfaces, rather than free-living.

Although the gravimetric approach is the most straightforward method for measuring decomposition rates, we found fairly large variations among replicates and low sensitivity. It was difficult to add identical weights to replicate incubations and to completely recover thousands of small particles for weight-loss determination. The measurement of bacterial growth rates via uptake of tritiated leucine was found to be a more sensitive approach, although this measure provides an instantaneous growth rate that has to be interpolated between time points, and it only provides information on cellulose converted to bacterial biomass; mineralization losses must be calculated based on and estimate of the efficiency of bacterial biomass production.

The respiration method was found to be the most appropriate approach for measuring cellulose decomposition in this study. Measurements are cumulative and precision among replicates are good. This method was chosen for the remainder of the decomposition studies using two types of respiration assays: 1) short-term assays (8 days or 30 days in length) to systematically examine factors likely to control the decomposition of cellulose in seawater (particle size, temperature, nutrients, water source); 2) long-term assay (three months) to examine the kinetics of decomposition and determine whether first order degradation is the appropriate model for paper slurry degradation.

Particle Size Studies. The cellulosic particles present in the waste slurries span a fairly large size range (from 30 μm to over 3 mm in diameter) and, upon release into the ocean, will sort in the water column based on size and sinking rate. Because bacterial decomposition of particles in the ocean is primarily a surface phenomenon, it is possible that large differences in the surface-to-volume ratio among the particles results in differences in specific decomposition rates. Thus, smaller particles with larger surface-to-volume ratios might degrade more rapidly, and have a larger decay constant, than larger particles with smaller surface-to-volume ratios.

Mixed paper slurry was size-fractionated into five size categories by resuspension in distilled water and sequential filtration through a series of sieves and polyethylene mesh screens with 2 mm, 1 mm, 500 μm and 150 μm openings. Particles caught on the 2-mm sieve were repeatedly resuspended and re-filtered to ensure that smaller particles were not attached to larger ones and that the sieve openings were not being occluded. Final size classes were as follows: >2000 μm, <2000 but >1000 μm, <1000 but >500 μm, and <500 but >149 μm.

Size fractionation of the mixed paper slurry into five categories showed that most of the particles did not pass the largest size sieve. We found that 97.8% of the particles (by weight) were retained on the 2 mm mesh. The 1-2 mm category contained 1.4% of the particle weight; the 500 μm to1 mm category contained 2.3% of the weight; the 150 to 500 μm category contained 1.1% of the weight; and the <150 μm category contained 0.4% of the weight.

To measure the effect of the size of cellulose particles on rates of decomposition of mixed paper wastes, bacterial respiration rates were measured individually for each of the particle size categories. Treatments were set up such that all size categories contained the same initial weight of mixed paper (0.1 mg cellulose·mL^{-1}) and five replicates of each size class were established. To measure decomposition, microbial consumption of oxygen was followed over an 8-day period.

Results of the first experiment showed no statistical differences (ANOVA; P=0.29; Fisher LSD) among size classes. Assuming first-order kinetics, rates were consistent with degradation of 12.4% of the cellulose in 30 days. In a second experiment, we included an additional treatment which contained the full range of particle sizes (i.e., unaltered mixed paper slurry). Again, there were no differences among the size classes or between the size classes and the unsized treatment (Figure 3.1.2-1) (ANOVA; P=0.35; Fisher LSD). Rates of respiration indicated a decomposition rate of 9.4% in 30 days, assuming first-order kinetics. Although accurate sizing of the particles was difficult (many particles are linear, so the angle at which they hit the screen has a significant effect on whether or not they pass through; screens clogged easily for the larger size classes), these experiments indicate that particle size is not a critical factor in determining decomposition rate. This is possibly due to the highly linear shape of most of the particles, which increases the effective surface area: volume ratio for all size classes, or to the ability of bacteria to access and colonize individual cellulose fibers within the particle matrix, regardless of its overall size.

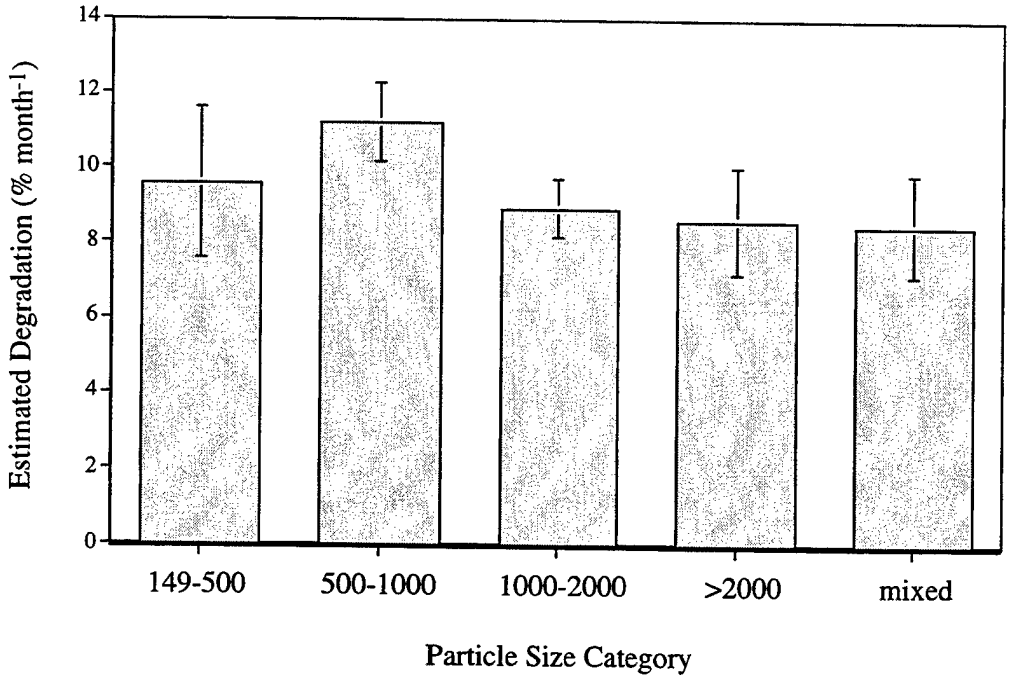

Figure 3.1.2-1. Results of particle size study #2. Bacterial respiration rates were measured for four different size classes of mixed paper particles and for unfractionated mixed paper slurry over an 8-day period.

Long-Term Decomposition Kinetics. A study was conducted to examine the kinetics of mixed paper slurry decomposition over a 3-month time frame to determine whether the first order kinetics apparent in shorter studies (8 days to 1 month) could be extrapolated to long-term degradation. Decomposition of the paper slurries was carried out in coastal Georgia seawater at 28°C with unlimited inorganic nutrient supply (starting concentrations of 100 μM N and 20 μM P). At intervals of 1 to 2 weeks, decomposition of the cellulose was determined from cumulative changes in oxygen concentrations in gas-tight incubation bottles (BOD bottles). After 11 weeks of decomposition, 30.7% of the paper slurry had been decomposed. The experiment was terminated at this point because oxygen concentrations inside the BOD bottles had dropped from 206 to 64 μM and there was concern that low oxygen availability might begin to affect decomposition rates.

Kinetics of decomposition generally followed a simple first-order decay model where k is the first-order decomposition constant and equals -0.0048 d^{-1}. The r^2 value for a natural log plot of the data fit with a linear model is 0.982. The equation predicts 50% decomposition of paper slurry in 145 days (21 weeks) and 90% decomposition in 480 days (69 weeks) when decomposition occurs in warm coastal seawater without nutrient limitation (Figure 3.1.2-2).

Effects of Bacterial Community Source on Decomposition Rates. Laboratory studies were conducted to explore inherent differences in bacterial communities from different marine environments to degrade the cellulose slurries. Degradation rates were determined by bacterial respiration (oxygen consumption) in 8-day bioassays. Seawater was collected in polyethylene carboys from a number of coastal and oceanic sites at a variety of depths (from surface to 3522 m). The water was shipped to our laboratory under refrigeration and used in decomposition studies within 2 days. Rates of cellulose decomposition were measured both with and without supplements of inorganic nutrients (ammonium and phosphate) to control for possible nutrient limitations on bacterial activity. For all samples, degradation rates were measured at 28°C to control for temperature effects on bacterial activity; for some samples, degradation rates were also measured at the ambient temperature at the time of collection.

Samples were collected from three oceanic sites in tropical, temperate, and arctic regions (Eastern Northern Pacific, Sargasso Sea, Bering Strait, and Chukchi Sea); from a continental shelf site in a temperate region (Southeastern U.S. shelf); and from a nearshore coastal site in a temperate region (Georgia coastal) (Table 3.1.2-2).

Results showed that cellulose was degraded slowly in all oceanic water samples (average = 0.85% in 30 d at 28°C) (Figure 3.1.2-3 and Table 3.1.2-3), with rates approximately 10-fold lower than those measured for the southeastern US shelf (8.21% in 30 days at 28°C) or coastal Georgia seawater (10.7% in 30 days at 28°C). Differences between oceanic samples and either the shelf or coastal samples were statistically significant (ANOVA; $P<0.001$; Fisher's LSD). These differences occurred despite the fact that temperature, cellulose slurry concentration, and nutrient availability were identical in all experiments. The low rates of degradation measured for oceanic water may be due to an absence of cellulolytic bacteria in the open ocean. Alternatively, it may be due to injury to bacteria when brought to 1 atmosphere pressure (for deep water samples), or to injury to or inactivity of bacteria when brought from low temperatures to 28°C.

We examined the possibility that the standard temperature chosen for these experiments (28°C) adversely affected rates of decomposition measured in oceanic samples, in which bacterial populations may be adapted to significantly lower ambient temperatures. In these decomposition experiments, water samples from the Chukchi Sea (Arctic 28 m) and Bering Strait (Arctic 5 m) were incubated at temperatures similar to the temperature of the seawater at the time of collection (4°C) during 8-day bioassays. Rates of

decomposition were determined to be 0.88% and 0.50% in 30 days, respectively, values which are not significantly different from those measured for these same samples at the higher temperature (0.46% and 0.46% at 28 °C, respectively) (T-tests; P=0.68 and P=0.58).

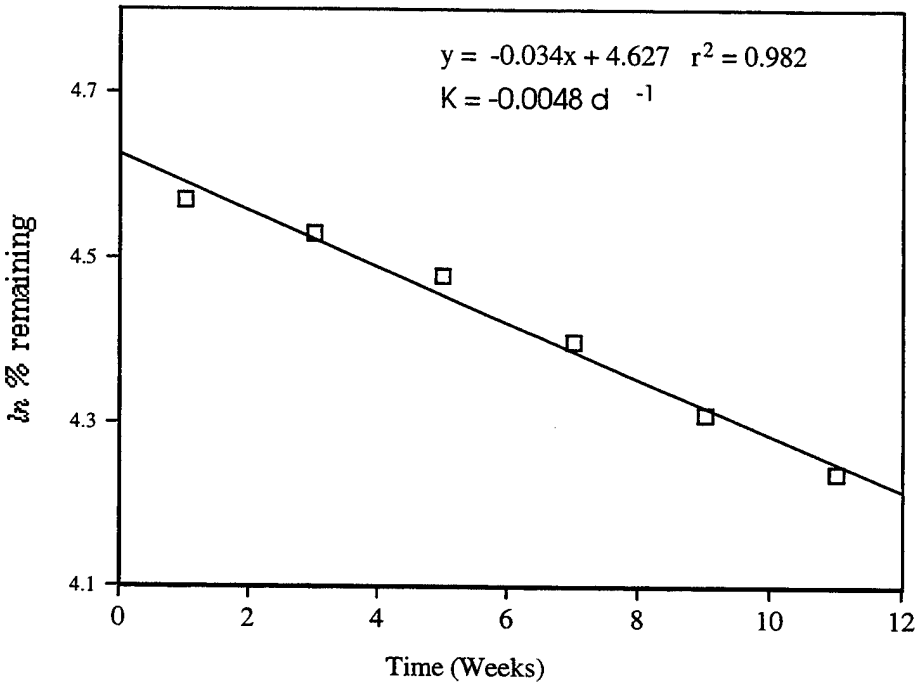

Figure 3.1.2-2. Results of long-term decomposition experiment. Cellulose decomposition was measured as changes in oxygen content in BOD bottles containing 0.01 mg mL^{-1} mixed paper slurry.

We also considered the possibility that injury to bacteria due to changes in pressure (when deep water samples were brought to the surface) adversely affected measured rates of cellulose decomposition for oceanic samples. Surface water samples from the Chukchi Sea (Arctic 28 m) and Bering Strait (Arctic 5 m) contained bacterial populations that were adapted to both cold temperatures (typical of deep ocean water) and surface pressures. Thus the bacteria in these water samples experienced no stress with regard to either temperature or pressure during cellulose decomposition experiments conducted at lower temperatures. Rates of cellulose slurry decomposition for these samples were 1.24% and 0.50% (in 30 days at 4 °C), which are similar to rates measured for deep water samples. For two samples collected at the same site (Chukchi sea), we found no statistical difference between rates in surface and deep water (T-test, P=0.75). Thus, low rates of degradation of cellulose by oceanic bacterial communities appear to be related to inherent differences in the community structure with regard to the ability to utilize cellulosic material, at least during the initial stages of decomposition, and not to effects of manipulating the temperature or pressure of the samples.

We found no effect on decomposition rates in these studies when inorganic N and P were added to seawater (5 μM NH_4^+ and 1 μM PO_4) for either surface or deep seawater. The lack of a nutrient effect likely results from sufficient N and P levels in the original seawater; for example, nitrate levels in the Eastern Tropical Pacific were 42 μM.

Table 3.1.2-2. Water samples collected for bacterial community source studies.

Site	Collection Date	Collection Temp (°C)	Collection Depth (meters)
Arctic (Chukchi Sea)	July, 1996	-1.5	28
Arctic (Chukchi Sea)	July, 1996	-0.3	3522
Arctic (Bering Strait)	July, 1996	0.9	5
Sargasso Sea #1	February, 1996	ND	surface
Sargasso Sea #1	February, 1996	ND	750
Sargasso Sea #2	May, 1996	7.5	1000
Northern Pacific Ocean	August, 1995	ND	1500
U.S. Shelf	April, 1996	17	surface
Coastal Georgia	May, 1995	18	surface

ND--Not determined.

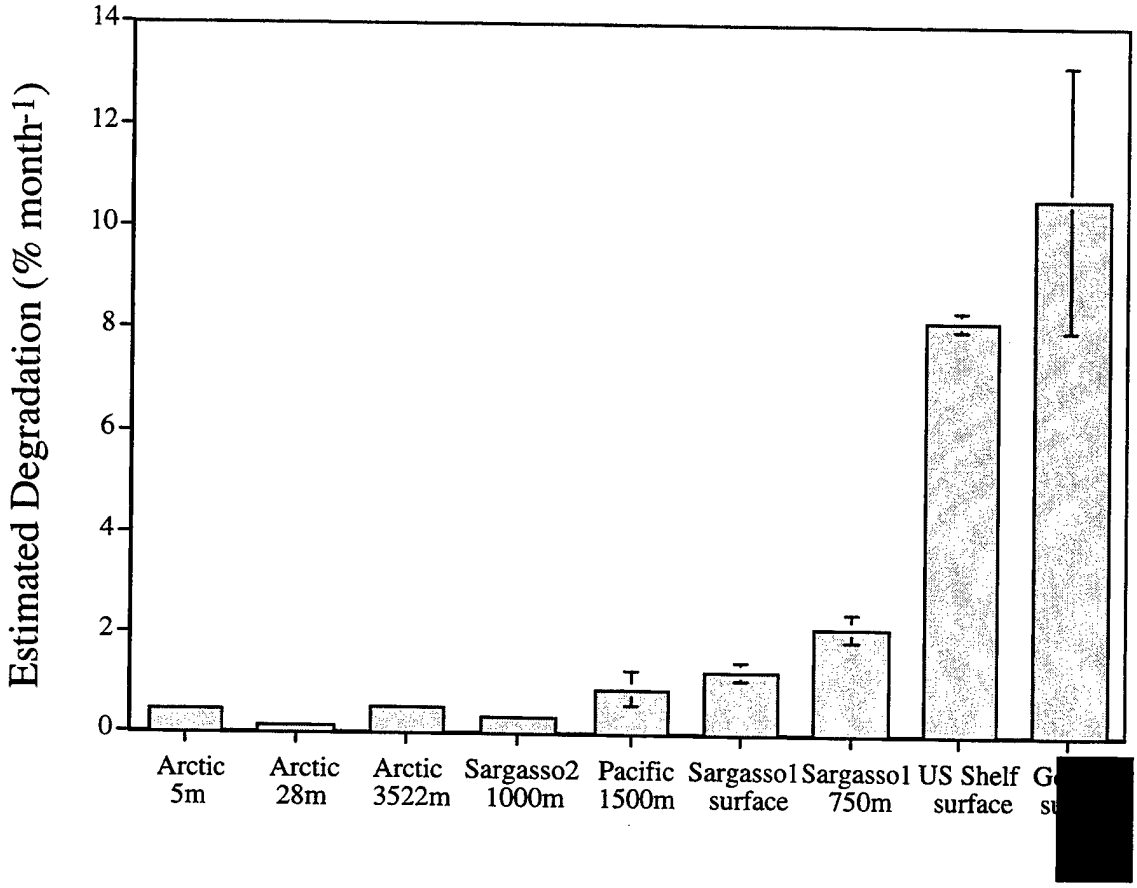

Figure 3.1.2-3. Rates of degradation of mixed paper cellulose slurry by bacterial populations from oceanic and coastal sites. Degradation was determined by measuring oxygen consumption in 8-day bioassays at 28°C; 5 mM N and 1 mM P were added to the seawater prior to incubation.

Table 3.1.2-3. Rates of degradation of mixed paper slurry by bacterial populations from oceanic and coastal sites. A "-" in the nutrient addition column indicates that inorganic nutrients were not added to the seawater; a "+" indicates the addition of 5 mM N and 1 mM P prior to incubation.

Site	Temperature (°C)	Nutrient Addition	% Decomposition (30 d)	k
Pacific 1500 m	28	-	1.38 ± 0.67	-0.00046
	28	+	0.88 ± 0.36	-0.00030
Sargasso #1, surface	28	-	1.72 ± 0.24	-0.00058
	28	+	1.25 ± 0.19	-0.00042
Sargasso #1, 750 m	28	-	1.58 ± 0.34	-0.00053
	28	+	2.12 ± 0.27	-0.00072
Sargasso #2, 1000 m	7.5	-	0.25 ± 0.09	-0.00008
	7.5	+	0.62 ± 0.25	-0.00021
	28	-	0.44 ± 0.18	-0.00015
	28	+	0.29 ± 0.11	-0.00010
Arctic, 5 m	4	-	0.49 ± 0.21	-0.00016
	4	+	0.50 ± 0.15	-0.00017
	28	-	0.50 ± 0.06	-0.00017
	28	+	0.46 ± 0.21	-0.00015
Arctic 28 m	4	-	1.24 ± 0.42	-0.00042
	4	+	0.88 ± 0.13	-0.00029
	28	-	0.24 ± 0.06	-0.00008
	28	+	0.11 ± 0.04	-0.00004
Arctic, 3522 m	4	-	0.49 ± 0.02	-0.00016
	4	+	0.56 ± 0.18	-0.00019
	28	-	0.54 ± 0.26	-0.00018
	28	+	0.50 ± 0.08	-0.00017
SE Continental Shelf	17	-	0.28 ± 0.16	-0.00009
	17	+	2.58 ± 0.33	-0.00087
	28	-	0.70 ± 0.38	-0.00023
	28	+	8.21 ± 0.2	-0.00286
Georgia Coastal	28	+	10.63 ± 2.6	-0.00375

Temperature and Nutrient Matrix Studies. Decay rates of cellulose particles were determined under the temperature and nutrient conditions representative of "special area" sites which were chosen by SSC SD as the focus of their modeling efforts. Conditions for these studies were based on seasonal variations and vertical profiles from the Baltic Sea, the Mediterranean Sea, and the Caribbean Sea. Chosen temperatures for these studies spanned a range of 4°C to 28°C, inorganic nitrogen concentrations ranged from 0 (trace levels) to 5 μM, and inorganic phosphorus concentrations from 0 (trace levels) to 1 μM.

The bacterial inoculum for all the experiments in this matrix was identical to eliminate any potential effects of differences in composition of the bacterial community among experiments. The inoculum was prepared by incubating 1.0 μm-filtered coastal seawater overnight in the laboratory to allow growth of the natural bacterial community in the absence of any protozoan grazers or metazoans. After incubation, the inoculum was divided up into a number of aliquots for long-term storage. Each seawater aliquot (800 μL) was mixed with glycerol (200 μL) in 1.5 mL plastic cryogenic vials and stored at -70°C. To obtain a fresh bacterial inoculum for each experiment, an aliquot was thawed, inoculated into fresh seawater, and allowed to grow for 48 hr. Bacterial cells were then harvested by centrifugation at 14,000 rpm for 20 minutes, resuspended in low-nutrient artificial seawater and used to inoculate each experiment.

Low-nutrient artificial seawater was made according to the procedures described above and inoculated with 0.8 mL of the standard bacterial inoculum. Cellulosic particles from mixed paper waste were added to the seawater to a final concentration of 0.001 mg mL^{-1}. Nutrient-free seawater/cellulose slurries were amended with inorganic nutrients to establish the following treatments: 5 μM N and 1 μM P; 3.75 μM N and 0.75 μM P; 2.5 μM N and 0.5 μM P; 1.25 μM N and 0.25 μM P; 0.064 μM N and 0.015 μM P (trace levels in the seawater preparation). Seawater of each nutrient concentration was dispensed into 60 mL glass BOD bottles; 30 replicate BOD bottles were set up for each nutrient treatment. Dissolved oxygen concentrations were measured by precision Winkler titrations in three replicate bottles at days 0, 3, 7, and then weekly for 3 additional weeks. In all cases, a "minus cellulose" control treatment was established in which paper slurry was not added; oxygen consumption in this treatment represented bacterial respiration at the expense of dissolved organic matter in the coastal seawater, and not at the expense of cellulose. Oxygen consumption in the treatments with cellulose were corrected for the consumption in the control treatments for final calculations of decomposition rate. Experiments were run at 28°C, 18°C, 8°C, and 4°C.

Rates of cellulose degradation for the temperature/nutrient matrix studies are shown in Tables 3.1.2-4 and 3.1.2-5. Temperature had a significant effect on rates of paper slurry degradation and is likely to be an important control on the rate at which paper is degraded in seawater. Rates of degradation at 28°C were approximately 10-fold those measured at 4°C. Inorganic nutrient concentrations were much less important in determining rates at which cellulose slurries degraded in seawater at most temperatures, and we observed little or no effect of 100-fold variations in N and P concentrations on decomposition rates at any temperature.

Table 3.1.2-4. Results of temperature/nutrient matrix studies presented as percent decomposition of paper slurry in 30 d. High = 5 mM N and 1 mM P; Medium High = 3.75 mM N and 0.75 mM P; Medium = 2.5 mM N and 0.5 mM P; Medium Low = 1.25 mM N and 0.25 mM P; and Low = 0.064 mM N and 0.015 mM P.

Temperature	High	Medium High	Medium	Medium Low	Low
28°C	11.13	11.19	11.71	10.99	11.22
18°C	5.55	5.87	6.04	5.56	5.20
8°C	3.52	3.25	3.09	3.83	3.03
4°C	1.32	0.53	1.00	1.59	1.13

Table 3.1.2-5. Results of temperature/nutrient matrix studies presented as the decomposition constant (k) assuming first order degradation kinetics. Nutrient treatments are as described in Table 3.1.2-4.

Temperature	High	Medium High	Medium	Medium Low	Low
28°C	-0.00393	-0.00396	-0.00415	-0.00388	-0.00397
18°C	-0.00190	-0.00202	-0.00208	-0.00191	-0.00178
8°C	-0.00120	-0.00110	-0.00105	-0.00130	-0.00103
4°C	-0.00045	-0.00018	-0.00033	-0.00053	-0.00038

For some experiments, seawater/cellulose slurries were incubated in 15-L aluminized mylar bags (with polyethylene inner coating) instead of BOD bottles to determine the effect of vessel type on measured decomposition rates. These gas-tight bags allowed measurement of decomposition via bacterial oxygen consumption, and sequential sampling from the same bag further increased sensitivity by providing cumulative measures of oxygen consumption. For these experiments, three BOD bottles were filled via a Tygon tube from the polyethylene bag just prior to dissolved oxygen measurements.

Rates of cellulose decomposition were similar in polyethylene bags compared to BOD bottles. At 28°C with high nutrient levels (5 μM N and 1 μM P), 9.58% of the paper slurry in the polyethylene bags was degraded after 30 days. By contrast, 10.39% and 11.93% of the paper in the BOD bottles was degraded in two separate experiments. Similarly, at 28°C with low nutrient levels (0.064 μM N and 0.01 μM P), rates of degradation were 3.89% in the bags and 4.46% in the bottles. Although there was a statistically significant difference between bags and bottles at high nutrient levels (P=0.05) [there was no difference at low nutrient levels (P=0.051)], the magnitude of the difference was low and we conclude that rates of degradation in the two types of incubation vessels are similar (Figure 3.1.2-4).

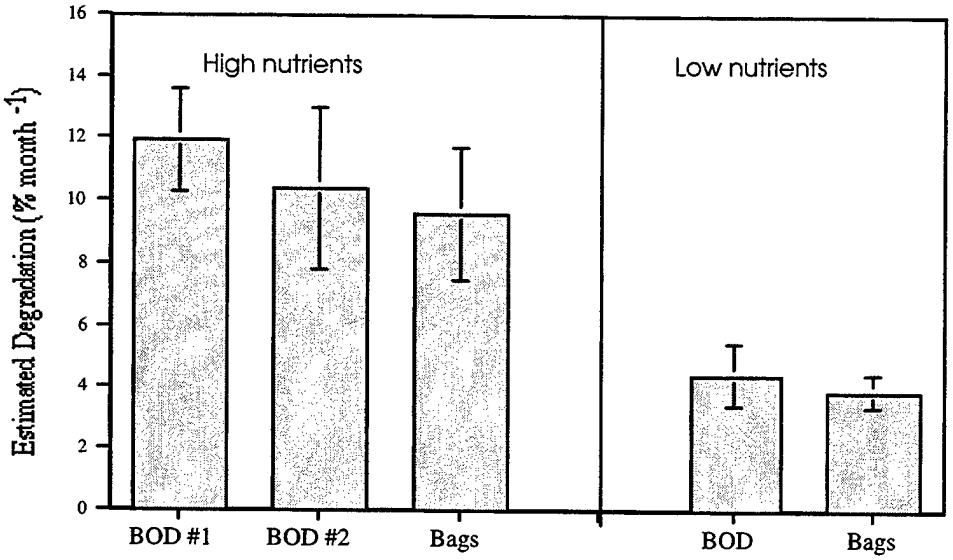

Figure 3.1.2-4. Comparison of degradation rates in two types of incubation systems: glass BOD bottles and 15-liter polyethylene/mylar bags.

CONCLUSIONS

1) Decomposition of mixed paper slurries in seawater follows first-order degradation kinetics. Decay constants (k) range from -0.004 d^{-1} at 28°C to -0.0004 $^{-1}$ at 4°C. These correspond to half-lives of 173 and 1733 days, respectively.

2) Q_{10} values for cellulose decomposition average 1.85 for temperatures between 8°C and 28°C. Between 4 °C and 8 °C, rates increase much more rapidly for a given rise in temperature.

3) Inorganic nutrient concentrations do not appear to significantly affect decomposition rates of paper slurries. Bacterial degradation is generally limited by temperature rather than nutrient availability over a range of nutrient concentrations representative of coastal and open ocean water.

4) Decomposition rates are not affected by the size of the paper particles; particles ranging from > 2 mm to < 500 µm are degraded at similar rates.

5) Bacterial communities from coastal seawater degrade cellulose more rapidly than communities from open ocean seawater in short-term (8 days) studies. Rates of decomposition under identical conditions differ by about 10-fold.

REFERENCES

Alldredge, A. L., and C. C. Gotshalk. 1990. *Bacterial Carbon Dynamics On Marine Snow.* Cont. Shelf Res. 10: 41-58.

Amann, R. I., B. J. Binder, R. J. Olson, S. W. Chisolm, R. Devereux, and D. A. Stahl. 1990. *Combination Of 16S Rrna-Targeted Oligonucleotide Probes With Flow Cytometry For Analyzing Mixed Microbial Populations.* Appl. Environ. Microbiol. 56:1919-1925.

Benner, R, A. E. Maccubbin, and R. E. Hodson. 1986. *Temporal Relationship Between The Deposition And Microbial Degradation Of Lignocellulosic Detritus In A Georgia Salt Marsh And The Okefenokee Swamp.* Microb. Ecol. 12:291-298.

Benner, R., S. Y. Newell, A. E. Maccubbin, and R. E. Hodson. 1984. *Relative Contributions Of Bacteria And Fungi To Rates Of Degradation Of Lignocellulosic Detritus In Salt Marsh Sediments.* Applied and Environmental Microbiology 48:36-40.

Benner, R., and R. E. Hodson. 1985. *Microbial Degradation Of The Leachable And Lignocellulosic Components Of Leaves And Wood From Rhizophora Mangle In A Tropical Mangrove Swamp.* Marine Ecology Progress Series 23:221-230.

Benner, R., M. A. Moran, and R. E. Hodson. 1985. *Effects Of pH And Plant Source On Lignocellulose Biodegradation Rates In Two Wetland Ecosystems, The Okefenokee Swamp And A Georgia salt marsh.* Limnol. Oceanogr. 30:489-499.

Chróst, R. J., and H. Rai. 1993. *Ectoenzyme Activity And Bacterial Secondary Production In Nutrient-Impoverished And Nutrient-Enriched Freshwater Mesocosms.* Microbial Ecology 25:131-150.

Ducklow, H. W., D. L. Kirchman, and G. T. Rowe. 1982. *Production And Vertical Flux Of Attached Bacteria In The New York Bight As Studied With Floating Sediment Traps.* Appl. Environ. Microbiol. 43:769-776.

Harrison, P.J., R. E. Waters and F. J. R. Taylor. 1980. *A Broad Spectrum Artificial Seawater Medium For Coastal And Open Ocean Phytoplankton.* J. Phycol. 16:28-35.

Lyman and Fleming, 1940.

Moran, M. A., R. Benner, and R. E. Hodson. 1989a. *Kinetics Of Microbial Degradation Of Vascular Plant Material In Two Wetland Ecosystems.* Oecologia 79:158-167.

Moran, M. A., and R. E. Hodson. 1989b. *Formation And Bacterial Utilization Of Dissolved Organic Carbon Derived From Detrital Lignocellulose.* Limnol. Oceanogr. 34:1034-1047.

Moran, M. A., R. J. Wicks, and R. E. Hodson. 1991. *Export Of Dissolved Organic Matter From A Mangrove Swamp Ecosystem: Evidence From Natural Fluorescence, Dissolved Lignin Phenols, And Bacterial Secondary Production.* Mar. Ecol. Prog. Ser. 76:175-184.

Moran, M. A., and R. E. Hodson. 1992. *Contributions Of Three Subsystems Of A Freshwater Marsh To Total Bacterial Secondary Productivity.* Microb. Ecol. 24:161-170.

Moran, M. A., and R. E. Hodson. 1994. *Dissolved Humic Substances Of Vascular Plant Origin In A Coastal Marine Environment.* Limnol Oceanogr., In press.

Pomeroy, L. R., J. E. Sheldon, and W. M. Sheldon. 1994. *Changes In Bacterial Numbers And Leucine Assimilation During Estimations Of Microbial Respiratory Rates In Seawater By The Precision Winkler Method.* Applied and Environmental Microbiology 60:328-332.

Simon, M., A. L. Alldredge, and F. Azam. 1990. Mar. Ecol. Prog. Ser. 65:205-211.

Smith, D. C., M. Simon, A. L. Alldredge, and F. Azam. 1992. *Intense Hydrolytic Enzyme Activity On Marine Aggregates And Implications For Rapid Particle Dissolution.* Nature 359:139-142.

3.2 CHEMICAL ANALYSIS OF INORGANIC PULPER MATERIAL

by Wayne Glad

The Code D662 materials laboratory received from Code D362 samples of a pulped paper material for the determination of major inorganic constituents. In order to get a qualitative understanding of the elements that were present in the pulp, a small sample was washed by a brief immersion in de-ionized water, placed in a quartz crucible and heated in a burner flame to destroy the organic constituents. Some of the powder that remained was placed with double stick tape on a Scanning Electron Microscope (SEM) stub and given a thin coating of gold. The sample was examined in the SEM, yielding the x-ray spectrum shown in Figure 3.2-1.

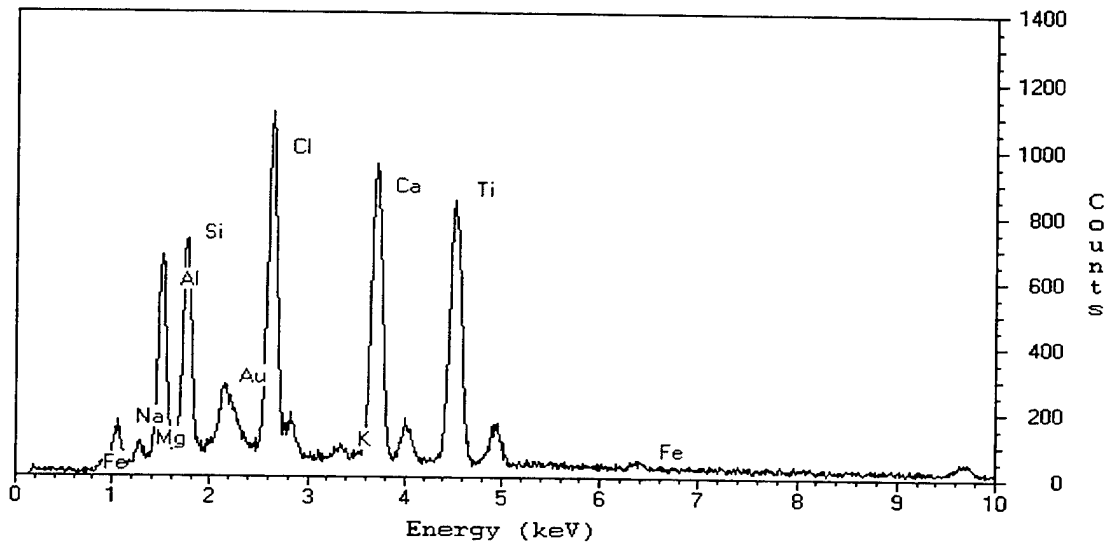

Figure 3.2-1. Pulped paper x-ray spectrum before extensive washing.

The major elements found were calcium, chlorine, titanium, silicon and aluminum. Somewhat smaller amounts of sodium, magnesium, potassium and iron were present. There may also be some sulfur present (as a shoulder on the right side of the gold signal from the coating). Most of these elements are filler materials in paper. Chlorine may be present as a remnant of the paper bleaching process.

To prepare samples for quantitative analysis using Inductively Coupled Plasma atomic emission spectroscopy (ICP) some pulp was washed extensively by placing the pulp in a büchner funnel and repeatedly adding de-ionized water and draining it through the pulp. The washed pulp was then dried overnight at 100 °C. Some of this dried, washed pulp was also heated in a burner flame and examined in the SEM. The x-ray spectrum from this sample is shown in Figure 3.2-2. The spectrum shows that the sodium and chlorine that were present in the lightly washed sample had been removed by the more extensive washing. The titanium, aluminum, silicon, and calcium appeared to remain in about the same relative concentrations.

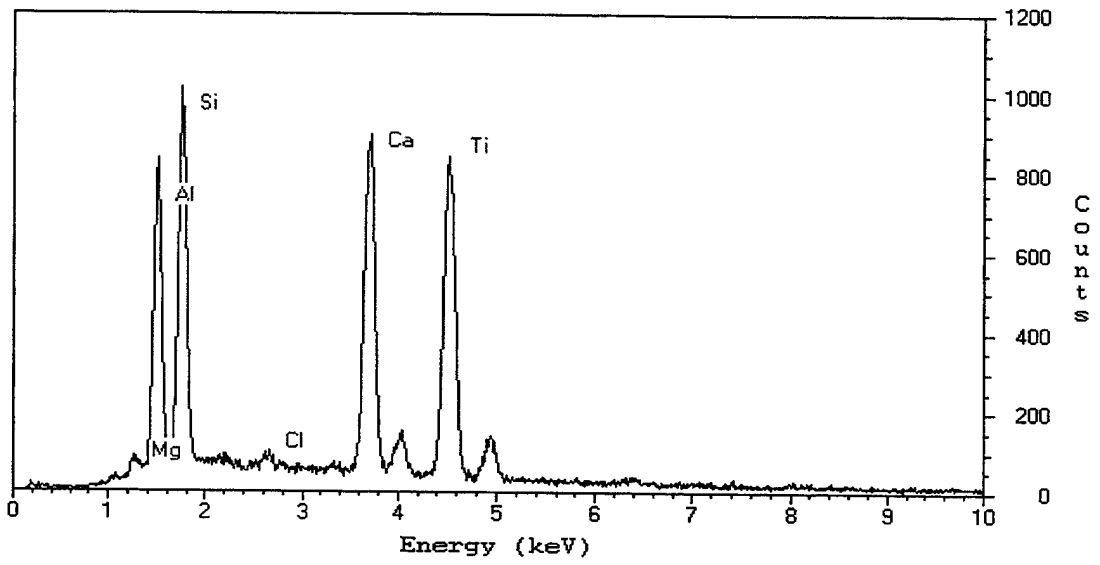

Figure 3.2-2. Pulped paper x-ray spectrum after washing.

Three dried pulp samples of about 0.25 gram were weighed into flasks and digested using concentrated sulfuric acid and nitric acid. The procedure involved heating the samples to fumes in sulfuric acid and then adding nitric acid drop-wise until the remaining liquid was clear. The samples appeared to digest completely. The samples were diluted to 100.0 mL and analyzed using ICP within 30 min of dissolution. The results of the analysis are shown in Table 3.2-1.

As was expected from the x-ray spectrum, the major inorganic components are calcium, titanium, aluminum and silicon. The concentrations of these major elements were consistent among the samples. Taking calcium as calcium carbonate, and the other major elements as their common oxides, these four major elements account for 5.7% of the total weight of the sample, which is near the 6-8% ash that was found by other investigators. Note that this may not represent complete recovery of all elements, since one would not expect complete solubility of titanium, aluminum and silicon oxides in the dilute acid solution produced by the final dilution. However, the recovery in these situations is often surprisingly good because the initial precipitation is of very small particles that are swept into and analyzed in the ICP as if they were in solution.

Table 3.2-1: ICP results (in weight percentage) of dried pulp

Sample	Ca	Mg	K	Fe	Si	Al	Ti	Na
1	0.91	0.064	0.028	0.083	0.34	0.58	0.88	0.16
2	1.00	0.060	0.00	0.07	0.34	0.58	0.88	0.10
3	0.97	0.070	0.00	0.05	0.34	0.54	0.90	0.19
Average	**0.96**	**0.065**	**0.009**	**0.068**	**0.34**	**0.57**	**0.89**	**0.15**

3.3 OCEAN BOTTOM TRANSPORT OF SHREDDED CANS: LABORATORY STUDY

by Dr. James Rohr, Dan Ladd, and Jeff Allen

SUMMARY

In order to estimate flow speeds necessary to initiate transport of shredded cans lying on the ocean bottom, a laboratory study was conducted to determine the laminar velocity profile, associated with their initial transport on a smooth, flat surface. From the laminar velocity profile the integrated stagnation pressure over the height of the sample can be determined. Although turbulent velocity profiles are anticipated at the ocean bottom, it is assumed that the stagnation pressures associated with initial motion will be similar. This approach should provide conservative estimates of threshold velocity because while the roughness effects the velocity profile, it does not increase bottom friction. Given the integrated stagnation pressure and assumed shape of the velocity profile, velocities 1meter above the ocean bed can be calculated. These velocities are compared with ocean-bottom velocity measurements reported in the literature in order to assess the likelihood of ocean-bottom trash transport. Several candidate turbulent profiles, each for a range of bottom roughness, are examined. Generally, the ocean-bottom flows calculated were subcritical for transporting bottom trash (i.e., shredded cans).

OVERVIEW

Five water tunnel tests were performed to estimate the hydrodynamic force initiating movement of shredded can samples. The samples were placed in laminar flow on a smooth, flat plate. The free stream velocity was slowly increased until motion was observed (see accompanying photograph). The corresponding Blasius velocity profile $u_B(x, y)$ were used to calculate the stagnation pressure $(^1/_2)\rho u_B^2$ at the leading edge of the sample. Integrating the stagnation pressure over the height of the sample provided an estimate of the hydrodynamic force per unit width. The integrated stagnation pressures from each laboratory experiment were then used to determine turbulent velocity profiles (more representative of oceanic bottom flows) which provided equivalent integrated stagnation pressures. Three candidate forms for the turbulent profile were chosen from the literature. Each was employed over a range of ocean bottom roughness heights. The mean velocity 100 cm from the ocean bottom, U_{100}, was calculated for each case. Oceanic estimates of U_{100}, derived from the water tunnel experiments, ranged from about $0.5 - 2.3$ m·s^{-1}. Values of U_{100} measured in the ocean generally vary between from about $0.01 - 1.0$ m·s^{-1}, with lower values reported more frequently. However, geological evidence and scattered observations do indicate that flows significantly exceeding critical transport speed occur intermittently. Analysis accounting for transport due to these atypical flows exceeds the scope of this effort.

The present analysis did not take into account lift, torque, bottom friction, sediment suspension, ripples or scouring effects. Scouring is thought to be the most important effect neglected as it would tend to bury the samples. Because scouring and bottom friction is neglected, the present analysis is thought to provide conservative estimates of U_{100}.

LABORATORY EXPERIMENTS

The experimental flow field chosen was a laminar boundary layer over a smooth, flat plate because it is well characterized (Blasius, 1908; Schlicting, 1979) and amenable with the full-scale samples we wished to test. A large processed tin can was obtained from a Navy shredder. It was 83.5 g and about 22.6 cm long, 13.3 cm wide and 6.35 cm at its highest point (henceforth referred to as H). This can, after being tested for two different orientations (Exps. #1 and #2; see Table 3.3-1), was cut into three smaller pieces (57.5, 21.3 and 3.9 gms) and tested again (Exps. #3, #4, and #5; see Table 3.3-1).

Table 3.3-1: Summary of water tunnel experiments

Experiment	Date	Mass (gms)	Location of Sample (cm)	Height of Sample (cm)	U_∞ ($cm \cdot s^{-1}$)
Exp. #1	9/11/95	83.5	24.3	6.35	50
Exp. #2	9/12/95	83.5	28.6	6.35	33.4
Exp. #3	9/13/95	57.5	28.6	6.35	34.4
Exp. #4	9/13/95	21.3	28.6	4.76	34.4
Exp. #5	9/13/95	3.9	28.6	3.49	32.5

The flat-plate experiments with the shredded can samples were tested in the NCCOSC high-speed recirculating water tunnel (see Figure 3.3-1) previously described by Ladd and Hendricks (1985). The facility has a 0.305-m diameter horizontal open jet test section which is 1 m long. Water velocities up to 14 $m \cdot s^{-1}$ are achieved with exceptionally low free-stream turbulence levels of 0.16% or less. A butterfly valve in the flow circuit was used to throttle the flow and achieve low speed velocities of $0.1 - 1.0$ $m \cdot s^{-1}$. The plate (see Figure 3.3-2) was smooth, flat, 53.41 cm long and mounted in a horizontal position along the jet centerline. The first 25.4 cm of the plate was supported by horizontal slots in a thick-walled acrylic pipe, with an inside diameter of 29.8 cm, which extends the origin of the open jet 29.0 cm into the test section.

An initial calibration of free-stream velocity above the flat plate boundary layer, U_∞, *vs* tunnel pump rpm was obtained using a TSI Laser Doppler Velocimeter mounted on a three-dimensional traverse with numerically controlled positioning. In subsequent experiments, U_∞ was inferred from the pump rpm. The entire velocity profile at a given location x downstream of the plate's leading edge was directly calculated assuming a Blasius profile. Transition from laminar to turbulent flow on a flat plate, while depending on the upstream turbulence, generally ranges from Reynolds numbers $3 \cdot 10^5$ to $3 \cdot 10^6$ (Schlicting, 1979). Here the Reynolds number Re is defined as $U_\infty x/\nu$, where ν is the kinematic viscosity of water. The maximum Reynolds number found necessary to initiate motion for the samples tested was less than $1.5 \cdot 10^5$, thereby ensuring laminar flow upstream of the samples.

By increasing the jet flow while recording the position of the samples, the impinging Blasius velocity profile $u_B(x, y)$ corresponding to the onset of motion could be determined. In incompressible flow the dynamic pressure, $(^1/_2)\rho u_B^2$ is equal to the stagnation pressure. Integrating the stagnation pressure for the Blasius profile over the height of the sample, provided an initial estimate of the critical hydrodynamic force per unit width required to initiate transport. (Better estimates must further consider the effect of lift, torque, bottom friction, sediment suspension, ripples and scouring effects.) Generally, the experiments show (see Table 3.3-1) that the critical free-stream velocity U_∞ for motion to commence did not show a strong dependence on the weight of the sample. This is consistent with the two-dimensional quality of the shredded can. Both the weight and the frontal area increased approximately proportional to

the square of the length and, therefore, nearly balanced each other (bigger pieces weighed more, but also had greater frontal area for stagnation pressure to act). The range of U_∞ for the water tunnel experiments was between 0.3 $m \cdot s^{-1}$ and 0.5 $m \cdot s^{-1}$.

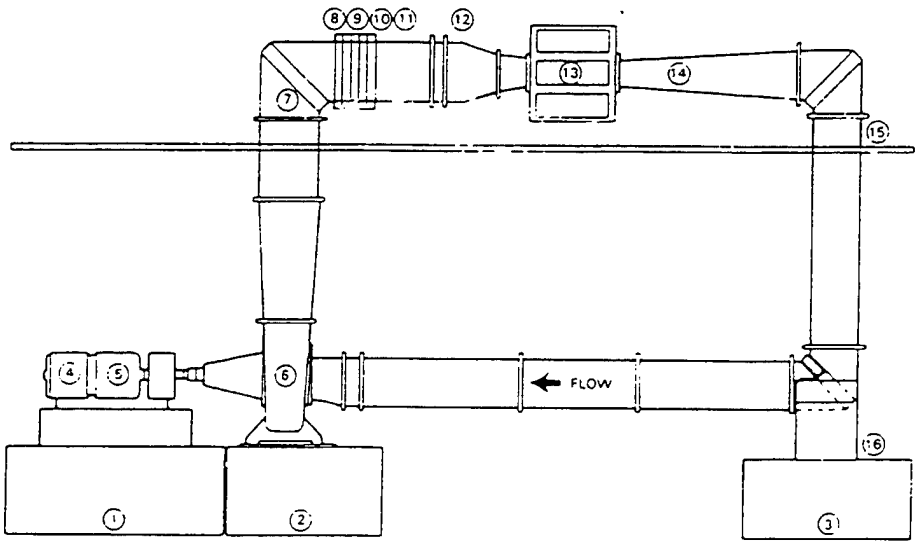

COMPONENTS

1, 2, 3	FOUNDATIONS	10	FINE HONEYCOMB
4	MOTOR	11	SCREENS
5	MAGNETIC CLUTCH	12	CONTRACTION
6	PUMP	13	TEST SECTION
7	TURNING VANES	14	DIFFUSER
8	FOAM	15	SECOND-FLOOR LEVEL
9	COARSE HONEYCOMB	16	FIRST-FLOOR LEVEL

Figure 3.3-1. Basic features of the SSC San Diego recirculating water tunnel.

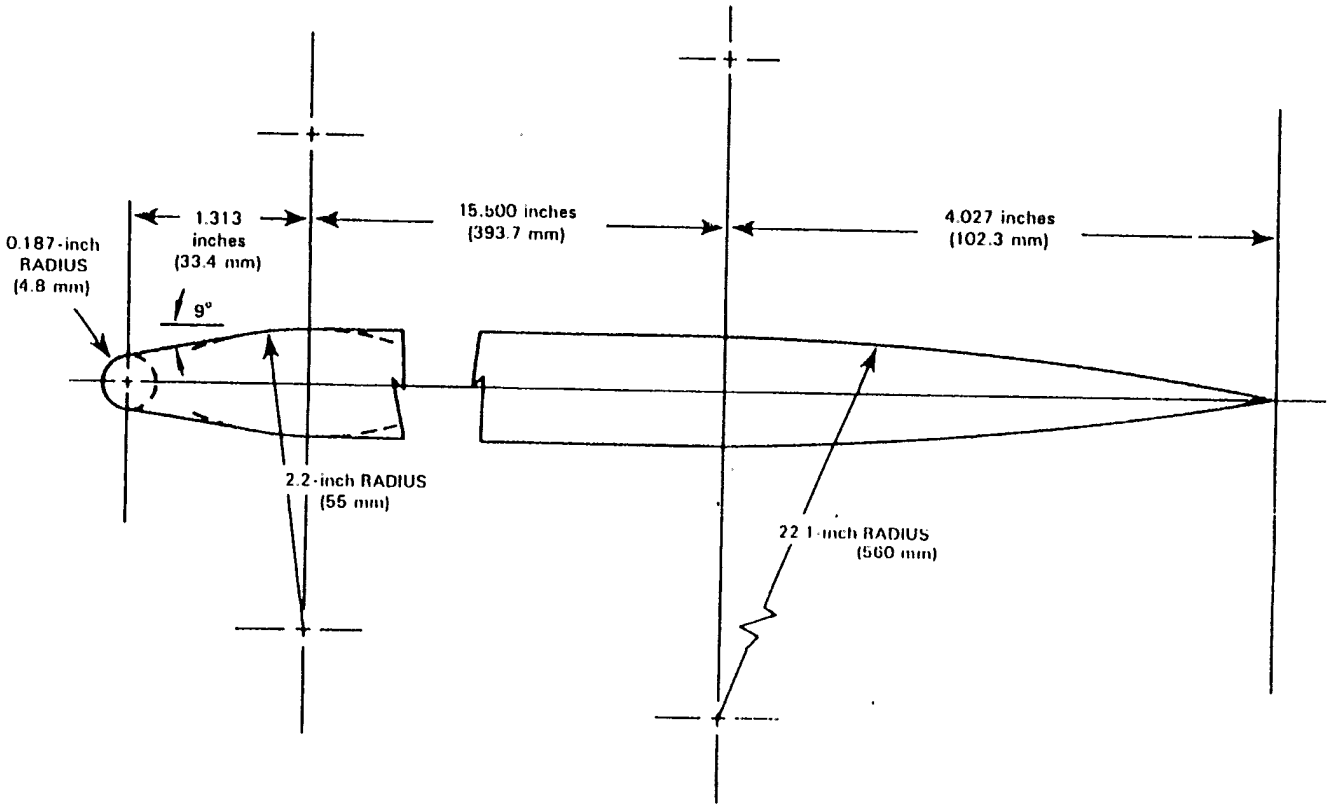

Figure 3.3-2. Streamwise dimensions of the flat plate on which the test samples were placed.

EXTRAPOLATION TO OCEANIC FLOW

The laminar velocity profiles associated with the onset of motion on the flat plate are not a good simulation of actual ocean bottom conditions. The bottom boundary layer in the sea is practically always turbulent (Soulsby, 1983). Mean velocity profiles above the sea floor have been generally found to be logarithmic in nature (Sternberg, 1968). There are several different logarithmic profiles to choose, each incorporating the effect of bottom roughness differently. In order to bracket the problem three different logarithmic profiles are employed in this analysis. The form of the profiles differ in how the roughness characteristics of the sea floor are incorporated. For each logarithmic profile a range of roughness values were chosen.

Profile 1. The first profile, equation (1a) tested evolved from Nikuradse's (1933) pipe-flow work with uniform sand grains. For fully rough flow, Nikuradse found that:

$$\frac{u}{u_*} = 5.75 \log_{10} \left(\frac{y}{k_s}\right) + 8.5 \qquad (1a)$$

where k_s is the mean diameter of the sand grains and y is the distance measured from the bottom surface. In fully rough flow, the resistance of a rough surface is characterized by the form drag of the roughness elements. The turbulent boundary layer is considered to be fully rough flow when the roughness Reynolds number, Re_*, is greater than 70 to 100 (Schlicting, 1979; Nowell and Jumars, 1984). The roughness Reynolds number is defined as u_*D/ν, where the friction velocity, u_*, is the square root of the ratio of the bottom shear stress to the water density ($u_* = [\tau_{bottom}/\rho]^{1/2}$), and D is the height of the roughness elements. For all the cases examined here, Re_* was always greater than 200, thereby ensuring completely rough flow.

Equation (1a) has been used to describe fluvial processes (Chang, 1988). The values of k_s used were 0.72 cm, representative of San Francisco Bay roughness (personal communication, Ralph Chang), and 1/4, 1/2 and 3/4 of the sample height, H. It was presumed that if the bottom roughness was larger than the height of the sample, the motion of the sample would be greatly impeded and for the purpose of this investigation could be neglected. Before equation (1a) determines a velocity profile, the value of u_* must be specified. The value of u_* was determined from the following equation:

$$\int_0^H (1/2)\ \rho\ u_B^{\,2}(y)\ dy =$$

$$\int_{k_s}^H (1/2)\ \rho\ u_*^{\,2}\{5.75 \log_{10} \left(\frac{y}{k_s}\right) + 8.5\}^{\,2}\, dy \qquad (1b)$$

where the integrated stagnation pressure determined in the water tunnel for the initiation of motion, is equated to the integral of the stagnation pressure derived from the assumed turbulent velocity profile, equation (1a). For the rough surface, the integral over the height, H, of the sample begins at k_s. Mean turbulent velocities at 100 cm from the ocean bottom, U_{100}, were calculated *via* equation (1a) for each water tunnel experiment and each value of k_s. The values of U_{100} can be found in Table 3.3-2 and ranged between 0.6 – 1.8 $m \cdot s^{-1}$.

Table 3.3-2: Oceanic Extrapolations via Equations 1a and 1b (beginning of turbulent velocity profile, $y = k_s$) (lam - Blasius laminar velocity profile associated with initial sample movement) (turb - turbulent profile providing same stagnation pressure)

Experiment	Friction Velocity (u_* ; $cm \cdot s^{-1}$)	Mean Velocity at 100 cm (U_{100} ; $cm \cdot s^{-1}$)	Roughness (k_s ; cm)
Exp. #1 (lam)	1.48	50.0	0.0
Exp. #1 (turb)	4.29	89.4	0.72
Exp. #1 (turb)	5.35	100.8	1.59
Exp. #1 (turb)	7.37	126.1	3.18
Exp. #1 (turb)	11.13	179.2	4.76
Exp. #2 (lam)	1.05	33.4	0.0
Exp. #2 (turb)	2.86	59.5	0.72
Exp. #2 (turb)	3.56	67.1	1.59
Exp. #2 (turb)	4.90	83.9	3.18
Exp. #2 (turb)	7.40	119.2	4.76
Exp. #3 (lam)	1.08	34.4	0.0
Exp. #3 (turb)	2.94	61.3	0.72
Exp. #3 (turb)	3.67	69.1	1.59
Exp. #3 (turb)	5.05	86.5	3.18
Exp. #3 (turb)	7.63	122.8	4.76
Exp. #4 (lam)	1.08	34.4	0.0
Exp. #4 (turb)	3.14	65.4	0.72
Exp. #4 (turb)	3.65	71.3	1.19
Exp. #4 (turb)	5.02	89.6	2.38
Exp. #4 (turb)	7.58	127.6	3.57
Exp. #5 (lam)	1.03	32.5	0.0
Exp. #5 (turb)	3.21	66.8	0.72
Exp. #5 (turb)	3.41	69.5	0.87
Exp. #5 (turb)	4.70	87.5	1.74
Exp. #5 (turb)	7.10	125.0	2.62

Profile 2. The frictional effect of individual sand grains on the flow may be quite small compared to that of larger roughness elements normally found on the sea floor (Sundborg, 1956; Vanoni and Brooks, 1957). Consequently, two additional turbulent velocity profiles, used more often in oceanic applications, were also employed. The first (Sverdrup et al., 1942; Sternberg, 1968) is the following:

$$\frac{u}{u_*} = 5.75 \log_{10}\left(\frac{y + k_0}{k_0}\right) \qquad (2a)$$

Although k_0 has units of height and depends on the roughness type, it has been referred to as a computational fiction having no clear physical significance (Denny, 1988). Therefore, it was not obvious at what height to start the vertical integrations of the velocity profiles. Compared to fully rough turbulent pipe flow with sand grains, k_0 has been empirically found to be approximately 1/30 of the sand grain diameter (Schlicting, 1979), while for gravel of various sizes in a rectangular channel, k_0 was 1/15 of the sand grain diameter (Kamphuis, 1974). To bracket the problem the turbulent profile, which rests on the roughness elements, was assumed to begin at $y = 0$, k_0 and $30k_0$ for the integrals in the following equation from which u_* is determined:

$$\int_0^H (1/2)\ \rho\ u_B^2(y)\ dy = \int_{0,\ k_o,\ 30\ k_o}^{H} (1/2)\ \rho\ u_*^2 \{5.75 \log_{10}\left(\frac{y + k_o}{k_o}\right)\}^2 dy \qquad (2b)$$

Some of the values of k_0 chosen were 0.024, 0.048, 0.053, 0.106 and 0.159 cm, 1/30th of those evaluated previously for k_s. Also included are the k_0 value of 0.18 cm, thereby spanning the range found by Sternberg, 1968 in tidal channels. The associated bottom topography in Sternberg's study ranged from fine sand deformed into irregular roughness elements approximately 2 cm high to a complex bed composed of gravel and rocks which protruded 6 to 10 cm above the surrounding sand (Sternberg, 1968).

The estimated values of U_{100} (using equation (2a) with y = 100 cm and determining u_* from equation (2b) using a lower integration limit of 0) are listed in Table 3.3-3 and range from 0.6 – 1.1 m·s^{-1}. There was essentially no difference in U_{100} whether the lower integration limit in equation (2b) was 0 or k_0. However, if 30 k_0 was used as the lower limit of integration of the velocity profile, equation (2a), U_∞ was significantly higher (see Table 3.3-4), ranging from about 0.6 – 2.3 m·s^{-1}.

Table 3.3-3: Oceanic Extrapolations via Equations 2a and 2b (beginning of turbulent velocity profile, $y = 0$) (lam - Blasius velocity profile associated with initial sample movement) (turb - turbulent profile providing same stagnation pressure).

Experiment	Friction Velocity (u_*; $cm \cdot s^{-1}$)	Mean Velocity at 100 cm (U_{100}; $cm \cdot s^{-1}$)	Roughness (k_o; cm)
Exp. #1 (lam)	1.48	50.0	0.0
Exp. #1 (turb)	1.83	87.6	0.024
Exp. #1 (turb)	2.13	93.6	0.048
Exp. #1 (turb)	2.18	94.6	0.053
Exp. #1 (turb)	2.61	102.9	0.106
Exp. #1 (turb)	2.95	109.1	0.159
Exp. #1 (turb)	3.06	111.3	0.180
Exp. #2 (lam)	1.05	33.4	0.0
Exp. #2 (turb)	1.22	58.3	0.024
Exp. #2 (turb)	1.42	62.3	0.048
Exp. #2 (turb)	1.45	62.9	0.053
Exp. #2 (turb)	1.74	68.5	0.106
Exp. #2 (turb)	1.96	72.6	0.159
Exp. #2 (turb)	2.04	74.0	0.180
Exp. #3 (lam)	1.08	34.4	0.0
Exp. #3 (turb)	1.25	60.1	0.024
Exp. #3 (turb)	1.46	64.2	0.048
Exp. #3 (turb)	1.50	64.8	0.053
Exp. #3 (turb)	1.79	70.5	0.105
Exp. #3 (turb)	2.02	74.8	0.159
Exp. #3 (turb)	2.10	76.3	0.180
Exp. #4 (lam)	1.08	34.4	0.0
Exp. #4 (turb)	1.33	63.5	0.024
Exp. #4 (turb)	1.49	67.0	0.040
Exp. #4 (turb)	1.56	68.5	0.048
Exp. #4 (turb)	1.78	73.0	0.079
Exp. #4 (turb)	2.01	77.7	0.119
Exp. #4 (turb)	2.30	83.5	0.180
Exp. #5 (lam)	1.03	32.5	0.0
Exp. #5 (turb)	1.33	63.7	0.024
Exp. #5 (turb)	1.39	65.1	0.029
Exp. #5 (turb)	1.58	69.5	0.048
Exp. #5 (turb)	1.67	71.4	0.058
Exp. #5 (turb)	1.88	76.1	0.087
Exp. #5 (turb)	2.40	87.3	0.180

Table 3.3-4: Oceanic Extrapolations via Equations 2a and 2b (beginning of turbulent velocity profile, $y = 30\ k_o$) (lam - Blasius velocity profile associated with initial sample movement) (turb - turbulent profile providing same stagnation pressure).

Experiment	Friction Velocity (u_* ; cm·s^{-1})	Mean Velocity at 100 cm (U_{100} ; cm·s^{-1})	Roughness (k_o ; cm)
Exp. #1 (lam)	1.48	50.0	0.0
Exp. #1 (turb)	1.863	89.27	0.024
Exp. #1 (turb)	2.244	98.61	0.048
Exp. #1 (turb)	2.318	100.5	0.053
Exp. #1 (turb)	3.187	125.6	0.106
Exp. #1 (turb)	4.81	178.3	0.159
Exp. #1 (turb)	6.318	229.7	0.18
Exp. #2 (lam)	1.05	33.4	0.0
Exp. #2 (turb)	1.239	59.39	0.024
Exp. #2 (turb)	1.493	65.61	0.048
Exp. #2 (turb)	1.524	66.88	0.053
Exp. #2 (turb)	2.12	83.53	0.106
Exp. #2 (turb)	3.2	118.6	0.159
Exp. #2 (turb)	4.203	152.8	0.18
Exp. #3 (lam)	1.08	34.4	0.0
Exp. #3 (turb)	1.277	61.18	0.024
Exp. #3 (turb)	1.538	67.59	0.048
Exp. #3 (turb)	1.589	68.9	0.053
Exp. #3 (turb)	2.185	86.05	0.106
Exp. #3 (turb)	3.296	122.2	0.159
Exp. #3 (turb)	4.33	157.4	0.18
Exp. #4 (lam)	1.08	34.4	0.0
Exp. #4 (turb)	1.363	65.31	0.024
Exp. #4 (turb)	1.584	71.25	0.048
Exp. #4 (turb)	1.691	74.31	0.053
Exp. #4 (turb)	2.164	88.91	0.106
Exp. #4 (turb)	3.27	126.6	0.159
Exp. #5 (lam)	1.03	32.5	0.0
Exp. #5 (turb)	1.391	66.67	0.024
Exp. #5 (turb)	1.477	69.19	0.048
Exp. #5 (turb)	1.817	79.85	0.053
Exp. #5 (turb)	2.028	86.92	0.106
Exp. #5 (turb)	3.047	123.5	0.159

Profile 3. The values of k_0 found in field studies are usually considerably larger than what would be predicted from the laboratory derived formulas, i.e. $k_0 = k_s/30$ or $k_0 = k_s/15$ (Soulsby, 1983). Naturally settled sediments may have a less even distribution than has been used in laboratory studies (Soulsby, 1983). The final mean turbulent velocity profile employed (equation (3); Soulsby, 1983) attempts to mitigate this problem by introducing the variable d_0.

Distances from the ocean bottom were now referenced to the displacement height, d_0, which, in effect, is the distance that the substratum has been lifted due to the presence of the roughness elements. This displacement height was the appropriate value for the lower limit of integration of the stagnation pressure for this velocity profile:

$$\int_0^H (1/2) \quad \rho u_B^2(y)\,dy =$$

$$\int_{d_0}^H (1/2) \quad \rho u_*^2 \{5.75 \log_{10}(\frac{y-d_0}{k_0})\}^2 dy \qquad (3)$$

For many bed geometries, d_0 is approximately 0.7 times the height of the roughness element (Denny, 1988; Soulsby, 1983).

The values of k_0 and d_0 reflect the following unrippled surfaces: silt (31 micron in diameter; $k_0 = .005$ cm; $d_0 = .002$ cm), sand (0.1 cm in diameter; $k_0 = .04$ cm; $d_0 = .07$ cm) and gravel (3.2 cm in diameter; $k_o = 0.3$ cm; $d_o = 2.24$ cm). The corresponding d_o values were calculated by multiplying 0.7 times the grain size associated with each surface roughness, as defined by its Wentworth size class (Wentworth, 1922). As before, after u_* was solved for each water tunnel experiment and a range of surfaces *via* equation 2b, the corresponding values of U_{100} were calculated using equation (3). Table 3.3-5 shows that U_{100} varied from 0.5 – 1.2 $m \cdot s^{-1}$.

Rippled Bottoms. This analysis ignores the effect of ripples on the sea bed. For sand beds covered by vortex ripples, the hydraulic roughness will be closely related to the ripple height (Nielson,1994). Current-generated ripples typically have wavelengths about 1000 grain diameters long (i.e., $\lambda = 1000\,d$), with a height to wavelength ratio of about 7 (Yalin, 1977). For the previously used grain size of 0.1 cm, the height of the ripple would be about 14 cm, significantly higher than the shredded material. Consequently, we conjecture that significant transport would not occur.

DISCUSSION

Historically, deep-water flows have been thought to be extremely slow, a fraction of a $cm \cdot s^{-1}$ (Stowe, 1987). However, these flow rates cannot explain the ripple and scour marks evident in many deep-sea floor photographs. More recent measurements (Nowell and Hollister, 1985) of the benthic boundary layer in the North Atlantic revealed typical velocities of 1 to 5 $cm \cdot s^{-1}$. However, higher velocities of 20 to 40 $cm \cdot s^{-1}$ have also been observed to exist for several days (Gross and Nowell, 1990). Eddy currents in the North Pacific at depths of 6200 m have been found in excess of 10 $cm \cdot s^{-1}$ (Imawaki and Takano, 1982). Deep-sea currents have shown velocities as high as 43 $cm \cdot s^{-1}$ at a depth of 4000 m (Capurro, 1970). In the vicinity of the Gulf Stream, velocities of 50 to 150 $cm \cdot s^{-1}$ have been observed at depths of 3000 – 4000 m (Schmitz, 1984). These currents, if extrapolated to the ocean bottom, may be strong enough to cause erosion of unconsolidated sediment particles (Komar, 1976). Sternberg (1968) studied the logarithmic nature of the velocity distribution within 1.5 m of the bed in six different tidal channels with

differing bed roughness. He found values of U_{100} between 30 and 50 cm·s^{-1}. Even under these extreme conditions, flow velocities do not exceed those estimated (50 cm·s^{-1} < U_{100} < 230 cm·s^{-1}) to be necessary to initiate motion of shredded cans in the ocean.

Table 3.3-5: Oceanic Extrapolations via Equations 3a and 3b (beginning of turbulent velocity profile, $y = d_o$). lam = Blasius velocity profile associated with initial sample movement. urb= turbulent profile providing same stagnation pressure)

Experiment	Wentworth Size Class	Diameter (cm)	Friction Velocity (u_*; cm·s^{-1})	Mean Velocity at 100 cm (U_{100}; cm·s^{-1})	Roughness (k_o; cm)	Velocity Profile Displacement (d_o; cm·s^{-1})
Exp. #1 (lam)			1.48	50.00		
Exp. #1 (turb)	Pebble gravel	3.2	1.38	78.53	0.005	0.002
Exp. #1 (turb)	Coarse sand	0.1	2.04	91.59	0.04	0.07
Exp. #1 (turb)	Medium silt	0.0031	3.48	116.60	0.3	2.24
Exp. #2 (lam)						
Exp. #2 (turb)	Pebble gravel	3.2	0.92	52.24	0.005	0.002
Exp. #2 (turb)	Coarse sand	0.1	1.35	60.94	0.04	0.07
Exp. #2 (turb)	Medium silt	0.0031	2.31	77.59	0.3	2.24
Exp. #3 (lam)						
Exp. #3 (turb)	Pebble gravel	3.2	0.95	53.82	0.005	0.002
Exp. #3 (turb)	Coarse sand	0.1	1.40	62.78	0.04	0.07
Exp. #3 (turb)	Medium silt	0.0031	2.38	79.93	0.3	2.24
Exp. #4 (lam)						
Exp. #4 (turb)	Pebble gravel	3.2	0.98	56.08	0.005	0.002
Exp. #4 (turb)	Coarse sand	0.1	1.48	66.72	0.04	0.07
Exp. #4 (turb)	Medium silt	0.0031	2.73	91.58	0.3	2.24
Exp. #5 (lam)						
Exp. #5 (turb)	Pebble gravel	3.2	1.38	78.53	0.005	0.002
Exp. #5 (turb)	Coarse sand	0.1	2.04	91.59	0.04	0.07
Exp. #5 (turb)	Medium silt	0.0031	3.48	116.60	0.3	2.24

SAMPLE CALCULATIONS

The following procedure was used to estimate the magnitude of oceanic-bottom flow necessary to commence motion. First, the free-stream, laminar velocity which initiated sample movement on a flat plate was experimentally determined. For example, in Exp. #1, a 83.5 gm piece of shredded can, 6.35 cm high and placed 24.3 cm downstream from the leading edge of the plate, first moved when U_∞ was 50 $cm \cdot s^{-1}$. (See accompanying photographs, in top photo there is no motion at U_∞ of 0.4 $m \cdot s^{-1}$. Continuing to increase U_∞ in 0.025 $m \cdot s^{-1}$ increments, the object is observed to first move at 0.5 $m \cdot s^{-1}$, as shown in bottom photograph.) Given x, ν and U_∞ the associated Blasius velocity profile can be determined (Schlicting, 1979). Next the stagnation pressure $(^1/_2)\rho u_B^2$ was integrated from the surface of the plate ($y = 0$) to the height of the sample ($y = H$). The resulting force per unit width is assumed to be the critical flow parameter governing the initial motion of the sample for its particular orientation in the flow field. Rotating the sample 90° results in a different frontal area and consequently a different force per unit width. In Exp.#2 the sample in Exp.#1 was rotated 90°, which increased its width from approximately 13.3 cm to 22.6 cm. This increase in frontal area resulted in a decrease in the free-stream velocity necessary to initiate motion (even though the sample was placed further downstream from the leading edge of the plate).

Having experimentally determined the stagnation pressure field associated with initial movement in laminar flow on a flat surface, it was next necessary to estimate turbulent flow velocity profiles on rough surfaces which resulted in an equivalent integrated stagnation pressure. This was accomplished by equating:

$$\int_0^H u^2_{\text{laminar-Blasius}}\,(y)\,dy \quad = \quad \int_{\text{roughness height}}^H u^2_{\text{turbulent}}\,(y)\,dy \qquad \text{(Eq.4)}$$

where the turbulent profile $u_{\text{turbulent}}$ was obtained from either equations (1a), (2a), or (3). A single choice of the roughness height used for the lower limit of integration for the turbulent profile was unrealistic. Consequently, a range of roughness heights were chosen for each turbulent profile tested.

The integrations for the turbulent velocity profiles were from the height of the bottom roughness to the top of the sample. Over this height it was assumed that the sample would be exposed to the flow. Substituting equations (1a), (2a), or (3) for $u_{\text{turbulent}}$ and setting this integral equal to the total stagnation pressure obtained experimentally (for the laminar, flat plate) allowed the friction velocity u_* to be determined. With u_* determined and either k_s, equation (1a), k_0, equation (2a), or d_o and k_o equation (3) known, the mean velocity at y = 100 cm could be calculated. These values could then be compared to oceanic measurements in order to assess the likelihood of transport.

REFERENCES

Blasius, H. (1908) Grenzschichten in Flussigkeiten mit kleiner Reibung. Z. Math. Phys., 56; English trans. NACA Tech Mem. 1256.

Capurro, L. (1970) *Oceanography for Practicing Engineers*. Barnes and Noble, New York.

Chang, H. (1988) *Fluvial Processes in River Engineering*. Krieger Publishing Company, Malabar, Florida.

Denny, M.W. (1988) *Biology and the mechanics of the wave-swept environment.* Princeton University Press, Princeton, N.J.

Gross, T.F. and Nowell, A.R.M. (1990) Turbulent suspension of sediments in the deep sea. Phil. Trans. R. Soc. Lond. A 331:167-181.

Imawaki, S. and Takano, K. (1982) Low-frequency eddy kinetic energy spectrum in the deep western North Pacific. Science 216:1407-1408.

Kamphuis, J.W. (1974) Determination of sand roughness for fixed beds. J. Hydraul. Res., 12, 193-203.

Komar, P.D. (1976) *Beach processes and sedimentation.* Prentice-Hall, Englewood Cliffs, N.J.

Ladd, D.M. and Hendricks, E.W. (1985) The effect of background particulates on the delayed transition of a 9:1 heated ellipsoid. Exp. Fluids 3, 113-119.

Nielson, P. (1994) *Coastal bottom boundary layers and sediment transport.* World Scientific Publishing Co. Singapore.

Nikuradse, J. (1933) Laws of flow in rough pipes. English trans., NACA Tech. Mem. 1292. (English translation).

Nowell, A.R.M. and Hollister C.D. (eds.) (1985) Deep ocean sediment transport - preliminary results of the high energy benthic boundary layer experiment. Marine Geology Special Issue 66:(1-4) 409 pp.

Nowell, A.R.M., and P.A. Jumars (1984) Flow environments in the aquatic benthos. Ann. Rev. Ecol. Syst.. 15: 303-328.

Schmitz, W.J.Jr. (1984) Abyssal eddy kinetic energy in the North Atlantic. J. Mar. Res. 42:509-536.

Schlicting, H. (1979) *Boundary-layer theory*. McGraw-Hill Inc., N.Y. 599.

Soulsby, R.L. (1983), The bottom boundary layer of shelf seas. *In Physical Oceanography of Coastal and Shelf Seas*. Ed. B. John, Elsevior, New York.

Sternberg, R.W. (1968), Friction factors in tidal channels with differing bed roughness. Marine Geol., 6, 243-260.

Stowe, K. (1987) *Essentials of Ocean Science.* John Wiley and Sons, New York, N.Y. 211.

Sunborg, , A. (1956) The River Klaraven: a study of fluvial processes. Geograf. Ann., 38, 127.

Sverdrup, H.U., Johnson, M.W. and Fleming, R.H. (1942) *The oceans, their physics, chemistry, and general biology.* Prentice-Hall, Englewood Cliffs, N.J. 1078.

Vanoni, V.A. and Brooks, N.H. (1957) Laboratory studies of the roughness and suspended loads of alluvial streams. Rept.. Sediment Lab., Calif. Inst. Technol., Pasadena, Calif. E-68, 121.

Wentworth, C.K. (1922) A scale of grade and class terms for classic sediments. J. Geol., 30, 377-392.

Yalin, M.S. (1977) *Mechanics of sedimentary transport* (2nd ed.). Pergamon, Oxford.

4. ADDITIONAL STUDIES FOR THE ENVIRONMENTAL IMPACT STATEMENT (EIS): U.S. NAVY SHIPBOARD SOLID WASTE DISPOSAL

4.1 SENSITIVE SPECIES AND HABITAT ECOLOGICAL ASSESSMENT IN MARPOL SPECIAL AREAS

by Merkel and Associates, Inc., San Diego, M&A Document No. 95-106-01

INTRODUCTION

In response to increasing international regulations regarding the discharge of solid wastes from maritime vessels, the U.S. Navy is conducting parallel efforts to both develop means for full compliance and to provide for ongoing Naval operations in the interim. Regulations developed under the International Convention for the Prevention of Pollution from Ships, 1973, as modified by the Protocol of 1978 (MARPOL 73/78) preclude the discharge of non-food solid wastes in coastal areas and designated Special Areas throughout the world. Designated and proposed Special Areas include the Antarctic region, Baltic Sea, Black Sea, Wider Caribbean region, Mediterranean Sea, the North Sea, the Gulfs region, and the Red Sea and associated Gulfs of Aden, Suez, and Aqaba (Figure 4.1-1).

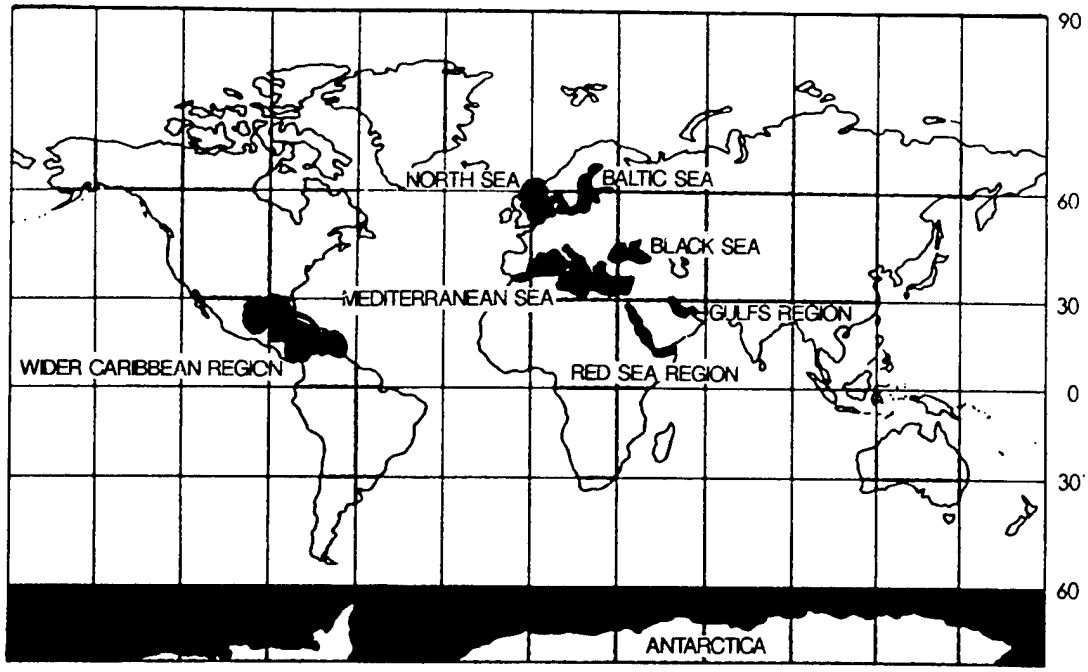

Figure 4.1-1. Geographic Distribution of MARPOL Special Areas. The eight areas included have been identified on the basis of ecological, oceanographic, and socio-political and economic factors. With the exception of the Antarctic, these areas are principally enclosed and semi-enclosed seas and shallow marginal shelf seas. Of the eight Special Areas, the International Maritime Organization (IMO) has adopted regulations in only the Antarctic, Baltic Sea, and North Sea.

While MARPOL 73/78 Annex V exempts discharges from public vessels, the U.S. Congress has enacted legislation through the Marine Plastic Pollution Research and Control Act of 1987 (MPPRCA) which prohibits all vessel discharges of plastics and solid wastes within 12 nmi (22.2 km) of land, or within Special Areas. The U.S. Navy has reviewed its current shipboard disposal practices and operational needs. It has proposed alternative mitigating measures and requested Congressional relief from these restrictions (NAVSEA 1993). The basic elements of the Navy's request are for relief in the following areas:

- An extension of the MPPRCA compliance deadline to 31 December 1998;
- Authorization to discharge non-plastic, non-floating processed solid wastes within Special Areas, and;
- Exemptions for submarines to allow continuation of the current practice of discharging wastes in sinkable compacted slugs.

As an alternative to the current restrictions, the Navy has proposed to implement the following discharge policies:

- The U.S. Navy will cease all shipboard discharge of plastics wastes;
- All non-plastic shipboard solid wastes will be processed into sinkable form prior to any discharge from surface ships operating within the open ocean, irrespective of designation as a MARPOL Special Area;
- No discharges will occur within 3 nautical miles (5.6 km) of U.S. or foreign shores;
- Pulped paper wastes and cardboard will be discharged beyond 3 nautical miles (5.6 km) of all shores, and;
- Non-floating solid wastes, including shredded metal and glass, will be discharged beyond 12 nautical miles (22.2 km) of all shores.

As a part of the effort to develop a shipboard waste disposal operations plan that would reduce potential impacts of discharge without impacting the Navy's ability to operate within designated Special Areas, the use of waste shredding and pulping equipment is being investigated. If implemented, equipment to be installed on all commissioned vessels by 1998 (except those capable of immediate compliance with MARPOL restrictions) would include a plastic processor, two pulpers for food and paper wastes, and a shredder for metal and glass.

The Naval Sea Systems Command (NAVSEA) has charged the SSC,San Diego with conducting an evaluation of the potential effects of continued solid waste discharges in Special Areas, assuming an implementation of pulping and shredding technology. This assessment includes an evaluation of the characteristics of the waste streams, a characterization of the receptor marine communities and species of special interest, and a discussion of potential ecological effects of the wastes within Special Area environments, and ultimate fates of the wastes.

Plastic wastes would not be discharged and food waste discharges are outside of the current purview of MARPOL. For this reason, these investigations focus specifically on pulped paper and cardboard waste and bagged discharge of shredded metal and glass waste.

A draft document entitled *Environmental Analysis of U.S. Navy Shipboard Solid Waste Discharges: Preliminary Report* (Chadwick et al., 1996) was prepared by the Marine Environmental Branch of SSC, San Deigo to address the general problem statement:

"*To what degree, if any, do the materials discharged adversely effect the marine environment?*"

This document reports preliminary analyses which have been completed to characterize the composition, dispersal, and degradation characteristics of the waste streams within the marine environment. In addition, this work includes a number of laboratory investigations to examine toxicity and other impacts of waste on representative organisms of the marine environment. As such, it lays the foundation for impact analyses within the marine ecosystem. To take the work a step further, Merkel and Associates, Inc. was retained by SSC, San Deigo to identify the potential environmental conditions and important ecological endpoints within each of the MARPOL Special Areas which may be susceptible to the proposed waste discharges.

STUDY OBJECTIVES AND SCOPE

This investigation has been undertaken to provide an analysis of potential pathways for ecological effects of shredded and pulped waste discharges within each of the Special Areas. The purpose of the effort is to identify specific biological communities and species of the designated MARPOL Special Areas. Due to time and funding limitations, the work effort has been conducted using existing, readily available information, experience with ocean waste disposal and marine community structure, and consideration of general ecological theory. The study focuses on habitats and high-interest species which are potentially at risk from the specific characteristics of the wastes to be discharged. Where information necessary to complete a detailed analysis was unavailable, assumptions have been made to complete the effort and data gaps have been identified. For this reason, information should be considered preliminary until further investigations can be completed to support or refute the assumptions made.

To approach the questions of potential risks of ecological impact, it is necessary to answer a number of questions regarding the characteristics of the receiving Special Areas. Not only is it important to understand the biological elements of the Special Areas, but also the physical and chemical characteristics which influence the ecology of the region. Specific questions which have been asked in this study include:

1) *What are the physical, chemical, and biological characteristics of the MARPOL Special Areas which may influence the distribution or effects of wastes in ecological systems?*

2) *Under what conditions might wastes interact with organisms in the marine environment and how might organisms be affected on an individual basis?*

3) *Given the characteristics of the materials to be discharged and the potential pathways of effects, what are the most sensitive ecological communities and/or important species resources of the Special Areas?*

DOCUMENT ORGANIZATION

This document is designed to be a supplement to other work efforts and, therefore, relies heavily on prior data collection. The second section of this document outlines the study methods and limitations of this work effort. This section discussed data sources, analytical procedures, and general programmatic study and data limitations.

The third section provides a brief summary of the characteristics of the two waste streams proposed to be discharged. Covered in this section are the physical and chemical properties of the wastes and the operational conditions of the discharge. Data for section on Characteristics of Waste Streams is

summarized almost exclusively from the SSC San Diego (previously NRaD) document (Chadwick et al., 1996).

The fourth section is devoted to an evaluation of the potential effects of the wastes in biological systems. The results of preliminary toxicity and physical interaction tests are considered (Chadwick et al., 1996). In this section, conceptual models of organism susceptibility to the proposed wastes and potential for ecological interactions are characterized on a theoretical basis.

The fifth section is the most extensive portion of this work effort and includes an analysis of each of the Special Areas. In these analyses the physical and chemical conditions of each Special Area are considered to the extent that they play a potential role in both short-term and long-term biological exposure of the waste streams. The current pressures on the ecology of the system, including fishing and pollutant loading, are considered. Finally, ecological factors of productivity, trophic structure and stability, sensitive receptor species, and high-interest habitats are considered.

The sixth section provides the synoptic conclusions of the ecological evaluations for the Special Areas and provides a summary of sensitive ecological endpoints in MARPOL Special Areas.

The seventh section provides a listing of the reference sources utilized in the preparation of this assessment.

STUDY METHODS AND LIMITATIONS

Approach to Investigation. The current investigation is designed to supplement existing preliminary work completed by others. The effort has been conducted as a literature review, theoretical modeling, and qualitative risk assessment exercise. To approach the basic questions, a three-part effort was undertaken: 1) the physical, chemical, and toxicity characteristics of the specific pulped and shredded wastes were reviewed, 2) the interactions of wastes and organisms were explored in greater detail, and conceptual models of waste effects on varying organisms were developed, and 3) the characteristics of each Special Area were examined and related to the waste streams and potential risks of ecological impact based on physical, chemical, and biological conditions, and structures of the system.

Characterization of Wastes and Waste Streams. Principally, information regarding the specific waste streams and their physical and chemical characteristics and effect on marine organisms, is derived from the *Draft Environmental Analysis of U.S. Navy Shipboard Solid Waste Discharges* document (Chadwick et al., 1996). This document and its appendices have been used extensively in the preparation of the current assessment. In order to assist a reader who does not have access to the Chadwick et al., 1996 document, or subsequent versions of this reference, and to follow the analyses, a brief summary of information has been prepared and provided in the third section on characteristics of waste streams.

No new analyses of the wastes or waste streams have been conducted for the current study effort. However, where specific physical and biological conditions which exist in various portions of the world, including some of the MARPOL Special Areas, violate generalities or assumptions made in the analyses of Chadwick et al., 1996, these have been addressed.

Identifying the Effects of Wastes in Ecological Systems. To address the effects of wastes in ecological systems, the NRaD (now SSC San Diego) preliminary report (Chadwick et al., 1996), serves as a point of departure for the present study. The NRaD report conducted a number of standard bioassay

and feeding interference tests for various organisms and characterized the potential risks of the proposed discharges on the basis of density and concentration- dependent impacts. This report focuses upon a variety of effects of solid waste disposal including pulped waste stream dispersal, the impact of packaged (bagged) shredded waste, and fates of waste on the sea floor. More specific questions relating to biological impact on key species, important ecological linkages, and numerically dominant taxa have been left for further study. The present study attempts to approach these questions through the following: 1) consideration of the results of the focused preliminary toxicity and organism interaction testing; 2) an evaluation of morphological, physiological, and ecological factors that would make some organisms more susceptible to waste impacts than others, and 3) application of ecological theory to develop conceptual models and susceptibility curves which would assist in linking general impact characteristics with specific conditions existing in the various MARPOL Special Areas being considered.

Special Area Characterization and Ecological Impact Assessment. In order to conduct ecological assessments on an area-by-area basis, efforts have been made to characterize the unique physical and biological features of each of the MARPOL Special Areas. Available oceanographic texts and papers were reviewed for physical and chemical data and an oceanographic profile for the region was developed. Key circulation, bathymetric, and seasonal patterns were identified. Technical papers were examined for data on regional and local productivity and ecological community structure. From these and other papers, data were assimilated to identify, on a regional scale, areas of specific ecological significance, general trophic relationships and food web linkages of the region, and key species and assemblages which either structure the communities of the area or provide important commercial or cultural benefits to the human population of the area. Where possible, species or organism groups which are recognized as threatened, endangered, rare, or protected under U.S. law or international treaties were also identified.

Given the massive undertaking any one Special Area could pose, addressing all eight has required some degree of subjective scoping to be completed to narrow the focus to a manageable effort. For this reason, coastal fringe habitats were generally excluded from consideration where the 12 nmi offshore discharge limit would clearly provide a considerable spatial separation between discharge areas and sensitive coastal habitats. Where offshore islands and small archipelagos, barrier reefs and seagrass beds, and shallow flats exist beyond the defined 12 nmi limit, communities typically considered to be coastal systems have been considered in this analysis. Conversely, while most pelagic systems have been addressed, a lesser amount of effort has been invested in characterizing those elements of the open pelagic systems which would not be expected to be adversely affected by the waste discharges proposed. For example, many of the seas investigated support developed neuston as well as mesopelagic assemblages. Because of the low potential for these assemblages to be affected, they have not been a focus of this study effort.

By applying such conceptual effect models of waste disposal impact on food webs, the authors of this study have attempted to make extrapolations from potential organismal level effects to community effects. This kind of comprehensive approach is particularly well suited in high-latitude areas where low diversity and high biomass trophic webs characterize the biota. It is also well suited in areas which are evolutionarily young, or stressed to the point of having a simplified community structure. In low latitude settings, many of the food webs have been outlined in enough detail to allow an application of this analysis approach; however, given the complex and multiple trophic linkages involved, such an analysis is inherently weaker in diverse tropical environments.

Because of the multiple variables of marine ecology, there can be no absolute conclusions regarding ecological impact of waste disposal in the analyzed environments. This study considers specific

quantifiable aspects of the wastes and waste streams, and then relates these factors to generalities and conceptual models of organismal biology. From this point, the oceanic and ecological conditions of the Special Areas including currents, temperatures, salinities, water density, productivity, as well as trophic relationships and community structure, are developed from averages, single localized studies, and generalized presentations. When it comes to quantifying oceanic or ecological conditions, almost no two data sources agree. As a result, it must be recognized that presentations which include numerical values are provided as a guide to the magnitude of effect rather than absolute numbers. Indeed, because of the meaninglessness of numerical presentations in this discussion, concerted efforts have been made to avoid quantification and focus more on qualitative presentations.

Data Collection and Sources. Time and financial constraints on this study have precluded conducting new field or laboratory studies. The study is based on a review of published literature and the combined scientific resources available to Merkel and Associates at the time of the work effort. Merkel and Associates staff is experienced in the fields of marine biology and oceanography. The authors of this study have drawn a majority of data from published scientific literature in the areas of marine ecology, geology and biology, as well as oceanography. Of the approximately 700 separate papers, documents, and publications reviewed during the course of the study, roughly 90% fall within the body of scientific literature in the general area of oceanography and the ocean sciences. Many of the publications not readily available from local colleges and universities in the San Diego area were kindly provided by the Navy. Some of the most informative and contemporary sources for physical data have been government publications such as those published by the Defense Mapping Agency and Department of Defense.

Limitations of Study and Extrapolation. It is difficult to assess many of the issues central to this study due to a lack of quantitative data and a paucity of studies that effectively model the environmental situations that arise from solid waste disposal in the oceanic environment. Good information on waste disposal in coastal and estuarine settings, while readily available, is invariably a poor analog for outer shelf, slope, or pelagic systems. Furthermore, most disposal studies which have been conducted have examined either settling and impact characteristics of unprocessed trash or dredged sediments, or effluent discharges from riverine systems or outfall pipes.

To approach the problems inherent in the evaluation of ship-generated wastes on biological systems, this study draws analogies from studies of dredge material, ocean disposal, pulp mill and sewage effluents, and natural inputs to marine systems. Although these analogs are clearly imperfect, they may represent the best available data on the subject. Because most documented waste sources are stationary, these frequently have a potential to affect localized areas. For this reason, impacts on a local scale would typically be anticipated to be more severe than would be seen in a mobile source such as a shipboard discharge. However, for the discharges on which detailed data exist, the location of the discharges have frequently been chosen based on an ecological risk assessment designed to protect highly sensitive areas. As a result, the most sensitive of habitats generally are spared and impact data for areas such as coral reefs and sponge communities are sparse or lacking altogether.

Within and between the range of MARPOL Special Areas there is such an extreme diversity of oceanic environments that specific conclusions regarding impact of discharge activities cannot be extended uniformly across even a single Special Area. Due to these limitations, narratives presented here are necessarily qualitative and somewhat subjective.

This report focuses on extremes in possible biotic disruption due to waste disposal. Given the scarcity of field and laboratory studies specifically aimed at this problem, conclusions and recommendations of this study are preliminary. With the focus on key, ecologically important species, consequences of waste

discharges on whole food webs have been extrapolated from reviews of well-known or classical studies pertaining to specific communities of organisms. These extrapolations weaken when applied to areas outside the focus of the original study; however, they are still useful as a general guide.

CHARACTERISTICS OF WASTE STREAMS

The following information was extracted largely from the *Environmental Analysis of U.S. Navy Shipboard Solid Waste Discharges*, prepared by Chadwick et al., 1996. Any supplemental sources are cited in the text. Shredded metal and glass wastes streams are treated separately from the mulched paper wastes due to the differing composition of the materials, discharge procedures, and dispersion.

SHREDDED METAL AND GLASS

It has been shown that the shredded metal waste to be produced on U.S. Navy vessels sinks at a more rapid rate than does compacted metal, which may retain air pockets. The increased sinking rate of shredded material will minimize excessive lateral transport in the water column and may reduce possible impacts in the coastal zone. Moreover, the shredded material will be enclosed in strong, but degradable burlap bags which will prevent the consumption of individual scrap pieces by fish and birds. Additionally, the burlap bags will further increase the sinking rate of the material.

The components of the burlap disposal bags by weight percentage will be as follows:

1.	Tin plated steel food cans	(71%)
2.	Glass	(13%)
3.	Burlap	(8%)
4.	Organic material	(6%)
5.	Paper labels and aluminum cans	(1%)

Metal and Glass Content and Characteristics. The steel cans to be shredded are comprised of iron (98%), tin (1%), manganese (0.5%), and trace carbon. In addition, organic enamels such as oleoresins or epoxies may be present as a coating on both aluminum and steel cans. The aluminum cans are comprised of aluminum (94%), magnesium (4% max), and manganese (1% max).

The major constituents of glass bottles by weight include oxides of silicon (75%), sodium (14%), and calcium (5%). Glass containers will be prepared for disposal by crushing them into granules. Glass is remarkably inert and has strong chemical bonds. At great depth, however, glass may fracture and dissolution of some silica will occur, resulting in physical and possibly chemical degradation.

The burlap sacks that will enclose the waste material are not indestructible; the discharge procedure must be carefully conducted to prevent the premature release and dispersion of waste materials. However, note that the burlap sacks have been chosen because of their durability; in recent field tests, the bags did not break upon impact with the water and proceeded, intact, to the bottom (S. Curtis and C. Katz, personal communication). Other constituents of the shredded waste will include organic material, such as food particles attached to cans. Paper labels, composed mainly of cellulose, will also be shredded. It is believed that the burlap sacks will degrade on the sea floor within months. Organic materials and paper will be subject to even faster microbial degradation and possible consumption by other organisms.

Frequency and Volume of Discharge. The frequency at which the bags will be discharged and the distribution of daily discharges will vary from ship to ship, and will depend on the number of shredders available and their processing rates. Typically, a processor is able to shred 275 kilograms of glass and metal per hour (NAVSEA, 1993). CV and CVN class ships will have two shredders installed; all other ships have only one. Therefore, the maximum shredding capacity per ship ranges from 275 to 550 $kg \cdot hr^{1}$. A typical burlap bag will hold 4.8 kg of shredded material. Ships shredding at maximum capacity will be able to discharge between 55 to 115 bags per ship per hour.

The number of burlap bags discharged per ship per day will depend on the size of the ship and the number of officers and crewpersons aboard. An estimate of the amount of metal and glass waste produced per person per day is 0.25 kg (NAVSEA, 1993). Therefore, ships with 50 to 6,300 persons would produce 12 to 1,575 $kg \cdot d^{-1}$ (or 3 -300 $bags \cdot d^{-1}$) of metal and glass waste.

Settling Properties, Diffusion, and Dispersal of Wastes. By minimizing the production of air pockets within the discharged bag, the shredding process will allow the bags to sink quickly. This method contrasts that of the disposal of compacted bags; during one survey, 60% of bags containing compacted metal and glass did not sink, regardless of the weight of the bags (Olson et al., 1989). The average settling velocity of the shredded metal and glass wastes to be utilized by navy vessels was 0.54 $m \cdot s^{-1}$, reaching constant settling velocity 2 seconds after discharge. In depths of 50 m, it will take 92 seconds for a bag to reach the bottom; in depths of 5000 m, it may take up to 2.6 hours for a bag to settle.

Because the burlap bags sink quickly, they are subject to minimal water column effects. Biological interaction is considered insignificant unless the bags break during descent. As mentioned above, this is possible, but improbable based on field test results. Thus, the main factors influencing the ultimate settling point of the bags are lateral currents and water depth. After bags have settled, further transport by currents is expected to be negligible. After settling, the burlap bag will decompose, the metals within the bag will corrode, and benthic organisms will be exposed to the waste. Once the burlap degrades, the contents of the sack will be released and small shreds of metal and glass may become subject to further transport by currents, chemical corrosion, biofouling, and burial. It is anticipated that burial (up to 5 cm in depth) of metal pieces via natural sedimentation would take 1 to 10 years. This, however, is an extremely general estimate since sedimentation rates, current, and mixing events vary with depth and vary from water body to water body.

The rate at which corrosion takes place in seawater is dependent upon several physical factors including pH, oxygen concentration, water pressure and temperature, biofouling, and the presence and thickness of organic enamels. Mid-range estimates suggest steel cans with a thickness of 0.01 inches and aluminum cans with a thickness of 0.004 inches could be entirely degraded in 2.5 to 4 years. This estimate reflects corrosion rates of 4 millimeters per year (mpy) for the steel and 1 mpy for the aluminum cams. However, the physical parameters of individual water bodies could significantly increase the time required for total degradation of the cans.

PULPED PAPER WASTES

Paper Content and Characteristics. The mulched paper waste streams to be generated by U.S. Navy vessels will consist primarily of white office paper and cardboard, and small amounts of magazines and newspapers. The paper, which will be composed of cellulose fibers combined with small amounts of inks, fillers, and dyes, will yield waste streams consisting of 92% organic material and 8% inorganic material. Since the main component of paper is cellulose $(C_6N_{10}P_5)_n$, the chemical composition of the waste stream is largely carbon with small amounts of nitrogen and phosphorous. The ratio of C:N:P of

the pulped paper is about 2000:1.3:0.15 (Redfield, 1934 cited in Chadwick et al., 1996). In studies conducted by the Navy, contaminants such as zinc, aliphatic hydrocarbons, and acetone, were not found in mulched paper samples.

Shredded paper particles will range from 16 to 6000 μm and will be in the form of single fibers, bundles, or matrices. A single fiber will typically have a diameter of 20 μm and a length of 200 μm, but these isolated fibers will comprise only about 5% of the waste stream; the remaining 95% of the mulched material will consist of bundles or matrices of fibers. The average density of the paper is 1.52 $g \cdot cm^{-3}$.

Frequency and Volume of Discharge. During the mulching process, water will be mixed with the paper until the ratio of solid phase to liquid phase is about 1:50 (2% solid phase by weight). This ratio is increased to 1:100 when the mixture is discharged by eduction with seawater. Simply put, one pound of solid waste will be vigorously mixed with 100 pounds of water and then discharged from the ship. The rate at which the waste is discharged will depend on the number of mulchers on a ship (which could be from one to three), the number of pulpers operating simultaneously, and the processing rate of the pulpers on individual ships. Small pulpers have a processing rate of 45 $kg \cdot hr^{-1}$, while large pulpers have a processing rate of 226 $kg \cdot hr^{-1}$ (NAVSEA, 1993). Thus, discharge rates could range from 45 to 680 $kg \cdot hr^{-1}$.

It is estimated that the rate of mulched paper generation per person aboard a Navy vessel is approximately 0.50 $kg \cdot person^{-1} \cdot d^{-1}$. The number of people aboard Navy vessels ranges from 50 to 6,286, depending upon the size of the vessel (NAVSEA, 1993). Therefore, the generation rate of paper waste per ship can range from 25 to 3,200 c. Because 100 pounds of water per one pound of solid phase are simultaneously discharged, 2,550 to 320,000 $kg \cdot hr^{-1}$ of water will be discharged with the paper waste. On a large ship, such as CVN 68, the discharge period would be approximately 4.6 $hrs \cdot d^{-1}$ with three pumpers operating, or 14 $hrs \cdot d^{-1}$ with one operating pumper.

The mulcher operation and discharge times will depend on each individual ship's operational practices. Waste will be discharged while ships are travelling at speeds between 10 to 30 kts with transit speeds of about 15 kts. Assuming a period of continuous discharge, a waste plume of CVN 68 could range from 130 to 400 km and contain 0.24 $g \cdot m^{-2}$ of solid phase, mulched paper.

Settling Properties, Diffusion, and Dispersal of Wastes. After being discharged, the mulched material will be further dispersed by ship wake. Optimal dilutions of up to 100 $mg \cdot kg^{-1}$ can occur when a ship travels at moderate speeds (about 15 kts). This mixing will occurs within minutes, and the waste will be concurrently introduced to organisms within the water column. Immediate toxicity and effects on particle feeders could occur.

Larger particles, which constitute up to 85% of the pulped solid phase by weight, will sink quickly to the bottom (820 $m \cdot d^{-1}$), while slow sinking (6 $m \cdot d^{-1}$) mid-sized particles comprise about 12% of the waste. The smallest particles will not sink. Settling tests have shown that about 95% of the waste stream will eventually reach the bottom of the water body into which it is introduced, about 5% will degrade in the water column, and much less than 1% will remain in the surface microlayer. During transit through the water column, the slow-sinking particles will be subjected to physical, chemical, and microbial degradation processes. The breakdown of the physical properties of the waste may alter the sizes of the particles; thus, the sinking rate of the particles. These chemical and microbial processes will consume oxygen and release nutrients and carbon dioxide. In an oxygen-limited area, oxygen depletion, heightened primary productivity, and localized eutrophication may result. In addition, biologically ingested waste particles may be assimilated and discharged as compacted fecal pellets, which will rapidly

sink. Lateral transport within the water column will be minimal due to the rapid settling rate of the majority of the pulped waste particles.

Once the material has settled to the bottom, the concentration of the wastes will be significantly lower than the concentration of the initial waste stream in the wake of the vessel. For example, based on the shallow waters of the North Sea (about 50 m), a worst-case scenario for dilution of settling material shows the concentration of the pulped waste to be reduced to about 0.033 $mg \cdot L^{-1}$ (a five-fold reduction from the wake concentration). In the Baltic Sea (200-m depth), the concentration of the benthic wastes would be about 0.017 $mg \cdot L^{-1}$. The substantially deeper Mediterranean and Caribbean basins may be expected to show much higher dilution factors of the benthic wastes.

Factors that influence the post-flocculation fate of mulched waste on the seafloor include resuspension, transport, vertical mixing, and degradation. Based on the characteristics of the particles, resuspension and lateral transport are more apt to occur in energy-rich environments such as shelf and coastal regions, and less apt to occur in regions where benthic currents are minimal (less than 20 $cm \cdot s^{-1}$). Burial and vertical mixing of the waste particles depend on the rates of bioturbation and natural sedimentation. Except in regions of high sediment input, such as river mouths, bioturbation is a prime controlling factor to burial and vertical mixing. Microbial degradation in aerobic conditions may occur in 1000 to 3000 days, while anoxic environments, such as that in the Black Sea, hinder degradation rates significantly.

It is not anticipated that the pulped waste stream will decrease water clarity to a large degree. Lab studies conducted by SSC San Diego show that the percent transmission of 767 nm wavelength light decreases linearly with increasing concentrations of pulped paper (SSC San Diego unpublished data courtesy of B. Chadwick). However, at concentrations of pulped paper below 1 $mg \cdot L^{-1}$, which is greater than actual discharge concentrations, the percent transmission of light decreases by only a few percent. Field studies conducted by NRaD show no measurable alteration of light transmission due to pulped waste along the wake of a ship as it discharges a waste stream into the water (B. Chadwick personal communication.).

The rate of degradation of the mulched paper will vary with particle structure and size, as well as the pressure, temperature, redox conditions, and presence and abundance of cellulolytic organisms in the receiving water body. A rough estimate of the degradation rate of mulched paper, especially in relation to temperature, is 0.01% of volume per day in cold water to 0.6% of volume per day in warm surface waters. However, the other physical factors mentioned above can have a considerable effect on these rates. Comparative data suggest that total annual input of pulped paper from all ships within a special area is roughly equivalent to spreading the entire yearly discharge from a single sewage treatment plant over the entire special area (Chadwick et al., 1996). Analysis of pulped paper waste input from U.S. Navy vessels suggests that potential long-term effects from nutrient loading or oxygen depletion are minimal. In addition, these effects are not likely to have a detectable effect on areas where these problems already exist.

SHIPBOARD WASTES IN ECOLOGICAL SYSTEMS

In order to assess the potential ecological effects of shipboard waste disposal, it is necessary to: 1) examine the effects of the wastes at an organismal level; 2) understand the degree of exposure of populations or groups of organisms to the waste streams, and; 3) evaluate the consequences of the impacts, considering the importance of potentially affected populations to the functioning of the overall biological system. The specificity which may be derived regarding the level of impact associated with

waste disposal is governed, to a great degree, by an understanding of the physical, chemical, and biological oceanography of a region and the characteristics and fate of the waste streams in the marine environment. In addition, the level of detail which may be accurately expressed is limited both by the degree of variability within the ecological system of a particular study area, and the level to which the biology of the region is understood.

This section provides an assessment of the effects of the two subject waste streams (*i.e.*, shredded metal and glass, as well as pulped paper) at the level of individual organisms. The majority of the tangible data supporting this assessment is derived from Chadwick et al., 1996. Other information as to the effects of wastes at an organismal level is derived from various studies involving similar waste streams, anecdotal field observations, and theoretical extensions of the data to groups of species with shared anatomy, physiology, or foraging ecology. The degree of potential opportunity for waste and organism interaction is conceptually modeled on a global ocean scale. Further refinements to the interaction opportunities evaluation, and a characterization of the affected environments of the various MARPOL Special Areas, is provided in section 5.

SHREDDED METAL AND GLASS WASTES

Shredded metal and glass waste under present disposal methods is unique in that it is a consolidated bagged waste. As a result, there is limited opportunity for wastes to interact with organisms within the water column. The principal opportunities which do exist for interaction would be localized around the descending bag and would include metal leachate, fine particulate metals and glass which escape the bags, as well as associated paper, food, and other incidental wastes which may be released. On the ocean bottom, a greater period of surface exposure exists as bags deteriorate and materials are slowly corroded, overgrown, or buried.

Chemical Effects. In order to evaluate worst-case conditions and determine thresholds of individual organisms to adverse effects, SSC San Diego investigations of leachate toxicity were conducted at concentrations and exposure times which were orders of magnitude greater than those expected within the water column. Through these investigations, it was determined that at the high leachate concentrations used (5% initial leachate), neither mysids, *Mysidopsis bahia*, nor fish minnows, *Menidia beryllina*, were adversely affected (Chadwick et al., 1996). Similarly, the diatom, *Skeletonema costatum* was not notably affected at a 5% concentration of the elutriate; however at higher concentrations, a reduction in chlorophyll florescence was noted. Similarly, bioluminescent activity of a dinoflagellate, *Gonyaulax polyedra*, was also reduced when exposed to metal elutriate. The SSC San Diego study noted that the tested elutriate concentrations were comparable only to the concentrations which may be found within the bag in the immediate proximity to the waste, and the exposure period of the studies (several minutes to 96 hours), would not occur during a free-fall to the bottom. Once on the ocean floor, exposure times would be lengthened, however, and the dilution of slowly dissolving metal wastes would remain extremely high, even within several centimeters of the waste.

Observations of metal or glass wastes within the marine environment, made by the authors of these studies, suggest that such wastes are commonly overgrown with organisms ranging from bacterial films and diatoms to sessile invertebrates and macroalgae. Similar observations were made by SSC San Diego in corrosion and degradation studies of bagged wastes. In these studies, conducted within San Diego Bay, shredded wastes were found to develop a fairly diverse and typical assemblage of cryptic community benthic organisms (Chadwick et al., 1996). This suggests that if toxic leachate were released

by the degradation of the shredded wastes, the rate of release, or concentration, was not likely to be lethal to most organisms.

Physical Effects. Another potential interaction between shredded waste and marine organisms relates to direct ingestion of the materials. Incidental releases of fine particulate material may occur upon the bags striking the water surface or during descent. It would be expected that with intact bags, the extent of released material would be minor and not ecologically meaningful. As mentioned previously, bag breakage, and subsequent large-scale release of shredded material into the water column, is possible but not probable based on field tests. However, many species of the photic zone are opportunistic and will ingest almost any material which flashes in the light as it drifts erratically. The presence of reflecting, particulate metallic silver in an ore spill has been observed to entice aggressive consumption by pink salmon fry (*Oncorhynchus gorbuscha*) which actively sought and ingested the silver flakes (Merkel, personal observation). Visually cued foraging is also the basis for use of artificial lures in the sport fishing industry, and it has been demonstrated that larger fish and other visual predators will readily attack and ingest non-prey, shiny materials. Due to the low density of discharged bagged wastes, the importance of incidental ingestion may be more pronounced when addressing specific high-interest species at the level of individual organisms, rather than at a population level. The concern with regards to ingestion of materials becomes limited to the worst-case scenario of bag breakage and release of larger metal and glass fragments, either during descent through the photic zone, or on the bottom within the photic zone, prior to a dulling of the metallic or glass sheen by the development of a bacterial film.

The extent of the potential ingestion problem has been documented for some species to be quite high. Plastic, metal, and oil have been inadvertently ingested by loggerhead turtles (*Caretta caretta*) foraging within the central Mediterranean Sea and as many as 20% of the turtles were found to have consumed waste litter (Gramentz, 1988). It is believed that the specific wastes ingested by the loggerheads were preferentially consumed as a result of their similarity to foods such as jellyfish and small baitfish. Such waste ingestion has been noted to cause death or illness if the materials are large enough to cause an intestinal blockage.

For the shredded wastes generated by military ships, it is likely that water column ingestion concerns would be limited to turtle, marine bird, shark, and some pinniped taxa. Most cetaceans are typically considered too large to be significantly affected; and no fish or invertebrates, including commercially important species, would likely be impacted in the numbers required to result in notable ecological affects.

Once on the bottom, ingestion of material would likely be dramatically reduced. Although the importance of its affect would be difficult to evaluate, it should be noted that several elasmobranchs, including sharks and rays, make use of electromagnetic fields in foraging. It is believed that deep-water species are particularly keen in this regard. Evidence of electromagnetic confusion in sharks has been demonstrated in several instances around metal structures in shallow waters. In deeper waters, the damage to trans-oceanic cables by sharks suggests that this group can be confused and even provoked into foraging or defensive behavior by electric fields. Such effects may result in preferential ingestion of bagged wastes by sharks or rays, or disruption of normal sensory capacity and reduced foraging efficiency by these fish.

PULPED PAPER WASTE

Unlike shredded wastes, the pulped wastes are proposed to be discharged as an unconfined stream, allowing for diffusion through the water column. In this instance, potential chemical, physical, and behavioral impacts to various organisms (both pelagic and benthic) are of concern. Factors governing the potential risks to organisms include: pulped waste concentration, period of exposure, susceptibility of individual organisms or species to the wastes, and behavior of the organisms.

Chemical Effects. Pulped paper wastes are predominantly cellulose with the majority of the pulp mass consisting of large particles of paper. Although the pulp includes incidental food and other wastes, the material contains low concentrations of nitrogen and phosphorus. With the exception of zinc (associated with a clay fraction used as a whitener and texturing material in writing paper), no designated priority pollutants occur in the waste to an appreciable level. Zinc is found at a concentration of 6 $mg \cdot kg^{-1}$, well below that currently used as a guideline for determining minimum toxicity levels in marine sediments (Chadwick et al., 1996).

Tests for chemical toxicity were conducted on a number of organisms including a mysid shrimp (*Mysidopsis bahia*), a minnow (*Menidia beryllina*), a dinoflagellate (*Gonyaulax polyedra*), a bacterium (*Photobacterium phosphoreum*), and a chain diatom (*Skeletonema costatum*). These were tested with 5% pulped waste leachates diluted in increments to determine the lethal concentration for 50% of the test organisms (LC_{50}) and the No Observable Effect Concentration (NOEC) (Chadwick et al., 1996). In preliminary tests, elutriate at even low test concentrations (still above normal anticipated exposure limits) was highly lethal to mysids and it was suspected that this result related to the presence of suspended solids within the liquid component of the waste. All subsequent tests were conducted on centrifuged supernatant to allow for an evaluation of chemical toxicity, absent confounding physical effects.

Mysids, dinoflagellates, and diatoms were found susceptible to chemical toxicity at intermediate and higher concentrations of the elutriate, while the minnow and the bacterium appeared unaffected at any tested concentration (Chadwick et al., 1996). The tested concentrations all exceeded the anticipated exposure concentrations by orders of magnitude; it is anticipated that actual concentrations of pulped discharge in Special Area environments would be well below the tested concentrations. It appears that chemical toxicity of the pulped waste is not likely to significantly affect typical marine organisms.

In studies examining the effect of leachate from pulped wastes on foraging activities of copepods, no significant change in ingestion rates were identified between control groups and copepods foraging in filtered water previously exposed to pulped wastes (Chadwick et al., 1996).

Physical Effects. The physical effects of pulped wastes on marine organisms is more difficult to evaluate. Particulate wastes may result in a number of ecological and physiological effects including interference with foraging behavior or efficiency, intestinal blockage or interference with nutrient absorption, and respiratory impairment.

In natural benthic systems, it is often possible to predict the community structure and trophic groups which will predominate based on the sediment stability and suspended particulate regime of the site. In areas of soft mud bottoms or high suspended matter, deposit feeders generally predominate over filter feeders and suspension feeders. In such communities, a considerable amount of suspended sediment has the effect of obstructing the fine filtering structures utilized by these groups to respire and capture planktonic and detrital food (Nybakken, 1982).

Investigations conducted by Chadwick et al., 1996 on the effects of the particulate component of the pulped waste on benthic organisms utilized an opportunistic omnivorous polychaete, *Neanthes aernaceodentata* (*N. caudata*), and a benthic amphipod, *Grandidierella japonica*, as test organisms. While these species are common bioassay test animals, both are animals found on soft marine bottoms including muddy estuary environments. As such, they are unlikely to be extremely susceptible to flocculent wastes. Therefore, it is not unexpected that even the heavy deposition of pulped waste resulted in no identifiable effects to these species. Furthermore, *Grandidierella* is an introduced species whose populations are increasing in intertidal mudflat areas at the expense of native species. This species has become extraordinarily common in such habitats as the *Spartina* flats of Willapa Bay in southern Washington, and there is some concern that it may be too hardy to serve as a good bioassay subject (J. Cordell, Univ. of Washington, School of Fisheries, personal communication).

Other observations of the effects of particulate wastes in benthic environments come from examination of static discharge points and associated receptor communities. These areas include designated ocean disposal sites for dredged materials, environments under aquaculture farms, and pulp mill and sewage effluent discharge zones. The applicability of these areas as indicators is limited. Most of these sites receive a much more prolific and consistent input of wastes than would be anticipated from shipboard disposal, and many of the discarded wastes also have nutrient concentrations which are vastly different than the pulped wastes considered in this study. Furthermore, some of the effluent wastes also include a fairly toxic component which can alter the community structure on a localized scale. These caveats being stated, it is also recognized that no exceptionally good analogs for the proposed waste disposal techniques currently exist. For this reason, it is necessary to cautiously apply some of the data collected from these "comparable" examples. H. Jones (personal observation) has noted that fiber mats near pulp mills support a relative paucity of suspension feeders or filter feeders, but a fair number of opportunists with few or no external gill structures. Similarly, communities established at ocean disposal sites also support primarily opportunistic detritivores and deposit feeding organisms (Merkel, personal observation). In estuarine regions and sheltered embayments where detrital silt input may be significant, and bottom sediments soft and unconsolidated, few, if any, species dependent upon filter-feeding may persist. Those filter or suspension feeding organisms that are found in these waters have typically developed growth forms such as stalks or elevated tubes which raise the feeding or gill structures well above the bottom to avoid the perils of fouling.

Perhaps of greater interest in evaluating the potential physical effects of the waste are the results of the copepod and clupeoid fish foraging studies, and the results of the early liquid-fraction investigations using mysid shrimp. In the NRaD studies of the foraging activity of copepods (*i.e., Calanus pacificus* and *Acartia* spp.) exposed to particulate wastes in the water column, an exponential decline in foraging activity occurred with increasing pulp slurry concentrations above 0.03% wet weight. Ingestion rates were not substantially different from control conditions at slurry concentrations of 0.05% and 0.1% (Chadwick et al., 1996). As stated previously, it is anticipated that actual concentrations of discharged material will be much lower than tested concentrations.

While the presence of slurry at high concentrations physically interfered with the foraging ability of copepods, the copepods quickly returned to pre-exposure ingestion rates upon removal of the particulate material. This post-exposure recovery is an indication that some impacts of the pulped wastes may be temporary and, depending upon exposure levels and period, may not result in any substantial impacts. However, for organisms which are short-lived or dependent upon continued ingestion to meet metabolic needs, prolonged exposure may be detrimental.

While not explicitly utilized as a test organism for the particulate fraction of the pulped waste, the preliminary results of liquid-phase bioassay tests using mysids would suggest this small crustacean may

be susceptible to the flocculent matrix material of the paper pulp. While studies did not focus on the mechanisms of impact, it is possible that this species suffered from suffocation brought on by fouling of the species' respiratory system, including both gills and swimmerets. If this is the case, species with external gills, as well as similar planktonic crustaceans such as krill may be similarly susceptible. A concern exists for most filter-feeding pelagic or benthic species, especially those living in persistently clean waters where gill purging mechanisms may be less well-developed.

In studies involving Pacific Sardine, *Sardinops sagax*, these clupeoid fish were found to exhibit reduced filter-feeding activity, slower growth, and higher levels of mortality with increased concentrations of pulped paper. However, at lower concentration levels, a greater degree of filter foraging occurred, and intestinal blockage by pulp resulted. Fish were found to be impacted at pulp concentrations falling between 0.1 and 1 $mg \cdot L^{-1}$. As with copepods, fish typically recovered to normal feeding activities when exposure to pulped paper ceased (Chadwick et al., 1996).

A final physical effect of pulped waste on marine organisms pertains to availability of light. Shallow benthic communities of seagrass, algae, and corals require good water clarity and a high level of light penetration to grow. A decrease in light penetration may result from increased suspended particulate matter that decreases water clarity or from a film of particulate matter that coats the blades or polyps of benthic organisms, effectively reducing the amount of light the reaches the organisms. As mentioned previously, neither lab nor field studies have revealed a large decrease in light transmission due to pulped waste material discharged from U.S. Navy vessels. Although unlikely, decreased light penetration, which may occur as a result of increased sedimentation, is discussed in this document.

Behavioral Effects. Foraging activities in most animals can be heightened by providing a stimulus such as added food resources. In many instances, a viable food need not be present to illicit a stimulus, only a component of the resource is required. For species which seek prey by sight, smell, or tactile means, a "super stimulus" from one factor may result in foraging behavior which is not supported by a true availability of food. As an example, filtering activity in the giant acorn barnacle (*Balanus nubilus*) can be stimulated by crushing an urchin and waving the body fluids over the barnacle. A similar response can also be obtained from the chemicals released in curing by some marine epoxies, even though no food is present (Merkel, personal observation). As discussed previously, an active foraging response can be elicited with visual consumers, including many species of fish. The importance of this foraging stimulus behavior to the evaluation of pulped waste effects relates to the operative concentration of the waste. A mobile consumer, or an active filter-feeder, has the ability to concentrate materials by selectively foraging over large areas, or by moving large volumes of water through feeding structures. For visual or tactile feeders exposed to a sparse cloud of pulped waste, an ability to actively pursue and capture pulp can enhance the effective concentration of the waste when species are affected by a super stimulus. As a result, even at low concentrations, an active and even preferential foraging on pulped material can result in considerable consumption by various organisms.

Studies conducted with clupeoid fish revealed not only a physical impediment to foraging with higher concentrations of pulped wastes, but also an apparent breakdown of normal schooling behavior (Chadwick et al., 1996). While this behavioral modification might be linked to the physical impairment of foraging, it may also relate to other factors such as reduction in visual acuity or dampening, or deflection of pressure waves generated by neighboring fish. While such behavioral changes are typically expected to be short-lived, they can also result in a greater susceptibility to predation or other risks. Such behavioral changes including avoidance, changes in foraging strategy, or other apparent behavioral effects, may also be early manifestations of a physiological effect such as respiratory distress. Again, it

should be noted that actual exposure concentrations in marine environments are anticipated to be much lower than the concentrations that were tested in laboratory situations.

General Trends in Organism Susceptibility to Wastes. It is necessary to recognize that each species will probably respond differently to similar levels of exposure to the various wastes. As a result, it is highly likely that some species will be more susceptible to wastes than the tested organisms, and some will be less affected. However, to address the possible affects of wastes in the natural environment, it is necessary to generalize affects to a larger group based on the occurrence of shared characteristics. In general, these characteristics may include taxonomic relationships, physiology, ecology, or morphology. It is assumed that an evaluation of the responses of the tested species, along with observations of organisms in other environments, can be used to create a generalized relationship between physiological or ecological traits and susceptibility to waste impacts. This basic relationship is necessary when examining the potential susceptibility of a community as a whole to the proposed waste stream. The primary characteristics currently believed to be important are foraging ecology, respiratory structures, and body size. To a far lesser degree, susceptibility to trace metal and other chemical toxicity is a factor when considering the shredded waste stream and the non-matrix component of the pulped wastes. Because of the flocculent, sticky, fibrous nature of cellulose, species which either filter water for feeding or respiration are expected to be most susceptible to pulped wastes. Species which rely on other means of respiration or foraging would be less susceptible to impacts. Figure 4.1-2 provides generalized curves expressing the anticipated degree of susceptibility of organisms to impacts from the waste streams based on respiratory anatomy and foraging mechanisms.

Relative to body size, extremely small organisms, especially those lacking cilia or flagella would be expected to escape any substantial effects associated with physical impairment; however, they may be more susceptible to chemical toxicity of waste stream leachates. Furthermore, species which are orders of magnitude larger than the waste particulates would be expected to be little affected by either the limited toxicity of the material or physical impairment of foraging or respiration. As an example, coarse grained respiratory organs such as the gills of large fish would be much less likely to become fouled than the gills of larval fish or small invertebrates. Figure 4.1-3 provides conceptualized curves expressing the potential degree of affects of wastes on organisms of increasing body size.

EXPOSURE OF ORGANISMS TO WASTE STREAMS

Two primary elements govern the extent of waste effects on organisms. As discussed earlier, the first is the magnitude of detriment to an organism's exposure to the wastes. The second is the degree to which the organisms come into contact with the waste streams. The characteristics of the waste streams including diffusion, material density, and the rate at which a material sinks, have been discussed in some detail within Chadwick et al. (1996). From this information, it has been demonstrated that under model and field circumstances, rapid diffusion of pulped wastes occurs within the upper water column and continues to disperse as it settles through the water. Conversely, bagged shredded waste maintains a constant, extremely low, dispersal concentration equal to the discharge concentration. To fully appreciate the significance of these diffusion characteristics relative to the ecology of the regions, it is necessary to consider the distribution of potential organismal receptors of the wastes.

With few exceptions, the vertical distribution of organisms within the oceans can be characterized on the basis of latitude and ocean depth profiles. Using biomass as an indicator of organism distribution, general curves can be created to characterize the vertical distribution of life in the sea.

Deep Ocean Environments. For both high and low latitude deep-ocean basins, the majority of the biological activity is associated with the photic zone in the uppermost portion of the water column (Figure 4.1-4). Phytoplankton provides the basis of a foodweb which ultimately feeds not only an epipelagic assemblage of organisms, but through detrital rain, provides for the presence of both deep water meso-, bathy-, and abyssopelagic assemblages as well as benthic communities. Below the photic zone, the biomass declines to relatively low levels, increasing once again within a relatively narrow band of animals which exhibit a diurnal migration between approximately 100 m and 80 m depth (deep scattering layer). Below the deep scattering layer, the biomass again declines, rising once more near the bottom where a detrital-based foodweb supports benthic infauna, epifauna, and demersal organisms.

Within deep, open ocean environments, the highest concentrations of pulped wastes would exist coincident with the greatest biomass of marine organisms. This condition can be further exacerbated by the presence of upwelling waters or shallow boundary currents or pycnoclines. In deeper waters, the concentration of both pulped waste and marine organisms would decline independently such that at depth, concentrations of wastes would be so low as to be difficult to measure and interactions of organisms with waste particles would be nominal and inconsequential (Figure 4.1-4).

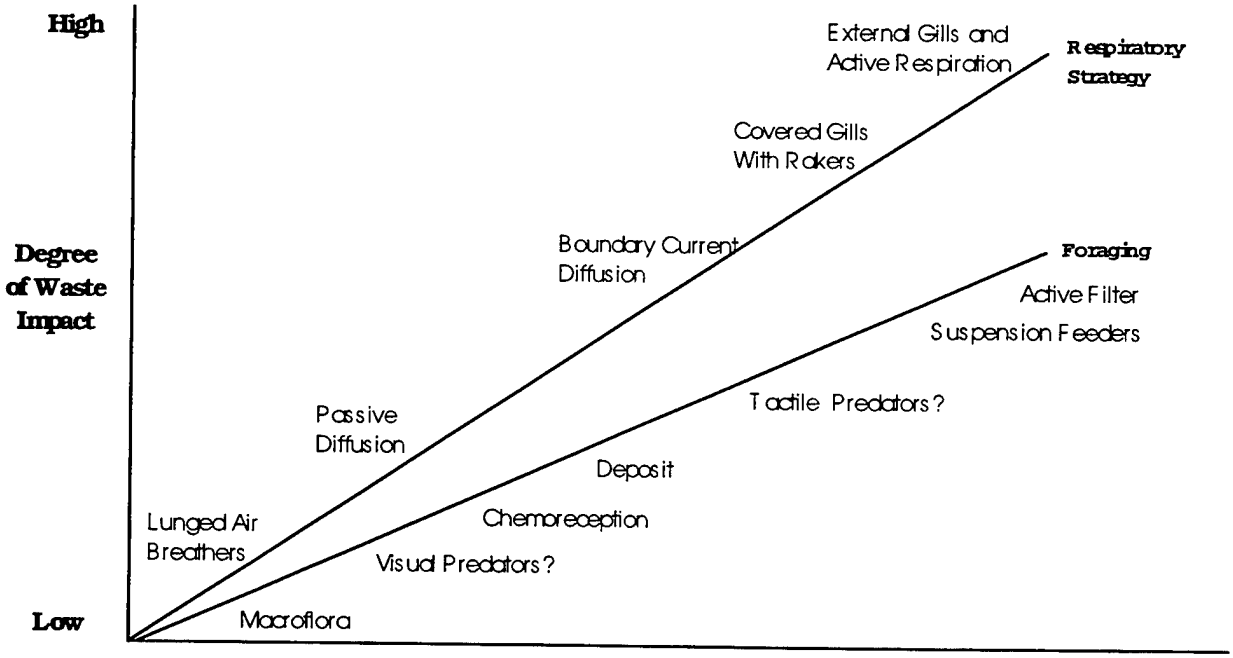

Figure 4.1-2. Relationship of respiratory strategy and foraging ecology of an organism to its potential susceptibility to impacts of pulped waste discharges

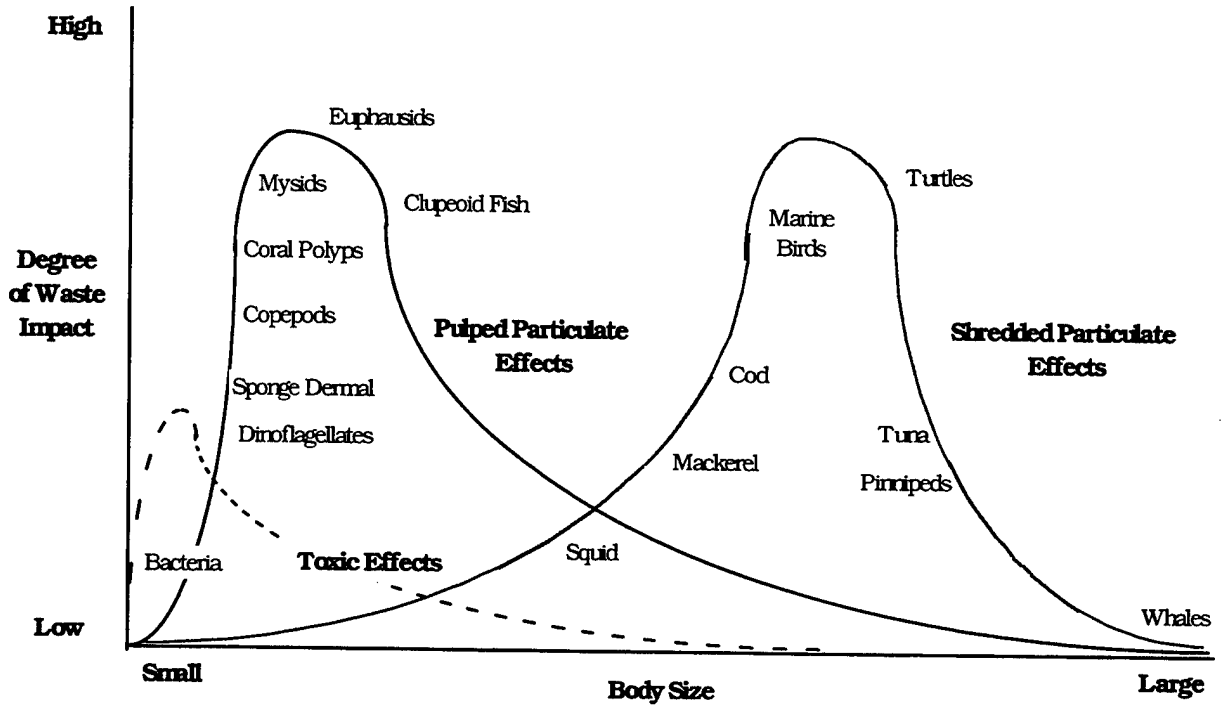

Figure 4.1-3. Generalized relationship of organism body size to potential susceptibility to impacts of shredded and pulped waste toxicity and particulate waste impacts

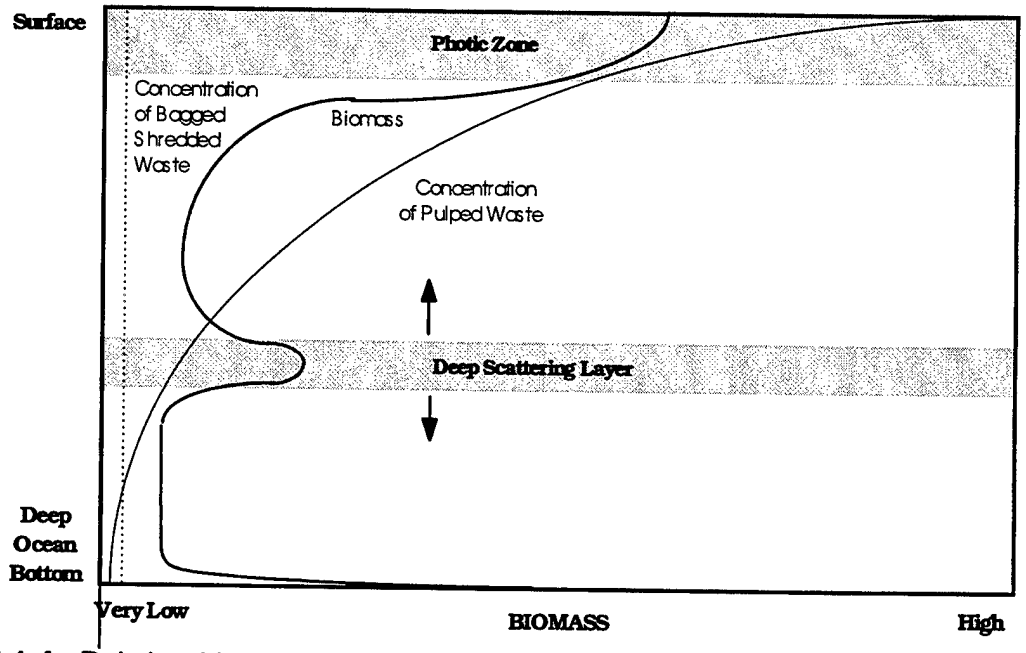

Figure 4.1-4. Relationship of biomass and waste stream concentration to depth in deep ocean environments. Biomass in both high- and low-latitude environments can be expressed with the same curve, recognizing that the entire curve is laterally shifted to the right for higher latitudes and to the left for lower latitudes.

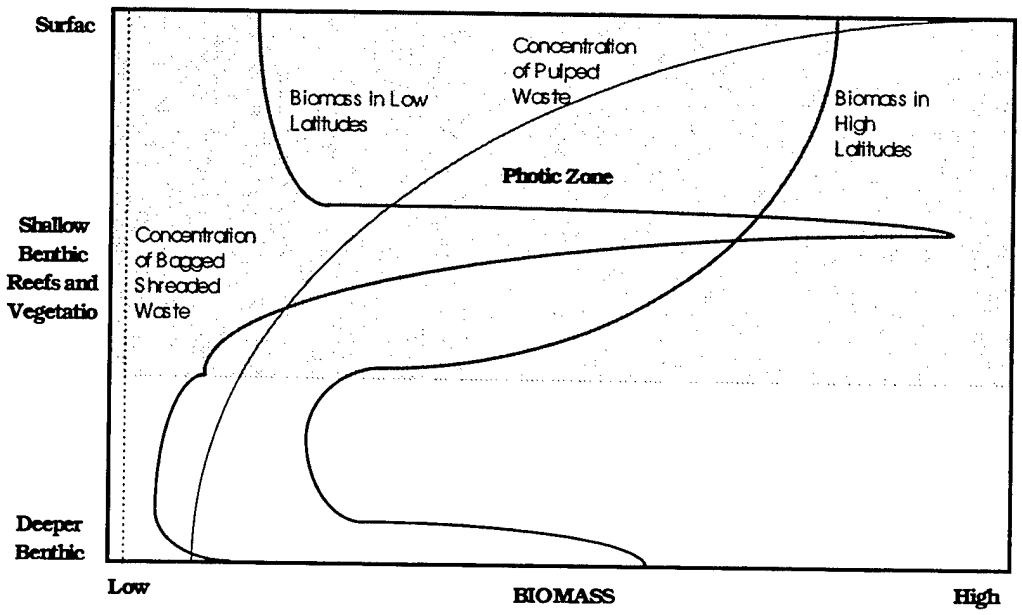

Figure 4.1-5. Relationship of biomass and waste stream concentration to depth in shallow sea environments. Biomass in low-latitude environments can be substantially lower than in high latitudes throughout the pelagic environment. However, benthic environments of low latitudes, which occur within the photic zone, can have an extremely high biomass as a result of the productivity of reefs, seagrass beds, and benthic algal communities.

Since the concentration of bagged waste would not change with depth, the potential for interaction between this waste and marine life is dictated exclusively by the density of organisms, rather than changes in the waste concentration as material sinks.

Shallow Seas- Low Latitudes. In shallow waters, the distribution of life varies from that of deeper oceanic basins in that benthic productivity may be substantial relative to phytoplankton productivity. This is especially true at tropical latitudes where coral reefs, seagrass beds, or algal flats may occur in shallow environments and support a considerable and diverse community (Figure 4.1-5). While biomass declines with increasing depth as a result of reduced light availability, the benthic and demersal community within this zone can often remain quite considerable. Below the photic zone, which may be quite deep as a result of low phytoplankton productivity and high sun angle, biomass declines, rising again at the sea floor where a detrital food-web exists.

Shallow Seas- High Latitudes. At higher latitudes the biomass curve follows that seen in deep oceans except for the absence or minimal occurrence of a deep scattering layer (Figure 4.1-5). High productivity occurs within the photic zone where phytoplankton dominate the system. Below the photic zone, biomass and diversity again decline and become dominated by opportunistic species dependent upon detrital rain and forays into the photic zone. The benthic and demersal communities of high latitude shallow seas can be extremely productive areas and support the predominant commercial fisheries of the world. These areas are home to cod, haddock, hake, halibut, sole, and a number of other fishes.

Within shallow seas, waste diffusion characteristics parallel those of deep oceans. However, in such shallow seas, the concentrations of pulped wastes may remain relatively high, down to a depth at which the material is deposited on the bottom. In such environments, unlike those found in the deep ocean, it may be possible to affect highly susceptible benthic communities. Because the concentration of bagged shredded waste does not change with depth, the relative shallowness of these areas is irrelevant to concentration of this waste stream. It should be noted, however, that at shallow depths there is more potential for spreading of the shredded wastes across bottom environments. Furthermore, bagged wastes may create microtopographic relief and provide hard surfaces for colonization by organisms which would otherwise have difficulty persisting in a particular region. These features are neither seen as detrimental nor particularly beneficial on an ecosystem scale.

MARPOL SPECIAL AREAS

The environmental characteristics of the MARPOL Special Areas which are most important to evaluation of potential effects of shipboard solid waste disposal are discussed in this section. At the end of the section on each Special Area is an analysis of the potential for adverse effects associated with a worst-case operational scenario within the region. In some instances, a worst-case scenario includes consideration of specific localized physical, chemical, or biological phenomena which create a potential for greater environmental risk than occurs over much of the basin. Where this is the case, conditions are discussed both for high-risk conditions and areas which typify the designated Special Area.

The following discussions are arranged by Special Area in order of descending latitude. For the sake of brevity, many of the later discussions reference back to similar conditions discussed in prior text.

ANTARCTICA

PHYSICAL AND CHEMICAL CONSIDERATIONS

Geography and Physiography. The Antarctic region is defined by the Antarctic Treaty of 1959 as the region below 60° South latitude (Figure 4.1-6). Other treaties and conventions have extended these limits to the north in order to include some of the more significant biological resources of the region. The boundary established for the Convention on the Conservation of Antarctic Marine Living Resources is based on the approximate location of the Antarctic Convergence and follows 60° South latitude over a portion of its length; however, it steps northward as far as 45° South latitude where Prince Edward Islands and Iles Crozet and Iles Kerguelen are located in the south Indian Ocean (Figure 4.1-6).

As a polar region, the Antarctic exhibits marked seasonal extremes. During the winter, darkness predominates for several months and the weather conditions in the Antarctic are among the most severe on earth. Most relevant to the current investigations are the persistent extreme cold conditions of the region and the prolonged light and dark seasons. These elements have a profound effect on terrestrial as well as oceanic environments. Approximately 98% of the continent is cloaked in a massive ice sheet (Defense Mapping Agency, 1992). Exposed land is dominated by rock and, in coastal plains and valleys, by mineral loams or glacial moraine sediments subject to deep dry permafrost conditions. Thus, even with the harsh winds that can predominate over the continent, the degree of erosion and wind transported sediment is relatively minor.

The Antarctic possesses approximately 65 to 70% of the world's fresh-water supply, yet almost all of this water is found within the massive continental ice (Defense Mapping Agency, 1992). Few streams exist, and these typically support small, seasonal flows of relatively clear water fed by low-elevation snow and ice melt.

Due to the persistence of a number of broad ice shelves, the continental shoreline in many areas is located several kilometers inland from the open sea. In the most extreme example, the Ross Ice Shelf extends over 700 km beyond the shoreline into deep waters of the Ross Sea. Seasonally, sea ice extends over vast portions of the southern oceans. During the late winter, sea ice can extend over as much as 20 million square kilometers, nearly doubling the size of the Antarctic ice pack. This has important physical and ecological considerations which are addressed later.

Bathymetry. Antarctica has a relatively narrow (approximately 30 kilometers width) and deep continental shelf. The shelf area reaches a depth of 500 to 900 m at its outer margins and is two to four times deeper than the world average shelf depth (Defense Mapping Agency, 1992). Continuing seaward, the continental slope drops to a depth in excess of 3000 m over a short 100km distance. Approximately 75% of the open water area of the Antarctic falls below 4000 m occurring within the Atlantic-Indian Basin, the South Indian Basin, the Southeast Pacific Basin, and a portion of the Southwest Pacific Basin. Oceanic basins contain deep marine and non-marine tertiary and younger sediment deposits as thick as 4 kilometers (Defense Mapping Agency, 1992). The continental slope and mid-oceanic ridges, including the Scotia Ridge, Cordillera, Macquarie Ridge, and Southeast Indian Rise, raise approximately 15% of the seafloor to a depth of 600 to 1200 m. Less than 10% of the open water of the Antarctic lies above 2000 m depth (American Geographical Society, 1970).

Currents, Tides, and Water Exchange. With the exception of the massive inlets formed by the Ross and Weddell seas and the long protrusion of the Antarctic Peninsula, the shoreline of the continent is relatively featureless from an oceanic scale perspective. Further, the smooth shoreline configuration and the position of Antarctica as an "island continent" centered on a rotational pole is important in shaping the major oceanic currents of the region (Figure 4.1-6). The unique characteristics of the area allow for a strong, persistent circumpolar oceanic flow which involves approximately 10% of the world's seawater and travels at about $0.5 m \cdot s^{-1}$ (Defense Mapping Agency, 1992). The Antarctic Circumpolar Current (West Wind Drift) is located predominantly around the Antarctic Convergence between 35° and 65°South latitude (Defense Mapping Agency, 1992). To the south, the Antarctic Divergence defines the boundary between the predominantly eastward flow of the Antarctic Circumpolar Current and a weaker nearshore westward flowing, wind-driven current called the East Wind Drift.

The Antarctic Convergence is centered around 50° South latitude in the Atlantic and ranges between 50° and 60° South latitude in the Pacific (Figure 4.1-6). This region of downwelling is found where the cold polar watermasses merge with the warmer waters of the bounding oceans and subduct beneath these less-dense tropical and subtropical waters. This subducted flow forms the Antarctic Intermediate Water which flows northward at a depth centered around the 900-m isobath (Thurman, 1975). The Antarctic Divergence zone is found between the predominant counter-current flows of the Circumpolar Current and the East Wind Drift. In this area, nutrient-rich warm waters, which were subducted in the North Atlantic and northern Indian Ocean, are forced up to replace the cooler subducting polar waters (Figure 4.1-7). The deep oceanic waters and narrow coastal shelf of Antarctica further define the circulation patterns which generate the Antarctic Divergence upwelling zone. It is important to note that the volume and location of upwelling is seasonal in nature and is also affected by prevailing atmospheric conditions.

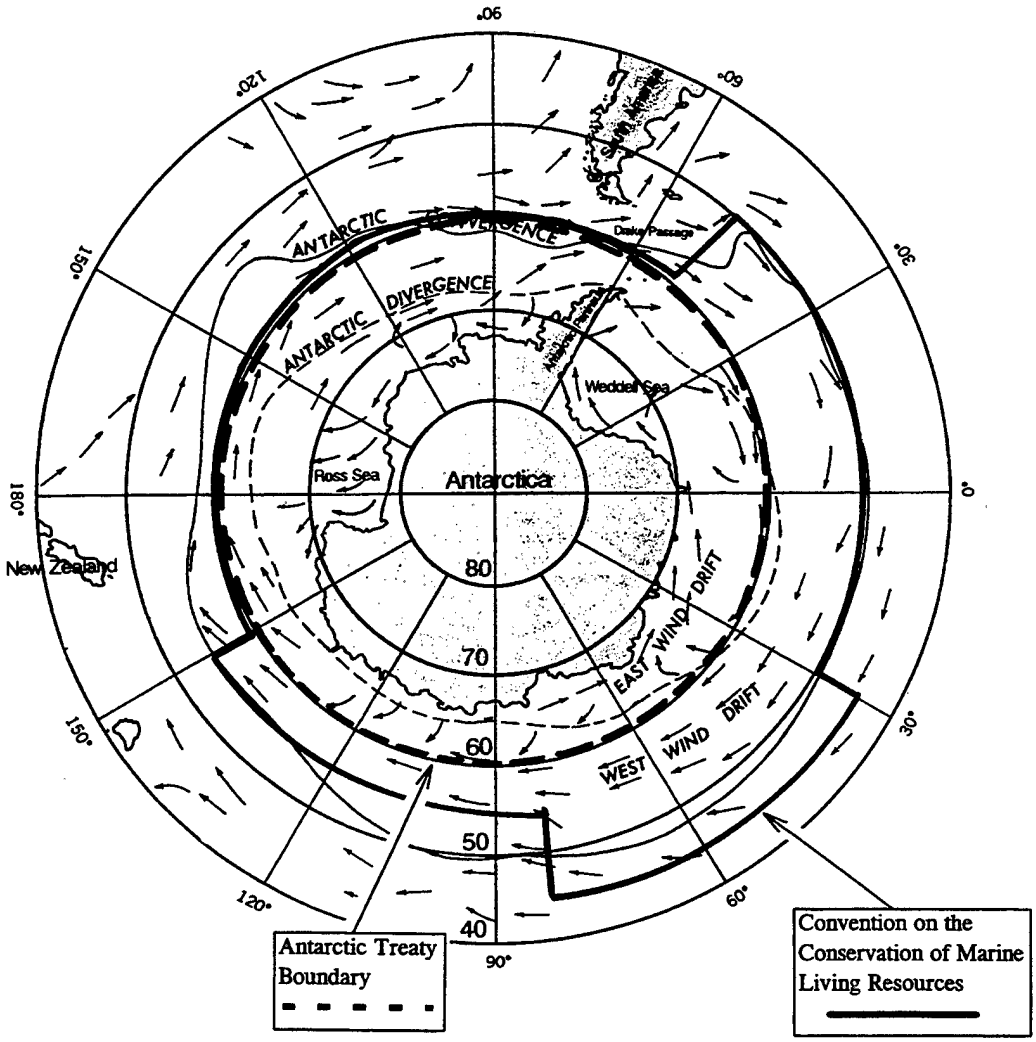

Source: Defense Mapping Agency, 1992

Figure 4.1-6. Major geographical, physical, and political features of the Antarctic region. The primary defining feature of the Antarctic region is the Antarctic Convergence where polar waters subduct below the warmer temperate and subtropical waters of the major oceanic bodies. Primary currents are the circumpolar West Wind Drift between the Antarctic Divergence and Antarctic Convergence, and the weaker East Wind Drift between the Antarctic Divergence and the continental land mass.

Unlike the majority of the designated and proposed MARPOL Special Areas, the Antarctic is not an isolated waterbody. In fact, the Antarctic is bounded on all sides by waters of the world's three largest oceans, the Pacific, Atlantic, and Indian Oceans. Interchange of waters with lower latitudes is highly significant, although most of the Antarctic coastal waters are moved northward near the seafloor rather than in surface water masses. The polar waters at approximately -1.9°C and 34.6 ppt (Thurman, 1975) become more dense and sink along the continental margin forming the Antarctic Bottom Water (El-Sayed, 1971). It is estimated that the Antarctic is responsible for replenishment of more than half of the bottom waters of the world's oceans (Defense Mapping Agency, 1992). The role of the Antarctic as a source for high-density, nutrient-rich waters or the origin point of thermohaline circulation makes it, in a biological sense, one of the most important bodies of water in the world.

Tides of the Antarctic are predominantly diurnal. Due to the excessive coverage of the continental shoreline with floating ice shelves, much of the shoreline tidal effects are muted. Further, due to the deep shelf and coastal waters, only limited, tidally driven circulation occurs.

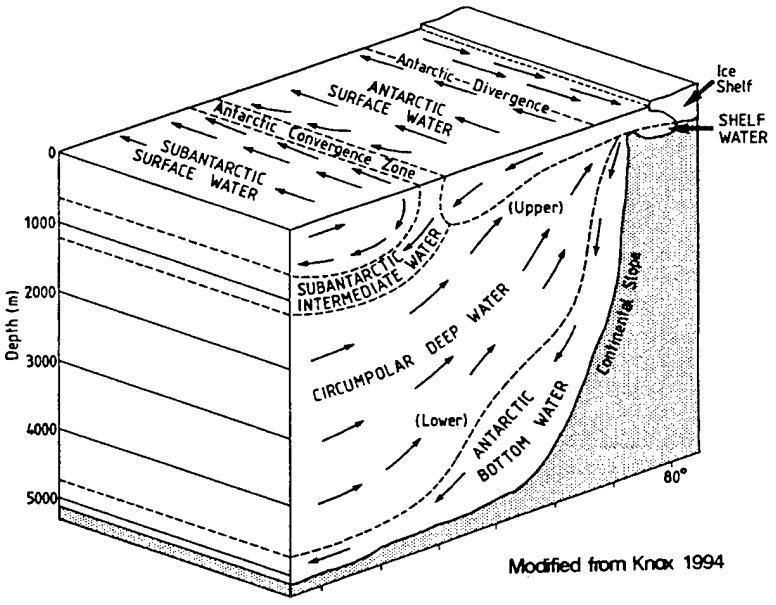

Source: Defense Mapping Agency, 1992

Figure 4.1-7. Diagram of major water masses of the Antarctic. Primary zones of upwelling and subduction include the Antarctic Divergence and Antarctic Convergence respectively. Antarctic Bottom Water generated on the shelf regions of marginal seas is conducted northward to the Pacific, Atlantic, and Indian Oceans.

Temperature and Salinity. Average annual surface water temperature below the Antarctic Convergence zone ranges from 1.1° to 2.2°C in the winter, to 2.8° to 5°C in the summer. Near the continental margin, temperatures vary from approximately -1.7° to -0.5°C (Defense Mapping Agency, 1992). The lowest large water mass temperatures within the Antarctic zone are -1.9°C; the freezing point of seawater at normal winter salinities (Thurman, 1975).

During the month of February (austral summer) surface water temperatures near the 60°S latitude boundary of the Antarctic Treaty range between 0° and 5°C (American Geographical Society, 1970). During the winter months, nearly the entire area designated as Antarctic waters may be covered in sea ice. Deep waters of the Antarctic region are often warmer than surface waters.

Surface salinity of the open ocean waters of the Antarctic, south of the Antarctic Convergence, varies on a seasonal basis as a result of freezing and thawing of ice. Salinities may range as low as 33.5 to 33.8 ppt during the summer ice melts (Defense Mapping Agency, 1992). To the north of the Convergence zone, salinities are more stable around 34.0 ppt. Good winter period salinity data are not currently available for many areas due to coverage by sea ice and a subsequent lack of sampling. It has been suggested that higher salinities may exist during the winter due to freezing of the freshwater, thus concentrating the salts into the remaining waterbody.

Oceanic Sedimentation. The Antarctic is notable for its low amounts of atmospheric dust associated with the dominance of ice over the continent. Similarly, the low wind and water erosion and transport of sediment has resulted in only limited mineral sedimentation in coastal and oceanic waters. Keys (1984) noted that suspended sediment within the Ross Sea ranged from 2-4 $mg \cdot L^{-1}$.

Both onshore and offshore, plankton-generated turbidity can be substantial on a seasonal basis. Areas of upwelling, as well as other areas of concentrated phytoplankton and zooplankton activity, generate significant amounts of organic particulate material within the water column. Much of this material ultimately settles to the bottom as an organic detrital rain. Diatom productivity in the Antarctic is so extensive that a belt of silica (opal) rich ooze forms much of the sediment floor. This diatom ooze, when viewed in submarine photographs, is studded with glacial dropstone pebbles ranging from less than one centimeter to over a meter in diameter.

CURRENT ENVIRONMENTAL STRESSES

Marine Pollution. In relative terms, the Antarctic may be viewed as one of the world's most pristine systems. Due to a virtual disinterest in the continent until relatively recent times, and the limited number of visitors who currently venture to the southern oceans, Antarctica has remained remarkably unpolluted. Recognizing the value of this undisturbed system, many countries have set about to protect the region through international treaties and guidelines for use of the area's resources. Such agreements have greatly benefited the protection of the area.

Currently, the continental Antarctic is visited primarily for scientific research purposes on a steadily increasing scale, while the Antarctic coastal waters attract scientific study as well as limited eco-tourism uses. Farther north, a limited amount of commercial fishing extends into the Antarctic waters. Associated with these uses are low levels of localized pollution.

Litter. Marine litter is limited by the lack of human activity within the region. On a small scale, garbage is discharged at various research stations along the coast and from commercial and scientific (private and military) research vessels operating within the southern ocean. Restrictions on the discharge of certain wastes were added to the Antarctic Treaty, particularly for such wastes as plastics. Seaborne litter which has washed up on sub-polar islands has been predominantly tied to commercial fishing activities (Chadwick et al., 1996). Anthropogenic materials deposited on the most-effected shores are non-degradable fishing nets and floats, styrofoam, milled and painted woods and aluminum, plastic, and

treated paper wastes. There is a notable gradient of increasing litter with decreasing latitude. Over much of the Antarctic coast, evidence of litter is non-existent.

While sinking litter discharges are difficult to document, it is expected that a similar latitudinal gradient would be noted with non-buoyant discharges and that much of the discharge would consist of material from fishing and commercial merchant ships. Due to the frequently stormy seas within the commercial shipping lanes of Drake Passage, it is likely that a considerable amount of cargo has been lost from ships traveling through these waters. Very limited solid waste discharges have likely occurred below 60° South latitude.

Toxic Materials. Like litter, toxic materials within the Antarctic environment are not well represented on a gross scale, although localized discharges do occur. Petroleum hydrocarbons are regularly discharged into Antarctic waters through small shipboard and shore station spills. Perhaps the largest reported discharge of petroleum products within Antarctic waters occurred in 1989 when a research supply vessel ran aground near Palmer Station on the Antarctic Peninsula, spilling 170,000 gallons of fuel into the sea (Defense Mapping Agency, 1992). Low levels of other contaminants including DDT, PCBs, and other organohalides have been found within krill, fish, birds, and mammals of the Antarctic, although levels are not considered to be high enough to form a health hazard (Defense Mapping Agency, 1992).

Metal concentrations within the Antarctic have been poorly characterized, and as such, it is difficult to derive any specific conclusions regarding the metal distribution in the area. Like other contaminants, it is anticipated that higher metal concentrations would be found locally in proximity to areas of settlements. Studies of trace metal concentrations within bivalves collected at three areas, including two bays with research stations and one bay which is hydrographically isolated, identified no specific trends between areas in proximity to stations and the more secluded area. In all areas, bioaccumulated metal levels were found to be lower than those typically reported for other areas of the world (Berkman and Nigro, 1992). While this may reflect differences in organismal biology as much as differences in metal exposure rates, the authors of this investigation pointed out that Antarctic studies may provide important baseline conditions for evaluating contaminant data collected in such worldwide programs as "Mussel Watch."

Organic wastes include ship and land-based sewage, food discharges, and fish processing wastes. These discharges raise the nutrient concentrations on a local scale, but due to the general low level of human activity within the region, the current level of these discharges is not likely to result in significant regional impacts.

Natural Input. Natural pollutant inputs from terrestrial sources within the Antarctic typically come from low levels of mineral sedimentation derived from ice melt which releases glacial flour and collected rocks and sediment. Due to the low productivity of the continental biosphere, nutrient influx into the oceans from terrestrial sources is believed to be minimal.

Organic enrichment of the oceans comes from upwelling of the deep ocean waters and the seasonal pulses and subsequent crashes of phytoplankton and krill blooms. These enrichment events are not believed to be detrimental to the region's ecology and, in fact, are the basis for much of the benthic community persistence. Eutrophication has not been demonstrated to be a threat in the context of Antarctic ecology.

While deep ocean sediments share characteristics with a number of oil-producing sediments found elsewhere in the world, there is currently no indication that natural oil seepage is extensive within the Antarctic.

Sea Traffic and Ports. Sea traffic within the Antarctic is extremely limited and seasonal in nature. Most commercial shipping occurs to the north of 60° South latitude within the marine shipping lanes of Drake Passage, between the southern tip of South America and the Antarctic Peninsula. Here, large commercial tankers and freighters pass from the Atlantic to the Pacific Oceans. A number of lesser shipping routes cross the fringes of the Antarctic region to reach Australia, New Zealand, and the southern tip of Africa (Defense Mapping Agency, 1992). These commercial routes are typically well-distanced from the continent and are only seasonally navigable due to the presence of considerable sea ice during the winter season.

Increasingly large numbers of cruise ships enter Antarctic waters during the austral summer season. These ships typically visit the Antarctic Peninsula rather than the more southerly portion of the region. Given the dearth of port facilities, most of the activities on these excursions consist of shipboard sightseeing and lectures with intermittent visits to highlight areas such as seal and penguin rookeries, as well as Antarctic research stations. Other sea traffic includes research expeditions throughout the Antarctic waters and to specific research stations. Curiously, significant numbers of research personnel are routinely ferried between the several research stations on the peninsula via commercial cruise ships.

FISHERIES AND AQUACULTURE RESOURCES

Commercial fisheries of the Antarctic have been historically focused on a rich whaling industry and fur trade which catastrophically depleted many of the top-level consumers of the region. Particularly hard-hit during 20th century whaling were the baleen whales including the fin (*Balaenoptera physalus*), blue (*Balaenoptera musculus*), humpback (*Megaptera novaeangeliae*), and Southern right whale (*Eubalaena australis*) (Defense Mapping Agency, 1992). During the peak of the whaling era, processing camps were established on some of the higher latitude islands of the southern oceans. Pinnipeds were likewise reduced by a well-developed fur trade and a demand for blubber in the 18th and 19th centuries. The most substantial species in these fisheries were the Southern fur seal and the elephant seal. Relatively recent regulations and restrictions on whaling and taking of marine mammals have greatly curtailed losses associated with these fisheries. The International Whaling Commission and the Convention for Conservation of Antarctic Seals provide levels of protection and sustainable harvest quotas for commercial, cultural, and scientific uses of these mammals.

Currently, most commercial fishing occurs north of the Antarctic Convergence in warmer waters. However, there is a limited commercial fishery for krill. There is a lesser fishery for squid and Antarctic fishes. It has been recently estimated that approximately 80,000 to 90,000 metric tons of krill are harvested per year. This is believed to be well below the sustainable yield (Defense Mapping Agency, 1992). Current constraints on the krill fishery are in finding an economical means of rendering krill into products for the world markets (Nasu, 1981). The ability to harvest krill from the Southern Ocean has been demonstrated, but problems of product quality remain unsolved.

Antarctic fish pose a number of problems as a commercial fishery. First, most species are demersal rather than pelagic. Few species occur in large schools, and most species are extremely small relative to normal commercial fisheries standards. Over one-half of the fish species known to occur in the Antarctic region do not obtain a length of over 25 cm (Everson, 1981). In addition, fishing access to this region is

seasonally restricted due to sea ice. These factors have served to limit most nations' interest in Antarctic finfish fisheries. However, as the oceans of the world are depleted, more and more interest is being focused on the sub-Antarctic areas and the outer island fisheries of the Antarctic continent. Fish catches have historically been poorly reported for the region and as such, it is not clear what trends in the fishery may exist (Everson, 1981). Fishing along the northern edge of the Antarctic Divergence is not uncommon; however, data on this fishery are sparse. Furthermore, poorly defined reporting regions for the Southern Ocean cloud the true picture of the extent of the Antarctic fishery. Roper (1981) reported that no commercial fishery for squid existed in the Southern Ocean, although a Japanese fishery was harvesting 20,000 metric tons per year out of New Zealand waters. Since the publication of that paper, small-scale sub-Antarctic fisheries have become established. Some extension of this fishery into waters south of the Antarctic Convergence occurs during the summer seasons. The exact catch was not determined in this review.

Phytoplankton. The Southern Ocean has often been regarded as one of the most highly productive regions of the world with estimates of primary productivity being reported as high as 3.0 $g \cdot C \cdot m^{-2} \cdot d^{-1}$ (Defense Mapping Agency, 1992). This productivity has generally been based on shipboard studies of productivity in waters taken during austral summer cruises and has been attributed to the extensive upwelling of nutrients along the Antarctic Divergence. However, more recently, it has been suggested that despite the nutrient-rich waters of the Southern Ocean, phytoplankton productivity is often limited by low water temperatures that inhibit growth, long winter dark periods and sea ice which limit light, and by poor availability of trace metals such as iron. Further, it has been shown that zooplankton grazing, especially by krill (*Euphausia superba*) can control and even eradicate entire phytoplankton blooms (Graneli et al., 1993; Lancelot et al., 1993). Additionally, nutrient mixing can occur in water too deep (and, thus, light-limited) to support large algal blooms (Graneli et al., 1993). Similarly, subduction of nutrient-rich waters also restricts phytoplankton productivity. Recently, a more conservative approximation of average primary production for the Antarctic has been figured to be 0.341 $gC \cdot m^{-2} \cdot d^{-1}$ (Defense Mapping Agency, 1992).

Studies suggest that although the entire primary production of the Southern Ocean is not significantly higher than that of other seas, the productivity in the southern region of the ocean, near marginal ice-edge zones, is seasonally quite high (Estrada and Delgado, 1990; Kang and Fryxell, 1993; Lancelot et al., 1993). This has been attributed to the presence of a shallow, vertically stable water layer on the surface of the marginal ice-edge zone. This layer forms in the late spring and early summer as ice melts, surface waters are warmed and illuminated by 24 hours of sunlight, and the water is seeded with actively growing sea-ice microbes. It has been suggested that the waters adjacent to the ice-edge contribute nearly 40% of the annual production south of the Antarctic Convergence (Smith and Nelson, 1986) with the majority of the remaining productivity being associated with upwelling along the Antarctic Divergence.

The phytoplankton of the Southern Ocean is made up predominantly of diatoms. Over 70 species of phytoplankton, dominated by two genera of diatoms (*Frugilariopsis* and *Pseudonitzschia*) and one of prymnesiophyte (*Phaeocystis*) have been located near the ice-edge of the Weddell and Ross seas and Prydz Bay (Kang and Fryxell, 1993). Approximately 60 species of dinoflagellates and silicoflagellates are secondary components of the phytoplankton assemblage. Productivity of these organisms contribute significantly to the bottom sediment content as a glassy siliceous ooze.

Zooplankton. Silicoflagellates, heterotrophic dinoflagellates, radiolarians, tintinnids, and microcrustaceans form the bulk of the protozooplankton (2-200μm) assemblage in the Southern Ocean. These species are distributed vertically throughout the water column with dinoflagellates occurring in the

shallow depths and microcrustaceans at greater depths (Boltovsky and Adler, 1992; Garrison and Buck, 1989). Garrison and Buck (1989) estimate the biomass of the protozooplankton in the Weddell Sea during spring and autumn to range from 55 to >650 $mgC \cdot m^{-3}$. Boltovsky et al., (1989) estimate that the average biomass of tintinnids, dinoflagellates, and silicoflagellates were 4.00 $mg \cdot C \cdot m^{-3}$, 1.02 $mgC \cdot m^{-3}$, and 0.39 $mgC \cdot m^{-3}$, respectively, in the Weddell Sea in the summer.

Unlike the macrozooplankton found in the other oceans of the world, the assemblage of the Antarctic Sea is dominated by relatively few species of euphausiid shrimp commonly known as krill. Copepods, amphipods, tunicates, and other euphausiids also exist in substantial numbers (Boysen-Ennen et al., 1991). Hempel (1985) describes several latitudinal zones of macroplankton including the ice-fee zone dominated by copepods, the seasonal ice-pack zone dominated by krill (predominantly *Euphausia superba*), and the permanent ice-pack zone dominated by the euphausiid ice krill (*Euphausia crystallorophias*). In pelagic waters, krill are widely distributed; however, a number of areas of high krill concentration have been identified (Figure 4.1-8).

Zooplankton productivity is governed by marked seasonal fluctuations in the availability of phytoplankton resources. It has been noted that many zooplankton species, including the krill (*Euphausia superba*), live under ice in the winter and shift to a pelagic existence in the summer; these species are, thus, able to exploit both ice algae and pelagic phytoplankton populations at different times during their development. The krill have been estimated to have an average biomass of 1 to 27 $g \cdot m^{-2}$ in the ice-edge portion of the Weddell Sea (Bergstrom et al., 1990). Additionally, concentrations of krill, although uncommon, have been recorded to have a density of 1000 to 10,000 $individuals \cdot m^{-3}$ (Johnson et al., 1984). During the austral spring, krill concentrated at the edge of the pack ice can form extremely dense narrow aggregations numbering in the billions of individuals.

Joiris (1991) has estimated that, based on the nutritional requirements of the top predators of the Antarctic, a minimum krill production rate of 16 $mgC \cdot m^{-2} \cdot d^{-1}$ is required within the Antarctic zone. Standing crop estimates of krill biomass vary from 125 million to 6 billion metric tons. Based on estimates of primary productivity for the Antarctic region, a standing crop of 250 million metric tons with an annual production of 300 million metric tons is probable (Defense Mapping Agency, 1992).

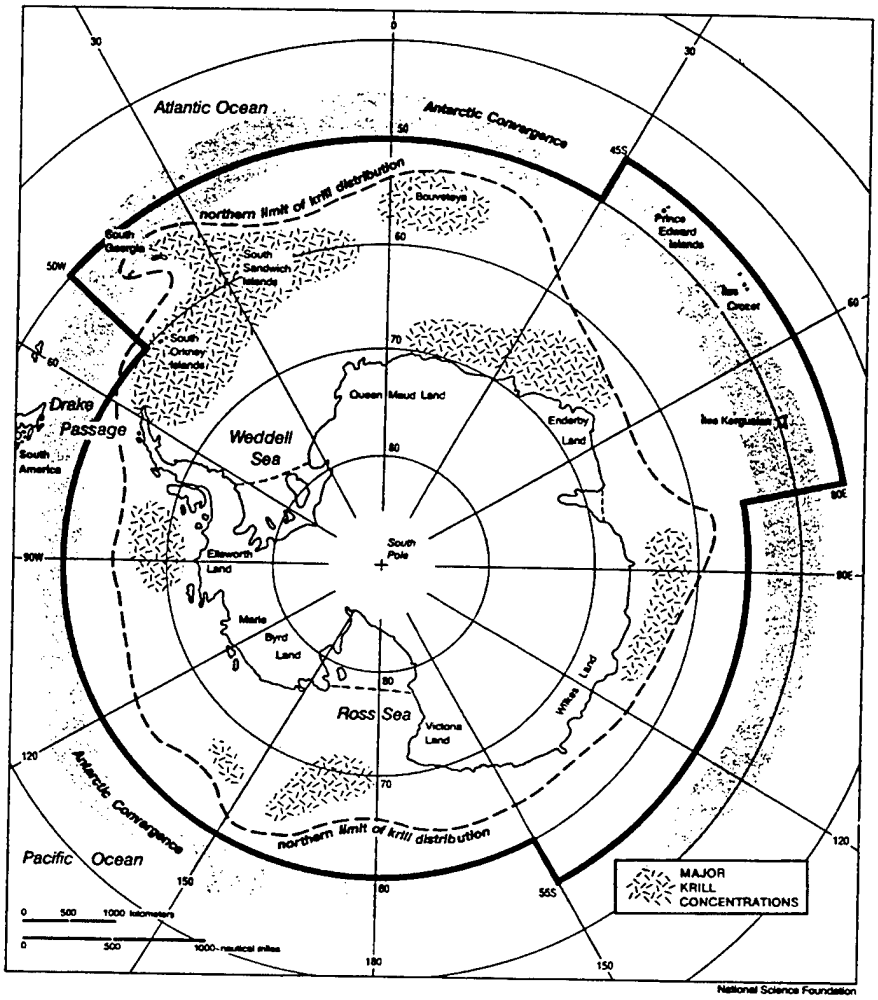

The boundary (solid line) of the Convention on the Conservation of Antarctic Marine Living Resources is determined by the approximate location of the Antarctic Convergence (shaded area). Within this area the convention protects all species of marine organisms and establishes a standard for rational use of these resources. By designating all populations, not just harvested ones, as resources the convention recognizes the interdependence of the components of the antarctic marine ecosystem.

Source: Defense Mapping Agency, 1992

Figure 4.1-8. Distribution of krill in the Antarctic region. Major aggregations of krill exist along the ice edge and in productive regions fed by the upwelling of the Antarctic Divergence. Individual aggregations may be several hundred meters in length and number in the millions of organisms.

TROPHIC RELATIONSHIPS

Pelagic Food Web. The Antarctic region is defined by a marked seasonal pattern of primary productivity and a short trophic web heavily dependent upon phytoplankton and one group of zooplankton. This trophic structure, while reducing the energy loss associated with multiple tiers of consumers, makes the system particularly vulnerable to disturbances that specifically affect key species in the trophic web.

Along with the primary production of phytoplankton, krill hold a keystone position in the Antarctic trophic web and have a direct effect on nearly every position in the food chain. Due to the abundance of krill in Antarctic waters, it is a readily available food source for not only first-order fish such as the Antarctic silver-fish (*Pleuragramma antarcticum*), but also for top predators, including pinnipeds, penguins, and cetaceans (Figure 4.1-9). In addition to the impact krill has on structuring the pelagic trophic web, this group also plays an important role as a primary source for detrital rain which feeds a short but substantial benthic food web as discussed later.

Another group which is key to the polar food web are the cephalopods. At least 47 species of cephalopods are known to occur in the Antarctic and sub-Antarctic region (Roper, 1981). Squid are the dominant organisms of this group; species including *Psychroteuthis glacialis* and *Todarodes filippovae* are among the most abundant and comprise a large portion of the diets of penguins, pinnipeds, and cetaceans. The standing stock of squid has been estimated to be 12.4 million tons with an annual production rate of 19 million tons (Defense Mapping Agency, 1992). This group holds an intermediate position in the food web and is consumed by many of the same organisms that eat krill. Perhaps one of the most important trophic linkages in the Antarctic region involves squid and toothed cetaceans. With this group, first order predators such as squid, fish, and other mammals and birds fully separate these whales from the primary food source of the Southern Ocean, krill.

It is generally believed that fish stocks in the Southern Ocean are not as abundant as those of other oceans (Defense Mapping Agency, 1992). The demersal fish fauna of the Southern Ocean consist of approximately 200 species dominated by the families of *Nototheniidae*, *Bathydraconidae*, *Channichthyidae*, and *Artedidraconidae* (Ekau, 1990; White and Piatkowski, 1993). Interestingly, the majority of species are small (less than 25 cm in length), have slow growth rates, lack swim bladders (and are, thus, demersal), and lack any respiratory pigment such as hemoglobin (Everson, 1981). Many species, due to their demersal nature, feed on benthic amphipods, isopods, molluscs, algae, and polychaetes. Some species, however, are pelagic feeders. The Antarctic silver-fish (*Pleuragramma antarcticum*) dominates catches in the waters of the high Antarctic shelves (White and Piatkowski, 1993; Boysen-Ennen et al., 1991). As mentioned previously, the silver-fish is a planktivorous species that feeds largely on copepods and krill. The silver-fish, in turn, forms a large portion of the diet of penguins, seabirds such as petrels, and pinnipeds (Joiris, 1991; Klages, 1989).

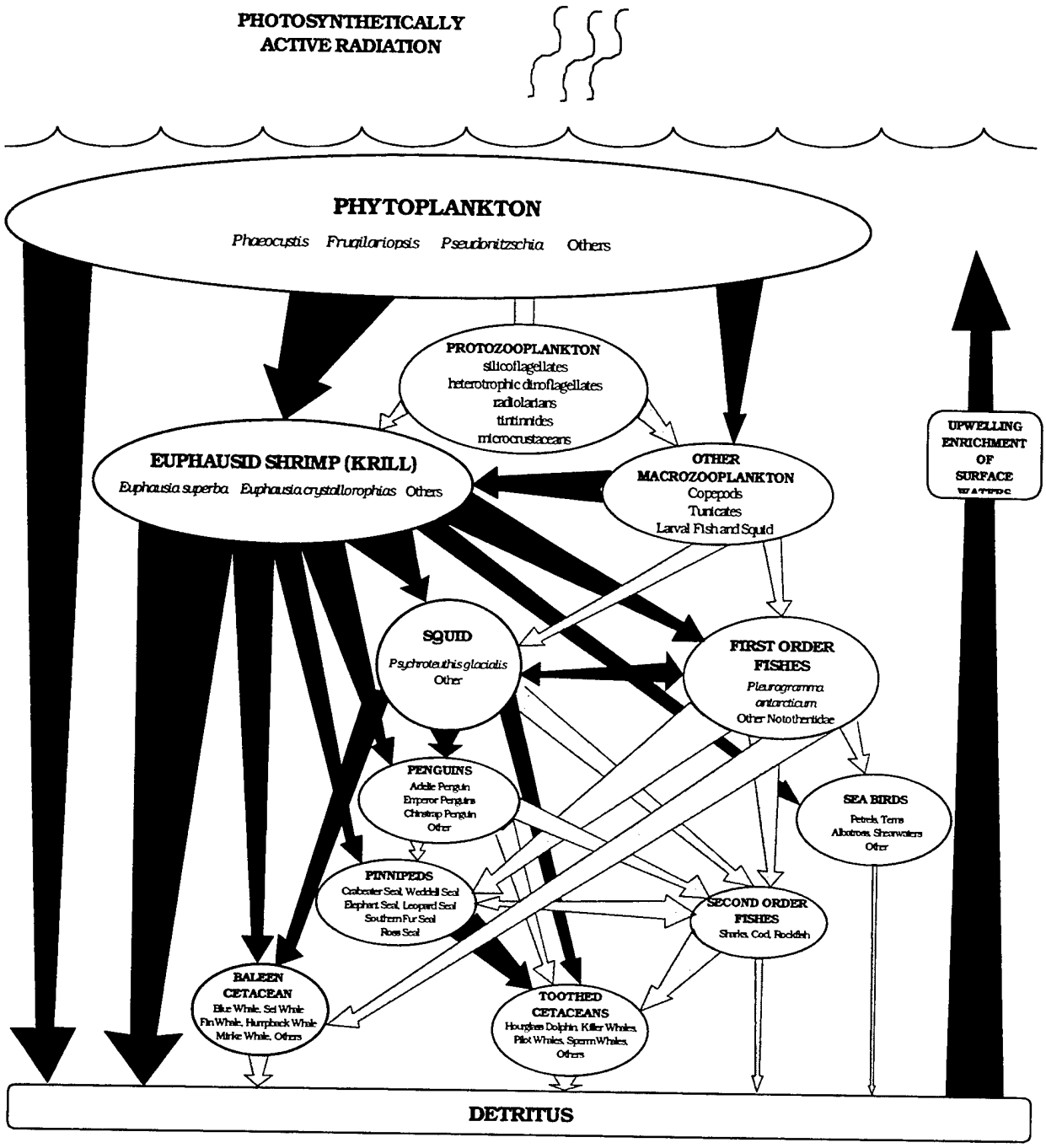

Figure 4.1-9. Pelagic food web of the Antarctic region. The open-water food web of the Antarctic is supported by high seasonal productivity of phytoplankton and secondary productivity of krill. Of note is the short trophic linkage between primary producers and even the highest level consumers. Dark arrows indicate the most significant linkages within the trophic web.

Only 11 avian species dominate the Antarctic region, with most of these being penguins and petrels (Prevost, 1981). An additional 35 species are found in the subantarctic region. The avifauna of the Southern Oceans and Antarctic continent have an estimated population of 350 million, 52% of which are penguins (Defense Mapping Agency, 1992). The numerically dominant penguin species include the Adelie penguin (*Pygoscelis adeliae*), the chinstrap penguin (*Pygoscelis Antarctica*), and the emperor penguin (*Aptenodytes forsteri*). These species feed largely on krill, small fish, and squid. Other species of penguins occurring in the region include the king (*Aptenodytes patagonicus*), rockhopper (*Eudyptes chrysocome*), macaroni (*Eudyptes chrysolophus*), and gentoo (*Pygoscelis papua*) penguins. Dominant seabird species include the Antarctic petrel (*Thalassoica Antarctica*), albatross (*Diomedea* spp.), and prion (*Pachyptila* spp.). In addition, several other species of petrels, shearwaters (*Puffinus* spp.), skua, cormorants, gulls (*Larus* spp.), and terns (*Sterna* spp.) are also present. Seabirds of the Antarctic forage mostly on krill, small fish, and squid. Prevost (1981) has estimated that penguins and seabird species consume 32 million tons of krill during the summer months. This is the equivalent of 10% of all krill available in Antarctic waters in the austral summer.

Six species of seals are found to occur in the Antarctic region. The most abundant of these, the crabeater seal (*Lobodon carcinophagus*), has an estimated population of 30 million. It is found in ice flow areas and feeds exclusively on krill. The Weddell seal (*Ommatophoca rossii*) has an estimated population of 1 million. It feeds primarily on notothenioid fish but has also been known to eat squid and krill (Ekau, 1990). The elephant seal (*Mirounga leonina*) has an estimated world population of 600,000, over half of which breeds on the island of South Georgia (McConnell et al., 1992). Gut content analyses have shown that these seals feed largely on cephalopods, including demersal squid and benthic octopods, and fish (McConnell et al., 1992). The leopard seal (*Hydrurga leptonyx*), which has an estimated population of 500,000, feeds primarily on krill and fish, but is also known to feed on penguins and even other seals. The Ross seal (*Ommatophoca rossii*) and Southern fur seal (*Arctocephalus gazella*) are thought to have populations of 200,000 each and feed on cephalopods, fish, and krill (Defense Mapping Agency, 1992).

Seven species of baleen whales occur at the top of the Antarctic pelagic food web and are as little as one trophic level removed from the primary producers. Feeding predominantly on the huge standing crop of krill occurring in Antarctic waters during the austral summer, migrating baleen cetaceans are more numerous in Antarctic waters than anywhere else in the world. In addition to consuming krill, these whales also eat large volumes of squid and a lesser volume of fish. Over the approximately 4 month summer stay in these waters, baleen whales can increase in weight by as much as 50 percent (Defense Mapping Agency, 1992). An adult blue whale can consume as much as 400 kg of krill per day over the course of a 120-day summer stay in the Antarctic region (Knox, 1994). The predominant species occurring within these waters include the blue (*Balaenoptera musculus*), fin (*B. physalus*), sei (*B. borealis*), humpback (*Megaptera novaeangeliae*), and minke (*B. acutirostrata*) whales. Also occurring to a lesser extent are the southern right whales (*Eubalaena australis*), a species typically found in temperate waters (Defense Mapping Agency, 1992).

Toothed cetaceans including whales and dolphins exist at the highest trophic level as the top carnivores. Consuming mostly fish, squid, penguins, and seals, these predators tend to occur along the edges of the ice pack. Twelve species of toothed whales occur in the waters of the Southern Ocean. The sperm whale (*Physeter macrocephalus*) is the largest of the toothed whales, numbers approximately 500,000, and feeds almost exclusively on squid. A number of smaller toothed whales, including the killer whale (*Orcinus orca*) and pilot whale (*Globicephala melaena*), as well as several species of dolphins, have diets comprised of various marine species including fish, seals, penguins, and only rarely, other cetaceans (Stonehouse, 1965; Defense Mapping Agency, 1992).

Benthic Food Web. The vertical zonation of the benthic community of coastal and shelf Antarctic waters, including both epifaunal and infaunal organisms and algae, is governed largely by physical disturbance. The shallow benthos of the Antarctic is seasonally disturbed by the formation of anchor ice, and the presence of ice scour. Therefore, relatively few species of sessile organisms and algae are able to survive in the shallow zone (0 to 33 m). This leaves the area bare with the exception of small numbers of motile predators and scavengers (Dayton et al., 1974). However, below 33 m, a unique benthic community exists that is rich in both biomass and density (Figure 4.1-10).

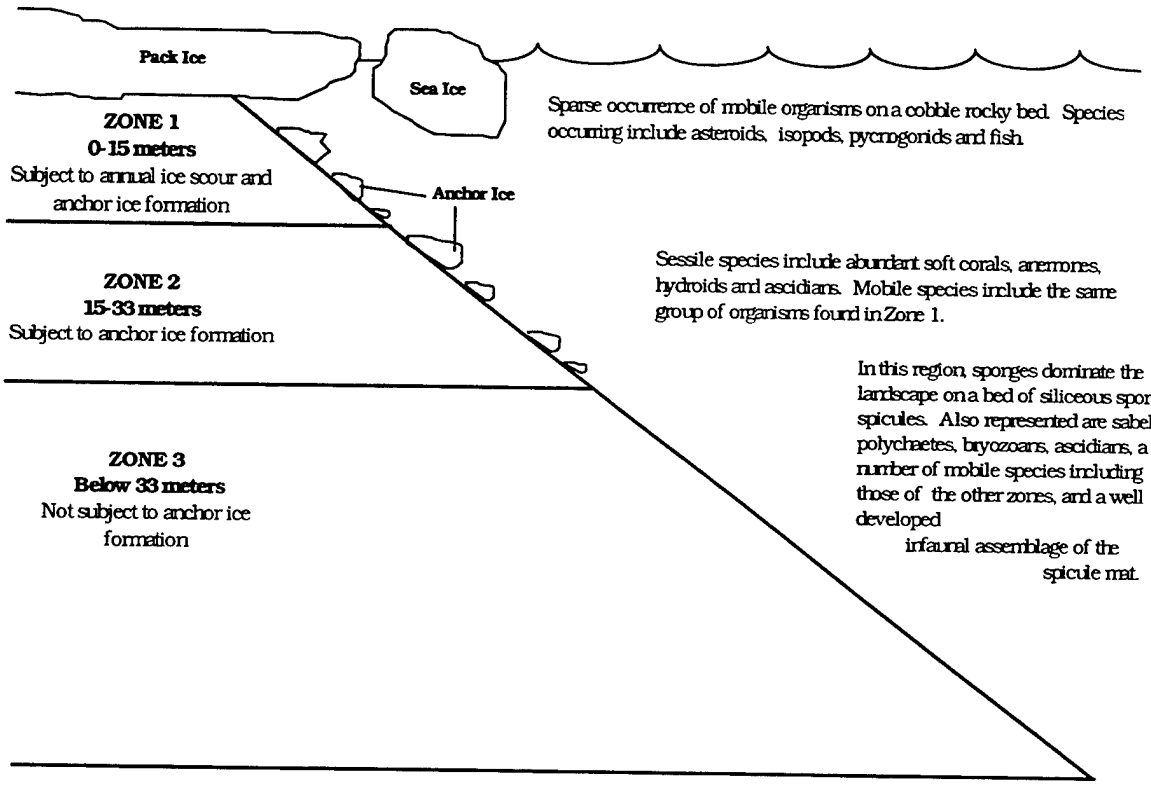

Figure 4.1-10. Antarctic Benthic Zonation. Benthic habitats along the continental and island areas are structured by the action of ice on the bottom. At McMurdo Sound, Dayton et al. (1970) described three zones which are governed by seasonal ice scour and the formation of anchor ice.

Approximately 700 species of macroalgae, belonging to 300 genera, are known to occur in the Southern Ocean, with 35% of the known species being endemic to the region (Knox, 1994). Algae growing in the ice scour and anchor ice zone are calcareous red algae, encrusting lichens, and brown algae that occupy crevices. Below the shallow ice zone, however, species richness and density of algae increases. Dominant species in the McMurdo Sound include shallow-growing species of *Iridaea* and *Leptosomia*, the deeper-growing species of *Desmarestia*, and the large, brown algae, *Himanothallus grandifolius* which occurs to depths of 50 m (Knox, 1994). Another large, brown algae common to the area is *Adenocystis utricularis* (Picken, 1985). Green algae species present include *Enteromorpha* spp., *Ulothrix* spp., and *Cladophora* spp. (Picken, 1985). The microalgal community consists of species that grow in the top few centimeters of the sediment, and species that are epiphytic, growing on rocks or macroalgal species. Limited studies of microalgae have been conducted. However, one study, conducted in the

South Orkney Islands, showed that benthic microalgal chlorophyll levels varied seasonally; the benthic primary productivity rate in the region ranged from 700.9 $mgC \cdot m^{-2} \cdot d^{-1}$ in December to 313.4 $mgC \cdot m^{-2} \cdot d^{-1}$ in July (Knox, 1994).

The deeper benthic faunal community is fed primarily by a detrital rain which emerges from the pelagic trophic web (Figure 4.1-11). This detritus feeds a deepwater protozooplankton assemblage, as well as a highly developed community of sessile filter feeders dominated by sponges. It has been estimated that the average biomass of benthos within shelf areas above 500 m may be as high as 400 to 500 $grams \cdot m^{-2}$ (Defense Mapping Agency, 1992). The low inorganic sedimentation rates and clear waters of the polar seas, combined with the dependent seasonal inputs of detrital rain are the primary factors which allow for the development of such a substantial filter-feeding and suspension feeding community (Dell, 1965).

Approximately 300 species of sponges, the majority of which are siliceous rather than calcareous, are known to occur in the Southern Ocean (Picken, 1985). In the McMurdo Sound region of the Ross Sea, for example, large colonies of sponges cover almost 55% of the benthic surface area and provide the majority of the vertical structure of the community (Dayton et al., 1974). Twenty-one species of sponges have been identified in the McMurdo Sound region, including *Rossella racovitzae*, several species of volcano sponges, and the fast-growing *Mycale acerata* (Dayton et al., 1974). Sponge communities, which thrive in hard substrate environments and often rest on a mat of glassy spicules, provide a kind of "second floor" for other benthic organisms by acting as refuge from predators and by providing elevated perches from which other organisms search for food (Gerdes et al., 1992). Other groups comprising the filter-feeding community are bryozoans, hydroids, actinians, gorgonaceans (including *Primnoela* spp.), tunicates, coldwater corals, and bivalves (dominated by *Limatula hodgsoni*, *Laternula elliptica*, and *Adamussium colbecki*) (Dell, 1965). Suspension-feeders include several species of ophiuroids and tubiculous polychaetes.

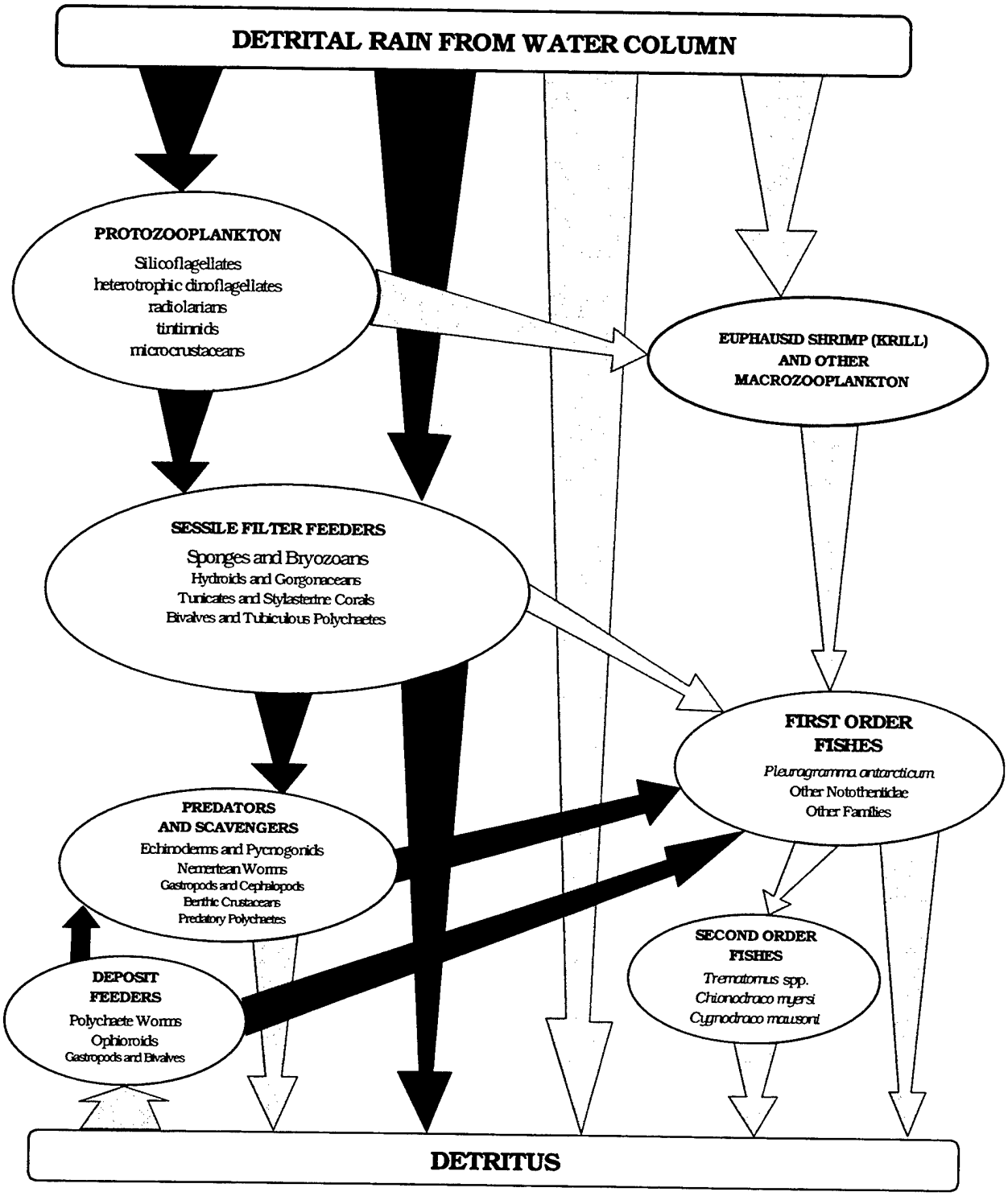

Figure 4.1-11. Benthic food web of the Antarctic region. The benthic trophic web of the Antarctic is supported predominantly by detrital rain from the pelagic system. Sessile suspension and filter feeders dominate the system and create both a food source and structured habitat for a number of opportunist as well as specialist consumers. Dark arrows indicate the most significant linkages within the trophic web.

The predators and scavengers of the Antarctic benthic community occur in low densities and have broad diets (Dayton et al., 1974). The majority of species are opportunistic and feed on sessile algae and sponges, other predators, detritus, and even suspended particulate matter. Scavengers, which feed largely on detritus, include crustaceans (isopods and amphipods), ophiuroids, and gastropods. Only eight species of decapod crustaceans exist in the Antarctic region, and all belong to the Natantia family (shrimp); no members of the Reptantia family (crabs and crayfish) have been observed (Arntz and Gorny, 1991). Isopods and amphipods are well represented and are often large in size; the isopod, *Glyptonotus antarcticus* can attain a length of 12 cm. Ophiuroids are abundant in the Antarctic region and have been well-documented in bottom photographs (Dell, 1965; Hedgpeth, 1971). Densities of these organisms have been reported to be as high as 100 million individuals per km^2 in the Ross Sea (Picken, 1985). Ophiuroids are opportunistic feeders and have been observed to grab prey from the water column, extend arms in order to collect suspended matter, and sift through bottom substrate in search of detritus.

As mentioned above, larger predators of the Antarctic region are often opportunistic feeders and will graze on sessile organisms and detritus, as well as hunt for motile prey. Dayton et al. (1974) identified several species of asteroids as predators in the McMurdo Sound. Dominant species include *Acodontaster conspicuus*, and *Odontaster validus*, a smaller species that preys on larval and adult *Acodontaster*. Large nemertean worms, pycnogonids, holothurians, and approximately 12 species of octopods are other predaceous species known to occur in the region. Additionally, many deeper water demersal fish forage on benthic fauna including crustaceans, polychaetes, and molluscs.

UNIQUE SPECIES AND ECOLOGICAL CONSIDERATIONS

Endangered/Threatened or Protected Species and Critical Habitat. The Antarctic region is home to several threatened and protected animal species. As mentioned earlier, whaling practices and fur trade during the 19th century decimated the populations of cetaceans and fur and elephant seals in the Antarctic. It is estimated that the fin whale population has been reduced from 400,000 to 90,000 while the blue whale population has been reduced from 200,000 to 2000 and humpback whales from 100,000 to 3000 (Defense Mapping Agency, 1992). Additionally, sperm and sei whales, which are still harvested, have populations that are currently half of what they were in the last century. The southern fur seal, the elephant seal, and the Ross seal now have special protected status and are no longer hunted. No critical habitat has been designated within the Antarctic.

Unique Ecological Phenomena. The Antarctic region is unique in its rich secondary productivity and an extremely short trophic web which is heavily reliant on krill. The majority of species that occur in the Antarctic depend directly on krill or supplement their diet, to varying degrees, with krill. As a result of the key role that krill play within the Antarctic, effects to these organisms can have the single greatest impact on the overall structure and stability of the entire system. A substantial decrease in the biomass of krill would affect the populations and feeding habits of fish, penguins and other seabirds, cetaceans, and pinnipeds, and would decrease the flow of detritus to the benthic food web.

Secondary to the interesting pelagic trophic web is the occurrence of the extensive benthic sponge community. Low sediment input and consumable detrital rain has lead to the development of an uncharacteristically well-developed sponge community. Relative environmental stability is critical to the maintenance of this system since modification of either the available nutrient influx or an increase in non-consumable sedimentation may either starve or smother the benthic organisms.

Important Breeding, Nursery, or Aggregation Areas. Surrounding the permanent Antarctic ice zone is the marginal or seasonal ice zone that consists of pack ice that partially thaws during the summer months and re-freezes during the winter months. This seasonal ice zone is an important ecological area. The majority of bird and mammal species known to occur in Antarctica inhabit the coastal areas of the continent, and utilize the rocky coastal areas and pack ice as breeding and loafing grounds. The abundant populations of krill, cephalopods, and fish in the adjacent waters are an easily accessible food source for pinnipeds, and penguins and other seabirds.

Additionally, as discussed earlier, large phytoplankton blooms are known to occur in the marginal ice zone. As the ice melts, the water temperature rises and a stable water layer forms that is ideal for large blooms. Swarms of krill, that live under the pack ice during the winter months, inhabit the marginal ice zone and feed on the phytoplankton blooms during the spring and early summer months. This highly productive marginal region is particularly relevant in that the ice pack can often extend well beyond the 12 nmi waste discharge restricted zone.

BALTIC SEA

PHYSICAL AND CHEMICAL CONSIDERATIONS

Geography and Physiography. The Baltic Sea, accessed via the North Sea through the narrow Danish Straits, is a shallow inland sea separating Denmark and Sweden on the west from Finland, Estonia, Latvia, Lithuania and Poland to the east and south. This remarkably brackish boreal seaway extends from Bothnian Bay at almost 66° North latitude southeast to the Bornholm Sea at 54° North latitude. It extends from 10° East longitude at the Danish Straits as far east as the Gulf of Finland at 30° East longitude (Figure 4.1-12). Three major basins, from the Bay of Bothnia in the north, through the Bothnian Sea and Baltic Sea proper in the south, comprise the Baltic; the narrow, elongate Gulf of Finland projects almost 500 kilometers to the northeast. To the east, the symmetrical Gulf of Riga extends almost 200 kilometers from the geographic center of the Baltic area. In total, the Baltic Sea covers 370,000 km^2 (Fitzmaurice, 1993).

Over 200 streams empty into the Baltic with eight of the major fluvial systems discharging a total of 6,890 $m^3 \cdot s^{-1}$ into the sea. Of these the largest are the Neva River (2,530 $m^3 \cdot s^{-1}$) at the extreme eastern margin of the Gulf of Finland, and the Vistula (1,030 $m^3 \cdot s^{-1}$) which empty into the Baltic proper from the south (Kaasik, 1989). Measuring 1.6 million square kilometers, the Baltic watershed covers slightly less than four times the areal extent of the Baltic Sea. The elongate north-south configuration of the seaway dictates substantial climatological variation throughout the area. On an annual basis, sea ice extends well southward, covering the Bothnian Sea, the central Baltic, and all of the Gulf of Finland. During the harshest of winters, the entire sea may be covered in ice.

Rocky coasts characterize most of the Sea's northern margins, and in the central Baltic, hundreds of islands dot the water's surface. Sandy beaches are common along the German coast. Despite its relatively shallow depths, the Baltic displays a rugged bathymetry across the floor of the basin where the physiography rivals that of the adjacent coastal vicinity (Winterhalter et al., 1981).

Geologically, the Baltic is extremely young. Its origins date less than 10,000 years ago when water filled a shallow basin recently vacated by massive continental glaciers. Three by-products of the extreme youth of the Baltic basin are glacial rebound, steadily increasing salinity, and extremely low biodiversity, even for a high-latitude marine water mass. Glacial rebound in Finland is as high as 9 $mm \cdot yr^{-1}$ where the crust is still rising after being buried under kilometers of ice for hundreds of thousands of years (Kaasik, 1989; Winterhalter et al., 1981). A striking aspect of this seaway, however, is the short residence time for water. Estimates for complete recycling of the limited volume of water in the Baltic Sea range from 20 to 40 years (Kaasik, 1989; Chadwick et al., 1996; Fitzmaurice, 1993; Zmudzinski, 1989; Thurow, 1989).

Figure 4.1-12. Baltic Sea region. The Baltic Sea is an extremely shallow inland sea which is separated from the North Sea by the island-dotted Danish Straits and a sill depth of only 8 m. A number of smaller basins separated by shallow sills and island archipelagos, comprise the sea; brackish condiions of the waterway are dictated by the numerous large rivers which flow to the Baltic.

Bathymetry. The Baltic Sea is very shallow, with most depths falling well below 100 m for most of the southern region. Shallower mean depths of 68 m and 43 m are found in the northern regions, including the Bothnian Sea and Bothnian Bay respectively. The gulfs of Riga and Finland average 28 and 38 m, respectively (Winterhalter et al., 1981). Maximum depths of the Baltic occur in limited geographic areas including the Gotland Deep (80 km east of Gotland) at 245 meters, the Landsort Deep (north of Gotland) at 459 meters, the Åland Sea at 300 meters, and the Harnosand Deep (northern part of the Bothnian Sea) at 230 meters. The average depth for the Baltic, which covers a total of 0.4 million square kilometers, is 52 meters and the volume is estimated at 22 thousand cubic kilometers (Jansson, 1972; Kaasik, 1989). The channel at the Danish straits is only 18 m deep while the basin's sill depth between Denmark and Sweden (The Darss Sill) is a mere 8 m. The sill depth between the Bothnian Sea and Bothnian Bay is 75 meters (Figure 4.1-12). Because of its shallow geometry, the Baltic accounts for 0.1% of the surface area of the world's oceans, but only 0.002% of their volume (Kaasik, 1989).

Currents, Tides, and Water Exchange. Excess fresh water supply dictates that permanent circulation in the Baltic is weak and most surface water velocities are only a few $cm \cdot s^{-1}$; velocities of subsurface waters are even less. Counterclockwise gyres in the Bothnian Sea and Bothnian Bay are poorly defined along the west coast but are more persistent on the east coast due to fluvial runoff and Coriolis effects. Even with the characteristic strong storm systems of the Baltic, average winds are weak and circulation is dominated by estuarine and thermohaline forces (Ehlin, 1981). Although some authors regard the Baltic as tideless owing to its extremely shallow nature, tidal flow is present, but very subdued, with both a mixed and diurnal characteristic and flow rates averaging 1 $cm \cdot s^{-1}$ (Thurow, 1989; Defense Mapping Agency, 1990; Kullenberg, 1981).

Water exchange for this seaway is a complex response to fluvial inflow, precipitation, and transport through the Danish Sound. Within the narrow Danish Sound there is an outflow of surface brackish water that varies from 8 ppt in the Baltic and increases to as high as 29 ppt in the northeast part of the North Sea after mixing has occurred (Figure 4.1-13). Deep transport across the sill back into the Baltic originates with North Sea water that has an approximate salinity of 34 ppt; salinities decrease to 17 ppt on the floor of the Baltic after mixing (Fitzmaurice, 1993; Ehlin, 1981). Sills in the Baltic impede deep circulation and much of the ocean bottom is relatively stagnant.

Temperature and Salinity. Hydrographic isolation and the wide latitudinal range of the Baltic results in a highly variable temperature/salinity profile. During the warmest month, the mean surface temperature of the Baltic is approximately 16°C (Jansson, 1972). Mean summer surface temperatures range from 14°C in Bothnian Bay to 18°C in the southern part of the Baltic proper while protected bays may have temperatures as high as 21°C. To the south, winter temperatures are approximately 1 to 2°C. The Bothnian Sea generally freezes over by early January; however, in severe years all but the southeastern Baltic freezes over. Empirically, higher temperatures are accompanied by higher salinity in the Baltic as fluvial mixing takes place primarily in surface waters. A strong summer thermocline develops in the Baltic proper at a depth of about 30 m (Kullenberg, 1981).

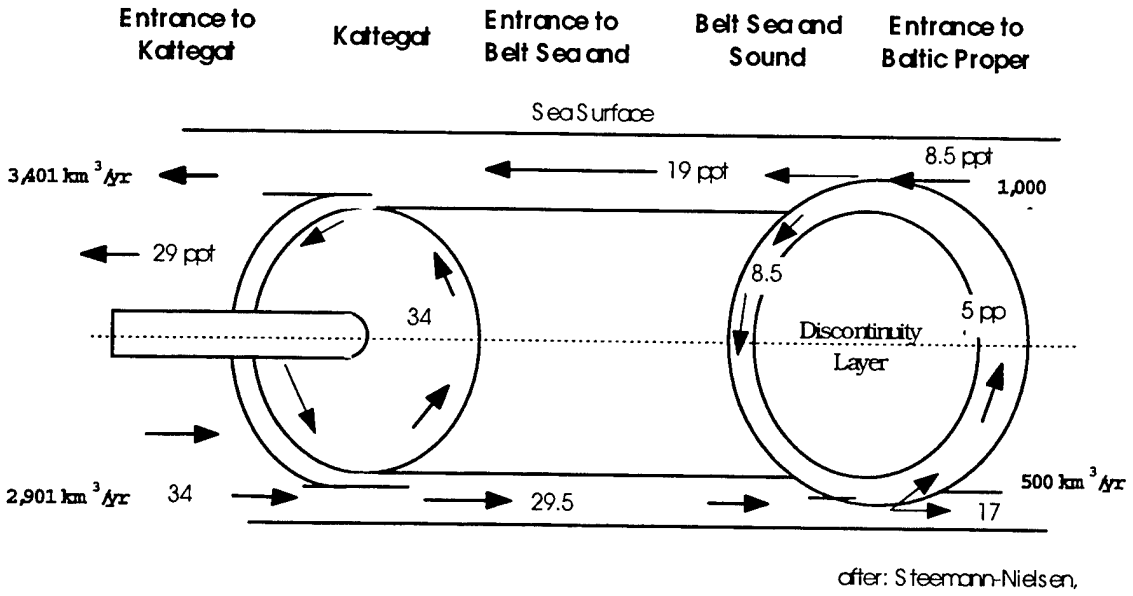

Figure 4.1-13. Schematic representation of the volume and salinity of water exchanged between the Baltic Sea and the North Sea. Strong salinity gradients and prevailing winds create a complex circulation pattern in which brackish water flows out at the surface while more saline water flows inward near the bottom.

Salinity stratification in the Baltic is permanent and throughout the area fresh-water inflow far exceeds evaporation. A permanent halocline 10 to 20 m thick occurs between 30 and 80 m, separating surface brackish layers from the deep saline interval (Kullenberg, 1981). Surface salinities vary from highs of 30 ppt in the Kattegat area between Denmark and Sweden, to 6 ppt in the central Baltic proper, down to 0.5 ppt in the Gulf of Finland and Bothnian Bay (Figure 4.1-14) (Jansson, 1972; Defense Mapping Agency, 1990). When the summer thermocline coincides with the location of a defined halocline, a strong density boundary (pycnocline) may form, creating an isolation of surface and deeper lying water masses and an impediment to settling of low density particulate matter.

One possible consequence of the relative youth of the Baltic Sea is the apparent long-term flux in salinity. Data from the past century suggest a slow increase in mean salinity values over the entire watermass although the process may be reversed in cycles up to 20 years in length (Zmudzinski, 1989).

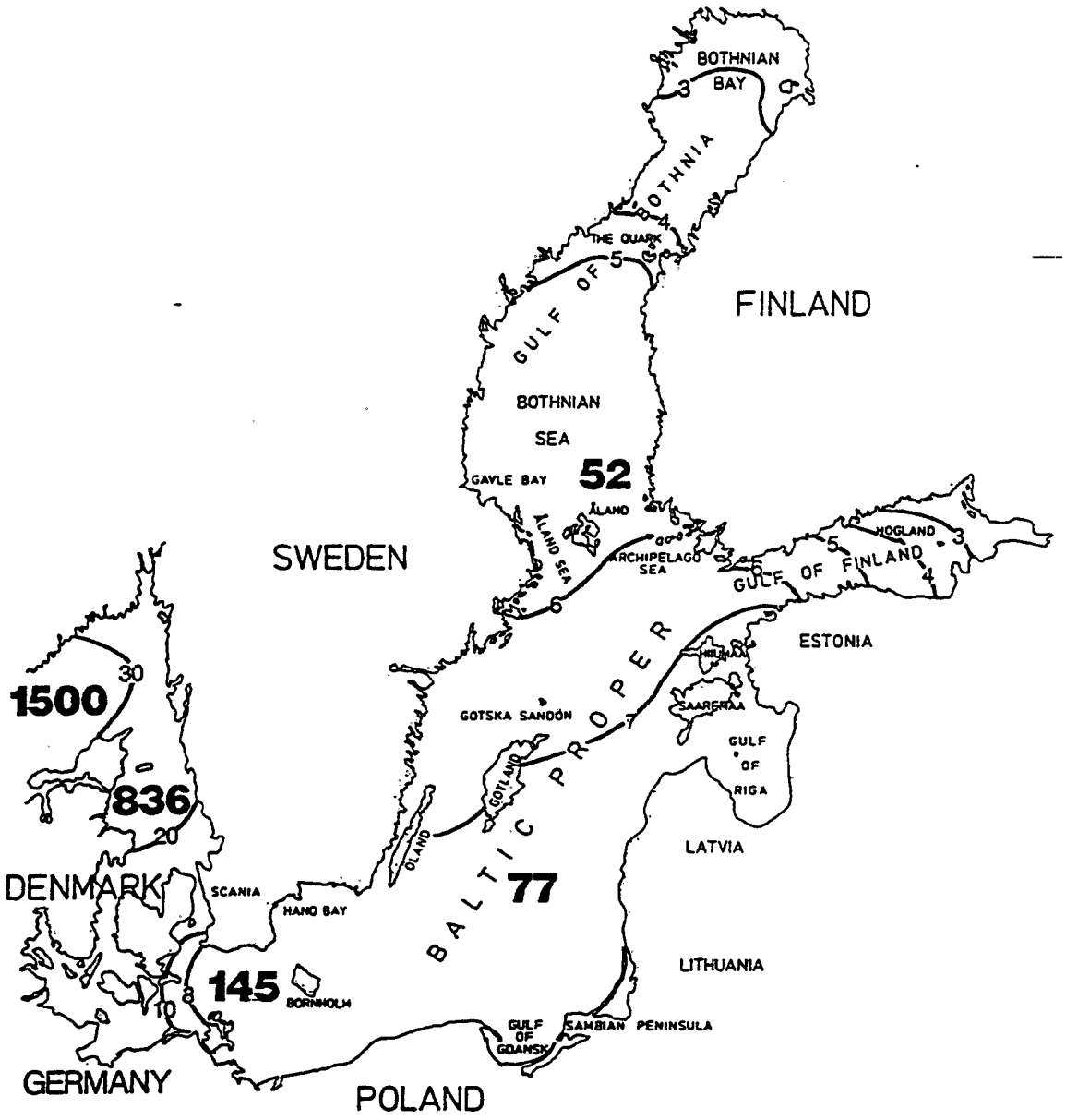

Figure 4.1-14. Salinity gradient and species richness of the Baltic Sea. Reaching conditions at or near fresh water conditions in the northern end of the Bothnian Bay and the eastern extreme of the Gulf of Finland, the Baltic Sea is a massive brackish watermass (isocline salinities in ppt). Species richness of the sea is extremely low with a maximum number of marine macrofauna species only reaching 145 at the southern end of the Baltic Sea near its connection to the North Sea (bold numbers).

Dissolved Oxygen. Periods of critical oxygen deficiency occur in the Baltic and short-term as well as intermediate period cyclic patterns exist. However, the apparent steady decline of dissolved oxygen within the deep waters of Gotland Deep and the Bothnian Sea from the 1890's through at least the late 1970s has been more alarming (Grasshoff and Voipio, 1981). A demonstrated trend in declining dissolved oxygen has received considerable attention in recent years (Kullenberg, 1983). The relative isolation of the deep Baltic basins by shallow sills and strong haloclines results in stagnation of the lower watermass. Organic material sinking from the euphotic zone and deposited organic sediments oxidize and consume available oxygen to the point of creating anaerobic reducing conditions under which hydrogen sulfide is produced. During periodic infusions of oxygen-rich bottom waters from the North Sea, much of the available oxygen is exhausted in oxidation of the accumulated hydrogen sulfide, leaving little for aerobic biological activity (Kullenberg, 1983).

While the reason for dissolved oxygen declines remains unclear, it is possible that the declines are related to either the natural increase in salinity which has been occurring since the formation of the Baltic, or an anthropogenic increase in organic inputs. While both factors may be operative, it is clear that the trend towards lower oxygen levels in deep basins has prevailed for at least the last century (Kullenberg, 1983). The cyclical development of increasingly anaerobic conditions within the Baltic suggest that deeper basins may eventually reflect conditions comparable to those seen in the Black Sea.

Baltic Sedimentation. Unconsolidated sediments on the floor of the Baltic conform to the classic pattern of coarse sediment (sand, gravel) in shallow, high-energy areas near the strands to increasingly finer grained material deep in the basins. The deepest areas at the bottom of discreet silled basins, well below the permanent halocline and wave base, display a layer of very fine clay mud (Winterhalter et al., 1981). Owing to the inherently aggressive nature of glacial erosion, most of the loose sediment in the Baltic Sea is of primary or secondary glacial origin, being vectored into the basin by fluvial systems. The average rate of sedimentation estimated over the entire Baltic Sea is approximately 0.079 $mm \cdot yr^{-1}$ with active areas being estimated to deposit 0.14 $mm \cdot yr^{-1}$ based on sediment loads in the water column (Winterhalter et al., 1981). Sedimentation rates within basins regions of Gotland Deep have been estimated by multiple means to be approximately 1 $mm \cdot yr^{-1}$ (Winterhalter et al., 1981). In coastal regions and enclosed embayments, sedimentation rates have been reported as high as 10 $mm \cdot yr^{-1}$. Pelagic diatoms characteristic of brackish environments undergo frequent blooms, augmenting offshore sediments with significant amounts of opaline silica after the plants die and the empty frustules (shells) settle to the bottom.

CURRENT ENVIRONMENTAL STRESSES

Marine Pollution. Over 70 million people live in the watersheds that feed into the Baltic Sea. The entire ocean rim is heavily industrialized with a wide variety of enterprises ranging from paper pulp mills, to chemical and metal refining operations, to mining and fossil fuel plants. In addition to toxins of every description and concentration, sewage and agricultural fertilizers supply the Baltic with a steady supply of nutrients (Grasshoff and Voipio, 1981; Cederwall and Elmgren, 1990; Zmudzinski, 1989). The political and socioeconomic structure of almost a dozen independent nations situated around the basin adds to the difficulty of controlling pollution.

Sewage is a major pollutant in the Belt Sea between Denmark and Sweden and in the Oresund area just to the east. The estimated discharge volume of domestic sewage alone exceeds 4.5 million cubic meters per day with much of this being untreated or receiving only primary treatment (Dybern and Fonselius, 1981). Nutrient inputs result in all coastal areas suffering heavy phytoplankton blooms during the

summer months. Forest industry products, mainly paper pulp and associated pollutants, characterize the margins of the Bothnian Sea and Bothnian Bay, as well as the Gulf of Finland. Industrially produced organochlorine compounds (*eg.*, DDT, HCB, PCBs) are found in toxic quantities throughout the Baltic and low temperatures of the water mass may retard the decomposition of these pollutants. Recent offshore dredging operations near Finland have apparently reintroduced into the environment organochlorine compounds that lay previously buried in coastal sand and gravel deposits (Defense Mapping Agency, 1990). Industrial production has also instilled alarming quantities of heavy metals into Baltic Sea waters and sediments. The latter pollutants eventually become concentrated in the tissue of fish, seals, and mussels.

The enclosed basin geography and low water temperatures aggravate the problems of petroleum spills and recovery. To date, the Baltic has not produced large amounts of commercial oil, but coastal refineries and oil transport by tankers have caused an ongoing, persistent problem with spills. Certainly one of the most curious anecdotes of pollution in the Baltic has to be the ongoing accidental recovery of explosive and mustard gas artillery shells dumped off Denmark after World War II (Dybern and Fonselius, 1981). In this case, ordinance disposed of over a half century ago is regularly exhumed by deep-dredge fishing operations, often with disastrous results.

Sea Traffic and Ports. As a main passage between the nations around the Baltic and the North Atlantic, the shipping lanes of the Baltic Sea are among the most heavily traveled in the world. For five Baltic nations, these shipping lanes represent the sole nautical link to global markets. However, for a portion of the year (late October through early March), approximately two thirds of the seaway is frozen over. Therefore, traffic is intensified during the spring, summer and fall months. Although shipping lanes have been long established within the Baltic, strict traffic lanes and speeds have recently been designated for the largest tankers and container ships due to increasing tanker collisions and spills in the area.

For most of the year, there are three possible routes to enter the Baltic Sea (Defense Mapping Agency, 1990). The most direct route lies between the island of Sjaelland and the Swedish coast. This is most favorable and passes by the Danish capital city of Kobenhavn. A central route between the islands of Sjaelland and Fyn is used by larger boats due to the depth of the channel. A very western route that passes between the Danish peninsula and the island of Fyn is rather shallow and is mainly used by local traffic. From January through March, the entrance may be completely blocked by ice, restricting all sea traffic from the Baltic Sea. The ports with the highest volume of sea traffic include Kobenhavn, Swinoujscie, Gdynia, Gdansk, Klaipeda, Liepaja, Riga, Leningrad, and Stockholm. The Soviet ports of Leningrad, Vysotsk, Vyborg, Tallinn, Novotallinskiy, Parnu, Riga, Ventspils, and Klaitpeda are open to calls by foreign vessels (Defense Mapping Agency, 1990).

FISHERIES AND AQUACULTURE RESOURCES

For commercial fishing, dredge nets, fixed nets, drift nets, dragnets, seines, lines, and wiers are all used. Although the fishery industry in the Baltic Sea is minimal, the largest concentration of vessels (mainly using drift nets) is found off the east coast of Gotland from June through November and in the early spring. In addition, trawling occurs throughout the year off the coasts of Oland, Gotland, St. Petersburg, and Bornholm. The diversity of fish and invertebrates in the Baltic is remarkably low. This is apparently due to the extreme youthfulness of the basin in geologic terms. The Baltic has been a major fishing are since the 12th century when herring were caught and processed (salted) for sale all over Europe. Salmon fishing was especially well established in the 1920s. Over 90 thousand tons of fish of several species

were recovered annually in the early 20th century. Mid-water trawling for herring, cod, and sprat began in the 1940s and continues today. Today, about 0.75 million tons of fish are taken annually in the Baltic region (Greenpeace: The Baltic, 1992). Herring, cod, and sprat are the most commercially important species, while flounder, salmon, ocean perch, and vendace make up the remainder of the large catch numbers.

Recently, catches have diminished due to the evolution of advanced fishing strategies, such as purse seines and trawls, that catch large quantities of fish, many of which are still in juvenile development stages. Reliable figures for catch tonnage only became available in 1970 and estimated Baltic fish stocks diminished by almost one-third, from 6.9 to 5 million tons, between 1970 and 1985 (Fitzmaurice, 1992). A clear trend in fisheries has been the development of more efficient fishing strategies followed by a surge in catches and, finally, a near crash in the stocks as overfishing ensues. The 1973 Gdansk Convention set guidelines for Baltic fishing in the form of quotas for each country, but the program began to collapse as figures set by political pressure were far above those recommended by biologists to maintain a sustained yield. As quotas were pushed ever higher, stocks began to collapse and in 1991 no quota was set for cod.

The history of the salmon fishery in the Baltic mimics that of the American Pacific Northwest. In 1927 fall fishing on a single estuary in Lithuania yielded 1000 fish daily with an average weight of almost 20 kg. However, scores of streams once available for spawning at the turn of the century have been destroyed by pollution and hydroelectric dams. By the 1980s, only a handful of streams had a sustained salmon life cycle and hatchery fish production has helped the once bountiful fishery recover only slightly.

Phytoplankton. A combination of high latitude and the geologically immature basin of the Baltic yields very low diversity figures for all major phytoplankton groups. The Baltic Sea experiences high seasonal variation in light levels and water temperatures, and phytoplankton blooms only occur during 4 to 5 months per year in the northern region (Bothnian Bay) and 9 to 10 months in the south (Baltic Sea proper). Primary productivity estimates are comparable to those for the Black Sea and range from 150 to 250 $gC \cdot m^{-2} \cdot yr^{-1}$ (Kullenberg, 1983). Productivity is governed in part by sea ice and nutrient level. The latter is regulated by fluvial inflow, waste water load, and phosphorous rich upwelling. During the winter, diatoms assemble under the ice imparting a characteristic yellow-brown coloration to the ice. Even with minimum light, *Chaetoceros* spp. and *Aphanizomenon* spp. blooms will develop. With sufficient light, vernal phytoplankton blooms dominated by "cold water" diatoms will develop (*eg.*, *Achnanthes* spp. *Melosira* spp. *Nitschia* spp. *Thalassiosira* spp.). Typically, dinoflagellates, such as the red-tide organism, *Gonyaulax catenataare*, are included in the bloom cycles.

Vernal bloom cycles begin in mid-April in the southern Baltic, in May in the central areas, and in June in the northern areas of Bothnian Bay (Hällfors et al., 1981). In the Baltic proper and Gulf of Finland, the low production stage begins in June and early July, but unlike earlier blooms, these are heavily regulated by consumers, principally the medusae, *Aurelia Aurita* and copepods. Blooms during this period consist primarily of diatoms, dinoflagellates, and blue-green algae, but typically diversity is low. Water clarity during the summer months drives the photic layer quite deep, however, little of the organic material produced reaches the bottom of the sea. Late summer, early fall blooms are rare, but are dominated by cryptomonads and large centric diatoms (*Actinocyclus* spp., *Cosinodiscus* spp.).

Zooplankton. Since it's origin less than 10,000 years ago, the Baltic basin has not had sufficient time for large numbers of endemic species to evolve. Intervals of catastrophic salinity flux from mid-range brackish to near fresh water conditions have characterized even the past 3000 to 4000 years and diversity

figures have remained very low. The number of zooplankton species in the Baltic is probably less than 60. Up to 95% of the Baltic biomass is made up of only six species of copepods, two rotifer species, two cladocerans, and one larvacean (Jansson, 1972). The medusa, *Aurelia aurita*, is also common among the surface waters of the Baltic. During the late summer and autumn *A. aurita* becomes extremely abundant to the degree that its biomass easily exceeds the sum of all other zooplankton species. Estimates of zooplankton biomass have been given at 1.1 $gC \cdot m^{-2} \cdot yr^{-1}$ with a production rate of 3.6 $gC \cdot m^{-2} \cdot yr^{-1}$ (Jansson, 1972). Often estimates of zooplankton production have been about 5 $gC \cdot m^{-2} \cdot yr^{-1}$ (Kullenberg, 1983).

The lack of species diversity in the Baltic is illustrated by the existence of relatively few species of copepods in the region. Approximately 800 species of copepods live in the world's oceans; however, only eight species are able to survive in the Baltic Sea. Yet, copepods remain one of the most important components of the Baltic food webs since they have a high productivity and relatively large standing stocks. Many of the copepods that exist in the Baltic are remarkably euryhaline. Species of the genera *Temora* and *Pseudocalanus* tolerate salinities as low as 6 ppt, while *Evande* spp. and *Pleopsis* exist in waters with salinities of 2 ppt (Hällfors et al., 1981).

The presence and distribution of a number of zooplankton species in the Baltic are affected by several physical factors. Temperature is an important factor in plankton life cycles and reproduction and biomass figures correspond well to temperature flux (Hällfors et al., 1981). Adaptability to salinity flux dictates, in part, the vertical distribution of plankton species. As a result, several species are confined to deep basins in the Baltic proper where salinity exceeds 14 to 15 ppt. Oxygen levels also controls, to a degree, distribution of plankton species and below the halocline area. With decreasing dissolved oxygen, diversity drops off drastically. During periods of anoxic bottom conditions characteristically deformed larval representatives of the taxon *Harmothoe sarsi* are present in bottom waters.

TROPHIC RELATIONSHIPS

Within the southern Baltic, less than 150 species of macroscopic fauna have been recorded and in the northern areas this number is reduced to 52 (Figure 4.1-15). Porifera and Echinoderms have no representatives in the Baltic, and the Bryozoa and Tunicates are known from only two to three species (Jansson, 1972). This is in contrast to approximately 1500 species of macroscopic marine animal species found in the adjacent North Sea at Skagerrak (Hällfors et al., 1981). The communities of the Baltic are extremely young and species depauperate. As such, trophic specialization has not occurred to any great degree and opportunism tends to dominate. Further, the extremely variable physical conditions of the surface watermass both on a seasonal and geographical basis also tend to support the development of opportunistic ecological strategies.

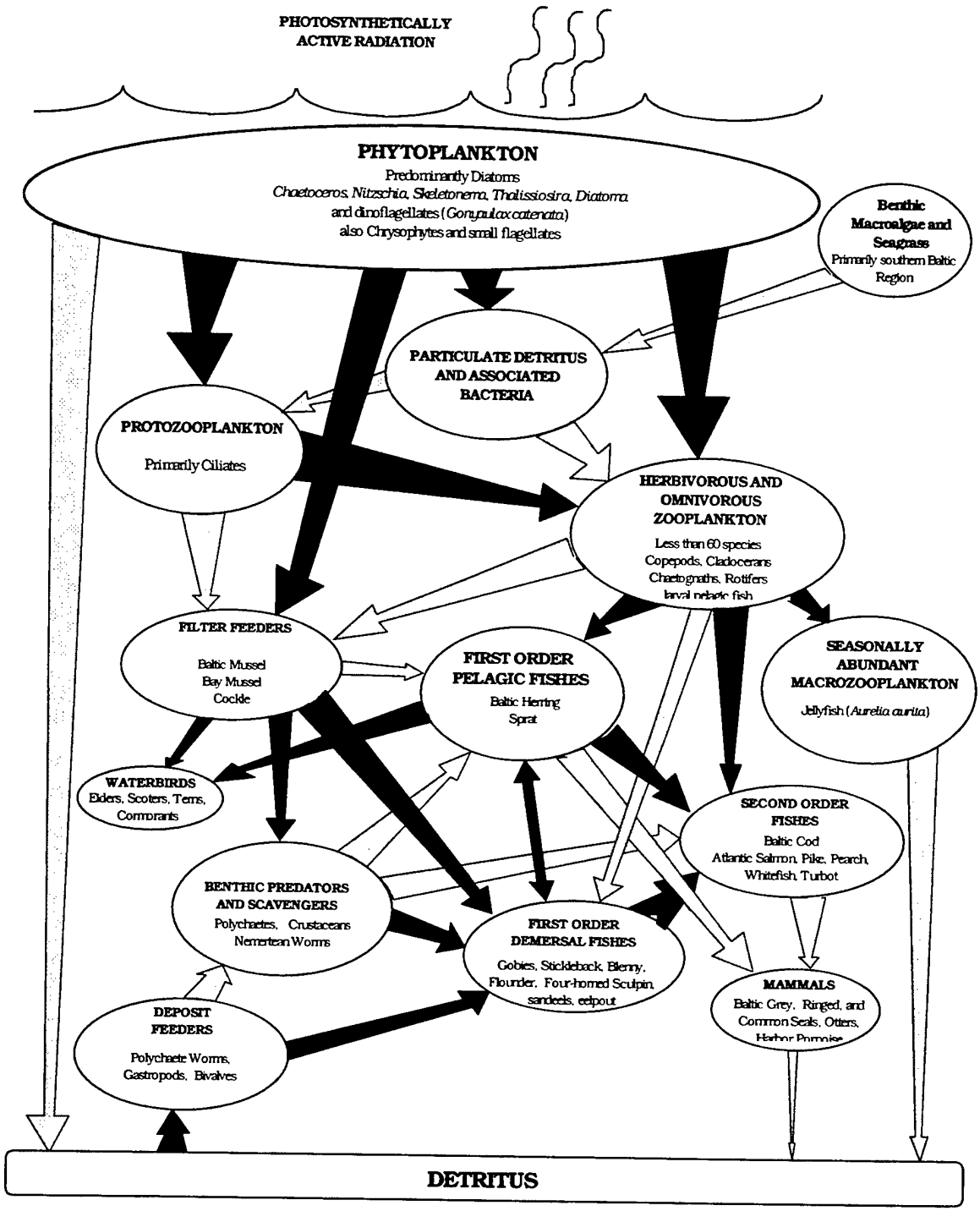

Figure 4.1-15. The Baltic Sea Trophic Web. The trophic assemblage of the Baltic Sea is marked by a complex web of opportunistic species surviving on seasonally cyclic phytoplankton production driven by riverine nutrient inputs and water temperature and light controls. Because of the euryhaline conditions persisting in the sea, not all species are represented in all regions. The trophic web presented has been simplified to reflect trophic group linkages and does not mean to infer that all species represented in a group are available at any given location.

Pelagic Food Web. The Baltic Sea region is defined by a marked seasonal pattern of primary productivity. In winter, primary production is heavily dominated by diatoms; in summer, by green algae and other organisms having short generation times and requiring high light levels; in the spring diatoms and dinoflagellates predominate, and in fall, the zooplankton biomass reaches its maximum. During the vernal bloom a large part of the primary production sinks to the bottom and is lost to the pelagic system.

Zooplankton support the pelagic fisheries and, as a result of tremendous seasonality, much of the fish fauna ecology is timed around plankton abundance. Pelagic fish fauna of the Baltic Sea are dominated by the spring and autumn herring and sprat recruitment. These fishes are smaller than their counterparts in the North Sea, generally due to a slower growth rate. Herring feed on copepod *nauplii* and plankton through the first year of life, later, plankton consumption decreases and is replaced by larger crustaceans (*Mysidae, Amphipoda*), and even fish (sprats, sticklebacks, etc.) for some populations of herring. Sprat larvae feed on eggs and young copepods, diatoms, and flagellates. Copepods are the most important food of sprat.

Due to the considerable variability in the physical environment of the Baltic, extreme mobility and the ability to switch between pelagic and demersal forage bases are critical to the pelagic fisheries. Fish distribution is seasonal and dependent upon species and physiological condition of the fish, food availability, temperature, salinity, and oxygen. Living in a massive estuary system, the need to exploit changing resource distribution forces a merging of principally fresh water species with oceanic species. Fresh water species include the garpike (*Belone belone*), perch, and pike, which feed primarily on fishes; and the 15-spined stickleback (*Spinachia spinachia*), which feeds on Amphipoda, Isopoda, vermes and young stages and eggs of other fishes; *Syngnathus typhle*, which feed on mysids, gastropod larvae and fish larvae; *Nerophis ophidion*, which feed on planktonic crustaceans. The most important ocean fish which have become adapted to brackish water are herring (*Clupea harengus membras*), cod (*Gadus morrhua*), sprat (*Sprattus sprattus*), and flounder (*Platichthys flesus*). Less-abundant marine pelagic fish include the anchovy (*Engraulis encrasicholus*) and mackerel (*Scomber scombrus*), which migrate primarily from the North Sea (Ojaveer et al., 1983).

Important anadromous and catadromous species of the Baltic include: Atlantic salmon (*Salmo salar*), brown (sea) trout (*S. trutta*), grayling (*Thymallus thymallus*), whitefish (*Coregonus lavaretus*), vimba (*Vimba vimba*), lamprey (*Lampetra fluviatilis*), and European eel (*Anguilla anguilla*) (Ojaveer et al., 1983).

More than 400 avian species are found in the Baltic region. The Baltic region is a major migratory route for waterfowl and other waterbirds. The Matsalu Nature Reserve on the west coast of Estonia is an important nesting spot for ducks, geese, and other aquatic birds. Three species of seals are found in the Baltic Sea. The most abundant of these is the gray seal (*Halichoerus grypus*). Also present are the hair seal (*Phoca vitulina*) and ringed seal (*Pusa hispida*) (Kaasik, 1989).

Characteristic of the Baltic food web is the presence of opportunistic feeders among the larger consumers. These organisms are typically fast swimmers and easily move to reach food supplies and serve to stabilize the system. A major problem with study of food webs of this type is the necessity of having good data for all seasons and at all levels in the water column. On a seasonal basis, considerable movement by certain taxa is apparent. Demersal fish migrate between hard and soft substrates; as gobies go offshore in the winter months, four-horned sculpins move to the shallows. Cod, as the great migrator in the Baltic, tie together several energy systems. Energy flow from coastal fringe algal belts to the open

pelagic and deep demersal systems as well as from phytoplankton/zooplankton assemblages to the deeper ocean and coastal regions are linked by this highly mobile predator.

Benthic Food Web. The role of benthic animals is significant in the food web. The biomass ratio of macrofauna to meiofauna is about 23:1 at depths between 3 m and 50 m. At these depths, ostracods make up 50 percent of the meiofauna biomass, while nematodes make up 90% of the abundance values. In oxygen-poor basins, only nematoda are found (Hällfors et al., 1981). The macrofauna is dominated by the crustaceans, *Pontoporeia* and *Mesidothea*, the worms, *Halicryptus* and *Harmothoe,* and the clam, *Macoma baltica*. Western and southern parts of the Baltic have a greater variety of polychaetes and clams and act as grazing areas for migrating bottom fish (*i.e.*, flounder and cod) (Jansson, 1972).

Marine algae dominates the vegetation of the outer and middle archipelago zones and along open coasts. Sheltered coastal bays support limnetic plants (*Phragmites austrialis* and *Potamogeton*) and charophytes which are home to tiny gastropods, juvenile bivalves, crustaceans, and permanent meiofauna such as Rotatoria, Oligochaeta, Turbellaria, and Nematoda. The most important macrofauna of these areas are the crustaceans, *Gammarus* spp., *Idotea* spp, and *Iarea albifrons*. (Hällfors et al., 1981) *Zostera* is of local importance in the southern Baltic. This vegetation is characterized by high numbers of clams and gastropods (*Macoma* spp.) (Jansson, 1972).

The highest biomass values of benthic macrofauna in the deep zone of the Baltic Sea are dependent upon oxygen content. In 1967, for the Arkona Basin, the three most dominant species of macrofauna accounted for 70 percent of the total number of individuals compared with corresponding percentages of 97 percent for the Gulf of Finland and 99 percent for the Gulf of Bothnia. Polychaetes predominate where oxygen conditions are critical (Hällfors et al., 1981).

Within the benthic system, plankton is consumed by filter-feeding organisms such as the Baltic mussel and the bay mussel (*Mytilus edulis*) which are subsequently consumed by benthic as well as pelagic predators including fish and crustaceans. Nemerteans are also important predators, consuming mantle tissues and eggs of the mussels. Detritus and associated bacteria form the basis for a deposit feeding community of meiobenthos dominated by harpacticoid copepods in coarse sediments and nematodes in finer sediments. The macrofauna of the southern Baltic is dominated by *Cyprina islandica, Abra alba, Astarte borealis* and *Macoma calcarea* which provide food for both demersal and opportunistic pelagic species (Kullenberg, 1983).

The demersal fish fauna of the Baltic include the Baltic cod (*Gadus morhua callarias*), the Atlantic cod (*Gadus morhua morhua*), flounder (*Platichthys flesus*), plaice (*Pleuronectes platessa*), turbot (*Scophtalmus maximus*), brill (*Scophthalmus rhombus*), dab (*Limanda limanda*), sandeel (*Ammodytes tobianus*, syn *A. lancea*), greater sandeel (*Hyperoplus lancolatus*) snake blenny (*Lumpenus lampretaeformis*), four-bearded rockling (*Rhinonemus cimbrius*), father lasher (*Myoxocephalus scopius*), sea scorpion (*Tarulus bubalis*), four-horned cottus (*Onococottus quadicornis*), eelpout (*Zoarces viviparus*), black goby (*Gobius niger*), sand goby (*Gobius minutus*), lumpsucker (*Cyclopterus lumpus*), sea snail (*Liparis liparis*), gold sinny (*Ctenolabrus rupestris*), and butterfish (*Pholis gunellis*). Most species at some life stage feed on crustaceans; many include polychaetes, and amphipods in their diet. The older flounder and turbot feed on bivalves. The smaller (or younger fish) such as sand goby, black goby, father lasher, sandeel, and cod serve as food for eel, sandeel, brill, turbot, cod, and sandab. Thirty-eight species of fresh water fish are common to the Baltic Sea; most are sporadic residents (Ojaveer et al., 1983).

UNIQUE SPECIES AND ECOLOGICAL CONSIDERATIONS

Endangered/Threatened or Protected Species. While there continue to be declines in a number of the fisheries and mammals of the Baltic region, the Baltic Sea supports no listed endangered or threatened species of marine life and no critical habitat has been designated within the sea.

Unique Habitats. The Baltic Sea as a whole is unique in its early stages of evolution as an ocean system. The limited diversity of the system allows for unique opportunities to examine species interactions and adaptations to cope with hostile environments. However, the euryhaline environment of the Baltic is not atypical of high-temperate estuaries, and from the standpoint of ecological systems, it shares some striking similarities with inner regions of the lower latitude Chesapeake Bay and Hudson Bay of similar latitudes in North America. Not withstanding the occurrence of comparable cold-temperate brackish systems, the young age of the system, the extreme barriers to circulation which are found at the various straits and sills of the Baltic, and the long history of human exploitation of the Sea, have created some of the more interesting field laboratories for the study of anthropogenic effects in the ocean environment.

NORTH SEA

PHYSICAL AND CHEMICAL CONSIDERATIONS

Geography and Physiology. The North Sea is located on a relatively large continental shelf area in the northwest of Europe. Semi-enclosed by highly industrialized nations, the North Sea ranks among the most studied marine systems in the world (Zijlstra, 1988). The North Sea is located between approximately 51° to 61° North latitudes and between 4° West longitude and 9° East longitude (Zijlstra, 1988) (Figure 4.1-16). The geographical limits of the North Sea cross the Strait of Dover and through the gaps separating Scotland and the Orkney and Shetland Islands. The boundary of the sea follows the 62nd North parallel, and falls between Norway and Denmark, following a line that connects Lindesnaes on the Norwegian coast with Hanstholm on the Danish coast.

The North Sea is a shallow, semi-enclosed sea located between the British Isles and the countries of Norway, Denmark, Germany, Holland, and Belgium with an area of approximately 575,300 km^2, a maximum length of 1100 km, a maximum width of 675 km, and an average depth of 94 m (Defense Mapping Agency, 1990). There are three main sea connections to the North Sea that include linkages between Scotland and Norway with the north Atlantic, to the east through Skagerrak with the Baltic Sea, and in the south with the English Channel (Zijlstra, 1988). The English Channel and Skagerrak linkages form an essential part of the natural system of the North Sea (Eisma, 1990).

Bathymetry. Two of the most prominent features of the North Sea shelf include the shallow Dogger Bank and the deep Norwegian Channel. The Dogger Bank is located in the south-central shallows of the North Sea with a minimum depth of approximately 15 m, whereas the Norwegian Channel is a deep corridor (250 to 600 m) that follows the Norwegian coastline and extends into the Skagerrak, where depths of almost 800 m have been recorded. Apart from these irregularities, the North Sea bottom gently slopes from the shallow southern part to the deeper northern region along the edge of the continental shelf at a depth of 200 to 250 m (Zijlstra, 1988).

Along the southern boundaries of the North Sea, the average depth seldom exceeds 30 m, receiving sediment inflows from some large continental rivers such as the Rhine, Meuse, Scheldt, Weser, and Elbe. The landward fringe of the northern periphery of the North Sea has averages depths between 100 to 150 m, and unlike the southern edge of the sea, is less affected by sediment inflows. Within the northwestern part of the North Sea, there are several isolated deep water holes formed by past glacial activity. Along the English coast, off Norfolk, an intricate system of submerged longshore banks is present, while to the south, a large estuarine area (Wadden Sea) forms the transition zone from land to the sea (Zijlstra, 1988). In addition, a large portion of the North Sea bottom is covered by sand, with occasional areas of gravel and stones, originating mainly from glacial periods. In some deeper parts, notably in the Norwegian Channel, on the Fladen ground in the north, and located southeast of the Dogger Bank, mud or sandy mud is present. Mud and debris also accumulate in the estuarine Wadden Sea area, and near the outflow of the large rivers, such as the Thames, in the southern North Sea (Zijlstra, 1988).

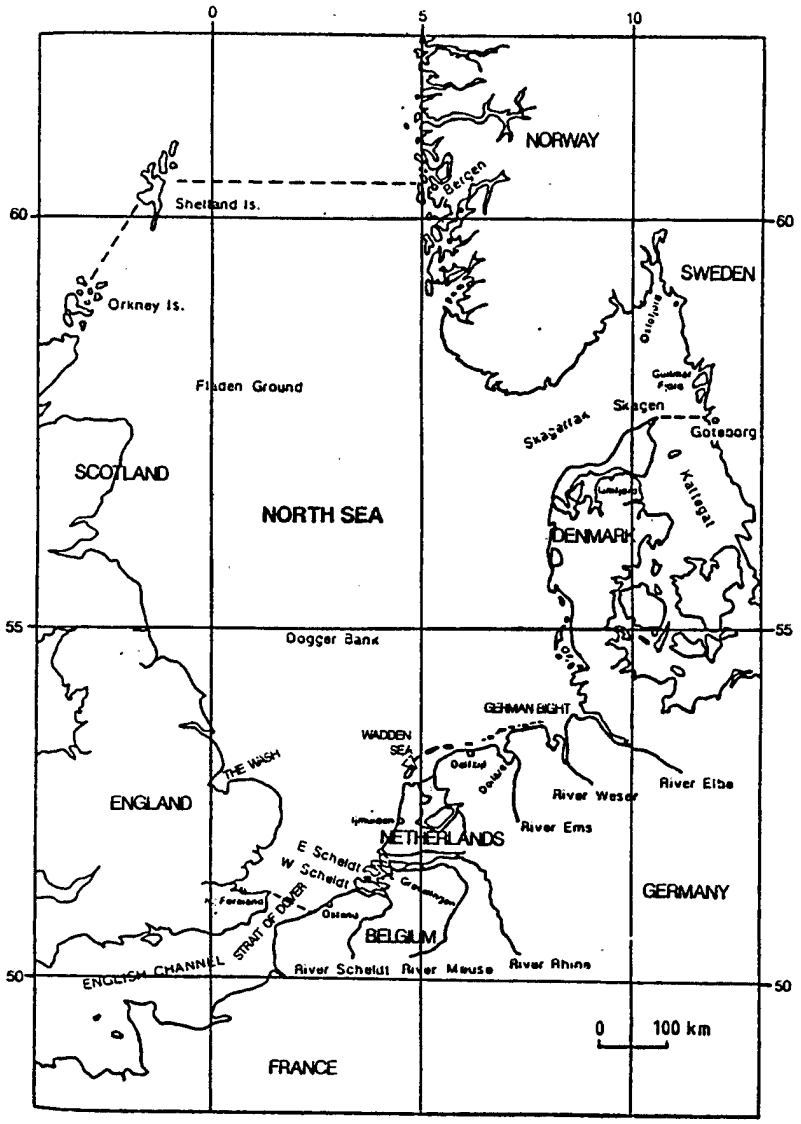

Figure 4.1-16. North Sea region. The North Sea is a shallow, open basin with connections to the North Atlantic Ocean, Baltic Sea, and English Channel.

Currents, Tides, and Water Exchange. Expansive continental shelf areas like the North Sea are characterized by presence of strong tidal currents and relatively large tidal extremes. Tidal currents are strongest along the western side of the North Sea and in the German Bight and decrease toward the east. Tides of the North Sea are predominantly semidiurnal with tidal waves entering the North Sea through the northern passage, while a much smaller wave train enters the Kattegat and passes into the Baltic (Defense Mapping, 1990). In the North Sea, seawater circulates counterclockwise from the North Atlantic between Scotland and Norway and in the south through the Straits of Dover (Eisma, 1990). Average residence time for water in the North Sea is less than one year. The Jutland Current enters the Kagerrak and follows the Norwegian Trench northward joining with the Baltic waters to form the Norwegian Coastal Current. Bottom currents in the North Sea are weak and variable in direction. The flow is generally topographically steered (Defense Mapping, 1990).

Corresponding with the three entrances of the North Sea, the major inflows consist of Atlantic water of high salinity from the north, between Scotland and Norway, and secondarily from the south through the Strait of Dover. In addition, there is inflow from the Baltic, which has a significantly lower salinity. Apart from these three primary water masses, five secondary water bodies are distinguishable within the Sea and include the English Coastal, Scottish Coastal, Northern North Sea, Continental Coastal, and Central North Sea. These water masses are derived from the primary oceanic waters and land run-off (Zijlstra, 1988).

The average residence time of the North Sea water is estimated to be approximately 6 to 9 months. Short residence time is beneficial because concentrations of pollutants can be quickly diluted. However, residence time in separate areas such as the southern North Sea and the German Bight are considerably longer (Zijlstra, 1988). The main outflow of North Sea water occurs in the northeast, where flushing times are significantly shorter than in other areas. Long flushing times are found near the major fresh water inflows in the western and southern North Sea and in the German Bight (Zijlstra, 1988).

Temperature and Salinity. Average annual surface water temperatures in the North Sea range from 3° to 8°C in the winter to 12° to 16°C in the summer (Defense Mapping Agency, 1990). The greatest variability occurs between the near-shore temperatures and the temperatures of the open sea bordering the Norwegian Sea. During the month of January, surface water temperatures range from 8°C in the north to 3°C off the eastern shores of Denmark. During the summer months, surface water temperatures range from 12°C in the north to 15°C near the central portions of the Sea, and 16°C off the eastern shores of Denmark (Defense Mapping Agency, 1990).

The salinity levels of the two Atlantic water masses, the North Atlantic and Channel, average >35 ppt while the Skagerrak averages <34 ppt. In principle, the water masses extend from surface to bottom, except for the low-salinity Baltic water which is restricted to the surface layers. This lower density water is thought to overlie North Atlantic water in the Norwegian Channel (Zijlstra, 1988). The North Atlantic inflow is estimated to be 20,000 to 45,000 $km^3 \cdot yr^{-1}$, the Channel inflow to be 1600 to 1800 $km^3 \cdot yr^{-1}$, and the Baltic inflow to be only 200 to 700 $km^3 \cdot yr^{-1}$; however, higher approximations of the Channel inflow have been estimated at 3400 $km^3 \cdot yr^{-1}$ (Zijlstra, 1988). Compared to the inflow from many other large sea areas, the contribution of rivers to the water of the North Sea is very moderate, at only 290 $km^3 \cdot yr^{-1}$. Although the contribution of river water to the North Sea is relatively small, the strongly polluted waters of some of these rivers may impact the biota in particular areas (Zijlstra, 1988).

Vertical mixing processes within the North Sea are dependent on both turbulence, induced by differences in current speed and direction with depth, and vertical density distribution. Within the majority of the

North Sea, areas typified by lower tidal current velocity have surface waters that are heated during the warmer season. Within these areas, a layer of warmer and less-dense water is formed in the spring, resting on the cold and deep water, separated by a thermocline. In such situations vertical mixing is greatly reduced, which has a profound effect on the biological productivity (Zijlstra, 1988). In the autumn, when the cooling of the surface waters reduces the vertical density differences, and turbulence is promoted by autumn gales, this stratification disappears again. Additional stratification occurs in areas heavily influenced by low-saline water, as for instance in the Skagerrak inflow. Within this area, low-salinity water with a reduced density will rest on the deeper, high-salinity water, separated by a halocline. Seasonal, or sometimes permanent, thermal stratifications are mainly found in the homohaline central and northwestern North Sea, whereas permanent, or sometimes seasonal, haline stratification is found in the northeastern North Sea, in and near the Skagerrak inflow (Zijlstra, 1988). In the shallow, well-mixed southeastern part, temperatures are lowest during winter, and highest during summer. The annual temperature range in the southeast is about 14 to 15°C, while in the northwest the range is only 5°C. Evidence suggests that a similar pattern may be found for the bottom temperatures, but due to stratification, the temperature range in the northern part of the North Sea is only about 0 to 2°C.

Oceanic Sedimentation. Despite the fact that a number of measurements of suspended sediment have been made in the North Sea and in the rivers supplying it, there is considerable uncertainty in the supply figures (McCave, 1988). For many rivers, not even the fluid discharge is well-known. Several discharge figures, which are partially based on reasonable specific discharge values for ungauged streams, lack any relevant quantitative or qualitative data. The North Sea sediment types (gravel, coarse sand, sand, fine sand, sandy mud, and mud) have patchy distribution. Most of the sediment is relictual and was supplied during the Pleistocene periods by rivers and ice flows. Present river discharges carry little sand or gravel, only suspended sediment (Eisma, 1990). Bottom sediments of the North Sea are chiefly of Holocene age and are only a few meters thick (Eisma, 1973). Primary external sources of nutrients are from river inflow, atmospheric exchange, and coastal discharges. Highest concentrations of nutrients are found during the winter when incoming solar radiation is low (Chadwick et al., 1996).

CURRENT ENVIRONMENTAL STRESSES

Marine Pollution. Since 1850, large-scale pollution in the North Sea has been linked with European industrialization. Most industrial and sewage contaminants are discharged into the rivers and streams which run into the open sea. River pollution with nutrients and chemical compounds is, together with atmospheric input, now noted as the main source of contamination of North Sea waters (Watermann and Kranz, 1992). Further, organochlorine contaminant levels rose in the 1940s as the concentrations of DDTs and PCBs increased (Dethlefsen, 1989). Sediment core samples have confirmed that North Sea contamination dates back to the last century and that the contamination has shown significant increases between 1915 to 1930 and 1954 to1974 (Watermann and Kranz, 1992).

The world's highest density of ship traffic is found in the southern section of the North Sea (Vauk and Schrey, 1987). This traffic has historically resulted in the deposit of large amounts of waste into the sea. Other primary pollution sources include sewage and industrial waste discharges, non-urban runoff from range, forests, agricultural, and mining lands (Colwell, no date), and atmospheric input of air pollutants (Watermann and Kranz, 1992).

Litter. Most marine litter in the North Sea is generated by routine waste discharges of travelling ships (Dixon and Dixon, 1983). The bulk of this litter includes plastics, such as cups, bottles, and packaging materials. Other litter includes wood items (i.e. fish boxes and planks), paper and cardboard objects,

metal, and glass containers, rope, and nylon netting. This litter causes polluted shorelines and environmental damage, including deaths of various marine mammals, seabirds, and other organisms. Large debris pollution such as plastic bags and containers may be a more directly lethal problem to individual marine mammals than chemical pollution. The latter reduces reproduction rate and longevity to some extent, but may only rarely lead to immediate death (Kastelein and Lavaleije, 1992).

In an attempt to reduce the volume of litter being deposited, garbage dumping has been prohibited and disposal facilities for North Sea ships have been established. Further, the discharge of synthetic materials, especially plastics, has been prohibited since 1989. Other litter, however, is still being dumped. These pollutants generally include paper products, glass, metals, and rags (Defense Mapping Agency, 1990).

Toxic Materials. Oil and natural gas are mined throughout the North Sea and the risk of spillage poses a major threat to the surrounding environment. Evidence suggests that marine benthos within a 1-km radius of oil platforms and production rigs are affected by mining activity. Severe effects to marine life can be found within a 500-m radius (Gray et al.,1990). Benthic macrofauna within 500 m have low diversity and biomass when compared to those outside the 500-m radius. Similarly, macrofauna within 500 m to 1 km have lower diversity and biomass than faunal communities outside a 1-km radius. Additionally, oil transport through the sea has resulted in several extremely damaging oil spills.

Heavy metal contaminants, as shown in sediment core samples, are the result of riverine deposits to the North Sea. In addition to terrestrial sources, atmospheric pollution from fossil fuel burning has contributed to increased levels of metal contaminants including mercury, lead, cadmium, zinc, and copper (Dominik et al., 1978; Kersten and Kronke, 1990 cited, in Watermann and Kranz, 1992). Primary sources for these metals are sewage and industrial wastes. Organisms located near sewage and industrial waste disposal sites are most impacted (Defense Mapping Agency, 1990).

Although numerous fish diseases and contaminants have been identified, definitive causal effect relationships are still debated (Dethlefsen, 1989). Untreated sewage is thought to be responsible for bacterial contamination in seafood, such as mussels (Johnstone, 1909,1913 cited in Watermann and Kranz, 1992). Anderson (1909) found a high concentration of coliform bacteria in fish around sewage disposal sites (Watermann and Kranz, 1992). Also, leucocytosis and abnormal gill conditions of mussels is related to unusually high concentrations of copper, zinc, and cadmium (Orton, 1923; Sunila, 1986, cited in Watermann and Kranz, 1992). Ulcers and tumors in various fish have been found and are attributed to toxic contaminants.

Sewage makes up the majority of the organic waste in the North Sea. Other organics include food and fishery wastes; however, these discharges are geographically restricted and are not likely to result in a significant impact on the region as a whole.

Nutrient loading from municipal waste water, agriculture, and terrestrial runoff is a serious pollutant in the North Sea. Nutrients, such as phosphorus and nitrogen, pollute coastal areas of some European countries. Increased nutrients cause periodic planktonic blooms results not only in depletion of the oxygen with subsequent damage to the aquatic biota, but in cases of a *Gonyaulax* bloom (i.e. "red tide"), may impact birds and mammals which ingest infected shellfish (Carter, 1973). In attempts to control nutrient loading, countries are working together to reduce the level of pollution being discharged into the sea. At the Second International Conference on the Protection of the North Sea in 1987, the countries agreed to reduce the total amount of contaminating nutrients by 50 percent (Ibrekk et al., 1991).

Natural Inputs. Although most localized planktonic blooms in the North Sea are anthropogenic, some occur naturally. Blooms of dinoflagellates producing toxic substances dominate the planktonic community and inhibit the grazing of non-toxic plankton. These toxins have killed numerous fish and have caused toxic contamination to other wildlife species that consume shellfish contaminated by these poisons. Further, additional blooms are manifested as a result of upwellings which bring essential nutrients to the shallow waters and which, together with sufficient light, encourage the production of red tides (Defense Mapping Agency, 1990).

The North Sea receives inflow from the Rhine, Meuse, Scheldt, Weser, and Elbe rivers. Mud accumulates in the estuarine Wadden Sea area, and near the outflow of the Scheldt and Thames rivers in the southern North Sea in the German Bight (Zijlstra, 1988). In addition, rivers are the major source of waterborne contaminants (Rees and Eleftheriou, 1989).

Sea Traffic and Ports. Sea traffic within the North Sea is distributed between multiple ports and transverses the ocean with the bulk of the traffic occurring in the northeast and southern regions of the North Sea. Numerous fishing vessels contribute to the large volume of traffic encountered in the North Sea. Trawlers may be met anywhere in the North Sea; driftnetters are usually found in groups of as many as 200 to 300 boats covering 40 to 160 square miles; seine fishermen are found between the latitudes of 53° and 58° North latitude throughout the North Sea; line fishing is generally limited to coastal areas. High-volume traffic ports include Aberdeen on the coast of Scotland; Newcastle, Hull, and London in England; Antwerpen, Rotterdam, and Amsterdam, in the Netherlands; Bremerhaven, Hamburg, and Cuxhaven in Germany; and Bergen and Oslo in Norway (Defense Mapping Agency, 1990). Further, several cruise ships enter North Sea waters during the summer season. These ships typically visit the Norway coastline; however, most European ports of call are readily accessible to such ships.

FISHERIES AND AQUACULTURE RESOURCES

The North Sea is considered one of the richest fishing areas of the world due to its biological and physical characteristics (McIntyre, 1988). Although the North Sea represents approximately 0.145% of the world's oceans surface area, it contributes about 5% to the world's fisheries yield (Zijlstra, 1988). The relatively high biological diversity and production can partially be attributed to a complete vertical overturn of the water column that distributes the nutrients at least once annually. In addition, the nutrient-rich water is supplemented by terrestrial inputs from several rivers.

The countries bordering the North Sea are the main exploiters of fishery resources. These countries include Norway, Denmark, the Netherlands, Belgium, Germany, and the UK. Other countries, such as France, the Faroe Islands, Sweden, and Poland fish these waters to a lesser extent. The desired species of plants and animals are those for which a market demand already exists or is predicted to arise. Currently, the majority of exploited resources are the pelagic and demersal fish, along with a wide range of shellfish. The pelagic and demersal fisheries' focus on the herring (*Clupea harengus*), cod (*Gadus morhua*), haddock (*Melanogrammus aeglefinus*), and mackerel (*Scamber scombrus*) have resulted in overfishing and depletion of stocks. Cod is an important resource in the southern sea while haddock dominates the catch in northern waters. Commercially important shellfish include molluscs (especially oysters, squid, scallops, mussels, and cockles) and crustaceans (crabs, lobsters, Norway lobsters, and shrimp). To maintain sufficient levels of capture for all species, fisheries now exploit waters beyond the North Sea. This trend mimics similar trends in virtually every other maritime setting, overlooking the obvious conclusion that edible fish foodstocks are finite (Zijlstra, 1988).

Initially, North Sea fisheries sought species for human consumption, but in the 1950s, industrial uses of fish reached an equal level of economic importance. Industrially fished species are used for fish oil, fish meal, pet foods, and mink or fish farms. Typically, these species include herring, sandeel, Norway pout, haddock, mackerel, and whiting, but excesses of other marketable foodfish may also be used for industrial purposes.

Due to overexploitation of fish since the 1970s, there has been an increasing emphasis on aquaculture. The topography and climate of the area limit the success of many species, but bivalve molluscs (particularly mussels) and North Atlantic salmon seem to thrive under such conditions. In 1984, the consumption of farmed salmon outnumbered the consumption of salmon caught in the wild, three to one (McIntyre, 1988).

Although regulations have been established to prevent further overexploitation of commercial species, the marine environment is still susceptible to extensive damage caused by fisheries. On going research is documenting these adverse effects and action is being sought to integrate environmental protection regulations with the fisheries regulations (Hey, 1992).

Phytoplankton. Primary production data for the North Sea is only available for certain restricted areas. In the northern North Sea, primary production is estimated at 70 to 90 $gC \cdot m^{-2} \cdot yr^{-1}$ (Steele, 1956 and1974; Wolf and Zijlstra, 1988). Comparable data was found by Joiris et al., 1982 and Radach (1983). Primary production in the German Bight has been estimated at 320 $gC \cdot m^{-2} \cdot yr^{-1}$ (Joiris et al., 1982; Gieskes and Kraay, 1975 cited in Wolf and Zijlstra, 1988). Production is higher further offshore, where freshwater traces are small, as determined by salinity measurements (Gieskes and Kraay, 1975 cited in Wolf and Zijlstra, 1988). Little data exist showing the annual fluctuations of primary productivity in the North Sea, but in the English Channel, the production varies between <100 to almost 300 $gC \cdot m^{-2} \cdot yr^{-1}$ (Boalch et al., 1978, cited in Wolf and Zijlstra, 1988).

Phytoplankton productivity is often limited by low water temperatures that inhibit growth and long winter dark periods and sea ice which limit light. The lower values of production in the northern North Sea may be a result of these factors. Other suggested limiting factors include copepod grazing in the northern sea and small heterotroph consumption in the southern sea (Joiris et al., 1982 cited, in Wolf and Zijlstra, 1988). Fransz and Gieskes (1984) suggest that a significant part of the planktonic blooms sinks or is consumed by microbial plankton.

The number of phytoplankton species in the North Sea is estimated to be much greater than 500. Of the larger species, 68 inhabit the entire North Sea in varying concentrations. Over 270 smaller species (nannoplankton and microplankton) are found in the German Bight alone (Lewis, 1985, cited in Wolf and Zijlstra, 1988).

Zooplankton. The population of zooplankton in the North Sea is diverse and includes five species of Branchiopoda, four species of planktonic gastropods, four species of tunicates, 22 species of calanoid copepods, a few species of chaetognatha, three genera of cyclopoid copepods, seven families of Malacostraca, and the genus *Tomopteris* (pelagic Polychaeta) (Anon., 1973, cited in Wolf and Zijlstra, 1988). The larger species, such as the Euphausiids and *Calanus*, are more dominant in the northern North Sea, while smaller species of copepods are more dominant in the southern sea (Colebrook et al., 1961; Colebrook and Robinson, 1965). The dominant species in the coastal areas are Scyphomedusae and the ctenophore, *Pleurobrachia pileus*. There are more than 300 species of zooplankton in the North Sea.

Mean annual standing crop biomass estimates of zooplankton are 12 to 19 $mg \cdot m^{-3}$ (Robertson, 1968 cited in Wolf and Zijlstra, 1988). Other studies found that the northern North Sea contained a mean annual biomass of 2.5 $gC \cdot m^{-2}$ (Steele, 1974, in Wolf and Zijlstra, 1988). Specifically, seasonal estimates include 0.4 $gC \cdot m^{-2}$ in March and 2.0 $gC \cdot m^{-2}$ in April, May, and November (Adams and Baird, 1970, cited in Wolf and Zijlstra, 1988). In the central North Sea, the biomass values are lower, ranging from 0.8 to 2.0 $gC \cdot m^{-2}$. The German Bight, along the Belgian coastal areas in the south North Sea, has an annual mean of about 0.3 $gC \cdot m^{-2}$ (Fransz and Gieskes, 1984, cited in Wolf and Zijlstra, 1988).

There are few estimates of zooplankton production. Cushing (1973) offered an estimate of 20 $gC \cdot m^{-2} \cdot yr^{-1}$, but it was considered to be an overestimate (Wolf and Zijlstra, 1988). For the northern North Sea, Steele (1974) found the production to be 18 $gC \cdot m^{-2} \cdot yr^{-1}$, while Fransz and Gieskes (1984) reported 20 $gC \cdot m^{-2} \cdot yr^{-1}$ in the northern waters and 10 $gC \cdot m^{-2} \cdot yr^{-1}$ in the German Bight. From these results, it was observed that biomass production of zooplankton was greater in the north, which is opposite the greater southern production of phytoplankton. Joiris et al., 1982 suggested that the difference may be due to a higher amount of energy being dissipated through a microbial food chain in the southern sea.

TROPHIC RELATIONSHIPS

Pelagic Food Web. Strong tidal mixing in the North Sea results in high primary and secondary productivity in the lower trophic levels. High annual production cycles normally occur in the summer and spring, but phytoplankton blooms are largely dependent on physical conditions such as water temperature, surface light, and the depth of the mixed upper water layer (Fransz et al., 1991). Pollution is also an important nutrient contributing factor. Increasing frequencies of phytoplankton blooms due to pollution, especially in the southern North Sea provide more food to pelagic fish, but may cause eutrophication and possible poisoning of other organisms.

Pelagic fish benefit from seasonal plankton blooms and flourish in all areas of the sea. Over 160 to 170 species of fish are common to the North Sea, a considerably greater number of species are sparsely distributed (Wheeler, 1969 and 1978, cited in Salomons, 1988). Of the common species, only 25 to 30 species are of extremely high abundance, about 80 species are widely distributed throughout the North Sea, 51 are found in colder and deeper waters, and 37 species occur mostly in the shallow waters of the southern North Sea. There are 11 commercially fished species which make up about 95% of the total yield (Cole and Holden, 1973, in Wolf and Zijlstra, 1988). Five of these species inhabit the coastal areas and make up about 40% of the total North Sea yield. The important species include sprat (*Sprattus sprattus*), herring (*Clupea harengus*), sole (*Solea solea*), dab (*Limanda limanda*), and plaice (*Pleuronectes platessa*). Other commercially important fish include mackerel (*Scomber scombus*), haddock (*Melanogrammus aeglefinus*), cod (*Gadus morhua*), Norway pout (*Trisopoterus esmarkii*), sandeel (*Ammodytidae* spp.), and whiting (*Merlangius merlangus*). Redeke (1941) theorized that as much as a third of North Sea fish are occasional or regular immigrants from the subarctic Atlantic, the English Channel, or the Bay of Biscay.

Most pelagic fish of the North Sea are generalists, eating anything of appropriate size (Figure 4.1-17). Little interspecific competition exists due to varying spawning times and individual adaptations to location and selection of food. During growth, food preferences tend to correlate with the developmental stage and size of the fish. Abundant fish species begin as eggs, and, as tiny larvae, most feed on zooplankton. In general, most pelagic fish are carnivores through the developmental stages of life (Daan et al., 1990). As adults, some species favor particular areas or food sources. For instance, herring remain

mainly planktivorous and many flatfish become dependent on the benthos. Also, the gadoids have a mixed diet of zooplankton, smaller fish, and benthic organisms.

Many avian species, grouped as seabirds, shorebirds, and wildfowl, utilize the North Sea shores for feeding, breeding, and molting. The total number of dependent species is 71, with 19 open-sea bird species and 21 winter breeders (Evans, cited in Goldberg, 1973). In addition, 68 avian species migrate along the coast of the Netherlands. Seabirds commonly found in the North Sea include gulls, petrels, shearwaters, terns, skuas, puffins, and guillemots. The avian diet exists of plants, zooplankton, shellfish, and marine fish.

The seabirds breed on the islands and coasts of the sea, where they acquire the majority of their food. For instance, coastal feeding gulls tend to be scavengers and carnivores, feeding on the sandhopper (*Talitrus saltator*) and the larvae of some Diptera. Two main species of shorebirds (oystercatchers and ringed plovers) consistently utilize the North Sea resources, both for breeding and feeding. Other shorebirds, such as the avocet, golden plover, lapwing, dunlin, curlew, redshank, and sanderling, use the North Sea as a food source during migration to replenish their fat stores (Carter et al., 1993). The invertebrates mainly preyed upon include *Mytilis edulis, Littorina littorea, Hydrobia ulvae, Macoma balthica, Carcinu maenas, Cardium edule,* and polychaetes. The only two species of wildfowl that consistently breed in large numbers on the islands and coast of the North Sea are shelduck and eider. After the breeding season, the coastal areas of western Denmark, Holland, and northwest Germany provide an important molting location for many species of wildfowl (Evans, in Goldberg, 1973). Such species include the common scoter, mallard, teal, eider, and shelduck.

Two species of seals, the grey seal and harbor seal, are commonly found in the North Sea region. Grey seals number over 100,000 animals and inhabit the northwestern and western regions of the Sea, but also appear off the northwest coast of Norway (Riejnders and Lankester, 1990). They were formerly common in the German Bight, but now are very rare. The harbor seal lives along the eastern shores of England and Scotland, and also along The Wash, the German Bight, and southern Norway. About 55,000 animals are thought to inhabit the North Sea areas (Harwood, 1978; Hauksson, 1987, cited in Reijnders and Lankester, 1990). The total food consumption of the grey seal is estimated to be 5 to 8 kg fish/day, while the total intake of the harbor seal is 5 kg fish/day. These figures combine to be 100,000 tons·yr^{-1} (Wolf and Zijlstra, in Salomons, 1988). The diet of the grey seal mainly consists of salmon and cod.

There are 18 known species of cetaceans inhabiting the North Sea. Of these, only seven are common and include the harbor porpoise (*Phocoena phocoena*), the white-sided dolphin (*Lagenorhynchus acutus*), the white-beaked dolphin (*Lagenorhynchus albirostris*), the bottlenose dolphin (*Tursiops truncatus*), the killer whale (*Orcinus orca*), the minke whale (*Balaenoptera acutorostrata*), and the pilot whale (*Globicephala melaena*). Little is known about the cetaceans of the North Sea, but evidence suggests that harbor porpoises are on the decline. In addition, harmful pollutants and fisheries, which trap mammals in nets and compete for fish, present hazards to all the cetacean species (Reijnders and Lankester, 1990).

Benthic Food Web. It is nearly impossible to produce a comprehensive picture of the North Sea benthos due to the lack of standard sampling methods and to the regional character of the studies. In the North Sea, two benthic communities are commonly found: a muddy sediment community dominated by a brittle star (*Amphiura filiformis*) and a number of worms (Polychaetes), and a sand-bottom community with typical bivalves (*Venus gallina*) and a sea urchin (*Echinocardium cordatum*). Off the Belgian-Dutch-German coast, where muddy sediment is subject to waves and currents, a separate community

characterized by smaller bivalves (*Abra alba*, *Nucula turgida*) and worms occurs. Additionally, in nearshore medium to coarse sand-bottom communities, a bivalve (*Spisula subtruncata*) and a small polychaete (*Goniadella bobretzki*) occur (Eisma, 1990). Near major estuaries, where salinity is variable, there may be widespread occurrence of a *Macoma balthica* community at depths of 0 to 15 m.
The vertical zonation of the benthic community of North Sea waters is governed primarily by depth, but may be related to differences in sediment properties (Eisma, 1990). However, there is no clear trend in abundance with depth (Zijlstra, 1988). Marine organisms occurring in the North and Baltic Sea regions drop drastically with reduction in salinity. Distribution of species are influenced by factors such as topography, aspect, and tidal range (Mitchell, 1987). In the shallow southern region of the Sea, relatively few species are abundant. It appears that benthic diversity is highest in the deep northern waters of the North Sea (Zijlstra, 1988). Biomass and production are related to environmental conditions. Food availability is one of the most important factors. The bulk of the food is provided by spring plankton bloom that can lead to the production of as much as 135 million metric tons of organic matter per year (Eisma, 1990).

Apart from contaminant concentration, the distribution of North Sea benthic fauna is strongly influenced by mud deposition. The presence or absence of many species is directly or indirectly related to sediment diameter. The basic common factor is assumed to be the selection of bottom sediment type by settling larvae. A few species with a pelagic stage can delay metamorphosis, necessary for settling, by a few days or weeks, while seeking the proper bottom sediment. Other factors influencing settling may include temperature, salinity, availability of light, and dissolved oxygen saturation. Temperature strongly influences the moment of metamorphosis (Eisma, 1990).

Once settled, distribution of benthos may be influenced by predation, food availability, and by patchy distribution of larvae and adults (Eisma, 1990). A large part of the organic matter is probably mineralized in the water column, but there may be considerable advection and deposition in some areas. Estimates of the amount of organic matter produced in the surface water of the North Sea that reaches the bottom waters vary from 20 to 30% to around 1% and are strongly governed by seasonal productivity.

Benthic macrophytes, are confined to rocky substrates in a belt extending from mean high water to a maximum of 50 m below the low water mark in the North Sea. Measurements of productivity of the fringing kelp forest is notably high. Figures for depths up to 10 m exceed those for intensive agriculture at the same latitude. Net production has been calculated at 299 $kg \cdot m^{-2} \cdot yr^{-1}$. with the bulk of this production passing to the detrital food chain (Bellamy et al., 1990).

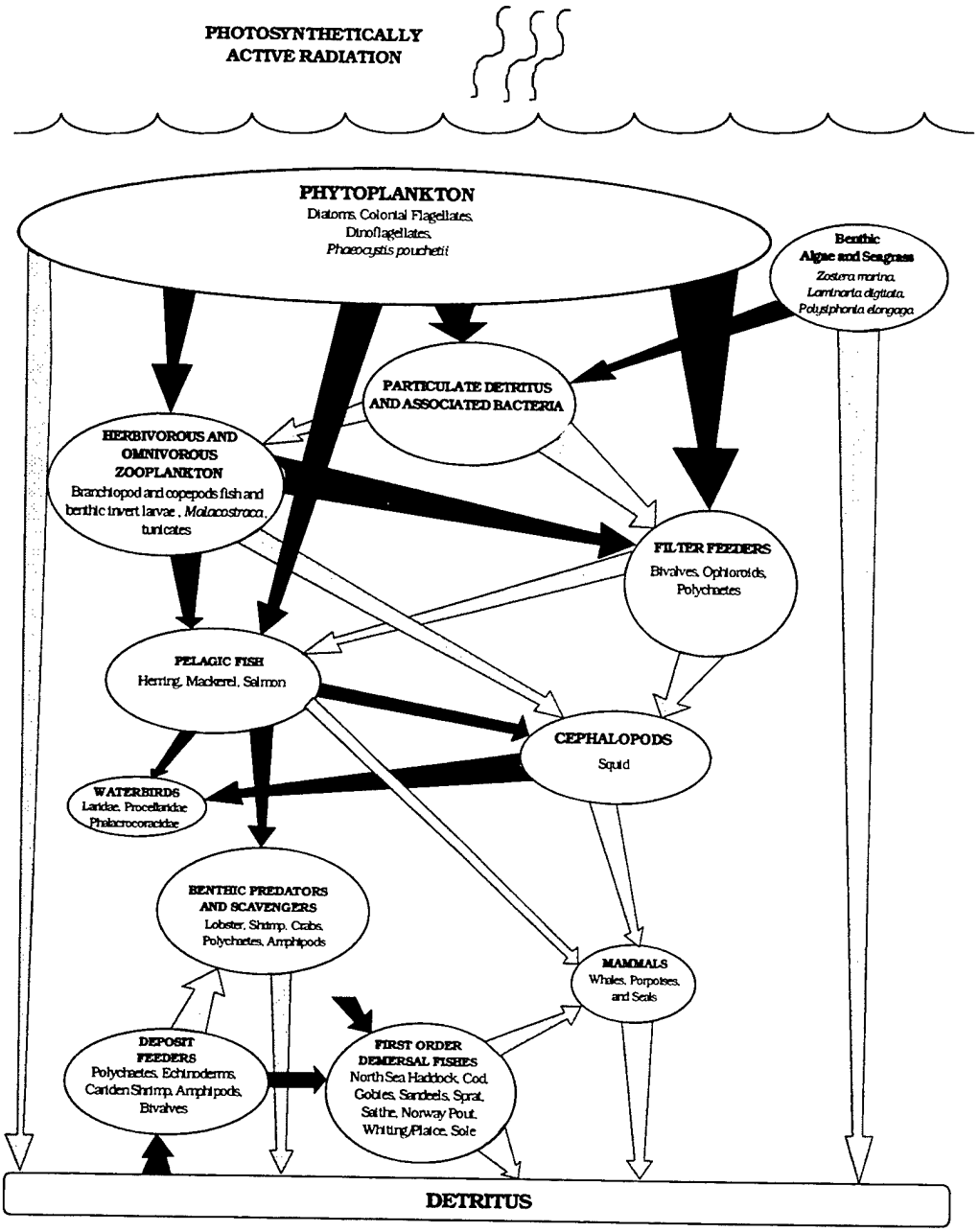

Figure 4.1-17. The North Sea Trophic Web. The trophic assemblage of the North Sea is marked by a highly productive web of opportunistic foraging. Relatively shallow and broad shelf environments are heavily exploited by a mix of demersal fishes and crustaceans which support an extremely important commercial fishery.

UNIQUE SPECIES AND ECOLOGICAL CONSIDERATIONS

Endangered/Threatened or Protected Species and Critical Habitat. The once-depleted North Sea population of the grey seals now stands in excess of 100,000. This species has undoubtedly recovered due the protection afforded by the Grey Seal Act of 1914 and 1938 and by the establishment of sanctuaries along the coast of England within the Farne Islands. In contrast, recent concerns over the

damage caused by the increasing seal population to fish important to adjacent salmon fisheries led to an amendment of the Act and to two test culls, both of which provoked a large public outcry. The most recent plan to cull 3500 seals in 1972 was, however, based on a detailed study which had indicated that increased crowding in the breeding sites leads to increased pup mortality (Bellamy et al., 1990). According to Bellamy (1990), the cull was recommended on grounds of "hygiene and sympathy for the suffering seals." Additional species of concern are the protected puffin populations of the Farne Islands that continue to suffer due to increased human related disturbance.

Unique Ecological Phenomena. The key ecological phenomena that characterizes the high productivity of the North Sea is the prolific fish population. The shallowness of a large portion of sea provides excellent breeding and spawning sites for many commercial fish species including the haddock, cod, and mackerel. Recent overfishing and oil spillage have potentially damaged this historically overexploited resource.

BLACK SEA

PHYSICAL AND CHEMICAL CONSIDERATIONS

Geography and Physiography. The Black Sea is an enclosed, brackish body of water located between 40°55' and 46°32' North latitudes and between 27°27' and 41°42' East longitudes (Figure 4.1-18). The Black Sea is the largest landlocked inland sea and is bordered by four European and Asian countries. Romania and Bulgaria bound the western portion of the Sea while the Ukraine lies to the north. The southern coastline is bordered by Turkey. The Black Sea is accessed from the Mediterranean Sea via the Dardanelles Strait into the Sea of Marmara, and finally through the narrow Bosporus Strait. The northeastern portion of the Sea is isolated by the Crimean Peninsula, forming a small body of water known as the Sea of Azov that is accessed through the Kerch Strait.

The Black Sea is situated in a semi-arid environment and evaporation (332 to 392 $km^3 \cdot yr^{-1}$) exceeds rainfall (225 to 300 $km^3 \cdot yr^{-1}$) (Balkas et al., 1990). However, the Sea is fed by an extensive fluvial system that adds approximately 350 km^3 of fresh water to the system per year. Therefore, there is a net inflow of freshwater into the Black Sea and a subsequent dilution of surface sea waters. Rivers that feed the Black Sea include the Danube, the Caucasian, the Anatolian, and several smaller Russian and Bulgarian rivers. The majority of river inflow comes from the Danube, which supplies the Black Sea with approximately 200 km^3 of water per year (Sorokin, 1983).

As the largest existing anoxic environment on earth, the Black Sea serves as a model of chemical and sedimentological evolution of early atmospheres and oceans. The Black Sea is characterized by unusual chemical and microbiological properties due to its stratified, anoxic deep waters. For the past 7000 years, decomposition, oxidation, sinking and accumulation of organic matter has led to a decrease in available oxygen in deep Black Sea waters (Balkas et al., 1990). Below a depth of 150 to 200 m, the waters of the Black Sea are completely anoxic and contain high concentrations of hydrogen sulphide (Sorokin, 1983). Today, since the percentage of Black Sea water shallower than 200 m comprises only 13% of the total water mass of the Sea, nearly 87% of the waters of the Black Sea are completely anoxic and, except for anaerobic bacteria, completely devoid of life.

Bathymetry. The Black Sea has an area of approximately 420,000 km^2, including the shallow Sea of Azov to the north (38,000 km^2), and a volume of 537,000 km^3 (Sorokin, 1983). The northwestern Black Sea is dominated by the wide, shallow shelf formed by sediments of the Danube fan (Figure 4.1-18). The waters of the Sea of Azov are also shallow. The coastal shelf of the southwestern Black Sea and eastern Black Sea is narrow with an average width of less than 15 km. From the shelf, the Sea floor drops down steep coastal slopes into a deeper central basin with a maximum depth of 2,206 m. The 31 km long Bosporus Strait, which connects the Black Sea to the Mediterranean Sea, is the world's narrowest strait and has an average width of 1.6 km (Balkas et al., 1990). The average depth of the Bosporus sill is only 36 m, which severely restricts water flow between the two seas. The Kerch Sill, that leads into the Azmov Sea is even shallower, with an average depth of 20 m.

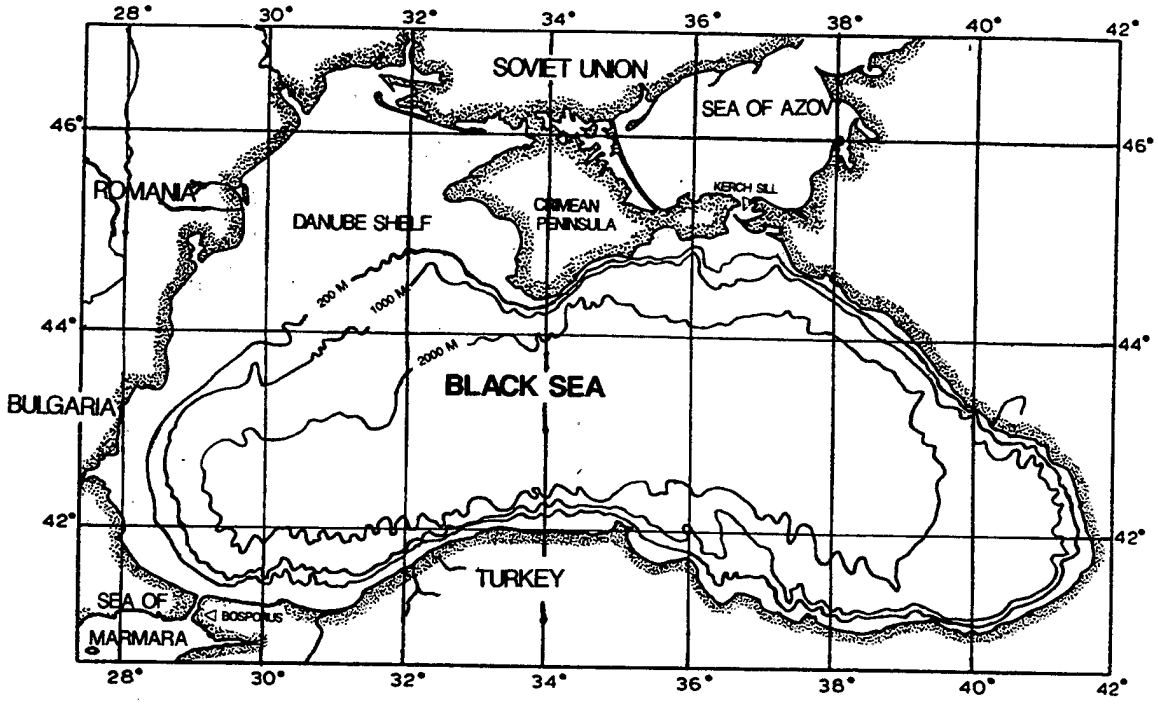

Figure 4.1-18. The Black Sea region. The Black Sea is poorly connected to the Mediterranean by the Marmara Sea and the Straits of the Bosporus. To the north is the Sea of Azov. The sea is a deep basin with extremely shallow sills restricting interchange with other water bodies. The primary shelf area occurs on the Danube Shelf, the flooded delta of the Danube River.

Currents, Tides, and Water Exchange. Surface currents of the Black Sea are controlled by a cyclonic boundary current which runs parallel to the basin's periphery and two cyclonic gyres located in the eastern and western portions of the central basin (Balkas et al., 1990). The larger cyclonic boundary current is presumed to converge south of the Crimean Peninsula and satellite imagery shows small eddies and countercurrents along the periphery (Neumann, 1942, cited in Hay, 1987). The velocities of Black Sea surface currents can be extremely high. The speed of the boundary current can travel 40 $cm \cdot s^{-1}$ in certain regions (Balkas et al., 1990). Due to the rapid velocities of surface currents, the deep currents of the Black Sea can travel as fast as 10 to 15 $cm \cdot s^{-1}$ at depths of 700 m (Sorokin, 1983). Velocities slow at extreme depths.

It is believed that, due to the extreme stratification of Black Sea water masses, water exchange in the Sea occurs at a very slow rate. The surface waters of the Sea are replenished by rain, and freshwater inflow from the large fluvial system that feeds the Sea. A bottom current flows from the Mediterranean Sea through the Bosporus Strait and into the Black Sea, carrying saltier, denser water northward. The result is a pronounced density gradient (pycnocline) that forms between 125 to 210 m in depth and a subsequent lack of seasonal mixing of Black Sea waters. Based on results from Carbon-14 age dating, it

has been estimated that the residence time of water in the Black Sea is between 935 and 2,250 years (Ostlund, 1974; Sorokin, 1983). Due to the enclosed nature of the Black Sea, tidal flow is minimal.

Temperature and Salinity. As mentioned previously, the waters of the Black Sea are permanently stratified as a result of the surface inflow of low density freshwater from rivers and rainfall and a deeper input of saline Mediterranean water. Average surface water salinities range from 18.0 to 18.5 ppt during the winter months, to 17.3 to 17.5 ppt in the summer. Due to increased river runoff, lower salinities (ranging from 14 to 16 ppt) are found in the northeastern shelf region during the summer months . In the central Black Sea, surface water salinity is approximately 18.5 ppt. The mean salinity of deep waters is distinctly higher and ranges from 22.2 to 22.4 ppt. (Balkas et al., 1990).

The surface temperatures of Black Sea waters display marked seasonal variation. Average annual surface water temperature ranges from 16°C in the southern Black Sea to 13°C in the northeastern Black Sea (Balkas et al., 1990). The mean temperature of the northwestern coastal and shelf region is as low as 11°C. During the summer months surface water temperatures can increase to 25°C in the southern portions of the Sea. However, while the Black Sea surface waters show seasonal fluctuation, deeper waters (50 to 70 m below the surface) remain constant throughout the year and have an average annual temperature of 9°C.

Oceanic Sedimentation. The Black Sea receives a high amount of sedimentation from river runoff. The Danube carries approximately 55% of the suspended sediment load to the Black Sea, the Caucasian rivers carry 29%, the Anatolian rivers carry 10%, and the remaining Russian and Bulgarian rivers carry 6% (Hay, 1987). A mean sedimentation rate of 15.8 to 17.0 cm per 1000 years has been estimated for the system (Calvert et al., 1991, cited in Chadwick et al., 1996).

Three main layers of sediment have been deposited in the Black Sea during the last 25,000 years. The most recently deposited layer consists of microlaminated sediments enriched with carbonate. The second layer, formed 3000 to 7000 years ago) consists of Black Sea sapropel sediments enriched with organic matter. The third, oldest layer consists of lutite sediments (Sorokin, 1983). Danube sediments contain low concentrations of heavy metals. The iron concentration increases in predeltaic marine sediments as the salinity of the water increases. Bulgarian coastal rivers do not carry significant amounts of sediments or polluting substances due to the presence of two large coastal lakes which function as purification plants (Balkas et al., 1990).

CURRENT ENVIRONMENTAL STRESSES

Marine Pollution. An estimated 165 million people from 16 countries live adjacent to the Black Sea drainage basin (FAO, 1994). The Black Sea has been affected by eutrophication and pollution in the inshore and shelf region communities (the Sea of Azov, the northwest shelf, the western and Caucasian coasts, and the area near the Bosporus) (Shushkina and Vinogradov, 1991). Few data are available pertaining to concentrations of marine contaminants in biota along the coast of Turkey. Land-based pollution, agricultural development, reductions in river discharges and overfishing have all contributed to eutrophication and subsequent ecological damage of the Black Sea environment (Salekhova et al., 1989; Shushkina and Vinogradov, 1991). Additionally, there is some evidence that the Black Sea may have served as a disposal site for nuclear wastes (Balkas et al., 1990).

Litter. Marine litter levels are likely high due to human activity within the region. Sixteen official dump sites exist in the western Black Sea, mostly on the continental shelf (Mee, 1992, cited in Chadwick

et al., 1996). Communities of the open sea are isolated to some extent by the convergence at the outer boundary of the main Black Sea current and are therefore less affected by pollution than the highly polluted inshore zones. (Shushkina and Vinogradov, 1991)

Toxic Materials. Nutrients make up a large part of the riverine discharge to the Black Sea. High concentrations of inorganic nutrients in the water are likely responsible for reduction of inshore meso-plankton (Shushkina and Vinogradov, 1991). The Danube River alone deposits 60,000 tons of total phosphorous and 340,000 tons of total inorganic nitrogen per year into the Black Sea (Mee, 1992 cited in Chadwick et al., 1996). Metal concentrations reaching the Black Sea have been poorly documented. Heavy metals such as copper, lead, cadmium, and zinc are discharged from such sources as wastewater outfalls and coal and ore mines. The most significant detrimental effects occur in coastal areas with highly developed industry (Balkas et al., 1990).

Organochlorine insecticides in samples of mussels and seven species of fish (*Engraulis encrasicolus, Merlangus merlangus exuxinus, Mugil auratus, Mullus surmuletus, Mullus barbatus, Trachurus trachurus, Scophthalmus maeoticus*) as well as in samples of fish oil and flour were examined by Akman et al. (1978). In the samples examined, the following substances were present: DDT (100% of the samples), BHC (100% of the samples), dieldrin (97% of the samples), aldrin (95% of the samples), and endrin (52% of the samples). (Akman et al., 1978 cited in Balkas et al., 1990).

Petroleum hydrocarbons are regularly discharged into Black Sea waters along navigation routes. Significant amounts of oil from bordering countries are transported in the Black Sea and extremely high hydrocarbon levels have been found from the Danube Fan to the Bosporus.

Organic wastes include ship and land-based sewage and food discharges and fish-processing wastes. These discharges raise the nutrient concentrations which may overburden areas subject to critical eutrophication; however, discharges into the open sea, where sinkable wastes would rapidly reach anoxic depths are far reduced from those in shallow coastal areas.

Natural Inputs. Natural pollutant inputs from terrestrial sources within the Black Sea are generated by the river discharges. The highest inputs come from Soviet rivers. Bulgarian and Turkish river inputs are lower (Balkas et al., 1990). Nutrients are most abundant in areas around the mouths of rivers and areas of upwelling. The two main periods of production are early spring from February to April, and late summer from August to September. Eutrophication is a serious threat in the context of Black Sea ecology. Rass (1982) noted that the recent decrease in water flow from the Black Sea through the Bosporus Strait testifies to the depletion of flow from rivers into the Black Sea. He stated that the decreased flow did not prevent pollution from entering the Sea. However, it did prevent water exchange and has resulted in further oxygen depletion and a reduction of flushing action in the surrounding water.

Sea Traffic and Ports. The Black Sea represents one of a small number of warm water ports that border the former Soviet states and is the only ocean access available to Romania and Bulgaria. Therefore, a high volume of sea traffic exists within the Black Sea. Most commercial shipping occurs within the marine shipping lanes of the Danube to the Bosporus. Here, large commercial tankers and freighters transport significant amounts of oil from bordering countries through the Bosporus Straits (Balkas et al., 1990). Approximately 300 warships travel annually through Black Sea waters. Additionally, 20,755 merchant ships traveled through the Strait in 1980. Major ports include Istanbul and Odessa.

FISHERIES AND AQUACULTURE RESOURCES

Commercially important Black Sea small pelagic fish include the European anchovy (*Engraulis encrasicolus*), horse mackerel (*Trachurus mediterraneus*), and sprats (*Sprattus sprattus*) (Balkas *et al.*, 1990). However, commercial fisheries of the Black Sea have declined drastically in recent years. Of the 26 species exploited during the 1960s, only six remain (Mee, 1992 cited, in Chadwick *et al.*, 1995). Recently, overfishing of these stocks along with abundant nutrient loading from adjacent fluvial systems produced an increase in zooplankton, which brought about an increase in the *Aurelia* jellyfish (from 50 million tons in the mid-1960's to 400 million tons from 1983 to 1984) (FAO, 1994). The abundance of jellyfish and zooplankton in the waters led to a 1988 outbreak of *Mnemiopsis leidyi*, an introduced ctenophore that is a remarkably efficient predator when high concentrations of zooplankton and other food sources are available. This species preys primarily on copepods and secondarily on fish eggs and larvae, particularly those of anchovy and mackerel. Due to the winter timing of sprat spawning, this species has not been as affected by the *Mnemiopsis* outbreak. Because of the large population of *Mnemiopsis leidyi*, spring blooms of zooplankton have been prematurely depleted and now, sufficient food does not exist for the small pelagic fish species. Thus, reproduction of stock species is low, and eggs and larvae produced are further susceptible to *Mnemiopsis leidyi* predation. In order to control the population of *Mnemiopsis leidyi*, two suggestions have been proposed. Because *Mnemiopsis* is an inefficient predator when food is scarce, low food levels brought about by the reduction of nutrient loading should decrease populations of the ctenophore. Additionally, sustaining high fish stocks by limiting exploitation for several years will be necessary to allow these species to better compete with *Mnemiopsis*.

The fisheries for larger pelagic fish, such as bonito and bluefish and for demersal species, such as sturgeon, mullet, turbot, and gobies have also declined since the 1970s (FAO, 1994). Increased eutrophication and changes in pelagic conditions have adversely affected the juveniles of these species. In addition, anoxia in the summer months has brought about inevitable fish kills of the demersal species. Moreover, a reduction in fresh water inflow has led to severe declines in fish and shellfish populations in estuaries. For instance, the fishing yield in the Dnepr estuary was five times less in the 1970s than in the 1950s. Also, certain important species (pike, roach, perch, vimba, and bream) have completely disappeared from these areas (Balkas *et al.*, 1990). Additionally, populations of oysters and mussels (*Mytilus* spp.), both formerly important commercial species, have been destroyed by anoxic bottom conditions and waste dumping, and by the disruption of larval settlement by the *Mnemiopsis* outbreak. The mussel stock of the Black Sea had decreased from 10 to 12 million tons in the northern Black Sea to half that size by the mid-1980s (FAO, 1994). Finally, the biomass of commercially and ecologically important phyllophora algae has decreased by 25% due to decreased river runoff, increased bottom trawling, and pollution.

The restoration of the Black Sea marine environment is essential for future exploitation of its resources. A complete halt on the fishery industry will result in a loss of $30 million/yr, but continued exploitation, without ecological recovery, would be even more costly and lead to a permanent loss of the fishing industry in the Black Sea (FAO, 1994). In the effort to restore fish stocks, hatcheries and rearing facilities are proposed for areas of minimal environmental damage. Beginning with local anadromous species (grey mullets, salmonids, and sturgeon), this effort may lead to breeding and release plans for turbot, contingent upon improved conditions that can sustain adult stocks. Additionally, sea ranching of several coelenterate predating, non-native species such as salmon, Baltic cod, haddock, and sparids, might reduce the *Mnemiopsis* populations and provide new fisheries resources.

Phytoplankton. Seasonal phytoplankton dynamics in the Black Sea are typical for a temperate marine basin. Nutrients are most abundant in areas around rivers mouths and in the peripheral areas of the Black Sea and the convergence zone of the large gyre (Hay, 1987). Two main phytoplankton blooms occur each year; the larger occurs during early spring (from February to April) and the smaller occurs in late summer (from August to September); more than 60% of the yearly primary production occurs during these months. Highest concentrations of phytoplankton are recorded in coastal regions, reflecting the influence of the general cyclonic circulation of the Black Sea and the presence of hydrogen sulphide zone in the central parts of the cyclonic circulations where the anoxic layer is closest to the surface. The lower limit of phytoplankton distribution occurs at the upper limit of the hydrogen sulfide zone.

Average yearly primary production estimates for the Black Sea range from 150 to 250 $gC \cdot m^{-3} \cdot yr^{-1}$and are comparable to estimates for fertile seas such as the Baltic (Balkas *et al.*, 1990). Estimates for the shallow northwest coastal areas are as high as 730 $gC \cdot m^{-3} \cdot yr^{-1}$, while those for the central basin are much lower at 36 $gC \cdot m^{-3} \cdot yr^{-1}$ (Sorokin, 1983). The biomass of phytoplankton is estimated at $3.7 \cdot 10^6$ t (8.8 $g \cdot m^{-2}$) (Christensen and Caddy, 1994).

Between 476 and 746 species of phytoplankton are found in the Black Sea (Sorokin, 1983; Cihangir and Tirasin, 1989). Populations are dominated by diatoms and dinoflagellates. The most abundant diatoms are the *Chaetoceros* spp. and the single oceanic diatom species found in the Black Sea is *Planktoniella sol.* Other dominant phytoplankton species include *Bacillariophyta* (more than 200 species) and *Pyrrophyta* (more than 150 species). Additional species include *Chlorophyta* (80 species), *Chrysophyta* (399 species), *Cyanophyta* (30 species), *Euglenophyta* (13 species), and *Xanthophyta* (3 species) (Sorokin, 1983; Cihangir and Tirasin, 1989).

Zooplankton. Like phytoplankton, zooplankton in the Black Sea exist only above the hydrogen sulfide zone. Vertical distribution of zooplankton is determined by temperature, salinity, currents, and the depth of the anoxic waters. (Cihangir and Tirasin, 1989) Most of the zooplankton accumulate in the upper 50 m of water, which contains 80% to 85% of the total zooplankton biomass (Sorokin, 1983). The biomass of protozoa has been estimated to range from 1.5 to 3.5 $g \cdot m^{-3}$ (Shuskina and Vinogradov, 1991). The biomass of zooplankton has been estimated to be 8.33 $g \cdot m^{-3}$ including *Sagitta*, a zooplanktivorous organism (Christensen and Caddy, 1994).

The Black Sea zooplankton are dominated by copepods. Copepod species include *Calanus* spp., *Acartia* spp., *Centropages* spp., *Oithona* spp., *Paracalanus* spp, *Pontella* spp., and *Pseudocalanus* spp. Other zooplankton include appendicularians (including *Oikopleura dioica*), cystoflagellates (including *Noctiluca miliaris*), and chaetognaths (Benli and Pilskaln, 1988). About 20 species of Mediterranean zooplankton enter the Black Sea through the Sea of Marmara, the majority of which are remarkably euryhaline (Sorokin, 1983).

The macrozooplankton assemblage of the Black Sea was dominated by the medusa *Aurelia aurita* in the 1970s and has since been superseded by *Mnemiopsis leidyi*, a predaceous ctenophore. The abundance of *Mnemiopsis* in 1989 was so great that the biomass was estimated to be close to 1 billion tons (Shuskin and Vinogradov, 1991). As mentioned previously, *Mnemiopsis* is predominantly zooplanktivorous and can survive long periods of reduced food availability through cannibalistic predation. Copepods, fish larvae, juvenile fish, and fish eggs are known to be potential prey of *Mnemiopsis* (Caddy and Griffith, 1994; Christensen and Caddy, 1994). Open sea productivity of *Mnemiopsis leidyi* in the Black Sea has been reported to be as high as 900 $g \cdot m^{-2}$ (September 1988) and as low as 1.2 $g \cdot m^{-2}$ (May through June 1989). This productivity has been based on data from expeditions over the course of the entire annual

cycle. *Mnemiopsis* individuals have even penetrated into the lower layers of the aerobic zone (Shuskina and Vinogradov, 1991). The representation of jellies in the Black Sea plankton accounted for 95% of the mesoplankton and 99.6% of the total biomass of the meso- and macroplankton in February/March 1991 (Shuskina and Vinogradov, 1991).

TROPHIC RELATIONSHIPS

Pelagic Food Web. The pelagic food chains of the Black Sea are fed by the abundant zooplankton dominated by the copepods (Figure 4.1-19). This trophic structure, which has already been severely weakened by eutrophication and pollutants and heavy nutrient enrichments from riverine discharges, as well as by proliferation of the *Mnemiopsis* ctenophore is nearly beyond repair. Due to the limited and even decreasing amount of oxygenated waters of the Black Sea, the system may be particularly vulnerable to disturbances which further the destruction of key species in the trophic web.

The macrozooplankton species, which feed on smaller zooplankton and the larval forms of fish, crustaceans and molluscs, include medusae (*Aurelia aurita*, *Rhizostoma plumo*, and *Sarsia setosa*) and ctenophores (including *Pleurobrachia pileus* and recently, *Mnemeopsis leidyi*), species which are little exploited by higher level consumers. As mentioned previously, the Black Sea currently faces a severe disruption of the natural trophic web due to the proliferation of ctenophores and jellyfish. These species presently consume 60 to 63% of the annual zooplankton production, while zooplanktivorous fish consume only 6.0 to 6.5% of the zooplankton (Christensen and Caddy, 1994). As a result, there is an energy transfer short circuit which combines with other factors to severely limit other resource links within the sea.

Fish stocks in the Black Sea are not as abundant as those of other oceans. The Black and Azov Seas include approximately 180 species of fish, 120 of which are exclusively marine, 22 of which are fresh water, and the rest of which are anadromous (Cihangir and Tirasin, 1989). Fifty-seven percent of the fish species are immigrants from the waters of the Mediterranean Sea (mackerel, bonito, mullet) (Balkas *et al.*, 1990). Zooplantivorous fish species include anchovy (*Engraulis encrasicholus*), horse mackerel (*Trachurus mediterraneus ponticus*), sprat (*Sprattus sprattus*), mullet (*Mugil cephalus* and *Liza aurata*), pipefish (*Syngnathus* spp.), and silverside (*Atherina* spp.). In 1984, the anchovy, sprat, and horse mackerel accounted for approximately 91% of the total annual catch (Cihangir and Tirasin, 1989). Larger, carnivorous species include bonito, mackerel (*Scomber scombrus*), bream (*Diplodus* spp.), and bluefish (*Pomatomus saltator*). These species feed mainly on planktivorous fish.

The top predators of the Black Sea waters include three species of dolphins, *Phoceana phoceana* (harbor porpoise), *Tursiops tursio*, and *Delphinus delphis* (common dolphin). Additionally, monk seals (*Monachus monachus*) were once common in the region, but it is doubtful whether viable populations are currently present. Dolphins feed primarily on anchovy, horse mackerel, mackerel, and bluefish. Although there is no quantitative data for fish consumption by dolphins in the Black Sea, it is estimated that at one time dolphins consumed half a million tons of food per year. However, current estimates of dolphin populations do not exceed 100,000 animals (FAO, 1994). It is improbable, therefore, that the current decrease in fish populations is related to depletion of stocks by cetacean predation. Populations of other top predators, bonito and bluefish, were reduced in the 1960s and 1970s due to overfishing and environmental degradation. These species, unlike the dolphins, migrate through the Bosporus and now only occasionally enter the Black Sea (Caddy and Griffith, 1994).

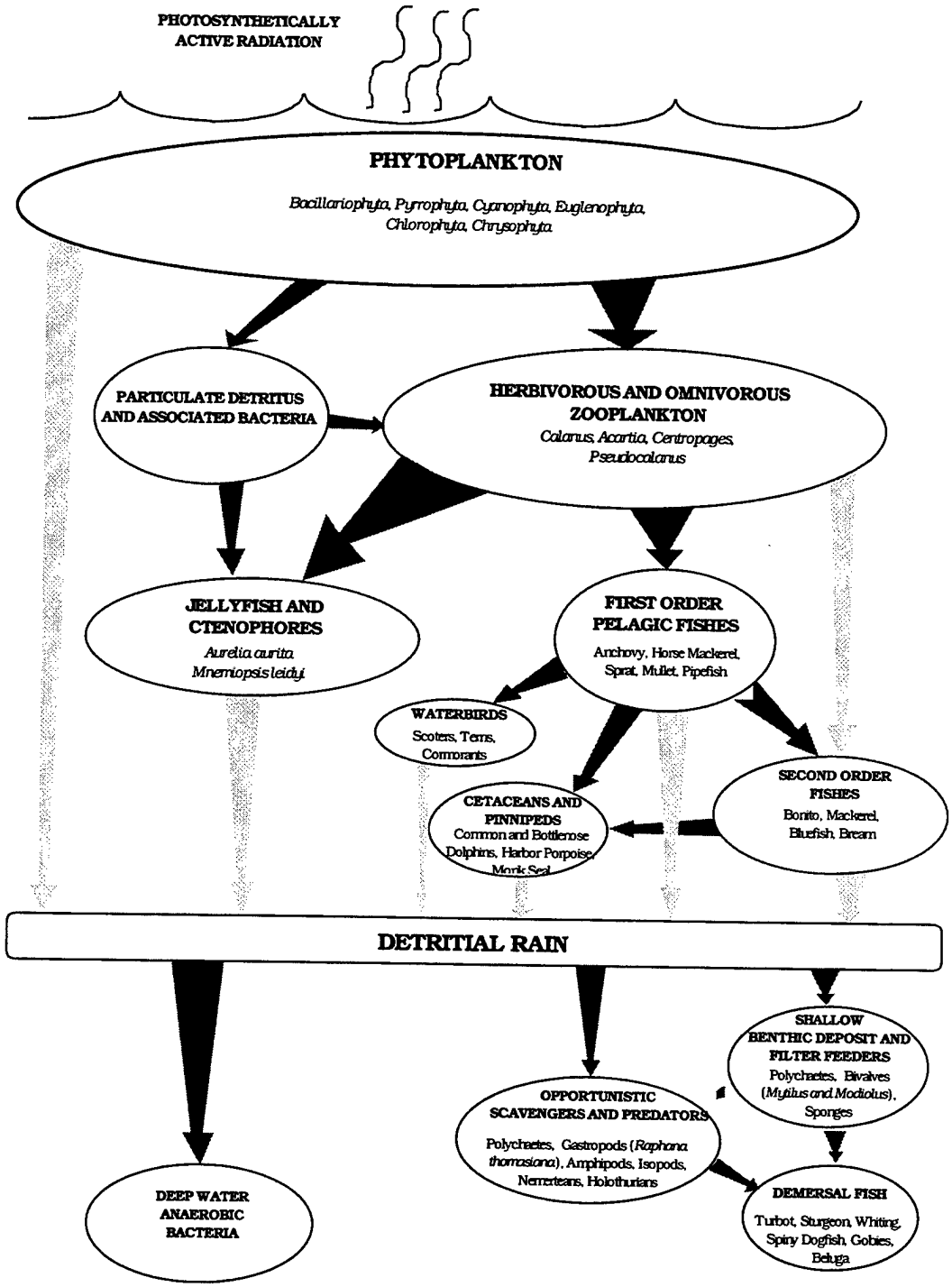

Figure 4.1-19. The Black Sea Trophic Web. The Black Sea system is highly stressed and well out of balance. Eutrophication of the surface waters has resulted in phytoplankton blooms followed by an overabundance of zooplankton and promotion of a handful of species of jellyfish and ctenophores. Massive seasonal pulses of these non-discriminate plankton consumers, along with fishing pressures, have reduced both larval and adult stocks of the Sea's fisheries. Anaerobic deep waters are occupied by bacteria while narrow shelf communities support a poorly developed opportunistic assemblage.

Benthic Food Web. The benthic communities of the Black Sea are restricted to shallow, oxygenated waters. Only 23% of the bottom of the Black Sea is inhabited by benthic flora and fauna (Sorokin, 1983). Benthic algae is found only in shallow waters (between 0 and 20 meters) and are represented by 304 species of mostly green, and some brown and red algae. The most common species include *Ulva* spp. *Cystoseira*, and *Phyllophora* (which is commercially harvested). About 90% of the total biomass of macrophytes in the Black Sea is comprised of *Phyllophora*. Two species of seagrass, *Zostera marina*, and *Zostera nana*, are found in shallow bays and lagoons. Within the seagrass beds, epiphytic algae, sponges, and bryozoans (such as *Lepralia* spp., and *Membranipora* spp.) thrive. These epiphytic species are an important food source for several demersal fish species.

The zoobenthos includes 1,520 invertebrate species. The most abundant species include Turbellaria (103 species), Nematoda (240 species), Gastropoda (118 species), Polychaeta (182 species), Ostracoda (109 species), Copepoda (154 species), and Amphipoda (103 species) (Cihangir and Tirasin, 1989). The members of these seven taxonomic groups represent 66% of the total benthic invertebrate species found in the Black Seas. Total annual production of the zoobenthos has been estimated to be $53.6 \cdot 10^6$ t (Cihangir and Tirasin, 1989).

Approximately 85% of the total benthic biomass of the Black Sea is found along in the shallow, northwestern waters of the Sea. The littoral zone of the Black Sea (wave splash area) is dominated by opportunistic scavengers including several species of amphipods, isopods, and mysids. The sandy and muddy near shore bottom is dominated by bivalves (*Cardium* spp., *Divaricella* spp., *Syndesmia* spp., and *Venus gallina*). Gastropods (*Nasa*, *Rissoa*), polychaetes (*Glyceria*, *Nereis*, *Spio*, and *Nerine*), nemerteans (*Eunemertes*, *Lineus*), and holothurians (*Synapta*) are also present in large numbers. The majority of these benthic invertebrates are filter or suspension feeders, or are opportunistic scavengers (Figure 4.1-19). In slightly deeper waters (50 to 70 meters), there are large populations of filter-feeding, commercially harvested mussels (*Mytilus galloprovincialis*). The shellfish species of the Black Sea have been replaced over much of their range by exotic species that are resistant to low oxygen conditions and nutrient-enriched water (Caddy and Griffith, 1994). The invasive predatory bivalve, *Raphana thomasiana*, has become quite common along Black Sea coasts in the last 40 years (Cihangir and Tirasin, 1989). In the deep waters below 70 meters, dense populations of the bivalve, *Modiolus phaseolinus*, are found. Additionally, the bulk of the deep benthos is comprised of tiny nematodes and harpacticoids that can occur in densities as great as $250 \cdot 10^3$ individuals$\cdot m^{-2}$ (Sorokin, 1983).

The Black Sea supports a wide diversity of shallow demersal fish fauna including turbot (*Psetta maxima maeotica*), whiting (*Merlangius merlangus euxinus*), spiny dogfish (*Squalus acanthias*), and gobies (*Gobius* spp.). Turbot and whiting prey on small fish and crustaceans and bivalves. Gobies feed on benthic invertebrates including crustaceans and polychaete worms. Spiny dogfish feed on various fish, molluscs, and some crustaceans (Cihangir and Tirasin, 1989). Currently, the turbot is subject to a ban on trawling by the Black Sea Fishery Commission. (Caddy and Griffith, 1994). Other demersal species include rays, eels, belugas (*Huso huso*), sturgeon (*Acipenser* spp.), sole, flounder, scorpionfish, blennies, and anglerfish.

UNIQUE SPECIES AND ECOLOGICAL CONSIDERATIONS

Endangered/Threatened or Protected Species. Currently, there are no threatened or endangered species in the Black Sea except for the monk seal. This species is listed as endangered under the U.S.

Endangered Species Act and is one of the most endangered of the marine mammals. The current status of this species within the Black Sea is unknown. No critical habitat has been designated within the Black Sea region.

Unique Habitats. The majority of the waters of the Black Sea are anoxic. Therefore, 100% of the marine flora and fauna inhabit less than 20% of the waters of the Black Sea. The shallow, nutrient-rich waters in the northwestern portion of the Sea, near the Danube delta, support the most diverse and extensive populations of organisms. If Black Sea fisheries are to recover, the high level of productivity in this region must be maintained. Other shallow, productive waters are located around the mouths of the other rivers that feed the Sea, and near the convergence of the large cyclonic gyre located near the Crimean peninsula.

Today the picture of the Black Sea is bleak. The waters of the Sea no longer support extensive fisheries. Overfishing, pollution, eutrophication, and ctenophore outbreaks have substantially decreased the stocks of numerous fish, mollusc, and algal species to the point that recovery appears improbable. The possibility of halting over-exploitation and of replenishing fish stocks has been discussed; however, populations continue to decline. Clean-up of the riverine discharges would play a significant role in reducing the rate of decline if not reversing it. However, barring correction of coastal inputs, little can be done within deep water areas of the cyclonic gyres to correct the situation.

MEDITERRANEAN SEA

PHYSICAL AND CHEMICAL CONSIDERATIONS

Geography and Physiography. The Mediterranean Sea is an almost land-locked sea ranging from 30° to 46° North latitude and 5° 50' West longitude to 36° East longitude (Figure 4.1-20). Its total area is close to $2.5 \cdot 10^6$ km^2. Separated from the western Atlantic by the narrow (5 km wide) Straits of Gibraltar, The Mediterranean is connected to the Black Sea at the eastern limits via the Dardanelles. Additionally, the Mediterranean Sea is connected to the Red Sea via the Suez Canal, completed in 1869. The total volume of the Mediterranean is $3.7 \cdot 10^6$ km^3 (Margalef, 1985). It is characterized by an irregular coastline of approximately 27,000 km punctuated by deep bays. An additional 19,000 km of coastline forms around the Mediterranean islands. The 18 countries surrounding the Mediterranean are directly and intensely influenced by the Sea. More than a third of the populations of these countries live in the coastal regions of the Mediterranean.

The Mediterranean is geologically a relatively young ocean basin spawned by the destruction and demise of an older east-west seaway (Tethys) that extended from the Americas on the west and transversed the Himalayas to the Pacific basin on the east (Margalef, 1985). A by-product of its geologic history may be seen even today as active geologic agents, including earthquakes and volcanoes, occur along the length of the basin. During several intervals within recorded history, destructive earth episodes have severely impacted and virtually wiped out entire cultures. The most compelling geologic aspect of the Mediterranean basin is that this ocean itself died as a seaway about six million years ago. For one million years, ending about five million years ago, this immense depression was an arid valley separating Europe from northern Africa. Within the Pliocene Epoch, the Atlantic Ocean breached the sill at Gibraltar to reestablish the Mediterranean as a sea. For this reason, and the fact that the main circulation of the Mediterranean goes into the Atlantic, these two oceans are closely related biologically (Maldonado, 1985).

Within the Mediterranean basin evaporation far exceeds fluvial influx, thus there is a strong recovery inflow of surface waters from the Atlantic through the Straits of Gibraltar and into the western Mediterranean (Maldonado, 1985). The intense evaporation drives Mediterranean surface waters well above the average marine salinity of 35 ppt. These warm, higher salinity waters sink to the floor and are extruded as bottom waters at the Gibraltar sill back into the eastern Atlantic (Maldonado, 1985). In contrast to its relatively young geologic history, the Mediterranean coast hosts some of the oldest civilizations on earth. More important is the diversity of cultures and political systems along the Mediterranean rim. These political realities, coupled with the geographic restrictions of the basin, make this area second only to the Baltic in its vulnerability to pollution. This has begun to manifest itself already by rapid depletion of fishing stocks and several of the hallmarks of ocean pollution that characterize this seaway.

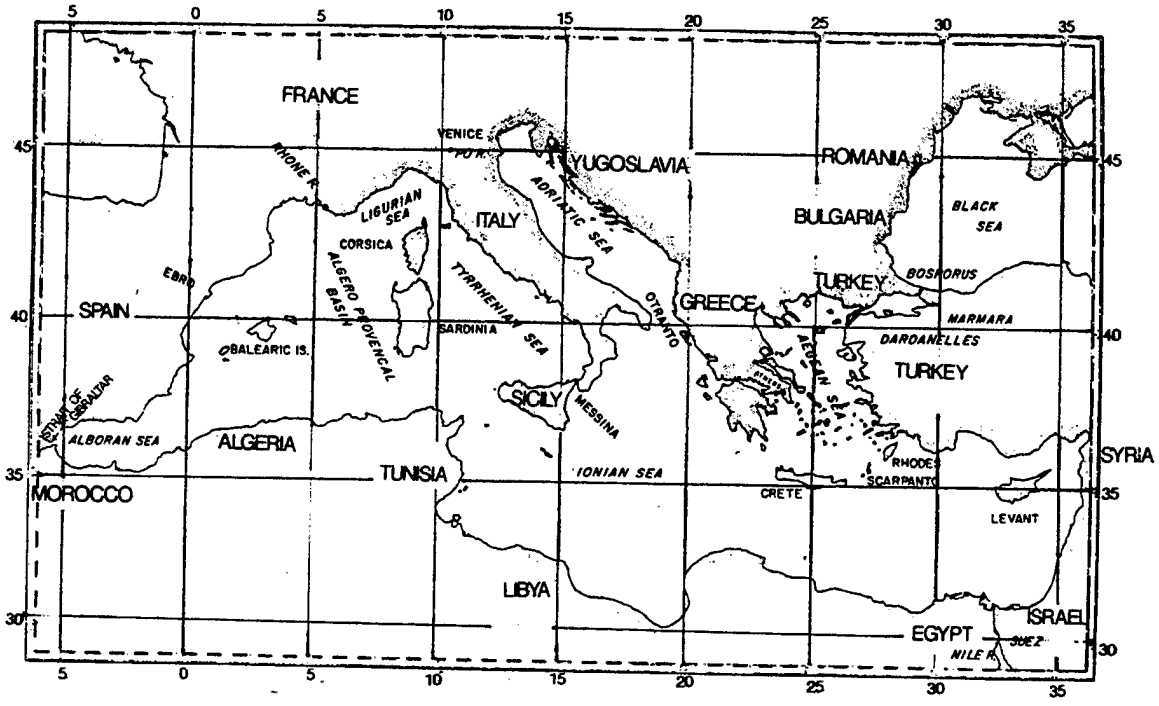

Figure 4.1-20 The Mediterranean Sea. The Mediterranean Sea extends from the Strait of Gibraltar on the west to the entrance of the Dardanelles on the east. It is connected to the Atlantic Ocean via the Strait of Gibraltar, to the Red Sea via the Suez Canal, and to the Black Sea via the Dardanelles.

Bathymetry. The Mediterranean is comprised of two major basins, the eastern and the western separated by a deep sill about 400 meters below the surface situated west of Sicily. The eastern Mediterranean is in turn subdivided into three basins, the Levantine on the east, the Ionian to the west, and the long isthmus of the Adriatic Sea projecting northwestward from the Ionian. In the western Mediterranean, the island of Sardinia separates the Tyrrhenian basin on the east from the Algerian basin on the west. Just east of the Gibraltar Strait, the Alboran basin separates Spain from Morocco. At its eastern extremity, the Mediterranean connects with the Black Sea at the Bosphorus Strait (Maldonado, 1985). This linear string of discrete basins separates areas of differing biology, sediments, and hydrology. Sill depth at the Bosphorus Strait in the area of the Dardanelles is only 75 m which minimizes but does not constrict hydrologic exchange between the Mediterranean and the Black Sea. In this vicinity, the Aegean Sea is a shallow depression separating Greece and Turkey. In concert with the relative youth and tectonic activity of the Mediterranean, continental shelves here are narrow, usually measured in tens of kilometers. These shelves are deeply scored by submarine canyons which were cut during the Mediterranean arid phase "the Messinian Crisis" and the basin floors are every bit as rugged as the surrounding coastal areas and highlands (Maldonado, 1985). Over 30% of the area of the Mediterranean waters have depths greater than 2000 m, while less than 20% of the area of the Sea has depths of less than 200 m (Miller, 1983).

Currents, Tides, and Water Exchange. Major water exchange systems in the Mediterranean are thermohaline-driven. High density, warm, high-salinity water sinks to the ocean floor to be driven across the bottom of the Gibraltar Sill into the Atlantic. A hydrological imbalance is induced by excess evaporation, 87% of which is compensated by surface inflows through the Gibraltar Strait. The

remaining 13% enters through the Dardanelles from the Black Sea (Maldonado, 1985). The Suez exchange is insignificant compared to the deeper, more profound, western exchange. Four major fluvial systems, the Rhone, Po, Ebro, and Nile, empty into the Mediterranean averaging $10 \cdot 10^3$ km^3 of input annually.

Surface currents throughout the multiple basins are invariably counterclockwise in their flow, the strongest of which is the surface inflow from the Atlantic eastward along the northern coast of Africa. This current is greatly enhanced during the summer months when Mediterranean evaporation is at a maximum (Maldonado, 1985). Components of this eastbound current can be identified in the Sicilian channel as well as in the eastern Mediterranean off the Levant coast. The frequency and density of the thousands of islands sprinkled across the basins are such that major currents are broken up into numerous small eddies.

Within recent time, the most profound anthropogenic event affecting the water exchange has been the construction of the Aswan High Dam, completed in 1970. This edifice has greatly impeded fluvial inflow and sedimentation. Ultimately, the nutrient loss to the eastern Mediterranean had by far the most serious regional impact while on a local scale, in Egypt, the dam had the consequence of reintroducing malaria to the Nile delta area on a grand scale.

Mediterranean tides are typically semidiurnal, with two high and two low waters during each day. Mean and spring tide ranges are small, averaging less than a meter. At Gibraltar, the tidal range is approximately 1 m, decreasing toward the east to less than a third of a meter. The tide range in the Tyrrhenian and Ionian Seas is measured in centimeters; however, the largest Mediterranean tides are to be found in the Gulf of Gabes just south of Tunis where the range is slightly less than 2 m. Further, much of the central Mediterranean is virtually tideless (Maldonado, 1985).

Temperature and Salinity. Thermocline and halocline horizons in the Mediterranean are among the best defined for the oceans of the world. Examples of these horizons in the Mediterranean have, in places, received such exhaustive study that they could be considered classic examples. Surface salinity values range from 36 ppt at Gibraltar to 37 ppt at the Sicilian Strait to as high as 39 ppt in the extreme eastern margin in the Levantine basin (Maldonado, 1985). These high-density and salinity-soaked waters sink in the eastern Mediterranean to form an intermediate water layer down to a maximum of 600 m which ultimately returns to the Gibraltar sill and pours back into the Atlantic. In the process of transit from the eastern to the western Mediterranean, sufficient mixing occurs to raise the salinity to 38 ppt as waters join the Atlantic. Inflow into the Atlantic across the Gibraltar sill from the Mediterranean has the effect of significantly raising eastern Atlantic temperatures and salinity values along the pathway of the propagating plume (Maldonado, 1985). Deep within the Mediterranean basin a third layer of water is found below the sill depths at 400 m down to basin maxima in excess of 4000 m. This very large water mass circulates only minimally and is characterized by an average temperature of 13°C and an average salinity of 38.5 ppt.

The temperatures of Mediterranean surface waters are characterized by marked seasonal variability. Temperatures average 13°C in winter to 26°C during the summer months. In general, temperature and salinity values for the deep water mass are remarkably homogenous (Maldonado, 1985).

Oceanic Sedimentation. In a general way, the Mediterranean basin conforms to the model energy versus sediment grain size model. In this model, proximal or shelf sediments are typically coarse grained while those in deep basins are fine-grained clay muds (Margalef, 1985). Adjacent to the fluvial effluents, deltas and fans of terrigenous origin are found. Approximately 90% of sediment deposited by fluvial

systems comes from the northern Mediterranean where these systems deliver $5 \cdot 10^7$ tons of sediment annually (Maldonado, 1985). In areas between major river mouths there is frequently a sizeable calcareous sediment component (Maldonado, 1985). Off the shelves, in continental slope waters, sediment supply alternates between massive gravity flows and hemipelagic settling from surface waters. The dominant Mediterranean sediments are fine-grained muds that vary from hemipelagic components along structural highs to turbidite muds on the abyssal plains of the deepest basins. An intriguing sidelight to Mediterranean deep-basin sedimentation is that many of the patterns are controlled by salt tectonics of the underlying Messinian evaporites. Diapirs driven by salt under pressure create a rugged ocean floor topography where distal turbidite flows are entrapped and ponded into discrete large and small basins.

Shelf carbonates are largely bioclastic, reflecting areas of local productivity in benthonic assemblages (Margalef, 1985). Generally, the Mediterranean is latitudinally zoned with carbonate-rich shelves on its southern margin and terrigenous sediment to the north. Unlike water, Mediterranean sedimentation is essentially a closed system with all transported particles becoming entrapped (Bas *et al.*, 1985).

CURRENT ENVIRONMENTAL STRESSES

Marine Pollution. With 18 countries surrounding the Mediterranean and more than 150 million people directly inhabiting the coastal areas, heavy industrialization, combined with human sewage, and agricultural fertilization by-products have all generated major pollution throughout the basin. Through the Po estuary alone, 65 tons of mercury, 243 tons of arsenic, and almost 500 tons of lead and other heavy metals are flushed annually into the Mediterranean (Pastor, 1991). Additional pollutants include petroleum and related hydrocarbons as well as thermal effluents from coastal industries.

Litter. Much of the information regarding litter in the Mediterranean is derived from estimates based on few quantitative studies (Chadwick et al., 1996). In 1970, Gerard Bellan (Station Marine d'Endoume - Marseille, France) tried to assess certain general aspects of pollution and litter in the Mediterranean. He found only two geographical sectors where pollution and litter studies had been conducted in a comprehensive manner: the regions of Marseille on the French coast and Trieste in the upper Adriatic. In the last two decades, subsequent studies have shown continued and overwhelming accumulation of persistent and non-persistent refuse in the Mediterranean Sea (UNEP, 1991). Further studies have shown the heterogeneous nature of the litter in terms of material type, size, units of measure, and the methods employed in quantification, result in a large variability in the estimates (Chadwick et al., 1996).

Although there is limited current quantitative estimates of the anthropogenic debris found in the Mediterranean, qualitative assessments of the litter found along the coastline show that the majority of the debris is believed to be land-based, in contrast to the reported marine-based litter on the western European shores (Gabrielides et al., 1990). The larger portion of this coastal debris is associated with tourism activities. The main source of marine-based debris is that which is discarded from ships. Of the $6.6 \cdot 10^8$ kg·yr^{-1} estimated for ship-borne trash, 97% was derived from merchant ships while 1.5% ($1 \cdot 10^7$ kg·yr^{-1}) was derived from military ship activity (Chadwick et al., 1996). Anthropogenic materials occurring within the debris washed up on the most-affected shores include non-degradable fishing nets and floats, styrofoam, milled and painted woods and aluminum, plastic, and treated paper wastes. Areas between Spain, France, and Italy bear approximately one-third of the debris load, while the north end of the Adriatic accumulates one-quarter of the Mediterranean's pollution.

Toxic Materials. Petroleum and related hydrocarbon pollutants enter the Mediterranean from three sources. Oil refineries around the Mediterranean rim have been a long standing problem. Within the decades of the 80s and 90s the Mediterranean has seen a great increase in exploration and offshore oil production. Finally, estimates of as much as a third of a million tons of waste oil flows into the Mediterranean annually via fluvial systems. The most profound problem has been related to the oil refineries found around the Mediterranean but the additional influx of petrochemicals from this industry has more serious potential for long-term damage than the relatively short-lived petroleum pollutants. The flushing of tankers, although prohibited, continues with only minimal abatement. Major spills have not occurred from this activity; however, a large number of minor accidental or deliberate spills occur each year in connection with transporting oil within the region (UNEP, 1989). Finally, estimates of as much as one million tons of waste oil flows into the Mediterranean annually via discharges from land-based and illegal activities (Chadwick et al., 1996).

Massive amounts of sewage with resultant overproduction and eutrophication are threatening the entire Mediterranean Sea. The Adriatic Sea is highly polluted by sewage. The Adriatic comprises only 5% of the total Mediterranean surface, but it receives fully one-third the fluvial inflow. Adriatic pollution reached critical levels for the first time in the summer of 1975 with sewage-induced algal blooms measuring tens of millions of cells per liter. The resultant eutrophication almost eradicated fish as well as all benthic invertebrates. This event turned out to be a harbinger of future disasters as large-scale blooms have recurred virtually every summer since. Another example of eutrophication occurred in 1983 in the Gulf of Trieste when overproductivity, triggered by sewage discharges, almost completely stripped the bottom waters of oxygen. Although the fauna has recovered somewhat, sewage effluent here remains a serious problem. Sewage pollution is additionally aggravated by the summer influx of as many as 100 million tourists. It is estimated that 85% of the waste water generated in the Mediterranean coastal cities flows into the sea untreated. This high figure is due in part to the fact that a significant amount of the modern equipment installed for the purification of waste water is either marginally functional or has failed completely (UN Environmental Programme, 1989).

Additional contaminants include agricultural pollution that may be subdivided into pesticides and excess fertilizer. The former category classically transmits and magnifies upwards through the food chain. The latter, like sewage, contributes to overproduction and eutrophication. Eutrophication tends to be more of a local problem, mainly occurring along the coastline as a result of land-based releases including river input, agricultural runoff, and domestic-industrial waste water input (Chadwick et al., 1996). River inflow of nutrients is by far the largest source, contributing 75% of the total estimated inputs of $8 \cdot 10^5$ $mtN \cdot yr^{-1}$ and $3.22 \cdot 10^5$ $mtP \cdot yr^{-1}$ (UNEP, 1989). Contrasting evidence suggests that the domestic and industrial inputs are only about 10 to 20% of the total input while agricultural runoff is about 10% of the total. Nutrient influx can influence large areas along the coast, particularly in areas with large sources and restricted circulation. The north-western portion of the Adriatic Sea is usually used as an example, with its large nutrient source from the Po River (Waste Discharge into the Marine Environment, 1982).

Two final toxic pollutant sources include bulk dumping of inert products comprised of everything from polypropylene to styrofoam, and thermal pollution. Bulk dumping interferes with biologic systems both by smothering and fouling (Venizelos, 1990). Thermal pollution in an already warm basin is perhaps even more insidious. Frequently, excess calories generated by industrial processes including nuclear power plants seriously impact localized biologic systems particularly those with stages in their life cycles that are triggered by thermal signals. However, these impacts are usually restricted to a very short distance from the points of discharge (Albaiges, 1985).

Natural Inputs. Eutrophication can be caused by natural upwellings common in the Mediterranean Sea. Upwellings can be caused by winter low-pressure systems that move the surface water outward from a cyclonic gyre and push deeper waters toward the surface. Even highly stratified water can have upwellings of this sort. Upwelling can occur as a result of evaporation as well. The Mistral-Tramontana wind, for example, is cool and extremely dry. As it blows across the Sea, surface water evaporates and the remaining dense, more-saline water sinks. This dense, sinking water pushes deep, nutrient-rich waters toward the surface. This rapid transformation is a common phenomenon in February and March in the northwest Mediterranean. Another upwelling region is located in the Alboran Sea, which has an anticyclonic gyre between the Iberian and African coasts.

Sea Traffic and Ports. Dense populations on the Mediterranean margins coupled with heavy industrialization, particularly on its northern shores contribute to very heavy maritime traffic within this basin. Annual traffic in the Mediterranean of ships that are more than 100 gross registered tons is estimated at 220,000 vessels (The World Bank, 1990). This problem is especially aggravated at the several straits, nautical choke-points, that separate the multiple subdivisions of the Mediterranean. The mild climatological regimen dictates near uniform traffic density on an annual basis.

FISHERIES AND AQUACULTURE RESOURCES

The limiting environmental conditions of the Mediterranean, namely the low concentration of phosphates and nitrates so necessary for the maintenance of marine pastures, together with the poor standing crop of bottom-dwelling organisms, provide no opportunity for the evolution of a large commercial fishing trade (Bas et al., 1985). In total, the Mediterranean fisheries produce about 800,000 tons of fish or 1.0% of the world's fish production. Although the general lack of large concentrations of fish has prevented the development of large-scale operations, the high prices of fresh fish in most Mediterranean countries have favored the development of a large number of small-scale fisheries. Though the boats used are rather small, rarely exceeding 70 feet long, their numbers are sufficient enough to deplete local stocks through overfishing. The tendency to over-exploitation is strengthened by the use of trawl nets with very small mesh size that retain even the smallest individuals (UNEP, 1989).

Trawling in the Mediterranean has been the main contributor to high levels of overfishing. As technological innovations have revolutionized the trawl fishing industries, the relative increase in fishing tonnage has increased. The steady increase in fishing capacity has produced competition between vessels for the scant resources available. This competition is motivated by the high economic value of the catches, which more than compensate for the high costs involved (Bas *et al.*, 1985). Artisan fisheries vary greatly in extent. They are still important in many localized areas, but they have lost their former importance off most of the coasts, including that of Spain. However, in Spain, artisan fishing is now making some recovery. This is seen in the improved fishing technology used on the numerous small boats still engaged in these fisheries. The catches include a variety of general coastal species, primarily sea breams and large hake which are taken by longlining or by handlining (Bas et al., 1985).

The Mediterranean fisheries exhibit an important trend: a continuing tendency for the replacement of the pilchard (*Sardina pilchardus*) by various species of the anchovy. Both are taken along the Mediterranean coast, especially in inshore areas. Evidence suggests that both of these species are underexploited over almost the entire Mediterranean, especially off the coast of Africa, where maximum sustainable yield for pilchard in this region is estimated at some 75,000 to 85,000 tons, mostly from Algeria. The maximum sustainable yield is lower off the coasts of Spain, France, and Italy (Bas et al., 1985).

Recently, certain carangid species have become commercially important, particularly the horse mackerel (*Scomber scombrus*), some 18,000 to 23,000 tons of which, on average, have been taken yearly over the period from 1968 to present (Bas et al., 1985). Among the demersal fish, hake (*Merluccius merluccius*) is one of the more important in all countries bordering the Mediterranean. In addition, rocky coasts provide a valuable harvest of various species of lobsters, crabs, shrimp, and prawns. Oysters are more common on shallower alluvial coasts. The brackish lagoons and deltas provide various species of anchovies and the red mullet (*Mullus* spp.). Additionally, of the larger fish species, there is one of moderate commercial value, the bluefin tuna (*Thunnus thynnus*). This species moves into the Mediterranean from the Atlantic and disperses in several directions, toward the coasts of Spain, Italy, and Libya. Related species of economic value are the bonitos (*Sarda sarda*) and the mackerels (Encyc. Brit., 1974).

Aquaculture is an emerging industry in the Mediterranean region. Mild water temperatures, in addition to a number of areas which are particularly well-suited for aquaculture, including abandoned salt works, coastal lagoons, and river deltas, make it a promising industry (Bas et al., 1985). Also noted is a long-standing practice of semi-culture of molluscs, such as the raft culture of mussels and the retaining of certain species in lagoons so that they can grow under favorable conditions. Extensive aquaculture is also being carried out along the coasts of France and Corsica with a goal to produce approximately 100 tons of various species of mullets, eels, basses, breams, and soles (Bas et al., 1985).

Several specialized fisheries have been in existence in the Mediterranean region for thousands of years; although these fisheries do not attain high levels of production, they do generate substantial economic value (Bas et al., 1985). Throughout the Mediterranean bivalve molluscs have historically been the most commonly harvested species. Species such as the common oyster (*Ostrea edulis*), blue mussel (*Mytilus edulis*), and Mediterranean mussel (*Mytilus galloprovincialis*) are heavily collected from shallow and sandy bottoms along the French, Italian, and Spanish coasts. Crustaceans continue to be a heavily exploited resource in the Mediterranean, with species such as *Macropipus* and *Carcinus* as the most commonly taken. In addition, certain species that were exploited in the past, like the red coral (*Corallium rubrum*), continue to be harvested (Bas et al., 1985). However, evidence suggests that large populations of the red coral have been depleted in many areas such as Italy and France, a victim of mass exploitation and a slow growth rate. Due to the species recent decline, large populations of the coral have been set aside off the coasts of Algeria and Morocco, where they are protected by stringent conservation measures (Bas et al., 1985). Further, sponges have also been considerably exploited in the Mediterranean, with *Spongia officinalis*, *Spongia zimicca*, and *Hippospongia communis* being the most important commercial species (Bas et al., 1985).

Phytoplankton. The Mediterranean Sea as a whole, and the western basin in particular, has a relatively low productivity rate, with high mean temperature and salinity (Bas et al., 1985). However, this productivity rate, especially in the western Mediterranean, is far from uniformly poor. During the winter months, nutrient-rich surface waters cool and sink creating a deep watermass. When these waters resurface, productivity increases. Therefore, the productivity rate varies with seasonal and annual changes; warmer years tend to be less productive than the colder years. Cooler years tend to be more productive due to the higher concentrations of nutrients in the water (Estrada et al., 1985).

Inventories on the annual phytoplankton and primary production cycles are available for several zones of the western Mediterranean basin, but information on offshore areas is scarce and based on sporadic surveys (Estrada et al., 1985). The highest primary production values reported in unpolluted areas have been measured in the area of divergence of the Gulf of Lions in April (Estrada et al., 1985). Productivity estimates for this area are 438 $gC \cdot m^{-2} \cdot yr^{-1}$. The comparison of data from different places is difficult,

because of the year-to-year fluctuations and small-scale variability related to local topographic and hydrographic factors, or to the influence of discharges of fresh water. Estimates of primary production along the coast of Spain range from 76 to 85 $gC \cdot m^{-2} \cdot yr^{-1}$ and along the coast of France range from 86 to 142 $gC \cdot m^{-2} \cdot yr^{-1}$. Assuming that 60% of the measured production is based on recycled nutrients, the average total primary production of the Mediterranean would be 90 $gC \cdot m^{-2} \cdot yr^{-1}$ (Estrada et al., 1985).

In the Mediterranean there are generally two maxima of phytoplankton biomass and production during the year: one in autumn, when the thermocline disappears, and another in late winter and spring, after nutrients have been supplied by upwelling or by mixing and stability of the water column is sufficient to allow the development of phytoplankton populations (Estrada et al., 1985). The seasonal variation of the phytoplankton populations in the Mediterranean is tightly linked to the annual alternation of periods of stratification and of mixing of the water column. When the supply of nutrients is adequate and the stability of the water is high (conditions not commonly found in the Mediterranean, except in the enclosed bays and polluted harbors) dense populations of phytoplankton may accumulate, with the result that the water appears reddish or otherwise colored. Such events are generally caused by dinoflagellates whose growth and secondary concentration contribute to this effect (Estrada et al., 1985). The most prominent organisms are dinoflagellates (*Scrippsiella*, *Cochlodinium*, and the non-photosynthetic *Noctiluca scintillans*), but *Chattonella subsalsa* and other flagellates have also been recorded. No significant toxic effects have been reported from Mediterranean red tides.

Sea Grasses and Benthic Algae. Four key factors limit and define the benthic primary production in addition to the nature of the substrate and different stress conditions (Ros et al., 1985). These include the nutrient concentration, intensity and quality of light, temperature effects on photosynthesis and respiration, and water agitation. All these factors can vary seasonally, and are affected by the physical and hydrographical features of the coast (Ros et al., 1985). These features each fall into recognizable zones according to their primary production.

Sources suggest that no reliable data estimates on primary producers exist for the supralittoral zone; however, estimates of 5 $gdw \cdot m^{-2} \cdot yr^{-1}$ have been suggested (Ros et al., 1985). This equals 2 $gC \cdot m^{-2} \cdot yr^{-1}$ using organic carbon weight as a reference. In the intertidal zone the energy flow is high and the populations have a high turnover rate, with a production of 700 $gdw \cdot m^{-2} \cdot yr^{-1}$, and a biomass around 250 $gC \cdot m^{-2} \cdot yr^{-1}$. In the lower and upper infralittoral zones, where the immersion is constant and the environmental conditions are less fluctuating, there is still enough wave movement to favor production. Evidence suggests that primary production may reach 4000 $gdw \cdot m^{-2} \cdot yr^{-1}$ and the biomass up to 1000 $gC \cdot m^{-2} \cdot yr^{-1}$ in this area (Peres, 1982). Based on these estimates, evidence suggests that the primary production of the Mediterranean benthos approaches the primary production of plankton occupying the coastal band of only about 1500 meters width (Ros et al., 1985). This emphasizes that the benthic contribution to the total marine primary production is small, but secondly, that its contribution to the littoral system economy must, nevertheless, be considered (Ros et al., 1985).

Zooplankton. A great homogeneity of neritic and oceanic zooplankton has been noted in the Mediterranean both quantitatively and qualitatively (Chadwick et al., 1996). The dominant species includes copepods and cladocerans (Moraitou, 1985). Only a few species constitute the bulk of the neritic community. Within this community almost 300 species of copepods and over 350 species radiolarians are found (Estrada et al., 1985). Some species from deeper waters can survive in the community during upwellings or homothermal periods (Gaudy, 1985). The oceanic fauna contains, besides several species common with the neritic area, a varied assemblage of species with low abundance. The deep-water fauna consists mainly of mesopelagic species. Only few species account for the bulk of this community which seems uniform over the entire Mediterranean (Gaudy, 1985). In

addition, the preponderance of the zooplankton species found in the Mediterranean are also found in the Atlantic.

TROPHIC RELATIONSHIPS

Pelagic Food Web. The pelagic food web of the Mediterranean is fed by the moderate amount of zooplankton that are able to survive in the Sea's waters. The western waters of the Mediterranean contain nutrients flushed in from the Atlantic Ocean, and are slightly more productive. Thus, the species diversity, and richness of the western waters are greater than those of the eastern waters. Despite a lack of zooplankton, a small, but relatively complex trophic structure exists for the region (Figure 4.1-21). Endemic species make up a moderate percentage of the total species present in the Mediterranean including 25 to 50% of the sessile groups, 13% of the crustaceans, and 10% of the fishes (Chadwick et al., 1996).

A group which is key to the Mediterranean food web are the cephalopods. Several species of cephalopods are widely distributed in the Mediterranean. This includes the commercially exploited cuttlefish (*Sepia*) and squids (*Loligo and Illex*), as well as octopus (*Octopus* and *Eledone*), which have a wider distribution range (Bas et al., 1985). These species comprise a large portion of the diet of second-order fishes, marine mammals, and waterbirds. diets of penguins, pinnipeds, and cetaceans. An often overlooked importance of the cephalopods is their contribution to detrital rain in the form of molts and carcasses. This group holds an intermediate position in the food web and is consumed by many of the same organisms that eat zooplankton.

The current environmental status of the Mediterranean already described, namely, the low concentration of phosphates and nitrates so necessary for the maintenance of marine pastures, together with the poor standing crop of bottom-dwelling organisms, provide no opportunity for the evolution of a big fisheries industry. The fish fauna of the Mediterranean is basically related to the fauna of the subtropical Atlantic with a large diversity of species. A total of 550 species is now admitted and 60 species appear to be endemic to the Mediterranean (Tortonese, 1985). The diverse first-order pelagic fish such as the blue whiting (*Micromesistius poutassou*) and pilchard serve a vital role in the pelagic food web as both consumers of phytoplankton and zooplankton, and as sustenance for many second-order pelagic fish and marine mammals. Second-order pelagic fish include the hake, bonito, bluefin tuna, horse mackerel, and pouting (*Trsipterus minutus capelanus*). These species feed not only on first-order pelagic fish but also on grazers (e.g., gastropods, nudibranchs, and crustaceans), cephalopods, benthic predators and scavengers (e.g., lobster, shrimp, crabs, and polychaetes), and first order demersal fish. Demersal fish such as the gobies (*Gobidae*), sole (*Solea solea*), and red mullet serve a dual role as consumers of the benthic predators and scavengers and as sustenance for the second-order pelagic fishes and marine mammals.

The most common seabirds belong to the families Laridae, Procellaridae, and Phalacrocoracidae. Thespecies of Laridae are among the most abundant in the region. The herring gull (*Larus argentatus*) is found living in groups in cliffs, beaches, and estuaries (Bas et al., 1985). The parent population is estimated to be 40,000 pairs. The black-headed gull (*Larus ridibundus*) is also common along the western coastline, particularly in France, and breeding population is evaluated to be 9000 pairs. The endangered Audouin's gull's (*Larus audouinii*) primary nesting location is found in the western Mediterranean, with a breeding population of approximately 4000 pairs (Bas et al., 1985). Other species, such as the common tern (*Sterna hirundo*) is estimated at approximately 4000 breeding pairs, mostly in France and Ebro Delta (Bas et al., 1985). The family Procellaridae is important in the region, in

particular the large breeding colonies (10,000 pairs) of the Cory's shearwater (*Procelaria diomedea*) usually found along the Mediterranean's many islands. The shag *(Phalacrocorax aristotelis*) shows a similar behavior, living on islands with a breeding population estimated at 1500 pairs (Bas et al., 1985).

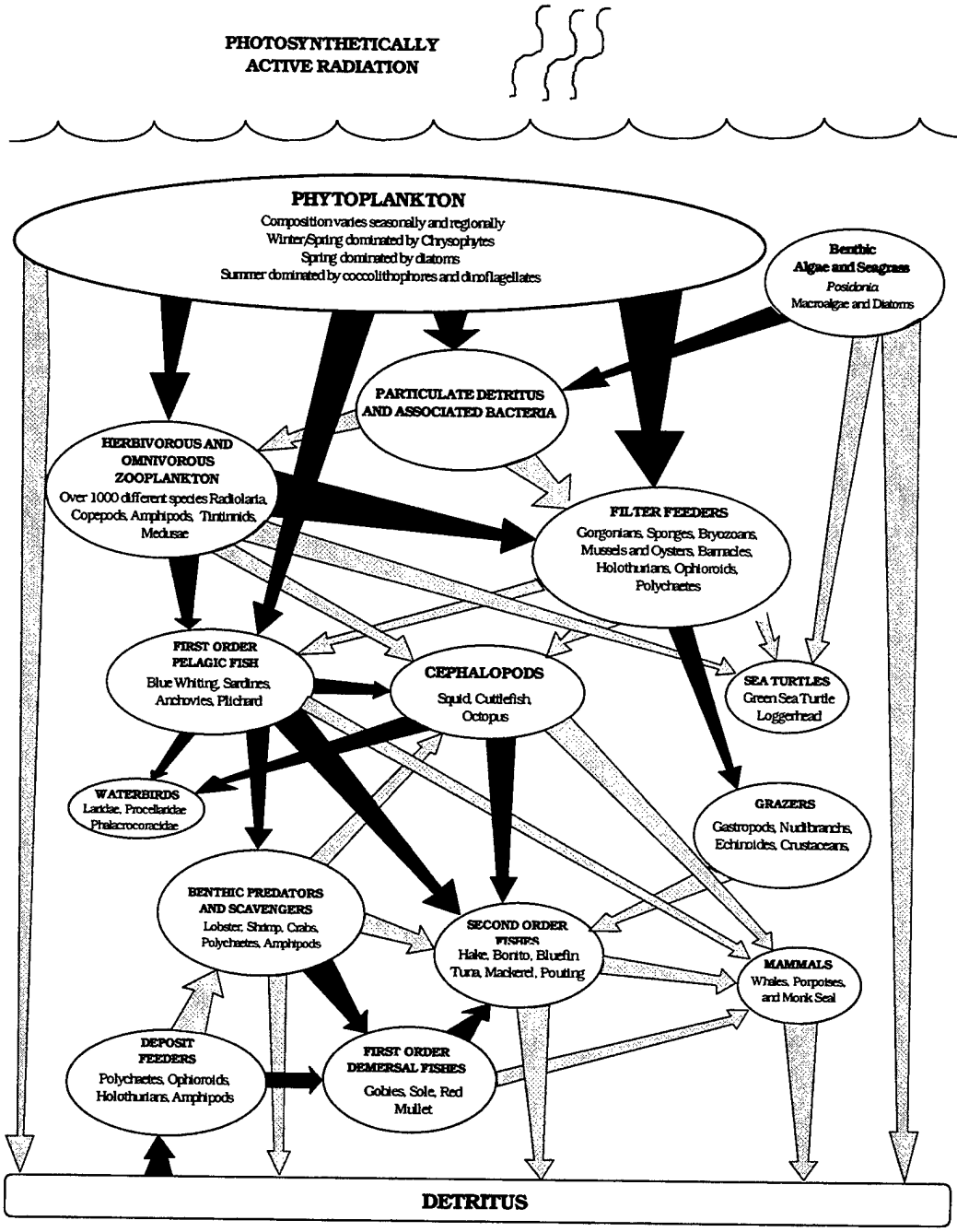

1985).

Figure 4.1-21. The Mediterranean Sea Trophic Web. The trophic assemblage of the Mediterranean Sea is marked by a highly diverse web of low species dominance and considerable opportunistic foraging. While limited in productivity relative to more open ocean environments, the Sea reflects considerable diversity and a resilience to trophic web pertebations. Deep benthic communities are depauperate compared to the Atlantic Ocean. Shallow benthic environments are limited but relatively productive.

Two species of pantropical marine turtles are found in the Mediterranean, the loggerhead turtle (*Caretta caretta*) and the green turtle (*Chelonia mydas*). Recent evidence suggests that these species are declining in numbers (Venizelos, 1990). Within the food web these species serve a minor role as consumers of herbivorous and omnivorous zooplankton, benthic algae and seagrass, and various filter-feeding organisms (Bas et al., 1985).

Several species of mammals are found in the Mediterranean region. The most abundant of these include five Mysticeti species, twelve Odontoceti species, and one Pinnipedia species (Casino et al., 1976). Of the marine mammals, the long-finned whale (*Globicephalla melaena*), striped dolphin (*Stenella coeruleoalba*), common dolphin (*Delphinus delphis*) are found along the entire Mediterranean coastline. Rare and restricted species include the bottlenosed dolphin (*Tursiops truncatus*), rough-toothed dolphin (*Steno bredanensis*), monk seal (*Monachus monachus*), sperm whale (*Physeter catadon*), Cuvier's beaked whale (*Ziphius cavirostris*), false killer whale (*Pseudorca crassidens*), killer whale (*Orcinus orca*), Risso's dolphin (*Grampus griseus*), and harbor porpoise (*Phocoena phocoena*). Within the pelagic food web, these species perform the role of consumers, feeding on cephalopods and first- and second-order pelagic fish.

Benthic Food Web. Although rich in species diversity, it is generally accepted that the Mediterranean benthos is poorer in biomass than the Atlantic coast of Europe. Historic studies sampled the western Mediterranean and the eastern Atlantic. More-recent studies have shown the calculated biomass expressed as live weight, on the average, very low near Naples and Salerno (6 $g \cdot m^{-2}$), three times higher in the Bay of Algiers and about 40 times higher (226 $g \cdot m^{-2}$) in the Atlantic off Faro and Lisbon (Ben-Tuvia, 1983). The biomass is higher in the western Mediterranean and in the north Adriatic than in other sections of the Mediterranean. The Levant Basin, Libyan Coast and Aegean Sea seem to have the lowest biomass. High biomass has been recorded near the deltas of rivers like the Rhone, Po, and Nile (Ben-Tuvia, 1983). Polychaetes and molluscs usually contribute the greatest share of individuals and biomass of circumlittoral communities in the region of Marseilles (Peres, 1967).

Within the Mediterranean's marine benthos there are several wide-ranging categories of primary producers that include seagrasses (*Posidonia*) and the microphytobenthos (diatoms). The substrate functions as the indicator of the prevalence of one or another group. On hard bottoms, macroscopical algae including Chlorophyceae, Phaeophyceae, and Rhodophyceae dominate, while the seagrass meadows are found on sandy bottoms. Microbenthos, made up chiefly of diatoms, can be dominant on soft silt substrates (Jackson, 1977).

Within the euphotic zone along the shallow coastal shelf and in protected lagoons and bays, coral reefs and seagrass beds thrive. Seagrass beds are common throughout much of the Mediterranean. The dominant seagrass of the Mediterranean is *Posidonia oceanica*. *Posidonia* is an endemic seagrass that forms luxuriant submarine "prairies" or meadows that can be considered as the archetype of the Mediterranean seagrass formations (Ros et al., 1985). *Posidonia* offers substrate for settlement and colonization by many sessile organisms and stabilizes the shallow sediment. *Posidonia* also influences chemical properties of the water and sediment (Ros et al., 1985). From an ecological perspective, the Posidonia meadows can be considered as mature ecosystems; both biomass and production are higher than on other sandy bottoms, as are the residence time of the elements and the species diversity (Ros et al., 1985). In addition, *Posidonia* meadows contain a highly diverse ecosystem with numerous hydrozoans, copepods, nematodes, bivalves, polychaetes, and decapods inhabiting the multi-layered seagrass beds. Further, several species of fish, including *Sarpa sarpa* and various species of Syngnathidae, use the meadows for feeding, courting, and spawning.

Today, some of the *Posidonia* meadows in the Mediterranean seem to be in regression. There is no general agreement on the causes; however, chemical or organic pollution, suspension of sediment in water, and mechanical degradation by fishing trawls have all been hypothesized to contribute to the losses (Ros et al., 1985). The disappearance of the *Posidonia* communities from the vicinity of harbors and estuaries indicates the high sensitivity of this seagrass to environmental disturbances (Ros et al., 1985).

On the hard substrates of the bathyal zone, an assemblage of "white-corals" generally form scattered clumps (Peres, 1985). These corals are consumers of living organic matter and are dominated by two large-branched species, *Lophelia pertusa* and *Madrepora oculata*, which are associated with solitary species such as *Caryophyllia armata* and *Desmophyllum cristagalli*. Sometimes the colonies of the two pilot species are dead; in other places with a large input of fine sediment, ramified corals become increasingly buried by fine silt. Individual colonies compensate for such silting by increasing vertical growth (Peres, 1985). Among the associated fauna, sponges are relatively scarce; however, several unique assemblages may be found within the western basin. Other reef species include filter-feeding colonial bryozoans and hydrozoans, anemones, and various bivalves. Additional filter and suspension feeders include the soft corals and tubiculous polychaetes.

Within the deeper environments, a variety of demersal scavengers and predators occupy the diverse biocenoses of the Mediterranean. These bottom-dwelling species vary in density and diversity along the continental slope (comprising the deep and rocky submarine canyons found near Italy and Algeria), to the gently sloping continental shelf (such as found near the Gulf of Lions), and finally to those located over shallow rocky or sandy bottoms running along the entire coastline. Additional special habitats of note include the large river deltas (e.g., Ebro, Nile, and Rhone) and the Alboran Sea, which contains a number of Atlantic species as a result of the currents flowing through the Strait of Gibraltar (Bas et al., 1985). There is, thus, a wide variety of benthic species in the Mediterranean, distributed according to the different types of continental shelf. The most abundant species on the slope include the hake, blue whiting, greater forkbeard (*Phycis blennioides*), and pouting, among others, which make up the greater part of the biomass.

Norwegian lobsters (*Nephrops norvegicus*) typically inhabit and form shoals at depths between 300 and 400 m (Bas et al., 1985). This species has been heavily exploited by commercial fisheries for many years; nevertheless, it may still be found where suitable burrowing habitat exists. Below these depths, principally around 600 m, the slope supports several species of shrimp, some common to the Mediterranean and nearby Atlantic waters, such as the rose shrimp (*Parapenaeus longirostris*), pink shrimp (*Aristeus antennatus*), and red shrimp (*Aristeomorpha foliacea*).

Together with hake, blue whiting, greater forkbeard, and pouting, other demersal species are typically found on the slope at depths greater than 100 m, such as pandora (*Pagellus*), sargo bream (*Diplodus*), and, closer inshore, dentex (*Dentex*), Couch's sea bream (*Pagrus*), gilthead (*Sparus*), gurnards (*Trigla*), and others. The red mullet, also an inshore species, is common throughout the lower levels of the Mediterranean. The former species dwells over sandy and muddy bottoms and the latter in rockier areas; juveniles form concentrations near the coast during the spawning season, later scattering. There is also a relatively large variety of Pleuronectidae, most notably the common sole (Bas et al., 1985).

Among the shallow-water species that inhabit the demersal reaches, prawns (*Penaeus* spp.) occur near river mouths, where populations are presently in decline. In addition, large crustaceans like the European lobster (*Homarus*) may be found in addition to the more common spiny lobster (*Panulirus*). Spider crabs (*Maja*) are encountered less frequently (either in shallow water or below 300 m) and a similar genus (*Paromola*) is more common along the Mediterranean bottom. Finally, cephalopod species, which are

widely distributed along the coast, include the cuttlefish (*Sepia*) and squids (*Loligo* and *Illex*), as well as octopus (*Octopus* and *Eledone*), which are distributed throughout most demersal reaches of the Mediterranean (Bas et al., 1985).

UNIQUE SPECIES AND ECOLOGICAL CONSIDERATIONS

Endangered/Threatened or Protected Species. Once abundant throughout the Mediterranean and the North African Atlantic, the Mediterranean monk seal is now confined to a few isolated stretches of coastline. Approximately 200 individuals remain in the Aegean and along the Mediterranean coast of North Africa and, perhaps a further 450 or more individuals remain near the Atlantic coast of Morocco and Mauritania. The Mediterranean monk seal was at one time commercially exploited. Its decline over the past 30 years has been attributed to human disturbance (including tourism) and increased coastal development. This has caused the monk seal to abandon many breeding beaches in favor of caves, where breeding success is usually poor. The species may still be found in several protected areas, but more protected areas are required to safeguard its future.

The island of Zakynthos lies off the northwest coast of the Peloponese in the Ionian Sea and, in Laganas Bay, has the largest remaining concentration of nesting loggerhead sea turtles in the Mediterranean (Venizelos, 1990). Evidence suggests that the primary reasons that the loggerhead is endangered is due to loss of habitat from beach development, entanglement within persistent marine litter, and accidental or intentional collection by commercial fishermen. Additional species of concern include the endangered Audouin's gulls, found primarily in the western Mediterranean, and the green turtle, which has seen great reductions in its numbers due to habitat destruction and illegal collection. The monk seal, the loggerhead and green turtles, and the Audoin's gull are all listed as threatened and endangered under the Federal Endangered Species Act (50CFR 17.11 and 17.12, USFWS, 1993).

Unique Habitat. The continental shelf is home to several unusual ecosystems. Within the western basin marine life flourishes along the interior shelf, with large sponge populations found in the shallow intertidal zones. In addition, *Posidonia* meadows are found throughout the Mediterranean and act as a biologically distinct "prairie" for a diverse assemblage of floral and faunal marine species.

RED SEA

PHYSICAL AND CHEMICAL CONSIDERATIONS

Geography and Physiography. The Red Sea is an elongated, narrow body of water that separates the African continent from the Arabian Peninsula (Figure 4.1-22). The Sea extends from 30° North latitude to 12°30' North latitude. In the north, the Red Sea branches into two narrow gulfs, the Gulf of Suez and the Gulf of Aqaba. In 1869, with the completion of the Suez Canal, the Red Sea was joined to the Mediterranean Sea via a narrow passage that cuts across the Sinai Peninsula; the completion of the Suez Canal has made the Red Sea one of the most important shipping routes in the world (Head, 1987a). In the south, the Red Sea flows through the narrow Straits of Bab al Mandab, into the Gulf of Aden, and finally into the Indian Ocean. Seven countries have coasts that border the Red Sea. Egypt, Sudan, and Ethiopia share the western, African coastline. Israel and Jordan have strategic ports along the northern coastline. Saudi Arabia and the North Yemen share the eastern coastline of the Red Sea. To the south, the African countries of Djibouti and Somalia, and the Arab country of South Yemen border the Gulf of Aden.

Despite its wide latitudinal distribution, the Red Sea and Gulf of Aden (hereafter known as the Red Sea region) experience minimal climatic variation. The countries that border the Red Sea region are hot and arid, and rainfall in the region rarely exceeds 10 mm per year (Edwards, 1987). The land bordering the region is dominated by sandy soils and sparse, semi-arid vegetation. The mean air temperatures during the winter months (November to February) range from 20°C in the north to 29°C in the south. In the summer (June to September), temperatures range from 35°C to 40°C. The arid climate of the region makes the surface waters of the Red Sea region unusually warm. The arid conditions also cause a high rate of evaporation of the surface waters of the Red Sea, resulting in both salty water and extreme humidity over the water. The rate of evaporation of the surface waters exceeds 200 $cm \cdot yr^{-1}$ (Thurman, 1975). Over the open sea, the average annual humidity is 70%; humidity is slightly lower along the coasts (Edwards, 1987).

Bathymetry. The Red Sea is 1,932 km long and averages 280 km wide (Head, 1987a). At its widest, the Sea is 354 km wide and narrows to 29 km wide at the Straits of Bab al Mandab. It is estimated that the total surface area of the Red Sea is $4.5 \cdot 10^5$ km^2 while the volume of the Sea is between $2.15 \cdot 10^5$ and $2.51 \cdot 10^5$ km^3 (Head, 1987a). It is probable that the Red Sea has formed during the last 30 million years and is a product of the divergence of the African and Arabian continental plates (Braithwaite, 1987). It lies along the axis of a large rift system formed by the Carlsburg Ridge, which cuts through the northwest Indian Ocean into the Gulf of Aden and into the Red Sea.

Despite its small size and isolated location, the Red Sea is deep. In the north, the shallow, coastal shelf extends only a few km offshore while to the south, the shelf is wider and exceeds 100 km in width at the Farasan Bank (Price et al.,1988). At its distal edge, the shelf drops gradually into a central trough that exceeds 100 m in depth along its entire length (Head, 1987a). From the trough, the bottom deepens further to a rift with depths in excess of 2,850 m. The Gulf of Suez is shallow with depths no greater than 80 m. The Gulf of Aqaba is over 1300-m deep, with the exception of a shallow sill (250 m-deep) located at the southern boundary of the Gulf. The depth at the Straits of Bab al Mandab is approximately 300 m; however, a shallow sill measuring 100 m in depth exists some 140 km to the north. All water entering the Red Sea from the Gulf of Aden must pass over this sill. Approximately 24% of the open water area of the Red Sea has a depth of 50 m or less, 32% has a depth of between 50 and 500 m, 30% has a depth of between 500 and 1000 m, while only 13% has a depth of greater than 1000 m (Head, 1987a).

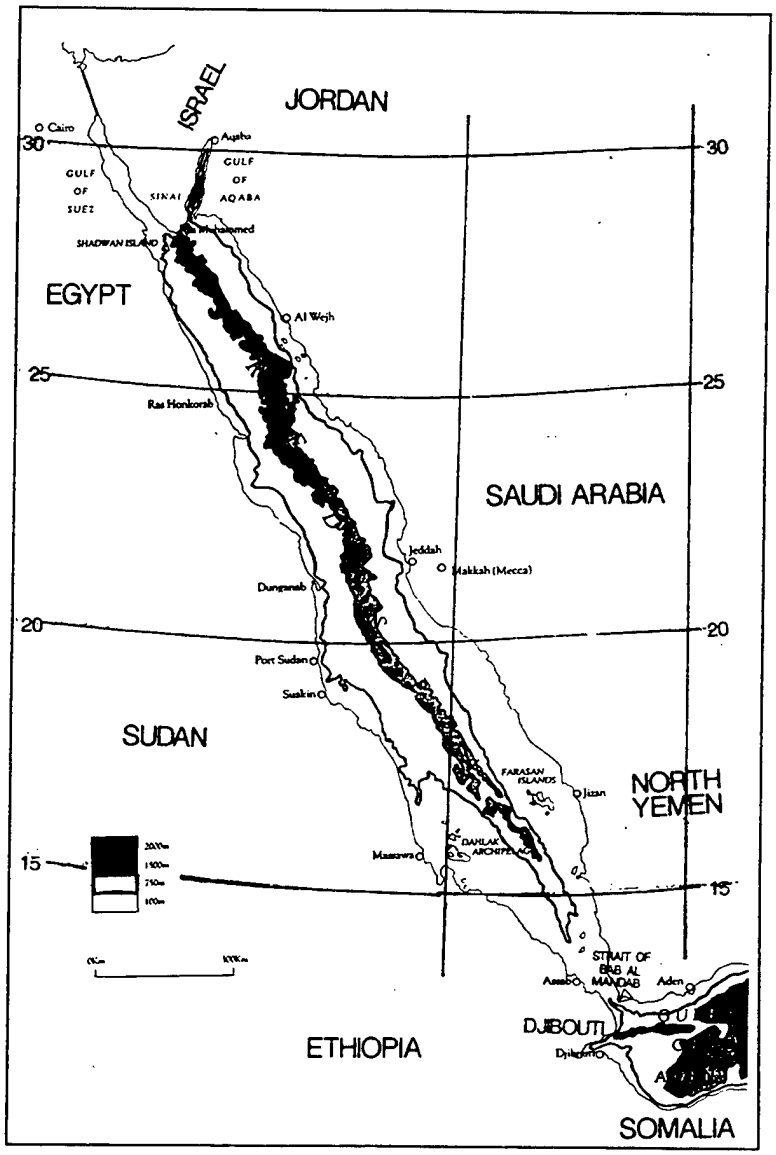

Figure 4.1-22. The Red Sea and Gulf of Aden. The Red Sea is a long, narrow basin that separates northeastern Africa from the Arabian Peninsula. It is connected to the Indian Ocean through the Gulf of Aden and to the Mediterranean Sea via the Suez Canal.

Currents, Tides, and Water Exchange. The surface currents in the Red Sea and Gulf of Aden are largely wind-driven. During the summer months, the prevailing winds blow from north to south across the entire Red Sea. The winds originate from a low pressure area over northwest India, known as a "monsoon low," and travel in a counterclockwise direction through the Red Sea, Gulf of Aden, and Arabian Sea (Edwards, 1987). During the winter months, winds continue to blow from the north across the northern portion of the Red Sea. However, the southern portion of the Sea experiences southerly winds that originate over the eastern Indian ocean and travel across the Gulf of Aden, through the Straits

of Bab al Mandab, and into the Red Sea. The central part of the Red Sea, where the air masses meet during the winter months, experiences calm seas with little wind.

Water circulation patterns follow the prevailing winds. Very little water enters the Red Sea from the Mediterranean Sea. This is due to very low flow conditions across the narrow Suez Canal and to the fact that the mean sea level at the southern end of the Canal is higher than that at the northern end for most of the year. Therefore, the majority of the water that replenishes the evaporated waters of the Red Sea comes from the Indian Ocean, via the Gulf of Aden. During the winter months, currents are aided by southerly winds and water flows north across the shallow sill beyond the Straits of Bab al Mandab and into the Red Sea. However, the subsurface waters of the Red Sea are cooler and more saline and, therefore, more dense than the incoming Indian Ocean waters. Therefore, as surface waters flow into the Red Sea, there is a simultaneous outflow of subsurface waters into the Gulf of Aden creating a two-layer system of water flow during the winter months (Edwards, 1987; Thurman, 1975). During the summer months, the dominant northerly winds force surface waters out of the Red Sea at a rapid rate. Underneath the rapid flowing surface waters, the two-layer winter water system remains in effect, creating a total of three water layers during the summer months (Figure 4.1-23).

Because the Red Sea is enclosed by land, with only a narrow passage to the Indian Ocean, tides within the Sea do not rise and fall in accordance with the Gulf of Aden and the Indian Ocean. Instead, the Red Sea experiences a local, small-scale tide with a semi-diurnal period; when the water is high at one end of the Sea, it is low at the opposite end (Edwards, 1987). In the south, near the Straits of Bab al Mandab, the influence of the Gulf of Aden tides becomes greater. In the north, the tides at the gulfs of Suez and Aqaba are influenced directly by Red Sea tides. The range of tides is greatest at the ends of the seaway, ranging from 0.6 m to 0.9 m at the north and south ends of the Sea, respectively. Horizontal flow, known as "tidal streams," can run as fast as 6 to 7 kts in restricted bays; however, it is not known to what extent these streams are tidally driven or wind-driven (Edwards, 1987). Tidal streams are not noticeable in the open waters.

Temperature and Salinity. The temperature of the Red Sea is very warm and remarkably constant at most depths. Average annual surface water temperature in the Red Sea during February ranges from 17.5°C in the Gulf of Suez to 27°C near the Straits of Bab al Mandab. During the month of June, the average annual surface water temperature ranges from 26°C in the Gulf of Suez to 32°C near the Straits (Edwards, 1987). In shallow coastal waters (less than 50-m deep) and lagoons, water temperatures can be as high as 36°C to 38°C; and temperatures as high as 45°C have been recorded in the coastal waters of the Red Sea.

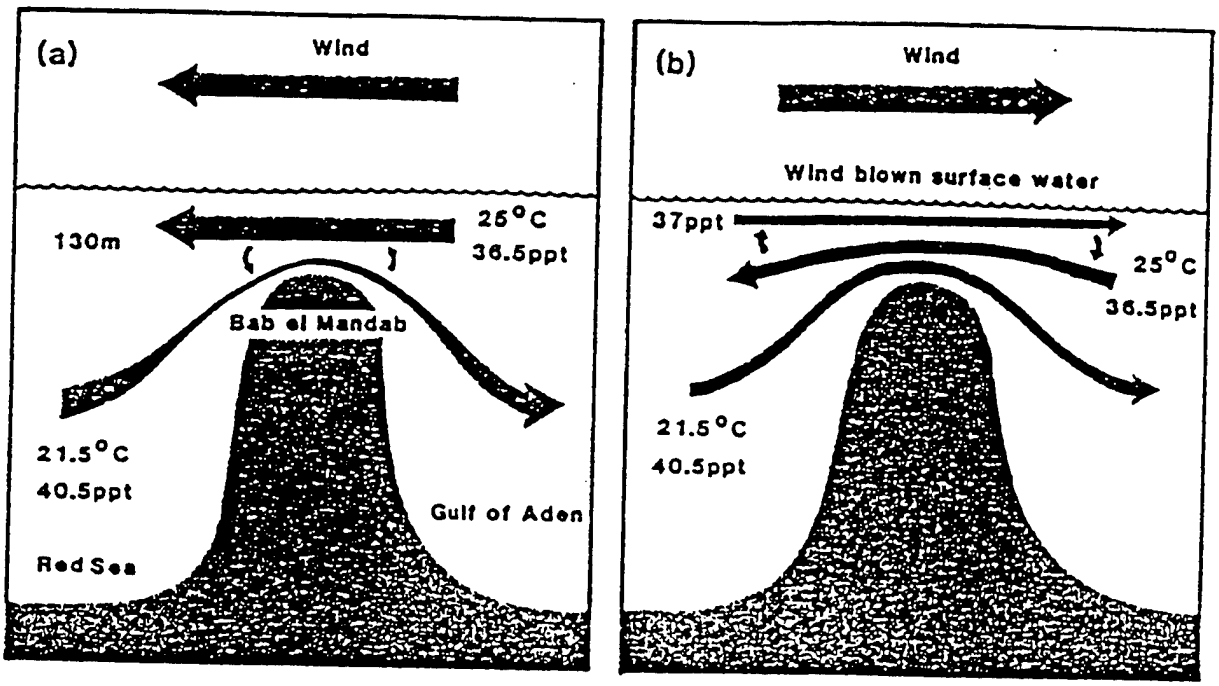

Figure 4.1-23. Winter (a) and summer (b) water flow through the entrance into the Red Sea. Adapted from Sheppard et al., (1960).

The temperature of subsurface waters (below 300-m deep) of the Red Sea remain constant between 21.5°C to 21.6°C for most of the year. It is believed that the cooler water originates in the Gulf of Suez where it is cooled by northerly winds, sinks, and flows south into the Red Sea. Between the warm surface waters and the cooler, but stable, subsurface waters exists a thermocline of varying thickness (located 90 to 150-m deep) where the major drop in temperature occurs.

Due to a high rate of evaporation and a low rate of precipitation and fresh water runoff, surface salinity values of the waters of the Red Sea are the highest in the world. Annual mean salinity of the surface waters near the Straits of Bab al Mandab is similar to that of the Gulf of Aden (about 36.5 parts per thousand). The salinity of the surface waters increases steadily towards the north, reaching 40.5 ppt at the mouth of the Gulf of Suez. The salinity of shallow, inshore waters and lagoons less than 10 m deep is estimated to be as high as 50 ppt (Edwards, 1987). The subsurface water mass of the Red Sea, along with a stable mean temperature, also has a stable mean salinity of between 40.5 and 40.6 ppt. This salinity, which is similar to that at the mouth of the Gulf of Suez, provides further evidence that subsurface waters flow from the Gulf into the Red Sea.

One unique feature of the Red Sea is the presence of hot brines located in the deep central basin of the Sea. In 1963, the Woods Hole Oceanographic Institution vessel, *Atlantis II*, retrieved a water sample from a deep ocean basin that had a temperature of 26°C and a salinity of 43.3 ppt (Karbe, 1987; Thurman, 1975). Subsequent research has identified the presence of 18 deep brine pools in the Red Sea. The brines, which can be as warm as 60°C with salinity in excess of 257 ppt, have densities great enough to prevent them from mixing with the surface water layers of the Red Sea. In addition to high salinity, the majority of the brines are enriched with heavy metals including manganese, zinc, copper, iron, and cadmium, and some contain high concentrations of hydrogen sulphide and carbon dioxide (Karbe, 1987). It is believed that the brines are formed as hot mantle fluids rise out of the deep, central trough of the Red

Sea. These fluids, which bear high concentrations of heavy metals, mix with fossil waters that have been trapped in the sea floor. As the hot mantle generates convection currents, the waters, enriched with salts leached from fossil soils, rise to the sediment surface forming the brines. So far, little is know about the existence of life in the brine pools. During the 1970s the Arabian nations began to explore the possibility of mining the metal-rich muds associated with the brines. Although a successful mining operation was established, the project was abandoned after several years due to the toxicity of the tailings which were discharged directly back into the Sea, raising the water salinity and harming sensitive reef systems and benthic communities.

Oceanic Sedimentation. Clear, tropical waters with high levels of light penetration are required for the establishment and survival of reef systems and seagrass beds. The Red Sea, which is noted for its reefs and benthic communities, has clear water with little suspended sediment or plankton. Seasonally, winds can cause sand storms that originate in the surrounding desert and blow over the water. However, the storms are infrequent and the long-term effects are minimal (Edwards, 1987). Very low precipitation levels and a lack of major rivers joining the Sea prevent significant runoff; mangroves act as a coastal stabilizer and trap sediments that may run into the neighboring waters.

The countries that surround the Red Sea region are rapidly modernizing and human-generated sedimentation effects are becoming more apparent. Coastal construction work, including the development of harbors, jetties, industrial sites, and roads, leads to increased levels of sedimentation (Ormond, 1987). The tendency to "strip-develop," or build in a narrow band along the coast where cooling water and easy waste disposal sites are available, is slowly but steadily degrading littoral and sublittoral communities (Ormond, 1987).

CURRENT ENVIRONMENTAL STRESSES

Marine Pollution. The Red Sea is one of the most traveled shipping routes in the world and is surrounded by a number of rapidly developing countries. The effects of environmental stress due to development, traffic, and pollution are increasingly apparent in the region. Due to the Red Sea's geography as a semi-enclosed body of water, pollutants tend to accumulate in the shallow waters instead of dispersing and degrading into the open ocean (Ormond, 1980). Therefore, pollutants tend to wash from coast to coast in the narrow Sea, settling on beaches, intertidal communities, mangroves, and coral reefs.

Dicks (1987) lists the sources of contaminants in the Red Sea region under three convenient headings: urbanization and tourism, oil, and other industrial inputs. The major pollutants associated with urbanization are sewage and garbage. Disturbance associated with tourism includes increased boat traffic, coral breakage due to anchor damage and diving activities, spear fishing, and shell collection. The Red Sea suffers from oil pollution along most of its coasts and in its offshore waters. Oil pollution stems from frequent spills associated with traffic through the Suez Canal, repeated spills from coastal oil fields, refineries, pipelines, and spills from offshore oil platforms (Awad, 1989). Industrial inputs include sedimentation from construction activities, brine from desalination plants, fertilizers, and heavy metals.

Urbanization and Tourism. Sewage is the most serious form of pollution input into the Red Sea region from coastal urban areas. It is convenient for residential and industrial developers to build near the sea to save money by discharging directly into the neighboring waters. Sewage is commonly discharged (treated or untreated) into the Sea just below the intertidal zone via pipelines (Dicks, 1987). Although no figures on the amount of sewage pumped into the Red Sea region are available, health

problems due to coliform bacteria levels near beaches have been reported. Additionally, due to the lack of open ocean circulation in the Red Sea, sewage tends to be retained by fringing coral reefs. Eutrophication from increased levels of nitrates, phosphates, and other nutrients begins with large algal blooms and the subsequent depletion of dissolved oxygen in the water. The blooms smother coral colonies directly, trap sediment that blocks light reaching the coral, and attract increased numbers of grazers that eat corals and algae and further destroy reefs (Walker and Ormond, 1982). Evidence suggests that high phosphate concentrations inhibit calcification and slow or stop coral growth (Walker and Ormond, 1982). Suspended solid wastes decrease the amount of light that reaches the reef, slowing coral growth and damaging the community.

Marine litter is extensive due to the increase of human activity within the region. Garbage consists primarily of plastics that enter the Sea from recreational and coastal urban areas, ship traffic, and offshore oil mining platforms (Dicks, 1987). Coastlines, such as that of Saudi Arabia, that receive offshore winds for most of the year are seriously polluted by plastics. Oil drums, buoys, plastic containers, and wood scraps are not uncommon along beaches and are not only damaging to littoral communities, but are truly unpleasant to look at. Additionally, plastic bags and containers, when lodged on reefs, can physically smother corals and seriously retard light penetration onto the reef.

International tourism has been increasing in Egypt, Israel (near Elat), Sudan, and other Red Sea countries. A majority of the tourism is related to recreational diving and it is estimated that as many as 10,000 divers visit the Sinai coast each year (Ormond, 1987). Breakage to corals occurs as a result of dropping anchors on reefs and walking on and kicking corals with fins. Riegl and Velimirov (1991) found that as many as 11% of shallow growing reef corals at several locations near Israel experienced tissue loss and algal growth associated with breakage; while 5% of shallow growing corals were damaged near Egypt. Other tourism-related damage stems from shell collection and spear fishing that decreases species diversity and richness on the reefs.

Oil. The Red Sea is one of the most oil-polluted water bodies in the world. While each square kilometer of the world's oceans receives an average of 9.17 $kg \cdot yr^{-1}$ of oil, the Red Sea receives 14.61 $kg \cdot yr^{-1}$ (Awad, 1989). Repeated spills from coastal refineries and oil fields, and from offshore platforms have made black bands of oil a common site on Red Sea shores. Additionally, tanker traffic in the region is estimated to be as high as 3700 vessels per year carrying 650 million tons of oil (Awad, 1989). Spills from these tankers add to the oil pollution. The most heavily polluted areas in the Red Sea region include the Gulf of Suez (especially along the western coast), Rabigh and Jeddah (along the Saudi Arabian coast), Port Sudan, and Elat (in the Gulf of Aqaba).

The effects of repeated oil spills on fringing reefs, mangroves, and seagrass beds are severe. Corals exposed to oil can have abnormal feeding behavior and mucus secretion, decreased growth rates, increased rates of tissue damage, disturbance of larval settlement, and decreased oxygen exchange (Mergner, 1984; Dicks, 1987). Additionally, floating oil has a shading affect, blocking light necessary for coral and seagrass growth. Oil that coats the pneumatophores (breathing roots) of mangroves effectively prevent oxygen exchange and suffocate the plants. Oil incorporated into sediment can damage root systems and ultrafiltration processes. Oil pollution also affects the eggs and larvae of many pelagic fish and can cause developmental abnormalities. Birds are particularly affected by oil spills that render them unable to fly, swim, and forage for food.

Other Industrial Inputs. Increased development along the coasts of the Red Sea region has led to other forms of pollution. As discussed above, coastal sedimentation is an increasingly problematic form of marine pollution in the Red Sea region. For example, the infilling of one coastal road near Jeddah,

Saudi Arabia effectively destroyed a healthy fringing reef. Now, 10 years later, the reef is bare except for a turf of green algae and scattered coral heads (Ormond, 1987). Other sources of pollution include injection of hot brines into the coastal waters from desalination plants. It is anticipated that by the year 2000, some 50 desalination plants will be in operation along the Saudi Arabian coast (Dicks, 1987). Finally, fertilizers and heavy metals are commonly discharged from coastal industrial sites.

Sea Traffic and Ports. In 1869, the Suez Canal was completed and the Red Sea became one of the most important shipping routes in the world. Ships carrying goods from Europe and oil from the Red Sea nations travel through the region extensively. In 1980, Egypt earned $US660 million in dues collected from ships using the Canal (Horton, 1987). Approximately 50 ships per day travel through the Straits of Bab al Mandab. The largest ports of the Red Sea are the Saudi Arabian port of Jeddah, whose close vicinity to the religious capital of Mecca makes it an important economic center, and the Sudanese port of Port Sudan.

Boat traffic on the Red Sea consists of large tankers and freighters, along with a limited fishing fleet from bordering nations. Oil is the most transported good on larger vessels, with nearly 10% of Europe's oil coming through the Red Sea (Couper, 1983). Other transported items include cotton, grains, and manufactured goods. The fishing fleets of Red Sea nations are relatively small and fishing methods remain traditional. Many of the fishing boats are small, one and two man vessels, and are often still powered by sail.

FISHERIES AND AQUACULTURE RESOURCES

The fisheries of the Red Sea region account for only 0.07% of the world total fisheries (Head, 1987b). Although fishing has always been important to the economies of the nations surrounding the Red Sea, most of the catch has, historically, been of a subsistence nature and has been maintained well below the maximum sustainable yield. Despite the fact that tropical waters have an extremely low rate of primary productivity, reef areas and seagrass beds are extremely productive and are estimated to support 9% of the world's fisheries (Head, 1987b). The majority of the fishing that occurs in the Red Sea is located over or adjacent to reefs.

To date, fishing in the Red Sea region has been characterized by small boats carrying one or two fishermen armed with cast nets, hand lines, pots, and spear guns; however, larger vessels carrying trawls and purse seines have recently appeared. Groupers, jacks, mackerel, snappers, mullets, sardines, and emperors are the main fish caught by local fisherman (Vine, 1985; Head, 1987b). Game fish, such as sailfish, barracuda, sharks, and tuna are also popular. Smaller catches of prawns, lobster, and turtles have been reported. Despite the fact that turtles have protected status in the region, they are still hunted aggressively and eggs are routinely gathered by local fishermen. Egypt has a total catch of approximately 14,000 metric tons of fish per year; Saudi Arabia has an annual catch of 8000 metric tons, while North Yemen, Sudan, and Ethiopia have catches of 22,000 tons, 1,050 tons, and 350 tons, respectively (Vine, 1985; Head, 1987b). Estimates of Somalian fish catches in the Gulf of Aden and neighboring Indian Ocean are 4000 metric tons by small fishing boats and 12,000 metric tons by the industrial fishing fleet (Stromme, 1987). Less than 5% of the total catch for the entire region is exported.

Several non-food fisheries have been in existence in the Red Sea region for thousands of years. The most well-known of these is the mother-of-pearl fishery. Buttons were cut from the shells of the molluscs, *Trochus dentatus*, *Trochus niloticus*, and *Pinctada margaritifera*, and a modest industry still exists for the collection of these species. Other species of molluscs, especially cowries, giant clams, and spider

conch, are collected and sold for jewelry and decoration (Mastaller, 1987). Additionally, the operculum of some gastropods is ground into a powder called "dufra" and sold as an aphrodisiac (Ormond, 1987). Other non-food fisheries include black coral for jewelry and tropical fish collection for the aquarium trade.

Phytoplankton. The Red Sea is not highly productive. Due to a lack of river inputs and a lack of upwelling areas, and due to the shallow sill that separates the Sea from the Gulf of Aden and Indian Ocean waters, the Red Sea does not contain high levels of nutrients. Levels of phosphate and nitrate in the surface waters of the northern Red Sea can be as low as 0.01 $\mu mol \cdot L^{-1}$ and 0.1 $\mu mol \cdot L^{-1}$, respectively (Weikert, 1987). Additionally, high temperature and extreme salinity make the Red Sea waters uninhabitable for all but a few species of planktonic organisms. During the winter months, prevailing winds drive water into the Red Sea from the Gulf of Aden and nutrient and production levels increase slightly; nutrient levels and primary productivity in the southern portion of the Sea exceed that of the northern portion of the Sea for most of the year. A marked decrease in productivity and biomass of plankton occurs north of 19° North latitude.

Estimates of primary production in the Red Sea vary greatly. An average estimate of productivity for the entire sea is 100 $mgC \cdot m^{-2}d^{-1}$ Weikert, 1987; Thiel and Weikert, 1984). However, numbers well above this have been reported. In the Gulf of Aqaba, primary production can range from 200 to 900 $mgC \cdot m^{-2}d^{-1}$, while in the southern portion of the Red Sea production can range from 500 to 1000 $mgC \cdot m^{-2}d^{-1}$ (Kimor, 1973; Weikert, 1987). Despite the variation in study results, it is apparent that primary productivity increases from north to south in the Red Sea.

There is a low diversity of plankton species in the Red Sea. Many of the organisms that wash into the Red Sea from the Gulf of Aden die when they are exposed to the warm salty waters of the Red Sea. Species that are able to survive are remarkable euryhaline. In one study, Natour and Nienhuis (1980) found only 49 species of dinoflagellates in the water of the Gulf of Aqaba. Phytoplankton stocks consist largely of dinoflagellates and blue-green algae. In reef areas, diatoms, such as *Chaetoceros* spp., *Nitzschiaceae* spp., and *Naviculaceae* spp. can dominate the phytoplankton assemblage. Large blooms of the blue-green algae, *Oscillatoria (Trichodesmium) erythraeum*, are common in the central Red Sea (Weikert, 1987; Vine, 1985). Blooms can be as thick as $9 \cdot 10^5$ $cells \cdot L^{-1}$ and can account for 70% of the total phytoplankton cell number of the Sea.

Seagrass and Coral Reefs. Seagrass beds line the shallow lagoons along the Red Sea coasts. Eleven species of seagrass are known to occur in the Red Sea. In the extreme northern portion of the Gulf of Aqaba, temperature and salinity extremes render the area inhabitable for only two of the eleven species. Estimates of the standing crop biomass for seagrasses in the Red Sea range from 70 kg $dw \cdot m^{-2}$ for *Thalassodendron ciliatum* on the Sinai coast, to 0.23 $kgdw \cdot m^{-2}$ for *Halodule uninervis* (Jones et al., 1987). For comparison, standing crop biomass for temperate grasslands can range between 0.2 and 5 $kg-dw \cdot m^{-2}$. Estimates of primary productivity for seagrass beds has been estimated to be as high as 1000 $gC \cdot m^{-2} \cdot d^{-1}$ in the Caribbean Sea (Jones et al., 1987). In the Red Sea, productivity of seagrass beds can range from 1326 $gC \cdot m^{-2} \cdot yr^{-1}$ for *Halodule uninervis*, to 617 $gC \cdot m^{-2} \cdot yr^{-1}$ for *Halophila stipulacea*, to 11 $gC \cdot m^{-2} \cdot yr^{-1}$ for sparse growths of *Halophila ovalis* (Wabeh, 1980, cited in Jones et al., 1987).

Coral reefs are considered to be among the most productive environments in the world. Soft and hard coral species, as well as some colonial bryozoans and some bivalves carry symbiotic algae in their tissue. These microscopic brown algae, known as zooxanthellae, are thought to provide the coral with nutrients necessary for calcium carbonate deposition; the coral, in turn, provide the algae with nutrients and shelter (Barnes, 1987). Additionally, below the surface of living corals there exists a layer of endolithic, blue-

green algae. Finally, several species of benthic macroscopic algae live on reef structures. Due to the symbiotic relationships of a number of species associated with reef systems, these systems have the capacity to recycle nutrients and are, as a result, very productive. Estimates of reef productivity can be as high as 10,000 $gC \cdot m^{-2} \cdot yr^{-1}$ when the productivity of the surrounding waters is as low as 20 to 50 $gC \cdot m^{-2} \cdot yr^{-1}$ (Lewis, 1977). A more conservative estimate of reef productivity is 500 to 2500 $gC \cdot m^{-2} \cdot yr^{-1}$.

Zooplankton. Like the diversity of phytoplankton, the diversity of zooplankton in the Red Sea is also low. Again, temperature and salinity extremes, and a rapid degradation of organic matter prevent all but the most tolerant species to die as they enter the Red Sea waters from the Gulf of Aden. For example, of the more than 300 species of copepods known to exist in the Indian Ocean, only 65 species have been identified in the southern Red Sea and only 35 species have been identified in the Gulfs of Suez and Aqaba (Weikert, 1987). Near coral reefs, copepods dominate the zooplankton taxa. Other dominant groups are amphipods, isopods, mysids, euphausiids, and larval forms of molluscs, polychaetes, and crustaceans. Of the 22 species of euphausiids known to occur in the Indian Ocean, only 10 species are found in the Red Sea; two of these, *Euphausia sanzoi* and *Pseudoeuphausia colosi*, are endemic to the Red Sea region.

The numbers and biomass of Red Sea zooplankton decrease from south to north and as depth increases. The zooplankton of the surface waters of the southern and northern Red Sea regions can have a wet weight of 81 $mg \cdot m^{-3}$ and 48 $mg \cdot m^{-3}$, respectively (Kimor, 1973). Below 1400 m, the wet weight biomass concentrations of zooplankton can be as low as 0.04 $mg \cdot m^{-3}$ (Weikert, 1987). These low biomass concentrations are not reached until depths of 4000 to 6000 m in other tropical seas. Additionally, due to the isocline, halocline, and varying dissolved oxygen concentrations with depth, less diel migration of zooplankton species occurs in the Red Sea than in other tropical oceans.

TROPHIC RELATIONSHIPS

Pelagic Food Web. The pelagic food web of the Red Sea is fed by a small amount of zooplankton that are able to survive in the Red Sea waters. The southern waters of the Red Sea contain nutrients washed in from the Gulf of Aden, and are slightly more productive. Thus, the species diversity and richness of the southern waters are greater than those of the northern waters. Despite a lack of zooplankton, a small, but relatively complex trophic structure exists for the region (Figure 4.1-24).

Nearly 1000 species of fish are found in the Red Sea. Small, planktivorous species include herrings and sardinellas (family Clupeidae), anchovies (family Engraulidae), and silversides (family Atherinidae). All have a similar, silvery appearance and congregate in large schools. Common species include the anchovies (*eg., Stolephorus heterolobus* and *Thryssa baelama*), the silverside (*Atherinomorus lacunosus*), and the herrings (eg., *Herklotsichthys punctatus* and *H. quadrimaculatus*) (Ormond and Edwards, 1987). These small schooling species are an important food source for jacks, needlefish, horsemackerel, and seabirds such as terns. The only large planktivorous fish species that occur in the Red Sea are the giant manta (*Manta birostris*) and the whale shark (*Rhincodon typus*).

Larger predacious fish species known to occur in the region include several species of jacks and horsemackerels (*Caranx* spp. and *Carangoides* spp.). These species are stream-lined with forked tails and are fast, efficient predators on smaller schooling fish and reef fish. They hunt by swimming along the sides of reefs and surprising stray fish and by charging and breaking up schools of fish and attacking separated individuals. Other predacious fish include tuna, including the species *Euthynnus affinis* and *Gymnosarda unicolor*, mackerel (*Scomberomorus commerson*), barracuda (*Sphyraena barracuda*), and

several species of needlefish and halfbeaks. Additionally, two game fish, the dolphin fish (*Coryphaena hippurus*) and sailfish (*Istiophorus platypterus*) are common.

The largest predators in Red Sea pelagic waters include sharks and cetaceans. Thirty species of sharks have been found in Red Sea waters. The four largest predatory species include the tiger (*Galeocerdo cuvier*), mako (*Isurus glaucus*), and two species of hammerhead sharks (*Sphyrna* spp.). Other common species include the whitetip reef shark (*Triaendon obesus*) and the blacktip reef shark (*Carcharhinus melanopterus*). Sharks are scavengers and predators and will consume bony fish, turtles, seabirds, cetaceans, and, as with the nurse shark (*Nebrius ferrugineus*), crustaceans, cephalopods, and even coral (Ormond and Edwards, 1987).

Of the 44 species of cetaceans found in the Indian Ocean, only nine have been identified in Red Sea waters (Frazier et al., 1987). Due to the lack of abundant plankton, the high salinity, and probably to the shallow sill that separates the Red Sea from the waters of the Indian Ocean, no baleen whales are found in Red Sea waters. Instead two species of toothed whales, the killer whale (*Orcinus orca*) and the false killer whale (*Pseudorca crassidens*), and approximately seven species of dolphin are known to occur. Dolphin species include Risso's (*Grampas griseus*), plumbeous (*Sousa chinensis*), spotted (*Stenella attenuata*), Indian Ocean bottle-nosed (*Tursiops t. aduncus*), Gill's bottle-nosed (*Tursiops t. gilli*), Atlantic bottle-nosed (*Tursiops t. truncatus*), and rough-toothed (*Steno rostratus*) dolphins. These cetaceans consume mainly schooling fish and some cephalopods. Killer whales consume fish as well as marine mammals, such as dugong (*Dugong dugong*) and other cetaceans.

Numerous species of seabirds live and breed in the Red Sea region. Red Sea birds include species that breed toward the Mediterranean in the north and winter in the Red Sea region, species that breed in the Indian Ocean region and venture north to the Red Sea, and those species that breed in the Red Sea region (Vine, 1985). Sixteen species of true seabirds breed in the Red Sea region. These include seven species of terns, two species of gulls, two species of boobies, and one species each of pelican, cormorant, noddy, shearwater, and tropic-bird. The majority of these species feed by diving on schools of small fish. Some species, such as the shearwater and gulls, will also eat planktonic crustaceans and molluscs. Other bird species that are found in the Red Sea region include herons, plovers, spoonbills, sanderlings, curlews, ospreys, and flamingos.

All five species of pantropical marine turtles are known to occur in the Red Sea region and all are protected from fishing by local laws. The hawksbill turtle, *Eretmochelys imbricata*, is the most abundant turtle of the Red Sea. It eats sponges, soft corals and sessile, soft invertebrates. There is evidence that it may graze on seagrass beds as well. The hawksbill nests during the spring; interestingly, large percentages of the eggs laid per clutch are yolkless and infertile (Frazier et al., 1987). *Chelonia mydas*, the green turtle, is the second most abundant species found in the Red Sea. This turtle grazes on seagrass. Although the green turtle rarely nests in the Red Sea, large populations nest in the Gulf of Aden. The loggerhead turtle, *Caretta caretta*, is the rarest Red Sea turtle. It feeds on molluscs and crustaceans that it crushes with its beak and nests in the Arabian Sea. The olive Ridley turtle, *Lepidochelys olivacea*, and the leatherback sea turtle, *Dermochelys coriacea*, are also rare in the Red Sea. The olive Ridley apparently feeds on shrimp and other crustaceans while the leatherback turtle is known to consume jellyfish. Neither species is found to breed in the region.

Benthic Food Web. As mentioned above, despite the fact that the waters of the Red Sea are not highly productive, the shallow benthic communities of the Sea are extremely productive and support a complex food wed (Figure 4.1-25). Within the euphotic zone along the shallow coastal shelf and in protected lagoons and bays, coral reefs and seagrass beds thrive. Seagrass beds are common along much

of the eastern and western coastline of the Red Sea and are also found in the Gulfs of Aqaba and Suez. Eleven species have been identified in the region. These include four species of *Halophila*, two of *Cymodocea*, and one species each of *Halodule*, *Enhalus*, *Syringodium*, *Thalassia*, and *Thalassodendron*. The wide, shallow shelf and unconsolidated sediments of the southern Red Sea allow for a wider diversity of seagrass species, as well as an increasing number of mangrove communities (species include *Avicennia marina*, *Rhizophora mucronata*, and *Bruguiera gymnorrhiza*), to thrive along the southern coasts (Price et al., 1988; Behairy et al., 1992).

Seagrasses stabilize reef sediments, serve as an important nursery ground for numerous species of fish and crustaceans, and comprise an important food and nutrient source for a number of reef species. Numerous epiphitic species of sponges, hydrozoans, bryozoans, tunicates, and spirorbid polychaetes are found on seagrass blades. Several gastropod species, including conch (*Strombus* spp.), urchins (*Tripneustes gratilla*), and a few species of surgeonfish and rabbitfish have been found to graze on seagrasses. Additionally, seagrasses provide a major food source for dugongs (*Dugong dugong*) and green turtles. The dugong, related to the manatee, can weigh up to 320 kg and are thought to exist in very small numbers in the Red Sea. It is also possible that the hawksbill turtle consumes seagrass. Coral reefs are another highly productive shallow benthic community common in the Red Sea. Fringing reefs occur along the coasts of the Gulfs of Suez and Aqaba. Further south, soft substrate dominated by seagrass beds and occasional patch reefs is more common. Additionally, in the southern waters, a small barrier reef thrives 5 to 20 km offshore, parallel to the Saudi Arabian coastline. Several small atoll reef structures and reefs surrounding islands are present off of the Sudanese, Saudi Arabian, Ethiopian, and North Yemen coasts (Head, 1987c).

The Red Sea and Gulf of Aden contain a rich diversity of corals and 177 species of reef building coral belonging to 53 genera are found in the Red Sea region. At least 15 of these species are known to be endemic to the region. Corals compete with each other for light and substrate and a distinct pattern of zonation is found on all reefs (Behairy et al., 1992; Head, 1987c; Goreau et al., 1979). Several zones exist on the typical Red Sea fringing reef. These include the wave crest dominated by branching corals such as *Acropora* spp., *Millepora* spp., and *Pocillopora* spp.; the calm backreef dominated by *Stylophora* spp., *Favia* spp., and *Porites* spp.; and the reef slope dominated by large heads of *Porities* spp. and *Goniastrea* spp. (Mergner, 1984; Head, 1987c).

Corals grow slowly, with growth rates ranging between 1 $cm \cdot yr^{-1}$ for boulder-like species to 39 $cm \cdot yr^{-1}$ for branching species; upward growth of an entire reef system does not exceed 0.2 to 0.7 $cm \cdot yr^{-1}$ (Head, 1987c; Goreau et al., 1979). As mentioned above, reef building corals contain symbiotic algae, known as zooxanthellae, within their tissues. This association appears to provide the corals with nutrients necessary to facilitate calcium carbonate deposition. Coral polyps obtain food by collecting plankton and organic debris in their tentacles and by sweeping the reef with exuded mesenterial filaments that search for detritus; there is also evidence that corals may also absorb dissolved nutrients directly through their body wall (Goreau et al., 1971; Barnes, 1987). Very few species are known to consume coral polyps. Many fish species, such as parrot fish, were once thought to eat large quantities of coral; however, they apparently feed more often on reef algae. One conspicuous species, the crown of thorns starfish (*Acanthaster planci*), is known to eat corals and can seriously limit coral growth (Campbell, 1987). It is possible that other asteroids and some urchins graze on coral polyps.

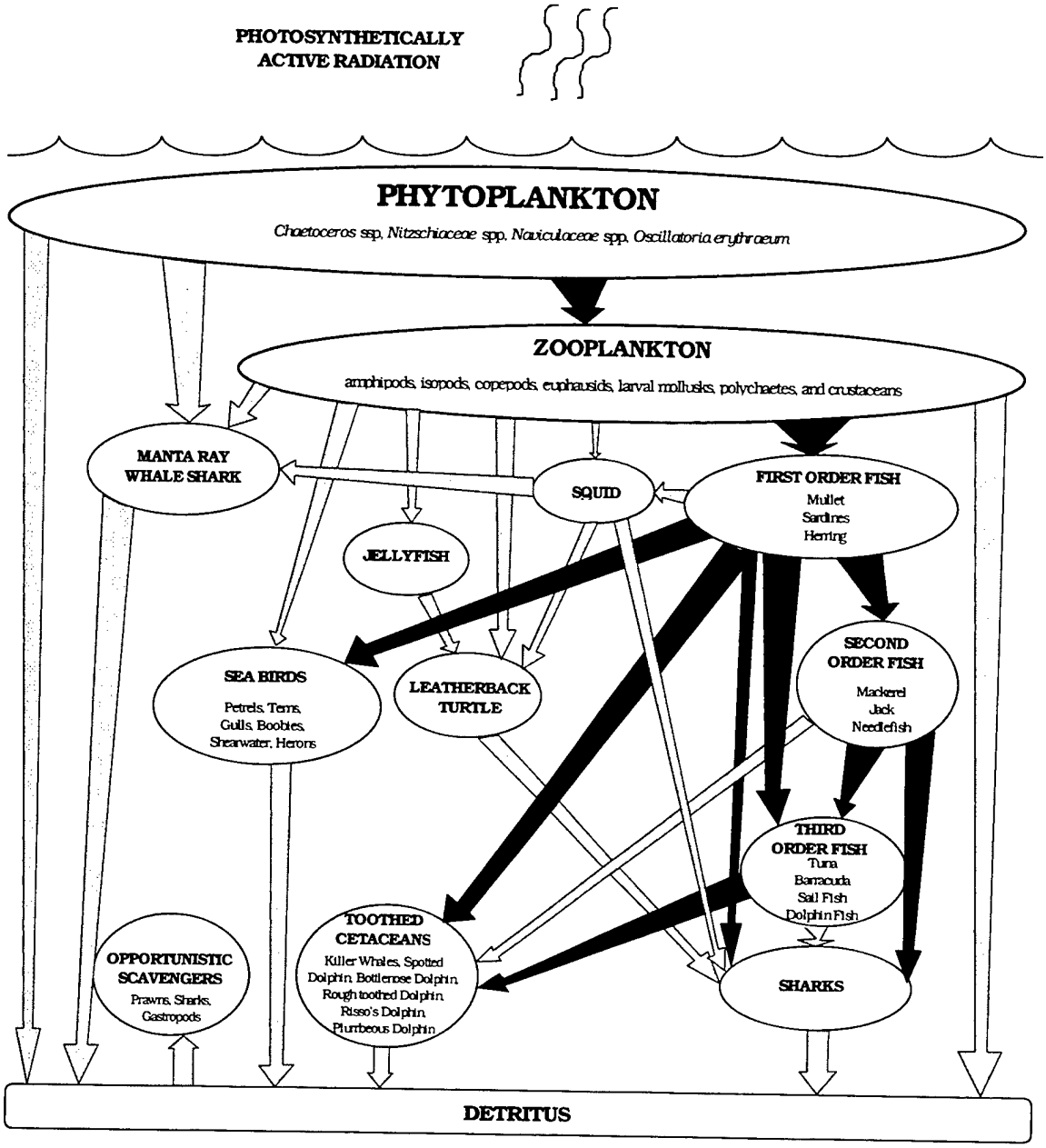

Figure 4.1-24. Pelagic trophic web of the Red Sea. The open water food web of the Red Sea is comprised of a diverse array of species ultimately dependent upon a limited phytoplankton crop. Biomass of the pelagic system is extremely low when compared to most oceanic areas including other open ocean tropical areas. So little of the pelagic production reaches the deep ocean that the abyssal benthos supports only scavenging opportunists.

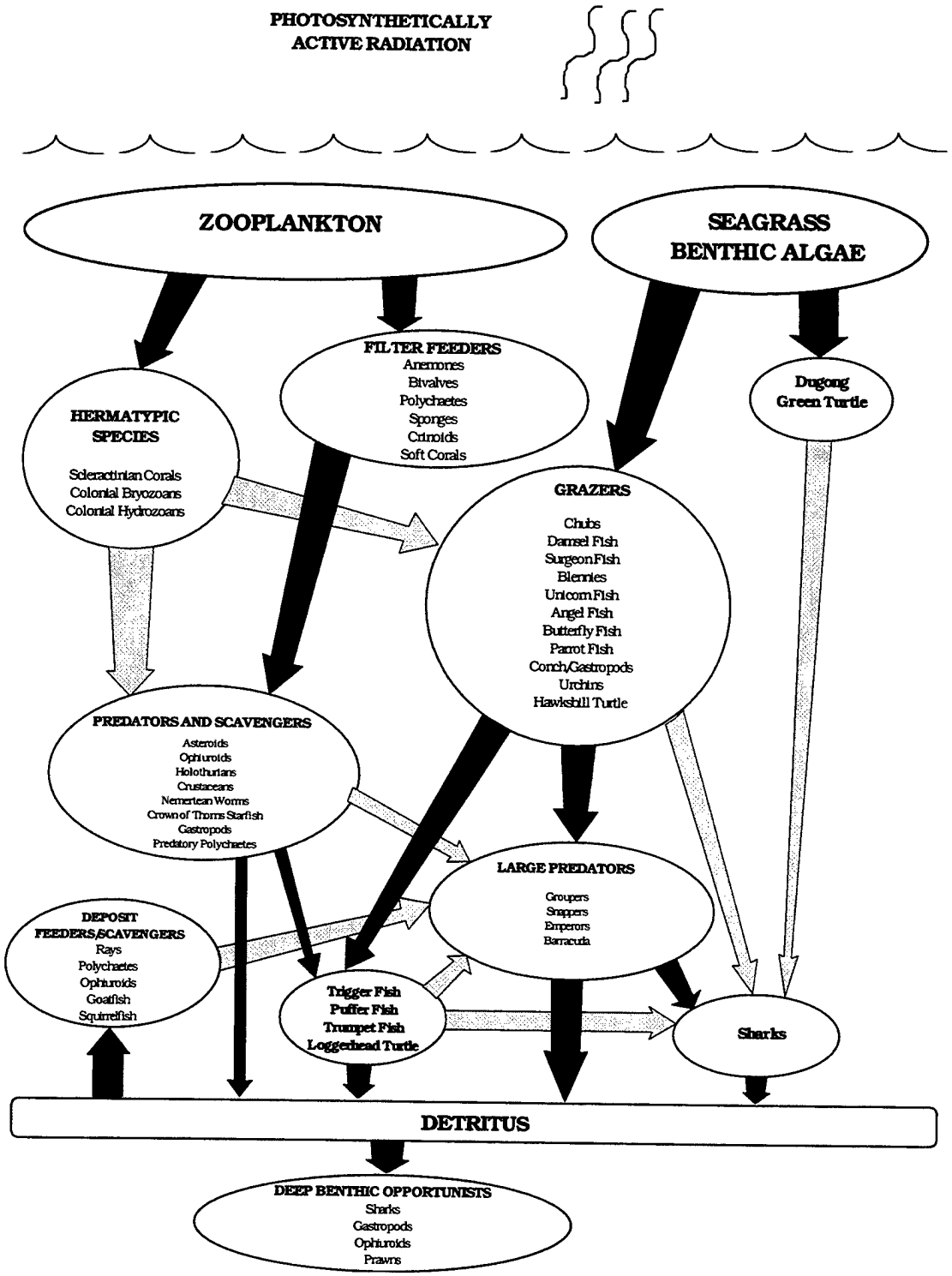

Figure 4.1-25. Benthic food web of the Red Sea. The benthic food web of the Red Sea is supported by highly productive coral and seagrass communities. The majority of shallow benthic organisms rely upon reefs and seagrasses for food, shelter, and as breeding grounds and shelter for juveniles. The deep benthos is fed by relatively little detrital material and consists largely of opportunistic scavengers and predators.

Other reef species that include zooxanthellae and that filter feed for plankton include colonial bryozoans and hydrozoans, zooanthids, anemones, and bivalves such as the giant clam (*Tridacna squamosa*). Sponges are another common filter feeder found on Red Sea reefs. One important group of sponges, of the genus *Cliona*, bore into coral substrate and dead coral skeletons. By breaking down dead coral, the sponge provides new substrate for colonization and reef expansion (Head, 1987d; Barnes, 1987). Other filter and suspension feeders include soft corals, tubiculous polychaetes such fan worms (*Sabellastarte* spp.), bivalves, and crinoids.

Numerous species of reef fish graze algae that grows on the reef. Fish known to feed on reef algae include several species of surgeon fish, unicorn fish, blennies, angel fish, butterfly fish, parrot fish, chubs, and damsel fish. Some species of damsel fish, including the whitebar (*Plectroglyphidon leucozona*), jewel (*P. lacrymatus*), and black damsel fish (*Stegastes nigricans*), are extremely territorial and cultivate small algae gardens for their own consumption (Ormond and Edwards, 1987). Additional, non-fish grazers include urchins, the best known of which are the long-spined urchins (*Diadema* spp.), conch and other herbaceous gastropods, and some species of crabs (Mergner and Mastaller, 1980).

Scavenger and predator invertebrate species common to the Red Sea region include asteroids, ophiuroids, holothurians, octopods, and nemertean worms. Several shrimp and lobster species are common on reefs. Both spiny and shovel-nosed lobster are found; the spiny lobster, *Panulirus penicillatus*, is the most common. The largest family of shrimp is Alpheidae; other shrimp include the banded cleaner shrimp (*Stenopus hispidus*) that eats by grooming ectoparasites from fish. Several species of carnivorous gastropods inhabit Red Sea reefs including tritons, cowries, and marine snails of the subdivision Neogastropoda (these include whelks, spindle shells, murex shells, mitres, cones, turrets, and basket shells). The feeding habits of carnivorous gastropods are diverse and include drilling and boring, injecting digestive enzymes into prey, and in the case of the cone shell, *Conus textile*, by shooting poisonous darts into fish and other prey (Mastaller, 1987).

Larger predators and scavengers that live in or around Red Sea reefs include fish such as groupers, snappers, rays, emperors, barracuda, trumpetfish, and triggerfish. The majority of larger reef fish feed on a combination of small reef fish, crustaceans, worms, and echinoderms. In the absence of the large triton (*Charonia tritonis),* triggerfish (*Balistoides viridescens*) are the major consumers of the crown of thorns starfish and urchins that can consume and damage reef corals. Loggerhead and hawksbill turtles also occur near reefs and consume crustaceans, molluscs, and other invertebrates. Finally, as mentioned above, several species of sharks inhabit Red Sea waters and are among the largest scavengers and predators on the reef.

Unlike that of Antarctica, the deep sea benthos of the Red Sea is sparse. A low level of surface water productivity coupled with a rapid degradation rate make the detrital material that reaches the depths of the Sea scarce. Therefore, filter feeders, such as sponges, bivalves, and tubiculous polychaetes, are rare at Red Sea depths. Due to the relatively warm, homogenous waters of the Red Sea, the majority of species that are present in the deep waters are not specially adapted to their environment, but instead are colonists from shallower waters (Thiel, 1987). Among the most abundant deep sea demersal and benthic species are prawns, such as *Haliporus steindachneri* and *Parapandalus adensameri*, several species of amphipods, and fish including the dagger-tooth (*Muraenesox cinereus*) and shark (*Iago omanensis*). Additionally, small numbers of scavengers including ophiuroids, asteroids, and gastropods have been found.

UNIQUE SPECIES AND ECOLOGICAL CONSIDERATIONS

Endangered/Threatened or Protected Species. Turtles and dugong are among the most threatened species that occur in the Red Sea. All five of the sea turtles occurring within the Red Sea are listed as threatened or endangered under the federal Endangered Species Act (50CFR 17.11 and 17.12, USFWS, 1993). There is evidence that turtles were hunted extensively in the Red Sea region during the last century for meat, oil, eggs, tortoise-shell, and leather. During the 1960s a canning factory was in operation in Somalia and in 1 year 6800 turtles were caught in Somali waters (Stromme, 1987). Despite the fact that the turtles are now protected species, local fishermen still collect eggs and hunt for adults. In addition, the dugong is listed as endangered. There is little knowledge about the state of the dugong population in the Red Sea; however, the lack of sighting and catches seems to support the belief that they are rare. As coastal development continues and heavy sedimentation flows into surrounding seagrass beds, dugongs will lose their only food source. Additionally, the infrequent reproductive periods and low reproductive rates of turtles and dugong make them particularly susceptible to environmental pressures.

No critical habitat for endangered species has been designated within the Red Sea or Gulf of Aden regions.

Unique Habitat. Due to the lack of surface water productivity in the Red Sea, coral reefs and seagrass beds that surround the Red Sea coasts are very important habitats. Both habitats have high levels of production and are a valuable food source of fish, invertebrates, reptiles, and marine mammals. Further, they are important nurseries and breeding grounds for fish and invertebrates and they provide shelter to numerous species. Additionally, coral reefs and seagrass beds stabilize sediment and prevent erosion.

Unfortunately, a majority of reefs and seagrass beds occur near the coast. Both of these habitats are currently threatened by increased coastal development that causes increased sedimentation and sewage spills on nearshore benthic communities. Oil spills from coastal refineries and wells further damage these communities. Finally, increased tourism, fishing, and shell and fish collection places strain on the reef environment. As coral reefs and seagrass beds disappear in the Red Sea region, species diversity and numbers will diminish significantly in the area.

WIDER CARIBBEAN REGION

PHYSICAL AND CHEMICAL CONSIDERATIONS

Geography and Physiography. The Caribbean Sea forms a large channel located between 9° and 25° North latitudes and between 60° and 90°West longitudes (Figure 4.1-26). It is bounded to the east by the waters of the Atlantic Ocean and to the west by the Gulf of Mexico. The 51 mile long Panama Canal, opened in 1914, connects the Caribbean Sea to the waters of the Pacific Ocean. The countries of Mexico, Belize, Guatemala, Honduras, Nicaragua, Costa Rica, Panama, Colombia, and Venezuela all share the southeastern coast of the Caribbean Sea. The United States, which borders the Gulf of Mexico, has a small coastline along the northern boundary of the Caribbean Sea. The islands of Cuba, Jamaica, Hispaniola (Haiti and the Dominican Republic), and Puerto Rico, as well as the island chains of the Bahamas, and the Turks and Caicos, form the northern border of the Sea. The Lesser Antilles island chain forms an arc (extending from the Virgin Islands to Trinidad and Tobago) that creates the eastern border of the Sea.

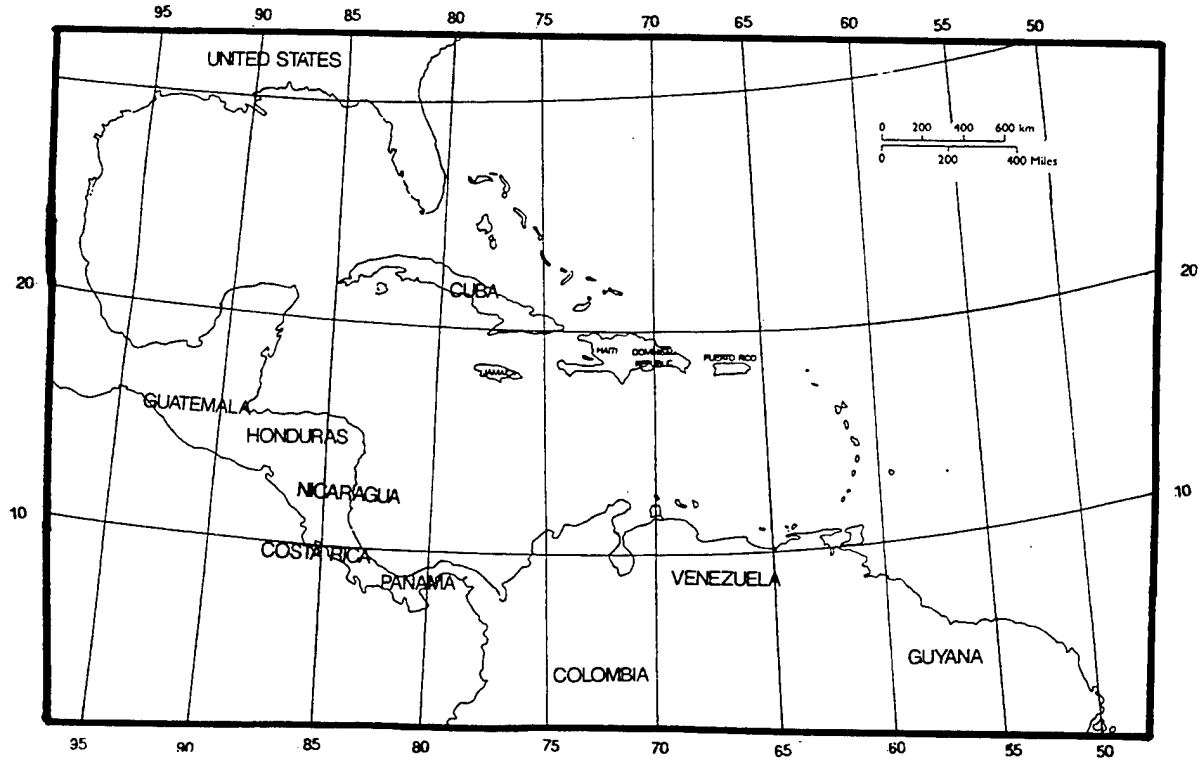

Figure 4.1-26. Wider Caribbean Region. The Caribbean Sea consists of a series of deep basins surrounded by numerous island chains. The Gulf of Mexico lies to the west and the Atlantic Ocean lies to the east.

Bathymetry. The greater Caribbean Sea, with area of $4.2 \cdot 10^6$ km^2, is comprised of a string of four increasingly deeper basins, all of which exceed 4000 m in depth (Underwood, 1989). Compared to other semi-enclosed ocean basins, the Caribbean is remarkably deep. At the northwest margin, the Gulf of Mexico, averaging 4400 m depth, is characterized by wide shelves of carbonate origin to the south and east (Yucatan and East Florida) and by terrigenous sediment to the north (Mississippi and Rio Grande deltas). The Yucatan Basin, between Cuba and the Gulf of Honduras, averages 4600 m in depth and is

bounded on the south by the Cayman Trough. The Cayman Trough has a depth of 7100 m and is predominately a carbonate regime. The Columbia Basin, northwest of Columbia, averages 4500 m in depth and is dominated by carbonate sedimentation. The Venezuela Basin, with an average depth of 6500 m, is bordered on its eastern margin by an active arc-trench system of oceanic volcanoes that forms the Lesser Antilles Island chain atop a crescent shaped ocean ridge. In addition to the volcanic influence, the latter basin receives substantial pelagic clay input from the prolific Oronoco and Amazon fluvial systems. Major sills separating this string of Caribbean basins have depths of 1000 m or less and peripheral sills in and out of the Caribbean area (Straits of Florida, Windward sill, Jungfern Sill, St. Lucius Sill, and the Grenada/ St. Vincent's Sill), similarly, have depths between 16 m and 1000 m.

Within this comparatively deep system of basins 80% of the water exceeds 1800 m depth while over 50% of its floors are over 3600 m deep (Clark, 1992). Most of the Caribbean water lies well below sill depth. With the exception of the Yucatan Gulf and Eastern Florida, continental shelves are narrow and much of the eastern margin in the Lesser Antilles Archipelago lacks a shelf entirely. Rapid uplift of the eastern margin of the Caribbean yields a subaerial topography virtually devoid of coastal lowlands where volcanic sources stand like pedestals above the sea floor. Nearer the strands of islands, carbonate sedimentation in the form of reefs or as precipitation has smoothed out the rugged narrow shelves to almost a glasslike finish. Carbonates from reef systems veneer volcanic islands and pave continental shelves around the margin, particularly in the southern reaches. At the basinward edge of these limestone platforms, submarine topography often drops off as sheer cliffs of carbonate rubble.

Currents, Tides, and Water Exchange. Surface circulation in and out of the greater Caribbean follows a general southeast to northwest to eastward clockwise pathway (Thurman, 1975; Svedrup et al., 1942). In the southern portion of the Sea, the west-flowing Guiana and North Equatorial currents feed directly into the Caribbean Current which enters the Gulf of Mexico between Cuba and the Yucatan area to initiate a clockwise loop current in that water body. That system, in turn, becomes the Florida current that rejoins the warm Antilles and Gulfstream Currents and reenters the Atlantic at the shallow Florida Straits. Within the Greater Caribbean surface current system, currents as strong as 2.5 knots have been reported (along the main axis of the Caribbean Current), but average surface flows rarely exceed 1 knot (Thurman, 1975). Eddy currents develop south of the Caribbean current in a counterclockwise system along the southern part of the Columbia Basin in the Gulf of Panama. Somewhat weaker counterclockwise currents form north of the main Caribbean current in the northern Venezuela Basin. The open circulation system of the Caribbean area yields very low estimates for surface water residence time above depths of 800 m. However, the majority of the water in the Caribbean basins lies below the depths of the major sills that connect the Caribbean waters to the Atlantic waters. Therefore, flushing or renewal of the deep regions of the Caribbean is limited (Underwood, 1989).

Caribbean tides are low to minimal, ranging from 1 m in the southeastern end down to less than 0.5 m in areas of the north. At the southeastern extreme of the area, the Amazon River has the world's longest estuarine system affected by tides. Here, very small tides can be measured up to 800 km upstream but even more spectacular are the tidal bores in this channel. At maximum these propagating waves move up river to 12 kts with a tidal bore as high as 5 m. As this bore advances up river it has the appearance of a rapidly moving waterfall (Thurman, 1975).

Temperature and Salinity. Four identifiable water masses are recorded in the Caribbean Sea, two above 200 m and two below (Thurman, 1975). The thin veneer of north equatorial current water entering the Caribbean is very warm with very little seasonal fluctuation; temperature here ranges between 26°C and 28°C. The surface waters of the northern Gulf of Mexico, however, can drop as low as 16°C during the winter months. Deep water masses are characterized by their lower temperature. A well-developed

thermocline at about 150 m separates surface and deep water masses. Below the thermocline, water drops to around 4°C with virtually no seasonal variation. The effect of this remarkably stable, layered temperature regime is an almost complete lack of mixing of surface and deep water. Significant upwelling does not occur and nutrients are supplied largely from estuarine mouths.

In the eastern part of the Caribbean, the minimum surface water salinity is 34.7 ppt while in the Yucatan Channel, minimum salinity averages around 34.9 ppt (Svedrup et al., 1942). Deep water masses include a subantarctic deep water mass with salinity values of 34.5 ppt. In the Gulf of Mexico, surface water salinity in the western portion may be as high as 36.6 ppt, but in the vicinity of the Mississippi, effluent surface salinities may drop to as low as 25 ppt while the salinity of deeper masses are around 35.5 ppt (Thurman, 1975).

Oceanic Sedimentation. The larger Caribbean Basin may be characterized as a carbonate regime which is fed terrigenous sediments from three major point sources, the Mississippi, Rio Grande, and Magdalena Rivers. Pelagic sediment from the Orinoco and the Amazon effluents is borne into the system by the strong tropical equatorial current. Major sediment transport into the area comes from the Mississippi mouth in the Gulf of Mexico (estimated at 222 million tons annually) and from the Magdalena River of Columbia (234 million tons annually) (Timberlake, 1983). Adjacent to these terrigenous systems, large sediment-dominated prograding deltas typically form and basinward of these structures, massive submarine fans extend across the slope rise and onto the abyssal plain. Discharge from these two fluvial systems moves through the greater Caribbean area from the southeast to the northwest.

The discreet Caribbean basins away from terrigenous sources conform to a model with carbonate shelves often dotted by extensive bioherm systems which give way in slope and abyssal waters to very fine deep sea clay. In the vicinity of the Lesser Antilles the prevailing tradewinds carry volcanic ash a short distance to deposit on the leeward side of the islands.

The majority of knowledge pertaining to sedimentation and geology in the Caribbean region, stems from offshore petroleum exploration. Continental self sediments in the Gulf of Mexico are a basinward extension of tertiary and quaternary geologic units that crop out above the strand along the continental shelf. Offshore petroleum exploration and production, so prevalent in northern Mexico, is targeted in tertiary rocks that have been structurally deformed into oil trapping features by much older salt layers that form the very bottom of this basin. By contrast petroleum resources around the Yucatan Peninsula are buried Mesozoic reef structures. Oil and gas structures drilled with some success near the Island of Trinidad in the southeastern corner of the area target a variety of environments including ancient buried shoreline sands.

CURRENT ENVIRONMENTAL STRESSES

Marine Pollution. To date, there is little coastal urbanization in the Caribbean region and, with the exception of petroleum spills, little wide-spread effects due to pollution. However, due to the open, well-flushed nature of the Caribbean Sea, any pollution generated by ship traffic or coastal industry and development is likely to be transported to the neighboring islands. Due to the surface current system into the area from the southeast, the Gulf of Mexico forms a near perfect natural trap for pollutants. In addition, the virtual lack of vertical exchange between surface and deep waters and the abundance of turbulent wakes and eddies prevent rapid water turnover and means that there is little relief when pollution does occur.

Urbanization and Tourism. Increasing urbanization and tourism put a strain on the surrounding marine communities of the Caribbean in a number of ways. The populations of a majority of Caribbean, Central and South American countries are increasing. Additionally, an estimated 100 million tourists vacation in the region annually (Timberlake, 1983). Tourism accounts for approximately 40% of the gross domestic income of the Caribbean Island nations (Bleaching of Coral Reefs in the Caribbean, 1988). Sewage is the largest source of pollution due to increased urbanization and tourism. It has been estimated that only 10% of the sewage produced in the region is treated (Timberlake, 1983). As discussed previously, sewage can decrease water clarity and thus reduce the light penetration necessary for growth of seagrasses and corals and can increase eutrophication and subsequent algal blooms that deplete dissolved oxygen concentrations (Goenaga, 1991).

Due to the active surface flow conditions in the Caribbean, marine debris from ships, coastal ports, and river inputs becomes concentrated and washes from shore to shore of the Caribbean nations. Garrity and Levings (1993) analyzed the litter along beaches at nineteen sites in Panama. They found that 82% of the debris found was styrofoam and other plastics. Metal and wood were less abundant. The majority of the debris came from Panama sources. However, at least 16% was from the United States, and 10% was from other sources.

Tourism damages the surrounding marine environment of the Caribbean in several ways. One source of damage is increasing anchor damage to reefs. The number of cruise ships that tour the Caribbean rose from 35 to 82 between 1982 and 1987 (Allen, 1992). Medium and large sized cruise ships have anchors weighing 5 tons or more that are periodically dropped on coral reefs. In one incident that occurred in 1985, an anchor and its chain destroyed a patch of reef that measured 2100 m^2 (Allen, 1992). Other sources of damage associated with tourism include divers that carelessly kick and stand on corals, shell collection, and even the use of dynamite and crowbars to collect tropical fish and shells from reefs.

Oil. Undoubtedly the largest sources of pollution in the Caribbean region are associated with petroleum production and transport. Petroleum enters the Sea in three ways, as runoff from fluvial sources, from tanker spills and flushing, and from oil exploration and production spills. At this point, the Caribbean, and in particular the Gulf of Mexico, endure the largest number of natural submarine oil and gas seeps in the world (Orr personal communication). The principal oil-producing areas in the region are Trinidad and Tobago, Venezuela, and the Gulf of Mexico (Clark, 1992). Nearly 2000 offshore oil platforms exist in the United States sector of the Gulf alone. Currently, it is estimated that tankers loaded with oil in excess of 5 million barrels pass through Caribbean waters each day (Underwood, 1989). Tankers, carrying oil from the Middle East to the United States, from Alaska to Europe, and from South America to Europe travel through the region. An estimated 7 million barrels of hydrocarbons from ballasting, ship cleaning, tank washing, and docking operations are deposited in the Caribbean Sea each year (Underwood, 1989).

To date the largest oil spill in the Caribbean region occurred from June 1979 to March 1980 when a blow-out occurred in the Ixtoc I oil field in the Bay of Campeche off of the coast of Mexico. Before the spill was capped off, 350,000 tons of crude oil had dumped into the Sea (Clark, 1992). Cleanup costs for the spill exceeded $US219 million dollars. Oil spills can have catastrophic effects on neighboring reef, mangroves, and seagrass beds can kill fish, birds, and mammals, and can damage breeding grounds of endangered species. After a 1986 spill in Panama, for example, colonies of the reef-building coral, *Siderastrea siderea*, either died or showed decreased reproductive ability (Guzman and Holst, 1993).

Other Industrial Inputs. Despite the fact that industrial development in the Caribbean is still minimal, industrial pollution is brought into Caribbean waters from the large watershed that feeds into the Sea. Pesticides and fertilizers, heavy metals, such as mercury, and bauxite from nearby mines enter rivers and eventually enter the Sea. It is estimated that by the year 2000, the Magdalena River will be so polluted that it will be devoid of oxygen or life for over 155 miles (Timberlake, 1983). Industrial wastes are dumped directly into the Sea from Puerto Rico and Trinidad. Heavy metals (including copper, zinc, iron, cadmium, and manganese) have been found in increasing quantities in the skeletons of reef corals (Guzman and Jimenez, 1992). Another source of industrial pollution is thermal effluent generated mainly by coastal power plants. These heated effluents can raise the adjacent waters 5°C above ambient sea temperature (Clark, 1992).

Increased sedimentation due to coastal development and dredging poses an additional threat to shallow benthic communities. Each year, 18,000 km^2 of Caribbean rainforest is destroyed to grow crops (Timberlake, 1983). As a result, adjacent estuaries, mangroves, seagrass beds, and coral reefs have faced an increase in sedimentation, a decrease in water clarity, and a subsequent increase in mortality. It is estimated that 75% of Colombian land is affected by erosion and that in Haiti, more than 50% of the soil has washed away down to bedrock (Timberlake, 1983). Other sources of sedimentation stem from the dredging of shallow bays and shipping channels, the extraction of beach sand for construction, and the filling of coastal shoreline for construction of hotels, houses, and industrial plants.

Sea Traffic and Ports. As mentioned previously, the majority of shipping activity in the Caribbean region is related to oil transport. On any one day there can be as many as 25 loaded supertankers and 75 loaded medium-sized tankers in Caribbean waters (Timberlake, 1983). Additional traffic consists of cruise ships, fishing boats, and supply ships that bring goods to the many populated islands of the region. Exports from the region include sugar and fiber, fruit, and some manufactured goods (Couper, 1983).

Due to the proximity of the Panama Canal to Caribbean waters, the Caribbean has become one of the most important shipping routes in the world. Shipping lanes are established through most of the major island passages in the region. The most traveled channels separating the Caribbean islands include the Windward Passage, between Cuba and Hispaniola, the Mona Passage, between Hispaniola and Puerto Rico, and the Anegada Passage, between the British and U.S. Virgin Islands (Suarez-Caabro, 1990). Approximately 200 million people inhabit the coastal cities in the Caribbean region (Suarez-Caabro, 1990). Major Caribbean island ports include San Juan, Puerto Rico; Havana and Santiago, Cuba; Port of Spain, Trinidad; and Santo Domingo, Dominican Republic.

FISHERIES AND AQUACULTURE RESOURCES

The waters of the Caribbean are characterized by low levels of primary productivity. Therefore, the Caribbean does not support the same large scale pelagic fisheries as those that are found in more temperate waters. Fishing practices in the Caribbean region are largely artisanal in nature; each island often contains a small fleet of canoes or outboard motor-powered skiffs that are manned by one or two people who set traps and pots or that dive on the reefs in search of shellfish. However, several nations including Cuba, the United States, and Mexico, have much larger fleets that fish commercially. The United States fishing fleet is responsible for 62.8% of the total catch in the Caribbean region while Mexico is responsible for 13.8%, Colombia and Venezuela for 11.9%, and the islands of the region for 8.3% of the total catch (Suarez-Caabro, 1990). In 1988, the total catches of the nations in the Caribbean region totaled 7.9 million tons of fish and shellfish (Suarez-Caabro, 1990).

The largest fishery in the Caribbean is the penaeid shrimp fishery along the northern Gulf of Mexico, the coasts of Mexico and Central America, and off the coast of Cuba. The spiny lobster, *Panulirus argus*, is found on reefs and is a commercially important shellfish species for Central American countries and for a number of small Caribbean islands. In Florida in 1982, the value of spiny lobster caught in local waters amounted to $15 million dollars (Bleaching of Coral Reefs in the Caribbean, 1988). Commercially important pelagic fish species include tuna, anchovies, mackerel, mullet, and menhaden. Important reef fish species include groupers, jacks, snappers, grunts, parrot fish, and trigger fish (Munro, 1983; Rodriguez, 1974). Additionally, the queen conch, *Strombus gigas*, is harvested by local island populations for sale, mainly in the United States. Timberlake (1983) estimated that the number of conch exported from Haiti amounted to 60,000 per month in 1979. Finally, a small sport fishing industry, thrives in the Caribbean with bonefish (*Albula vulpes*) and tarpon (*Megalops atlantica*) as important species.

Phytoplankton. Like other tropical seas, the waters of the Caribbean Sea are characterized by high water clarity and low levels of productivity. Due to a lack of mixing of surface and deep water layers, the Caribbean waters contain low levels of nutrients. The most productive waters of the region include the upwelling area located along the Venezuelan coast, where the tilt of water layers brings nutrient-rich waters into the euphotic zone, and along littoral zones, where nutrients are washed into the Sea from the river systems that flow into the Caribbean (Rodriguez, 1974). Levels of phosphate and nitrate in the surface waters of the Caribbean Sea can be as low as 0.2 $\mu mol \cdot L^{-1}$ and 0.06$\mu mol \cdot L^{-1}$, respectively (Chadwick et al., 1996).

Estimates of primary production in the Caribbean Sea vary from area to area depending on the location of river inputs and upwellings. In the central region of the Sea, productivity can be as low as 50 to 100 $mgC \cdot m^{-2} \cdot d^{-1}$ (Margalef, 1971). Along the upwelling region near the coast of Venezuela, production is higher and can range between 1 to 3 $gC \cdot m^{-2} \cdot d^{-1}$. In general, important commercial fisheries are located in regions of higher productivity while coral reefs are found in areas of lower productivity with clearer waters.

Unlike the Red Sea, the Caribbean Sea contains a large diversity of plankton species. The rapid circulation and lower salinity of Caribbean waters facilitate the colonization and survival of plankton species. An estimated 450 species of diatoms and 460 species of flagellates are found in Caribbean waters (Wood, 1971). Diatom species commonly found include *Chaetoceros* spp., *Nitzschiaceae* spp., *Coscinodiscus* spp., *Thalassiosira* spp., and *Rhizosolenia* spp. (Wood, 1971). Dinoflagellates include *Ceratium* spp., *Goniaulax* spp., *Gymnodinium* spp., *Peridinium* spp., and *Phalacroma* spp.

Seagrass and Coral Reefs. Similar to the waters of the Red Sea, Caribbean waters are characterized by areas of high benthic productivity. Seagrass beds line the shallow lagoons along the coasts of Florida, the Yucatan peninsula and Central America, and numerous Caribbean islands. Seagrass beds are dominated by turtle grass, *Thalassia testudinum.* Other common species include *Syringodium filiforme* (manatee grass), *Diplanthera wrightii* (shoal grass), *Halodule wrightii*, *Halodule beaudettei*, *Halophila baillonis*, *Halophila decipiens*, and *Halophila engelmannii*. Beds of *Thalassia* and associated algae can contribute as much as 3000 $gC \cdot m^{-2} \cdot yr^{-1}$ of primary production (Clark, 1992). *Thalassia* productivity in Puerto Rico has been estimated to be lower, at 900 $gC \cdot m^{-2} \cdot yr^{-1}$ (Humm, 1973).

Caribbean waters are home to 14% of the world's coral reefs. As mentioned previously, coral reefs are considered to be among the most productive environments in the world. Coral reefs are characterized by high rates of nitrogen fixation and nutrient recycling; additionally, because benthic communities are fixed in space, large quantities of nutrients, in low concentrations, are carried to them, thus facilitating

productivity (D'Elia, 1983). This recycling ability, enhanced by the symbiotic relationship of reef organisms and the brown algae known as zooxanthellae, leads to very high productivity estimates for reef systems. Estimates of reef productivity, as stated earlier in this document, can range between 500 to 2500 $gC \cdot m^{-2} \cdot d^{-1}$, with some estimates as high as 10,000 $gC \cdot m^{-2} \cdot d^{-1}$ (Lewis, 1977).

Zooplankton. The zooplankton assemblage of the Caribbean Sea is dominated by grazing copepods. More than 300 species of copepods have been identified in the region (Owre and Foyo, 1971). Common copepod species include *Paracalanus aculeatus*, *Clausocalanus furcatus*, *Undinula vulgaris*, *Calanus minor*, *Farranula gracilis*, *Temora* spp., and *Oithona plumifera* (Michel and Foyo, 1976). Other dominant groups include siphonophores, euphausiids, chaetognaths, mollusc, crustacean, and polychaete larva, tintinnids, and salps. Medusae such as *Aglaura* spp., *Liriope* spp, and *Rhopalonema* spp. have also been identified.

The numbers and biomass of Caribbean zooplankton are greater in areas of higher primary productivity. In the upwelling region near Venezuela copepod densities can be as great as 1200 individuals$\cdot m^{-3}$; off the coast of Cuba densities as high as 4000 individuals$\cdot m^{-3}$ have been reported (Margalef, 1971). Margalef (1971) and Hopkins (1973) estimate the wet weight of zooplankton to be 0.03 to 0.1 $g \cdot m^{-3}$ in areas of lower productivity to 0.3 $g \cdot m^{-3}$ in areas of higher productivity, reaching as high as 1 $g \cdot m^{-3}$ near river mouths such as the Mississippi.

TROPHIC RELATIONSHIPS

Pelagic Food Web. The pelagic food web of the Caribbean, like that of the Red Sea, is fed by a small amount of zooplankton dominated by copepod species. The upwelling area adjacent to the coast of Venezuela and the waters in the vicinity river inputs are more productive; therefore, species diversity and richness in these areas are greater than those of the central Sea waters. The pelagic food web for the Caribbean region is similar to that of the Red Sea region (Figure 4.1-27). One notable difference is the presence of baleen whales and increased numbers of other cetaceans in the Caribbean waters.

Small, planktivorous Caribbean fish species include herrings and sardinellas (Clupeidae), and anchovies (Engraulidae). Small, schooling species are an important food source for jacks, needlefish, horsemackerel, and seabirds. Four species of squid are common in Caribbean waters; these include Plee's striped squid (*Loligo pleii*), brief thumbstall squid (*Lolliguncula brevis*), Pickford's squid (*Pickfordiateuthis pulchella*), and atlantic oval squid (*Sepioteuthis sepioidea*) (Kaplan, 1982). Large planktivorous fish species that occur in the Caribbean Sea are the giant manta (*Manta birostris*) and the whale shark (*Rhincodon typus*). Baleen whales including humpback (*Megaptera novaeangliae*), blue (*Balaenoptera musculus*), fin (*B. physalus*), sei (*B. borealis*), minke (*B. acutirostrata*), and black right (*B. glacialis*) whales have all been observed in Caribbean waters.

The larger predacious fish species known to occur in the Caribbean region are the same as those known to occur in the Red Sea and include several species of jacks and horsemackerels (*Caranx* spp. and *Carangoides* spp.), tuna, mackerel, barracuda (*Sphyraena barracuda*), and several species of and needlefish and halfbeaks. The largest predators in Caribbean Sea pelagic waters include sharks and cetaceans. Among the most common shark species of the Caribbean include the tiger (*Galeocerdo cuvier*), shortfin mako (*Isurus oxyrinchus*), lemon (*Negaprion brevirostris*), and six species of hammerhead sharks (*Sphyrna* spp.). Other common species include the spinner shark (*Carcharhinus brevipinna*), the bull shark (*C. leucas*), the blacktip shark (*C. limbatus*), and the reef shark (*C. perezi*). Sharks are scavengers and predators and will consume bony fish, turtles, seabirds, cetaceans, and, as with

the nurse shark (*Nebrius ferrugineus*), crustaceans, cephalopods, and even coral (Ormond and Edwards, 1987).

Other than sharks, the largest predators of the Caribbean Sea are the toothed cetaceans and a few species of pinnipeds. Toothed whale species identified in the waters of the Caribbean include the killer whale, the false killer whale, and the pygmy killer whale, the sperm whale, the pygmy sperm whale, the short-finned pilot whale, and Cuvier's beaked whale. Dolphin species include spotted, Atlantic Ocean bottle-nosed, rough-toothed, common, bridled, Risso's, and long-snouted dolphins. These cetaceans consume mainly schooling fish and some cephalopods. Killer whales consume fish and marine mammals, such as pinnipeds, manatees and cetaceans. Species of pinnipeds that have been identified in Caribbean waters include the Caribbean monk seal (*Monachus tropicalis*) and the California sea lion (*Zalophus californianus*). Pinnipeds mainly eat fish and cephalopods.

Numerous species of seabirds live and breed in the Caribbean region. Over 400 avian species have been recorded in or flying over the Gulf of Mexico (Woolfenden and Schreiber, 1973). Common species that live near the water and that rely on the water for food include white and brown pelicans, cormorants, frigate birds, herons and egrets, ospreys, grebes, plovers, turnstones, brown noddies, and several species of gulls and terns. The majority of these species feed by diving on schools of small fish. Some species will also eat planktonic crustaceans and molluscs.

Finally, all five species of pantropical marine turtles are known to occur in the Caribbean region. As discussed in the Red Sea portion of this document, species include the hawksbill turtle, *Eretmochelys imbricata*; the green turtle, *Chelonia mydas;* the loggerhead turtle, *Caretta caretta;* the olive Ridley turtle, *Lepidochelys olivacea;* and the leatherback turtle, *Dermochelys coriacea*. There is evidence that Caribbean turtle populations are declining. In 1947, 40,000 marine turtles hatched in the Gulf of Mexico; however, in 1976, only 700 were found, and in 1977 the number decreased further to 450 (Timberlake, 1983).

Benthic Food Web. A majority of the ecological data that pertains to the Caribbean region addresses the interrelationship of three important shallow benthic and coastal communities: mangroves, seagrass beds, and coral reefs. As mentioned above, despite the fact that the waters of the Caribbean Sea are not highly productive, these shallow benthic communities of the Sea are extremely productive. These species form an integrated web in which the health of each of the three communities is affected by the health of the other two (Figure 4.1-28). The benthic food web of the Caribbean is supported by thriving reefs, mangroves, and seagrass beds (Figure 4.1-29).

Mangrove forests or swamps form between the high and low tide marks on flat, swampy, tropical shorelines that are rich in sediments and loose mud. Dense populations of mangroves occur along the Magdalena and Orinoco river deltas in South America, along the eastern shores of the Gulf of Mexico, and on numerous Caribbean islands. Four species of mangroves are common in the Caribbean region; these include black mangrove (*Avicennia germinans*), white mangrove (*Laguncularia racemosa*), red mangrove (*Rhizophora mangle*), and buttonwood (*Conocarpus erectus*). Mangrove forests serve an important ecological role by trapping pollutants and silt washed from adjacent land (Ogden and Gladfelter, 1983; Underwood, 1989; Timberlake, 1983). By stabilizing coastal sediment, mangroves maintain water clarity and promote reef and seagrass growth. Additionally, mangroves provide a source of nutrient-rich detritus and dissolved organic material (DOM) to reefs and seagrass beds. Finally, mangrove stands and neighboring seagrass beds serve as habitat for a number of epiphytic algae species and are important nursery and feeding ground for commercially important reef species such as the spiny

lobster (*Panulirus argus*), the pink shrimp (*Penaeus duorarum*), and various grunts and snappers (*Haemulon* spp., and *Lutjanus* spp.) (Ogden and Gladfelter, 1983).

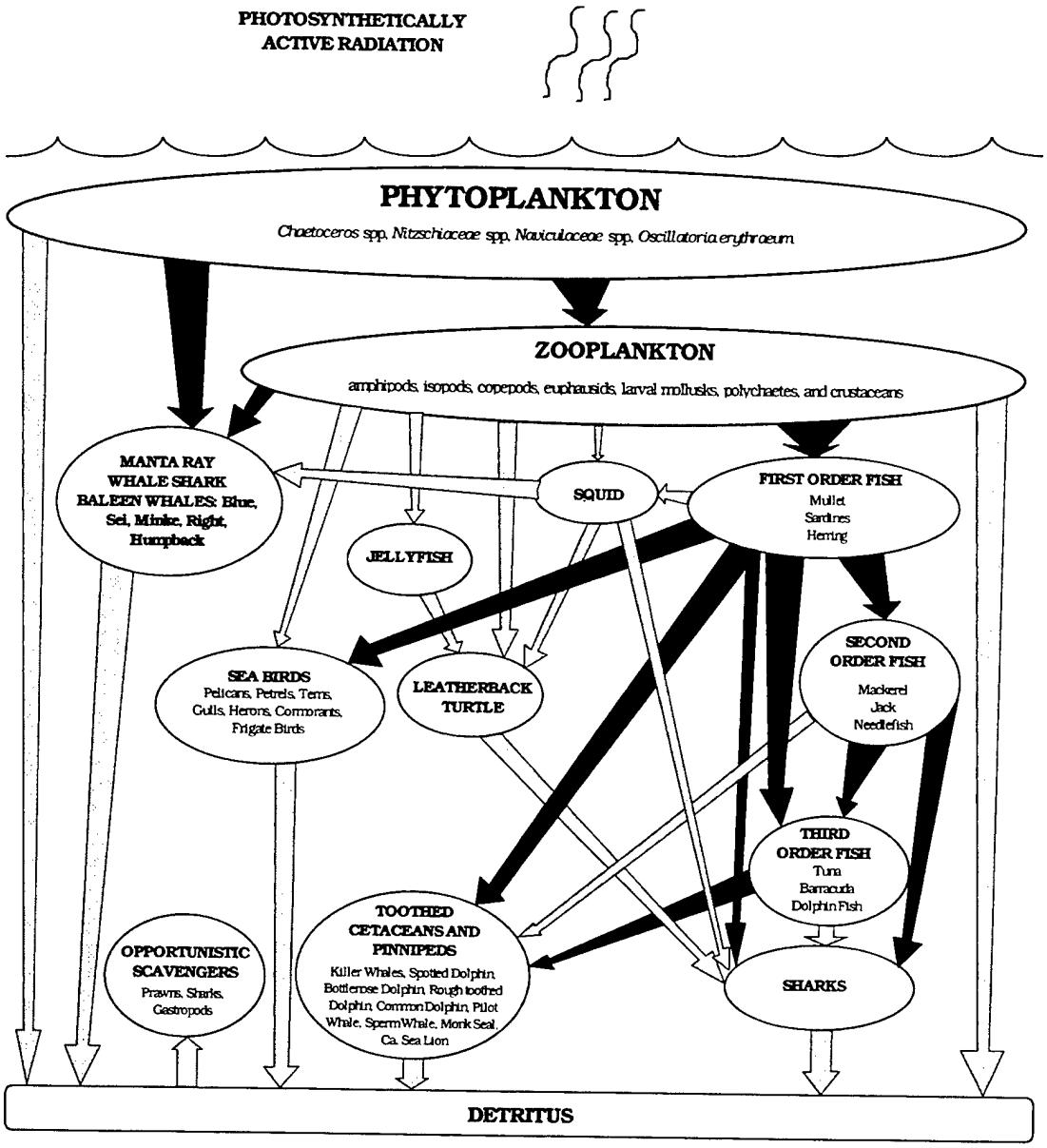

Figure 4.1-27. Pelagic trophic web of the Caribbean Sea. The open water food web of the Caribbean Sea is comprised of a diverse array of species ultimately dependent upon a limited phytoplankton crop. Like that of other tropical seas, biomass of the pelagic system is extremely low when compared to most oceanic areas.

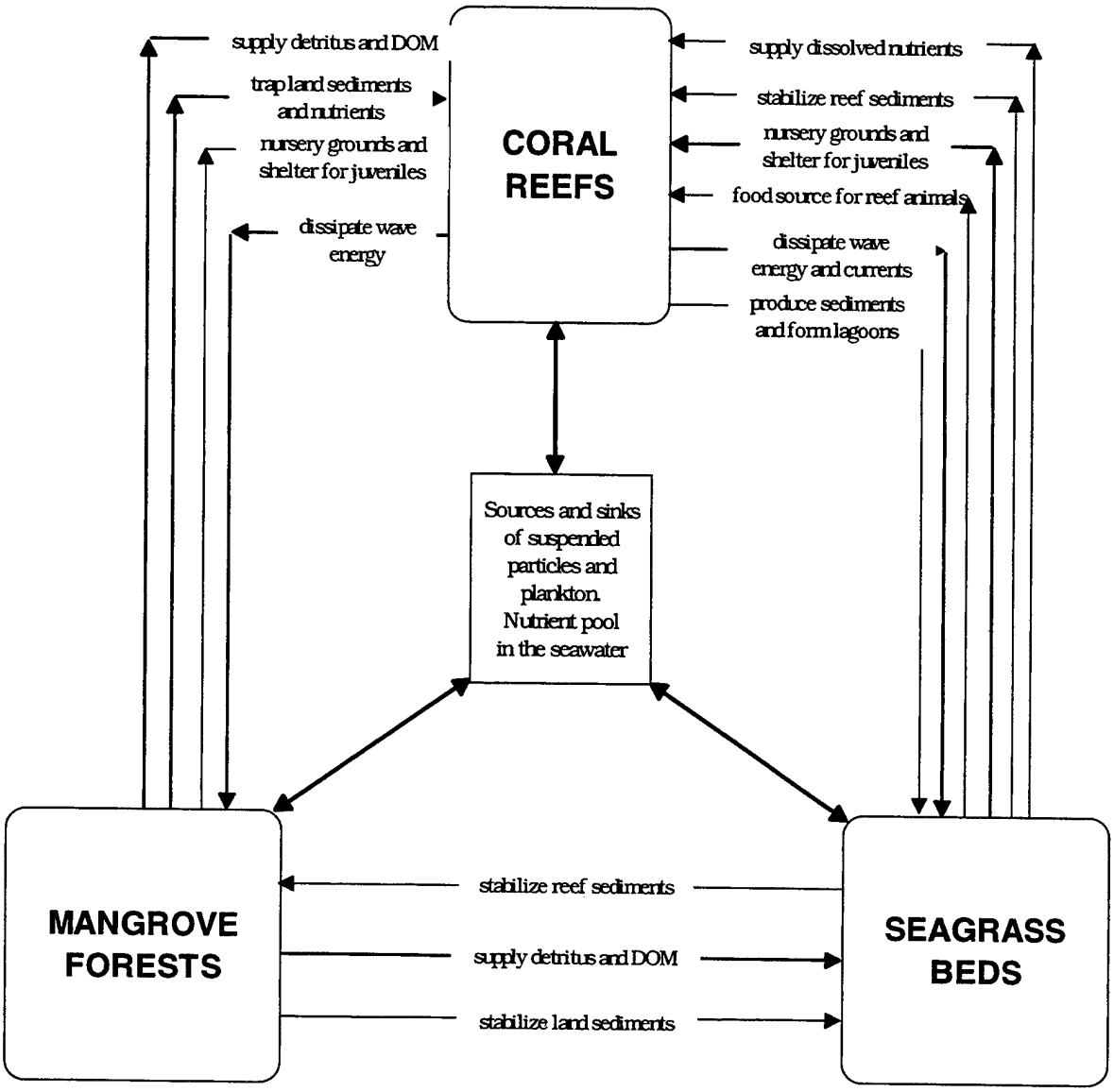

Figure 4.1-28. Interrelationship of shallow benthic Caribbean communities. Principal interactive mechanisms between coral reefs, seagrass beds, and mangrove forests are illustrated by beneficial feedback loops and nutrient exchange pathways. The most significant relationships are denoted by thick arrows.

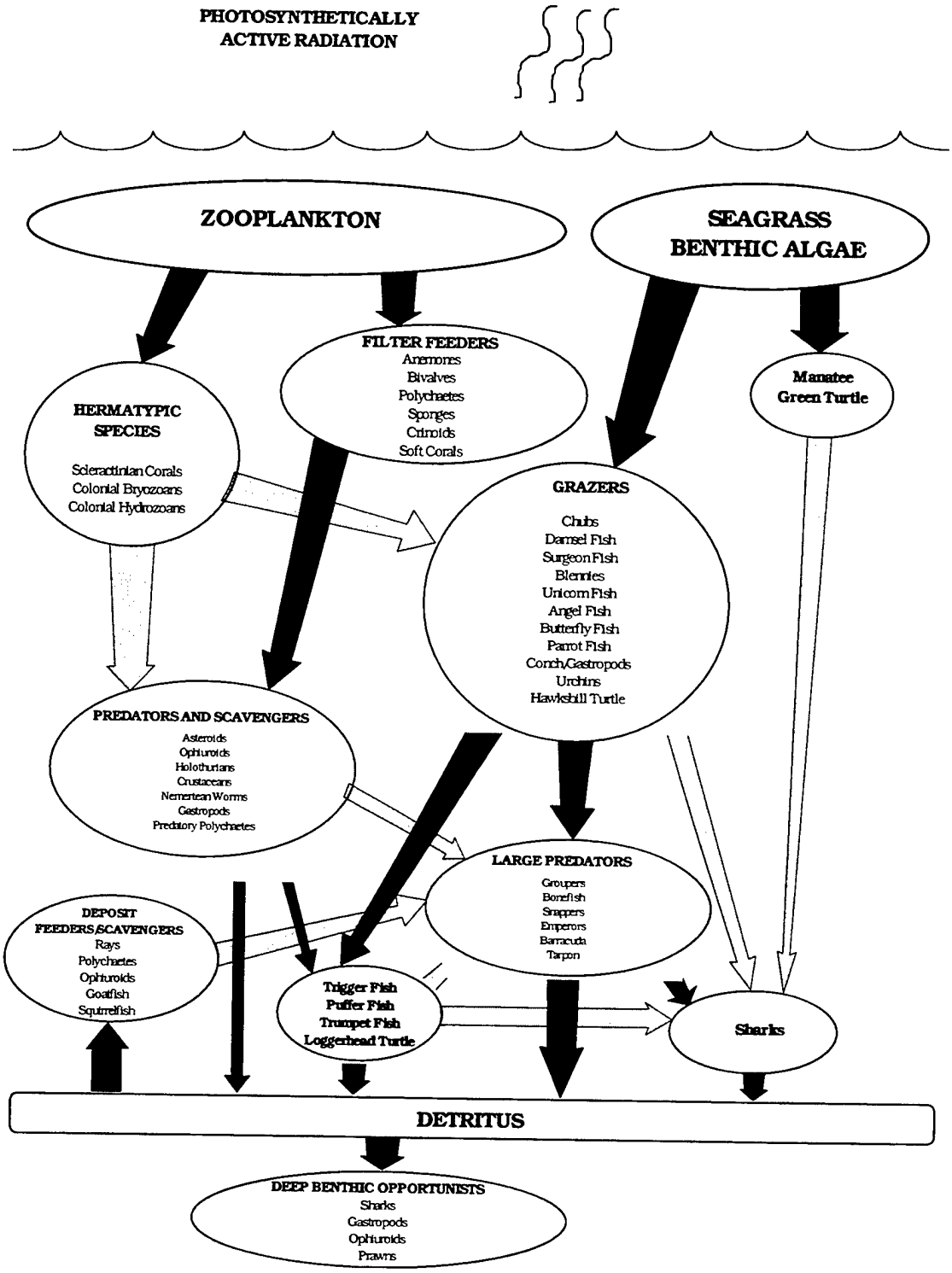

Figure 4.1-29. Benthic food web of the Caribbean Sea. The benthic food web of the Caribbean Sea is supported by highly productive coral, seagrass, and mangrove communities. The majority of shallow benthic organisms rely upon reefs and seagrasses for food, shelter, and as breeding grounds and shelter for juveniles. The deep benthos is fed by relatively little detrital material and consists largely of opportunistic scavengers and predators.

Seagrass beds, dominated by turtle grass (*Thalassia testudinum*) are common along in the calm shelf waters and shallow lagoons along the coasts of the Gulf of Mexico, the Yucatan peninsula and Central America, and numerous Caribbean islands. Caribbean seagrass systems are generally connected on the landward side to mangrove forests and salt marshes and on the seaward side to coral reefs (Underwood, 1989). Seagrasses, which spread by sending out rhizomes, or runners, stabilize reef sediments and help maintain the water clarity necessary for reef growth. Additionally, they provide a source of nutrients in the form of dissolved organic matter and particulate organic matter to adjacent reefs. Seagrass beds serve as an important nursery ground for numerous species of fish and crustaceans; many species of reef organisms breed and seek protection in seagrass beds. Often organisms migrate to the nearby reef when they become too large to be afforded sufficient protection by seagrasses (Ogden and Gladfelter, 1983).

Numerous epiphytic species of algae, sponges, hydrozoans, bryozoans, tunicates, and spirorbid polychaetes are found on seagrass blades. Additionally, seagrasses provide a major food source for manatees (*Trichechus manatus latirostris*), green turtles (*Chelonia mydas*), several species of reef fish, and urchins such as *Diadema antillarum*, *Lytechinus variegatus*, and *Tripneustes ventricosus* (Humm, 1973).

The coral reefs of the Caribbean region form a complex and diverse benthic community. Coral reefs are located on the shallow banks that surround the majority of Caribbean islands. Fringing reefs occur along the coasts of Florida, Mexico, Colombia, and Venezuela. The barrier reef off the coast of Belize is second in size only to the Great Barrier Reef of Australia. Coral reefs protect inshore seagrass beds and mangrove forests by dissipating wave energy and current force from the open waters. Behind the reef crest exists the calmer waters of the backreef and reef lagoon, perfect habitat for seagrass growth. Reefs serve as shelter and food for numerous species of fish and invertebrates. Nearly 300 species of Caribbean fish, over 180 of which are landed for human consumption, are associated with reefs as adults (Environmental Agenda for the 1990s 1991). A number of reef species, such as the long-spined urchin (*Diadema antillarum*), and parrot fish (*Sparisoma* spp.) utilize the reef for protection and venture out to graze on the seagrass and algae that surround the reef, creating a bare patch of sediment, or halo, around the reef (Ogden and Gladfelter, 1983).

A detailed narrative of coral reef zonation, coral growth rates and feeding mechanisms, and associated species dynamics has been prepared for the Red Sea portion of this document. Like the Red Sea region, the Caribbean region contains a rich diversity of corals. Kaplan (1982) provides a good description of Caribbean reef zonation. Common reef building corals include the branching corals, *Acropora palmata* and *A. cervicornis* found along reef crests. Boulder-shaped corals such as *Montastrea annularis*, *M. cavernosa*, *Agaricia agaricites*, *Siderastrea siderea*, *Porites asteroides*, and brain corals including *Diploria* spp. and *Colpophyllia* spp. dominate the mixed reef slope area. Calmer backreef waters and sheltered patch reefs are dominated by smaller branched corals such as *Porites porites*, and *Madracis mirabilis*, and by small flower and mound-shaped corals such as *Favia fragum*, *Eusimilia fastigiata*, and *Manicina areolata*. Soft coral communities are dominated by sea rods (*Plexaura* spp., *Plexaurella* spp. *Muricea* spp.), sea plumes (*Pseudopterogorgia* spp.) and sea fans and whips (*Gorgonia* spp. and *Pterogorgia* spp). Relatively few species are known to feed on corals. Some grazing reef fish, such as parrot fish, may consume coral in small amounts. Additionally, the colorful gastropod, *Cyphoma gibbosum*, commonly known as flamingo tongue, and the stinging fireworm, *Eurythoe complanata*, are known to graze on sea fans and other gorgonians (Diehl et al., 1988).

Other Caribbean filter-feeding reef species include a diverse community of sponges, including the large vase sponge (*Ircina campana*) that can grow as tall as two feet and as wide as three feet, and branching sponges such as *Verongia longissima*. Common anemones include the pink-tipped anemone (*Condylactis gigantea*), and the ringed anemone (*Bartholomea annulata*). Filter-feeding polychaetes

include fan worms and Christmas tree worms (*Sabellastarte* spp. and *Spirobranchus* spp.). Echinoderms such as crinoids and basket stars (*Astrocaneum* spp.) often use hard corals as elevated platforms on which to filter feed.

The reef fish assemblages of the Caribbean Sea are similar to those of the Red Sea. Algae-grazing fish include several species of surgeon fish, tangs, blennies, angel fish, butterfly fish, parrot fish, chubs, and damsel fish. Additional, non-fish grazers include urchins, herbaceous gastropods, and some species of crabs (Diehl, 1988). Commercially important conch species including *Strombus gigas* and *Stombus pugilis* are known to graze on *Thalassia* beds.

Scavenger and predator invertebrate species common to the Caribbean Sea region include asteroids, ophiuroids, holothurians, octopods, and nemertean worms. Several shrimp and lobster species are common on reefs. Both spiny and shovel-nosed lobster are found, and the spiny lobster, *Panulirus argus*, and slipper lobsters, *Scyllarides* spp. are the most common. Common shrimp species include the mantis shrimps (*Gonodactylus* spp.) and cleaning shrimps (*Periclimenes* spp. and *Stenopus* spp.) Several species of carnivorous gastropods inhabit Caribbean reefs including cowries, whelks, and some species of helmets.

Larger Caribbean reef predators include fish such as groupers, snappers, rays, emperors, barracuda, trumpet fish, scorpion fish, and trigger fish. As in the Red Sea, the majority of larger Caribbean reef fish feed on a combination of small reef fish, crustaceans, worms, and echinoderms. Octopods, which find shelter in the nooks, and cracks of the reef, hunt for crustaceans, echinoderms, and small fish. The five species of octopods common to Caribbean reefs are the briar octopus, the seaweed octopus, Joubin's octopus, the white-spotted octopus, and the common Atlantic octopus (Kaplan, 1982). Loggerhead and hawksbill turtles also occur near Caribbean reefs and consume crustaceans, molluscs, and other invertebrates. Finally, as mentioned above, several species of sharks inhabit Caribbean waters and are among the largest scavengers and predators on the reef.

Like the waters of the deep Red Sea, deep Caribbean waters do not mix rapidly with surface waters. Therefore, with the exception of a few regions of mixing and upwelling, deep Caribbean waters do not receive a large supply of detrital matter from upper water layers. Therefore, filter feeders, such as sponges, bivalves, and tubiculous polychaetes, are not common at Caribbean depths. However, a number of Caribbean islands are situated on narrow shallow banks; steep walls drop from the edge of the banks into deep waters. These walls can support extensive sponge and gorgonian filter-feeding communities that grow out from the wall and pull organic matter from the currents. Additionally, the deep waters are well-oxygenated (5.0 to 6.0 $mg \cdot L^{-1}$ at a depth of 2600 m in some areas) and have a stable temperature of approximately 4°C (Svedrup et al., 1942). Therefore, the deep demersal fish populations of the Caribbean are relatively abundant with about 200 species identified to date (Rass, 1971). Other deep water organisms include shrimp, and some gastropods and echinoderms.

UNIQUE SPECIES AND ECOLOGICAL CONSIDERATIONS

Endangered/Threatened or Protected Species. Turtles and manatees are among the most threatened species that occur in the Caribbean Sea. The manatee and all five of the sea turtles occurring within the Caribbean Sea are listed as threatened or endangered under the federal Endangered Species Act (50CFR 17.11 and 17.12, USFWS, 1993). As mentioned previously, there is evidence that numbers of turtles hatched in the region is declining. There is also evidence that the manatee population is declining. These slow-swimming grazers inhabit lagoons and waterways that contain abundant seagrass

beds and that, unfortunately, also contain large numbers of boats. Despite the fact that Florida Manatees are protected by state and national law, they are often hit by boats and cut by props, shot by vandals, and harassed by divers (Caldwell and Caldwell, 1973). Finally, the baleen whale species that spend a potion of the year in Caribbean waters have, in the past, been decimated by a large whaling industry. The humpback, blue, fin, sei, minke, and right whales are all endangered under the federal Endangered Species Act (50CFR 17.11 and 17.12, USFWS, 1993). No critical habitat for endangered species has been designated within the wider Caribbean region.

Critical Habitat. Due to the lack of surface water productivity in the Caribbean, coral reefs, mangroves, and seagrass beds that surround the Caribbean islands and coasts are very important habitats. As discussed previously, each habitat is a valuable food source for fish, invertebrates, reptiles, and marine mammals. Further, they are important nurseries and breeding grounds for fish and invertebrates and they provide shelter to numerous species. Additionally, the three habitats form a unique interdependent web, whereby the health of each habitat affects the health of the other two. Therefore, damaging coral reefs will harm seagrass and mangrove communities as well, and vice versa. Currently there are several marine reef parks, such as those in the Cayman Islands, the Florida Keys, and off the coast of Honduras, located in Caribbean waters. Additional parks, such as one located in the Turks and Caicos Islands, are planned for the future.

As discussed in the Red Sea portion of this document, a majority of reefs, mangroves, and seagrass beds occur near the coast. Each habitat is currently threatened by increased coastal development that causes increased sedimentation and sewage spills on nearshore benthic communities. Oil spills from offshore wells and ship spillage further damages these communities. Finally, increased tourism, fishing, and shell and fish collection place a strain on the reef environment. As coral reefs, mangroves, and seagrass beds disappear in the Caribbean region, species diversity and numbers will diminish significantly in the area.

THE GULFS REGION

PHYSICAL AND CHEMICAL CONSIDERATIONS

Geography and Physiography. The Persian Gulf, or Arabian Gulf as it is sometimes known, is a sedimentary basin separating the Zagros Mountains of Iran and the main body of the Asian continent from the Arabian Peninsula (Figure 4.1-30). The formation of this shallow gulf is thought to have been allied to plate tectonic forces that also created the Red Sea, and which within several tens of thousands of years may result in a complete closure from the Arabian Sea at the Straits of Hormuz. During the late Pleistocene, the basin completely dried out, a circumstance which may figure prominently in its present relatively low biological diversity.

The present Gulf lies between latitude 23°9' and 30°25' North latitude, and between 48° and 56° East longitude. In the east, the Persian Gulf flows through the narrow Straits of Hormuz, into the Gulf of Oman, and eventually into the Indian Ocean. Eight countries have coasts that border the Persian Gulf: Oman, the United Arab Emirates, Qatar, Bahrain, Saudi Arabia, Kuwait, Iraq, and Iran. The peninsula of Qatar is the most sizeable landform encroaching into the Gulf; the most significant among many small islands are Bahrain, Khark, Qeys, and Qeshm. Steep slopes, mountains, and sometimes precipitous cliffs predominate on the Iranian side of the gulf; while the Arabian shoreline, with the exception of the Musandam Mountains of Oman at the extreme eastern end, is a low-lying desert.

Despite its wide latitudinal distribution, the Persian Gulf and adjacent Gulf of Oman (hereafter known as the Persian Gulf region) experience only sporadic climatic variation (Sheppard, 1993). The countries that border the Persian Gulf region have hot, arid climates, and rainfall in the region is sparse. The land bordering the Gulf is dominated by sandy soils and sparse, semi-arid vegetation. The xeric climate and shallowness of the sea can make the surface waters of the Persian Gulf region unusually warm. The arid conditions also cause a high rate of evaporation of the surface waters of the Persian Gulf, resulting in both atypically high water salinity, as well as seasonally high humidity over the water.

Bathymetry. The Persian Gulf extends 984 km from northwest to southeast. At its widest, the Gulf reaches a maximum of 336 km, with the Straits of Hormuz varying from 48 to 96 km in width. The Gulf's basin becomes shallow in the northwest and towards the west coast, with an isolated trough extending northward from the Straits of Hormuz along the Iranian coast for approximately 100 km. This trough collects denser bottom water and impedes the exit of bottom flow. The total surface area of the Persian Gulf is approximately 240,000 km^2. An average depth for the Gulf is 35 m, and a maximum depth of approximately 100 m occurs in the Straits of Hormuz. Deepest waters are found along the Iranian coast; conversely, a broad shallow area, usually less than 37 m, is found along the Arabian coast. Near shore waters abutting the western shoreline average 25 m in depth, and with the exception of a few coral reefs north of Ras Tanura, the offshore benthic environment is primarily a vast low relief of sand/silt substratum interspersed with seagrass beds (Coles and McCain, 1990).

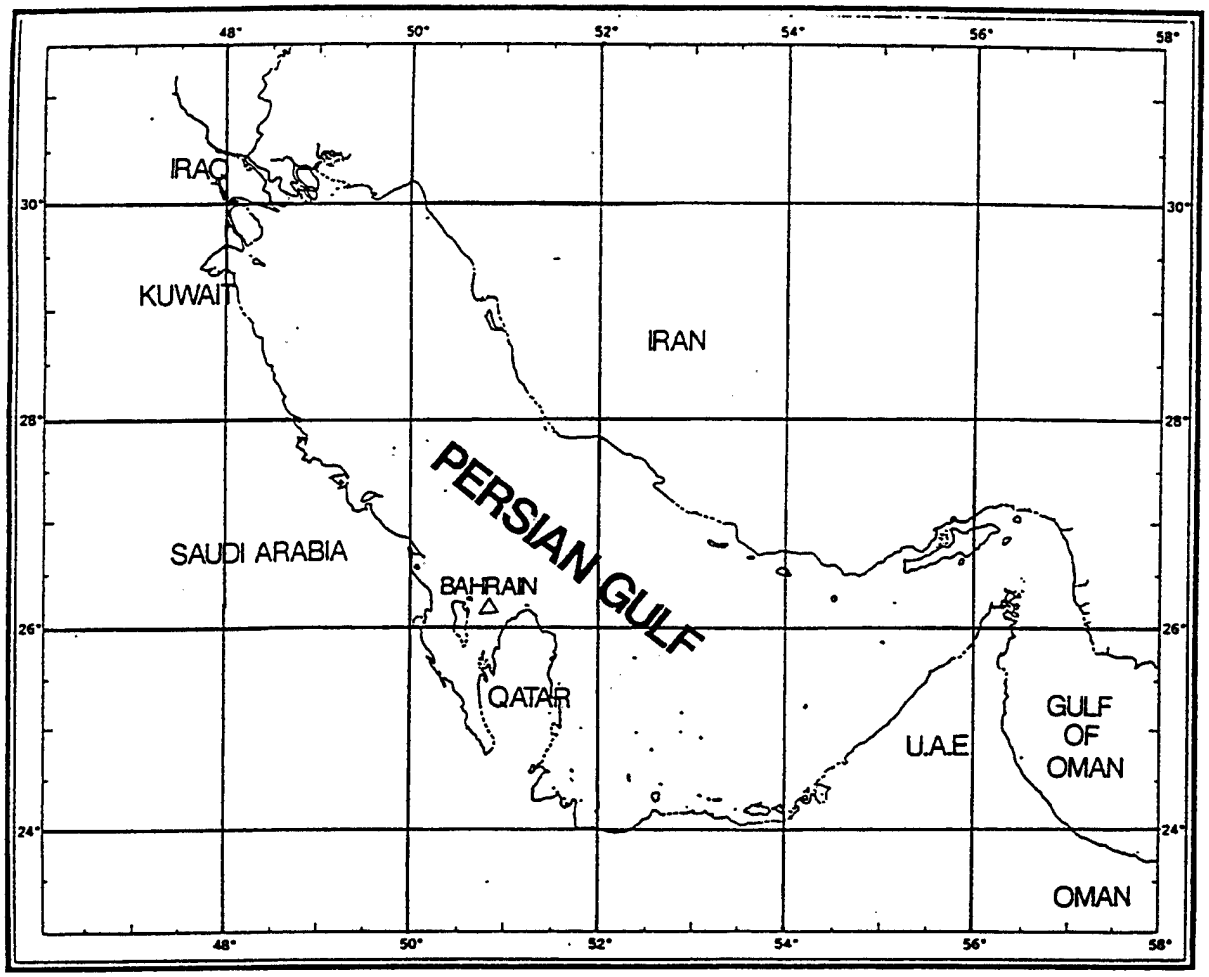

Figure 4.1-30. The Gulfs region. The Persian Gulf (Arabian Gulf) separates the Zagros Mountains of Iran and the main body of the Asian continent from the Arabian Peninsula. The formation of this shallow gulf is attributed to plate tectonic forces that may also have created the Red Sea.

Currents, Tides, and Water Exchange. The general hydrological regime of the Persian Gulf consists of surface waters movement westward towards the coasts from the Arabian Sea via the Gulf of Oman, evaporating and sinking at the margins, and leaving the Persian Gulf at depth (Ross and Stoffers, 1978). The main body of water is well-mixed throughout most of the year; at the mouth of the Gulf there is a high-salinity flow outward along the bottom of the Straits of Hormuz which is balanced by a surface influx from the Indian Ocean that passes along the eastern coast (Nelson-Smith, 1988 in UNEP Studies #44). This results in a weak, counterclockwise circulation. Tides have a range of 0.5 m in mid-gulf to about 3 m towards both the head and mouth of the Gulf. Along the shallow western coast, expanses of several kilometers of sand and mud flat may be uncovered at low tide. Currents are usually tidally generated in the western Gulf with water movement toward the south-southeast during ebb and west-northwest during flood tides (KFUPM/RI, 1988). The waters in the inner sea are more turbid than generally found in the Red Sea or Indian Ocean (Nelson-Smith, 1988 in UNEP Studies #44).

Prevailing north-northwest winds (i.e., the well publicized shamal) off the eastern coast of Saudi Arabia flow at an acute angle to the coastline, and the surf meets the beach at an angle. As a result, there is a constant wave-driven movement of water along the shore in a southeasterly direction. Sand grains washed off the beach by one wave, in effect, are deposited a little further to the southeast by the next wave. This "longshore transport" of beach sediment is a nearly universal feature of these coastlines; such movements regularly create long, hook-shaped sand spits running southeasterly from the major headlands or coastal projections (Basson et al., 1977). Turbulent waters at the Straits of Hormuz can result from strong winds meeting countervailing currents. Dust storms are common and conditions are frequently hazy in the Gulf in summer, with autumn winds reaching velocities as high as 95 mph in relatively short spans of time. These winds deposit substantial quantities of dust onto the surface of the Gulf.

Water circulation patterns are primarily counterclockwise. Water exchange between the Gulf of Oman and the Persian Gulf, via the Straits of Hormuz, is limited. The majority of the water that replenishes the evaporated waters of the Persian Gulf comes from this eastern link with the Indian Ocean. Fresh water influx is primarily from the Rud-e Karun, Euphrates, and Tigris rivers in Iraq (via the Shatt al Arab estuary), supplemented by lesser seasonal drainages from the Zagros Mountains of Iran. Fresh water influx from the southwestern side of the Gulf is minimal. The average rainfall into the Gulf is less than 7 $cm \cdot yr^{-1}$ while the average evaporation rate is on the order of several (up to 5 or more) meters per year (Ross and Stoffers, 1978). An unusual oceanographic phenomenon occurs in a submarine spring off Bahrain; the source of this artesian water is reputedly the Jabal Tuwayq in Arabia.

Residence time for parcels of waters within the Gulf prior to exchange, via the Straits of Hormuz, with waters in the Gulf of Oman is estimated to be 2 to 5 years. Longer residence periods are presumed for the shallow northern areas where movement is governed by river outflow and wind friction. At the approximate longitude of the Qatar Peninsula, density-driven, negative estuary conditions prevail. High evaporation in the shallows adjacent to the United Arab Emirates provides much of the saline bottom water feeding the bottom outflow through the Straits of Hormuz (Reynolds, 1993).

Temperature and Salinity. The water temperature of the Gulf is relatively warm, but can fluctuate substantially from season to season. Local extremes can provoke damaging effects to coral assemblages, and may be a primary reason for the absence of coral in some portions of the Gulf which might otherwise provide suitable growing conditions and substrate. Average annual surface water temperature in the Persian Gulf is 32°C in August and 18°C in February. Bottom water ranges from nearshore temperatures of 16 to 36°C to offshore temperatures of 17 to 34°C; these can reach as low as 11°C inshore (Coles and McCain, 1990).

The salinity of the Gulf generally ranges between 37 to 40 ppt, but increases to over 50 ppt in several embayments (Hashim, 1993). In the region between Ras Tanura and the entrance to the Gulf of Salwah a pronounced pycnocline is formed by high-salinity water from the Gulf of Salwah moving northward and underlying the less saline water of the open Gulf (KFUPM/RI, 1988).

Due to a high rate of evaporation and a low rate of precipitation and fresh water runoff, surface salinity values in the waters of the Persian Gulf can be very high. Surface salinities ranging from 38 to 42 psu in the region north of Al-Khobar increase dramatically southward, so that salinities in the Gulf of Salwah near Qatar range from 52 psu in the north to 59 psu in the more sheltered south, with no indications of vertical salinity stratification. Water movement in the Gulf of Salwah is partially constricted by a reef complex at its northern end. Tidal streams commonly exceed 1 to 2 $m \cdot s^{-1}$ past islands and other constrictions, providing local mechanisms for food replenishment of filter feeders. Water enters the Gulf through the Straits of Hormuz with a salinity of 36.5 to 37 psu (Sheppard, 1993).

Oceanic Sedimentation. The total average input for the fluvial system that enters the northern Persian Gulf is 1100 $km^3 \cdot yr^{-1}$ (Reynolds, 1993). Sediments carried from extensive riverine systems in Iraq are primarily captured in the extensive marshes at the mouth of the Shatt al Arab. These sediments have been gradually filling the northwest end of the Gulf, while a submarine delta has spread across the periphery of these marshlands. About one-third of Gulf sediments consist of wind transported sand and dust carried by the prevailing northwest winds across up to 800 miles of desert (Pilkey and Nobel, 1966 cited in Ross and Stoffers, 1978). Sediment studies show that grain-size increase is often directly correlated to deeper water depth, with sand-sized material concentrated along the southern and central portions of the Gulf as opposed to the Iranian coast (Ross and Stoffers, 1978).

A counterclockwise current in the southern part of the Gulf may be responsible for the redistribution of sediments and total organic carbon; such currents are not of similar strength in the northern part of the Gulf (Al-Ghadban et al., 1994). Dissolved inorganic nutrients in the western Gulf have low concentrations which decrease in proximity to the shoreline, suggesting a significant nutrient depletion of oceanic water as it moves through the Gulf (Grasshof, 1976).

The countries that surround the Persian Gulf region are rapidly modernizing and human-generated sedimentation effects are increasing. Coastal construction work, including the development of harbors, jetties, industrial sites, and roads, is leading to increased levels of sedimentation (Ormond, 1987).

CURRENT ENVIRONMENTAL STRESSES

Marine Pollution. The Persian Gulf includes some of the most traveled, commercial shipping routes in the world, and supports a number of rapidly developing ports. The effects of environmental stress due to shoreline development, ship traffic, and associated pollution are increasingly apparent in the region. Due to the Persian Gulf's geographical configuration and narrow outlet to the Gulf of Oman and the Arabian Sea, pollutants tend to accumulate in its shallow waters instead of dispersing and degrading into the open ocean. As a result, pollutants tend to wash from coast to coast in the narrow Gulf, particularly to the west, settling on beaches, intertidal communities, mangroves, and coral reefs.

Shoreline beach tar abundances of 10 to 100 times values reported for other areas of the world have been determined for sites along the Saudi coastline (Coles and Gunay, 1989). Major sources of effluent that might negatively effect marine biota are sewage treatment plants at Al-Khobar and Dammam, oil

refineries at Ras Tanura and Safaniyah, electrical and desalinization plants at Al-Uqayr, Aziziyah, and Jubail, as well as near shore oil fields at Abu Ali, Manifa, and Safaniyah (Coles and McCain, 1990).

The Persian Gulf suffers from varying levels of oil pollution along most of its coasts and within its offshore waters. The hydrocarbon input in the marine habitat is estimated to be 47 times more per unit area than the world average (Golob and Brus, 1984 cited in Al-Ghadban, 1994). Massive spills were suffered during the 1991 Gulf War; initial studies show surprisingly limited and localized short-term impacts. However, most studies recommend follow-up work which is expected to show more subtle and insidious long-term problems associated with this pollution. On going oil pollution stems from spills associated with tanker traffic through the still heavily mined waters; repeated spills from coastal oil fields, refineries, and pipelines; and spills from offshore oil platforms (Awad, 1989). Industrial inputs include sedimentation from construction activities, brine from desalination plants, fertilizers, and heavy metals.

Urbanization and Tourism. The build-up of basic infrastructure needed to develop rapidly urbanizing ports around the Persian Gulf has led to drastic changes in consumption patterns, and an exponential increase in litter originating in Gulf waters. The counterclockwise circulation of the Gulf has exacerbated litter deposition on the western beaches.

One result of recent Gulf region hostilities has been an additional increase in man-made debris accumulating on these western beaches. "Gash" thrown overboard by offshore vessels has been a continuing problem. Plastic bags and containers, when lodged on reefs, can physically smother corals and seriously retard light penetration onto the reef. One limited study counting debris on approximately 100 meters of relatively isolated beach, at two locales on opposite sides of the Oman Peninsula, noted substantial and varied items of discarded debris on both coastlines (Bourne, 1989). The source for most of this material was apparently off-shore dumping by various watercraft.

A more extensive study (Khordagui and Abu-Hilal, 1993) estimated $1.35 \cdot 10^6$ man-made items stranded along 800 km of Arabian Gulf and Gulf of Oman shorelines in the United Arab Emirates (UAE); an associated focused survey accounted for 22,771 separate items. Plastic fragments constituted 27.1% of the debris. Additional litter included 16.4% bottles, 10.9% tins, 10.1% wood logs, 8.5% polystyrene blocks used in fishing, 8.4% ropes and nettings, 7.1% plastic bags, 6.6% cardboard, 2.3% footwear, 1.9% lamp bulbs, and 0.5% rubber. Plastic fragments (excluding industrial plastic pellets) originated primarily from embrittled plastic bottles, cups, and containers. According to Dixon and Dixon (1981 cited in Khordagui and Abu-Hilel, 1993), bottles made from major thermoplastics, particularly high-density polyethylene, are photodegradable out of water. The photodegradation initially causes embrittlement followed by substantial fragmentation (but not necessarily disintegration) of the plastics, generally within 2 years of its being discarded. Most of the large plastic fragments found on the beaches were presumed to have been present less than 2 years. Polystyrene floats were often marked as made in Iran, indicating regional rather than local origin of this material. Plastic bags tended to occur closer to population centers, while in more remote areas, thicker plastic sheets associated with cargo packaging were found. Large numbers of weapons and ammunition crates were found, mostly labeled as made in the United States. While some local food packaging apparently originated in the UAE, much similar material was presumed to have been discarded from shipping originating outside of the region. Most of the litter found on the UAE beaches was from marine-based sources and primarily attributable to fishing activities and offshore oil field workers, as well as boat, ship, and tanker traffic. Additionally, it was noted that litter was almost double on beaches in the Persian Gulf in comparison to beaches in the Gulf of Oman.

Agricultural chemicals such as urea fertilizer, which are dissolved in run-off, contribute to eutrophication in some coastal areas. However, levels of aldrin, lindane, dieldrin, and DDT in marine sediments and biota are generally low in the Persian Gulf compared to other regional seas (Price, 1993).

Oil. The massive spill of oil into the Persian Gulf during the 1991 Gulf War resulted in approximately 10,816,701 barrels of oil being released directly into the water (Tawfiq and Olsen, 1993). The spill was at least three times the size of the Ixtoc blowout in the Gulf of Mexico, the largest previous spill known. It was over 40 times larger than the *Exxon Valdez* spill in Alaska. Additionally, an estimated 500 million barrels of oil were emitted or ignited in the oil fields, releasing oil aerosols, soot, toxic combustion products, and gases into the atmosphere. A substantial portion of these emissions undoubtedly settled out onto the Gulf's waters.

A study of sediments and molluscs (Redman et al., 1992, in Tawfiq and Olsen, 1993) found that concentrations of hydrocarbon fractions derived from the spill were restricted to the shoreline of Saudi Arabia within 400 miles of the release site. Particularly hard hit was Dawhat ad Dafi where millions of gallons of oil ended up in sheltered halophyte marshes and algal mat complexes within the intertidal region. Significant damage to coral reefs was not observed during the *Mt Mitchell* research cruise assessing biological impacts in the region, or during IUCN follow-up investigations. Some very localized damage to three reefs in Kuwait may either represent a response to the oil spill, or bleaching mortality associated with natural weather fluctuations that included reduced sea-surface temperatures (Gerges, 1993). Histological analysis of total lipid levels in seven genera of shallow-water corals suggested that oil pollution had no significant effect on lipid synthesis and photosynthesis (Al-Sofyani, 1993, in Tawfiq and Olsen, 1993). No significant effects on the respiration rates or photosynthesis of seagrasses were noted; three species of *Halodule* were tested. The oil appears to have had little effect on the subtidal seagrasses in the northern part of the Gulf (Gerges, 1993). One area also hard hit was Gurmah Island where an extensive mangrove system was heavily oiled; on-going deterioration of this habitat has occurred despite clean-up efforts. Following the spill, the Saudi shrimp fishery collapsed with prawn stock abundance at only 10% of 1988 to1989 levels. High mortality of fish was observed in localized areas, particularly around Gurmah Island.

Oil pollution impacts from the Gulf War also severely affected four seabird species found in high numbers in the region. Great Crested Grebe (*Podiceps cristatus*), Black-necked Grebe (*Podiceps nigricollis*), Great Cormorant (*Plalacrocorax carbo*), and Socotra Cormorant suffered extensive mortality (22 to 50%+) (Evans, Symens, and Pilcher, 1993). At least 30,000 birds of various species died as a result of exposure to oil (Gerges, 1993).

Laboratory experiments have shown toxic effects of petroleum fractions on holoplanktonic and meroplanktonic crustaceans (Linden, 1976, in Price et al., 1993), including postlarval penaeid shrimp (which are locally common and the focus of an important fishery in the Gulf region). The effects of oiling on zooplankton are also well documented (Teal and Howarth, 1984, in Price et al., 1993). Noticeable declines in the Gulf's shrimp fishery following the 1991 Gulf War (0.275 individuals$\cdot m^{-3}$ in 1992 versus 6.77 individuals$\cdot m^{-3}$ in 1976) have been attributed to a mix of factors including oil pollution and the massive smoke plumes that locally reduced light and temperatures over a portion of the Persian Gulf (Price et al., 1993).

The effects of repeated oil spills on fringing reefs, mangroves, and seagrass beds can be severe. Corals exposed to oil can have abnormal feeding behavior and mucus secretion, decreased growth rates, increased rates of tissue damage, disturbance of larval settlement, and decreased oxygen exchange (Mergner, 1984; Dicks, 1987). Additionally, floating oil has a shading affect, blocking light necessary

for coral and seagrass growth. Oil that coats the pneumatophores (breathing roots) of mangroves effectively prevents oxygen exchange and suffocates the plants. Oil incorporated into sediment can damage root systems and ultrafiltration processes. Oil pollution also affects the eggs and larvae of many pelagic fish and can cause developmental abnormalities. Birds are particularly affected by oil spills when oil coatings render them unable to fly, swim, and forage for food.

Other Industrial Inputs. Dust precipitation from Arabia can include metal pollutants from industry which are strongly adsorbed onto the dust particles, with vigorous winds serving as a transport mechanism of these pollutants to the marine environment. Similarly, adsorbed hydrocarbon pollutants form southern Iraq can be significant components of dust-blown pollution in the northern Gulf (Sheppard, 1993).

Sea Traffic and Ports. Boat traffic on the Persian Gulf consists primarily of large tankers, freighters, and naval vessels, along with a local fishing fleet from bordering nations. Oil is the most transported good on larger vessels. The fishing fleets of the Persian Gulf nations are relatively small, but traditional fishing methods are evolving under the more efficient techniques reflected elsewhere. Many of the traditional fishing boats are small, one and two man vessels, and are often still powered by sail.

The Gulf is a principal world shipping lane for oil and oil products with more than half the world's petroleum transported through the area. The principal ports are Abadan, Bandar-e Khomeini, and Bushire in Iran; Doha in Qatar; Kuwait City in Kuwait; Ras Tanura and Damman in Saudi Arabia; Manama in Bahrain; and Dubai and Sharjah in the United Arab Emirates.

FISHERIES AND AQUACULTURE RESOURCES

Fisheries for shrimp in the Persian Gulf are of global, as well as regional importance. In 1986, total landings in the Gulf for shrimp were over 13,600 tons, and for shellfish and finfish over 335,500 tons. Target species included penaeid shrimp (*Penaeus semisulcatus*) and other crustaceans such as *Thenus orientalis*, in addition to finfish such as grouper, Spanish mackerel, and caranjids (Price and Sheppard, 1991). Two species of pearl oyster are important commercially: *Pinctada radiata* and *Pinctada margaritifera*. The latter is considered commercially threatened, but adequate population data is lacking.

Like those of the Red Sea, the fisheries of the Persian Gulf region account for a very limited percentage of the world total. Although fishing has always been important to the economies of the nations surrounding the Persian Gulf, most of the catch has historically been of a subsistence nature, and has been maintained well below the maximum sustainable yield. Despite the fact that tropical waters typically have an extremely low rate of primary productivity, reef areas and seagrass beds are extremely productive and are estimated to support 9% of the world's fisheries (Head, 1987b). The majority of the fishing that occurs in the Persian Gulf is located over, or adjacent to reefs or seagrasses.

Phytoplankton. The Gulf is one of the more productive bodies of water in the world when one examines benthic rather than pelagic production. Primary reasons for this productivity are the shallowness of the Persian Gulf seabed which typically lies within an illuminated zone and the nutrient input from the northern fluvial system. Western portions of the Gulf have diverse planktonic habitats that include sheltered bays, saline lagoons, shallow exposed coastal waters, and offshore open waters. Primary productivity is greatest in mixed central waters and shallow bays, as well as areas under the influence of the Shatt al Arab estuary and its nutrient enhanced waters. General chlorophyll *a* values in Gulf water have been reported at 0.2-0.86 $mg \cdot m^{-3}$, a figure which is not particularly high (Sheppard,

1993). Some locales such as Kuwait Bay register high chlorophyll values (9.6 $mg \cdot m^{-3}$) and this supports an assessment of high productivity for the area. In one study, plankton in Kuwait Bay were found to be richer in protein and fat than in adjoining Kuwaiti waters (Yamani et al., 1993).

Approximately 100 taxa of phytoplankton are found in the Gulf of Oman; densities range from 555 to 45,973 $cells \cdot L^{-1}$ (Grice and Gibson, 1978). Summer populations in the Gulf are dominated by diatoms reaching lowest densities between 5 and 10 m deep, and becoming progressively denser closer to the sea bed. The average density of individuals is usually lower offshore than either nearshore or in bays. This contrasts with winter where dinoflagellates provide the highest productivity (Basson et al., 1977); densities are highest at about 10 m in depth (approximately 185 to 352 dinoflagellate individuals per milliliter). The Gulf pelagic zone is apparently more productive than either the northern or central Red Sea, but 1 to 2 orders of magnitude less than the Arabian Sea (Sheppard et al., 1992, in Sheppard, 1993).

Seagrass and Coral Reefs. At least four seagrasses occur in the Persian Gulf with the dominant species being *Halodule uninervis*, a eurythermal species tolerant of high salinity. Occasional beds of *Halocule stipulacea* and *Halodule ovalis* are found in the region. A 1970s study found more than 530 species of plants and animals among the seagrasses of the Gulf (Basson et al., 1977, cited in Sheppard and Roberts, 1993); a number which should be substantially increased on the basis of more recent research. Particularly heavy seagrass beds occur around Bahrain, primarily in waters less than 8 meters in depth. Abundant tracts of seagrass are also found in the shallow waters off the coast of Saudi Arabia. Seagrasses here extend into deeper waters (approximately 10 m) where they eventually become patchy in their distribution. Biomass of *Halodule uninervis* dominated communities ranges from 0.05 to 0.24 $gdw \cdot m^{-2}$ and is comparable to figures for similar species in the Red Sea and elsewhere (Price and Coles, 1992 cited in Sheppard and Roberts, 1993). For comparison, standing crop biomass for temperate grasslands can range between 0.2 and 5 $kgdw \cdot m^{-2}$. Estimates of primary productivity for seagrass beds has been estimated to be as high as 1000 $gC \cdot m^{-2} \cdot d^{-1}$ in the Caribbean Sea (Jones et al., 1987). Benthic fauna in Gulf seagrasses and sand/silt habitats are predominantly filter feeders, utilizing organic particulates which are more abundant in the Persian Gulf than in the clearer waters of the northern Red Sea. Gulf seagrasses have a smaller portion of seagrass "specialists" and a larger portion of "generalists." Extensive Gulf macroalgal beds are locally important in the life cycles of the postlarvae of shrimp (*Penaeus semisulcatus*) and spat of pearl oysters (*Pinctada* spp.) (Price and Coles, 1992).

Due to seasonal temperature fluctuations and turbid waters in some areas of the Gulf, coral diversity is not as high as that of the Red Sea and other Indo-Pacific reefs. However, no shallow waters of the Gulf contain coral reefs. As stated previously, coral reefs are considered to be among the most productive environments in the world. Estimates of reef productivity can be as high as 10,000 $gC \cdot m^{-2} \cdot yr^{-1}$ when the productivity of the surrounding waters is as low as 20 to 50 $gC \cdot m^{-2} \cdot yr^{-1}$ (Lewis, 1977). A more conservative estimate of reef productivity is 500 to 2500 $gC \cdot m^{-2} \cdot yr^{-1}$.

Zooplankton. Zooplankton productivity exhibits substantial temporal and geographic variation, with diversity lower than in the Arabian Sea (Price, 1979, in Sheppard, 1993). In general, zooplankton is more abundant in the interior bays than in nearshore waters. The summer populations of Tarut Bay are dominated by calanoid copepods and gastropod larvae (Basson et al., 1977).

A 1992 study (Al-Yamani et al., 1993) of zooplankton groups from Qatar to Kuwait along the southwestern Gulf indicated these groups were not homogeneously distributed as previously suggested (Grice and Gibson, 1978). Significant differences from station to station were noted for nauplii, copepods, tintinnids, larvaceans, gastropod larvae, cladocerans, and total zooplankton. No significant differences were observed for pelecypod larvae, larval decapods, fish eggs, and larvae. In Saudi Arabian

waters highest concentrations of zooplankton were found at stations closest to Kuwait, while lowest mean zooplankton densities occurred near Bahrain and areas northward such as Rennie Shoals.

Quantitative zooplankton samples collected throughout the Persian Gulf and the Gulf of Oman noted biomass ranges from 0.11 to 2.00 $cm^3 \cdot m^{-3}$ in the former, and 0.52 to 2.27 $cm^3 \cdot m^{-3}$ in the latter. Numerical abundance of zooplankton in the Persian Gulf ranged from 79-5098 individuals$\cdot m^{-3}$ copepods were most abundant, followed by doliolids, larvaceans, cladocerans, and chaetognaths. No significant differences were found between diurnal and nocturnal comparisons of zooplankton. The highest zooplankton biomass values were found in the central region of the Gulf. The Persian Gulf maintains an indigenous and diverse pontellid fauna (Grice and Gibson, 1978).

Low diversity of zooplankton species in the Persian Gulf is tied to the shallowness of the basin which precludes mesopelagic and bathypelagic species which, for example, are important elements of the planktonic communities in the deeper-basined Red Sea (Kimor in Zeitzschel, 1973).

TROPHIC RELATIONSHIPS

Pelagic Food Web. The pelagic food web of the Gulfs region is fed by a moderately productive plankton assemblage (Figure 4.1-31). Over 465 species of fish are found in the Persian Gulf (Hashim, 1993). Small, planktivorous species include herrings and sardinellas (family Clupeidae), anchovies (family Engraulidae), and silversides (family Atherinidae). These species have a similar, silvery appearance and congregate in large schools. Common species in the gulf (Basson et al., 1977) include a silverside (*Allanetta forsskali*), which occurs in dense shoals in shallow coastal waters and bays as well as the commercially important anchovy (*Stolephorus* spp.). These small schooling species are an important food source for King Mackerel, tuna (*Thunnus obesus*), jacks, and seabirds such as terns.

Recent sampling of the western Gulf using demersal trawls, line fishing, and fish traps reported the dominant fish to be slipmouth (*Leiognathus fasciatus*), pigface bream (*Lethrinus kallopterus*), and therapon (*Therapon puta*) (Hashim, 1993). Plankton netting for fish larvae during 1964 to 1965 reported Gobiidae and Apogonidae most common in the southern Gulf, and gobies, Clupeidae, and Pomadasyidae most common in the northern Gulf. In a regional assessment that included the Arabian Sea, herring-like larvae were relatively common and abundant in the Persian Gulf along with anchovy (W. Nellen in Zeitzschel, 1973). In a comparison of the Persian Gulf with the substantially deeper Red Sea, the former is considered significantly poorer in fish species due to the largely absent bathypelagic and abyssal species, and the paucity of endemic littoral species (H. Steinitz in Zeitzschel, 1973).

Larger predacious fish species known to occur in the region include barracuda (*Sphyraena japonica*) which is found around artificial structures and at the edge of coral reefs, the king mackerel or Chana'ad (*Scomberomorus commersoni*) which grows to at least 180 cm, and the bream (*Acanthopagrus cuvieri*) which regularly is found in the coastal shallows near sandy beaches (Basson et al., 1977).

The largest predators in Persian Gulf pelagic waters include sharks and cetaceans. Common in the Gulf (Basson et al., 1977) are the nurse shark (*Chiloscyllium griseum*), lemon shark (*Negaprion brevirostris*), and a particularly common miniature reef shark (*Carcharhinus menisorrah*). Sharks are scavengers and predators; they will consume bony fish, turtles, seabirds, cetaceans, crustaceans, and cephalopods (Ormond and Edwards, 1987). Forty-four species of cetaceans are found in the Indian Ocean. Noted occasionally in the shallower Persian Gulf region are several baleen (*i.e.*, toothless) whales including Bryde's Whale (*Balaenoptera brydei*) and the Humpback Whale (*Megaptera novaeanliae*). Locally

common is a bottlenose dolphin (*Tursiops aduncus*), a common dolphin (*Delphinis delphi*), spinner dolphin (*Stenella logirostris*), and other species such as the Indo-Pacific Humpbacked Dolphin are occasionally reported (Basson et al., 1977).

Numerous species of seabirds live and breed in the Persian Gulf region. The Gulf is particularly important for breeding seabirds, wintering waders, and passage migrants. A recent winter survey (Zwarts et al., 1991, cited in Price, Sheppard, and Roberts, 1993) noted 21 species of wading birds representing approximately 30,000 individuals. Mud flats, extremely well-developed on the western Gulf coast, were observed to support greater wader feeding densities than either sand flats or rock flats. Particularly high quality intertidal mud flat habitat is found in Saudi Arabia at Tarut Bay, Dawhat ad Dafi, and the northwestern part of Musallamiyah. Each year as many as a quarter of a million wading birds winter in the Saudi portion of the Gulf, and numbers for the entire Gulf region may be as high as 1 to 2 million. Offshore major nesting sites for at least three species of tern include the lesser crested tern with an estimated 25,000 pairs breeding on five Saudi islands.

Two species of pantropical marine turtles are important faunal components of the Persian Gulf. The hawksbill turtle (*Eretmochelys imbricata*) eats sponges, soft corals and sessile, soft invertebrates. There is evidence that it may graze on seagrass beds as well. The hawksbill nests during the spring (Frazier et al., 1987). *Chelonia mydas*, the green turtle, is the other common species encountered in the Persian Gulf. This turtle grazes on seagrass. Very sizeable nesting colonies of green turtles (approximately 6000) occur at Ras al Hadd in the Gulf of Oman. It is possible that the commercially important turtle production of India and Pakistan is based on the Persian Gulf region's breeding sites. Hawksbill turtles occur in smaller numbers with rookeries found on Hormuz, Shedvar, and Lavan islands (Iran), and also on Masirah Island in Omani waters (Price, Sheppard, and Roberts, 1993). Occasional to the Gulf are a leatherback turtle (*Dermochelys coriacea*) and a loggerhead turtle (*Caretta caretta*).

Benthic Food Web. The benthic food web of the shallow Gulfs region is reliant upon highly productive coral reefs and seagrass communities (Figure 4.1-32). Coral reefs and seagrass beds thrive within the euphotic zone along the shallow coastal shelf, as well as in protected lagoons and bays. Seagrass beds are common along much of the western coastline of the Gulf and are sporadically distributed in shallower locales well into the central Gulf. The wide, shallow shelf and unconsolidated sediments of the western Gulf provide substrate for four seagrass species, as well as limited opportunities for mangrove communities dominated by *Avicennia marina*. Additionally, seagrasses provide a major food source for dugongs (*Dugong dugong*), green turtles and numerous reef fish. The dugong, related to the manatee, can weigh up to 320 kg and is locally common in the waters near Qatar. Populations of dugong in the Gulf are locally abundant and concentrated near the Gulf of Salwah region. The population in the Gulf between Ras Tanura and Abu Dhabi is estimated to be 7,310 ± 1300 (Preen, 1989 in Price and Sheppard, 1991). It is also possible that the endangered hawksbill turtle consumes seagrass.

Coral reefs are another highly productive shallow benthic community common in the Persian Gulf. True reefs, which are presently accreting carbonate limestone, are localized in the Persian Gulf region. Better developed examples are found around the offshore islands as coral cays. The cays are fringed by broad buffering reefs, with extensive reef flats at the low tide level, as well as diverse reef slopes extending to the soft substrate at 10 to 20 meters in depth. Six of these island cays occur in Saudi Arabian waters and a few are found in Kuwait, Bahrain, and Qatar. Most of the more common reef patches do not support the cays, and cover considerably greater areas. One chain north of Bahrain provides more sublittoral hard substrate than all the island cays combined. These broader patch reefs are subject to greater scouring and do not support the same high biological diversity, but can support vigorous stands of macro-algae and some well developed coral communities (Price, Sheppard, and Roberts, 1993). Additional,

coastal coral reefs occur around the Musandam Peninsula near the Strait of Hormuz and along the coast of Oman in the Gulf of Oman.

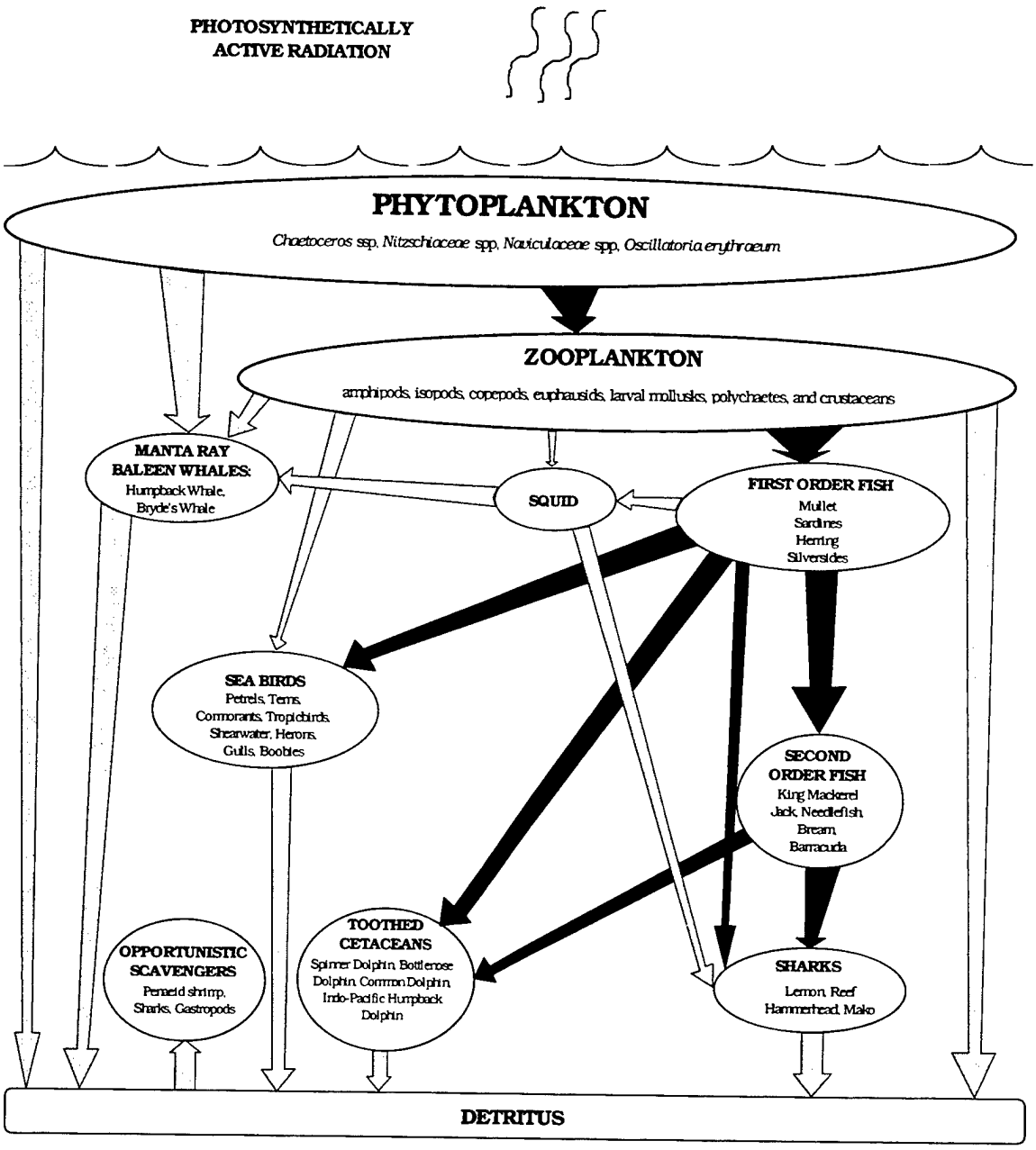

Figure 4.1-31. Pelagic trophic web of the Gulf region. The open water food web of the Gulfs region is comprised of a diverse array of species ultimately dependent upon a limited phytoplankton crop. Biomass of the pelagic system is higher than that of the Red Sea. However, due to extreme temperatures and salinities and to the relative youth of the shallow Persian Gulf basin, species diversity is low when compared to open ocean tropical areas.

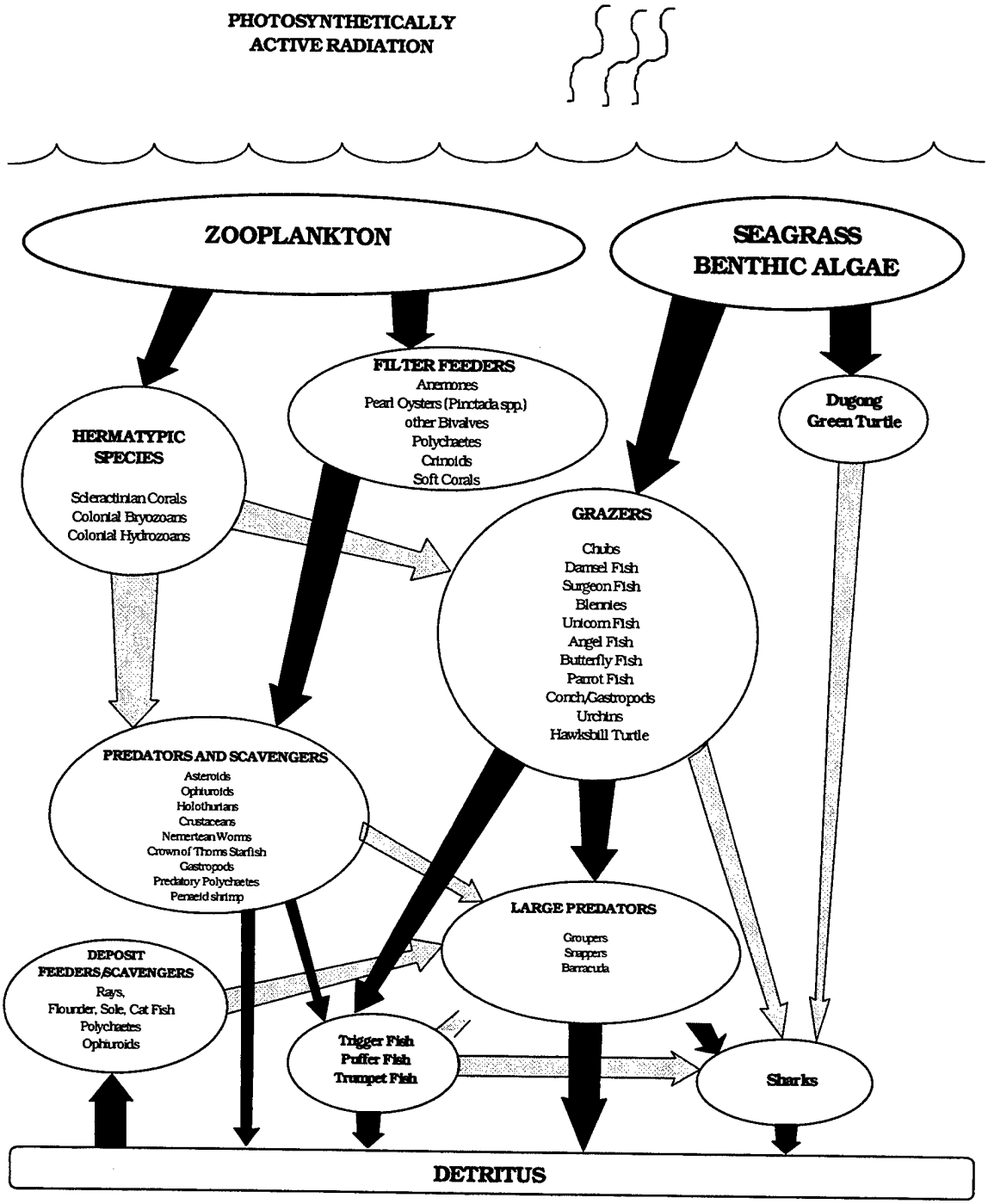

Figure 4.1-32. Benthic food web of the Gulfs region. The benthic food web of the shallow Gulfs region is supported by highly productive coral and seagrass communities. The majority of shallow benthic organisms rely upon reefs and seagrasses for food, shelter, and as breeding grounds and shelter for juveniles. Other benthic communities include mudflats and deeper mud/silt bottom environments dominated by filter-feeding bivalves and opportunistic scavengers.

Coral species diversity in the Gulf is low in terms of Indo-Pacific reefs. Approximately 50 to 60 zooxanthellate species are known, compared with nearly 200 species in the Red Sea and possibly double that number in the Indian Ocean. The Indian Ocean has been the colonizing source of corals since the Holocene transgression. Important factors limiting growth and possible barriers to recruitment of additional species include seasonal fluctuations in water temperature, and cold water upwelling in the Arabian Sea. Upwelling, combined with an extensive seafloor devoid of suitable hard substrate, separate the entrance of the Gulf from higher diversity reef areas in the Indian Ocean. Local seasonal fluctuations within the Gulf of up to 28°C also limit access by pioneering species (Price, Sheppard, and Roberts, 1993).

Coral species including *Stylophora* spp., *Acropora* spp., and *Porites* are the dominant builders of framework reefs in the Persian Gulf region. As previously mentioned, reef building corals contain symbiotic algae, known as zooxanthellae, within their tissues. This association appears to provide the corals with nutrients necessary to facilitate calcium carbonate deposition. Coral polyps obtain food by collecting plankton and organic debris in their tentacles, and by sweeping the reef with exuded mesenterial filaments that search for detritus. There is also evidence that corals may absorb dissolved nutrients directly through their body wall (Goreau et al., 1971; Barnes, 1987). Very few species are known to consume coral polyps. Many fish species, such as those of the parrot fish family, were once thought to eat large quantities of coral; however, they apparently feed more often on reef algae. The crown of thorns starfish (*Acanthaster planci*) is locally absent from some coral communities in the Persian Gulf; however, the starfish is known to graze on reefs near Oman (Salm et al., 1993). It is possible that other asteroids and some urchins graze on coral polyps.

Other reef species that include zooxanthellae and that filter feed for plankton include colonial bryozoans and hydrozoans, anemones, and bivalves. Other filter and suspension feeders include soft corals, tubiculous polychaetes, bivalves, and crinoids.

Several mud bottom animal assemblages have been investigated off the Saudi coast. The commoner of the two is generally found at depths from 6 to 15 meters and is dominated by the cockle *Cardium papyraceum*, a filter feeder occurring in average populations of 5 to 10 per square meter. Also found in this relatively diverse community are a sea urchin (*Temnopleurus toreumaticus*), a burrowing crab (*Dorippe dorsipes*), pen shells belonging to the genus *Pinna*, and a snail (*Murex kusterianus*). The second community is dominated by a heart urchin (*Brissopsis persica*) and a brittle star (*Amphioplus seminudus*), with an accompanying low diversity of additional species (Basson et al., 1977).

The Gulf reef fish are limited in variety in comparison to the reef fishes of the Red Sea or Indian Ocean. Nevertheless, numerous species of fish graze algae that grows on the reefs. Fish known to feed on reef algae include several species of surgeon fish, unicorn fish, blennies, angel fish, butterfly fish, parrot fish, chubs, and damsel fish. Three species of colorful butterfly fish in the Gulf feed on living coral polyps or on small, associated zooplankton: the brilliant orange *Chaetodon melapterus*, the russet-brown *Chaetodon nigropunctatus*, and the flag fish *Heniochus acuminatus*. Particularly abundant in the region are species such as the green wrasse (Thalossoma lunare) and a blue butterfly fish (*Pomacanthus maculosus*).

A detailed study of the benthic communities in the western Gulf (Coles and McCain, 1990) collected over 144,000 benthic organisms; 835 species were identified in the samples. The most frequently occurring species were several pelecypods, *Timoclea aracaria*, *Ctena bella*, and *Ervillia* sp., as well as two polychaetes, *Onuphis* sp. and *Prionospio* sp. Overall pelecypod and gastropod molluscs accounted for 60% of the total abundance; polychaetes, 26%; crustaceans 6%; and echinoderms 1%.

Rocky intertidal areas of the Saudi coast are not particularly productive, primarily due to the intense heat and desiccation in the summer, which precludes vigorous stands of algae. Most sessile animals in this zone are filter feeders. Among the vagile animals, important grazing gastropods include a top-shell (*Trochus erythraeus*), a turban (*Turbo coronatus*), and a limpet-like pulmonate (*Siphonaria rosea*). Common denizens of the mudflats include a herbivorous grazing crab (*Metapograpsus messor*), an ocypodid crab (*Cleistostoma dotilliforme*), as well as a burrowing crab (*Macrophthalmus depressus*). The last mentioned often dominates a broad expanse of mud flat, which even at low tide has a thin, adherent film of water. The lowest level of the intertidal mud flats often has dense populations of the snail *Cerithidea cingulata*. Sand flats feature another small crab, *Scopimera scabricauda* (Basson et al., 1977).

UNIQUE SPECIES AND ECOLOGICAL CONSIDERATIONS

Endangered/Threatened or Protected Species. Marine turtles and dugong are among the most threatened species that occur in the Persian Gulf. Green and hawksbill turtles and dugong are all classified as endangered or threatened under the Endangered Species Act of 1973. Regardless of regional prohibitions on the commercial exploitation of turtles, local fishermen are continuing to target nesting beaches. In November 1991 a survey assessing litter on the south shores of the Gulf found 14 carcasses of seas turtles lying upside down on their shells close to the water line near Ras Al Khaimah. Man made holes were dug in the same beach in search of turtle eggs (Khordagui and Abu-Hilal, 1993). As coastal development continues around Qatar and heavier sedimentation flows into surrounding seagrass beds, dugongs will gradually see their only food source dwindle. The infrequent reproductive periods and low reproductive rates of turtles and dugong make them particularly susceptible to environmental pressures. Also of regional conservation interest is the level of endemism found in the Persian Gulf. 12% of the echinoderms and 10% of all fish species present are endemic to the Gulf (Price and Sheppard, 1991).

Critical Habitat. Areas identified as critical habitat in the Gulf region include coral reefs and seagrass beds, and vast areas of intertidal mud flats. All have disproportionately high productivity in comparison to the limited areas they occupy. Seagrass beds are significant habitat for juvenile shrimp and pearl oysters, as well as pasture for herbivores such as dugong and green turtles. Mangrove habitat, never abundant, is now substantially diminished throughout the Gulf. Along the extensive stretch of Saudi Arabian coastline, it is reduced to only about 4 km^2 (Price and Sheppard, 1991). *Avicennia marina* is the only species occurring naturally in the Persian Gulf; this contrasts with the much greater diversity found of mangrove species on contiguous shorelines of northern India, or the four species occurring in the Red Sea. Dawhat Dafi is near the northern latitudinal limit of mangal ecosystems in the Gulf. Mangroves are often stunted in the Persian Gulf (i.e., 1 to 2 m) whereas the same species reach six meters on the Gulf of Oman.

A majority of reefs and seagrass beds occur short distances from the coast. Both habitats are currently threatened by increased coastal development and port expansion, and are subject to increased sedimentation and sewage spills on near shore benthic communities. Oil spills from coastal refineries and wells further damage these communities. In addition, increased tourism, fishing, and shell and fish collection place strains on such reef environments. As coral reefs and seagrass beds disappear in the Persian Gulf region, species diversity and numbers will diminish significantly in the area.

CONCLUSIONS

The approach taken in this section has been to review the basic study objectives as stated in Chapter 1.0 in relation to discussions provided throughout this report. Conclusions have been drawn from individual section discussions which generally provide a more detailed rationale than the statements and findings set forth below.

UNIQUE SPECIES AND ECOLOGICAL CONSIDERATIONS

Table 4.1-1 provides a summary of the critical habitats, unique ecological phenomena, and endangered, threatened, and sensitive species of the eight MARPOL Special Areas as discussed in Section 5 of this document. Analyses have been focused on keystone or indicator species, species that are adequately addressed in the literature pertaining to each region, and on species which could be the most likely to be negatively affected by U.S. Navy waste discharges. Critical habitats and unique ecological phenomena include essential breeding and loafing grounds for listed species, important food sources and highly productive communities, and sensitive resource areas that are important to the economies of the local region (including heavily-visited tourist areas and important fishing grounds).

Table 4.1-1. Summary of unique species and ecological considerations for each MARPOL designated Special Area.

	CRITICAL HABITATS AND UNIQUE ECOLOGICAL PHENOMENA	ENDANGERED AND THREATENED SPECIES
ANTARCTICA	The marginal/seasonal ice zone contains the most important breeding and loafing grounds in the region. Additionally, this area supports large krill populations which feed a majority of Antarctic animal species. Another zone of important productivity is the Antarctic Divergence where krill support a rich pelagic marine community.	**cetaceans:** the blue, fin, humpback, sperm, sei, southern right, and minke whales. **pinnipeds:** the southern fur seal, elephant seal, and Ross seal.
BALTIC SEA	The Baltic Sea is unique in that it is an evolutionarily young ocean system, has extreme barriers to circulation with neighboring water bodies, and has a low salinity. As such, the limited diversity of the system allows for unique opportunities to examine species interactions and adaptations.	**pinnipeds:** the grey seal.

	CRITICAL HABITATS AND UNIQUE ECOLOGICAL PHENOMENA	ENDANGERED AND THREATENED SPECIES
NORTH SEA	The shallow North Sea has historically provided excellent breeding and spawning grounds for numerous commercially important fish species. Recent overfishing has damaged this resource, but the fish of the region still constitute a major food source for surrounding nations.	**pinnipeds:** the grey seal. **birds:** the puffin populations of the Farne Islands.
BLACK SEA	The Black Sea is largely anoxic and marine flora and fauna inhabit only 20% of the waters of the Sea. The shallow, nutrient-rich waters near the Danube in the northwest support the most diverse and extensive populations of organisms.	**pinnipeds:** the monk seal.
MEDITERRANEAN SEA	The continental shelf regions in the north and south portions of the Sea support ecologically important *Posidonia* seagrass meadows, and economically important corals and sponge assemblages.	**cetaceans:** the long-finned, and sperm whales. **pinnipeds:** the Mediterranean monk seal. **birds:** the Audouin's gull. **turtles:** the loggerhead and green turtles.
RED SEA	The Red Sea contains highly productive, shallow benthic, seagrass and coral reef communities that provide habitat and food for numerous species, stabilize bottom sediments and prevent erosion, and are locally important fishing grounds and tourist destinations.	**turtles:** the green, loggerhead, hawksbill, olive Ridley, and leatherback turtles. **marine mammals:** the dugong.
WIDER CARIBBEAN REGION	The Caribbean Sea contains highly productive, shallow benthic, seagrass and coral reef communities that provide habitat and food for numerous species, stabilize bottom sediments and prevent erosion, and are economically important fishing grounds and tourist destinations.	**cetaceans:** the humpback, blue, sei, fine, minke, and right whales. **turtles:** the green, loggerhead, hawksbill, olive Ridley, and leatherback turtles. **other marine mammals:** the manatee.

	CRITICAL HABITATS AND UNIQUE ECOLOGICAL PHENOMENA	ENDANGERED AND THREATENED SPECIES
GULFS REGION	The Gulfs Region contains highly productive, shallow benthic, seagrass and coral reef communities that provide habitat and food for numerous species, stabilize bottom sediments and prevent erosion, and are locally important fishing grounds.	**cetaceans:** the humpback, and Bryde's whales. **turtles:** the green, and hawksbill turtles. **other marine mammals:** the dugong.

SIGNIFICANT CHARACTERISTICS OF MARPOL SPECIAL AREAS

The characteristics of the marine environments in each of the Special Areas have been discussed previously in Chapter 5. In that these are rudimentary summaries, they have not been reiterated here. The MARPOL Special Areas which have been reviewed range from polar to tropical seas. Water temperatures, salinities, and dissolved oxygen levels run the gamut of extremes. Water temperatures within considered seas can range from below zero, (in the Antarctic), to greater than 30°C, (in the Red Sea). Salinities range from nearly freshwater conditions in the northern Baltic Sea, to salinities in excess of 40 ppt (and locally above 50 ppt) in shallow regions of the Red Sea and the Gulfs region. Dissolved oxygen can exceed extreme saturation levels within the cold Antarctic waters where phytoplankton may receive sunlight for 24 hours a day during the austral summer; conversely, portions of the Baltic and the entire deep basin of the Black Sea are completely anoxic.

One of the fundamental conclusions which has been derived from this investigation is that physical, chemical, and biological characteristics vary considerably between Special Areas and, in many cases, within a single study area. Further, both spatial and temporal variability can be important factors which complicate the characterization and analysis of potential ecological effects of waste disposal within a MARPOL Special Area. As a result, attempting to address impacts on Special Area-wide or basin-wide scale (several of the Special Areas such as the Mediterranean, the Baltic, and the Caribbean include more than one basin) may result in conclusions which must either ignore or be driven by localized features of the larger region.

This paradox of scale and the lack of ability to completely predict details of future operational scenarios has made it necessary to address impacts on a general basis. Further, it is necessary to select an appropriate scale on which to base an impact assessment. To assess effects, the authors have opted to fall back on the most manageable scale and analyze impacts primarily at the organism level and secondarily on a local trophic web level. Using this approach, it is hoped that local effects can be brought into focus without sacrificing the ability to project upward to a larger scale analysis.

SUMMARY OF SENSITIVE ECOLOGICAL ENDPOINTS IN MARPOL SPECIAL AREAS

As has been an issue in the current evaluation, the assessment of significant, potential risk or impacts is often relative to the scale on which the assessment is conducted. For individual organisms that happen to be in the wrong place at the wrong time, interaction with discharged wastes may be lethal. For the most part, these interactions have not been considered significant, except where endangered or threatened species may be adversely impacted.

Looking beyond the organismal scale, to the ecology of a local area, the loss of individual organisms would not be considered significant; however, significant impacts may occur if enough organisms are impacted and if those organisms impacted are important to the structure of the ecological communities of the local area. To be considered significant on a local-scale, impacts such as relatively large local die-offs or detrimental impacts to community structuring organisms, or commercially, socially, or scientifically important species should be reasonably likely to occur under regularly recurring circumstances. It is not anticipated that all locations within a Special Area are likely to be susceptible to equal levels of local impacts. It is also realized that there are several other sources, such as fishing activities and presence of stationary terrestrial effluents, that cause locally significant impacts. Further, it should not always be assumed that a given location will be consistently subject to the same level of susceptibility to impacts. In fact, seasonal factors may play extremely important roles in the distribution and susceptibility of organisms to impacts or in establishing ambient physical conditions which favor the increased interaction of organisms and wastes. It is at the local-scale that most of the potential significant impacts would be anticipated to occur. This is also the scale on which most stationary effluent impacts are assessed and such impacts are recognizable.

Beyond the local-scale, and looking at a regional-scale, an impact would have to be extremely widespread (covering many hundreds to thousands of square kilometers) or be distributed along an extensive linear band of the ocean before being considered significant. This is the scale at which large oil spills such as the Exxon Valdez spill in Prince Williams Sound or the Amoco Cadiz off of the Brittany coast of France are assessed. It is also the scale at which large river (i.e. the Mississippi River, the Nile, or the Danube) inputs of sediment, contaminants, and nutrients are assessed. Few, if any, of the proposed discharges are anticipated to result in regional-scale, significant impacts.

Given the relatively low volume of wastes being discharged at any given time, it is unlikely that discernable significant impacts would occur over large regions of an ocean at any given time. This being said, it is important to identify the conditions which would be required to result in such regional impacts and to note that such conditions may occur in some portions of a few of the Special Areas considered, during some periods of time. First, there must be sufficient ship traffic to provide enough waste to result in widespread impacts. However, ships need not be present at all times and traffic may be spread over very long periods-decades. Second, impacts at a local-scale must be prolonged either by very slow ecological recovery, permanent habitat modification, or regular reactivation or resuspension of wastes through time. Finally, there must be enough local-scale events to depress the ecology of the region in excess of the actual, local effects or to saturate the region with overlapping local-scale impacts. Areas with the potential for such regional effects have low turnover rates, such as the slow-growing reef communities of the southern end of the Red Sea and the Gulf of Aqaba and the slow-growing sponge communities of the Antarctic, marginal seas. Again, the improbable coincidence of conditions necessary to result in regional effects make such occurrences unlikely.

On a basin-scale, or Special Area-wide scale (differentiated because several of the Special Areas support multiple and very different basin conditions), no impacts of the proposed dumping practices can be

viewed as having significant adverse effects. At this scale, natural and anthropogenic inputs, both offshore and terrestrial, dominate the identifiable conditions. Thus, it would be relatively impossible to detect effects relative to activities of the U.S. Navy beyond the existing system responses to the underlying parameters and variability.

In light of these thresholds, impact assessment has been focused at the local level. Unless otherwise specified, impacts and significance determinations are presumed to be operative under the threshold conditions defined for local-scale impacts. The following tables provide a summary of potentially sensitive endpoints for each of the MARPOL designated Special Areas. Tables address the pulped paper (Table 4.2-2) and shredded metal and glass wastes (Table 4.2-3) separately because the potential effects may vary considerably for any given area. The tables focus on organisms and communities that have the perceived potential to experience adverse effects as a result of waste discharges. These include organisms such as clupeoid fish, large copepods, and euphausiids that could experience fouling of respiratory apparatus as a result of pulped waste discharge. Also included are benthic filter feeders, such as coral polyps, polychaetes, and sponges, that could experience a disruption of feeding mechanisms as a result of discharges. Additionally, highly productive shallow benthic communities such as coral reefs and seagrass beds, and larger endangered and threatened mammals, birds, and reptiles have been included. Each of these organisms and communities has been discussed in detail in the section on ecological systems in this document.

Table 4.1-2. Sensitive biological communities associated with pulped paper waste discharge within MARPOL Special Areas.

	PELAGIC WATERS	SHALLOW BENTHIC WATERS	DEEP BENTHIC WATERS
ANTARCTICA	Potentially sensitive communities include krill populations, especially in the marginal ice zone. Mechanism of potential impact includes respiratory fouling. A large food web reliant upon krill as a major food source.	Potentially sensitive communities include complex associations of sponges, colonial bryozoans, and other filter- and suspension-feeding organisms that are adapted to low, suspended sediment loads.	No sensitive biological communities. Deep water benthic communities consist largely of mobile, opportunistic scavengers and predators.
BALTIC SEA	Potentially sensitive communities include local populations of clupeoid fish (including herring, sardines, and anchovies). Mechanisms of potential impact include short-term behavioral, feeding, and respiratory responses.	No sensitive biological communities. A majority of benthic filter-feeding communities are of estuarine origin and are adapted to high particulate influence.	No sensitive biological communities. Mobile scavengers and predators are not likely to be impacted; however, a lack of cellulose-digesting macrofauna could result in

	PELAGIC WATERS	SHALLOW BENTHIC WATERS	DEEP BENTHIC WATERS
			accumulation of pulped waste on the sea floor.
NORTH SEA	Potentially sensitive communities include local populations of clupeoid fish (including herring, sardines, and anchovies). Mechanisms of potential impact include short-term behavioral, feeding, and respiratory responses.	No sensitive biological communities. No large communities of sponges exist in the North Sea; most species of filter feeders are adapted to high particulate influence.	No sensitive biological communities. Mobile scavengers and predators are not likely to be impacted.
BLACK SEA	No sensitive biological communities. Clupeoid fish and large copepod populations are sparse and are not likely to be affected.	No sensitive biological communities. Benthic organisms are adapted to high particulate influence from river inputs.	No sensitive biological communities. Deep benthic waters are completely anoxic and devoid of all but bacterial life forms.
MEDITERRANEAN SEA	No sensitive biological communities. Clupeoid fish populations are sparse and zooplankton is dominated by smaller copepods that are unlikely to be affected.	Potentially sensitive communities include commercially important sponge and cool water coral communities along the northern and southern shelves. Mechanism of potential impact includes filter-feeding capability.	No sensitive biological communities. Mobile scavengers and predators are not likely to be impacted.
RED SEA	No sensitive biological communities. Clupeiod fish populations are small and relatively few species of larger zooplankton inhabit the Sea.	Potentially sensitive communities include ecologically important seagrass beds and coral reefs located along the coasts and in the shallow southern waters. Mechanism of potential impact includes filter-feeding capability.	No sensitive biological communities. The deep benthic population is sparse and is composed largely of mobile, opportunistic foragers that are not likely to be impacted.

	PELAGIC WATERS	SHALLOW BENTHIC WATERS	DEEP BENTHIC WATERS
WIDER CARIBBEAN REGION	No sensitive biological communities. Clupeiod fish populations are small and relatively few species of larger zooplankton inhabit the Sea. Commercially important fish and prawns existing near upwellings and river inputs are adapted to high particulate influence.	Potentially sensitive communities include ecologically important seagrass beds and coral reefs located adjacent to numerous island chains and along the Central American barrier reef. Mechanism of potential impact includes filter-feeding capability.	No sensitive biological communities. The deep benthic population is sparse and is composed largely of mobile, opportunistic foragers that are not likely to be impacted.
GULFS REGION	No sensitive biological communities. Clupeiod fish populations are small and relatively few species of larger zooplankton inhabit the Sea.	Potentially sensitive communities include ecologically important seagrass beds and coral reefs located along the western coasts of the Persian Gulf, the Straits of Hormuz, and the southern coast of the Gulf of Oman. Mechanism of potential impact includes filter-feeding capability.	No sensitive biological communities. No deep waters exist in this area. The floor of eastern waters is muddy and benthic organisms are adapted to high particulate influence.

Table 4.1-3. Sensitive biological communities associated with shredded waste discharge within MARPOL Special Areas.

	PELAGIC WATERS	SHALLOW BENTHIC WATERS	DEEP BENTHIC WATERS
ANTARCTICA	Although risk is minimal, endangered or threatened mammal and bird species that may accidentally ingest wastes are considered to be sensitive endpoints.	No sensitive biological communities. Bag waste damage to sponge communities or other shallow-water benthic habitats is likely to be minimal.	No sensitive biological communities.
BALTIC SEA	Although risk is minimal, endangered or threatened mammal and bird species that may accidentally ingest wastes are considered to be sensitive endpoints.	No sensitive biological communities.	No sensitive biological communities.
NORTH SEA	Although risk is minimal, endangered or threatened mammal and bird species that may accidentally ingest wastes are considered to be sensitive endpoints.	No sensitive biological communities.	No sensitive biological communities.
BLACK SEA	Although risk is minimal, endangered or threatened mammal and bird species that may accidentally ingest wastes are considered to be sensitive endpoints.	No sensitive biological communities.	No sensitive biological communities.

	PELAGIC WATERS	SHALLOW BENTHIC WATERS	DEEP BENTHIC WATERS
MEDITERRANEAN SEA	Although risk is minimal, endangered or threatened mammal, turtle, and bird species that may accidentally ingest wastes are considered to be sensitive endpoints.	Potentially sensitive communities include endangered green and loggerhead turtles that may ingest waste from seagrass beds and foraging areas. Although risk is minimal, wastes may damage sessile sponges and corals.	No sensitive biological communities.
RED SEA	Although risk is minimal, endangered or threatened mammal, turtle, and bird species that may accidentally ingest wastes are considered to be sensitive endpoints.	Potentially sensitive communities include endangered turtles and dugong that may ingest waste from seagrass beds and foraging areas. Although risk is minimal, wastes may damage sessile sponges and corals.	No sensitive biological communities.
WIDER CARIBBEAN REGION	Although risk is minimal, endangered or threatened mammal, turtle, and bird species that may accidentally ingest wastes are considered to be sensitive endpoints.	Potentially sensitive communities include endangered turtles and manatees that may ingest waste from seagrass beds and foraging areas. Although risk is minimal, wastes may damage sessile sponges and corals.	No sensitive biological communities.
GULFS REGION	Although risk is minimal, endangered or threatened mammal, turtle, and bird species that may accidentally ingest wastes are considered to be sensitive endpoints.	Potentially sensitive communities include endangered turtles and dugong that may ingest waste from seagrass beds and foraging areas. Although risk is minimal, wastes may damage sessile sponges and corals.	No sensitive biological communities.

REFERENCES

Al-Ghadban, A.N., Jacob, P.G. and Abdali, F. 1994. *Total Organic Carbon in the Sediments of the Arabian Gulf and Need for Biological Productivity Investigations*. Marine Pollution Bulletin, V28 N6. pp. 356-374.

Al-Yamani, F.Y., Al-Rifaie, K. and Ismail, W. 1993. *Post-Spill Zooplankton Distribution in the NW Gulf*. Marine Pollution Bulletin, V27. Great Britain. pp. 239-243.

Albaigés, J., Aubert, M. and Aubert, J. 1985. *The Footprints of Life and of Man*. In: Key Environments: Western Mediterranean. Margalef, R. (Ed.) International Union for Conservation of Nature and Natural Resources. Oxford, New York, Toronto, Sydney, Frankfurt. pp. 317-351.

Allen, W. 1992. *Increased Dangers To Caribbean Marine Ecosystems* - Cruise Ship Anchors and Intensified Tourism Threaten Reefs. Bioscience, V42 N5. pp.330-335.

American Geographical Society. 1970. *Antarctica Map*. Prepared by the American Geographical Society of New York for the United States Antarctic Research Program. A. Hoen and Co., Baltimore Md.

Arntz, W. and Gorney, M. 1991. *Shrimp (Decapoda, Natantia) Occurrence and Distribution in the Eastern Weddell Sea, Antarctica*. Polar Biology, V11 N3, pp. 169-177.

Awad, H. 1989. *Oil Contamination in the Red Sea Environment*. Water, Air, and Soil Pollution, V45. Kluwer Academic Publishers. pp. 235-242.

Balkas, T., Dechev, G., Mihnea, R., Serbanescu, O. and Unlüata, U. 1990. *State of the Marine Environment in the Black Sea Region*. UNEP Regional Seas Reports and Studies. N124.

Barnes, R.D. 1987. *Invertebrate Zoology, 5th Edition*. Saunders College Publishing. Fort Worth, USA.

Basson, P.W., Burchard, J.E.Jr., Hardy, J.T. and Price, A.R.G. 1977. *Biotopes of the Western Arabian Gulf: Marine Life and Environments of Saudi Arabia*. Aramco Department of Loss Prevention and Environmental Affairs. Dhahran, Saudi Arabia.

Behairy, A.K.A., Sheppard, C.R.C. and El-Sayed, M.K. 1992. *A Review of the Geology of Coral Reefs in the Red Sea*. UNEP Regional Seas Reports and Studies N152.

Bellamy, D. J, Edwards, P., Hirons, M.J.D., Jones, D.J. and Evans, P.R. 1973. *Resources of the North Sea and Some Interactions*. In: North Sea Science. Goldberg, E.D. (Ed.) MIT Press, Cambridge, MA and London, England, pp. 383-399.

Bellan, G. 1985. *Effects of Pollution and Man-Made Modification on Marine Benthic Communities in the Mediterranean*: A Review. In: Mediterranean Marine Ecosystems. Moraitou-Apostolopoulou, M. and Kiortsis, V. (Eds.) NATO Scientific Affairs Division. New York, London. pp. 163-194.

Ben-Tuvia, A. 1983. *The Mediterranean Sea, B. Biological Aspects.* In: Ecosystems of the World 26: Estuaries and Enclosed Seas. Ketchum, B. (Ed.) Elsevier Scientific Publishing Company. Amsterdam, Oxford, New York. pp. 239-251.

Benli, H.A. and Pilskaln, C.H. 1988. *Plankton Community.* In: Woods Hole Oceanographic Series, V88 N35-40, pp. 103-105. Honjo, S. (Ed.)

Bergstrom, B.I., Hempel, G., Marschall, H-P, North, A.W., Siegel, V and Stromberg, J-O. 1990. *Spring Distribution, Size Composition and Behaviour of Krill Euphausia superba in the Western Weddell Sea.* Polar Rec., V26, pp. 85-89.

Berkman, P.A. and Nigro, M. 1992. *Trace Metal Concentrations in Scallops around Antarctica: Extending the Mussel Watch Programme to the Southern Ocean.* Marine Pollution Bulletin, V24 N6, pp. 322-323.

Bleaching of the Coral Reefs In The Caribbean. 1988. United States Congress Senate Committee on Appropriations Subcommittee On Commerce, Justice, State, The Judiciary, and Related Agencies. Hearing Before a Subcommittee of The Committee on Appropriations, United States Senate, One Hundredth Congress, First Session: Special Hearing, Washington.

Boltovsky, D. and Alder, V. 1992. *Microzooplankton and Tintinnid Species-Specific Assemblage Structures - Patterns of Distribution and Year-to-Year Variations in the Weddell Sea (Antarctica).* Journal of Plankton Research, V14 N10, pp. 1405-1423.

Boltovsky, D., Alder, V. and Spinelli, F. 1989. *Summer Weddell Sea Microplankton - Assemblage Structure, Distribution and Abundance, With Special Emphasis on the Tintinnia.* Polar Biology, V9 N7, pp. 447-456.

Bourne, W.R.P. 1989. *Oil and Garbage in the Gulf.* Marine Pollution Bulletin, V20 N2. Great Britain. p. 90.

Boysen-Ennen, E., Hagen, W., Hubold, G. and Piatkowsi, U. 1991. *Zooplankton biomass in the Ice-Covered Weddell Sea, Antarctica.* Marine Biology, V111 N2, pp.227-235.

Braithwait, C.J. 1987. *Geology and Paleogeography of the Red Sea Region.* In: Key Environments: Red Sea. Edwards, A.J. and Head, S.M. (Eds.) Pergamon Press. Oxford, New York, Beijing, Frankfurt, São Paulo, Sydney, Tokyo, Toronto. pp. 22-44.

Caddy, J.F. and Griffiths. 1994. *Environmental Management and Protection of the Black Sea.* General Fisheries Council for the Mediterranean, Report of the Second Technical Consultation on Stock Assessment in the Black Sea. FAO Fisheries Report, Rome, pp. 166-190.

Caldwell, D.K. and Caldwell, M.C. 1973. *Marine Mammals of the Eastern Gulf of Mexico.* In: Summary of Knowledge of the Eastern Gulf of Mexico, 1973. Jones, J.I., Ring, R.E., Rinkel, M.O. and Smith, R.E. (Eds.) State University of Florida System. pp. III-I-1 - III-I-23.

Calvert, S.E., Karlin, R.E., Toolin, L.J., Donahue, D.J., Southon, J.R. and Vogel, J.S. 1991. *Low organic carbon accumulation rates in Black Sea sediments.* Nature, 350, pp. 692-695.

Campbell, A.C. 1987. *Echinoderms of the Red Sea.* In: Key Environments: Red Sea. Edwards, A.J. and Head, S.M. (Eds.) Pergamon Press. Oxford, New York, Beijing, Frankfurt, São Paulo, Sydney, Tokyo, Toronto. pp. 215-250.

Carter, I.C, Williams, J.M, Webb, A., and Tasker, M.L. 1993. *Seabird Concentrations in the North Sea: An Atlas of Vulnerability to Surface Pollutants.* Offshore Animals Branch, Joint Nature Conservation Committee.

Casinos, A. and Vericad, J.R. 1976. *The cetaceans of the Spanish coasts.* Mammalia, V40 N2. pp.267-289.

Cederwall, H. and Elmgren, R. 1990. *Biological Effects of the Eutrophication in the Baltic Sea, Particularly the Coastal Zone.* Ambio, V19 N3. pp. 109-112.

Chadwick, D.B., Katz, C.N., Curtis, S.L., Rohr, J., Caballero, M., Valkirs, A. and Patterson, A. 1995. *Environmental Analysis of U.S. Navy Shipboard Solid Waste Discharges: Preliminary Report*, 25 July 1995.

Christensen, V. and Caddy, J.F. 1994. *Reflections on the Pelagic Food Web Structure in the Black Sea.* General Fisheries Council for the Mediterranean, Report of the Second Technical Consultation on Stock Assessment in the Black Sea. FAO Fisheries Report, Rome, pp. 84-101.

Cihangir, B. and Tirasin, E.M. 1989. In: Black Sea Oceanography. Izdar, E. and Murray, J.W. (Eds.). NATO Series C: Mathematical and Physical Sciences. Kluwer Academic Publishers. V351.

Clark, R.B. 1992. *Marine Pollution, Third Edition.* Clarendon Press. Oxford, New York.

Coles, S.L. and Gunay, N. 1989. *Tar pollution on Saudi Arabian Gulf beaches.* Marine Pollution Bulletin, V20. Great Britain. pp. 214-218.

Coles, S.L. and McCain, J.C. 1990. *Environmental Factors Affecting Benthic Infaunal Communities of the Western Arabian Gulf.* Marine Environmental Research, V29. pp. 289-315.

Colwell, R.R., *Microbiological Effects of Ocean Pollution.* University of Maryland, USA. pp. 375-389.

Cormaci, M., Furnari, G. and Scammacca, B. 1992. *The Benthic Algal Flora of Terra Nova Bay (Ross Sea, Antarctica).* Botanica Marina, V35 N6, pp. 541-552.

Couper, A. 1983. *The Times Atlas of the Oceans.* Van Nostrand Reinhold, New York.

D'Elia, C.F. 1983. *Gradients in Factors Limiting Primary Productivity.* In: UNESCO COMAR project for Coastal Ecosystems of Latin America and the Caribbean. pp. 9-13.

Daan, N., Bromley, P.J., Hislop, J.R. and Nielsen, N.A. 1990. *Ecology of North Sea Fish.* Netherlands Journal of Sea Research, V26, pp. 343-386.

Defense Mapping Agency. 1990. *Ocean Basin Environment. Sailing Directions (Planning Guide) for the North Sea and Baltic Sea*, Defense Mapping Agency, Pub.190, 3rd Edition.

Defense Mapping Agency. 1991. *Ocean Basin Environment. Sailing Directions (Planning Guide) for the Mediterranean*, Defense Mapping Agency, Pub.130, 5th Edition.

Defense Mapping Agency. 1992. *Ocean Basin Environment. Sailing Directions (Planning Guide) for Antarctica*, Defense Mapping Agency, Pub. 200, 2nd Edition.

Dell, R.K. 1965. *Marine Biology*. In: Antarctica.. Trevor Hatherton (ed.) The New Zealand Antarctic Society. Fredrick A. Praeger, Inc. New York, NY. pp. 129-152.

Dethlefsen, V. 1989. *Fish in the Polluted North Sea.* Dana - A Journal of Fishes and Marine Research, V3, pp. 109-129.

Dicks, B. 1987. *Pollution.* In: Key Environments: Red Sea. Edwards, A.J. and Head, S.M. (Eds.) Pergamon Press. Oxford, New York, Beijing, Frankfurt, São Paulo, Sydney, Tokyo, Toronto. pp. 383-404.

Diehl, F., Mellon, D., Garrett, R. and Elliott, N. 1988. *Field Guide to Invertebrates of San Salvador Island, Bahamas*. Bahamian Field Station.

Dixon, T.J and Dixon, T.R. 1990. *Marine Litter Distribution and Composition in the North Sea.* Marine Pollution Bulletin, V14 N4, pp. 145-148.

Dybern, B.I. and Fonselius, S.H. 1981. *Pollution.* In: The Baltic Sea. Voipio, A. (Ed.) Elsevier Scientific Publishing Company. Amsterdam, Oxford, New York. pp. 351-381.

Edwards, F.J. 1987. *Climate and Oceanography*. In: Key Environments: Red Sea. Edwards, A.J. and Head, S.M. (Eds.) Pergamon Press. Oxford, New York, Beijing, Frankfurt, São Paulo, Sydney, Tokyo, Toronto. pp. 45-69.

Ehlin, U. 1981. *Hydrology of the Baltic Sea.* In: The Baltic Sea. Voipio, A. (Ed.) Elsevier Scientific Publishing Company. Amsterdam, Oxford, New York. pp. 123-134.

Eisma, D. Dr. 1973. *Sediment Distribution in the North Sea.* In: North Sea Science. Goldberg, E.D. (Ed.) MIT Press, Cambridge, MA and London, England. pp. 131-150.

Eisma, D. Dr. 1990. *Transport and Deposition of Suspended Matter in the North Sea and the Relation to Coastal Siltation, Pollution, and Bottom Fauna Distribution.* Aquatic Sciences, V3 N2-3. pp. 181-216.

Ekau, W. 1990. *Demersal Fish Fauna of the Weddell Sea, Antarctica.* Antarctic Science, V2 N2, pp. 129-137.

El-Sayed, S.Z. 1971. *Dynamics of Trophic Relations in the Southern Ocean.* In: Research in the Antarctic. L.O. Quam.(ed.) American Association for Advancement of Science, Wash. D.C. 1971 Pub. No. 33.

Environmental Agenda for the 1990's. 1991. A Synthesis of the Eastern Caribbean. Country Environmental Profile Series. The Caribbean Conservation Association. The Island Resources Foundation.

Estrada, M. and Delgado, M. 1990. *Summer Phytoplankton Distributions in the Weddell Sea.* Polar Biology, V10 N6. pp. 441-449.

Estrada, M., Vives, F. and Alcaraz, M. 1985. *Life and Productivity of the Open Sea.* In: Key Environments: Western Mediterranean. Margalef, R. (Ed.) International Union for Conservation of Nature and Natural Resources. Oxford, New York, Toronto, Sydney, Frankfurt. pp. 148-197.

Evans, M.I., Symens, P. and Pilcher, C.W.T. 1993. *Short-term Damage to Coastal Bird Populations in Saudi Arabia and Kuwait Following the 1991 Gulf War Marine Pollution.* Marine Pollution Bulletin, V27. Great Britain. pp.157-161.

Everson, I. 1981. *Fish.* In: Biological Investigations of Marine Antarctic Systems and Stocks (Biomass): Volume II: Selected Contributions to the Woods Hole Conference on Living Resources of the Southern Ocean 1976. Univ. Library, Cambridge, Feb. 1981. ,pp. 78-97.

FAO (Food and Agriculture Organization of the United Nations). 1994. *FAO Fisheries Report N495.* General Fisheries Council for the Mediterranean. Report of the Second Technical Consultation on Stock Assessment in the Black Sea. Ankara, Turkey, 15-19 February 1993.

Fitzmaurice, M. 1992. *International Legal Problems of the Environmental Protection of the Baltic Sea.* Braham and Trotman; Norwell, Kluwer Academic Publishers. Massachusetts, USA.

Fransz, H.G, Mommaerts, J.P. and Radech, G. 1991. *Ecological Modeling of the North Sea.* Netherlands Journal of Sea Research, V28. pp. 67-140.

Frazier, J.G., Bertram, G.C. and Evans, T.G.H. 1987. *Turtles and Marine Mammals.* In: Key Environments: Red Sea. Edwards, A.J. and Head, S.M. (Eds.) Pergamon Press. Oxford, New York, Beijing, Frankfurt, São Paulo, Sydney, Tokyo, Toronto. pp. 288-314.

Garrison, D. and Buck, K. 1989. *Protozooplankton in the Weddell Sea, Antarctica - Abundance and Distribution in the Ice-Edge Zone.* Polar Biology, V9 N6. pp. 341-351.

Garrison D. and Buck K. 1989. *The Biota of Antarctic Pack in the Weddell Sea and Antarctic Peninsula Regions.* Polar Biology, V10 N3. pp. 211-219.

Garrity, S. and Levings, S. 1993. *Marine Debris Along The Caribbean Coast Of Panama. Marine Pollution Bulletin.* V26 N6. pp. 317-324.

Gaudy, R. 1985. *Features and Peculiarities of Zooplankton Communities from the Western Mediterranean.* In: Key Environments: Western Mediterranean. Margalef, R. (Ed.) International Union for Conservation of Nature and Natural Resources. Oxford, New York, Toronto, Sydney, Frankfurt. pp. 279-307.

Gerdes, D, Klages, M., Arntz, W.E., Herman, R.L, Galeron, J. and Hain, S. 1992. *Quantitative Investigations on Macrobenthos Communities of the Southeastern Weddell Sea Shelf Based on Multibox Corer Samples.* Polar Biology, V12 N2. pp. 291-301.

Gerges, M.A. 1993. *On the Impacts of the 1991 Gulf War on the Environment of the Region: General Observations.* Marine Pollution Bulletin, V27. Great Britain. pp. 305-314.

Goenaga, C. 1991. *The State Of Coral Reefs in The Wider Caribbean.* Interciencia, V16 N1. pp. 12-20.

Golob, R. and Brus, E. 1984. *Statistical Analysis of Oil Pollution in the Kuwait Action Plan Region and the Implications of Selected World-Wide Oil Spills to the Region.* In: Regional Seas: Combating oil pollution in the Kuwait Action Plan Region. UNEP Regional Seas Reports and Studies #44. United Nations Environment Programme. pp. 7-34.

Goldberg, E. (Ed.) 1973. *North Sea Science.* NATO North Sea Conference. The MIT Press, Cambridge, MA.

Goreau, T.F., Goreau, N.I. and Goreau, T.J. 1979. *Corals and Coral Reefs.* Scientific American, V241. pp. 124-136.

Goreau, T.F., Goreau, N.I. and Yonge, C.M. 1971. *Reef Corals: Autotrophs or Heterotrophs?* Biol. Bull, V141. pp. 247-260.

Graneli, E., Graneli, W., Rabbani, M. and Daugbjerg, N. 1993. *The Influence of Copepod and Krill Grazing on the Species Composition of Phytoplankton Communities from the Scotia-Weddell-Sea - An Experimental Approach.* Polar Biology, V13 N3. pp. 201-213.

Grasshoff, K. 1976. *Review of the hydrological conditions of the Gulf Region.* UNESCO Rep. Mar. Aci., V28. pp. 37-45.

Grasshoff, K. and Voipio, A. 1981. *Chemical Oceanography.* In: The Baltic Sea. Voipio, A. (Ed.) Elsevier Scientific Publishing Company. Amsterdam, Oxford, New York. pp. 183-274.

Gray, J.S., Clarke, K.R., Warwick, R.M. and Hobbs, G. 1990. *Detection of Initial Effects of Pollution on Marine Benthos: An Example from the EkoFisk and Eldfisk Oilfields, North Sea.* Marine Ecology Progress Series, V66. pp. 285-299.

Greenpeace The Seas of Europe: The Baltic. 1992. Leithe-Eriksen, R. (Ed.) Collins and Brown Limited, London, U.K.

Grice, G.D. and Gibson, V.R. 1978. *Report B: General Biological Oceanographic Data from the Persian Gulf and Gulf of Oman.* Woods Hole Oceanographic Institution. Technical Report: Unpublished Manuscript.

Guzman, H. and Holst, I. 1993. *Effects Of Chronic Oil-Sediment Pollution On The Reproduction Of The Caribbean Reef Coral Siderastrea-Siderea.* Marine Pollution Bulletin, V26 N5. pp. 276-282.

Guzman, H. and Jimenez, C. 1992. *Contamination Of Coral Reefs By Heavy Metals Along The Caribbean Coast of Central America - (Costa Rica and Panama).* Marine Pollution Bulletin, V24 N11. Great Britain. pp. 554-561.

Haagensen, D.A. 1976. *Thecosomata.* In: Caribbean Zooplankton. Office of Naval Research. Department of the Navy.

Hällfors, G., Niemi, Å., Ackefors, H. Lassig, J. and Leppäkoski, E. *1981 Biological Oceanography.* In: The Baltic Sea. Voipio, A. (Ed.) Elsevier Scientific Publishing Company. Amsterdam, Oxford, New York. pp. 219-274..

Hashim, O.A. 1993. *Fisheries Study in the Gulf.* Marine Pollution Bulletin, V27. Great Britain. pp. 279-284.

Hay, B.J. 1987. *Particle Flux in the Western Black Sea in the Present and Over the Last 5,000 Years:* Temporal Variability, Sources, Transport Mechanisms. Woods Hole Oceanographic Institution and The Massachusetts Institute of Technology. Doctoral Dissertation.

Head, S.M. 1987a. *Introduction.* In: Key Environments: Red Sea. Edwards, A.J. and Head, S.M. (Eds.) Pergamon Press. Oxford, New York, Beijing, Frankfurt, São Paulo, Sydney, Tokyo, Toronto. pp. 1-21.

Head, S.M. 1987b. *Red Sea Fisheries.* In: Key Environments: Red Sea. Edwards, A.J. and Head, S.M. (Eds.) Pergamon Press. Oxford, New York, Beijing, Frankfurt, São Paulo, Sydney, Tokyo, Toronto. pp. 363-382.

Head, S.M. 1987c. *Corals and Coral Reefs of the Red Sea.* In: Key Environments: Red Sea. Edwards, A.J. and Head, S.M. (Eds.) Pergamon Press. Oxford, New York, Beijing, Frankfurt, São Paulo, Sydney, Tokyo, Toronto. pp. 128-151.

Head, S.M. 1987d. *Minor Invertebrate Groups.* In: Key Environments: Red Sea. Edwards, A.J. and Head, S.M. (Eds.) Pergamon Press. Oxford, New York, Beijing, Frankfurt, São Paulo, Sydney, Tokyo, Toronto. pp. 233-250.

Hempel, G. 1985. *On the Biology of Polar Seas, Particularly the Southern Ocean.* In: Marine Biology of Polar Regions and Effects of Stress on Marine Organisms. Gray, J.S. and Christiansen, M.E. (Eds). J. Wiley and Sons. pp. 3-33.

Herman, R.L. and Dahms, H.U. 1992. *Meiofauna Communities Along a Depth Transect off Halley Bay (Weddell Sea-Antarctica).* Polar Biology, V12 N2. pp. 313-320.

Hey, Ellen. 1992. *A Healthy North Sea Ecosystem and a Healthy North Sea Fishery: Two Sides of the Same Regulation?* Ocean Development and International Law, UK, V23 N2-3. pp. 217-238.

Hopkins, T.L. 1973. *Zooplankton.* In: Summary of Knowledge of the Eastern Gulf of Mexico, 1973. Jones, J.I., Ring, R.E., Rinkel, M.O. and Smith, R.E. (Eds.) State University of Florida System. pp. IIIF-1 - IIIF-10.

Horton, M. 1987. *The Human Settlement of the Red Sea.* In: Key Environments: Red Sea. Edwards, A.J. and Head, S.M. (Eds.) Pergamon Press. Oxford, New York, Beijing, Frankfurt, São Paulo, Sydney, Tokyo, Toronto. pp. 339-362.

Humm, H.J. 1973. *Seagrasses.* In: Summary of Knowledge of the Eastern Gulf of Mexico, 1973. Jones, J.I., Ring, R.E., Rinkel, M.O. and Smith, R.E. (Eds.) State University of Florida System. pp. IIIC-1 - IIIC-9.

Ibrekk, H.O., Molvoer, J, Faafeng, B. 1991. *Nutrient Loading to Norwegian Coastal Waters and its Contribution to the Pollution of the North Sea.* Water Science and Technology, V24 N10. pp. 239-249.

Jackson, J.B.C. 1977. *Competition on Marine hard substrata: the adaptative significance of solitary and colonial strategies.* American Nat, V3. pp. 743-767.

Jansson, Bengt-Owe. 1972. *Ecosystem Approach to the Baltic Problem. Bulletins From the Ecological Research Committee.* Swedish Nat. Sci. Res. Council. Stockhom, Ekologikommitten, Statens.

Johnson, M.A., MacAulay, M.C., and Biggs, D.C. 1984. *Respiration and Excretion Within a Mass Aggregation of Euphausia superba: Implications for Krill Distribution.* Journal of Crustacean Biology, V4. pp. 174-184.

Joiris, C. 1991. *Spring Distribution and Ecological role of Seabirds and Marine Mammals in the Weddell Sea, Antarctica.* Polar Biology, V11 N7. pp. 415-424.

Jones, D.A., Ghamrawy, M. and Wahben, M.I. 1987. *Littoral and Shallow Subtidal Environments.* In: Key Environments: Red Sea. Edwards, A.J. and Head, S.M. (Eds.) Pergamon Press. Oxford, New York, Beijing, Frankfurt, São Paulo, Sydney, Tokyo, Toronto. pp. 169-193.

Kaplan, E.H. 1982. *A Field Guide to Coral Reefs Caribbean and Florida.* Peterson, R.T. (Ed.) Houghton Mifflin Company. Boston, MA.

Karbe, L. 1987. *Hot Brines and the Deep Sea Environment.* In: Key Environments: Red Sea. Edwards, A.J. and Head, S.M. (Eds.) Pergamon Press. Oxford, New York, Beijing, Frankfurt, São Paulo, Sydney, Tokyo, Toronto. pp. 70-89.

Kaasik, T.O. 1989. *The Geography of the Baltic Region.* In: Comprehensive Security for the Baltic. Sage Publications. Westroy, A.H. (Ed.) London, Newbury Park, New Delhi.

Kang, S.H. and Fryxell, G.A. 1993. *Phytoplankton in the Weddell Sea, Antarctica: Composition, Abundance, and Distribution in the Water-Column Assemblages of the Marginal Ice-Edge Zone During Autral Autumn.* Marine Biology, V116. pp. 335-348.

Kastelein, R.A. and Lavaleije, M.S.S. 1992. *Foreign bodies in the stomach of a female Harbour porpoise (Phocoena phocoena) from the North Sea.* Aquatic Mammals, V18 N2. pp.40-46.

KFUPM/RI. 1988. *Marine Monitoring and Baseline Survey, V4, Oceanographic Studies.* Final Report prepared for the Australian Trade Commission by the Water Resources and Environment Division, Research Institute, King Fahd University of Petroleum and Minerals.

Khordagui, H.K. and Abu-Hilal, A.H. 1993. *Man-Made Litter on the Shores of the United Arab Emirates on the Arabian Gulf and the Gulf of Oman.* Water, Air, and Soil Pollution, V76. Kluwer Academic Publishers. pp. 343-352.

Kimor, B. 1973. *Plankton Relations of the Red Sea, Persian Gulf and Arabian Sea.* In: Ecological Studies 3: The Biology of the Indian Ocean. Zeitzschel, B. (Ed.) Springer-Verlag. New York, Heidelberg, Berlin. pp. 221-232.

Klages, N. 1989. *Food and Feeding Ecology of Emperor Penguins in the Eastern Weddell Sea.* Polar Biology, V9 N6. pp. 385-390.

Kullenberg, G. 1981. *Physical Oceanography.* In: The Baltic Sea. Voipio, A. (Ed.) Elsevier Scientific Publishing Company. Amsterdam, Oxford, New York. pp. 135-181.

Lancelot, C., Mathot, S, Veth, C. and Debaar, H. 1993. *Factors Controlling Phytoplankton Ice-Edge Blooms in the Marginal Ice-Zone of the Northwestern Weddell Sea During Sea Ice Retreat 1988 - Field Observations and Mathematical Modelling.* Polar Biology, V13 N6. pp. 377-387.

Lewis, J.B. 1977. *Processes of organic production on coral reefs.* Biology Review, V52. pp. 205-247.

Maldonado, A. 1985. *Evolution of the Mediterranean Basins and a Detailed Reconstruction of the Cenozoic Paleoceanography.* In: Key Environments: Western Mediterranean. Margalef, R. (Ed.) International Union for Conservation of Nature and Natural Resources. Oxford, New York, Toronto, Sydney, Frankfurt. pp. 17-59.

Margalef, R. 1985. *Introduction to the Mediterranean.* In: Key Environments: Western Mediterranean. Margalef, R. (Ed.) International Union for Conservation of Nature and Natural Resources. Oxford, New York, Toronto, Sydney, Frankfurt. pp. 1-16.

Margalef, R. 1971. *The Pelagic Ecosystem of the Caribbean Sea.* In: UNESCO-FAO Symposium on Investigations and Resources of the Caribbean Sea and Adjacent Regions, Curaçao, November 1968. UNESCO, Paris. pp. 483-496.

Mastaller, M. 1987. *Molluscs of the Red Sea.* In: Key Environments: Red Sea. Edwards, A.J. and Head, S.M. (Eds.) Pergamon Press. Oxford, New York, Beijing, Frankfurt, São Paulo, Sydney, Tokyo, Toronto. pp. 194-214.

McConnell, B.J, Chambers, C. and Fedak, M.A. 1992. *Foraging Ecology of Southern Elephant Seals in Relation to the Bathymetry and Productivity of the Southern Ocean.* Antarctic Science, V4 N4. pp. 393-398.

McIntyre, A.D. 1988. *Fisheries Resources.* In: Pollution of the North Sea: An Assessment. Salomons, W., Bayne, B.L., Duursma, E.K. and Forstner, U. (Eds). Department of agriculture and Fisheries for Scotland. Berlin; New York; Springer-Verlag. pp. 152-162.

Mee, L.D. 1992. The Black Sea in crisis: A need for concerted international action. AMBIO. V21. pp. 278-286.

Mergner, H. 1984. The Ecological Research on Coral Reefs of the Red Sea. Deep-Sea Research, V31A. pp. 855-884.

Mergner, H. and Mastaller, M. 1980. *Ecology of a Reef lagoon Area Near Aqaba (Red Sea).* In: Proceedings of the symposium on the coastal and marine environment of the Red Sea, Gulf of Aden and tropical western Indian Ocean Vol. III. The Red Sea and Gulf of Aden environmental programme. Jedah (ALESCO). pp. 39-76.

Mitchell, R. 1987. *Conservation of Marine Benthic Biocenoses in the North Sea and the Baltic: a Framework for the Establishment of a European Network of Marine Protected Areas in the North Sea and the Baltic.* European Committee for the Conservation of Nature and Natural Resources.

Munro, J.L. (Ed.) 1983. *Caribbean Coral Reef Fisheries Resources.* ICLARM, Manila, Philippines.

Nasu, K. 1981. *Recent Japanese Investigations of the Living Resources of the Southern Ocean.* In: Biological Investigations of Marine Antarctic Systems and Stocks (Biomass): Volume II: Selected Contributions to the Woods Hole Conference on Living Resources of the Southern Ocean 1976. Univ. Library, Cambridge, MA. pp. 99-105.

Natour and Nienhuis. 1980. *Some Phytoplanktonic Studies in Aqaba: Gulf of Jordan.* In: Proceedings of the symposium on the coastal and marine environment of the Red Sea, Gulf of Aden and tropical western Indian Ocean Vol. III. The Red Sea and Gulf of Aden environmental programme. Jedah (ALESCO). pp. 489-515.

NAVSEA 1993. *U.S. Navy Shipboard Solid and Plastics Waste Management Program Plan.* Naval Sea Systems Command.

Nelson-Smith, A. 1984. *Effects of Oil-Industry Related Pollution on Marine Resources of the Kuwait Action Plan Region.* In: Regional Seas: Combating oil pollution in the Kuwait Action Plan Region. UNEP Regional Seas Reports and Studies #44. United Nations Environment Programme. pp. 35-52.

Nybakken, J.W. 1982. *Marine Biology: An Ecological Approach.* Harper and Row, New York, New York.

Odium, H.T. 1972. *Ecosystem Approach to the Baltic Problem.* Bulletin from Ecological Research Committee of NFR, the Swedish Natural Sciences Research Council. N6.

Ogden, J.C. and Gladfelter, E.H. 1986. *Caribbean Coastal Marine Productivity*: Results of A Planning Workshop At Discovery Bay Marine Laboratory. University of The West Indies. Jamaica, Paris: UNESCO.

Ojaveer, E., Lindroth, A., Bagge, O., Lehtonen, H. and Toivonen, J. 1983. *Fishes and Fisheries.* In: The Baltic Sea. Voipio, A. (Ed.) Elsevier Scientific Publishing Company. Amsterdam, Oxford, New York. pp. 275-350.

Olson, T.M., Gill, S.E. and Alig, C.S. 1989. *Study of Solid and Plastic Waste Management Aboard USS Emory S. Land (AS 39).* David Taylor Research Center, Bethesda, MD. p. 45.

Ormond, R.F.G. 1987. *Conservation and Management.* In: Key Environments: Red Sea. Edwards, A.J. and Head, S.M. (Eds.) Pergamon Press. Oxford, New York, Beijing, Frankfurt, São Paulo, Sydney, Tokyo, Toronto. pp. 405-423.

Ormond, R.F.G. 1980. *Introduction.* In: Management and Conservation of Red Sea Habitats. Proceedings of the symposium on the coastal and marine environment of the Red Sea, Gulf of Aden and tropical western Indian Ocean Vol. III. The Red Sea and Gulf of Aden environmental programme. Jedah (ALESCO). pp. 135-162.

Ormond, R.F.G. and Edwards, A.J. 1987. *Red Sea Fishes.* In: Key Environments: Red Sea. Edwards, A.J. and Head, S.M. (Eds.) Pergamon Press. Oxford, New York, Beijing, Frankfurt, São Paulo, Sydney, Tokyo, Toronto. pp. 251-287.

Owre, H.B. and Foyo, M. 1971. *Studies on the zooplankton in the Caribbean Sea.* In: UNESCO-FAO Symposium on Investigations and Resources of the Caribbean Sea and Adjacent Regions, Curaçao, November 1968. UNESCO, Paris. pp. 503-508.

Pérès, J.M. 1967. *The Mediterranean Benthos.* In: Oceanography Marine Biology Annual Review 5. Barnes, H. (Ed.) pp. 449-533.

Pérès, J.M. 1982. *Major benthic assemblages.* Marine Ecology, V7. John Wiley, Chichester, London. pp. 523-582.

Pernetta, J. 1994. *Philips Atlas of the Oceans.* Reed Int. Books, Ltd. London.

Prevost, J. 1981. *Population, Biomass and Energy Requirements of Antarctic Birds.* In: Biological Investigations of Marine Antarctic Systems and Stocks (Biomass): Volume II: Selected Contributions to the Woods Hole Conference on Living Resources of the Southern Ocean 1976. Univ. Library, Cambridge, MA. pp. 125-137.

Price, A.R.G. 1979. *Temporal variations in abundance of penaeid shrimp larvae and oceanographic conditions off Ras Tanura, western Arabian Gulf.* Est. Coastal Marine Science, V9. pp.451-465.

Price, A.R.G. 1993. *The Gulf: Human Impacts and Management Initiatives.* Marine Pollution Bulletin, V27. Great Britain. pp. 17-27.

Price, A.R.G., Crossland, C.J., Shephard, A.R.D., McDowall, R.J., Medley, P.A.H., Smith, M.G.S., Ormond, R.F.G. and Wrathall, T.J. 1988. *Aspects of Seagrass Ecology along the Eastern Coast of the Red Sea.* Botanica Marina, V31. pp. 83-92.

Price, A.R.G., Mathews, C.P., Ingle, R.W. and Al-Rasheed, K. 1993. *Abundance of Zooplankton and Penaeid Shrimp Larvae in the Western Gulf*: Analysis of Pre-War (1991) and Post War Data. Marine Pollution Bulletin, V27. pp.273-278.

Price, A.R.G. and Sheppard, C.R. 1991. *The Gulf: Past, Present and Possible Future States.* Marine Pollution Bulletin, V22 N5. Great Britain. pp. 222-227.

Price, A.R.G., Sheppard, C.R. and Roberts, C.M. 1993. *The Gulf: Its Biological Setting.* Marine Pollution Bulletin, V27. Great Britain. pp. 9-15.

Rass, T.S. 1971. *Deep-Sea Fish in the Caribbean Sea and the Gulf of Mexico (the American Mediterranean Region).* In: UNESCO Symposium on Investigations and Resources of the Caribbean Sea and Adjacent Seas. Paris. pp. 509-526.

Rass, T.S. 1987. *Present Status of the Composition of the Black Sea Ichthyofauna.* Institute of Oceanology, Academy of Sciences of the USSR - IOAN, Moscow, V27 N3. pp. 64-72.

Rees, H.L. and Eleftheriou, A. 1989. *North Sea Benthos: A review of Field Investigations into the Biological Effects of Mans' Activities.* Journal du Conseil, V45. pp. 284-305.

Reijnders, P.J. and Lankester, K. 1990. *Status of Marine Mammals in the North Sea.* Netherlands Journal of Sea Research, V26 N2-4. pp.427-435.

Reynolds, R.M. 1993. *Physical Oceanography of the Gulf, Strait of Hormuz, and the Gulf of Oman - Results from the Mt Mitchell Expedition.* Marine Pollution Bulletin, V27. Great Britain. pp. 35-59.

Riegl, B. and Velimirov, B. 1991. *How many damaged corals in Red Sea reef systems? A quantitative survey.* Hydobiologia, V216/217. Kluwer Academic Publishers. pp. 249-256.

Rodriguez, G. 1974. *The Living Resources of the Caribbean and the Gulf of Mexico.* In: Caribbean Study and Dialogue *Pacem in Maribus.* International Oceanic Institute, Malta University Press.

Roper, C.F.E. 1981. *Cephalopods of the Southern Ocean Region: Potential Resources and Bibliography.* In: Biological Investigations of Marine Antarctic Systems and Stocks (Biomass): Volume II: Selected Contributions to the Woods Hole Conference on Living Resources of the Southern Ocean 1976. Univ. Library, Cambridge, MA. pp. 99-105.

Ros, J.D., Romero, J., Ballesteros, E. and Gili, J.M. 1985. Diving in Blue Water. *The Benthos.* In: Key Environments: Western Mediterranean. Margalef, R. (Ed.) International Union for Conservation of Nature and Natural Resources. Oxford, New York, Toronto, Sydney, Frankfurt. pp. 233-295.

Ross, D.A. and Stoffers, P. 1978. Report C: *General Data on Bottom Sediments Including Concentration of Various Elements and Hydrocarbons in the Persian Gulf and Gulf of Oman.* Woods Hole Oceanographic Institution. Technical Report: Unpublished Manuscript.

Salekhova, L.P., Kostenko, N.S., Bogachik, T.A. and Minibaeva, O.N. 1989. *Composition of Ichthyofauna in the Region of the Karadag State Reserve (Black Sea).* Journal of Ichthyology, V28 N2. pp. 16-23.

Salomons, W., Bayne, B.L., Duursma, E.K. and Förstner, U. (Eds.) 1988. *Pollution of the North Sea: An Assessment.* Berlin; New York; Springer-Verlag.

Sheppard, C.R.C. 1993. *Physical Environment of the Gulf Relevant to Marine Pollution: An Overview.* Marine Pollution Bulletin, V27. Great Britain. pp. 3-8.

Sheppard, C.R.C., Price, A.R.G. and Roberts, C.M. 1992. *Marine Ecology of the Arabian Region: Patterns and Processes in Extreme Tropical Environments.* Academic Press. London.

Shushkina, E.A. and Vinogradov, M.Y.E. 1991. *Long-Term Changes in the Biomass of Plankton in Open Areas of the Black Sea.* Oceanology, V31 N6. pp. 716-721.

Siegel, V., Bertstrom, B., Stromberg, J.O. and Schalk, P.H. 1992. *Distribution, Size Frequencies and Maturity Stages of Krill, Euphausia superba, in Relation to Sea-Ice in the Northern Weddell Sea.* Polar Biology, V10 N7. pp. 549-557.

Sorokin, Y.I. 1988. *The Black Sea.* In: Ecosystems of the World. Postma, H. and Zijlstra, J.J. (Eds) Elsevier Science Publishers. Amsterdam, Oxford; New York; Tokyo. pp. 231-278.

Smith, W.O. and Nelson, D.M. 1986. *Importance of Ice Edge Phytoplankton Production in the Southern Ocean.* Biological Science, V36. pp.251-257. (cited in Kang and Fryxell, 1993)

Stromme, T. 1987. *Annex IV Sectoral Report on Marine Living Resources.* In: Coastal and Marine Environmental Problems of Somalia. UNEP Regional Seas Reports and Studies #84. Annexes. pp. 88-110.

Suarez-Caabro, J.A. 1990. *An Overview of the Fisheries of the Caribbean and Adjacent Seas.* Proceedings of the 43rd Gulf and Caribbean Fisheries Institute. pp. 292-305.

Sverdrup, H.U., Johnson, M.W. and Feming, R.H. 1942. **The Oceans**. Prentice Hall, New Jersey.

Tawfiq, N.I. and Olsen, D.A. 1993. *Saudi Arabia's Response to the 1991 Gulf Oil Spill.* Marine Pollution Bulletin, V27. Great Britain. pp. 333-345.

The World Bank. 1990. *The Environmental Program for the Mediterranean: Preserving a Shared Heritage and Managing a Common Resource.* World Bank; Luxembourg: European Investment Bank, Washington D.C., USA.

Thiel, H. 1987. *Benthos of the Deep Red Sea.* In: Key Environments: Red Sea. Edwards, A.J. and Head, S.M. (Eds.) Pergamon Press. Oxford, New York, Beijing, Frankfurt, São Paulo, Sydney, Tokyo, Toronto. pp. 112-127.

Thiel, H. and Weikert, H. 1984. *Biological Oceanography of the Red Sea Oceanic System.* Deep-Sea Research, V31A. pp.829-831.

Thurman, H.V. 1975. *Introductory Oceanography.* Charles E. Merrill Publishing Company, Columbus Ohio.

Thurow, F. 1989. *Fishery Resources of the Baltic Region.* In: Comprehensive Security for the Baltic. Westroy, A.H. (Ed.) Sage Publications. London, Newbury Park, New Delhi.

Timberlake, L. 1983. *The Improbable Treaty: The Cartagena Convention and the Caribbean Environment.* Tinker, J. and Cheney, B. (Eds.) Earthscan. London, England.

Tortonese, E. 1985. *Distribution and Ecology of Endemic Elements in the Mediterranean Fauna (Fishes and Echinoderms).* In: Mediterranean Marine Ecosystems. Moraitou-Apostolopoulou, M. and Kiortsis, V. (Eds.) NATO Scientific Affairs Division. New York, London. pp. 57-83.

Underwood, P.C. 1989. *The Marine Environment and Ocean Development in the Eastern Caribbean.* In: New Law of The Sea For The Caribbean - An Examination Of Marine Law and Policy Issues In The Lesser Antilles. Gold, E. (Ed.) **Lecture Notes on Coastal and Estuarine Studies**, V27. Springer-Verlag. pp. 112-142.

Vauk, G. and Schrey, E. 1987. *Litter Pollution from Ships in the German Bight.* Marine Pollution Bulletin, V18 N6B. pp. 316-319.

Venizelos, L.E. 1990. *The Endangered Loggerheads of Zakynthos (Greece): A Part of the Mediterranean Sea Turtle Conservation Issue.* The Formation of MEDASSET (Mediterranean Association to Save the Sea Turtles). Thalassographica. V13, suppl. 1. pp. 53-59.

Vine, P. 1985. *The Red Sea.* IMMEL Publishing. London, Jeddah.

Wabeh, M.I. 1980. *Studies on the ecology and productivity of the seagrass Halophila stipulacea, and some associated organisms in the Gulf of Aqaba (Jordan).* Ph.D. Thesis, University of New York, U.K.

Walker, D.I. and Ormond, R.F.G. 1982. *Coral Death from Sewage and Phosphate Pollution at Aqaba, Red Sea.* Marine Pollution Bulletin, V13 N1. Pergamon Press, Ltd. pp. 21-25.

Watermann, B. and Kranz, H. 1992. *Pollution and Fish Diseases in the North Sea; Some Historical Aspects.* Marine Pollution Bulletin, V24 N3, pp. 131-138.

Weikert, H. 1987. *Plankton and the Pelagic Environment.* In: Key Environments: Red Sea. Edwards, A.J. and Head, S.M. (Eds.) Pergamon Press. Oxford, New York, Beijing, Frankfurt, São Paulo, Sydney, Tokyo, Toronto. pp. 90-111.

White, M.G. and Piatkowski, U. 1993. *Abundance, Horizontal and Vertical Distribution of Fish in Eastern Weddell Sea Micronekton.* Polar Biology, V13 N1. pp. 41-53.

Winterhalter, B., Flodén, T., Ihnatius, H., Axberg, S. and Niemistö, L. 1981. *Geology of the Baltic Sea.* In: The Baltic Sea. Voipio, A. (Ed.) Elsevier Scientific Publishing Company. Amsterdam, Oxford, New York. pp. 1-117.

Wolf, P.DE. and Zijlstra, J.J. 1988. *The Ecosystem.* In: Pollution in the North Sea: An Assessment. Salomons, W., Bayne, B.L., Duursma, E.K. and Forstner, U. (Eds.) Berlin; New York; Springer-Verlag. pp. 118-144.

Woolfenden, G.E. and Schreiber, R.W. 1973. *The Common Birds of the Saline Habitats of the Eastern Gulf of Mexico: Their Distribution, Seasonal Status, and Feeding Ecology.* In: Summary of Knowledge of the Eastern Gulf of Mexico, 1973. Jones, J.I., Ring, R.E., Rinkel, M.O. and Smith, R.E. (Eds.) State University of Florida System. pp. IIIJ-1 - IIIJ-22.

Zijlstra, J.J. 1988. *The North Sea Ecosystem.* In: Ecosystems of the World. Postma, H. and Zijlstra, J.J. (Eds.) Elsevier Science Publishers. Amsterdam; Oxford; New York; Tokyo. pp. 231-278.

Zmudzinski, L. 1989. *Environmental Quality in the Baltic Region.* In: Comprehensive Security for the Baltic. Westroy, A.H. (Ed.) Sage Publications. London, Newbury Park, New Delhi.

4.2 ANALYSIS OF POTENTIAL EFFECTS OF U.S. NAVY SHIPBOARD SOLID WASTE DISCHARGES ON MARINE THREATENED AND ENDANGERED SPECIES

by Dr. D. Bart Chadwick, Stacey L. Curtis, Charles N. Katz

INTRODUCTION

As part of a fate and effects study of U.S. Navy shipboard solid waste discharges (Chadwick et al., 1996), SSC San Diego has examined some of the available information relevant to assessing the potential for impacts to endangered species in MARPOL Special Areas and in the world's oceans. This work was initiated by concerns as to whether burlap bags containing shredded metal and glass discharged from U.S. Navy ships could pose a significant risk to endangered species through ingestion. The assessment included the following primary objectives relevant to shredded waste discharges: 1) to identify threatened and endangered species found in the world's oceans and specifically those found within MARPOL Special Areas; 2) to identify behavioral patterns inherent for each listed species which would influence their potential to encounter and ingest wastes; 3) to determine the abundance and distribution of proposed solid waste discharges given historical U.S. Navy operations; and 4) to qualitatively evaluate the potential for impact to threatened and endangered species populations given the estimated likelihood of exposure. The findings represent a qualitative review of relevant information needed in assessing the likelihood of impact. The assessment is based on the potential for detrimental effects arising from ingestion. In general, quantitative analysis of impacts of solid waste discharges on endangered species is limited by a lack of applicable data.

BACKGROUND

Effects of trash on marine species to date have been primarily caused by coastal sources, fishing, oil, or plastics (for review see Ridgway and Harrison, 1985). The concerns that are generally raised in the literature include:

Ingestion of plastics, other debris, tar balls or sharp objects such as fish hooks

Entanglement of species from fishing nets or litter

Toxicity due to contaminants associated with debris or oil spills

Collision with ships (whales)

Some marine species have been known to ingest or become entangled with debris such as plastics or impacted by oil (Gramentz, 1988; Venizelos, 1990). The risk of harm from ingestion is partly a function of size of the organism, its feeding characteristics, and its proximity to the discharged waste (Merkel and Associates, Inc., 1996).

Results of work performed on U.S. Navy Shipboard solid waste discharges indicate that burlap bags containing metal and glass wastes sink rapidly to the sea floor (0.5 $m \cdot s^{-1}$) in all seas (Chadwick et al., 1996). As a result, the waste stream has a minimal impact in the water column and, thus, processes occurring on the sea floor will determine its potential effects. Furthermore, the high sinking rate minimizes lateral transport of burlap bags from the discharge point which will occur in waters outside a 12-nmi discharge limit from shore. The filled burlap bags weigh approximately 5 kg and have the approximate diameter of 0.6 m. The average bag components by percent weight are as follows: tins

cans, 80.76%; burlap 8.75%; glass 4.50%; organics 2.31%; aluminum 1.92%; and paper 1.76%. Once deposited on the ocean bottom, the burlap bag and its contents are subject to corrosion, burial, and fouling. Given these general findings, only threatened and endangered species likely to come into contact with the sea floor are expected to have potential for exposure.

The issue of toxicity of the shredded metal and glass is not seen as relevant to threatened and endangered species. The waste stream was subjected to toxicity testing on a wide range of organisms including marine bacteria, phytoplankton, zooplankton, benthic invertebrates, and fish (Chadwick et al., 1996). The toxicity tests performed showed only limited effects to plankton causing an inhibition of light output or a reduction in growth rates. It was estimated that these effects were unlikely to be seen outside the burlap bag itself. There is no evidence to suggest that these effects would be significant to larger marine organisms through ingestion.

APPROACH

The first step in this assessment was to review U.S. and foreign endangered species lists to identify those species living in the marine environment and to obtain their general distribution in the ocean or in Special Areas. Only oceanic species were considered and birds were excluded from consideration because studies have shown that the material packaged in burlap bags does not break on impact with the sea surface and sinks rapidly through the water column (Chadwick et al., 1996). The next step was to identify typical feeding or other behaviors for each species to qualitatively assess the likelihood that these behaviors might lead to ingestion of the solid waste. The third step was to assess the likelihood of exposure to animals potentially at risk from ingestion. The final step was to qualitatively summarize the overall likelihood of an individual encountering the waste in its environment and being harmed during its normal range of behaviors.

The data used in this analysis come primarily from the following sources:

- ***Identification and General Distribution of Threatened and Endangered Species:*** U.S. and Foreign threatened and endangered species lists were obtained from the United States Fish and Wildlife Service database, 1996
- ***Typical Behavior Patterns:*** Available information on typical feeding habits and movements common to the species of concern which may influence their exposure to U.S. Navy solid waste discharges were obtained from the scientific literature (see reference list).
- ***Navy Operations and Discharge Quantities:*** Ship operations within Special Areas and generation rates of shredded waste were obtained from the CNO EMPSKD database and Chadwick et al., 1996. At the time of this assessment data on U.S. Navy ship operations outside of Special Areas were unavailable.

IDENTIFICATION AND GENERAL DISTRIBUTION OF THREATENED AND ENDANGERED SPECIES

Threatened and endangered species found in the world's oceans (USFWS, 1996) and those common in each of the Special Areas are listed in Tables 4.2-1 and 4.2-2 (for review see Merkel and Associates, Inc., 1996; and Ridgway and Harrison, 1981a, 1981b, 1985, 1989). Some species, particularly whales and sea turtles, can be migratory and their distribution and abundance is not precisely known. Historically, species have become threatened or endangered due to over hunting, habitat destruction from coastal development, or interference with nursing or nesting areas. There are still many unknowns with regard to some species and assumptions in this report are based on the best data currently available. For a concise reference of the threatened and endangered species distribution, habitat preferences, feeding behaviors, and current population status see Table 4.2-5 at the end of the report.

COMMON BEHAVIORS OF THREATENED AND ENDANGERED SPECIES

Sea Cows. Much of the information on Dugongs (*Dugong dugong*) used in this analysis comes from the work of Nishiwaki and Marsh, 1985. Dugongs are found primarily in tropical and subtropical coastal and island waters of the Indo Pacific. Aerial surveys have shown that dugongs tend to occur in warm (~18-33°C) shallow, sheltered inshore and reef areas where extensive beds of seagrasses occur. Dugongs usually remain offshore during daylight hours and come inshore to feed only at night. Analysis of stomach contents indicates that dugongs consume a wide variety of tropical and subtropical seagrasses. Algae are also eaten but only in small quantities if seagrasses are abundant. Exploitation includes netting for food, and to make products with medicinal and aphrodisiac properties. The total population size is unknown. Dugongs are benthic feeders, however, they generally feed inshore and are relatively selective in their food choices. They are therefore considered to have a very low likelihood of encountering and ingesting solid waste.

West Indian manatees (*Trichechus manatus*) are found throughout the Wider Caribbean Basin, the Gulf of Mexico, and the Atlantic coast. West African manatees *(Trichechus inunguis)* range from Senegal to Angola on the west coast of Africa. They generally inhabit coastal areas, as well as estuaries and rivers. They are mostly herbivorous, opportunistic feeders. They are not known to be a deep-water species, with approximately 10 m being the greatest depth to which an individual has been seen diving (Hartman, 1971). The manatee has been taken for food, oil and leather. Indirectly, manatees have been harmed by alterations in their habitat including the disposal of sewage and other wastes from shore, dredging and fill projects, and potentially by oil spills from offshore drilling and shipping. The population of the West Indian manatee is estimated to have been several thousand when the Europeans arrived in what is now the United States. Surveys done in Florida in the 1970's estimated a population of approximately 800 to 1000 individuals (Brownell et al., 1978). Population studies of West African manatees are inadequate to determine reliable population numbers. Manatees, even more so than dugongs, prefer to dwell in inshore areas and the likelihood of encountering and ingesting discharged waste is considered to be very low.

Table 4.2-1. Listed U.S. and Foreign Threatened and Endangered Species in the world oceans. (Source: U.S. Fish and Wildlife Service, Division of Endangered Species, July 1996).

Species Category	Common Name	Threat status	General Distribution
Sea Cows	Dugong	Endangered	Indo-Pacific tropical and subtropical shallow coastal and island waters: northern Indian Ocean from Madagascar to Indonesia; Philippines; Australia; southern China; Palau.
	West African Manatee	Threatened	West Coast of Africa from Senegal River to Cuanza River.
	West Indian Manatee	Endangered	Coastal waters of Atlantic Ocean, Gulf of Mexico, and Caribbean Sea from southeastern United States to northeastern Brazil and Greater Antilles and Trinidad and Tobago Islands.
Otters	Marine Otter	Endangered	Southeast Pacific coast from Peru to Straits of Magellan.
	Southern Sea Otter	Threatened	Northeast Pacific Coast from Pribilof Islands to California.
Seals/Sea-Lions	Stellar/Northern Sea-Lion	Threatened	Central Kuril Islands to Ano Nuevo Island, California (primarily Gulf of Alaska and Aleutian Islands).
	Guadalupe Fur Seal	Threatened	Guadalupe Island, 200km west of Baja California, to southern California Channel Islands (primarily San Miguel and San Nicolas Islands).
(EXTINCT?)	Caribbean Monk Seal	Endangered	Western Caribbean to Bahamas to Florida Keys.
	Hawaiian Monk Seal	Endangered	Hawaiian Islands
	Mediterranean Monk Seal	Endangered	Southern and western Black Sea to Atlantic coast of Morocco and Mauritania to Madeira Islands.
Turtles	Green Sea Turtle	Threatened	Global tropical to subarctic ocean waters. Endangered on the Florida coast.
	Hawksbill Sea Turtle	Endangered	Global tropical to subtropical ocean waters (juveniles pelagic, adults primarily inhabit reef and mangrove areas).
	Kemp's Ridley Sea Turtle	Endangered	Coastal waters and bays of Gulf of Mexico and Atlantic Ocean.
	Leatherback Sea Turtle	Endangered	Global ocean waters. Primarily nesting on Pacific shores of the American tropics, in the Guianas and tropical West Africa.
	Loggerhead Sea Turtle	Threatened	Global temperate, subtropical and tropical waters along continental shelves, and in bays, estuaries and lagoons.
	Olive Ridley Sea Turtle	Threatened	Global ocean waters. Primarily nesting on Pacific shores of the American tropics, in the Guianas and tropical West Africa.
Whales	Blue Whale	Endangered	Global ocean waters.
	Bowhead Whale	Endangered	Arctic waters >50° N.
	Finback Whale	Endangered	Global ocean waters.
	Gray Whale	Endangered	Northwest Pacific coast (Korean stock)
	Humpback Whale	Endangered	Global ocean waters.
	Northern Right Whale	Endangered	25°-60° N (Pacific) 30°-75° N (Atlantic) ocean waters.
	Southern Right Whale	Endangered	20°-50° S ocean waters.
	Sei Whale	Endangered	Global in temperate ocean waters.
	Sperm Whale	Endangered	Global in temperate and tropical ocean waters, generally between 50° N and 50° S. Known to enter the Mediterranean Sea.

Table 4.2-2. Listed U.S. and Foreign Threatened and Endangered Species found within MARPOL Special Areas.

Special Area	Species
Antarctica	fin whale, blue whale, humpback whale, sperm whale, sei whale
Baltic Sea	loggerhead turtle, possibly fin whale, blue whale, and sei whale
North Sea	leatherback and possibly other turtles, and possibly fin whale, blue whale, and sei whale
Black Sea	monk seal
Mediterranean Sea	loggerhead turtle, monk seal, green turtle, fin whale, blue whale, sei whale, and sperm whale
Red Sea	dugong and five species of turtles
Wider Caribbean Basin	manatees, all six species of turtles, fin whale, blue whale, humpback whale, sei whale, right whale
The Gulfs Area	dugong, hawksbill turtle, green turtle, fin whale, blue whale, sei whale

Sea Otters. The sea otters listed on the U.S. and foreign endangered species lists are the southern sea otter and the marine otter. Southern sea otters (*Enhydra lutris nereis*) inhabit coastal regions in the North Pacific from as far south as Baja California and extending along North American and Canadian coasts out past the Aleutian Islands to Kamchatka and the Kurii Islands. The marine otters (*Lutra felina*) generally occur along the coasts of Peru south to Straits of Magellan. Little information is available on species of marine otters but they are assumed to have the same general behaviors as sea otters. Sea otters are not migratory, however, individuals can wander long distances along the coastlines (Kenyon, 1981a). They generally feed on sea urchins, molluscs, mussels, clams, and sometimes fish. They dive for food and typically remain underwater for approximately 1 minute, bringing their prey back to the surface where they crush it with their paws and pass it to their mouths. Where food is abundant they, feed in shallow waters of approximately 3- to 9-m depth. During aerial surveys, Kenyon (1981a) has found that the majority of otters are within the 55 m curves, although they have been known to dive to 75 m and there is a record of one diving to 97 m. Sea otters have been primarily exploited for their fur. By the time they were put under protection, some believed that their population was so depleted that they would not recover. However, they have survived on the most remote and hostile shores and have increased in population over the past several decades. The total population in the late 1970s was estimated to be at least 100,000 and may be as high as 150,000 currently (Kenyon, 1981a). Although they do feed on the bottom, they are typically in shallow in-shore waters. Additionally, their feeding behavior is fairly specialized and if they were to encounter trash, they are not likely to mistake it for food which they crack open on the surface. Thus, they have a very low likelihood of ingesting solid wastes from the sea floor.

Sea- Lions and Seals. The Steller or northern sea lion (*Eumetopias jubatus*) was recently added to the U.S. threatened list in 1990. Its centers of abundance and distribution are the Gulf of Alaska and Aleutian Islands although they are found as far east as Kamchatka and the Kurii Islands and as far south as San Miguel Island off of southern California. Steller sea lions feed near land, from approximately 5 to 20 nmi offshore. They generally feed at night but also have been known to hunt during the day. They

are opportunistic predators, and although their food preferences and feeding behaviors have not been studied in depth, they are known to feed on fish, squid, octopus, bivalves, shrimp and crabs. Most of the prey found in the stomachs of Steller sea lions indicates that they dive to depths of approximately 180 m (Fiscus et al., 1966).

Sea lions, reported to be abundant along the California coast and offshore islands before 1860, were exploited for food, oil, and clothing. In addition, until passage of the MMPA in 1972, commercial and sport fishermen were allowed to kill sea lions that interfered with their fishing operations. Their populations still seem to be decreasing. Species abundance estimates during the late 1970s ranged from 248,000 to 300,000 adult and juvenile animals. However, counts at rookeries and haulout sites throughout most of Alaska and the USSR in 1989, plus estimates from surveys conducted in recent years at locations not counted in 1989, provide a range-wide Steller sea lion population estimate of about 116,000 (NMFS, 1996). They are known to be able to dive up to 180 m and do occasionally wander out to sea, however, they are fairly selective feeders and the majority of their feeding grounds are near shore giving them a very low likelihood of ingestion.

Three genera of monk seals are on the U.S. and foreign threatened and endangered species lists, the Caribbean monk seal (*Monachus tropicalis*), the Hawaiian monk seal (*Monachus schauinslandi*), and the Mediterranean monk seal (*Monachus monachus*). Hawaiian monk seals inhabit and breed regularly on the Leeward (Northwestern) Hawaiian Islands. Mediterranean monk seals have traditionally lived near remote coastlines and offshore islands which were free from human intervention. They feed usually in less than 30-m depth on a variety of organisms including barouni, synagrida, gopa, kephalos, chicharres, pargo, ray, and octopus, although there have been reports of diving to deeper depths (Kenyon, 1981b). Additionally, the Hawaiian monk seals are thought to prey on pelagic species while traveling long distances in the open ocean. They seem to be pushed near extinction by increased accessibility to their habitats, which brings growing intensity of fishing and entanglement and disturbance of pregnant females, thereby reduced reproduction. The Mediterranean monk seal probably numbers in several hundred to one thousand including the Mediterranean and the Black Sea areas (Kenyon, 1981b), the Hawaiian monk seal is thought by NMFS to number approximately 1400, and although the Caribbean monk seal is still listed on the endangered species list it is apparently extinct. Monk seals, in general, are selective feeders in shallow water, which gives them a very low likelihood of ingesting solid waste.

The Guadaloupe fur seal (*Arctocephalus townsendi*) is the only southern fur seal known to inhabit waters north of the equator. The species was thought to be extinct until living fur seals were sighted at Guadaloupe Island off the coast of Baja California in 1954 (Bonner, 1981a). Southern fur seals generally live in colonies on isolated rocks or islets, or on oceanic islands. Fur seals eat a wide variety of food, ranging from marine invertebrates to pelagic schooling fish to penguins. Stones are often found in the stomachs of seals and their function is unknown (Bonner, 1981a). They feed at various levels in the sea, some species eating primarily in the surface waters and others capturing bottom-dwelling forms, at times, such as octopus and rock-lobsters. It is not known how deep they can dive, however, divers have sighted them at 39 m and they probably can go as deep as 120 m. Early exploitation decreased southern fur seal populations throughout their range. Currently, threats to existing stocks include destruction by fishermen and tourists, and occasionally by illicit hunters. A population count as of 1979 estimated approximately 500 individuals (Hubbs, 1979). As with the other pinnipeds, these seals are considered to have a very low likelihood of ingestion due to their feeding habits.

Turtles. Sea turtles are generally migratory and inhabit most of the world's oceans. Under the Endangered Species Act, all marine turtles are listed either as endangered or threatened on the U.S. list, and one, the olive ridley turtle, is listed on the foreign list. Historical data on sea turtle numbers are

limited. In addition, the length of time that data have been collected has been short when compared with the long life and low reproductive rate of all turtle species. Therefore, it is difficult to assess their long-term status. Much of the information below on sea turtle species comes directly from The Endangered and Threatened Species of the Southeastern United States (The Red Book) and from the U.S. Fish and Wildlife Service.

Green Sea Turtle (*Chelonia mydas*). The green turtle is found in tropical and temperate seas and oceans. They are generally found in fairly shallow waters (except when migrating) inside reefs, bays, and inlets, and are attracted to lagoons and shoals with an abundance of marine grass and algae. Adult green turtles feed primarily on marine algae and grasses in very shallow water areas. They may also occasionally consume small molluscs, sponges, crustaceans, and jellyfish; however, they are generally known to be vegetarians. They are not known to feed during migrations (NMFS, personal communication). Hatchlings have been observed to seek refuge and food in sargassum clumps. Green turtles have an estimated population of no more than 600,000 adults worldwide (USFWS, 1996). Because green turtles are primarily non-selective benthic feeders, it is uncertain whether they would ingest the bagged waste, thus the likelihood of ingestion can only be assessed based on their potential for exposure to solid wastes.

Hawksbill Sea Turtle (*Eretmochelys imbricata*). The hawksbill is found in tropical and subtropical seas of the Atlantic, Pacific, and Indian Oceans. Hawksbills frequent coral reefs, shallow rocky areas, coastal areas, lagoons or oceanic islands, and narrow creeks and passes. They are seldom seen in water deeper than 20 m (NMFS/USFWS, 1993), and hatchlings are often found floating in masses of sea plants. Hawksbills feed on the bottom and forage close to shores and reefs. This species is omnivorous, but has a preference for invertebrates. The diet has been observed to include algae, mangrove, fish, barnacles, molluscs, sponges, sea urchins, hydroids, and ectoprocts. The hawksbill has been heavily exploited primarily for its' shell and, secondarily, for eggs, meat, and use of the skin for leather. Continued trade of products from this species suggests that further declines are possible. Although no population estimates are available, total numbers are known to be low. Because hawksbill turtles are primarily non-selective benthic feeders, it is uncertain whether they would ingest the bagged waste, thus the likelihood of ingestion can only be assessed based on their potential for exposure to solid wastes.

Kemp's (Atlantic) Ridley Sea Turtle (*Lepidochelys kempii*). Adults are restricted to the Gulf of Mexico, but juveniles have been observed along the Atlantic coast as far north as Massachusetts. Outside of nesting, the major habitat for Kemp's ridleys is the nearshore and inshore waters of the northern Gulf of Mexico, especially Louisiana waters, and they are often found in salt marsh habitats. They are primarily inshore benthic feeders in less than 100 to 200 m and they feed in the water column when they are migrating (NMFS, personal communication). This turtle's diet consists primarily of invertebrates, mostly crabs, but it also includes shrimp, snails, sea urchins, sea stars, medusae, fish, and occasionally, marine plants. Over harvesting of both eggs and adults for food and the skin has been a major factor in the decline. Currently the major threat is drowning when inadvertently caught in shrimp nets. In 1947, on a single day, 40,000 females were seen nesting on one beach alone. Currently, only about 700 to800 female Kemp's Ridley turtles nest annually along a limited portion of Mexico's Gulf coast. Because Kemp's Ridley turtles are primarily non-selective benthic feeders, it is uncertain whether they would ingest the bagged waste, thus the likelihood of ingestion can only be assessed based on their potential for exposure to solid wastes.

Leatherback Sea Turtle (*Dermochelys coriacea*). The leatherback turtle is distributed worldwide in tropical and temperate waters of the Atlantic, Pacific, and Indian Oceans. It is also found in small numbers as far north as British Columbia, Newfoundland, and the British Isles, as far south as Australia, Cape of Good Hope, and Argentina. The leatherback is the most pelagic of the sea turtles and is often observed near the edge of the continental shelf. However, they are also observed just offshore of the surf

line. They feed in the water column and are known to dive deeply, down to 900 m and commonly to 300 to 400 m (NMFS, verbal communication). The principal food is jellyfish, but the diet is also known to include sea urchins, squid, crustaceans, tunicates, fish, blue-green algae, and floating seaweed. The decline is considered primarily to be the result of exploitation by humans, mostly through consumption of the eggs, although the meat is also eaten. Exposure and vulnerability while nesting make the turtles highly susceptible to overuse. Increasing beach development and utilization are also detrimental, as sea turtles require relatively undisturbed beaches for nesting. Further losses occur through drowning when the turtles are accidentally caught in the nets of commercial shrimping and fishing trawlers, and by capture in longline and driftnet fisheries. The world female breeding population is about 29,000 to 40,000 turtles. Numbers on total populations are inconclusive. Because leatherback turtles are primarily water column feeders it is unlikely that they would ingest bagged waste on the sea floor.

Loggerhead Sea Turtle (*Caretta caretta*). The loggerhead is found in temperate and subtropical waters, worldwide, with major nesting beaches in eastern Australia, Sultanate of Oman, and the southeastern United States. The loggerhead is widely distributed within its range. It may be found hundreds of miles out to sea, as well as in inshore areas such as bays, lagoons, salt marshes, creeks, ship channels, and the mouths of large rivers. Nesting occurs mainly on open beaches or along narrow bays having suitable soil, and it is often in association with other species of sea turtles. Loggerheads apparently migrate over long distances with tagged specimens being recaptured 1200 to 1500 nmi from the point of release. Coral reefs, rocky places, and ship wrecks are often used as feeding areas. They are primarily benthic feeders in less than 100 to 200 m and they feed in the water column while migrating (NMFS, personal communication). This species feeds on molluscs, crustaceans, fish, and other marine animals. Threats include loss of nesting beaches to various types of human activities, excessive natural predation in some areas, inadvertent drownings when the turtles become trapped in fishing and shrimping trawls, marine pollution from oil, plastics, and styrofoam; and the lack of adequate regulatory mechanisms. Current worldwide nesting estimates range from 40,000 to 50,000 nests annually. Because loggerhead turtles are primarily non-selective benthic feeders, it is uncertain whether they would ingest the bagged waste, thus the likelihood of ingestion can only be assessed based on their potential for exposure to solid wastes.

Olive (Pacific) Ridley Sea Turtle (*Lepidochelys olivacea*): The olive ridley sea turtle is found in global ocean waters. The primary nesting areas are on the Pacific shores of the American tropics, in the Guianas and tropical West Africa. Like the loggerhead and other Kemp's Ridley turtles, they are primarily benthic feeders in less than 100 to 200 m and feed in the water column during migration (NMFS, personal communication). They feed primarily on crabs, shrimp, rock lobsters, jellyfish, tunicates, and reportedly algae. Both eggs and adults are being heavily exploited. Olive Ridleys in Mexico have been over harvested for international trade with Japan. There is evidence that the turtles are often being captured in shrimp trawls and gill nets. There are no available data on worldwide populations. Because Olive Ridley turtles are primarily non-selective benthic feeders it is uncertain whether they would ingest the bagged waste, thus the likelihood of ingestion can only be assessed based on their potential for exposure to solid wastes.

In general, sea turtles prefer coastal regions and estuaries, bays, lagoons and, sometimes, even marshes and fresh water areas (Brown, 1976) although they are known to migrate long distances across the ocean. The leatherback seems to be an exception to this and, although sighted in inshore waters, is thought to usually reside off shore. Most sea turtles are omnivorous and feed on seaweeds and eelgrasses as well as small crustaceans, molluscs, jellyfish, some fish, snails, sea urchins, and even squid and octopus, although the green turtles are primarily vegetarian. They mostly forage non-selectively in relatively shallow bottom areas or feed in the water column during migration (depending on the species). Threats to turtles have historically been from fishermen and shrimp trawlers, and commercial uses. The greatest current threat to sea turtles probably is beach destruction which interferes with habitats used for nesting

(Brown, 1976). Coastal development is reducing nesting, egg incubation, and foraging habitats. Other factors also contribute to the low population total. These include the increasing number of snorklers and scuba divers who spear turtles for sport or profit and the large scale loss of eggs and hatchlings to natural predators. Also, turtles are known to mistake plastics for jellyfish, and do ingest other pollutants such as tar balls and oil, etc. Floating tar balls and plastics, if eaten, can harm or kill sea turtles. The magnitude of these problems is not fully known, but they occur worldwide, and prompt international cooperation for marine turtle protection and recovery (NMFS, 1996). Because all of the turtles, except the leatherback, are primarily non-selective benthic feeders, it is uncertain whether they would ingest the bagged waste, thus the likelihood of ingestion can only be assessed based on their potential for exposure to solid wastes.

Whales. Much of the anecdotal and biological data discussed below have comprehensive reviews taken directly from a National Marine Fisheries Service (NMFS) report entitled "The Status of Endangered Whales" (Marine Fisheries Review, 1984), reports from Hubbs Sea World, and "The Handbook of Marine Mammals" (Vol. 3, Ridgway and Harrison, 1985; Vol. 4, Ridgway and Harrison, 1989).

There are currently seven species of cetaceans in U.S. waters that are protected under the Endangered Species Act. They are the blue whale, the bowhead whale, the fin whale, the humpback whale, the northern right whale, the sei whale, and the sperm whale. All seven species are listed as endangered. The gray whale was taken off the U.S. list in 1993, however, due to a small population in the Northwest Pacific (the Korean stock), they remain on the foreign list.

Except for the sperm whale, which is a toothed whale, all of the listed whales are baleen whales. Baleen whales have a unique adaptation for feeding which consists of a series of plates arranged inside the mouth, and bristles which intertwine to form a mat that is used as a sieve. Baleen whales generally feed by sifting water through these plates and collecting small invertebrates in the process. They usually feed in the upper water column at various levels of the food chain except the gray whale, which is known to be primarily a bottom feeder. There are variations in their feeding habits according to the individual species. Many species feed on zooplankton such as copepods and small crustaceans such as amphipods, euphausiids, and mysids. Some are also known to feed on squids and fishes. The type of prey may determine how a specific species feeds. Baleen whales typically feed by one of three ways (as reviewed in Leatherwood and Reeves, 1983):

1) "by opening the mouth wide, taking in a large quantity of water, and then closing the mouth, forcing the water out and collecting on the mat of bristles the plankton or fish the water contains" (known as "lunging or gulping");

2) "by swimming through the water, mouth ajar, allowing the water to flow in through the gap at the front of the mouth between the two rows of baleen plates, and out through the gaps between the side plates, leaving the particles of food behind" (known as "skimming"); and

3) "by using the suction created when the tongue is pressed against the palate to draw water and food into the mouth, then squeezing the water out with another movement of the tongue."

Variations in the typical feeding methods can be seen in some species such as the humpback and gray whales. The humpback whale has been observed to construct bubble nets around a school of fish and then lunge up through the bubble net to get their food. The gray whale feeds off the sea floor by "scooping" material up into their baleen.

The baleen whales are found worldwide and most of them are migratory. Currently, their abundance varies from a few hundred to over a hundred thousand, depending on the species. Two species in particular show the opposite extremes of what can happen with regard to recovery of the populations. Both the gray whale off of the west coast of North America and the right whale off of the east coast were hunted to the verge of extinction. The gray whale population has now recovered and has been removed from the U.S. list of endangered species. On the other hand, the right whale population, despite being protected from hunting for over 50 years, numbers less than 400 animals. Humans still present a problem for the slow-moving right whale, one of the major causes of death for this species is collisions with ships (NMFS, 1984). Below is a general description of each listed whale species:

Blue Whale (*Balaenoptera musculus*). Blue whales are found throughout the global oceans and they feed on small shrimp-like crustaceans in the upper water column, mostly within 100 m of the surface (for review, see Leatherwood and Reeves, 1983). The number of blue whales in the southern hemisphere was severely depleted by whaling. Due to commercial whaling, the size of the population is less than 10 percent of what it was originally, numbering, in total, approximately 14,000 (NMFS, 1994). Because blue whales are primarily upper water column feeders, it is unlikely that they would ingest bagged waste on the sea floor.

Bowhead Whale (*Balaena mysticetus*). Bowhead whales are found primarily in Arctic waters and have a diet similar to that of right whales. They are known to be "skimmers" and eat small crustaceans such as copepods and euphausiids (krill). They have been observed with mud streaming from their mouths, and benthic amphipods and stones in their stomachs, which indicate that they do occasionally feed at or near the bottom in shallow areas (Lowry et al., 1978). However, they are primarily known to be upper water column feeders. As with other species, the bowhead whale was severely depleted by commercial whaling. Their numbers currently range around 7500 (NMFS, 1996). Because bowhead whales are primarily water column feeders it is unlikely that they would ingest bagged waste on the sea floor.

Fin Whale (*Balaenoptera physalus*). They are found throughout the global oceans. Depending on where they live, fin whales eat both fish and small crustaceans. In the Antarctic, their prey is almost exclusively krill. In northern areas they often eat small schooling fish such as herring or anchovies. They are known to be able to dive deeply, up to approximately 230 m (Gambell, 1985), but are not known to feed off or near the bottom. Like the other great whale species, the population of fin whales was severely depleted by whaling. Their current populations are estimated to be approximately 120,000. Because fin whales are primarily water column feeders it is unlikely that they would ingest bagged waste on the sea floor.

Gray Whale (*Eschrichtius robustus*). There are two stocks of gray whales in existence currently, the California and the Korean. The California stock is no longer listed on the U.S. endangered species list, whereas the Korean is still included on the foreign list. Most gray whales summer in Chukchi, Bering, Okhotsk, and Bering Seas where they feed in shallower areas of the continental shelf with high benthic biomass. They are primarily, although not exclusively, benthic feeders and they do have the capability to dive deeply, not uncommonly to 120 m (Wolman, 1985) and perhaps up to 600 m. They are thought to feed primarily on garmmaridean amphipods. Limited representation of other benthic species such as polychaete worms and molluscs suggest to researchers that they are selective feeders (Mizue, Ray and Schevill, Rice and Wolman, Sund, Walker, 1981). It is possible that gray whales stir up bottom sediments and filter the turbid water from which heavier species settle out (Wolman, 1985). During migration and in calving areas the gray whales usually swim in shallow water and may even swim in the surf zone. A population estimate for the Korean gray whale is thought to number only 100 to 200 (NMFS, 1996). Because gray whales are primarily non-selective benthic feeders, it is uncertain whether they would ingest the bagged waste, thus the likelihood of ingestion can only be assessed based on their potential for exposure to solid wastes.

Humpback Whale (*Megaptera novaeangliae*). The humpback whale is found throughout the global oceans. In the southern hemisphere its primary food is krill. In the northern hemisphere it eats schooling fish such as anchovies, cod, sand lance, and capelin. It generally feeds by "lunging", however, is also known to have a unique method of creating a bubble column which they rise through to feed. They have also been known to dive near the bottom, and benthic organisms have been found in their stomachs. Scientists estimate that there are 10,000 humpbacks worldwide-only about 8% of its estimated initial population. Considerable numbers are still found entangled in fishing gear each summer. Because humpback whales are primarily water column feeders, it is unlikely that they would ingest bagged waste on the sea floor.

Right Whale (*Eubalaena glacialis*). Right whales are found throughout the world's oceans in the middle latitudes. They feed on large schools of crustaceans, specifically copepods and krill, and may feed on small fish. Right whales are not known to dive deeply, generally up to only 50 m. The right whale got its name because it was the "right" whale to hunt-it was slow moving and floated after being killed. It is the most endangered species of whale off of the U.S. coasts. It was the first whale hunted by American whalers, and it was so depleted that it has not recovered despite being protected for over 50 years. One of the major causes of death for right whales currently seems to be collisions with ships. Because right whales are primarily water column feeders, it is unlikely that they would ingest bagged waste on the sea floor.

Sei Whale (*Balaenoptera borealis*). They are in the temperate regions of the worlds oceans. They feed primarily on krill and other small crustaceans, but also feed at times on small fish. They are not known to dive deeply. Although less is known about the numbers of sei whales than some other species, they were also severely impacted by commercial whaling. Current estimates of worldwide populations are 54,000 (IWC, 1994). Because sei whales are primarily water column feeders, it is unlikely that they would ingest bagged waste on the sea floor.

Sperm Whale (*Physeter macrocephalus*). Unlike the other great whales on the endangered species list, the sperm whale is a toothed whale. Sperm whales are found in tropical and temperate regions of the world's oceans and have been known to enter the Mediterranean Sea and Antarctica at times. Toothed whales are generally more selective feeders than baleen whales. Sperm whales feed mainly on squid, including the giant squid, and they have also been known to eat skates and small sharks. Sperm whales are noted for their dives, which can last up to an hour and a half and go as deep as 3.3 kilometers under the surface. Although they are not thought to "scoop" material off the bottom as the gray whales do, researchers have found unusual things in their stomachs, including stones, coconuts and glass balls in addition to benthic organisms (Tinker, 1988). One theory is that these whales rid themselves of indigestible objects by belching or regurgitating them (Berzin, 1972). It has an estimated population of two million. Because sperm whales are primarily water column feeders, it is unlikely that they would ingest bagged waste on the sea floor.

Beaked whales (a family in the suborder of toothed whales), although not listed on the endangered species lists, are also thought to feed occasionally in the benthic zone as well as the water column. The family of beaked whales includes approximately 18 species which are distributed through six genera, and there are variations to the general behaviors mentioned below. Beaked whales are found worldwide but are uncommon everywhere (Tinker, 1988). Of the little that is known, they tend to travel alone or in small groups, avoid ships and shorelines, and prefer deep waters. Much of the information available today has come from beached specimens and very little is known about their habits. Prey items found in the stomachs of a Cuvier's beaked whale (*Ziphius cavirostris*) are either open ocean, mesopelagic, or deep-water benthic organisms, supporting the idea that it is an offshore, deep-diving species (Heyning,

1989). Other species are thought to have similar tendencies due to inspecting stomach contents, and sightings or lack of. Beaked whales are generally thought to feed primarily on squid, however, fish, crustacean, sea stars, and sea cucumbers have also been found in their stomachs. They are not thought to "scoop" off the bottom as the gray whales do, and their relatively limited benthic exposure suggests that it is unlikely that they would ingest bagged waste from the sea floor.

The listed whales became endangered because they were hunted so heavily that the populations were severely reduced. During the 19th century, whales were hunted primarily for oil and baleen. They were traditionally taken for oil, blubber, ivory, and other commercial products. As recently as 20 years ago, products from whales were used for everything from machine oil to women's cosmetics. Because of the passage of the Marine Mammal Protection Act (MMPA) in 1972, it became illegal to import products containing materials from whales. Current concerns regarding the health and longevity of whales have been outlined by NMFS and others. Although commercial whaling currently does not present a threat to the survival of the baleen whales, loss of habitat and other human activities may make recovery more difficult. Collisions with vessels, oil spills and other changes in water quality, coastal development, and increasing noise created from the use of oceanic resources may all affect the whales. Fisheries may affect whales in two ways. First, whales may become entangled in fishing gear. As an example, each year, several humpback whales are entangled in fishing gear along the east coast of the United States and Canada. Second, fisheries may compete with whales for food, such as herring. Increased noise or boat traffic may cause whales to alter their behavior. There is evidence that humpback whales in Hawaii may have changed their use of near-shore waters where calves are raised by their mothers because of increasing human activity. Migrating bowhead whales may move further offshore to avoid human-caused noise. Although we do not have a full understanding of the possible impacts, pollution could also affect whales. Many contaminants are stored in a whale's blubber for long periods of time. Pollutant loads are usually lower in baleen whales than in dolphins and porpoises. Deterioration of the environment could possibly affect the whales in another way; if pollution and other factors reduce the number of fish and crustaceans, the food available to the whales could also be reduced. (NMFS, 1984).

QUALITATIVE ASSESSMENT OF INGESTION POTENTIAL

Species which do not feed off the bottom are highly unlikely to ingest solid waste on the sea floor. Likewise, species that are selective in their food choices are also unlikely to ingest these materials. Therefore, those species which clearly have feeding behaviors which are selective or non-benthic are considered to be very unlikely to be adversely impacted from solid waste discharges. These species are therefore ruled out from subsequent exposure analysis using estimates of density of burlap bags on the sea floor given historical data of ships traffic in Special Areas and estimated solid waste generation figures (Chadwick et al., 1996).

A qualitative assessment of ingestion potential is summarized in Table 4.2-3. The table qualitatively describes the likelihood that feeding behaviors of the various threatened and endangered species might lead to ingestion of shipboard solid wastes. It indicates which species are known to be benthic feeders and which are known to be non-selective feeders. The final column indicates only those species that are both benthic feeders and are not selective, thus placing them at potential risk of ingestion.

Table 4.2-3. Summary table of species feeding behavior (benthic feeding and non-selective feeding) and overall assessment of whether a species has a potential for ingestion.

Species Category	Species Common Name	Status	Benthic Feeder	Non-selective Feeder	Potential Ingestion
Sea Cows	Dugong	Endangered	X		
	West African Manatee	Threatened	X		
	West Indian Manatee	Endangered	X		
Otters	Marine Otter	Endangered	X		
	Southern Sea Otter	Threatened	X		
Seals/Sea-Lions	Stellar/Northern Sea-Lion	Threatened	X		
	Guadalupe Fur Seal	Threatened	X		
(EXTINCT?)	Caribbean Monk Seal	Endangered	X		
	Hawaiian Monk Seal	Endangered	X		
	Mediterranean Monk Seal	Endangered	X		
Turtles	Green Sea Turtle	Threatened	X	X	X
	Hawksbill Sea Turtle	Endangered	X	X	X
	Kemp's Ridley Sea Turtle	Endangered	X	X	X
	Leatherback Sea Turtle	Endangered			
	Loggerhead Sea Turtle	Threatened	X	X	X
	Olive Ridley Sea Turtle	Threatened	X	X	X
Whales	Blue Whale	Endangered		X	
	Bowhead Whale	Endangered		X	
	Finback Whale	Endangered		X	
	Gray Whale	Endangered	X	X	X
	Humpback Whale	Endangered		X	
	Northern Right Whale	Endangered		X	
	Southern Right Whale	Endangered		X	
	Sei Whale	Endangered		X	
	Sperm Whale	Endangered		X	

U.S. NAVY OPERATIONS IN MARPOL SPECIAL AREAS

To determine the extent of naval operations and potential shredded waste discharges into MARPOL Special Areas, a survey of historical ships employment schedule (EMPSKD) data was conducted using the CNO archived EMPSKD database (OSD N311ND). The information used to calculate potential ship discharges included ship traffic of all ship classes within the Special Areas from 1984 to 1993, ship complements, and estimated waste generation rates (Chadwick et al., 1996). The database suggests that U.S. Navy Ships generally transit in random patterns throughout these seas. Discharges are therefore expected to occur randomly in these seas and outside the 12 nmi discharge limit.

On an annual basis, the number of burlap bags expected to be discharged within each Special Area ranges from 400 in the Black Sea to 179,000 in the Mediterranean (in the past 10 years there have been no U.S. Navy operations in Antarctica). On an annual basis, the amount of surface area occupied by burlap bags is a small fraction of the sea floor available in each area, ranging from $2 \cdot 10^{-10}$ in the Black Sea to $6 \cdot 10^{-8}$ in the Gulfs Area (see Table 4.2-4). This annual discharge would result in a density of about one burlap bag in an area of between one bag/nmi^2 and 300 bags/nmi^2, depending on Special Area. It would, therefore,

take between 170,000 and 50,000,000 years of U.S. Navy discharges to cover 1% of the sea floors of Special Areas neglecting losses due the effects of corrosion. Thus, for all seas, the probability of encountering these wastes on the sea floor, is therefore, exceptionally low.

Table 4.2-4. Annual U.S. Navy Shredded Metal and Glass Discharges in MARPOL Special Areas.

Annual Averages:	Gulfs Area	Red Sea	Mediterranean Sea	Caribbean Region	Baltic Sea	North Sea	Black Sea
Mandays	1418000	465600	3437000	2550000	23000	32300	8216
Discharge of Bags (mt)	344.9	113.3	859.0	638.0	5.8	8.1	2.0
Discharge of Bags (bags)	71900	23600	179000	132900	1200	1700	400
Surface Area of Discharged Bags (m^2)	14400	4700	35800	26600	240	340	83
Total Special Area Surface Area (m^2)	$2.4 \cdot 10^{11}$	$4.5 \cdot 10^{11}$	$2.5 \cdot 10^{12}$	$4.2 \cdot 10^{12}$	$4.0 \cdot 10^{11}$	$5.8 \cdot 10^{11}$	$4.2 \cdot 10^{11}$
Bag Surface Area / Total Surface Area	$6.0 \cdot 10^{-8}$	$1.0 \cdot 10^{-8}$	$1.4 \cdot 10^{-8}$	$6.3 \cdot 10^{-9}$	$6.0 \cdot 10^{-10}$	$5.9 \cdot 10^{-10}$	$2.0 \cdot 10^{-10}$
Bag Density (nmi^2/bag)	1.0	5.6	4.1	9.3	96.5	99.4	296.2
Years to Cover 1% of Sea Floor	$1.7 \cdot 10^{5}$	$9.5 \cdot 10^{5}$	$7.0 \cdot 10^{5}$	$1.6 \cdot 10^{6}$	$1.7 \cdot 10^{7}$	$1.7 \cdot 10^{7}$	$5.1 \cdot 10^{7}$

U.S. NAVY OPERATIONS OUTSIDE MARPOL SPECIAL AREAS

The distribution of operations of U.S. Navy ships outside MARPOL Special Areas was not researched as part of the original fate and effects study of Chadwick et al. (1996) and, thus, the extent and distribution of operations is not characterized at this time. However, given the much larger areal extent and greater average depth of the oceans relative to Special Areas, coupled with a 12-nmi discharge limit and random pattern of discharge, the relative amount of sea floor impacted is expected to be similar to or less than what is found within Special Areas. Given a low density of sea floor coverage, the probability of encountering these wastes on the sea floor is exceptionally low.

QUALITATIVE ASSESSMENT OF EXPOSURE POTENTIAL

The potential for impacts to threatened or endangered species from U.S. Navy shipboard solid wastes is based on a qualitative assessment of the likelihood of exposure to those species having a potential risk of ingestion. Exposure to the waste is categorized based on the probability of overlap between a species' typical distribution and feeding habitat and the deposition location of solid wastes discharged during typical Navy operations. The primary consideration for exposure is that discharges will occur at a distance of >12 nmi from shore and is based on sinking rates that are unlikely to be transported closer to shore by more than 0.1 nmi from the discharge point (Chadwick et al., 1996). Species that feed primarily within the 12 nmi limit from shore would, therefore, have a very low potential for exposure.

Determining exposure also requires comparing the depths to which organisms likely dive for food with water depths in which the burlap bags are likely deposited. Although some Special Areas are relatively shallow (e.g., the Persian Gulf has a mean depth of 36 m) only 8% of the world's oceans are less than 200 m deep (Sverdrup et al., 1942). Taking the 12-nmi limit into consideration decreases this percentage

even further. Thus, only a small fraction of the seas are potentially available for exposure to shallow feeding animals. Only organisms capable of feeding at significant depths are, therefore, potentially exposed.

A final consideration used in estimating potential exposure is that only a tiny fraction of sea floor area is likely to be covered with burlap bags. The highest density of bags estimated to be discharged annually in Special Areas is in the Persian Gulf at 1 bag per nmi^2. This number is not expected to be higher in open ocean areas. The density will increase each year of discharge although the processes of corrosion and burial will effectively remove the materials over time. Analysis in Chadwick et al. (1996) suggests that steady-state, from corrosion alone, is reached in about 7.5 years implying that the number of bags available is 7.5 times the annual discharge rate. In the case of the Persian Gulf, this implies a maximum density of 7-8 bags per nmi^2.

Of the listed species, only five species of turtles and one species of whale were found to have feeding behaviors which could place them at risk for ingestion of bagged waste. These include: the Green Sea Turtle, the Hawksbill Sea Turtle, Kemp's Ridley Sea Turtle, the Loggerhead Sea Turtle, the Olive Ridley Sea Turtle, and the Gray Whale. The following sections are a qualitative assessment of the potential for exposure of each of these species in order to identify their overall likelihood to be impacted from the discharge of U.S. Navy shipboard solid wastes.

Green and Hawksbill Sea Turtles. Green and hawksbill sea turtles are grouped together here because they have similar feeding habitats. Green sea turtles primarily feed in shallow waters inside reefs, bays, inlets, lagoons and shoals with an abundance of marine grass and algae. Although they migrate long distances, they are not known to feed while doing so. Similarly, the hawksbill sea turtle frequents rocky areas, reefs, shallow coastal areas, lagoons, oceanic islands, and narrow creeks or passes. They are seldom seen in water deeper than 20 m, where they forage on the bottom. These types of feeding grounds are most likely to be found inside of the 12-nmi limit or in water depths that preclude ship traffic. Therefore, the areas where these turtles forage will not generally overlap with regions where U.S. Navy ships would discharge. In the limited cases where overlap might occur, the likelihood of a turtle encountering the solid waste materials remains very low as a result of the exceptionally low sea floor density of burlap bags. Because of this combination of factors which limit their exposure, the likelihood of impact to green and hawksbill sea turtles is very low.

Kemp's Ridley, Olive Ridley, and Loggerhead Sea Turtle. These sea turtles are grouped together because their feeding habitat extends well offshore and into moderate depths which may include areas outside the region bounded by the 12-nmi discharge limit. All three turtles are primarily benthic feeders in less than 100 to 200 m and, typically, feed in the water column during migration. The Kemp's Ridley and Olive Ridley sea turtles predominantly live nearshore. While the loggerhead is commonly found hundreds of miles out to sea, its primary feeding areas include coral reefs and rocky places in areas such as bays, lagoons, salt marshes, creeks, ship channels, and the mouths of large rivers.

The habitat of these turtles may have some overlap with bagged wastes discharged from U.S. Navy ships. These turtles also have the ability to dive deep enough to encounter the wastes although they would not preferentially seek out the bagged material. Therefore, the likelihood of encounter would be controlled by the density of the bags on the sea floor. In this limited case where overlap might occur, the likelihood of a turtle encountering the solid waste materials remains very low as a result of the exceptionally low sea floor density of bags. Because of this combination of factors which limit their exposure, the likelihood of impact to Kemp's Ridley, Olive Ridley and loggerhead sea turtles is very low.

Gray Whale. Gray whales (Korean Stock) are found in the Bering Sea, the Chukchi Sea, the sea of Okhotsk, and the western Beaufort Sea in the summer and migrate south along the western Pacific for the winter. The northern latitudes are considered gray whale feeding grounds. Although they do have the capability to dive to a depth of 600 m, they typically feed in shallower areas of the continental shelf, which contains high benthic biomass. Gray whales typically feed minimally during their annual migrations to more southern latitudes (although exceptions are noted such as in pregnant females and those wintering at the Farallon Islands). Based on anecdotal knowledge, these northern seas are only occasionally visited by U.S. Navy ships. This would suggest that the burlap bag density in these areas are even reduced from the low density already suggested by estimates for Special Areas. Furthermore, the filtering mechanism by which gray whales obtain their food are thought by some to preclude them from ingestion large and/or heavy materials. Minimizing the chances of ingesting the generally heavy solid waste materials, along with the exceptionally low bag densities expected where gray whales feed, suggests that their likelihood for impact is very low.

SUMMARY AND CONCLUSIONS

The likelihood of impacts to threatened and endangered species has been assessed based on consideration of species behavior and potential exposure. Of the listed species, only gray whales and five species of turtles were found to have feeding behaviors which could place them at risk for ingestion of bagged waste. For these species it is uncertain whether they would ingest the waste if they encountered it. Although there is no specific evidence for ingestion of this type of waste, the fact that they feed off the sea floor in a relatively non-selective manner indicates that they might inadvertently consume the waste if they came across it.

The likelihood that these species would encounter the waste was, therefore, assessed on the basis of typical feeding behavior, habitat, and diving capabilities of the animals in relation to expected discharge locations, depths, and densities of the waste from the ships. In general, it is expected that the 12-nmi discharge limit, the extremely low spatial density of shredder burlap bags on the sea floor, the burial of bagged waste by natural sedimentation processes, and the slow deterioration of the waste materials due to corrosion will all serve to minimize the likelihood of exposure to all threatened and endangered species.

For turtles it was found that the limited overlap between feeding areas and discharge areas (coastal vs. >12 nmi offshore), limited diving depths of most species, and the very low spatial density of burlap bags in areas where encounters might possibly occur all combine to reduce the expected exposure to extremely low levels. On this basis, impact to sea turtles due to discharges of bagged solid waste was determined to be very unlikely. Similarly, for gray whales it was found that the overlap between the areas and depths where the whales generally feed and significant Navy ship traffic occurs will be very limited. In addition, the filtering mechanism by which gray whales obtain their food generally precludes them from ingestion of large and/or heavy materials. These factors, combined with the general characteristic of extremely low spatial density of bagged waste on the sea floor indicate that the likelihood of impact to gray whales from shredder discharges would be very low.

In conclusion, there are only a limited number of listed species which display feeding behaviors which could place them at risk for ingestion of bagged waste. For these, the extremely low chance of exposure indicates that the likelihood of impact is very low.

TABLE 4.2-5: KNOWN ENDANGERED AND THREATENED SPECIES WORLDWIDE

Common Name	Species	Type	Threat status	Source designating species status	Distribution/Habitat	Feeding Habits/Behaviors	Current Population Status	Notes
Dugong	*Dugong dugong*	Dugong	Endangered	FOREIGN	Indo-Pacific tropical and subtropical shallow coastal and island waters: northern Indian Ocean from Madagascar to Indonesia; Philippines; Australia; southern China; Palau.	Shallow water herbivore (primarily of sea grasses).		
West African Manatee	*Trichechus senegalensis*	Manatee	Threatened	FOREIGN	West Coast of Africa from Senegal River to Cuanza River.	Shallow water (<10m) herbivore (primarily of vascular plants). Reported to feed on mangrove leaves and palm fruits.		
West Indian Manatee	*Trichechus manatus*	Manatee	Endangered	US	Coastal waters of Atlantic Ocean, Gulf of Mexico, and Caribbean Sea from southeastern United States to northeastern Brazil and Greater Antilles and Trinidad and Tobago Islands.	Shallow water herbivore (<10m).	1900 Florida, 1992	
Marine Otter	*Lutra felina*	Otter	Endangered	FOREIGN	Southeast Pacific coast from Peru to Straits of Magellan.			
Sea Otter	*Enhydra lutra*	Otter	Threatened	US	Northeast Pacific Coast from Pribilof Islands to California.	Predator of fish and marine invertebrates (e.g. sea urchins, clams, crabs, mussels). Known to dive to 75m.	100,000 Alaska; 2000 California (University of Michigan, 1996)	
Steller/Northern Sea Lion	*Eumetopias jubatus*	Sea-lion	Threatened	US	Central Kuril Islands to Ano Nuevo Island, California (primarily Gulf of Alaska and Aleutian Islands).	Opportunistic predator of fish, cephalopods, bivalves, shrimp and crabs. Reported to dive to 180m.	116,000 (NMFS, 1996)	
Guadalupe Fur Seal	*Arctocephalus townsendi*	Seal	Threatened	US	Guadalupe Island, 200km west of Baja California, to southern California Channel Islands (primarily San Miguel and San Nicolas Islands).	No data. Probable predator of fish, cephalopods, crabs and spiny lobsters. May dive to 120m.		
Caribbean Monk Seal	*Monachus tropicalis*	Seal	Endangered (extinct?)	US	Western Caribbean to Bahamas to Florida Keys.		Believed extinct since 1952 (NMFS, 1996)	
Hawaiian Monk Seal	*Monachus schauinslandi*	Seal	Endangered	US	Hawaiian Islands.	Selective benthic predator of spiny lobsters, moray and conger eels, scorpaenids, bothids, and octopi.	1400 (NMFS, 1996)	
Mediterranean Monk Seal	*Monachus monachus*	Seal	Endangered	FOREIGN	Southern and western Black Sea to Atlantic coast of Morocco and Mauritania to Madeira Islands.	Selective predator of fish, rays and octopi. Known to dive to 75m.	500-1000, 1978 (1985)	

TABLE 4.2-5: KNOWN ENDANGERED AND THREATENED SPECIES WORLDWIDE (Continued)

Kemp's Ridley Sea Turtle	*Lepidochelys kempii*	Turtle	Endangered	US	Coastal waters and bays of Gulf of Mexico and Atlantic Ocean.	Feeds primarily on crabs.	Nesting population estimated at 700-800 (NMFS, 1996)	Known to ingest plastic, rubber, fishing line and hooks, tar, cellophane, rope, string, wax, styrofoam, charcoal, aluminum cans and cigarette filters resulting in interference of metabolism or gut function and absorption of toxic byproducts (NMFS, 1996).
Leatherback Sea Turtle	*Dermochelys coriacea*	Turtle	Endangered	US	Global ocean waters. Primarily nesting on Pacific shores of the American tropics, in the Guianas and tropical West Africa.	Feeds primarily on medusae.	Nesting population estimated at 29,000-40,000 worldwide (NMFS, 1996)	Known to ingest plastic bags, plastic and styrofoam pieces, tar balls, balloons and plastic pellets resulting in interference of metabolism or gut function and absorption of toxic byproducts (NMFS, 1996).
Loggerhead Sea Turtle	*Caretta caretta*	Turtle	Threatened	US	Global temperate, subtropical and tropical waters along continental shelves, and in bays, estuaries and lagoons.	Feeds primarily on crabs, medusae and molluscs.	40,000 - 50,000 (NMFS,1996)	Known to ingest plastic bags, plastic and styrofoam pieces, tar balls, balloons and raw plastic pellets resulting in interference of metabolism or gut function and absorption of toxic byproducts (NFMS, 1996).
Olive Ridley Sea Turtle	*Lepidochelys olivacea*	Turtle	Threatened	US	Global ocean waters. Primarily nesting on Pacific shores of the American tropics, in the Guianas and tropical West Africa.	Feeds primarily on crabs, shrimp, rock lobsters, jellyfish, tunicates and, reportedly, algae.	No estimate available.	Known to ingest plastic bags, plastic and styrofoam pieces, tar balls, balloons and raw plastic pellets resulting in interference of metabolism or gut function and absorption of toxic byproducts (NFMS, 1996).
Blue Whale	*Balaenoptera musculus*	Whale	Endangered	US	Global ocean waters.	Planktivore (almost exclusively euphausids) in coastal waters by "gulping" or "lunging."	Severely Depleted (NFMS): 14,000 (IWC, 1994); 11,200 (Department of Commerce, 1983); 500 Antarctic (NMFS, 1996)	
Bowhead Whale	*Balaena mysticetus*	Whale	Endangered	US	Arctic waters >50° N.	Planktivore (primarily euphausids and copepods) by "skimming" (surface feeding). Some evidence of bottom feeding (on gammarids) by foraging in mud. Estimated to dive >1400m (unconfirmed).	Severely Depleted (NMFS): 7500 (NMFS, 1996)	
Finback Whale	*Balaenoptera physalus*	Whale	Endangered	US	Global ocean waters.	Planktivore by "gulping" or "scooping" (primarily euphausids) in Antarctic waters; schooling fishes in northern Atlantic and Pacific. Known to dive to 230m.	Severely Depleted (NMFS): 120,000 (IWC, 1994); 5200 northwest Atlantic, 1982 (NMFS, 1996); 20,000 northern Pacific, 1980 (1985), 103,000 southern hemisphere, 1980 (1985)	

TABLE 4.2-5: KNOWN ENDANGERED AND THREATENED SPECIES WORLDWIDE (Continued)								
Gray Whale	*Eschrichtius robustus*	Whale	Endangered	FOREIGN	Northwest Pacific coast (Korean stock),	Bottom feeder (primarily gammarids) by re-suspending and staining bottom sediments. Some evidence of feeding on small schooling fish reported. Known dive to 600m	Recovered (NMFS): 20,850+ eastern Pacific, 100-200 Korean stock, 1988 (NMFS, 1996)	
Humpback Whale	*Megaptera novaeangliae*	Whale	Endangered	US	Global ocean waters.	Plankton/small fish feeder in coastal waters by "gulping," "lunging" and use of "bubble behaviors." Some bottom feeding evidence reported.	Severely Depleted (NMFS): 10,000 (IWC, 1994); 9,310+ (1985); 1400-2000 northern Pacific (NMFS, 1996)	
Northern Right Whale	*Balaena glacialis*	Whale	Endangered	US	25º-60º N (Pacific) 30º-75º N (Atlantic) ocean waters.	Coastal water planktivore (primarily of copepods euphausids) by "skimming" and "gulping." Known to dive to 50m.	Severely Depleted (NMFS): 1000 (IWC, 1994); 350 western Atlantic, 5-7 sightings eastern Pacific (NMFS, 1996)	
Southern Right Whale	*Balaena australis*	Whale	Endangered	US	20º-50º S ocean waters.	Coastal water planktivore (primarily copepods and euphausids) by "skimming" and "gulping." Known to dive to 50m.	Severely Depleted (NMFS): 3000 (IWC, 1994); 1000-4300 (1985)	
Sei Whale	*Balaenoptera borealis*	Whale	Endangered	US	Global in temperate ocean waters.	Planktivore (primarily copepods, euphasids, amphipods and small fish). Not known to dive deeply.	Severely Depleted (NMFS): 54,000 (IWC, 1994); 37,000 southern hemisphere, 14,000 north Pacific, 2000 north Atlantic (1985)	
Sperm Whale	*Physeter catodon*	Whale	Endangered	US	Global in temperate and tropical ocean waters, generally between 50º N and 50º S. Known to enter the Mediterranean Sea.	Predator, primarily of squid, with sharks and skates reported. Known to dive to 1000m.	At or Above Optimum Sustainable Population (NMFS): 2,000,000 (NMFS, 1996)	Known to injest stones and other non-food objects.

REFERENCES

Berzin, A.A., *The Sperm Whale*, Israel Program for Scientific Translation, Jerusalem. (Translated from Russian: Berzin, 1971).

Bonner,W.N., in Ridgway, S.H., Harrison, R.J. (Eds.), *Handbook of Marine Mammals Volume 1: The Walrus, Sea Lions, Fur Seals and Sea Otter*, Chapter 8, pp. 161-208, London: Academic Press, 1981a.

Brown, V., *Sea Mammals and Reptiles of the Pacific Coast*, New York, Macmillan Publishing Co., 1976.

Brownell, R.L., Jr., Ralls, K., Reeves, R.R. (Eds), Report of the West Indian manatee workshop, Orlando, Florida, cosponsored by the Florida Audubon Society, Florida Dept. Nat. Res., Natl. Fish and Wildlife Lab. of the U.S. Fish and Wildlife Serv., and Sea World of Florida, 27-29 March 1978.

Chadwick, D.B., Katz, C.N., Curtis, S.L., Rohr, J., Caballero, M., Valkirs, A., Patterson, A. *Environmental Analysis of U.S. Navy Shipboard Solid Waste Discharges: Report of Findings.* Technical Report 1716, Naval Command, Control and Ocean Surveillance Center, RDT&E Division, California, 1996.

Fiscus, C.H., Baines, G.A., *Food and feeding behavior of Steller and California Sea Lions*, J. Mammal 47, 195-200, 1966.

Gambell, R., in Ridgway, S.H., Harrison, R.J. (Eds.), *Handbook of Marine Mammals Volume 3: The Sirenians and Baleen Whales*, Chapter 7, Fin Whale, pp. 171-192, San Diego, Academic Press, 1985

Gramentz, D., *Involvement of Loggerhead Turtle with the Plastic, Metal, and Hydrocarbon Pollution in the Central Mediterranean*, Great Britain: Marine Pollution Bulletin, V19, No. 1, pp. 11-13, 1988.

Harrison, R.J., King, J.E., *Marine Mammals*, London: Hutchinson and Co. LTD, 1965

Hartman, D.S., *Behavior and Ecology of the Florida Manatee, Trichechus manatus latirostris (Harlan), at Crystal River, Citrus County*. Unpublished Ph.D. Dissertation, Cornell University, Ithaca, New York, 1971.

Hubbs, C.L., Gualalupe Fur Seal. In *"Mammals in the Seas"*, pp. 24-27, FAO Fish. Ser. (5) Vol. 2, 1979.

Kenyon,K.W., in Ridgway, S.H., Harrison, R.J. (Eds.), *Handbook of Marine Mammals Volume 1: Seals*, Chapter 9, Sea Otter, pp. 209-223, London, Academic Press, 1981a.

Kenyon,K.W., in Ridgway, S.H., Harrison, R.J. (Eds.), *Handbook of Marine Mammals Volume 2: Seals*, Chapter 8, Monk Seals, pp. 195-220, London, Academic Press, 1981b.

Littell, R., *Endangered and Other Protected Species: Federal Law and Regulation*, Washington, D.C.: The Bureau of National Affairs, 1992.

Leatherwood, S., Reeves, R.R., *The Sierra Club Handbook of Whales and Dolphins*, Sierra Club Book, San Francisco, 1983.

Lowry, L.F., Frost, K.J., and Burns, J.J., *Food Of Ringed Seals And Bowhead Whales Near Point Barrow, Alaska*. Can. Field Nat., 92, 67-70, 1978.

Merkel and Associates, Inc., *Ecological Assessment of U.S. Navy Shipboard Solid Waste Discharges with MARPOL Special Areas: Draft Final*, M&A Doc. No. 95-106-01, 1996.

Mizue, K., *Gray Whales in the East Sea Area of Korea*, Sci. Rep. Whales Res. Inst. 5, 71-79, 1951.

National Marine Fisheries Service, *The Status of Endangered Whales, Marine Fisheries Review*, National Marine Fisheries Service Scientific Publications Office, Seattle, Washington, 1984.

National Marine Fisheries Service, *Our Living Oceans Annual Report*, National Marine Fisheries Website, 1996.

Nishiwaki, M.and Marsh, H., in Ridgway, S.H., Harrison, R.J. (Eds.), *Handbook of Marine Mammals Volume 3: The Sirenians and Baleen Whales*, Chapter1, Dugong, pp. 1-31, San Diego, Academic Press, 1985.

Pritchard, P.C.H., *Living Turtles of the World*, Neptune City, N.J.: T.F.H. Publications, 1967.

Ray, G.C., Schevill, W.E., *Feeding of a Captive Gray Whale (Eschrichtius robustus)*, Mar. Fish. Rev. 36(4), 31-38, 1974.

Reilly, S.B., *Population Assessment and Dynamics of the California Gray Whale (Eschrichtus robustus)*, Ph.D. dissertation, University of Washington, Seattle, 1981.

Rice, W.D., Wolman, A.A., *Life History and Ecology of the Gray Whale (Eschrichtius robustus)*, Am. Soc. Mammal., Sprec. Pulb. 3, 142 pp., 1971.

Ridgway, S.H., Harrison, R.J. (Eds.), *Handbook of Marine Mammals Volume 1: The Walrus, Sea Lions, Fur Seals and Sea Otter*, London: Academic Press, 1981a.

Ridgway, S.H., Harrison, R.J. (Eds.), *Handbook of Marine Mammals Volume 2: Seals*, London, Academic Press, 1981b.

Ridgway, S.H., Harrison, R.J. (Eds.), *Handbook of Marine Mammals Volume 3: The Sirenians and Baleen Whales*, San Diego, Academic Press, 1985

Ridgway, S.H., Harrison, R.J. (Eds.), *Handbook of Marine Mammals Volume 4: River Dolphins and the Larger Toothed Whales*, London, Academic Press, 1989.

Sund, P.N., *Evidence of Feeding During Migration and of an Early Birth of the California Gray Whale (Eschrichtius robustus)*, J. Mammal 56(1), 265-266, 1975.

Sverdrup, H.U., M.W. Johnson, R.H. Feming. The Oceans. Prentice Hall, New Jersey, 1942.

Tinker, S.W., Whales of the World, pp. 100-300, Honolulu, Bess Press, 1988.

United States Fish and Wildlife Service, *List of U.S. and Foreign Threatened and Endangered Species*, Internet, 1996.

Venizelos, L.E., *The Endangered Loggerheads of Zakynths (Greece): A Part of the Mediterranean Sea Turtle Conservation Issue. The Formation of Medasset (Mediterranean Association to Save the Sea Turtles)*, Greece: Thalossographica, V13, Suppl.1, pp. 53-59, 1990.

Walker, L.W., *Nursery of the Gray Whales,* Nat. Hist. 58(6), 248-256, 1949.

Wolman, A.A., in Ridgway, S.H., Harrison, R.J. (Eds.), *Handbook of Marine Mammals Volume 3: The Sirenians and Baleen Whales*, Chapter 3, Gray Whale, pp. 67-90, San Diego, Academic Press, 1985

The following references were taken from reports used from the Internet

Dodd, C. K., Jr., *Synopsis of the Biological Data on the Loggerhead Sea Turtle Cavetta cavetta (Linnaeus 1958)*, U.S. Fish Wildl. Serv., Biol. Rep. 88(14), 110 pp., 1988.

Ehrhart, L. M., *Status Report of the Loggerhead Sea Turtle*, Pages 122-139 in L. Ogren (ed.), Proceedings of the Second Western Atlantic Symposium. NOAA Tech. Memo. NMFS - SEFC - 226, 1989.

Marquez, R., *Status report of The Kemp's ridley turtle*, Pages 159-168 in L. Ogren (ed.), Proceedings of the Second Western Atlantic Symposium, NOAA Tech. Memo - NMFS - SEFC-226, 1989.

Meylan, A., *Status Report of the Hawksbill Turtle*. Pages 101-115 in L. Ogren, F., Berry, K., Bjorndal, H., Kumpf, R., Mast, G., Medina, H., Reichart, and R. Witham (eds.), Proceedings of the Second Western Atlantic Turtle Symposium. NOAA Tech. Memo. NMFS/SEFC-226, 1989.

National Marine Fisheries Service and U.S. Fish and Wildlife Service, *Plan for Hawksbill Turtles in the U.S. Caribbean Sea, Atlantic Ocean, and Gulf of Mexico*, National Marine Fisheries Service, St. Petersburg, Florida, 52 pp., 1993.

Ogren, L., *Status Report of the Green Turtle*, Pages 89-94 in L. Ogren (ed.), Proceedings of the Second Western Atlantic Symposium. NOAA Tech Memo. NMFS - SEFC -226, 1989.

Pritchard, P., *Status Report of the Leatherback Turtle*, Pages 145- 152 in L. Orgren (ed.), Proceedings of the Second Western Atlantic Symposium, NOAA Tech. Memo. NMFS-SEFC-226, 1989.

U.S. Department of the Interior, *Species Accounts for the Sensitive Wildlife Information System (SWIS). Fish and Wildlife Service*, National Wildlife Laboratory, Gainesville, Florida, 1977.

4.3 ANALYSIS OF POTENTIAL EFFECTS OF U.S. NAVY SHIPBOARD SOLID WASTE DISCHARGES ON CORAL REEFS

by Dr. D. Bart Chadwick, Stacey L. Curtis, Charles N. Katz

INTRODUCTION

As a component of the SSC San Diego assessment studies, the potential exposure and effects of solid waste discharges on coral reefs were examined. The coral reef assessment included the following primary objectives: 1) to determine the general distribution of coral reefs in MARPOL Special Areas; 2) to determine the extent of Navy operations in areas where coral reefs exist; and 3) to evaluate, based on estimated exposure levels, the potential impact of Navy solid waste discharges on coral reefs in MARPOL Special Areas. The study focuses primarily on potential effects of pulper discharges, however, some estimates of the potential exposure and area of impact from shredder bags are also included. Originally, this assessment was done using historical port visit information in each of the MARPOL Special Areas and then subsequently using historical ship transit information.

APPROACH

Prior to this study, a characterization and environmental analysis of U.S. Navy shipboard solid waste discharges was conducted to identify the possible fate and effects of both the pulped and shredded solid waste streams (Chadwick et al., 1996). This assessment of impacts to coral reefs takes into account the conceptual models developed in the previous analysis, including the specific nature of the waste streams, along with the overall environmental parameters associated with coral reef systems. The conceptual model previously used for the local scale is the most pertinent in this case. It takes into account physical processes (near-field mixing, advection or transport, and settling), first-order processes within the water column and sediment (degradation, deposition, burial, and resuspension), and potential effects (toxicity, damage due to physical impacts, smothering and stress due to particle clearance, direct and indirect mortality, and degradation due to light reduction). The approach taken to accomplish the above objectives for the coral reef assessment can be summarized as follows:

General Distribution of Coral Reefs. Areas where coral reefs exist within the world oceans and seas were evaluated to determine which Special Areas have significant occurrences of coral reefs. Three Special Areas were identified as having significant coral reef habitat: the Red Sea, the Gulfs Region, and the Wider Caribbean Basin. The location of coral reefs within the Special Areas were determined from published reports and nautical charts.

Extent of Naval Operations. Ship operations within the three Special Areas were analyzed to determine the proximity and frequency of naval vessels transiting near coral reef systems. First, the number of ship visits to ports within each Special Area was estimated using archived employment schedule information. Ports in the vicinity of coral reefs with 10 or more ship visits per year were then included for further analysis. Analysis of impact to coral reefs based on port visits is presented first. Subsequently, ships positions within Special Areas were estimated using historical ship movement information to determine more precisely the amount of naval operations near known coral reefs. A comparison of the two methods is made, and the potential effects to coral reefs systems is discussed on the basis of expected exposures versus background and literature effects levels.

Exposure Levels. For the analysis based on port visit data, sedimentation due to the discharge of various ship classes was estimated using the waste generation rate for each applicable ship class and the wake dilution formula of Csanady (1973). From the ship sedimentation and number of visits, an average daily sedimentation rate was estimated. The sedimentation rate is based on the assumption that the ships all pass along the same track while entering and leaving port and discharge uniformly in both directions. Similarly for the analysis based on historical ship transits, sedimentation was estimated using the waste generation rate for each applicable ship class and the wake dilution formula of Csanady (1973). However, in this case the average daily sedimentation rate was estimated using historical ship positions within each of the Special Areas. In both cases, the assumptions were highly conservative in that the calculations are based on the vessels always discharging near the coral reef locations.

In addition, acute exposure was evaluated based on the passing of a single CVN class ship (worst-case total suspended load concentration). Potential reductions in light levels which might affect reef health were evaluated based on laboratory measurements of light transmission with actual pulped paper samples and compared with expected CVN pulped discharges. Direct toxicity was assessed based on previous toxicity and chemical characterization studies described in Chadwick et al. (1996).

GENERAL DISTRIBUTION OF CORAL REEFS IN MARPOL SPECIAL AREAS

The best available data source for geographical locations and spatial extent of coral reefs within the Special Areas was found to be the reports developed by UNEP (1988), although not all are fully known. Information was also used from the recently compiled "ReefBase" database (McManus et al., 1996); however, the resolution of the geographical content appears to be similar to the UNEP reports. The information summarized below is based on both of these sources. This approach provided information with which to determine the areas where coral reefs and Navy operations overlapped.

Of the eight existing and proposed Special Areas, the three which have significant coral reef systems are the Red Sea, the Gulfs Region, and the Wider Caribbean Basin. Within these areas, the factors controlling exposure to the coral reefs include the presence and distribution of the reefs, the extent that the reefs reside outside the restricted discharge limits from shore, and the extent of typical vessel operations. Worldwide, the coral reefs are generally distributed in tropical and subtropical regions between the latitudes of 30° N and 30° S. They thrive in warm temperatures between 20° to 28° C and have evolved to require abundant light in shallower waters of typically 50 m, although some are found at depths up to approximately 200 m when sufficient light is present.

The Gulf Region. The Gulfs Region includes the Persian Gulf, the Gulf of Oman, and part of the Arabian Sea. The Gulf proper is a shallow, enclosed sea which slopes downward from the low coastline of Saudi Arabia to a shallow trench (80-100 m) close to the mountainous coast of Iran. The Gulfs Area has less developed reef systems than the Red Sea, with few reef building corals in the north but some extensive and diverse shelf and island reefs in the southwest (see Figure 4.3-1).

The Red Sea. The Red Sea is situated in an elongated depression with a central trough which reaches depths of 2000 m. Exceptionally clear waters exist as a result of limited riverine input and sediment trapping within the deep trough. In addition, the relative calmness and lack of severe storms in the region provide for coral growth which is not restricted by wave action. Well developed fringing reefs exist in the north and central regions extending approximately 3 to 10 km offshore. The southern region has a much wider shelf with shallower water which permit corals out to approximately 100 km offshore,

although increased turbidity and freshwater inflows lead to less extensive reef development than in the north (see Figure 4.3-1).

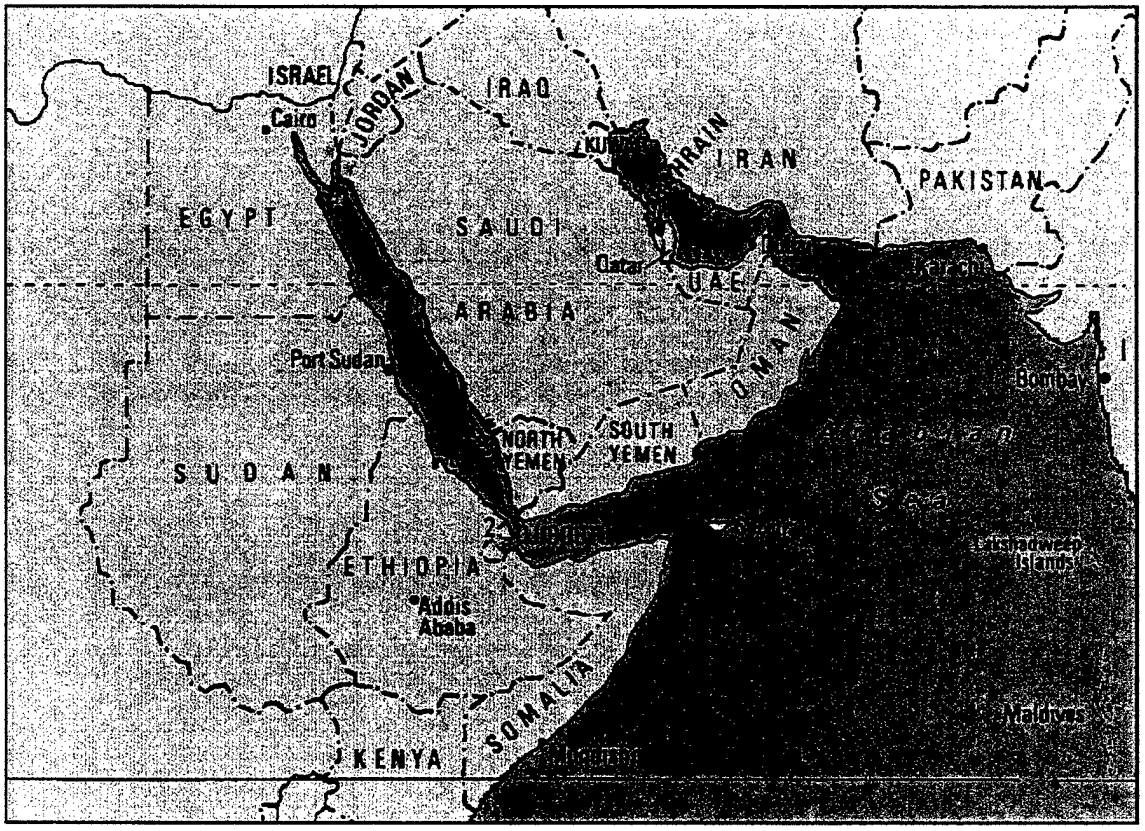

Figure 4.3-1. The distribution of coral reefs in the Red Sea and Gulf Region. Coral reef areas are indicated in red. Stars indicate parks and preserves (Coral Reefs of the World UNEP, 1988).

The Wider Caribbean Basin. The Wider Caribbean Basin (including the Gulf of Mexico and the Caribbean Sea) comprises a semi-enclosed body of water consisting of several deep basins. The region lacks extensive shallow continental shelf areas except off the Yucatan Peninsula and part of South America. Fringing and patch reefs are the most common formations. Shallow reefs surround the majority of Caribbean Islands, fringing reefs occur along the coasts of Florida (eastern shore), Mexico, Columbia, and Venezuela with a large barrier reef off the coast of Belize. Localized regions of significant reef development are found off Columbia, Honduras, Panama, and particularly Belize (UNEP, 1988). See Figure 4.3-2.

Some of the most extensive reefs occur in the Antilles which form an arc from Cuba on the north to the Netherlands Antilles on the south. Reefs in this region are typically better developed along the sheltered Caribbean shores and less developed along the exposed Atlantic shores. The Gulf of Mexico is characterized by high levels of terrigenous sedimentation with only scattered reef development. Reef development in the Caribbean waters off Central and South America is limited by large influxes of freshwater from mainland river systems.

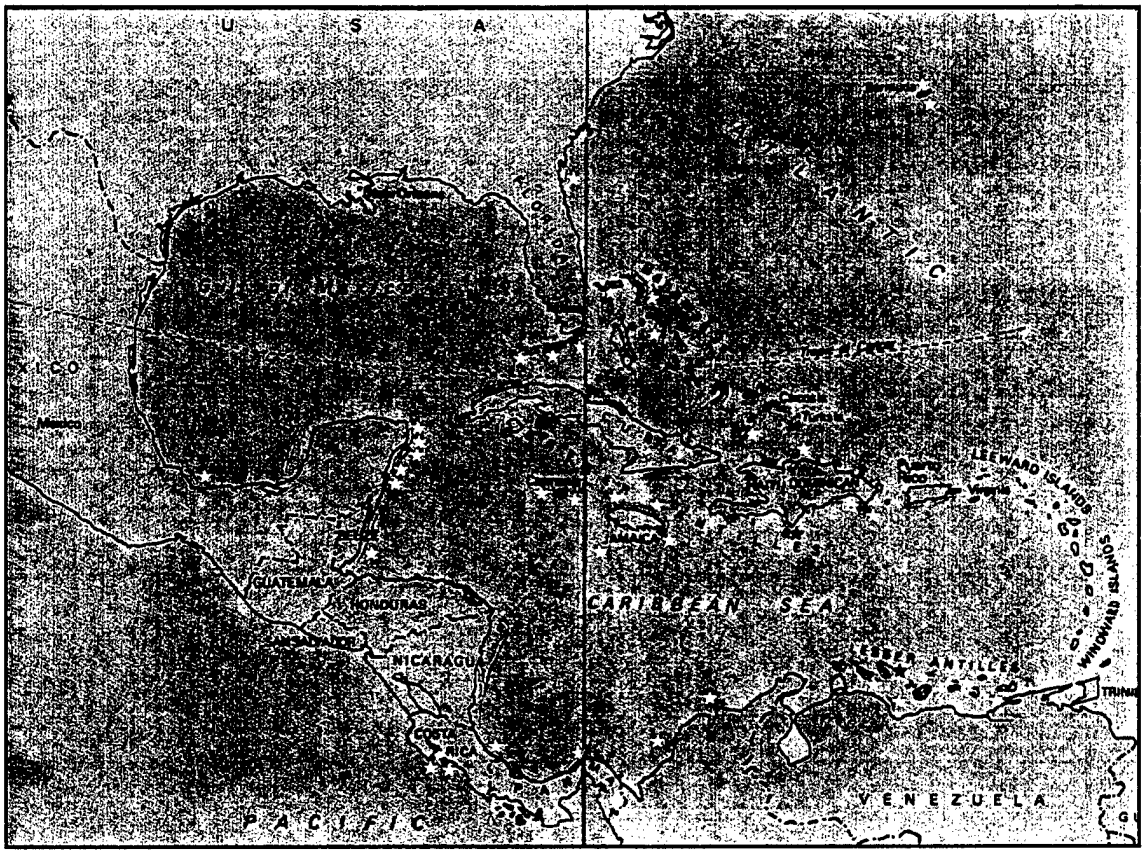

Figure 4.3-2. Distribution of coral reefs in the Wider Caribbean Basin. Coral reef areas are indicated in red. Stars indicate parks and preserves (Coral Reefs of the World UNEP, 1988).

NAVAL OPERATIONS NEAR CORAL REEFS

Quantifying the extent of naval operations near coral reefs is required in determining the overall mass loading in these sensitive regions. Ship employment databases were obtained and used to calculate historical traffic. Naval operations near coral reefs were evaluated using two different sets of ship traffic data: 1) visits to ports in the vicinity of coral reefs and, 2) historical ship tracks which provide a more precise picture of naval operations near reef systems. This was done because initial port visit estimations came from the same databases used in the overall environmental assessment. However, to address specific concerns raised by regulatory agencies, more precise location data were subsequently obtained and analyzed.

Naval Operations Near Coral Reefs Using Port Visit Data. Originally, to determine the extent of naval operations near coral reefs, a survey of port visits in the three Special Areas was conducted using data from the Chief of Naval Operations (CNO) archived EMPSKD database (OSD N311ND). The information acquired from the database included the ship class, the ship complement, the port visited, and the visit date for the years 1984-1993. Ports which were located within Special Areas with coral reef systems and had an average of 10 or more visits per year were selected for further analysis. There were seven ports from the Caribbean, six from the Gulfs, and one from the Red Sea selected under

this criterion (Figure 4.3-3). The highest number of yearly visits in each Special Area averaged 85 at Roosevelt Roads in the Caribbean, 55 at Sitrah Anchorage in the Gulfs area, and 13 at Hurghada in the Red Sea.

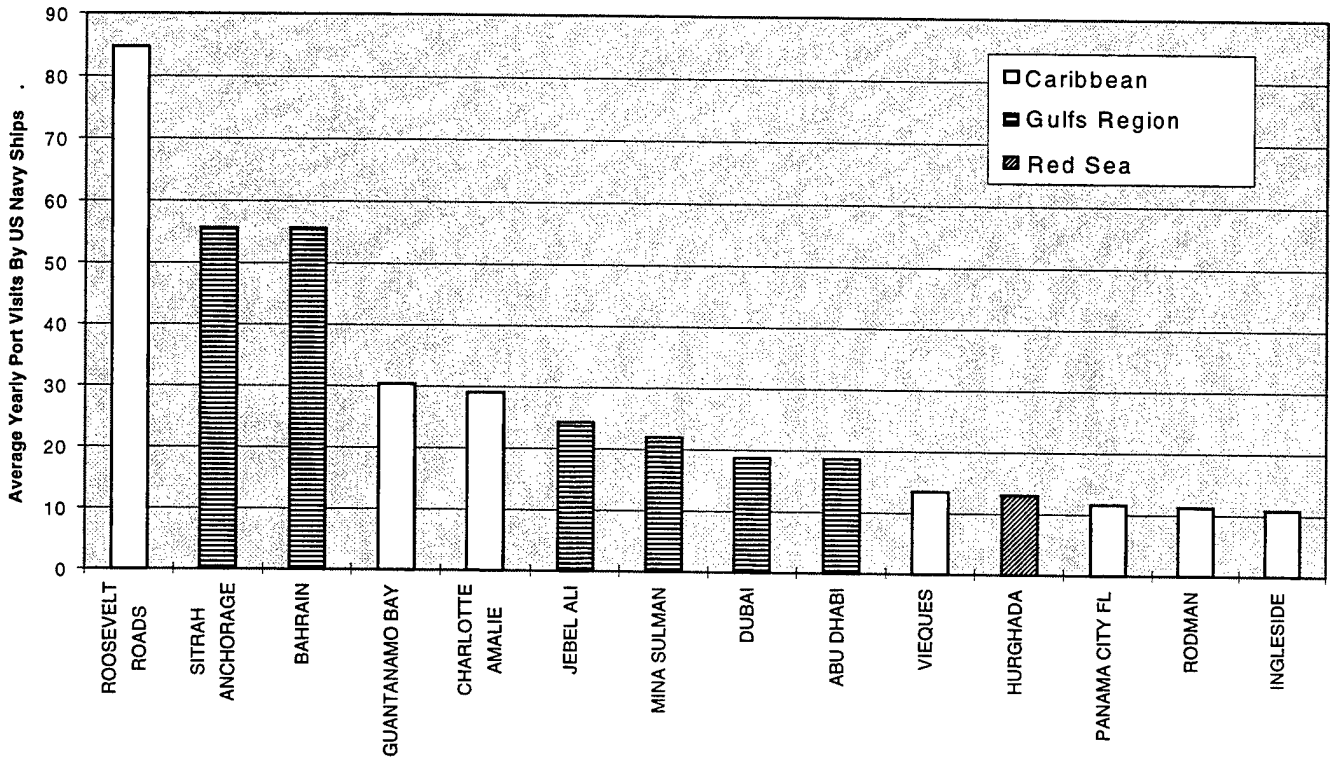

Figure 4.3-3. Average yearly port visits by Navy ships. Ten-year average (1984-1993) for the Caribbean, Red Sea, and Gulfs Region.

A wide range of ship types is included in these total number of visits. For example, at Roosevelt Roads, an average of 46 different ship classes visited the port each year with the number of visits per ship class ranging from a high of fourteen to a low of one (Figure 4.3-4). Other ports show similar patterns. This is important because different ship classes will carry different configurations of processing equipment, including one or more of the large or small pulpers which discharge at different rates. Additionally, the pulped material will be diluted differently depending on the wake geometry of the ship. The average discharge rate was estimated for each ship class using the ship complement (number of crew) times the waste generation rate ($lb \cdot crew^{-1} \cdot day^{-1}$). This information, along with the port visit data, was used to calculate estimated mass loading.

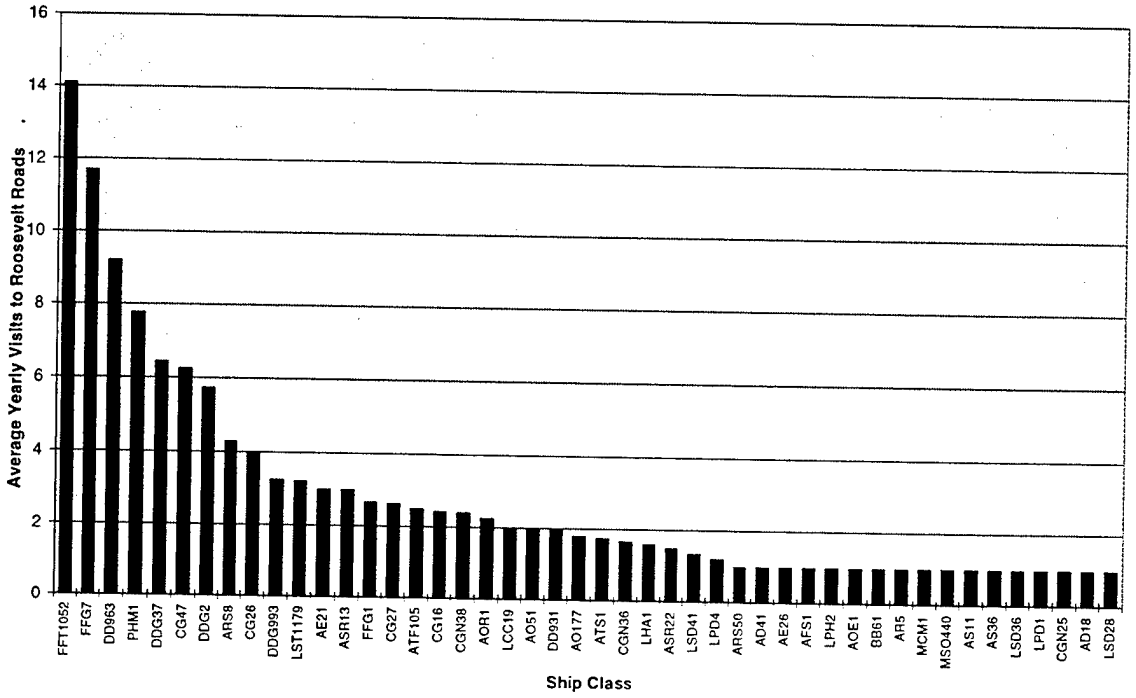

Figure 4.3-4. Average yearly port visits by various classes of Navy ships to Roosevelt Roads in the Caribbean based on a 10 year average (1984-1993).

Pulped Material. In order to account for worst-case loading of the pulped material, food waste (1.21 lb ·crew^{-1}·day^{-1}) was combined with the paper waste (1.11 lb·crew^{-1}·day^{-1}) and the discharge rate incorporated the sum of all pulped waste materials (2.32 lb·crew^{-1}·day^{-1}) even though discharge of food waste is not restricted under Annex V. The wake concentration associated with a single passage for each ship class was then estimated by dividing the discharge rate for that ship by the wake volume using the empirical formula of Csanady (1973):

$$V = 8BDU$$

where V is the wake volume per unit time, B is the ship breadth, D is the ship draft, and U is the ship speed. The true dimensions for each ship class were used for B and D, and a ship speed of 10 knots was assumed for all cases. Modeling and field results discussed in Chadwick et al. (1996) indicate that this gives a reasonable estimate of the wake dilution. The sedimentation for various ship classes based on this estimate are shown in Figure 4.3-5.

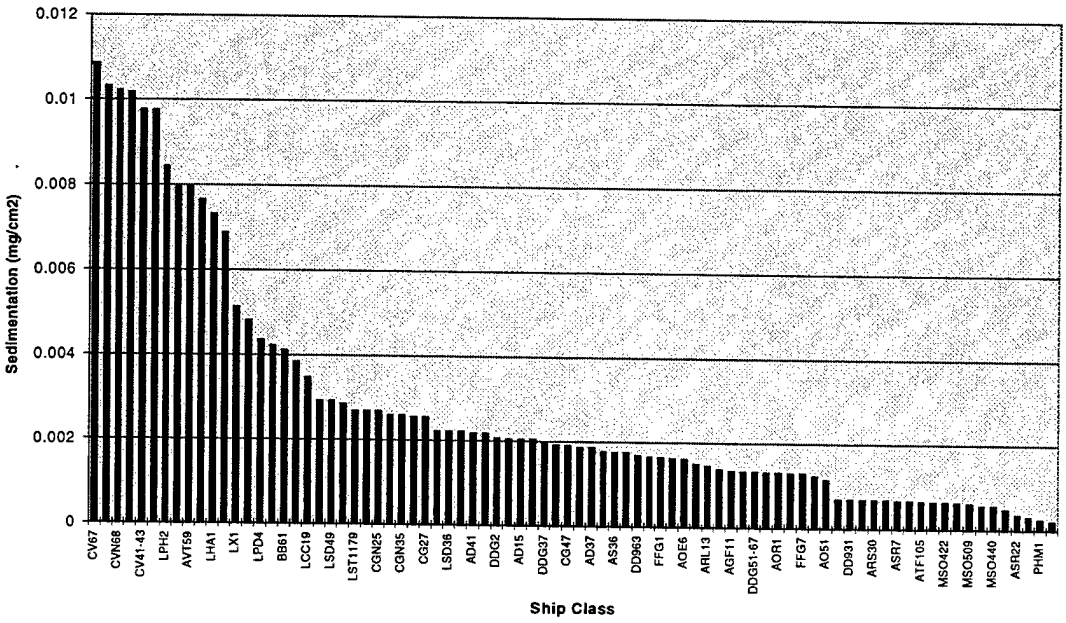

Figure 4.3-5. Estimated sedimentation rates for various Navy ship classes.

Final estimates of long-term sedimentation rates associated with pulper discharges were then determined by multiplying the sedimentation for each visit by the number of visits for each ship at each port and adding up the total sedimentation over the 10 year period 1984-1993. These totals were then doubled to account for the arrival and departure passages associated with each visit, and divided by 10 to obtain the yearly average (see Figure 4.3-6). This conservative approach assumes that the vessel will discharge along the same track while entering and leaving port. The section on potential effects of pulper discharges on coral reefs gives literature values of background and effects levels observed previously for coral reef sedimentation with which to make comparisons with daily sedimentation rates.

In addition to sedimentation estimates, maximum suspended loads in the wake obtained from previous laboratory and field measurements were found to be about 0.2 $mg \cdot L^{-1}$ for a CVN class vessel. This wake concentration provides a reasonable upper bound for the level of acute suspended load exposure for the reefs and assists in determining maximum light reduction.

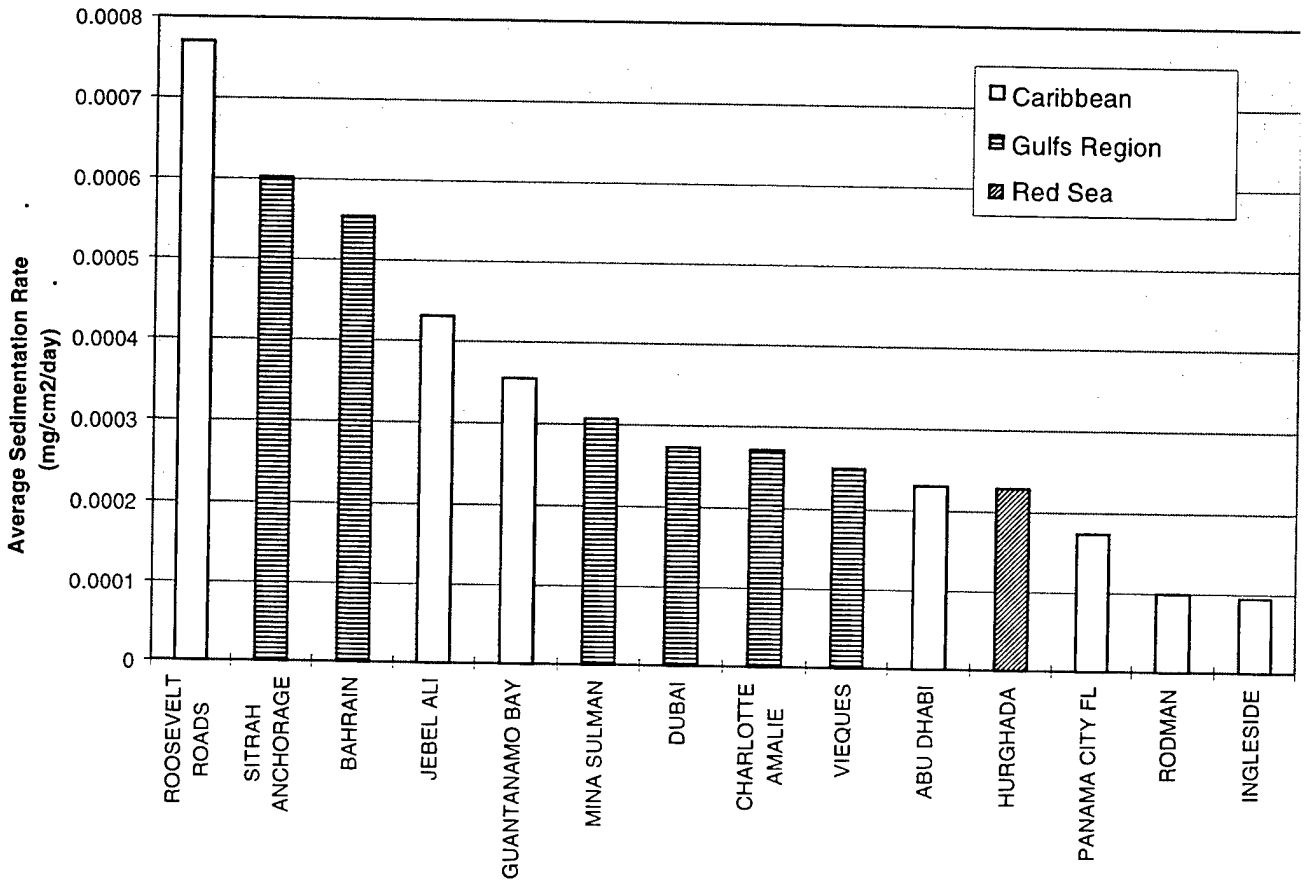

Figure 4.3-6. Estimated long-term sedimentation rates at ports in MARPOL Special Areas where coral reefs are found and Navy ships visit an average of 10 or more times per year.

Shredded Material. The operational analysis of the above port visit data can be used for the shredded material as well. The areal coverage of shredder bags discharged near coral reefs can be estimated based on the same port visit approach described above for estimating sedimentation rates for pulpers. The primary differences between the pulped material and the shredded material are that the generation rate for the shredded metal and glass are somewhat lower (0.25 $lb \cdot crew^{-1} \cdot day^{-1}$) and the waste is discharged in discrete units with a typical frontal area of about 0.2 m^2. Using these data, assuming that ships cross over the same path while entering and leaving port, and assuming the width of the shredder bag waste field to be restricted to the beam of the ship, we first estimated the areal coverage for each ship class for a single passage. Based on the ship operational data and discharge quantities for the appropriate ship class, we then estimated the average yearly areal coverage based on discharges both entering and leaving ports near coral reefs with at least 10 ship visits per year (see Figure 4.3-7). The port with the greatest number of visits, Roosevelt Roads, had an average annual areal ship track coverage of approximately 0.004%. Thus, it would take 250 years to cover only 1% of the sea floor along the track.

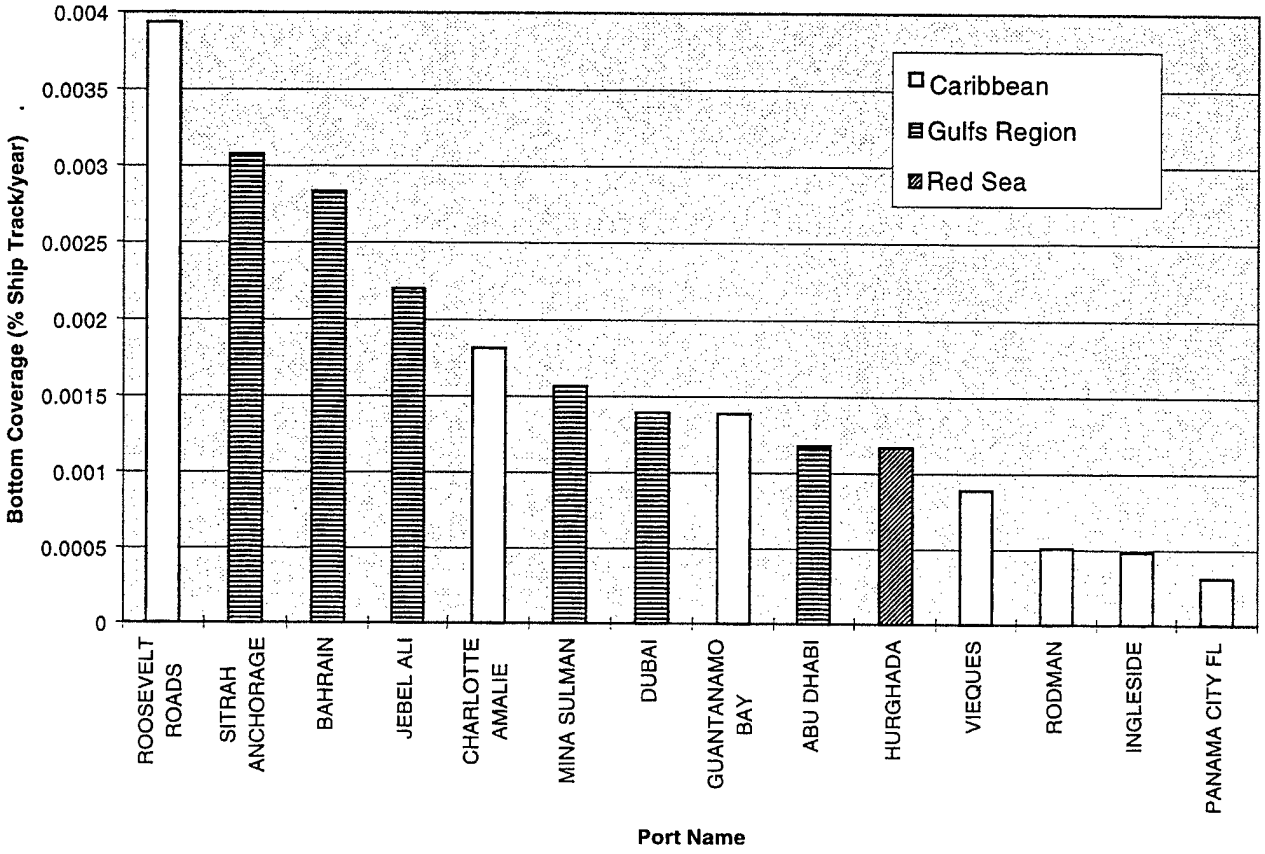

Figure 4.3-7. Estimated annual percentage of bottom beneath the ship track covered by shredder bags at ports where coral reefs exist and Navy ships visit an average of at least 10 times per year.

Naval Operations Near Coral Reefs Using Ship Transit Data. The results from the port visit data showed little potential for detrimental effects, however, it was decided that a more precise estimation of ship traffic near coral reefs was warranted. Therefore, a database containing historical ship movements (CHF_POSITION database) was obtained from CNO (OSD N311ND). This database contained the position (latitude and longitude of vessels traveling in each of the three Special Areas at 8-hour intervals for dates during 1991 to 1995, along with the ship class and ship complement. This time period included high-density traffic in the Persian Gulf during the Gulf War. Additionally, the locations of known coral reefs were evaluated with respect to overlap with ship traffic. For the pulper discharges, the ship footprint, the wake size and an estimated transport rate of 1 $m \cdot s^{-1}$ in an ocean current resulted in a potential overlap of the discharge with the reefs within a 3 nmi range. For the shredder discharges, the maximum resolution of the position data along with the vertical settling rate of 0.5 $m \cdot s^{-1}$ (Chadwick, et al., 1996) and the same transport rate of 1 $m \cdot s^{-1}$ resulted in a potential overlap within a 1 nmi range. In both cases, the position resolution was 1 nmi. Therefore, vessels using a pulper or shredder near a coral reef were considered to overlap or "visit" the reef if they were within 3 nmi and 1 nmi, respectively. After determining the overlap of ship traffic and coral reefs in each sea, the visits were charted by those locations, which had greater than 1, 10, or 100 visits per year. The quantities of discharges were based on the generation rates of each ship class (taking into account the ship complement); the pulper discharge concentrations were based on wake mixing specific to each ship class along with the generation rate, and the discrete shredder discharges were considered to be randomly distributed along the ships route.

For the Gulfs Area, 420 known coral reef positions and 19,194 ship position data records were evaluated (see Figure 4.3-8). For the Wider Caribbean Basin, 992 known coral reef positions and 36,156 ship position data records were evaluated (see Figure 4.3-9). For the Red Sea, 1149 known coral reef positions and 4242 ship position data records were evaluated (see Figure 4.3-10).

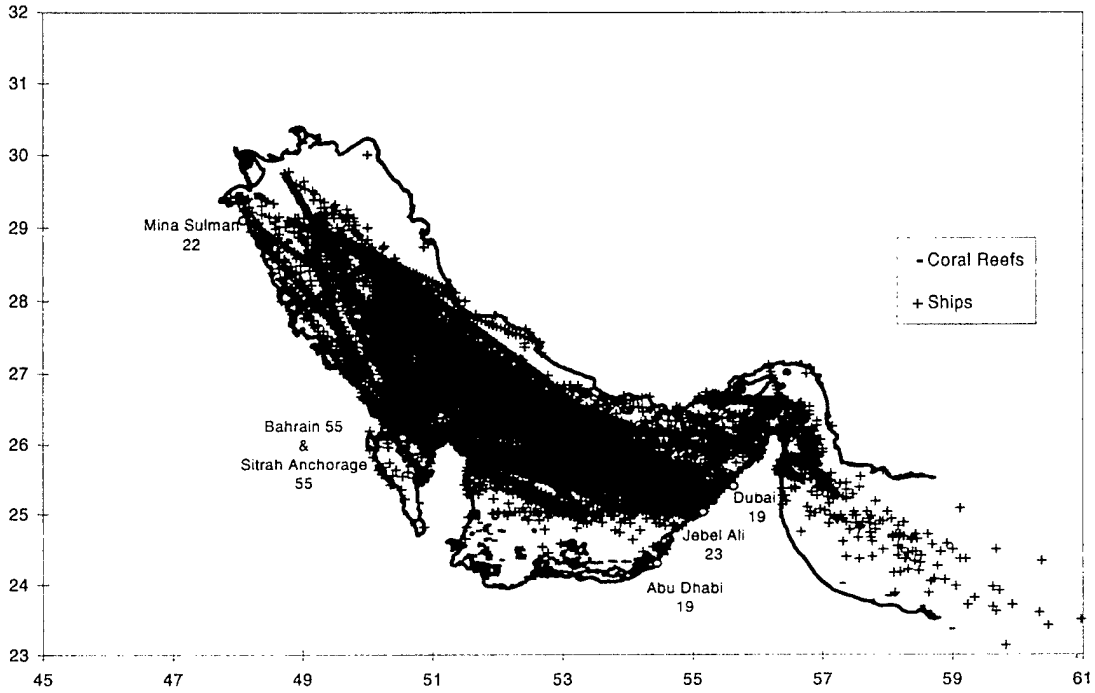

Figure 4.3-8. Ship traffic and reef positions in the Gulfs Area (CNO CHF_POSITION data, 1991-1995; Coral Reefs of the World UNEP, 1988; Reefbase, 1996)

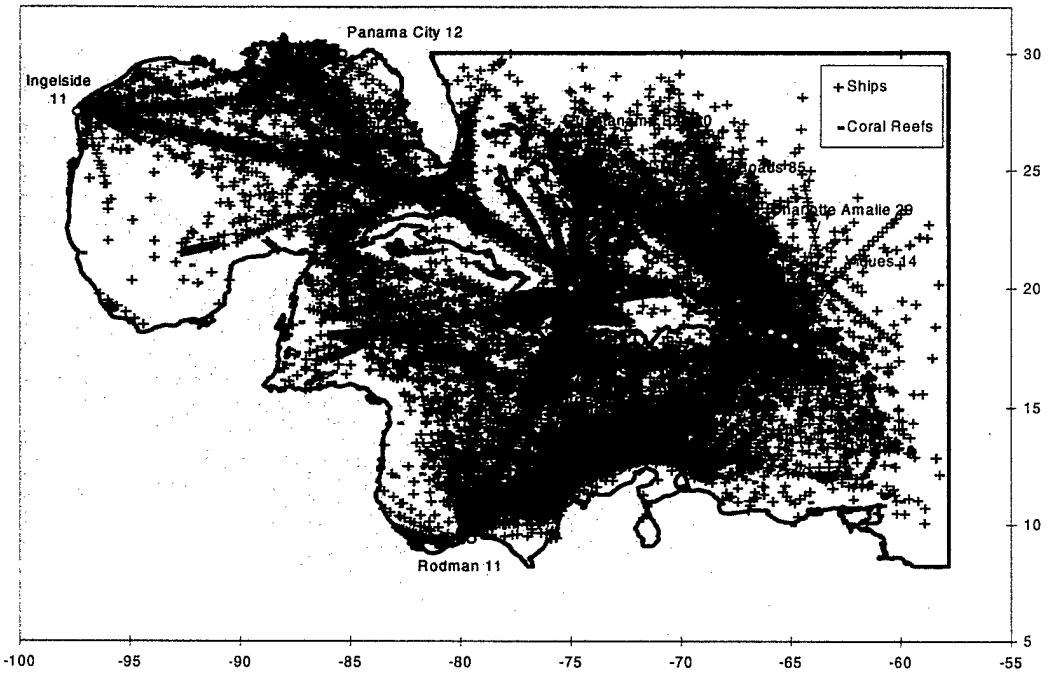

Figure 4.3-9. Ship traffic and reef positions in the Wider Caribbean Basin (CNO CHF_POSITION data, 1991-1995; Coral Reefs of the World UNEP, 1988; Reefbase, 1996)

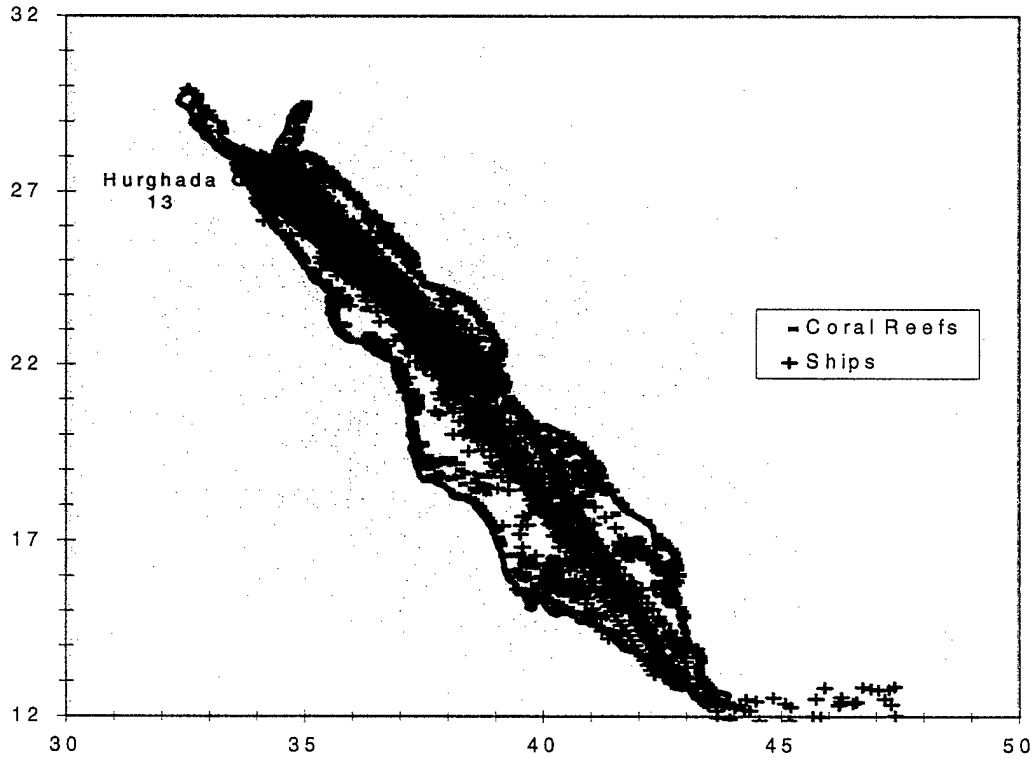

Figure 4.3-10. Ship traffic and reef positions in the Red Sea (CNO CHF_POSITION data, 1991-1995; Coral Reefs of the World UNEP, 1988; Reefbase, 1996)

Pulper Discharges. The maximum number of times a vessel came within 3 nmi of any reef was 414 visits per year in the Gulfs Area, 24 visits per year in the Wider Caribbean Basin, and 11 visits per year in the Red Sea. Table 4.3-1 displays the number of visits within a 3 nmi range in each Special Area. This information is displayed graphically in Figures 4.3-11, 4.3-12, and 4.3-13.

Table 4.3-1. Number of visits within a 3 nmi range in each Special Area.

Visits	Gulfs Area	Wider Caribbean Basin	Red Sea
Maximum	414	24	11
> 100	6	0	0
> 10	10	11	2
> 1	59	77	59

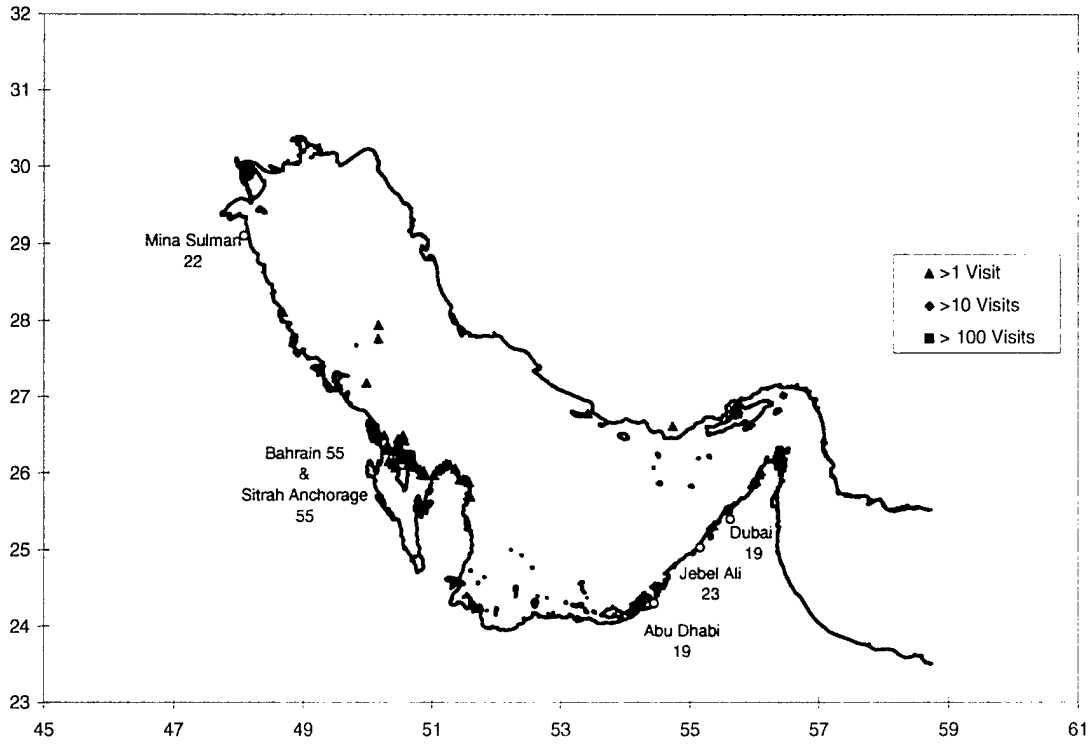

Figure 4.3-11. Overlap of ships and coral reefs within a 3 nmi range in the Gulfs Area (five-year average, 1991 to1995).

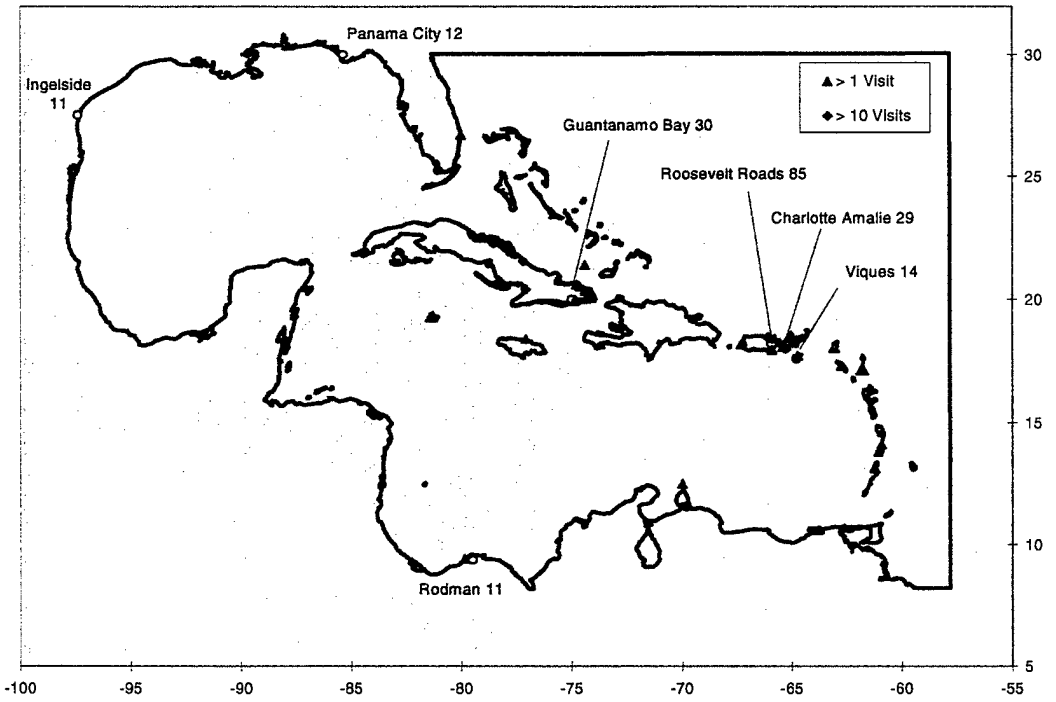

Figure 4.3-12. Overlap of ships and coral reefs within a 3-nmi range in the Wider Caribbean Basin (five-year average, 1991 to 1995).

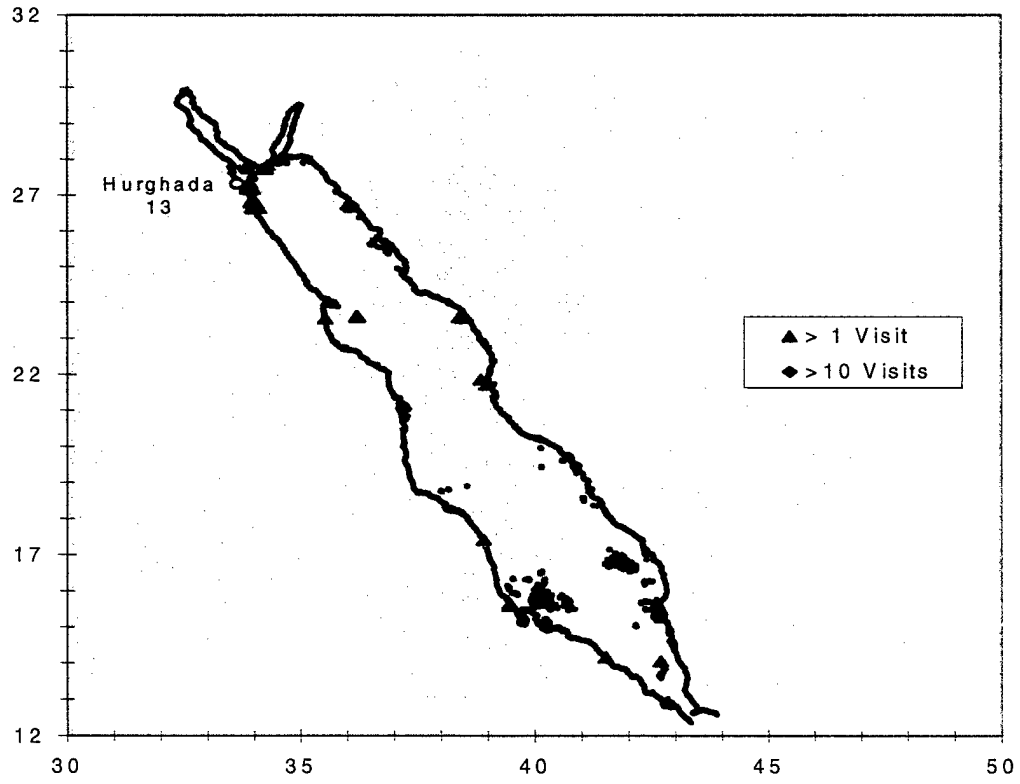

Figure 4.3-13. Overlap of ships and coral reefs within a 3-nmi range in the Red Sea (five-year average, 1991 to 1995).

As in the case using port visit information, there was a wide range of vessel types included in the coral reef visits in each of the Special Areas considered. Using the same discharge quantities (2.32 lb·crew^{-1}·day^{-1}) and the same empirical formula of Csanady (1973) for ship wake concentration, sedimentation rates for each visit location were calculated. The maximum sedimentation rates for the Gulfs Area, the Wider Caribbean Basin, and the Red Sea are $2.3 \cdot 10^{-3}$ mg·cm^{-2}·d^{-1}, $1.2 \cdot 10^{-4}$ mg·cm^{-2}·d^{-1}, and $7.0 \cdot 10^{-5}$ mg·cm^{-2}·d^{-1}, respectively. The section on Potential Effects of Pulper Discharges on Coral Reefs presents literature values of background and effects levels observed previously for coral reef sedimentation with which to make comparisons with these maximum values. The value used in assessing potential effects due to total suspended solids and light reduction remain the same at 0.2 mg·L^{-1} for the worst-case, single-ship discharge from a CVN class vessel.

Shredder Discharges. The maximum number of times a vessel came within 1 nmi of any reef is 71 visits per year in the Gulfs Area, 18 visits per year in the Wider Caribbean Basin, and 2.4 visits per year in the Red Sea. Table 4.3-2 displays the number of visits within a 1 nmi range in each Special Area. This information is displayed graphically in Figures 4.3-14, 4.3-15, and 4.3-16.

Table 4.3-2. Number of visits within a 1 nmi range in each Special Area.

Visits	Gulfs Area	Wider Caribbean Basin	Red Sea
Maximum	71	18	2.4
> 100	0	0	0
> 10	1	1	0
> 1	8	15	6

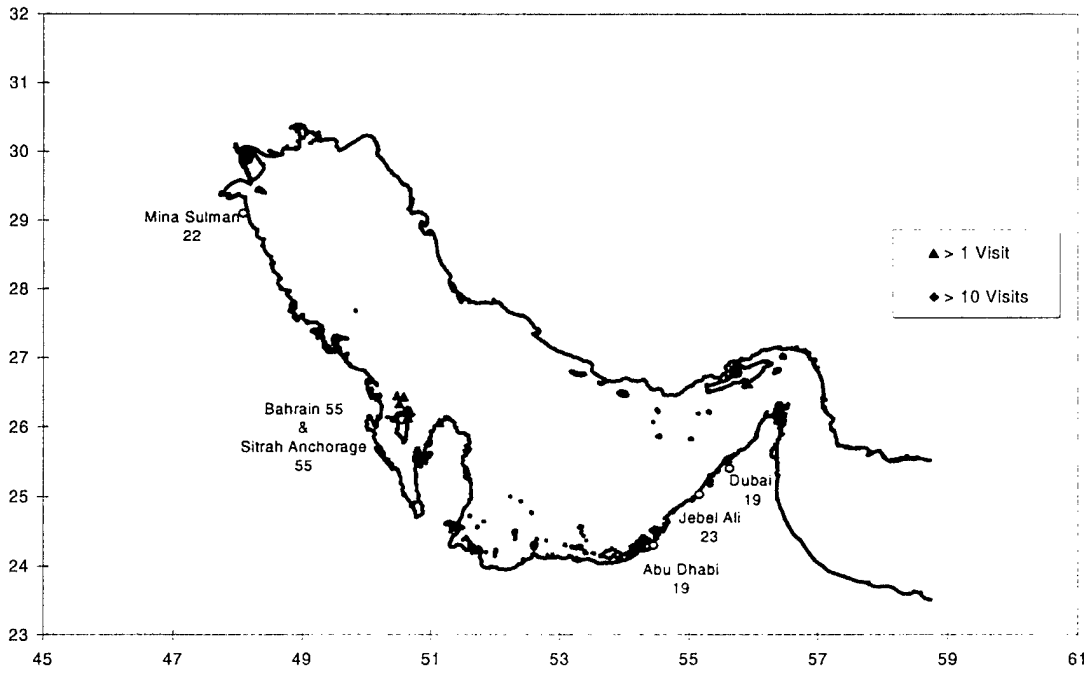

Figure 4.3-14. Overlap of ships and coral reefs within a 1-nmi range in the Gulfs Area (five-year average, 1991 to 1995).

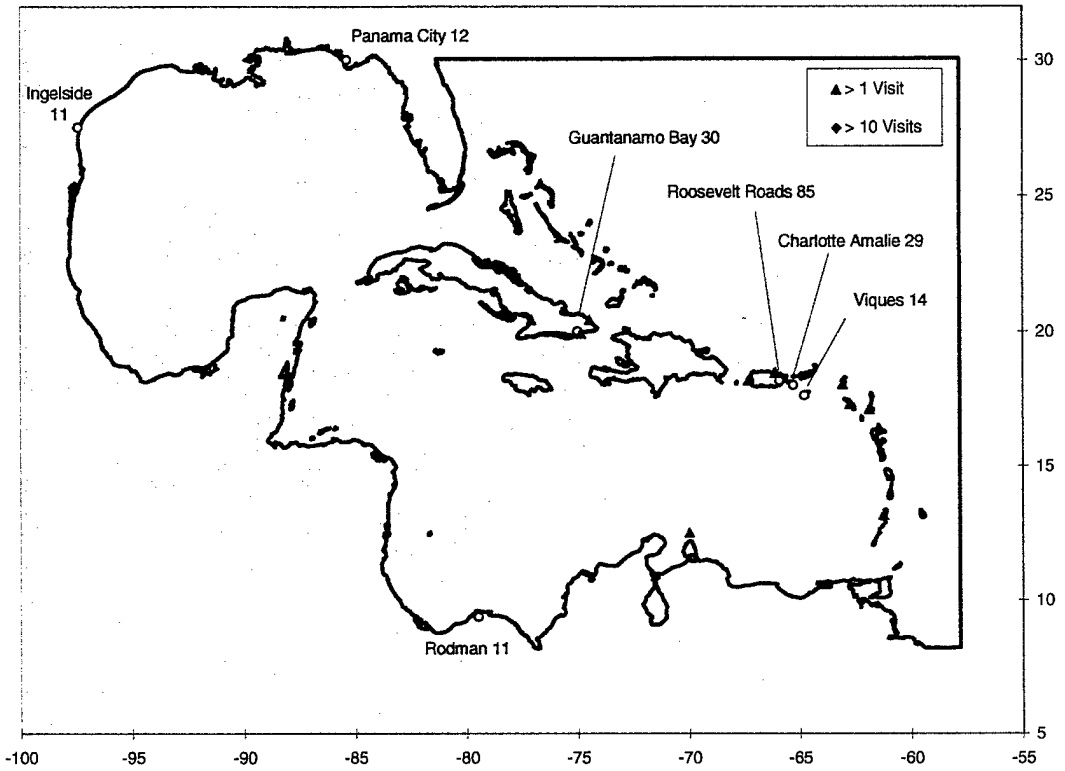

Figure 4.3-15. Overlap of ships and coral reefs within a 1-nmi range in the Wider Caribbean Basin (five-year average, 1991 to 1995).

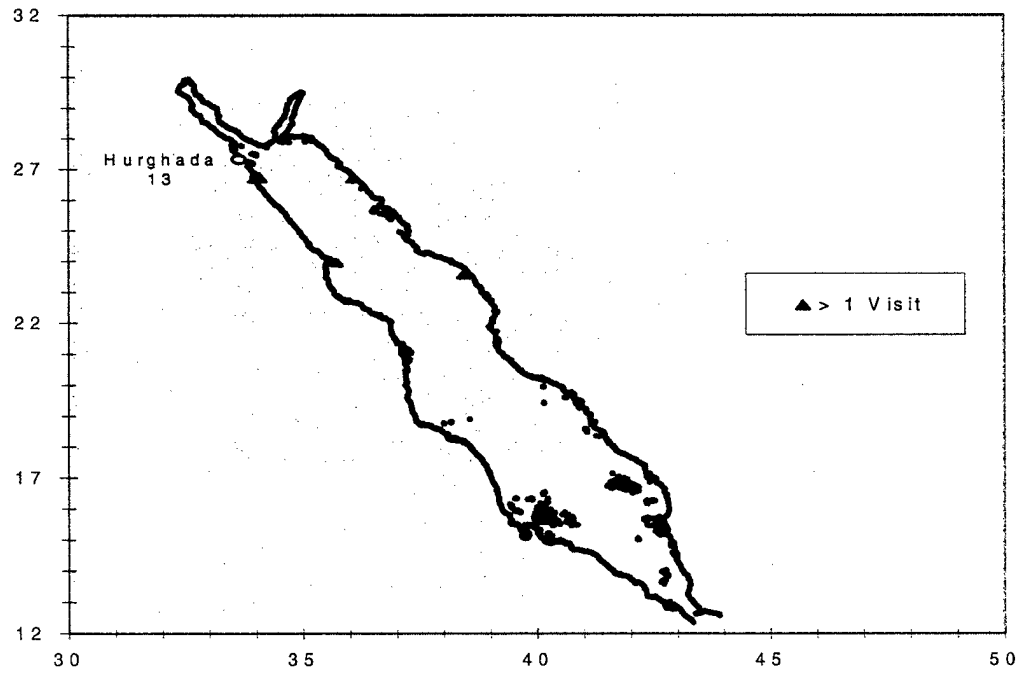

Figure 4.3-16. Overlap of ships and coral reefs within a 1-nmi range in the Red Sea (five-year average, 1991 to 1995).

As in the case using port visit information, ship class and crew complements were taken into account in calculating mass loading. Using the same discharge quantities for metal and glass (0.25 lb·crew^{-1}·day^{-1}) and the typical frontal area of 0.2 m^2, the average annual sea floor coverage was calculated. The maximum sea floor coverage for the Gulfs Area, the Wider Caribbean Basin, and the Red Sea are $2.7 \cdot 10^{-3}$ %·yr^{-1}, $1.1 \cdot 10^{-3}$ %·yr^{-1}, and $1.8 \cdot 10^{-4}$ %·yr^{-1}, respectively. Given the maximum coverage for each Special Area and neglecting any degradation of the material, the time it would take to cover 1% of the coral area would be greater than 370 years for the Gulfs Area, greater than 900 years for the Wider Caribbean Basin, and greater than 5500 years for the Red Sea.

Imposing 3 nmi And 12 nmi Discharge Limits. Because most coral reef systems lie in shallow water, and often close to shore, there can be a difference between the amount of overlap between the ships and coral reefs when distance-from-shore restrictions are implemented. The section on potential effects of shredder bag discharges will discuss transport and areal coverage of the shredder bags; however, a comparison from the standpoint of operational discharge restrictions is presented here. For the pulper, a 3-nmi distance restriction is imposed. Approximately 60% of the coral reefs lie within the 3-nmi limit, and the assumptions for transport of the pulped material (estimated to be 3 nmi) do not reduce the likelihood of overlap with coral reefs. However, because a 12-nmi distance restriction is imposed for the shredder, the actual overlap between vessels and coral reefs can be significantly lower than estimated using the 1-nmi range. Table 4.3-3 presents the effects on coral reef visits and maximum sea floor coverage by shredder bags when the 12-nmi discharge limit is applied. The 12 nmi discharge limit reduces the likelihood of overlap by at least a factor of 10, and much more in some instances.

Table 4.3-3. Comparison of Effects on Overlap of Ships and Coral Reefs from 3 nmi and 12 nmi Discharge Limits

Region	Reefs Outside 3 nmi Limit	Reefs Outside 12 nmi Limit	Max Visits per year		Max Sea Floor Coverage (%·yr^{-1})	
			12 nmi Limit	No Limit	12 nmi Limit	No Limit
Gulfs Area	38%	5%	1.4	71	$4.8 \cdot 10^{-5}$	$2.7 \cdot 10^{-3}$
Wider Caribbean	45%	10%	1.4	18	$6.6 \cdot 10^{-5}$	$1.1 \cdot 10^{-3}$
Red Sea	40%	5%	0.0	2.4	0	$1.8 \cdot 10^{-4}$

Comparison Of Port Visit And Ship Transit Data Relative To Coral Reef Overlap. When evaluating the overlap between Navy vessels and coral reefs, the only Special Area that shows an increase when using ship transit data versus port visit data is the Gulfs Area. The maximum number of visits in the Bahrain/Sitrah Anchorage area increased from 110 for the port visit analysis to 414 for the ship transit analysis. This translates to an increase in the sedimentation rate from 0.0006 mg·cm^{-2}·d^{-1} to 0.002 mg·cm^{-2}·d^{-1}. Estimates made in the other two Special Areas show a decrease in sedimentation rate. Because of the greater distance-from-shore restriction for the shredder discharges, all of the Special Areas show a decrease in sea floor coverage when using the ship transit data versus the port visit data. These numerical comparisons are shown in Table 4.3-4 below.

Table 4.3-4. Comparison of Using Port Visit Data Versus More Precise Ship Transit Data.

Region	Maximum Number of Potential Overlaps of Ships and Coral Reefs				Sedimentation ($mg \cdot cm^{-2} \cdot d^{-1}$)		Sea Floor Coverage (%/Year)	
	3 nmi Discharge Limit			12 nmi Disch. Lim.				
	Port Visits	Ship Transits			Pulper (3 nmi Discharge Limit)		Shredder (12 nmi Discharge Limit)	
	3 nmi Range	3 nmi Range	1 nmi Range		Port Visits	Transits	Port Visits	Transits
Gulfs Area	110	414	71	1.4	0.0006	0.002	0.003	0.00005
Caribbean	170	24	18	1.4	0.0008	0.0001	0.004	0.00007
Red Sea	26	11	2.4	0	0.0002	0.00007	0.001	0

POTENTIAL EFFECTS OF PULPER DISCHARGES ON CORAL REEFS

Effects of particulate discharges on coral reefs have been examined in a number of previous studies (Dodge et al., 1974; Rogers, 1990). The concerns that are generally raised in the literature include:

Direct toxicity to coral polyps due to contaminants associated with the particulates. Many contaminants are preferentially bound to particles and polyps may be exposed to these as the particles settle.

Smothering of corals under high sedimentation rates. Sessile coral polyps cannot move in response to large particulate influxes and may thus be smothered in areas of high sedimentation.

Stress and mortality due to increased clearing requirements in high particulate environments. Many corals are adapted to clear particles however increasing sediment loads may lead to a disproportionate energy expenditure on clearance, placing the animals under stress which may eventually lead to mortality.

Reduction in light levels due to increased suspended particulate loading. Coral polyps are often very sensitive to light levels because of their symbiotic dependence on photosynthetic zooxanthellae.

Toxic Effects. The pulped paper waste stream has been subjected to toxicity testing on a wide range of organisms including marine bacteria, phytoplankton, zooplankton, benthic invertebrates, and fish. None of these tested showed significant effects at the concentrations expected in the environment (Chadwick et al., 1996). In addition, detailed chemical analysis of the pulped paper waste stream indicates that it is composed primarily of non-toxic organic materials with low nutrient content. Only zinc was found at detectable levels and these levels were significantly below published toxicity thresholds (Chadwick et al., 1996). Although no direct tests have been performed on corals (no standardized tests exist), the evidence above suggests that the likelihood of toxic effects to corals is very low.

Smothering and Particle Clearance: The potential effects of smothering and increased particle clearance are both a function of the increase in suspended particle load and sedimentation associated with ship discharges. Background sedimentation rates and suspended loads were determined for a number of coral reefs from a review of the literature. These values are summarized in Table 4.3-5. In addition, suspended loads and sedimentation rates at which adverse effects on corals have been observed previously were also obtained from the literature review (Table 4.3-6). These values can then be compared to the estimated suspended loads and sedimentation rates associated with pulper discharges. The underlying assumption in this analysis is that pulper particles behave in a similar manner to sediment particles with respect to their potential physical effects on corals. Fibrous organic material could potentially behave in different ways than sediment, however, this is the closest data from the literature for comparison with regard to particle size and non-toxic nature.

Table 4.3-5. Background sedimentation and suspended sediment loads near coral reefs from a review of published studies. Source references are listed in the first column.

Study	Sedimentation Rate ($mg \cdot cm^{-2} \cdot d^{-1}$)	Suspended Solids ($mg \cdot L^{-1}$)	Extinction Coefficient ($1 \cdot m^{-1}$)	Reef Type and Depth
Maragos (in Rogers, 1983)	35 - 41,096			
Dodge *et al.* (in Rogers, 1983)	0.5 - 1.1			
Rogers 1982	0.1 - 5.8			
Cintron *et al.* (in Rogers, 1983)	1 - 15			
Rogers, 1983	2.5 - 9.6	0.8		Backreef 4m deep
Rogers, 1990	<1 - 10	<10		No stress levels
Dodge *et al.* (in Rogers, 1990)	0.5 - 1.1			Reef Lagoon 4m deep
Rogers 1982	0.8 - 5.8			Five reefs 3-5m deep
Cortes and Risk (in Rogers, 1990)	30 - 360			
Tomasck and Sander (in Rogers, 1990)	<1 to >40	4.3 - 73		
Ott (in Rogers, 1990)	ca 5 - 10			Barrier reef 13.5-45m
Rice and Hunter, 1992		15.1 - 26.2		Gulf of Mexico 7-26m
Stafford-Smith, 1993	>200			Australian fringing reefs
Roy and Smith, 1971		0.3 - 3.5	0.13 - 0.28	Fringing reef outside Fanning Island

Table 4.3-6. Effects levels for sedimentation and suspended sediment loads on coral reefs from a review of published studies. Source references are listed in the first column.

Study	Sedimentation Rate ($mg \cdot cm^{-2} \cdot d^{-1}$)	TSS ($mg \cdot L^{-1}$)	Light Transmission Reduction (%)	Species	Measured Responses
Roy and Smith, 1971		3.5		*Montipora*, *Acropora* sp.	Reduced abundance, diversity
Loya, 1976	3-15			*Montastrea cavernosa*, *M. annularis*, *Siderastrea radians*, *S. siderea*, *Diploria strigosa*, *Meandrina meandrites*, *Agaricia agaricites*	Diversity, coverage
Rogers, 1983	200			*Diploria strigosa*, *Acropora cervicornis*, *Montastraea annularis*	Daily application - no effect - 38 days
Rogers, 1983	200-800			*Acropora palmata*, *Montastraea annularis*, *D. clivosa*	Death, bleaching
Dallmeyer et al., 1982		175		*Montastrea annularis*	Reduction in chlorophyll content and production rate
Bak, 1978			99%	*Porites astreoides*, *Madracis mirabilis*, *Agaricia agaricites*	Death; Temporary 33% reduction in growth rate
Rice and Hunter, 1992		49-199		*Cladocora arbuscula*, *Manicina aereolata*, *Solenastrea hyades*, *Phyllangia americana*, *Isophyllia sinuosa*, *Scolymia lacera*, *Stephanocoenia mitchelinii*	No effect on survival 10 days; Growth effects at 165 $mg \cdot liter^{-1}$
Stafford-Smith, 1993	>100			*Montipora equituberculata*, *Porites lobata*, *P. lutea*	Bleaching after 6 days

Previous modeling and field studies indicate that the highest suspended load in the wake of a ship occurs for the CVN class ships at concentrations of about 0.2 $mg \cdot L^{-1}$, while typical background levels range from 0.8 to 73 $mg \cdot L^{-1}$, and observed effects levels range from 3.5 to 200 $mg \cdot L^{-1}$. For long-term sedimentation rates, the highest estimate occurs in the Gulfs Area at about 0.002 $mg \cdot cm^{-2} \cdot day^{-1}$ using the ship transit data. Typical background sedimentation rates range from 0.1 to 360 $mg \cdot cm^{-2} \cdot day^{-1}$ and adverse effects have been observed at rates ranging from 3 to 800 $mg \cdot cm^{-2} \cdot day^{-1}$. From comparative exposure, background, and effects levels summarized in Table 4.3-7, it is clear that the probability of significant smothering of corals or clearance stress is very low. In comparison, the sedimentation rates

for both the Caribbean Region and the Red Sea are reduced when using the more precise ship transit data. Only the Gulfs Area indicates an increased sedimentation rate (see Table 4.3-4).

Table 4.3-7. Comparison of pulper discharge levels to background and effects levels.

	Sedimentation Rate ($mg/cm^2/d$)	TSS (mg/L)	Light Transmission Reduction (%)
Estimated Inputs			
Single CVN Wake	0.04 mg/cm^2	0.2	0.02
Port Visits:			
Caribbean - 85 Visits/Year	0.0008		
Gulfs - 56 Visits/Year	0.0006		
Red Sea - 19 Visits/Year	0.0002		
Ship Transits:			
Caribbean	0.00007		
Gulfs Area	0.002		
Red Sea	0.0001		
Background Levels	0.1 - 360	0.8 - 73	
Effects Levels	3 - 800	3.5 - 200	

Reduction in Light Levels. The potential reduction in light levels was evaluated based on laboratory tests of the relationship between light transmission and pulped paper concentrations. As described in Chadwick et al. (1996), the majority of the pulped paper waste stream (85% by mass) is contained in large particles which sink rapidly (typically within one day). Thus the only fraction of the waste stream which is likely to affect light levels is the smaller size particles for extended durations, generally made up of individual fibers. These particles are small enough to remain in the water column for several days. In the laboratory tests, increasing levels of paper particles were added to reference seawater and pumped through a standard 25-cm pathlength transmissometer. Assuming that the worst-case wake concentration for the CVN is about 0.2 $mg \cdot L^{-1}$, and that particles remaining in the water column comprise about 15% of the total mass, the highest expected concentration of small particles would be about 0.03 $mg \cdot L^{-1}$. Because light attenuation in the sea is a function of depth, a relationship between the concentration of paper particles and light transmission was established (Figure 4.3-17). A regression line of light vs. paper concentration from Figure 4.3-17 indicates a reduction in light transmission from about 84.58% for the reference seawater to about 84.56% for the seawater with pulped paper. Based on the conservative assumption that the entire water column down to the 1% light level depth (typical limit for photosynthetic activity) contained small particles at this concentration, the change in depth of the 1% light level can be estimated from

$$\Delta Z_{1\%} = ln(0.01)*(1/K_{ocean} - 1/K_{paper})$$

where $\Delta Z_{1\%}$ is the change in the depth of the 1% light level, K_{ocean} is the extinction, or attenuation, coefficient for the reference ocean water, and K_{paper} is the extinction coefficient for the seawater with pulped paper added. From the laboratory experiment K_{ocean} is ~ 0.4351 m^{-1} and K_{paper} is ~ 0.4361 m^{-1} giving a value of $\Delta Z_{1\%}$ ~ 0.02 m. It seems highly unlikely that a change of 2 cm in the 1% light level would result in any effects on the health of coral reefs.

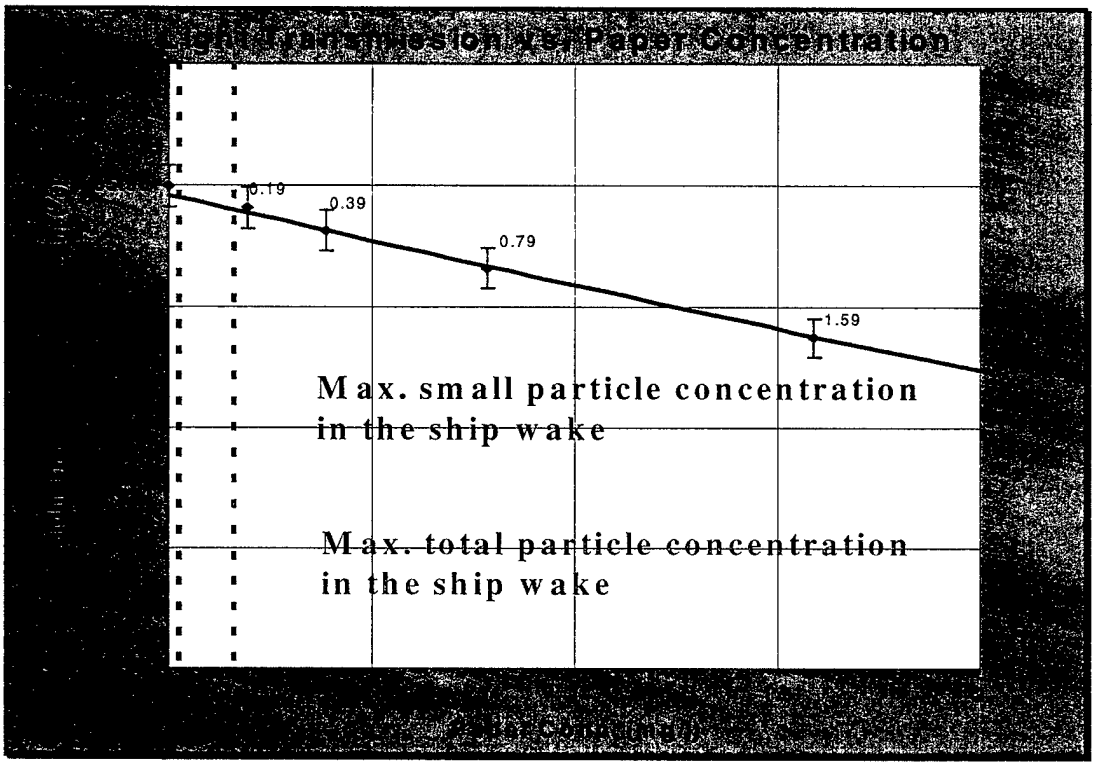

Figure 4.3-17. Effects of pulped paper on light transmission based on laboratory tests of the small particle fraction of the pulper waste stream.

POTENTIAL EFFECTS OF SHREDDER BAG DISCHARGES ON CORAL REEFS

The primary concern for effects of shredder bag discharges on coral reefs stems from the potential physical damage to reefs due to the initial landing, the smothering of reef areas beneath the bags, and the possible damage done by subsequent storm driven transport of the bags. Effects from shredder bags are localized to the vicinity of the bag itself.

The potential for physical damage and smothering of corals depends primarily on two factors which govern exposure. The first factor, as for the pulped waste, is the amount of time that Navy ships spend operating near coral reefs and discharge waste. The second factor is the amount of transport that takes place following discharge which determines just how close to a coral reef a ship must operate for the shredder bags to land on coral. Based on the toxicity studies described in Chadwick et al. (1996), it is unlikely that significant toxicity effects would be found beyond the localized region of the bag itself. Thus, the sections below focus on the lateral transport of the shredder bags following discharge, and the fractional area of sea floor that would be covered by shredder bags in areas where coral reefs are known to overlap with Navy ship traffic.

Transport of Shredder Bags. The shore-ward (or reef-ward) transport of shredder bags was examined in some detail in Chadwick et al. (1996). Field tests of the bagged waste showed that it sinks rapidly at a rate of about 0.5 $m \cdot s^{-1}$. The distance the bags might be transported toward a reef thus depends primarily on the strength of the onshore current and the water depth. This relationship is shown

in Figure 4.3-18. For example, based on this analysis we would estimate the maximum shoreward transport of a bag discharged in 200 m of water with a 1 $m \cdot s^{-1}$ shoreward current would be about 0.35 km (0.19 nmi). Although a typical shoreward transport of 0.19 nmi was estimated, the mapping resolution dictated that shredder bag discharges were considered any time a vessel came within 1 nmi of a coral reef. Using the 12-nmi discharge limit as described in the historical ship traffic analysis, ships came within 1 nmi of coral reefs only 1.4 times per year in the Gulfs Area and the Wider Caribbean Basin, and not at all in the Red Sea. Therefore, the likelihood of shredder bags landing on reefs is extremely small. And, in reality, the few vessels that do transit within 1 nmi of the coral reefs are unlikely to be directly over a reef or extremely close to a reef since reefs are generally avoided as navigational hazards.

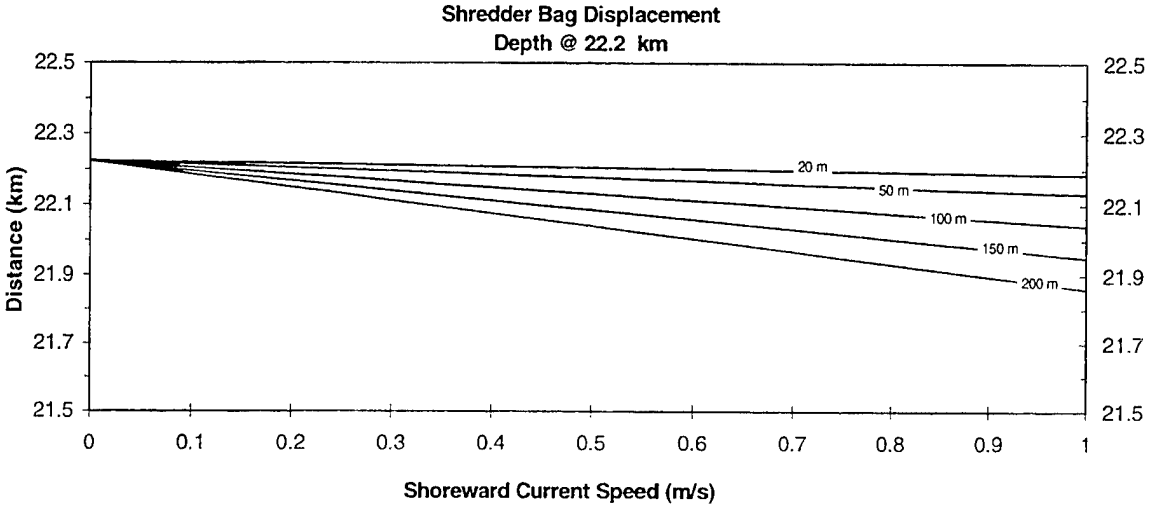

Figure 4.3-18. Shore-ward transport of shredder bags under varying conditions of shore-ward current speed and discharge depth. All values are based on a vertical settling velocity of 0.5 $m \cdot s^{-1}$.

Areal Coverage of Shredder Bags Near Coral Reefs. We have seen from the previous operational analysis that the worst-case sea floor coverage for the ship transit data, is estimated to be in the Gulfs Area at $2.7 \cdot 10^{-3}$ %/yr. However, legislation which was passed allowing the use of pulpers and shredders on naval vessels in Special Areas specified that the shredder bags must be discharged at greater than 12 nmi from shore. With this restriction, the areal sea floor coverage by shredder bags is further reduced to $4.8 \cdot 10^{-5}$ %/yr. Thus, given the historical traffic that has been in the Gulfs Area, even if the vessels discharged directly over coral reefs while transiting, it would take approximately 21,000 years to impact 1% of the coral reefs in the worst-case scenario. This result suggests that even in the unlikely event that ships transit over coral reefs, the area that would be effected by shredder bags would be extremely small.

SUMMARY AND CONCLUSIONS

Concerns regarding the potential effects of pulped and shredded waste streams from U.S. Navy ships on coral reefs have been assessed based on the most recent data available on waste stream characteristics, historical ship operations, coral reef distributions, and coral reef sensitivities. The analysis indicates that the potential effects of pulped paper waste are minimized by several factors including the high initial dilution of the waste stream, the non-toxic nature of the waste material, and the limited overlap between

ship operations and coral reef locations. Estimated maximum suspended particle loads following discharge and long-term sedimentation rates were found to be well below reported background and effects levels for a number of coral reef studies. Similarly, because the majority of the material settles rapidly, estimated reductions in light levels due to localized increases in suspended particle loads were shown to have negligible effects on the light penetration depths. Together, these results indicate the likelihood of significant effects on coral reefs in MARPOL Special Areas from pulper discharges is very low.

Potential effects of physical impacts from shredder bags are limited by the rapid settling of the bags, the non-toxic nature of the material, and the limited overlap between ship operations and coral reef locations. Maximum lateral transport of shredder bags from the discharge location was shown to be about 350 m indicating that bags will only be likely to land on coral reefs if the ships are transiting directly above them. This scenario is unlikely from an operational standpoint. Using the historical ship transit data at 1 nmi resolution, which is considered to be more precise than the port visit data, the highest input near Bahrain/Sitrah Anchorage in the Gulfs Area would take over 370 years to cover only 1% of the coral reef area. However, when the 12-nmi distance-from-shore restriction is applied, it would take approximately 21,000 years to cover only 1% of the coral reef area. As with the pulped waste stream, these results suggest that the likelihood of significant effects on coral reefs in MARPOL Special Areas from shredder discharges is very low.

REFERENCES

Bak, R.P. *Lethal and Sublethal Effects of Dredging on Reef Corals.* Marine Pollution Bulletin, pp. 14-16, 1978.

Chadwick, D.B., Katz, C.N., Curtis, S.L., Rohr, J., Caballero, M., Valkirs, A., Patterson, A. *Environmental Analysis of U.S. Navy Shipboard Solid Waste Discharges: Report of Findings.* Technical Report 1716, Naval Command, Control and Ocean Surveillance Center, RDTandE Division, California, 1996.

Cintron, G., McKenzie, F., Olazagasti, R. *Studies at the PRINUL Site, Final Report: Missions 3 and 5.* Department of Natural Resources, San Juan, Puerto Rico, 1974.

Cortes, J., Risk, M.J. *El Arrecife Coralino del Parque Nacional Cahuita, Costa Rica.* Revta Biol. Trop., V32, pp. 109-121, 1984.

Csanady, G.T. *Turbulent Diffusion in the Environment.* Journal of Atmospheric Science V26, pp. 414-426, 1973.

Dallmeyer, D.G., Porter, J.W., *Smith G.J. Effects of Particulate Peat on the Behavior and Physiology of the Jamaican Reef-Building Coral Montastrea annularis.* Marine Biology V68, pp. 229-233, 1982.

Dodge, R.E. Vaisnys, J.R. *Coral Populations and Growth Patterns: Responses to Sedimentation and Trubidity Associated with Dredging.* Journal Marine Research, V35, pp. 715-730, 1977.

Dodge, R.E., Aller, R.C., Thomson, J. *Coral Growth Related to Resuspension of Bottom Sediments.* Nature, London, V247, pp. 574-577, 1974.

Loya, Y. *Effects of Water Turbidity and Sedimentation on the Community Structure of Puerto Rican Corals.* Bulletin of Marine Science, V26(4), pp. 450-466, 1976.

Maragos, J.E. *A Study of the Ecology of Hawaiian Reef Corals.* Ph.D. thesis University of Hawaii, 1972.

Ott, B. *Community Patterns on a Submerged Barrier Reef at Barbados, West Indies.* International Revue ges. Hydrobiology, V60, pp. 719-736, 1975.

McManns, J.W., Ablan, M.C., *ReefBase: A Biological Database on Coral Reefs and Their Resources.* ICLARM, Manila, 1996.

Rice, S.A., Hunter, C.L. *Effects of Suspended Sediment and Burial on Scleractinian Corals From West Central Florida Patch Reefs.* Bulletin of Marine Science, V51(3), pp. 429-442, 1992.

Rogers, C.S. *The Marine Environments of Brewers Bay, Perseverance Bay, Flat Cay and Saba Island, St. Thomas, U.S.V.I. with Emphasis on Coral Reefs and Seagrass Beds: November 1978-July 1981.* Division of Natural Resources Management, Department of Conservation and Cultural Affairs, Government of the Virgin Islands, 1982.

Rogers, C.S. *Responses of Coral Reefs and Reef Organisms to Sedimentation.* Marine Ecology Progress Series, V62, pp. 185-202, 1990.

Rogers, C.S. *Sublethal and Lethal Effects of Sediments Applied to Common Caribbean Reef Corals in the Field.* Marine Pollution Bulletin, V14, N10, pp. 378-382, 1983.

Roy, K.J., Smith, S.V. *Sedimentation and Coral Reef Development in Turbid Water: Fanning Lagoon.* Pacific Science, V25, pp. 234-248, 1971.

Stafford-Smith, M.G. *Sediment-Rejection Efficiency of 22 Species of Australian Scleractinian Corals.* Marine Biology, V115, pp. 229-243, 1993.

Tomascik, T., Sander, F. *Effects of Eutrophication on Reef-Building Corals. III. Reproduction of the Reef-Building Coral Porites porites.* Marine Biology, V94, pp. 77-94.

UNEP. *Coral Reefs of the World: Volume 1 Atlantic and Eastern Pacific.* UNEP Regional Seas Directories and Bibliographies. IUCN, Gland, Switzerland and Cambridge, U.K./UNEP, Nairobi, Kenya. xlix + 329 pp., 30 maps, 1988.

UNEP. *Coral Reefs of the World: Volume 2 Indian Ocean, Red Sea, and Gulf.* UNEP Regional Seas Directories and Bibliographies. IUCN, Gland, Switzerland and Cambridge, U.K./UNEP, Nairobi, Kenya. xlix + 329 pp., 30 maps, 1988.

UNEP. *Coral Reefs of the World: Volume 3 Central and Western Pacific.* UNEP Regional Seas Directories and Bibliographies. IUCN, Gland, Switzerland and Cambridge, U.K./UNEP, Nairobi, Kenya. xlix + 329 pp., 30 maps, 1988.

5. FULL-SCALE FIELD TEST AND MODEL VALIDATION

5.1 FIELD MEASUREMENTS AND MODELING OF DILUTION IN THE WAKE OF A U.S. NAVY FRIGATE

by C. Katz, D. Chadwick, J. Rohr, M. Hyman, D. Ondercin

INTRODUCTION

This report describes a field effort by the Marine Environmental Quality Branch (Code D362) of SSC, San Diego designed to quantify dilution levels in the turbulent wake of a U.S. Navy frigate. This effort is a part of a larger study to assess the fate and effects of solid wastes discharged from U.S. Navy ships. One method proposed for disposing paper/cardboard solid wastes is to pulp and discharge it directly into the wake as a paper/cardboard seawater slurry. To assess the potential environmental impact of this mode of discharge, accurate estimates of the dilution capacity of the wake is necessary. Although there are sophisticated computational models that can simulate the wake behind naval surface ships and estimate ship-wake dilution levels, and there have been full-scale studies of the wake dilution behind barges and tankers, there have been no field measurements with full-scale naval surface ships. Therefore, to directly measure wake dilution and compare with model predictions, field experiments were conducted off the coast of San Diego, California, using the frigate, the USS *Vandergrift* (FFG48), as the test platform, and the RV Acoustic Explorer as the measurement platform. The specific objectives of the full-scale field study were to:

- Measure at various downstream locations and depths the cross-wake concentration of a passive scalar, fluorescein dye, discharged into the wake of a frigate moving at 8 and 15 kts. Estimate minimum and average cross-wake dye dilution levels as a surrogate of the liquid phase of the waste stream.
- Measure at various downstream locations and depths, the average cross-wake concentration of pulped paper and fluorescein dye, discharged into the wake of a frigate moving at 8 kts. Estimate average pulped paper dilution levels, the solid phase of the waste stream.
- Compare dilution results with computational model (TBWAKE) simulations to assess its capability to predict dilution levels under varying ship and sea conditions.

BACKGROUND

Regulations negotiated through the International Maritime Organization (IMO) have imposed restrictions to pollution discharge from ships in international waters (MARPOL 73/78). Regulation 5 of Annex V to the International Convention for the Prevention Of Pollution from Ships (1973) as modified by the Protocol of 1978 prohibits the discharge of non-food solid wastes into sensitive oceanographic and ecological areas, known as Special Areas. These MARPOL Special Areas include the Baltic Sea, the North Sea, the Mediterranean Sea, the Wider Caribbean Region, the Antarctic area, the Black Sea, the Red Sea, and the "Gulfs" area (including the Persian Gulf and Gulf of Oman). These restrictions were mandated by the U.S. Congress, requiring U.S. compliance by 31 December 2000 for surface ships and 31 December 2008 for submarines. These discharge restrictions could have a major impact on Navy

operations; therefore, the Naval Sea Systems Command (NAVSEA) studied alternative shipboard systems and procedures for full or partial compliance with these regulations.

One proposed solid waste discharge alternative consists of pulping paper and cardboard products in a seawater slurry and discharging it over the side of a ship. NAVSEA 03R16, tasked SSC San Diego to explore the fate and potential environmental effects of this discharge alternative (Chadwick et al., 1996). Initial dilution of the slurry in the wake of a ship is critical to identifying exposure levels (magnitude and duration) to organisms in the water column. The initial mixing is also important in determining the areal distribution of the material and understanding its eventual fate. To determine these parameters, SSC San Diego proposed both a modeling and field measurement effort. The modeling effort was performed in conjunction with the Naval Coastal Systems Station (NCSS) using a numerical model called TBWAKE. The field effort was performed with the Johns Hopkins University Applied Physics Laboratory (JHU/APL).

APPROACH

The basic test concept was for the USS *Vandergrift*, henceforth referred to as the frigate, to operate its solid waste pulper under controlled conditions while the measurement platform, the RV *Acoustic Explorer*, henceforth referred to as the AX, maneuvered behind making *in situ* and flow-through measurements. A specific type of white photocopy paper and fluorescein dye were discharged from the frigate's pulper at specified rates. The dye and paper were both measured using fluorescent measurement techniques while the paper particles were also measured gravimetrically. The specific photocopy paper employed had an inherent fluorescent intensity that was used for one method of particle quantification.

While the frigate was discharging paper and dye along a straight track, the AX transited in the wake in two geometries. In the first geometry termed "Follow-the-Leader" (FTL), the AX held position with its measurement equipment centered in the wake at three discrete distances behind the frigate: 5, 10, and 15 frigate ship-lengths. These measurements were designed to identify the average concentration of dye and paper particles at the specified distances back. In the second geometry termed "Serpentine" (SERP), the AX started close-in behind the frigate, then fell back over time as a result of criss-crossing the full lateral extent of the wake. These measurements were designed to look at maximum concentrations of dye and the cross-wake distribution as a function of distance back.

The tests were run under as close to standard operating conditions as possible given ship and measurement limitations. An exception to this was that all but one set of measurements were made while the frigate discharged paper at a nominal rate that was about 2.5 times normal (110 $kg \cdot hr^{-1}$) to enhance the ability to detect paper particles. On one occasion, the rate was lowered to the nominal operational discharge rate of 45 $kg \cdot hr^{-1}$. Measurements were made while the frigate was transiting at either 8 or 15 kts.

EXPERIMENTAL METHODS

Test Overview. The field test was conducted off the coast of San Diego, California, during the period 8 through 16 February 1996. The period 8 through 11 February was used for equipment-loading and checkout on both ships. Dedicated at-sea testing with the frigate was conducted on the afternoon of 12 February, the morning of 13 February, and all-day, 14 February. Pulped paper particle sampling efficiency tests were performed with the *AX* on 15 February. Equipment was removed from both ships

on 16 February. The test was conducted nominally 5 to15 nmi west of San Diego in at least 200 m of water (Figure 5.1-1).

The *AX* used the SSC San Diego pier as its home port. Each day the *AX* would leave San Diego and rendezvous with the frigate, which was spending the week at sea conducting shakedown and training exercises. Representatives from SSC San Diego and JHU/APL rode the *AX* to perform the dye and paper particle measurements (see Table 5.1-1). Representatives from Carderock Division Naval Surface Warfare Division Annapolis Detachment (CDNSWC/AD) and JHU/APL rode the frigate to coordinate operations with the ship's company, and to care for and feed the pulper and the dye-dispensing system (Table 5.1-1).

Daily operations began by performing hydrographic measurements aboard the *AX* to determine background water clarity and to determine the depth of the mixed layer. Once these measurements indicated appropriate field conditions, the full overboard sampling system (described below) was deployed and spun up to full operational status. Background particulate load and dye measurements were then made prior to arrival of the frigate. Upon arrival of frigate, the two ships positioned themselves appropriately in one of the two geometries and the tests began.

The ships traveled randomly in more or less straight lines within an operations area that was about 500 km^2. Multiple samples were collected under each test condition, and most test conditions were repeated at least twice. A summary of the test conditions, sample data collected, and test chronology can be found in summary section 4.6. At the end of each day's tests, hydrographic and background water clarity measurements were again made and the ships departed for their respective overnight destinations.

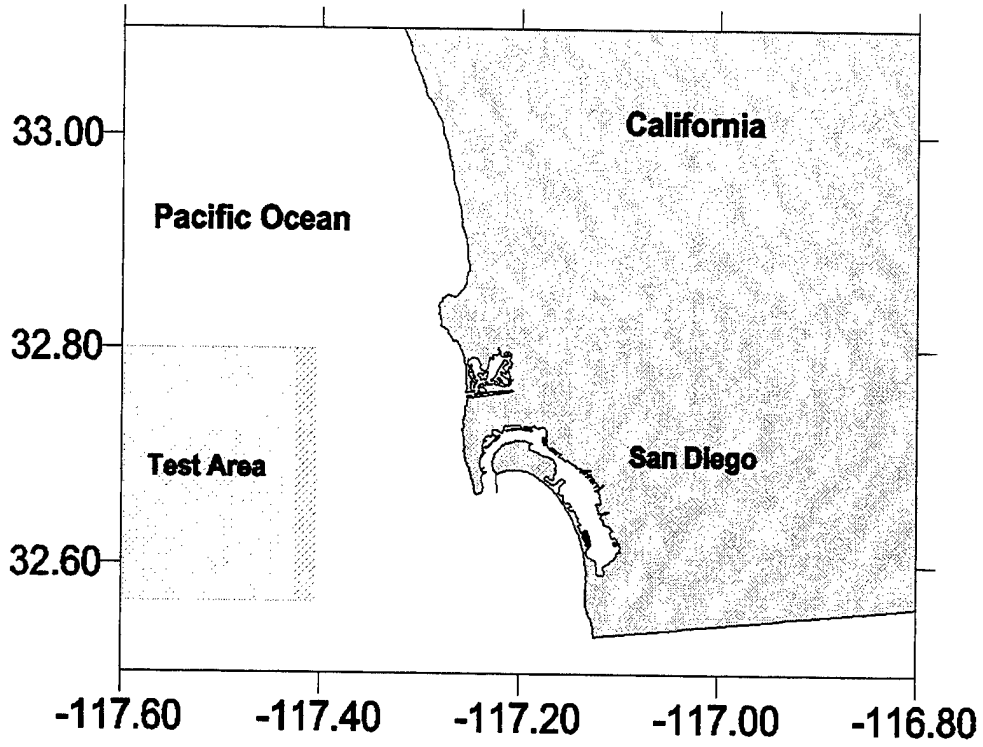

Figure 5.1-1. Field measurement test area of San Diego, California.

Table 5.1-1. Personnel involved in the field tests. Not all personnel were necessarily present for each day's tests.

Person	Affiliation	Primary Responsibility
Aboard RV *Acoustic Explorer*		
Charles Katz	SSC San Diego	Test Coordinator
Bart Chadwick	SSC San Diego	Bridge Comms/Control
Andy Patterson	SSC/Computer Sciences Corp	Data Acquisition
Brad Davidson	SSC/Computer Sciences Corp	Particle Sampling
Jon Groves	SSC/Computer Sciences Corp	Particle Sampling
Dan Ondercin	JHU/APL	Particle Analysis
Jim Velcky	JHU/APL	Particle Sampling
Charles Sarabun	JHU/APL	Data Acquisition
Aboard USS *Vandergrift*		
Gene Ward	JHU/APL	Test Coordinator
Steve Stetz	CDNSWC/AD	Pulper Operator
Todd Olson	CDNSWC/AD	Pulper Operator

Discharge Platform Configuration- Frigate. The frigate has, at waterline, a length, beam, and draft of 125.9 m, 13.7 m, and 6.7 m respectively. It has a displacement of about 3000 tons and is propelled by a single clockwise rotating screw. Its on-board "small" pulper was installed a few months before the tests were conducted. The "small" refers to its physical size as well as its pulped material discharge rate that is nominally 45 $kg \cdot hr^{-1}$.

Concentrated (40%) liquid fluorescein dye (Keystone Aniline Corporation, C.I. acid yellow 73) was delivered into the input side of the pulper using a peristaltic pump. The delivery rate of 0.8 $L \cdot min^{-1}$ was monitored using an in-line flow meter. White photocopy paper (Hammerhill 24-lb Premium Business Laser Paper) was delivered manually into the pulper. The input rate was determined on the basis of timing the number of reams (2.7 $kg \cdot ream^{-1}$) placed into the input side of the pulper. A concerted effort was made to maintain a uniform feed rate of paper into the pulper at either 45 or 110 $kg \cdot hr^{-1}$. The pulped paper/dye stream was then merged with the ship's seawater firemain, as per standard operating procedures, before being discharged amidships on the starboard side of the ship at a rate of 190 $L \cdot min^{-1}$. The resultant mixture at the point of discharge had a concentration of dye that was 2 $g \cdot L^{-1}$, equivalent to 6.7 $g\ s^{-1}$ (density=1.25 $g \cdot mL^{-1}$), and either 3.9 or 9.6 $g \cdot L^{-1}$ pulped paper.

Check samples of the discharge effluent, sampled just before the overboard port, were collected occasionally for confirmation of the discharge concentrations. These samples were stored frozen on board until analyzed gravimetrically as described below.

The pulper was run for approximately 3 minutes with dye and paper prior to the beginning of each test, to obtain a constant discharge condition. Once the discharge rate was stable, the ships positioned themselves appropriately and the measurements began. After a 10-minute time period during the FTL runs, the dye discharge was pulsed on and off, rather than fed continuously, as a way to mark the centerline of the wake rather than for data analysis purposes. A differential global positioning system (DGPS), placed onboard the frigate prior to the tests, was used to track its position during the tests.

Measurement Platform Configuration- AX. A suite of *in situ* and onboard measurement devices was installed aboard the AX to measure particle and dye concentrations. A towed array was assembled which consisted of a high-volume seawater pumping system to provide samples for pulped paper analysis and for flow-through dye measurements. The array also consisted of a chain of in-fairing fluorometers to provide *in situ* dye measurements. The array was towed 6 m off the starboard beam using the ship's service crane, which was a sufficient distance from the ship so that the data collection was not influenced by the AX's own wake. Onboard, computers were used to acquire data from the array instruments as well as from the ship's DGPS navigation system and flow-through dye fluorometers. Additionally, the ship's radar was used to monitor ship separation distances. The DGPS system clock provided the master clock used for all measurements.

Pulped Paper Particle Collection. The high-volume seawater-pumping system used to collect pulped paper particles consisted of three 2.5 cm internal diameter reinforced plastic hoses taped to a 5-mm hydrowire holding a 225 kg dead weight. The lengths of the three tubes were such that water was sampled from depths of about 1.0, 4.6, and 9.5 m when the system was towed at 8 kts during FTL runs (sampling was slightly deeper when doing SERP runs). A pressure transducer was installed at the end of each tube to monitor the intake depth at a 1-Hz rate.

Topside, the three hoses were plumbed into self-priming pumps that pumped water to a "tee" assembly. At the "tee" 80% of the water flowing up each hose was delivered to a net manifold while about 20% was delivered to a flow-through fluorometer. The measured flow rate through each net was 0.7, 0.6, and 0.5 L·s-1 for the shallow, mid, and bottom sample depths, respectively. The net manifold fed three 1-m long, 20-μm mesh plankton net stockings suspended in a large rubber trash container. Each plankton net was dedicated to one of the three sample hoses. At the bottom of each net was a PVC cod end where particles were collected.

During a typical sample-collection run, water was pumped through the nets for 10 min (6 min at the one-ship length separation distance and during SERP runs). At the end of that period, the nets were choked off near the bottom to prevent additional water/pulp sample from entering the cods. The cods were removed using a quick release mechanism and replaced with cleaned cod ends. During the cod end exchange, water was continuously being filtered in the net above the cod end, thus permitting continuous sample collection. All sample times were recorded using the DGPS synchronized clock.

The pulped material accumulated in the cod ends was processed immediately after collection. The fluorescent nature of the paper under black-light bulbs was used to ensure complete sample transfer into 125-mL jars. The cod was then washed and scrubbed with a brush before being used again. An identification label was fixed to each jar, and the sample was logged into a computer database. The samples were stored at room temperature until analysis without chemical preservation.

Pulped Paper Particle Concentration Analysis. The mass of pulped paper collected from the high-volume filtration system was determined by two independent methods, fluorometrically and gravimetrically, as described below. While the primary method employed was fluorometric, samples analyzed gravimetrically allowed an independent check on the analyses. The net-filtered samples were split after the fluorometric analysis to provide samples for gravimetric analysis, keeping track of the split sample volumes. Concentration of the material was then determined by dividing the total mass collected by the total seawater volume filtered, accounting for filtering efficiency and background fluorescence or particulate loads.

Fluorometric Mass Determination. The presence of optical bleaching agents in most white paper provided a unique marker for the detection of pulped paper. These fluorescent brighteners are added to white paper to improve their optical whiteness by absorbing ultraviolet (UV) light and converting it to the visible blue fluorescent light. Different paper brands were tested to determine the fraction of the fluorescent dye indelibly bonded to the paper, and its long-term stability in water. A premium Business Laser Paper produced by Hammermill was chosen because after several weeks, more than 95% of its dye was found to remain bonded to the paper.

A Turner Designs Model 10-000R fluorometer was used to determine the mass of the pulped paper by measuring its fluorescence in a blended slurry. A near-UV fluorescent lamp was used for pulped paper excitation between 310 and 390 nm, and appropriate optical filters were employed to measure the fluorescence emission between 420 and 490 nm. At these excitation/emission wavelengths, there was no interference with the fluorescence generated by fluorescein dye. The fluorometer was calibrated with a stock pulp solution, containing a known mass of the Hammermill Premium Business Laser Paper homogenized in a known volume of water with a blender. This mixture was serially diluted, and the resultant mass versus fluorescence calibration (Figure 5.1-2) was used to quantify the mass of the test samples. Background samples collected throughout the survey were used to correct for any fluorescence inherent in the natural background particulate load.

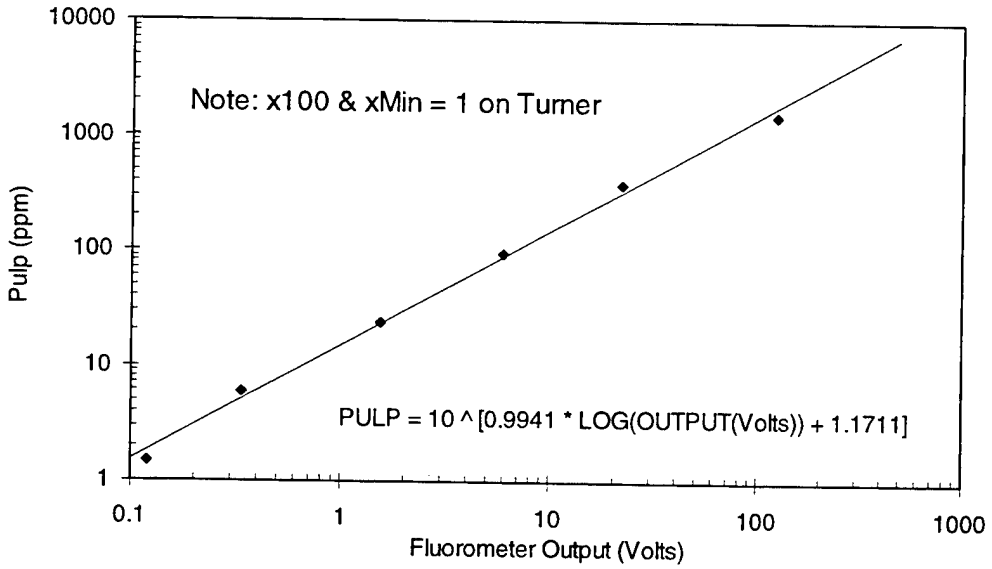

Figure 5.1-2. Relative fluorescence signal versus pulped paper concentration (APL, 1996.)

Gravimetric Mass Determination. Sample splits, already blended, were taken after fluorometric examination for routine gravimetric analysis. These samples were filtered through pre-weighed glass fiber filters (0.4 μm), dried, and weighed on an electronic balance. Mass of the pulped material measured in this way was corrected not only for filtering efficiency, but also for background particulate material. Background samples collected throughout the field tests were used to correct for the natural particulate load.

Additionally, 13 confirmation samples obtained from the frigate's pulper discharge were analyzed gravimetically. Approximately 50 mL aliquots of these samples were filtered through pre-weighed glass fiber filters (0.4 μm), dried, and weighed on an electronic balance. No background particulate load

corrections were made to these samples because of the high concentration of pulped paper directly out of the pulper.

Particle Sampling Efficiency. The filtering efficiency of the net manifold system was estimated by comparing the mass of pulped paper collected directly from the pulper (into a 20-L bucket) with those collected after pumping water through the filtration system. Eighteen 125-mL samples were taken from the collection bucket, six of which were further pumped through the net manifold.

Each pulp sample designated for pumping through the net manifold was pumped separately through the manifold by placing it into a 4-L container and submerging the container in a vat filled with 380 L of seawater. The pump intake to the manifold was placed in the small container first to ensure that all the pulp was pumped through the manifold. After most of the water had been pumped from the vat (about 10 min), the net was allowed to drain and the cod end removed. The pulp sample was removed from the cod end following the same sample-handling and analysis protocols used with the test samples.

The average mass (measured fluorometrically) of 12 samples pumped directly from the pulper was 79 ±11 mg. The average mass in the six samples pumped through the net system was 64 ±48 mg. Therefore, the estimated filtering efficiency was about 81% (gravimetric analysis placed the efficiency at 80%). This percentage was used to adjust the measured mass of the pulped paper when calculating final concentrations.

Fluorescein Dye Measurements. Two independent measures of fluorescein dye concentration were made during the field tests. The primary measurements were made using a chain of five *in situ* fluorometers deployed as part of the towed array. The second set of measurements were made on seawater flowing from the high-volume pumping system hoses through three separate onboard fluorometers. The *in situ* measurements provide the highest spatial and temporal resolution while the flow-through measurements provided more of an integrated measurement technique because of mixing that occurs in the hose system. Comparison data from the two sets of fluorometers were spatially matched by taking into account individual hose lags, and sample depth differences.

***In Situ* Dye Measurements.** The towed fluorometer chain system consisted of five in-fairing fluorometers developed at JHU/APL, five co-located pressure transducers, a signal conditioning subsystem, and a PC-based data acquisition system. The depths of the individual sensors depended on the cable catenary which changed with ship speed and run geometry, but were always monitored by an adjacent pressure transducer. For the FTL geometry, sample depths averaged: 1.0, 2.0, 4.5, 7.7, and 9.0 m. Sample depths during the SERP geometry averaged: 2.7, 4.5, 6.5, 9.5, and 11.5 m.

Seawater passing through the fluorometer sampling chamber was optically excited around 490 nm by a halogen lamp pulsed at 20 Hz. A photodiode synchronously sensed light emission near 525 nm. The fluorescence voltage data were digitized at 4 Hz and stored as a function of time (GPS synchronized clock).

The fluorometers were calibrated before and after the survey by placing them into a stock solution of fluorescein dye and serially diluting it, noting the fluorescence voltage at each known dye concentration. The calibration was performed over a range of dye concentrations between 0.3 and 300 $ug \cdot L^{-1}$ (or ppb). The log-log regression of the fluorescence voltage as a function of concentration was used to calculate sample concentrations (Figure 5.1-3).

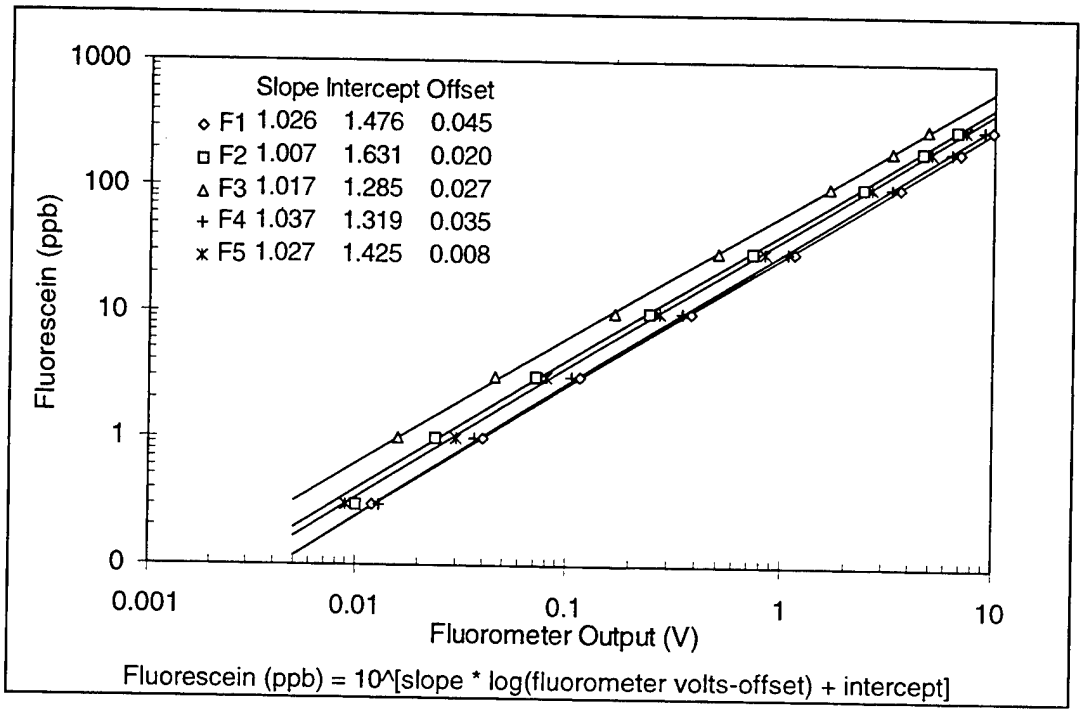

Figure 5.1-3. Relative dye fluorescence versus fluorescein dye concentration for five *in situ* sensors (APL, 1996).

Flow-through Dye Measurements. Water flowing up from the seawater sampling system was partially diverted through three flow-through Turner Model 10AU fluorometers, one for each depth. Sample depths for the FTL runs averaged 1.0, 4.6, and 9.5 m. During SERP runs the sampling depths averaged 1.4, 5.6, and 10.3 m. The seawater passing through the fluorometer flow cell was optically excited at 455-510 nm and resultant fluorescence emission was measured between 510 and 700 nm. The fluorescence output in volts was digitized at a 1-Hz rate and stored as a function of time (GPS synchronized clock).

Each of the flow-through fluorometers was calibrated before and after the surveys. This was done by recirculating seawater in the flow-through system and making serial additions of a primary fluorescein standard (0.026%), made from the 40% fluorescein dye used in the field tests. The resultant fluorescence signal in volts was recorded at each addition spanning a concentration range of 3 to 2700 $ug \cdot L^{-1}$. Dye concentrations of seawater measured during the field test was determined using a polynomial regression of the fluorescence signal in volts as a function of dye concentration (Figure 5.1-4).

Additional Measurements – AX. At the start and end of each day's test, background seawater characteristics were measured to determine the mixed layer depth and background water clarity. A standard conductivity, temperature, and depth (CTD) profiling system with 25 cm pathlength light transmissometer was deployed manually to obtain salinity, temperature, density, and light transmission values as a function of depth to 45 m.

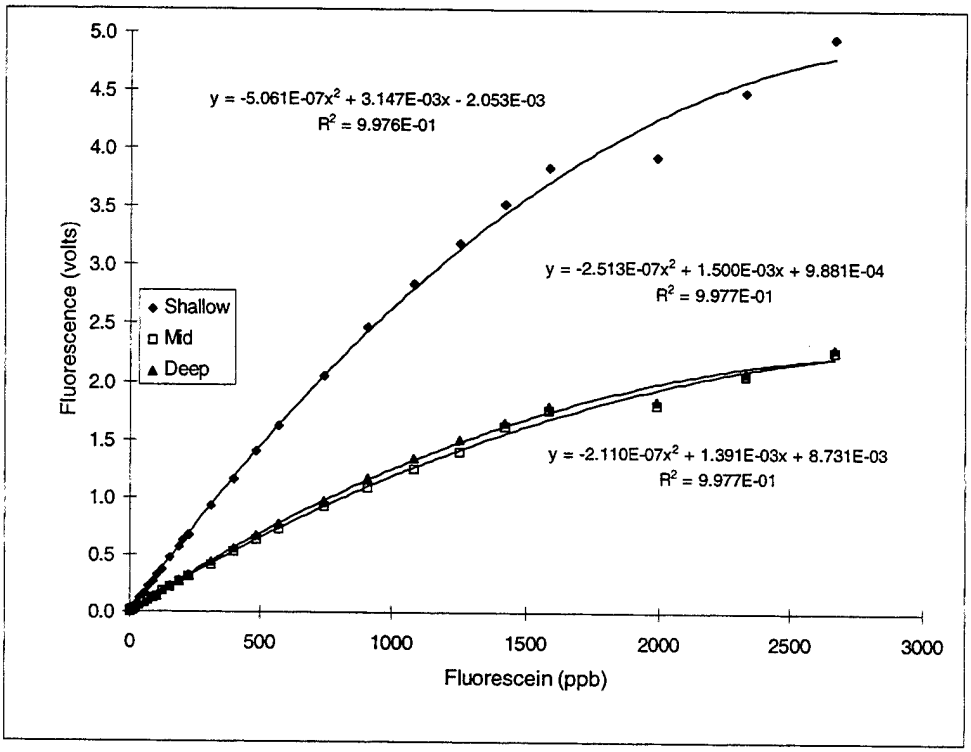

Figure 5.1-4. Relative fluorescence signal as a function of fluorescein dye concentration for three flow-through fluorometers.

DGPS navigation data were acquired a 1-Hz rate throughout the survey on both the frigate and AX. The AX's radar was also used to keep track of separation distances of the two ships. Because DGPS data from the frigate were lost on day 3 of the tests, the manual records of the radar measurements were used to reconstruct the frigates track.

The pressure transducers co-located with the *in situ* fluorometers and the hose at the end of the hoses were calibrated prior to and after the surveys independently and against each other to ensure accurate sample depth measurements. This was done by strapping them together and lowering them over the side and measuring their depth with a tape measure fixed to the assembly. The voltage versus depth was regression was generated for each transducer and used to calculate depth during the surveys.

DATA PROCESSING

Data Acquisition. Two real-time data acquisition computers were used to record and display navigation, fluorometer, and sample depth data.. The *in situ* fluorometer and depth data from the towed array were displayed and recorded at 4 Hz along with GPS time on one computer. The flow-through fluorometers, pressure transducers at the hose ends, and DGPS data were displayed and recorded at 1 Hz on a second data acquisition system. All measurements were merged using time to co-locate all data spatially (this includes hose lag times). While the computers were not used to record pulped paper sample data or radar records, these data were logged manually using the GPS time recorded on the computers.

Because the DGPS aboard the frigate was inoperable during the serpentine tests, the distance between the frigate and *AX* was determined from the radar record. Discrete radar measurements of distance were regressed as a function of time. The resulting regression line was used to calculate, at any time during the test, the relative locations of the frigate and *AX*. The surface location of the towed array was estimated visually and added to the ship separation data to estimate the distance between measurement location and frigate.

Data Visualization. Visualizations of the dye concentration data were generated using Golden Graphics Surfer® software. Using the true relative surface positions of the two ships, the calibrated dye data for each depth were gridded and interpolated to produce both plan and cross-sectional views of the dye for each of the SERP runs. Data from the plan views were interpolated on approximate grid size of 100x by 40y using an octant search radius of 1000x and 10y, and a correlation length scale of 1000x and 100y. Cross-sectional plots were produced for specific distances behind the frigate using the depth dependent data from each sensor. These data were interpolated on an approximate grid size of 100y by 40z using an octant search radius of 10y and 7z, and a correlation length scale of 20y and 10z. A threshold of 1 $ug \cdot L^{-1}$ was used as a cutoff value for display, a value that was roughly three standard deviations above background. Graphical representations of the computer simulations were produced in the same manner as described above.

SAMPLING SUMMARY

The following is a brief summary of the chronology, configurations, samples, and data collected during the field tests that are described in the results and discussion sections. These summaries are tabulated in Tables 5.1-2, 5.1-3, and 5.1-4.

Pulped Paper Data. Pulped paper samples were collected from three depths (1.3, 4.6, and 8.8 m) on a total of seven FTL runs as well as during 16 background runs. While pulped paper samples were also collected and analyzed on the serpentine runs, they were used only for qualitative interpretation purposes. All samples were measured both fluorometrically (primary method) and gravimetrically. The samples were collected at approximately 1, 5, 10, and 15 ship lengths downstream from the frigate. FTL runs were repeated three times at the five ship length separation distance (once at the lower discharge rate), and twice at 10 and 15 ship length distances. Two runs at one ship length back were also made, though these were coupled with the SERP runs. During each run, two to seven replicate net-filtered samples were collected, depending on the length of the run. Background net samples were collected before and/or after each of the FTL runs. A total of 177 samples from 59 sample sets (three depths) were collected. This total does not include pulped paper samples collected during the SERP runs. An additional 18 samples were also collected to determine the net sampling efficiency and another 13 check samples were collected and analyzed gravimetrically from the frigate's pulper discharge.

Table 5.1-2. Chronology of field tests performed. FTL=Follow-the-leader geometry.

Date	Time	Activity	Desired Ship Separation (frigate ship-lengths)	Actual Ship Separation (frigate ship-lengths)*
12 February	14:20 - 15:00	Background		
	15:52 - 16:42	FTL 8 kts	5	3.1 - 5.2
	16:57 - 17:07	Background		
	17:12 - 18:02	FTL 8 kts	10	8.5 - 9.1
	18:02 - 18:12	Background		
13 February	6:13 - 6:33	Background		
	6:44 - 7:54	FTL 8 kts	5	3.9 - 5.4
	7:57 - 8:07	Background		
	8:19 - 9:43	FTL 8 kts	10	10.1
	9:50 - 10:00	Background		
	10:12 - 10:52	FTL 8 kts	15	15.2
	10:56 - 11:06	Background		
	11:30 - 12:02	FTL 8 kts	15	15.2
	12:05 - 12:15	Background		
14 February	6:56 - 7:26	Background		
	7:48 - 8:48	FTL 8kts @ 45 $kg \cdot hr^{-1}$	5	
	8:48 - 8:58	Background		
	9:17 - 10:00	Serpentine 8 kts		1 - 23
	10:02 - 10:08	Background		
	10:32 - 11:02	Serpentine 8 kts		1 - 22.3
	11:02 - 11:08	Background		
	11:29 - 11:47	Serpentine 15 kts		1.9 - 26.8
	11:50 - 11:56	Background		
	12:23 - 12:29	FTL 8kts	1	1
	12:29 - 12:47	Serpentine 15 kts		1 - 26.2
	12:47 - 12:53	Background		
	13:40 - 13:52	FTL 8kts	1	1
	13:52 - 14:10	Serpentine 15 kts		1.4 - 29.9
	14:12 - 14:18	Background		
	14:37 - 14:49	FTL 8kts	1	1
	14:49 - 15:19	Serpentine 8 kts		1.9 - 22.4
	15:19 - 15:25	Background		

Table 5.1-3. Pulped paper sample collection summary. Sample sets were simultaneously collected at three depths: 1.3, 4.6, and 8.8 m.

Ship Separation Distance (Ship-Lengths)	Number of Runs	Sample Sets	Background Sample Sets	Nominal Pulper Feed Rate ($kg \cdot hr^{-1}$)
1	2	5	3	106 - 119
5	2	12	6	112 - 153
5	1	6	3	40 - 45
10	2	13	4	104 - 137
15	2	7	3	97 - 114

Fluorescein Dye Data. Fluorescein dye measurements were made were made on the seven FTL runs. The data during these runs were analyzed quantitatively for the flow-through fluorometers only. Dilution calculations were calculated over a 10- minute time period during each run when the dye was continuously pumped. Dye measurements made at all other times on the FTL runs were used only to qualitatively assess how well the centerline of the wake was tracked during the test.

A total of six serpentine runs were made, three each at frigate speeds of 8 and 15 kts. During these runs, the wake was crossed 12 to 29 times. Fluorescein dye measurements were made continuously on these runs using both the *in situ* fluorometer array (primary method) and the flow-through fluorometers. The array data were collected at five depths, averaging 2.7, 4.5, 6.5, 9.5, and 11.5 m, while the flow-through data were collected at three depths averaging 1.4, 5.6, and 10.3 m.

Table 5.1-4. Fluorescein dye sampling summary.

Ship Separation Distance (Ship-Lengths)	Frigate Speed (kts)	Wake Crossings	Average Sampling Depths (m)
1-26	8	28	
1-24	8	17	***In Situ*:** 2.7, 4.5, 6.5, 9.5, 11.5
1-29	15	12	**Flow-Through:** 1.4, 5.6, 10.3
1-29	15	14	
1-33	15	12	
1-24	8	17	

COMPUTATIONAL MODEL

Arguably the best available description of the turbulent flow field in a wake of a surface ship, has evolved from efforts to minimize the probability of ship detection through manifestations of its wake. A computational model, TBWAKE, which was originally developed to study ship microbubble wakes (Smith and Hyman, 1987; Hyman et al., 1987; Nguyen and Hyman, 1988a,b), was modified to study the dispersal of shipboard waste discharge in the near field (< 30 ship lengths) of the wake of a frigate. TBWAKE is well documented and has been at least partially verified with full-scale experiments on

many classes of U.S. Naval surface craft under a wide range of oceanic conditions (Hyman, 1990; Hyman, 1994). Near field wake mixing was considered for both a passive and paper-like discharge effluent in both unstratified and stratified ocean environments.

The near field numerical simulation of wake dispersion was based on standard convective-diffusive modeling of continuous fluid fields. The model used a parabolic Navier-Stokes solver in which the equations describing the instantaneous flow field were ensemble averaged. The result is a set of three-dimensional differential equations which are elliptic in character. These are solved by assuming that the streamwise pressure and stress gradients are negligible, and that there is no flow reversal. Because of the assumptions used, the simulations cannot be initiated until after about a half ship length (60 m). At this distance, all dependent variables are specified, forming what is termed the Initial Data Plane (IDP). The numerical algorithms then propagate those data downstream. Estimation of the IDP is the weakest link in the simulation process but should provide better than order of magnitude dilution estimates. A series of runs with different locations of the initial concentration field within the IDP showed little effect on the final concentration distribution at 3000 to 5000 m behind the ship.

The model discharge was considered as both a passive scalar and as composed of particles of pulped paper-cardboard. The model used the range of particle sizes from 100 to 3000 um, a density of 1.54 $g \cdot cm^{-3}$, and settling velocities described in Chadwick et al., 1996 (Table 5.1-5). A continuous particle population (with units $\#/m^3/\mu$), proportional to r^{-3}, was defined and discretized. Particles were not allowed to change size (coalesce, shear, or decompose), and they were presumed to be always falling at their (size dependent) terminal velocity.

The original algorithm was developed for simulating microbubble transport and employed a surface boundary condition of the zero gradient type. While a gradient-free boundary condition is appropriate for the passive scalar case, it is not suitable for the particle case, as it will result in particles being introduced at the ocean surface. Consequently, a zero flux condition was imposed at the surface to first order accuracy. The outcome of this approximation was a cumulative introduction of mass, 10-25 percent (increasing with ship speed), over the first 3000 m of the ship's wake.

Simulations were run for both 8-kt and 15-kt frigate speeds. The domains on which the computations were performed varied with ship speed. In general, the lateral dimension ranged to about 100 m and the vertical dimension ranged to about 30 m. The down-wake dimension was calculated from the IDP at 60 m behind the frigate out to 4000 m. The 200x91x41 (streamwise by horizontal by depth) grids had a high density near the surface and near the IDP but were uniform in the lateral direction. The total amount of mass flux through the IDP was determined by the rate of discharge from the ship, 6.7 $g\ s^{-1}$ of dye and either 3.9 or 9.6 $g \cdot L^{-1}$ pulped paper. For the paper/cardboard effluent, the concentration computation summed all sizes of paper/cardboard particles. The passive scalar simulations treated the discharge as if it was a neutrally buoyant dye. For both discharge cases, a relatively low background diffusivity of 10 $cm^2 \cdot s^{-1}$ was chosen, which was representative of the low sea state during which the field experiments were performed.

Table 5.1-5. Pulped paper characteristics used as model inputs.

Radius (μm)	Terminal Velocity ($cm \cdot s^{-1}$)	Cumulative Mass Fraction
200	0.0480	0.0884
500	0.2416	0.2004
800	0.2957	0.3053
1000	0.3910	0.3730
1200	0.6679	0.4393
1400	1.227	0.5046
1600	2.095	0.5689
1800	2.992	0.6324
3000	7.713	1.0000

RESULTS

Test Conditions. All field tests were conducted under excellent weather and in ideal sea-state 1 conditions Vertical profile data collected each day indicated a mixed layer depth of approximately 20 m with high, thoug variable, water clarity (see Figure 5.1-5). The variability in background water clarity, affecting only th gravimetric analyses, was accounted for by collecting background samples before and/or after each test run. O two occasions, ship transit directions were altered to keep clear of areas of patchy phytoplankton growth, based o visible inspection of the filtrate.

Pulped Paper Analyses. Two nominal pulping rates of 109 and 45 $kg \cdot hr^{-1}$ were chosen for the tests. However, the exact pulper rates varied slightly during each run. Specific rates measured during each run ranged from 78 to 127 $kg \cdot hr^{-1}$ for the high rate, and between 40 and 45 $kg \cdot hr^{-1}$ for the lower rate. Samples collected from the frigate's discharge stream and measured gravimetrically, independently confirmed that the measured discharge concentrations were within 11% of their expected values expected. To compare pulped paper concentrations data collected on the AX from test to test, variations in the measured discharge rates were normalized to the nominal rates. The concentrations were also corrected to reflect the filtering efficiency of the sampling method which was measured at 80% (see Table 5.1-6).

The concentration of pulped paper in samples collected at the three sampled depths and four separation distances was measured both fluorometrically and gravimetrically. Though the absolute numbers vary by method, several features can be seen in both data sets shown in Tables 5.1-7 and 5.1-8. The surface concentration of pulped paper decreases monotonically as a function of distance in the wake behind the frigate. Surface (1.3 m) concentrations decrease from a maximum value of 0.45 $mg \cdot L^{-1}$ at one ship length back to about 0.03 $mg \cdot L^{-1}$ at 15 ship-lengths back. While no measurable concentration of pulped paper was found at the 4.6 m sampling depth at 1 ship-length back, concentrations of about 0.03 $mg \cdot L^{-1}$ were observed at 10 ship-lengths. The concentration at this depth then dropped off to about 0.02 $mg \cdot L^{-1}$ at 15 ship-lengths. Similarly, samples collected at 8.8 m showed no measurable pulped paper concentration at 1 ship-length back, though concentrations of about 0.01 $mg \cdot L^{-1}$ were found at the other three downstream distances.

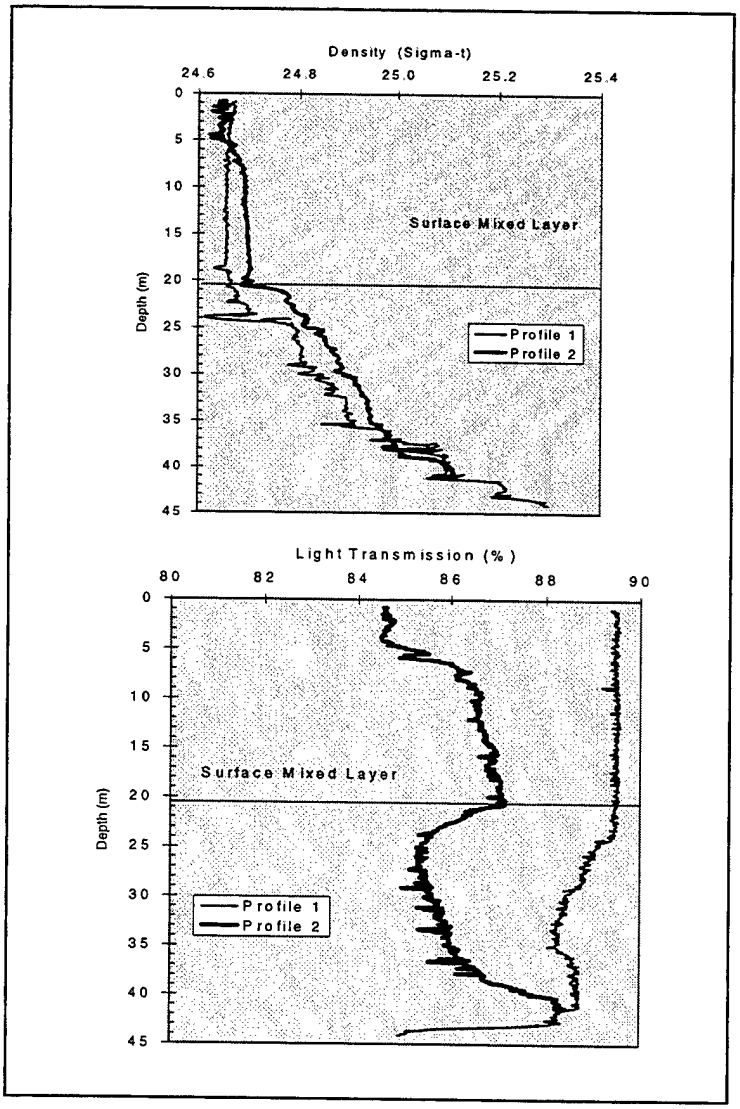

Figure 5.1-5. Density and light transmission as a function of depth for two vertical profiles made during the field experiments. The plots show very clear water and a mixed layer of about 20 m.

Table 5.1-6. Sample filtration efficiency as determined both fluorometrically and gravimetrically. Sample sizes were not equivalent for the two methods.

Analysis Method	Before Filtration (mg)	After Filtration (mg)	Efficiency (%)
Fluorometric	79 ±11	64 ±48	81
Gravimetric	34 ±8	27 ±10	79

The resultant concentration distribution can be attributed to both dilution and particle settling. As the distance behind the frigate increases, the wake volume grows resulting in a general decrease in pulped paper concentrations. However, because turbulent mixing diminishes as a function of distance behind the frigate, the

effect of natural particle settling results in an increased concentration of particles at depth the further back in the wake. This occurs until there is nearly a uniform distribution at 15 ship-lengths back.

The concentration of pulped material measured by both analytical methods should be considered an average valu rather than a maximum because each sample was collected over a 6 to 10-minute period while transiting through the apparent center of the wake. The accuracy of collecting samples along the centerline of the wake was dependent on the ability to maneuver the AX to the visual maxima of pulsed dye and was qualitatively monitored with the dye fluorometers. The fluorometer data suggest that the measurements were not always made at the wak center. As such, dilution estimates should also be considered as average values. Based on a 9.6 $g \cdot L^{-1}$ input, a maximum of 0.45 $mg \cdot L^{-1}$ of pulped paper measured at 1 ship-length represents a dilution of $2.1 \cdot 10^4$. Within eight minutes of discharge, at 15 ship-lengths back, average particle concentrations were less than 0.03 $mg \cdot L^{-1}$ throughout the water column, representing a dilution of $3.2 \cdot 10^5$. The full range of average dilution values measured for the pulped paper particles in the field tests was $2.1 \cdot 10^4$ to $1.2 \cdot 10^6$ (Table 5.1-9).

Table 5.1-7. Average pulped paper concentrations as a function of distance behind Frigate. Values derived from fluorometric analyses. Discharge concentration was 9.6 $g \cdot L^{-1}$).

Distance Back (ship-lengths)	Distance Back (m)	Pulped Paper Concentration ($mg \cdot L^{-1}$) Measured fluorometrically			
		n	1.3 m	4.6 m	8.8 m
1	126	5	0.45 ± 0.02	0.002 ± 0.003	0
5	630	12	0.10 ± 0.007	0.04 ± 0.02	0.009 ± 0.01
10	1260	13	0.03 ± 0.01	0.03 ± 0.01	0.008 ± 0.005
15	1890	7	0.03 ± 0.02	0.02 ± 0.009	0.01 ± 0.008

Table 5.1-8. Average pulped paper concentrations as a function of distance behind frigate. Values derived from gravimetric analyses. Discharge concentration was 9.6 $g \cdot L^{-1}$).

Distance Back (ship-lengths)	Distance Back (m)	Pulped Paper Concentration ($mg \cdot L^{-1}$) Measured gravimetrically			
		n	1.3 m	4.6 m	8.8 m
1	126	5	0.20 ± 0.06	0	0
5	630	9	0.08 ± 0.02	0.07 ± 0.02	0.02 ± 0.01
10	1260	10	0.04 ± 0.02	0.04 ± 0.01	0.03 ± 0.02
15	1890	4	0.02 ± 0.006	0.01 ± 0.002	0.008 ± 0.005

Table 5.1-9. Average dilution levels of pulped paper based on a discharge concentration of 9.6 $g \cdot L^{-1}$. Values were derived from fluorometric analyses.

Distance Back (ship-lengths)	Distance Back (m)	Average Particle Dilution Measured fluorometrically		
		1.3 m	4.6 m	8.8 m
1	126	$2.1 \cdot 10^4$	$4.8 \cdot 10^6$	-
5	630	$9.9 \cdot 10^4$	$2.5 \cdot 10^5$	$1.1 \cdot 10^6$
10	1260	$3.2 \cdot 10^5$	$3.2 \cdot 10^5$	$1.2 \cdot 10^6$
15	1890	$3.6 \cdot 10^5$	$4.8 \cdot 10^5$	$9.6 \cdot 10^5$

For the most part, the two analytical methods produced comparable numbers, typically within 25%. However, differences as much as a factor of two to three were observed for a few sample sets. These differences are reasonable given the low concentration levels observed throughout the tests. Because the fluorometric data were not affected by variability in the background particulate load, this method is considered to be the more accurate measure of the concentrations. In either case, the two data sets that were analyzed independently show good agreement of the pulped paper concentration distribution, with absolute values all nearly within a factor of two.

The sample set collected at a lower discharge rate of 45 $kg \cdot hr^{-1}$ was performed at a 5 ship-length distance. The normalized ratio of concentrations for these data and those collected at the higher 110 $kg \cdot hr^{-1}$ rate should, therefore, be a factor of 2.4. The normalized ratio of the samples analyzed at the two discharge rates averaged about 2.6 (Table 5.1-10), indicating that the experiments run at the higher discharge rate scaled exceptionally well.

Table 5.1-10. Comparison of the average *in situ* pulped paper concentrations measured at two discharge rates: 109 and 45 $kg \cdot hr^{-1}$ for samples collected 630 m aft of the frigate. The expected ratio was 2.4.

Sample Depth (m)	Normalized Concentration @ 109 $kg \cdot hr^{-1}$ ($mg \cdot L^{-1}$)	Normalized Concentration @ 45 $kg \cdot hr^{-1}$ ($mg \cdot L^{-1}$)	Measured Ratio
1.3	0.097 ± 0.07	0.042 ± 0.02	2.3
4.6	0.036 ± 0.02	0.013 ± 0.007	2.8
8.8	0.0087 ± 0.01	0.0033 ± 0.003	2.6

Fluorescein Dye Analyses. Fluorescein dye was used to quantitatively measure the along-track and cross-track spreading and dilution of the liquid phase of the pulper discharge as it became entrained in the turbulent wake of the frigate. During the FTL runs dye was discharged for a continuous period of 10 min then pulsed as a way of marking the wake. Dye concentration measurements made by the flow-through fluorometers during those continuous discharges (including those during SERP runs at 1 ship-length) provide an estimate of the dilution similar to those measured for the pulped paper. Concentrations ranged between 125 $ug \cdot L^{-1}$ at the surface for 1 ship-length to about 9.0 $ug \cdot L^{-1}$ at 15 ship-lengths (Table 5.1-11). The dilution levels calculated for these concentrations ranged between $1.6 \cdot 10^4$ and $9.1 \cdot 10^6$. Like the pulped paper, these measurements must be considered as average values because they were made over a variable wake width.

Most of the dilution values based on these dye measurements were within about a factor of two of those calculated from the pulped paper measurements (see Table 5.1-9). The difference between dilution values calculated for pulped paper and those for dye increased with depth and at the shorter distances back. This likely resulted from

the fact that while dye concentrations decrease because of mixing, pulped paper concentrations diminish from a combination of both particle settling and mixing.

Dye measurements made during the serpentine runs provide a three-dimensional full view of the wake development as a function of time and distance behind the frigate. Examples of the dye plume for the 8-kt case are visualized as planar surface views in Figure 5.1-6 and in vertical slices across the wake at varying distances behind the frigate in Figure 5.1-7a and b. It can be seen from these qualitative views that the vertical and horizontal boundaries of the wake generally increased with ship separation. The dye field closest to the frigate exhibited a highly concentrated region near the surface, with a concentration gradient monotonically decreasing with depth. As the wake aged, the dye spread both laterally and vertically, forming some localized patches of hig dye concentrations. The wake also meandered, presumably as a result of slight variation in the frigate's track. At approximately 60 m back, the width of the wake as measured by the dye was about 15 m and reached a depth of about 5 m. The maximum width of the wake was approximately 40 m, which on this run, occurred about 2025 m downstream (patchiness of the wake results in variations of the distance back for maximum wake width). At this distance back, the maximum depth of the dye was 8.5 m. Dye concentrations measured at the 9.5 and 11.5 m fluorometers were nearly all less than the threshold value of the analysis of 1 $ug \cdot L^{-1}$.

Table 5.1-11. Average dye concentrations and calculated dilution based on flow-through fluorometer measurements made during continuous dye discharge periods for FTL runs. Dilution is based on a discharge concentration of 2 $g \cdot L^{-1}$.

Distance Back (ship-lengths)	Distance Back (m)	Average Dye Concentration ($ug \cdot L^{-1}$)		
		1.3 m	4.6 m	8.8 m
1	126	124.5	8.8	1.3
5	630	38.8	15.0	0.3
10	1260	12.8	10.3	1.5
15	1890	9.0	7.9	2.0

Distance Back (ship-lengths)	Distance Back (m)	Average Dilution		
		1.3 m	4.6 m	8.8 m
1	126	$1.6 \cdot 10^4$	$6.1 \cdot 10^6$	$9.1 \cdot 10^6$
5	630	$5.2 \cdot 10^4$	$1.3 \cdot 10^5$	$6.8 \cdot 10^6$
10	1260	$1.3 \cdot 10^5$	$2.0 \cdot 10^5$	$1.4 \cdot 10^6$
15	1890	$2.2 \cdot 10^5$	$2.5 \cdot 10^5$	$9.9 \cdot 10^5$

Complementary examples of vertical and horizontal dye concentration profiles behind the frigate when moving at 15 kts are shown respectively in Figures 5.1-8 and 5.1-9. The number of crossings was less for the 15-kt case due to the increased speed of the frigate relative to the *AX*. As had been observed at 8-kts, the dye field closest to the frigate moving at 15 kts also exhibited a highly concentrated region near the surface with a concentration gradient monotonically decreasing with depth. Some patchiness and meandering were observed in these runs as well. Within about 1 ship length, the dye had spread to a width of about 10 m and to a depth of about 5 m. The maximum width of the wake was approximately 44 m, which on this run, occurred about 3025 m downstream. At this distance back, the maximum depth of the dye was about 6 m, slightly shallower than the 8-kt case. Dye concentrations measured at the 9.5 and 11.5 m fluorometers were almost all less than the threshold value of the analysis of 1 $ug \cdot L^{-1}$.

Maximum dye concentrations were almost always (~ 95%) found at the shallowest sensor location (2-3 m deep) and closest in to the frigate. For the 8-kt serpentine runs maximum dye concentrations measured by the *in situ* or flow-through fluorometers were around 350 ug·L^{-1}, approximately 5700 times less than the discharge concentration of 2 g·L^{-1}. The concentration of dye was reduced another order of magnitude within about 1500 m. At the furthest downstream measurement location of around 3500 m, concentrations were about 25 ug·L^{-1}, reflecting a total dilution of more than five orders of magnitude. Close to the frigate, mean concentrations in the wake (for values above 1 ug·L^{-1}) were about a factor of 20 less than the maximum, diminishing to about a factor of three or four at maximum distances back. A power law fit to the 8-kt data (Figure 5.1-10) shows maximum dye concentration, D (ug·L^{-1}), diminishing in the downstream direction, x (m), as: $D_{8\text{-kts}} = 9000\ x^{-0.77}$. This power law relationship falls roughly midway between that expected for dilution within a turbulent wake (exponent of -0.5) and dilution within a constant diffusive quiescent environment (exponent of -1) (Hyman, 1990).

At the start of the 15-kt serpentine runs, the frigate and *AX* were initially both moving at 8 kts (near the maximum speed of the *AX*). As the frigate accelerated to 15 kts, the *AX* began its serpentine geometry. Consequently, maximum concentration measurements obtained near the frigate for both 8- and 15-kt serpentine runs were similar (Figure 5.1-10). However, after a few hundred meters, the speed of the frigate increased to 15 kts and the dye concentration was, as expected, generally lower than that for the 8-kt runs. A maximum dye concentration observed during the 15-kt runs was 230 ug·L^{-1}. In general, the ratio of maximum dye concentrations for the 15 kt and 8 kt runs was close to the inverse ratio of their corresponding speeds (8/15). This may be at least partly attributed to the fact that the discharge rate remained the same for both speeds at 6.7 g·s^{-1}, and, thus, the amount of dye ejected per unit length of wake is inversely proportional to the speed of the frigate. Like the 8-kt case, mean concentrations in the wake (for values above 1 ug·L^{-1}) were about a factor of 20 less than the maximum in close to the frigate and diminished to about a factor of three or four at maximum distances back. A power law fit to the 15-kt at-sea data show maximum dye concentrations diminishing in the downstream direction as:

$$D_{8\text{-kts}} = 8200\ x^{-0.81}.$$

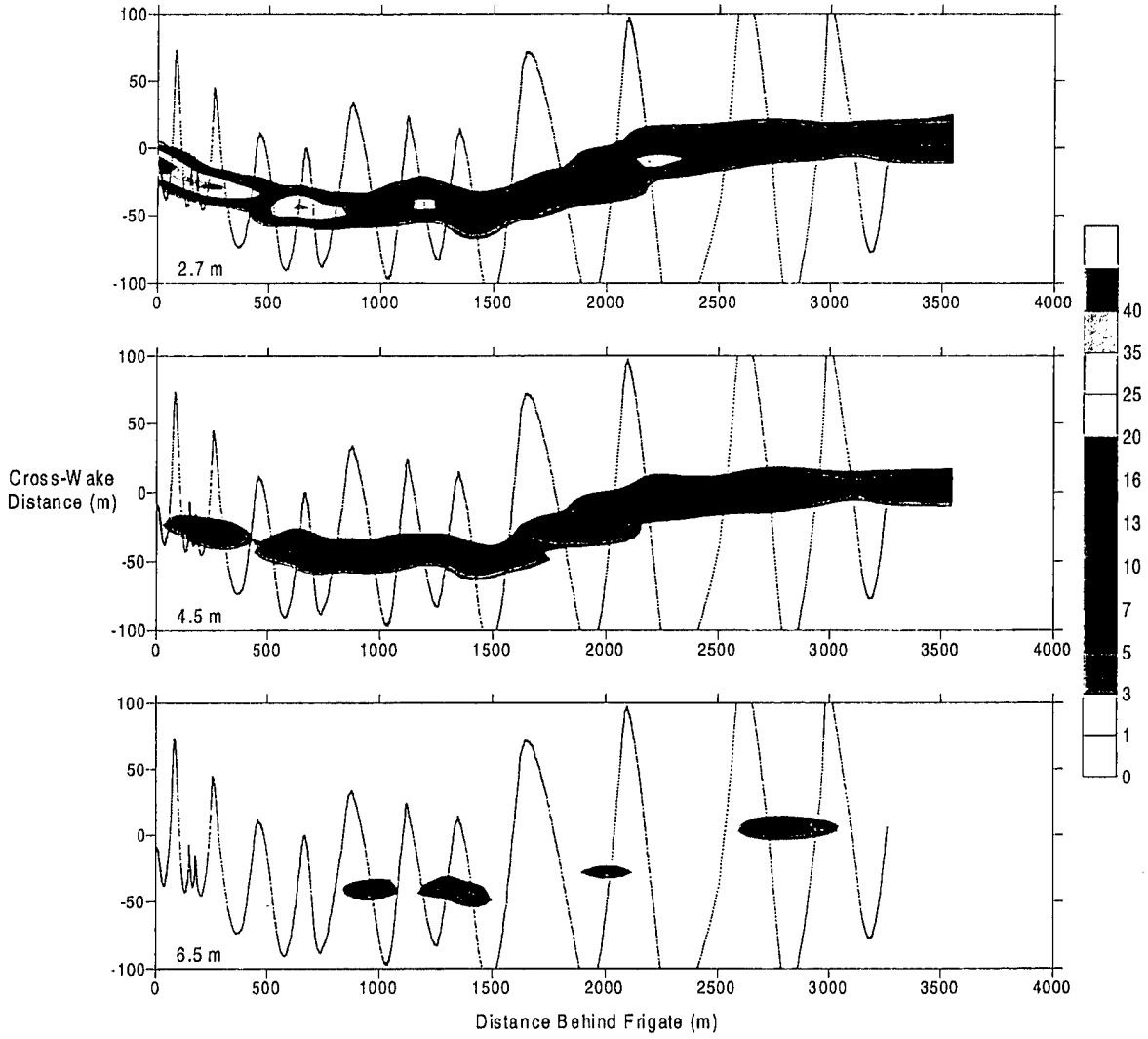

Figure 5.1-6. Plan view dye concentration (ug·L^{-1}) for Serpentine Run 1 (8 kts) at 2.7, 4.5, and 6.5 m depths as a function of distance behind the frigate. Concentrations were measured by the *in situ* fluorometer array. Dye concentrations measured at 9.5 and 11.5 m were virtually all below the 1ug·L^{-1} threshold of the analysis.

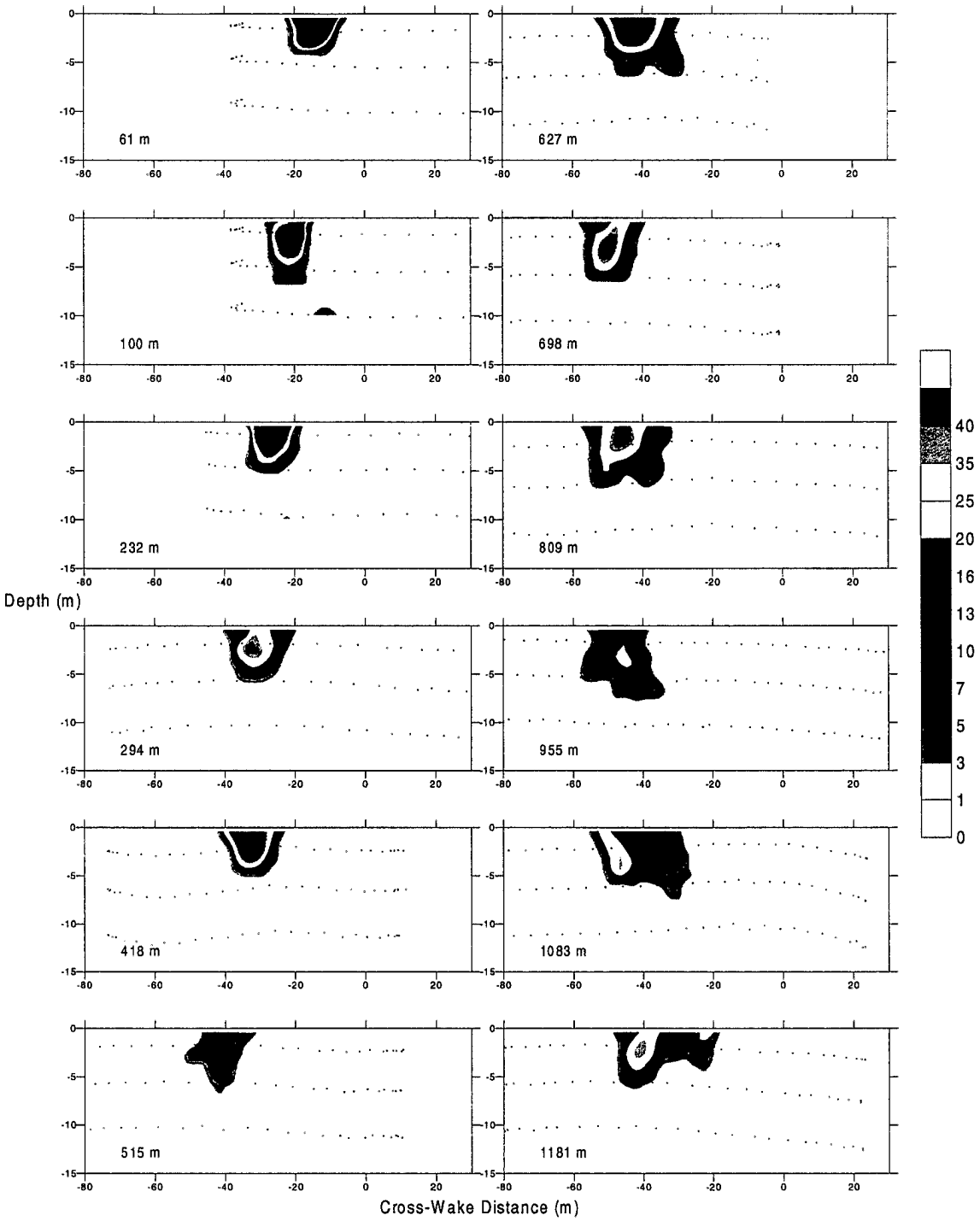

Figure 5.1-7a. Cross-sectional views (looking toward frigate from behind) of dye concentration ($ug \cdot L^{-1}$) for Serpentine Run 1 (8 kts) for first 12 full-wake crossings. The crossing distance behind the frigate is noted on each cross-section. Concentrations were measured by the *in situ* fluorometer array.

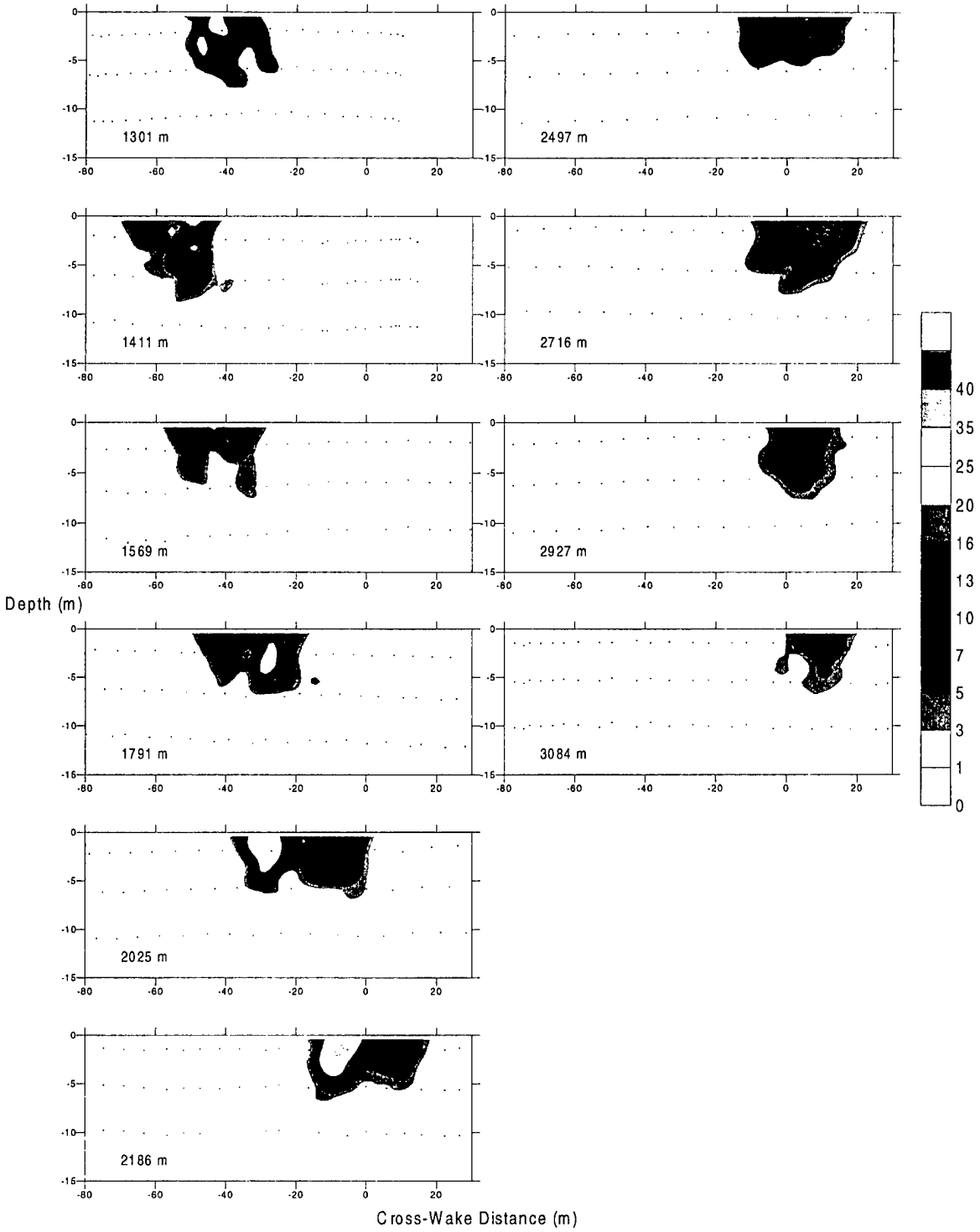

Figure 5.1-7b. Cross-sectional views (looking toward frigate) of dye concentration (ug·L^{-1}) for Serpentine Run 1 (8 kts) for last 10 full-wake crossings. The crossing distance behind the frigate is noted on each cross-section. Concentrations were measured by the *in situ* fluorometer array.

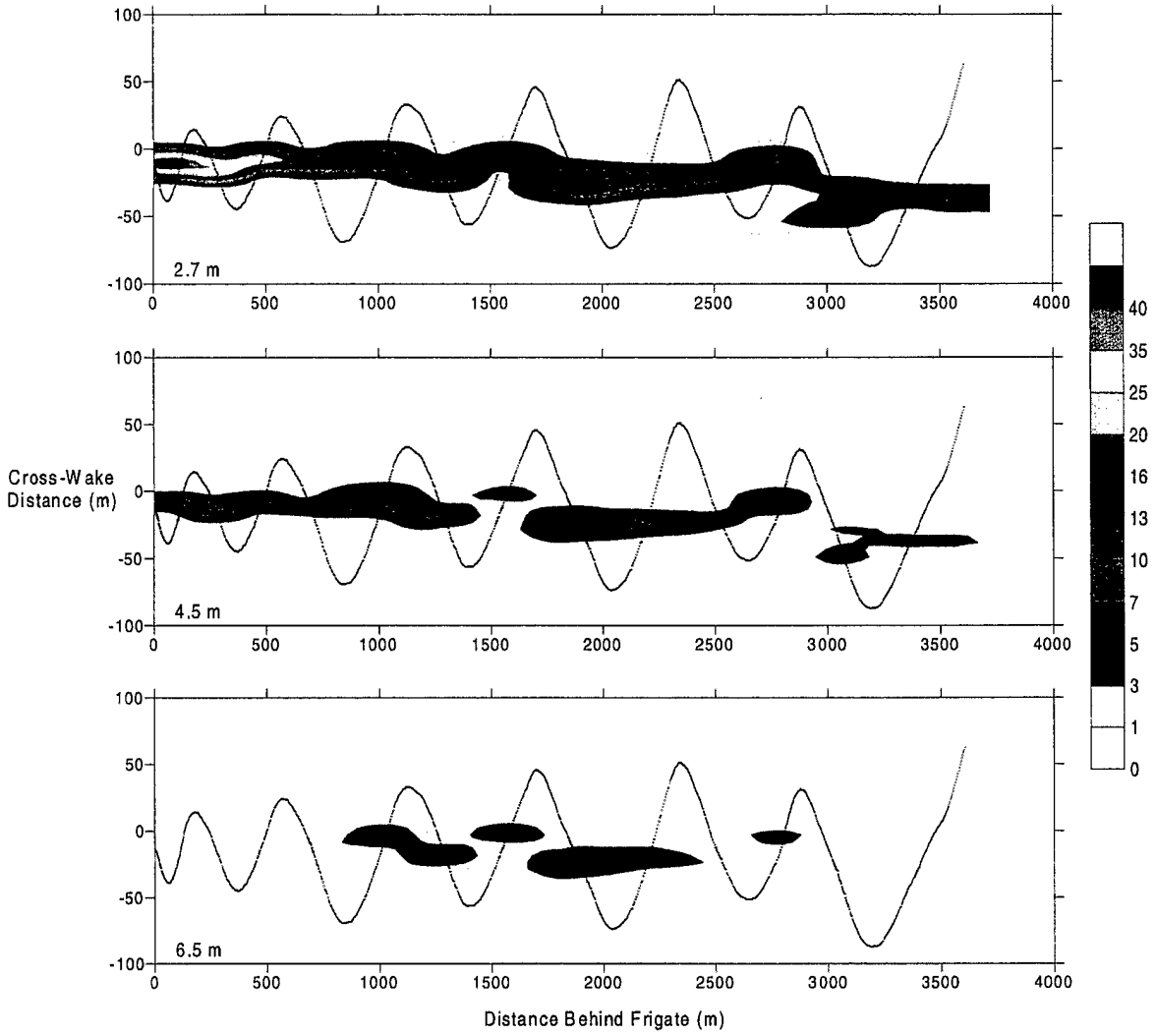

Figure 5.1-8. Plan view dye concentration (ug·L^{-1}) for Serpentine Run 4 (15 kts) at 2.7, 4.5, and 6.5 m depths as a function of distance behind the frigate. Concentrations were measured by the *in situ* fluorometer array. Dye concentrations measured at 9.5 and 11.5 m were virtually all below the 1ug·L^{-1} threshold of the analysis.

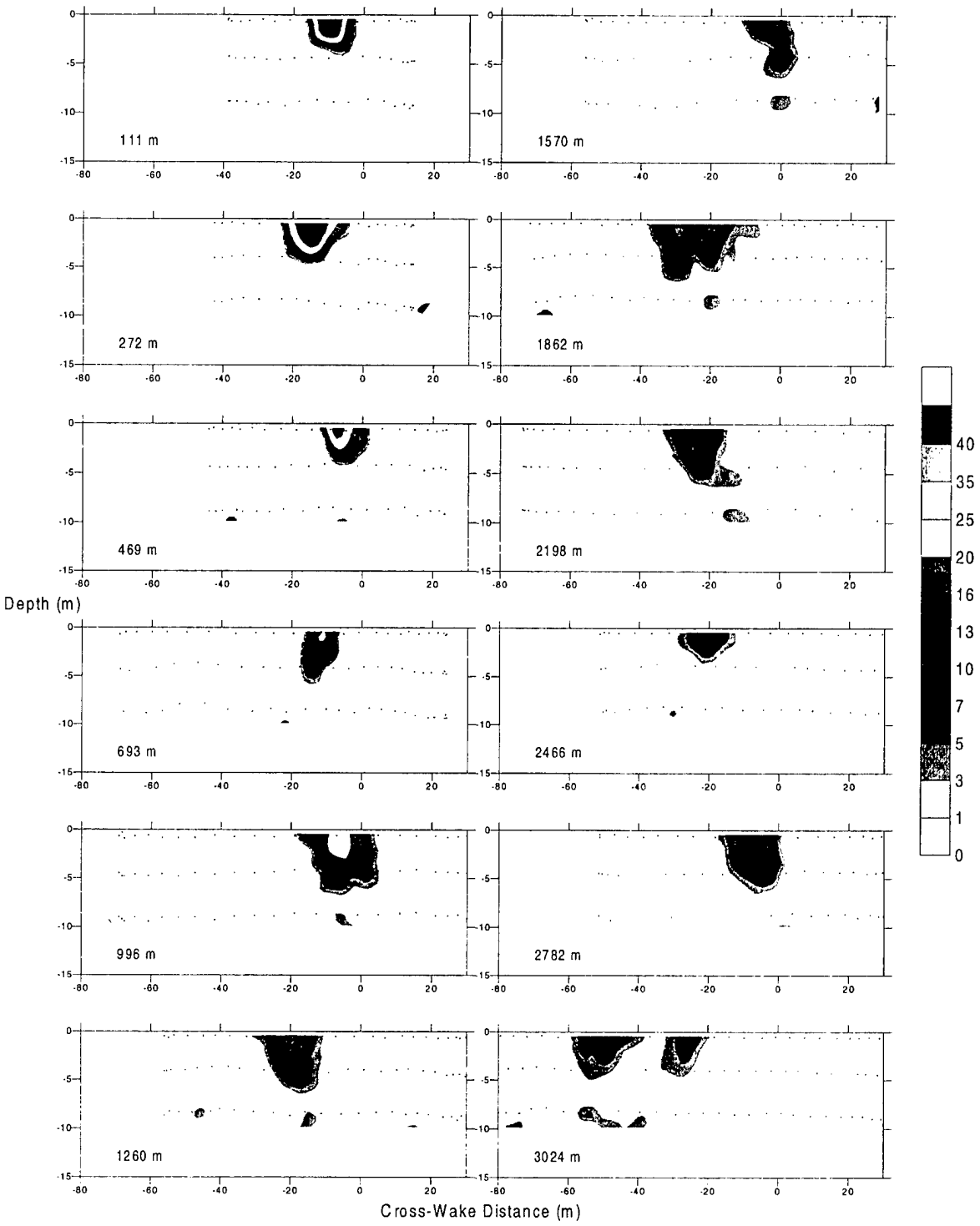

Figure 5.1-9. Cross-sectional views (looking toward frigate from behind) of dye concentration ($ug \cdot L^{-1}$) for Serpentine Run 4 (15 kts) for first 12 (of 13) full-wake crossings. The crossing distance behind the frigate is noted on each cross-section. Concentrations were measured by the *in situ* fluorometer array.

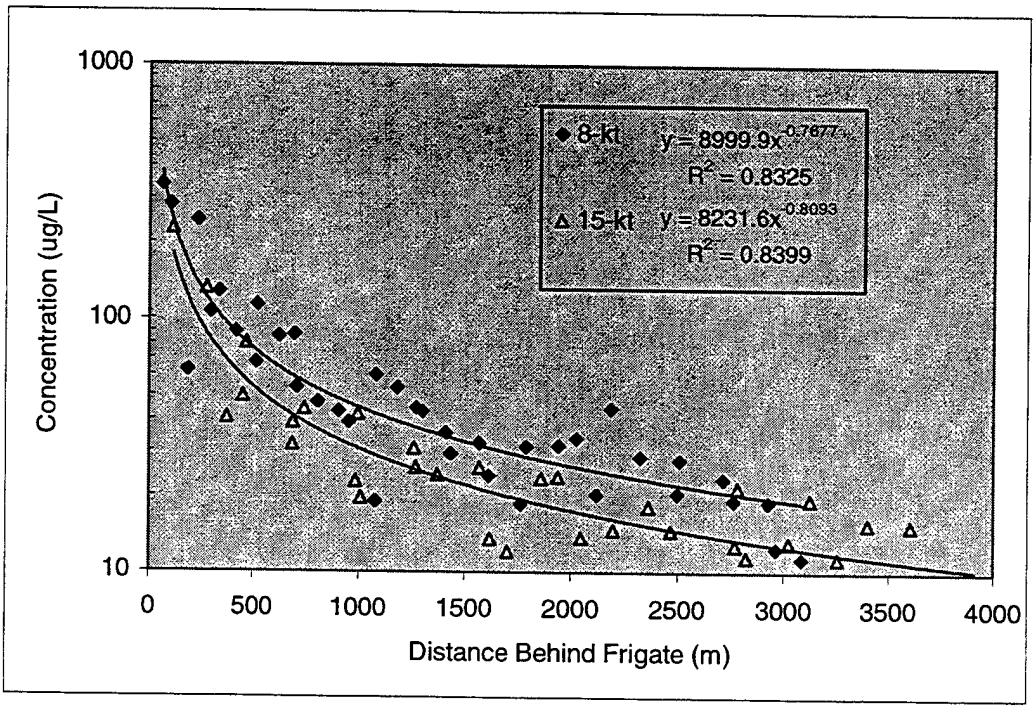

Figure 5.1-10. Maximum dye concentration as a function of distance behind the frigate for both 8-kt and 15-kt runs measured at each wake crossing.

Minimum dye dilution estimates were made by dividing the concentration of dye at discharge (2 $g \cdot L^{-1}$), by the maximum concentration measured at each wake crossing by the *in situ* fluorometer array. Figure 5.1-11 displays the minimum dye dilution as a function of frigate-*AX* separation distance for both frigate speeds of 8 and 15 kts. Minimum dilutions ranged from about $5.9 \cdot 10^3$ closest in to the frigate to roughly $2.3 \cdot 10^5$ at a down-wake distance of 3500 m for both the 8-kt and 15-kt case. The 15-kt dilution values were almost always lower than the 8-kt counterpart, though the differences were very slight.

The dilution data derived from the *in situ* fluorometer array are corroborated with the flow-through dye measurements. Figure 5.1-12 shows dilution as a function of distance back as measured by both fluorometer systems. As anticipated, close to the frigate, the flow-through fluorometers measured noticeably higher dilutions than the *in situ* system because of the additional mixing occurring in the sampling tubes. However, with increasing distance from the frigate, this difference generally decreased because the additional mixing in the flow-through tube became less important as the gradient in the wake was reduced.

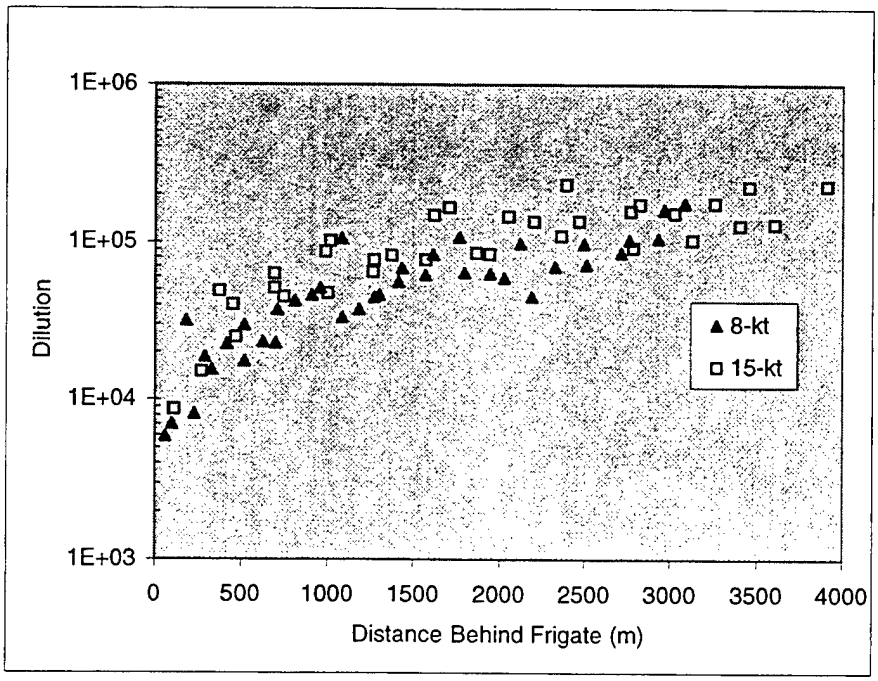

Figure 5.1-11. Minimum dye dilution for 8-kt and 15-kt data based on 2 $g \cdot L^{-1}$ discharge concentration.

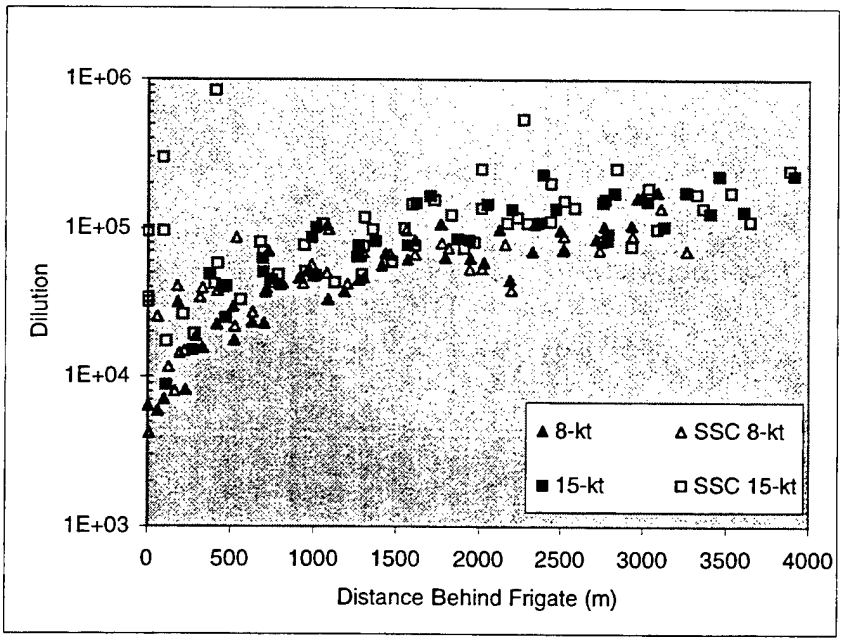

Figure 5.1-12. Minimum dye dilution for 8-kt and 15-kt data based on 2 $g \cdot L^{-1}$ discharge concentration. Results for data collected from both the *in situ* fluorometer array and flow-through array (SSC) are included.

MODEL RESULTS

Pulp. Model results for pulped material were generated as maximum and average concentrations as a function of distance behind the frigate for both the 8-kt and 15-kt case. The concentration data, based on an input rate of 110 $kg \cdot hr^{-1}$, are shown in Figure 5.1-13. For the 8-kt case, maximum concentrations dropped from 0.32 $mg \cdot L^{-1}$ at roughly 500 m, where model results are stabilized, to 0.055 $mg \cdot L^{-1}$ out at 4000 m. Average concentrations for the same distances behind the frigate were 0.062 to 0.011 $mg \cdot L^{-1}$, respectively. The corresponding minimum dilution, corresponding to the maximum concentration values, and a starting concentration of 9.6 $g \cdot L^{-1}$ ranged from $1.2 \cdot 10^4$ and $7.2 \cdot 10^4$. For the 15-kt case, maximum concentrations dropped from 0.20 $mg \cdot L^{-1}$ at roughly 500 m to 0.042 $mg \cdot L^{-1}$ out at 4000 m. Average concentrations for the same distances behind the frigate and at 15 kts were 0.035 to 0.009 $mg \cdot L^{-1}$, respectively. The corresponding minimum dilution for the maximum concentration values, using the starting concentration of 9.6 $g \cdot L^{-1}$, are $2.0 \cdot 10^4$ and $9.6 \cdot 10^4$.

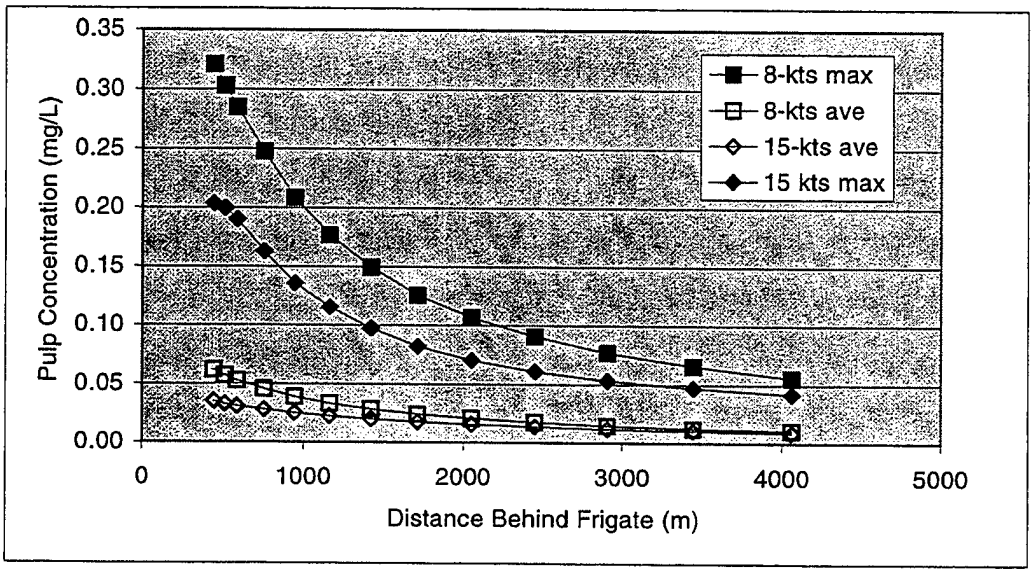

Figure 5.1-13. Model results for pulped material concentration as a function of distance behind the frigate.

Dye. Results of the model simulation for dye are shown qualitatively in Figures 5.1-14 and 5.1-15. A plan view of the 8-kt data shows growth of the wake from the IDP at about 60 m out to 4000 m for 2.5 m depth. The plot uses the same contour colors and intervals and a minimum threshold of 1 $ug \cdot L^{-1}$ as shown earlier for the field data. Though data are shown starting at the IDP, only values for distances greater than 500 m are considered fully stabilized. Unlike the measured data that showed patchiness and a meandering track, the concentration contours for the model output were smooth and straight throughout. Cross-sectional plots show the wake growing monotonically both laterally and with depth. Growth of the wake to the right of centerline in the plot results from the model taking into consideration the starboard discharge and clockwise rotation of the screw. The modeled wake width grew from its preset value of about 10 m at the IDP to about 30 m out at 3000 m. Over these distances, the depth of the dye increased from about 3 m to 10 m.

Maximum concentrations of dye decreased from 66 $ug \cdot L^{-1}$ at 500 m behind the frigate to 14 $ug \cdot L^{-1}$ out at 4000 m (Figure 5.1-16). A power law fit to the modeled 8-kt data show maximum dye concentrations diminishing in the downstream direction as: $D_{8\text{-kts}} = 5778 \cdot x^{-0.73}$, where x is measured in meters. Again, this relationship is midway between fully turbulent dilution (-0.5 exponent) and diffusive dilution (-1 exponent), Hyman, 1990. Mean dye

concentrations in the wake at each crossing (for values above the 1 ug·L^{-1} threshold) were about a factor of 4-5 less than maximum values throughout the wake. Minimum downstream dilutions, calculated by dividing the concentration of effluent at discharge (2 g·L^{-1}) by the maximum concentration of effluent computed in the corresponding wake cross section ranged from $3.0 \cdot 10^4$ to $1.4 \cdot 10^5$ over the 500 to 4000 m down-wake distance (Figure 5.1-17).

Corresponding model results for the 15-kt case are shown qualitatively in Figures 5.1-18 and 5.1-19. For this case, maximum dye concentrations decreased from an initial 42 ug·L^{-1} at 500 m behind the frigate to 8.6 ug·L^{-1} at 4000 m (Figure 5.1-15). These correspond to minimum dilution levels of $4.8 \cdot 10^4$ and $2.3 \cdot 10^5$. A power law fit to the modeled 8-kt data show maximum dye concentrations diminishing in the downstream direction as:

$$D_{15\text{-kts}} = 6410\ x^{-0.80}.$$

Because the governing equations were originally ensemble averaged, the maximum concentrations calculated are most likely less than those found in any single realization. It has been estimated for bubble concentrations that the difference between maximum concentrations found for single realizations and ensemble averages are typically less than 50 %. It is expected that a roughly similar relationship should hold for the present problem.

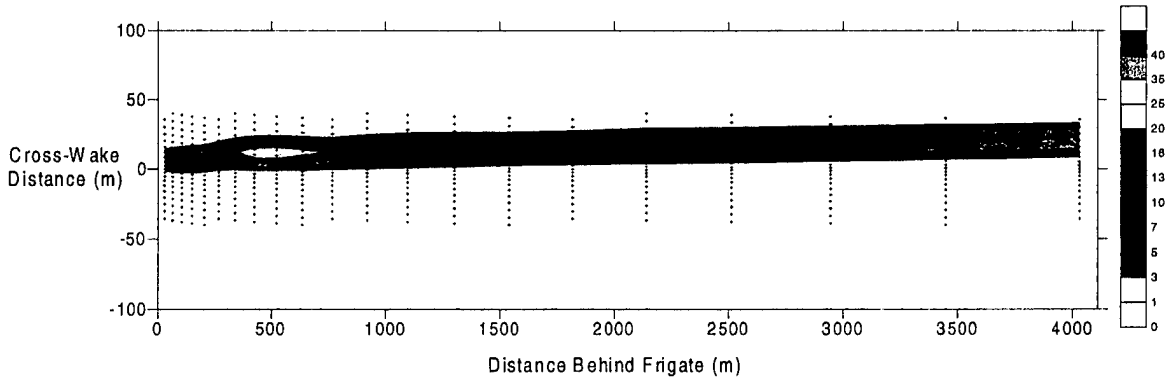

Figure 5.1-14. Plan view of modeled dye concentration (ug·L^{-1}) at 2.5 m depth, as a function of distance behind the frigate at 8 kts. The IDP was at about 60 m for this run.

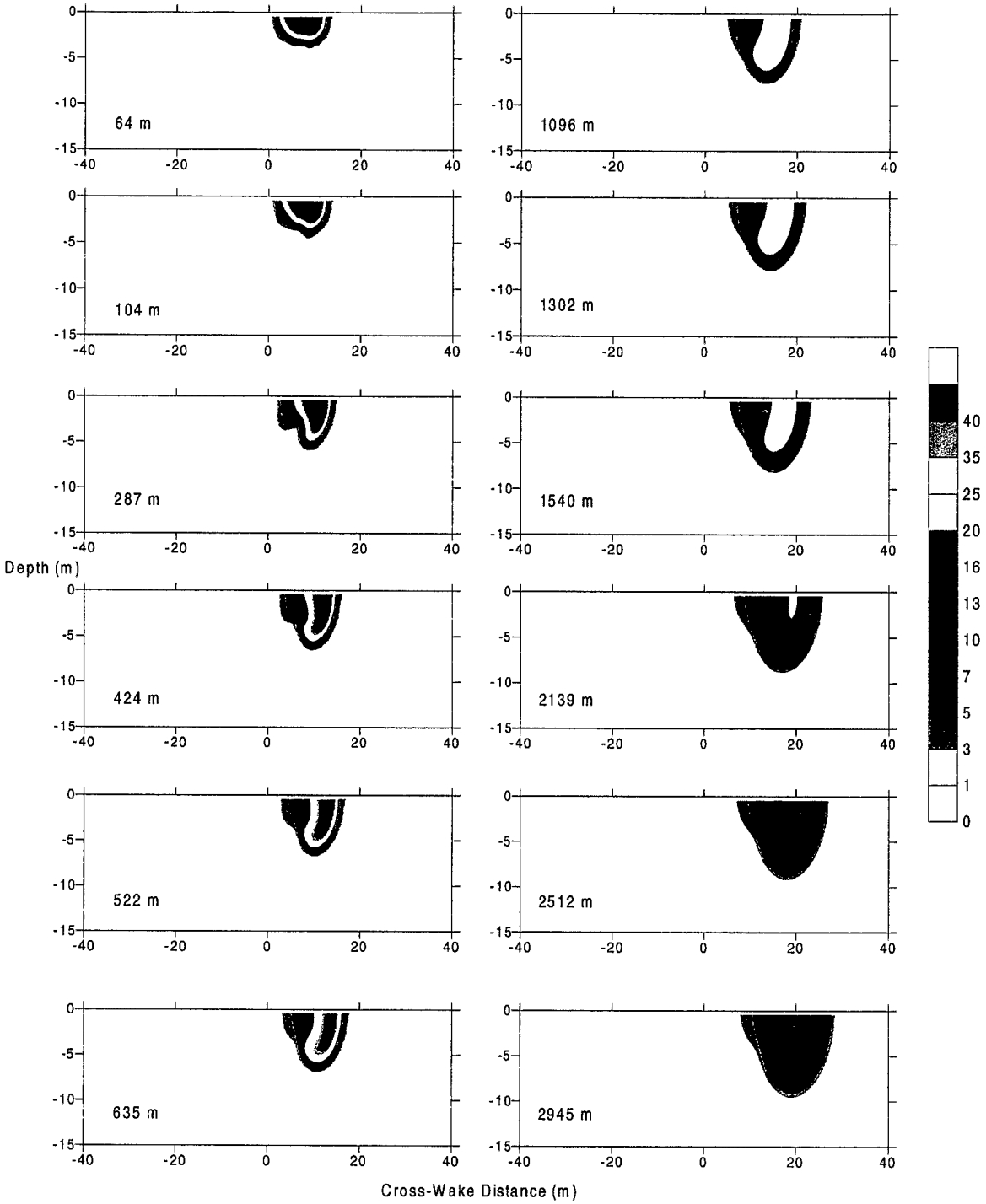

Figure 5.1-15. Cross-sectional views (looking toward frigate from behind) of model dye concentration ($ug \cdot L^{-1}$) at selected distances behind the frigate for the 8-kt case. The IDP was at about 60 m for this run.

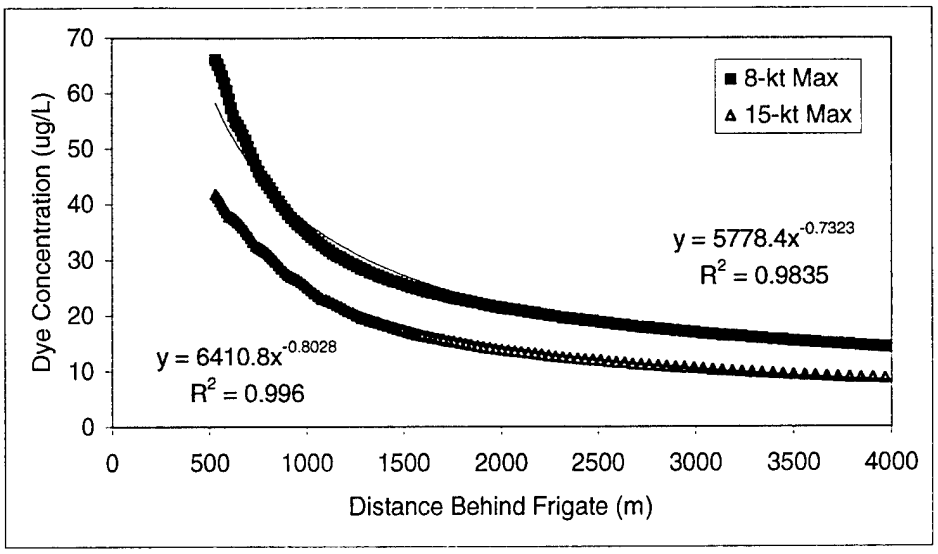

Figure 5.1-16. Model results for maximum dye concentration ($ug \cdot L^{-1}$) as a function of distance behind frigate.

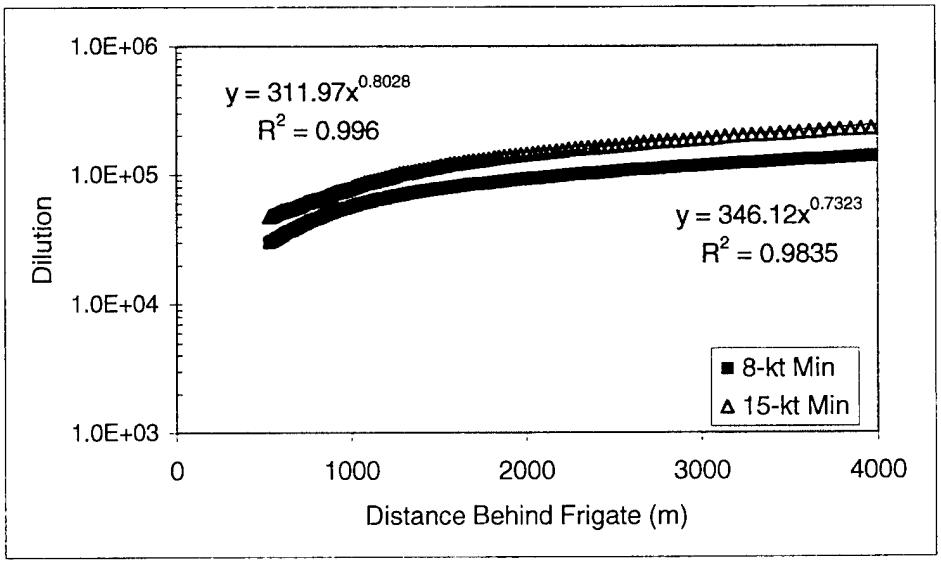

Figure 5.1-17. Minimum dilution for model dye results as a function of distance behind frigate.

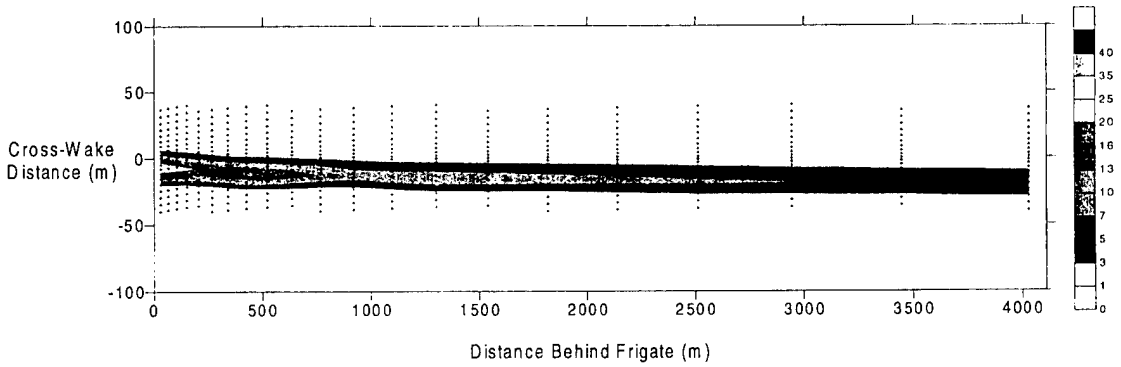

Figure 5.1-18. Plan view of modeled dye concentration ($ug \cdot L^{-1}$) at 1 m depth, as a function of distance behind the frigate at 15 kts. The IDP was at about 60 m for this run.

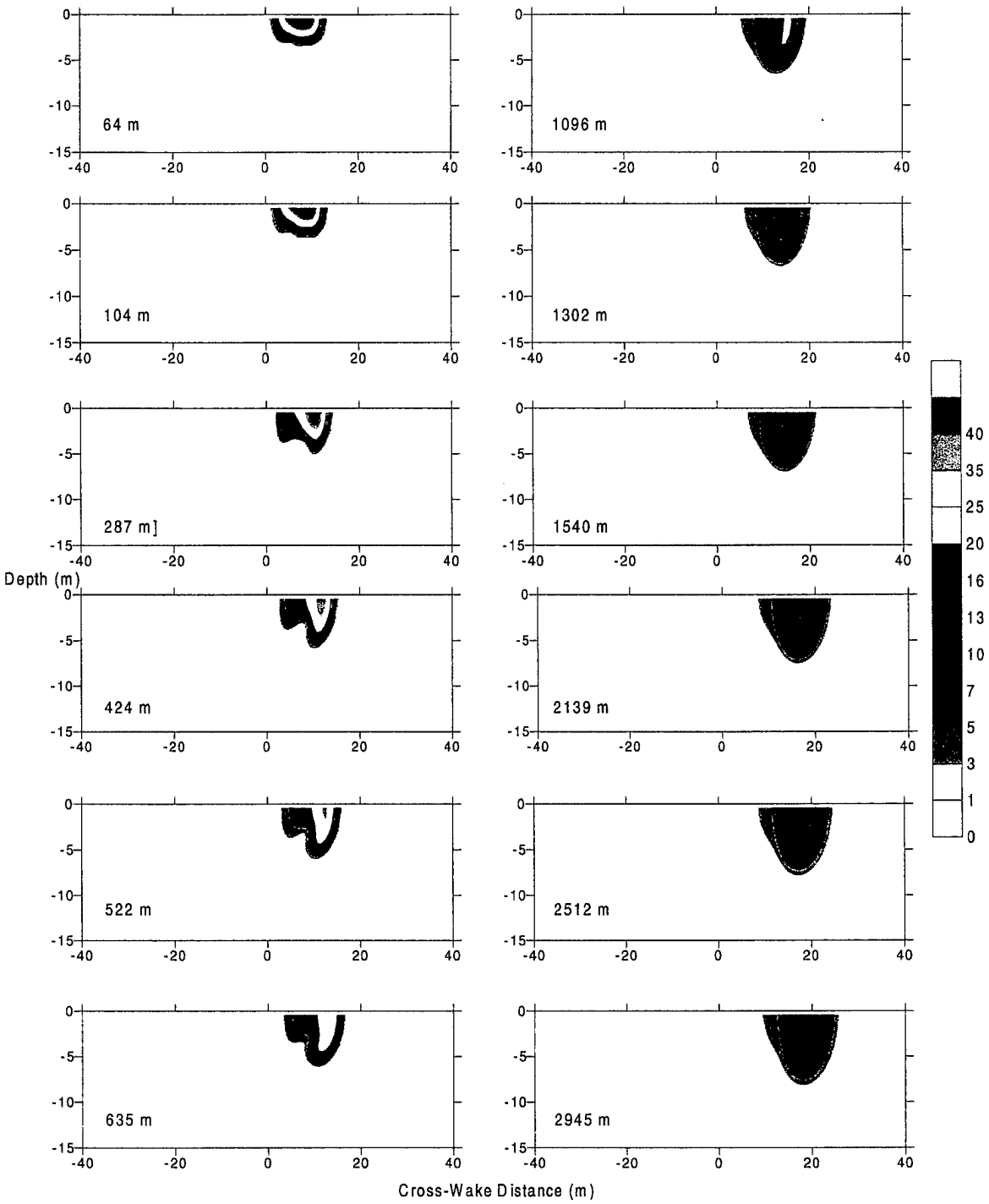

Figure 5.1-19. Cross-sectional views (looking toward frigate from behind) of model dye concentration ($ug \cdot L^{-1}$) at selected distances behind the frigate for the 15-kt case. The IDP was at about 60 m for this run.

DISCUSSION

One goal of the field effort was to measure the concentration and, therefore, dilution of pulped paper and dye as a function of time after discharge to characterize the exposure levels of the particulate and liquid phases of shipboard solid waste discharges in the ocean. A second goal of the effort was to validate a modeling effort that would be used to characterize exposure levels for a range of conditions that are not possible to measure. Both goals ultimately were required to assess the ecological impact of one of the Navy's proposed alternatives for solid waste discharges. In the following discussion, field data for pulped paper and dye are summarized, validated against physical laws governing wake growth and mass balance, and compared to model predictions.

Pulp. A summary of the measured and modeled pulp concentration data for the 8-kt case are shown in Figure 5.1-20. All concentrations of pulp measured in the field fell between modeled maximum and average values. This held true even for small distances behind even though the model results are not fully stabilized until about 500 m. While most measured data fell along the model average, the fluorometrically derived measurement made at 1 ship-length fell along the model maximum. The close agreement between model averages and measurements is expected because of the methods employed to collect the samples. The high data value derived fluorometrically close-in, indicates that this sample may actually have captured the maximum concentration in the wake, though the sample measured gravimetrically does not support this. However, excellent agreement between model and measured results at greater distances behind the frigate suggests that the dilution values calculated from the model are reasonable for predicting concentrations under standard discharge rates (45 $kg \cdot hr^{-1}$). This is particularly true given that the field results scaled well under varying discharge rates.

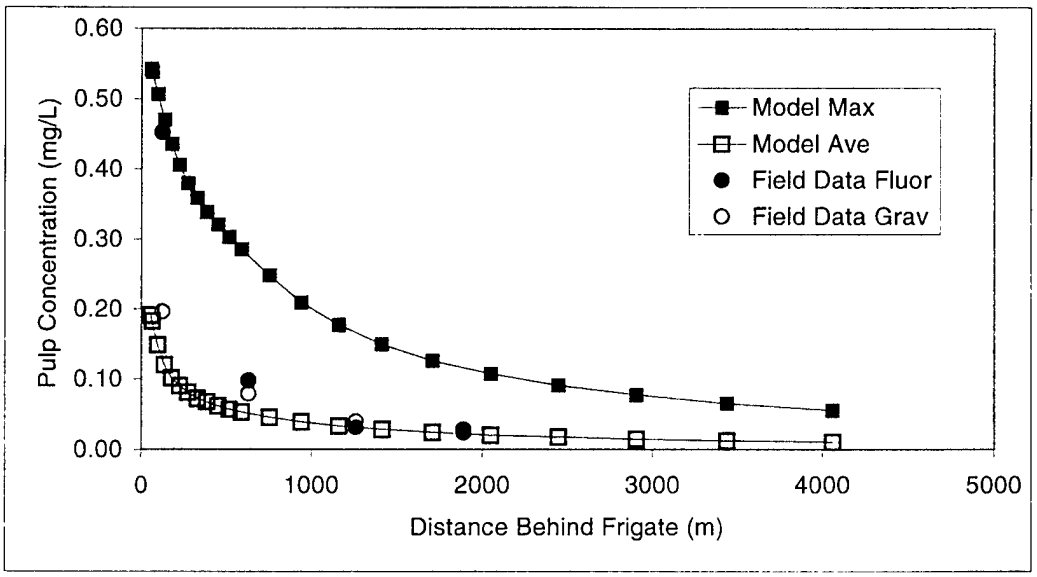

Figure 5.1-20. Modeled and measured pulp concentrations as a function of distance behind frigate. Field data "Fluor" refers to results determined fluorometrically while "Grav" refers to results determined gravimetrically.

Dilution at 8 kts as function of distance behind the frigate is shown in Figure 5.1-21. At 5 ship-lengths behind the frigate (630 m), the average dilution value measured was $9.9 \cdot 10^4$. By 15 ship-lengths (1890 m), the average pulp dilution value reached $3.6 \cdot 10^5$. Comparable model dilution values were $2.1 \cdot 10^5$ and $4.4 \cdot 10^5$, respectively. Close-in the differences are about a factor of 2 while out toward the end of wake mixing, the differences are within 20%. Given the standard operational discharge rate of 45 $kg \cdot hr^{-1}$, which represents a starting discharge concentration of 3.9 $g \cdot L^{-1}$, the model equation predicts an average concentration of pulped material 0.018 and 0.009 $mg \cdot L^{-1}$, at the

same distances back. The maximum concentrations predicted at these distances, using the minimum dilution curve, would be 0.088 and 0.048 $mg \cdot L^{-1}$, respectively. At 8 kts, these maximum concentrations would be reached within 8 mins of discharge. As seen previously (Figure 5.1-13), concentrations would be roughly half (8/15) for a frigate traveling at 15 kts.

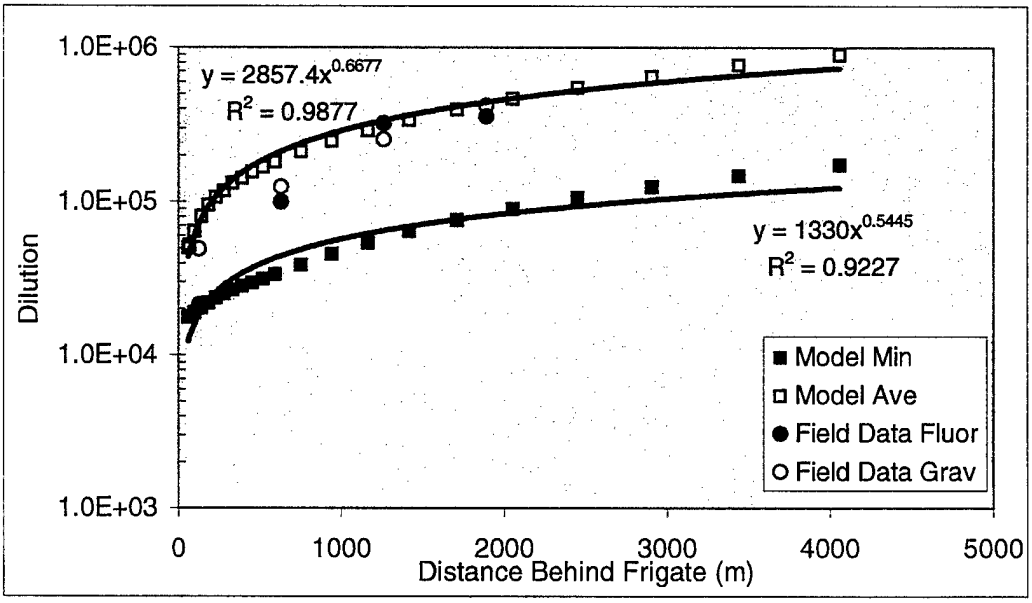

Figure 5.1-21. Modeled and measured dilution values as a function of distance behind frigate. Field data "Fluor" refers to results determined fluorometrically while "Grav" refers to results determined gravimetrically.

Dye. The field measurements and model runs of dye discharge provide a means to assess the dilution of the liquid phase of the discharge stream as well as to provide details of wake dilution not available from the sparse particle data. These data, in terms of dilution versus distance behind the frigate, are shown in Figures 5.1-22 and 5.1-23. For the 8-kt case (Figure 5.1-22), it can be seen that the measured and modeled data agree remarkably well with each other. This is true for both the *in situ* and flow-through field measurements. A regression equation using the *in situ* data predicts minimum dilution values of $3.1 \cdot 10^4$ and $7.3 \cdot 10^4$ at 5 and 15 ship-lengths back, respectively. For the same locations, the model equation predicts minimum dilution values of $3.9 \cdot 10^4$ and $8.7 \cdot 10^4$, respectively. Model predictions of average dilution values are roughly a factor of 4 higher at $1.7 \cdot 10^5$ and $3.4 \cdot 10^5$. The measured values and model predictions are typically within 20% of one another, though at 5 ship-lengths, the average dilution values differ from the model by 50%. The average dye dilutions predicted for the dye ($3.4 \cdot 10^5$) are comparable to those measured ($3.6 \cdot 10^5$) and predicted for the pulp and ($4.4 \cdot 10^5$).

For the 15-kt case (Figure 5.1-23), it can be seen that the *in situ* and flow-through field measurements agree well with one another as well as with the model results, particularly when looking at minimum dilution values. A regression equation using the *in situ* data predicts minimum dilution values of $2.8 \cdot 10^5$ and $4.5 \cdot 10^5$ at 5 and 15 ship-lengths back, respectively Using the model equation, the minimum dilution at 5 ship-lengths is $3.5 \cdot 10^4$, while at 15 ship-lengths back it is $6.3 \cdot 10^5$. The differences between model and measured values is about 20%. Average dilution values are about a factor of 5 higher for corresponding distances, at $5.5 \cdot 10^4$ and $1.3 \cdot 10^5$.

The exceptional agreement between field measurements made using multiple independent techniques for both the liquid phase (dye) and particulate phase (pulp) of the discharge suggests that wake dilution was very well

characterized by the field effort. The remarkable agreement of the field data with model predictions, supports a strong reliance on the model for use in predictions for conditions falling outside the specific measurement regime.

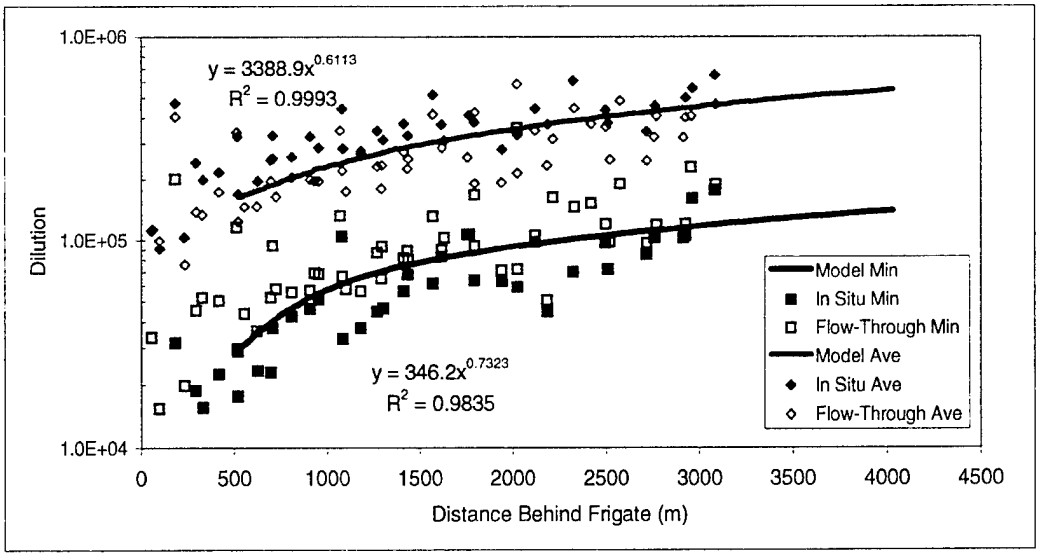

Figure 5.1-22. Modeled and measured minimum and average dilution values as a function of distance behind frigate for the 8-kt case. The equations shown are for the modeled data.

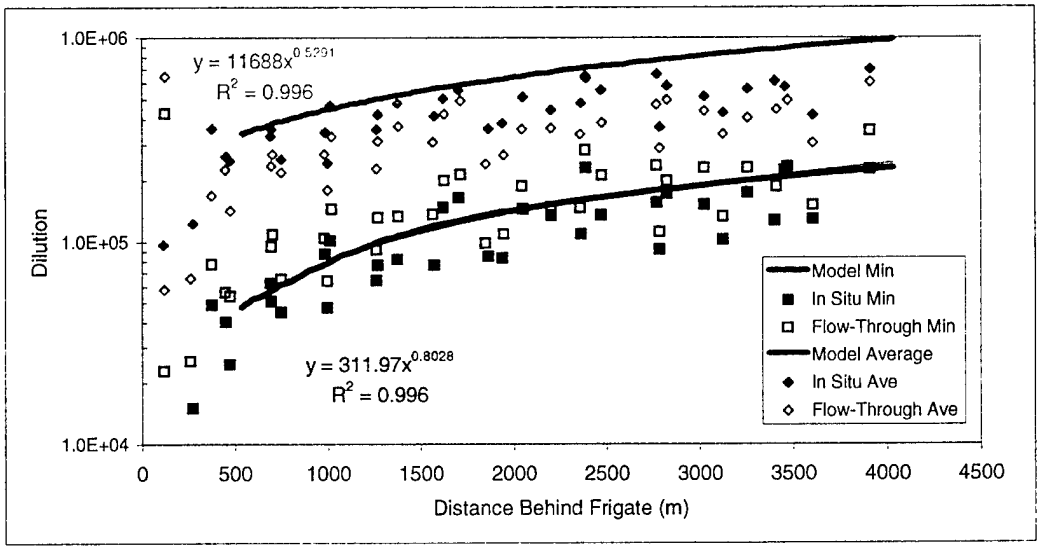

Figure 5.1-23. Modeled and measured minimum and average dilution values as a function of distance behind frigate for the 15-kt case. The equations shown are for the modeled data.

Wake Width. Dye measurements made during the serpentine runs provide sufficient data for validating physical laws governing wake growth. Estimates of the dye stream width as a function of distance behind the frigate, for the 8-kt and 15-kt runs are shown in Figure 5.1-24. The dye stream width at each downstream location was determined as the greatest lateral extent of dye throughout the measurement plane for concentrations of dye greater than or equal to 1 ug·L^{-1}. The width, W (m), of the dye stream for all the data for both ship speeds increased with downstream separation from the frigate, (x, in meters), approximately as: $W \sim x^{0.25}$ at 8 kts and $W \sim x^{0.31}$ for 15 kts. Though the regression equation for the 8-kt case had an r^2 of 0.7, noise in the 15-kt case resulted in a regression equation r^2 of only 0.36. Computer simulations, which represent an average result acquired over many realizations, predict that the width of the dye plume should increase downstream as $W \sim x^{0.20}$ and $W \sim x^{0.18}$ for the 8-kt and 15-kt runs, respectively.

The observed power law increase of wake width with downstream distance for both the field experiments measurements and model simulations lie well within the range of exponents reported for various types of wakes studied in the laboratory. Investigations conducted in tanks with unstratified flows have reported growth rates for the width of submerged, momentumless wakes, ranging from $W \sim x^{0.25}$ (Naudascher, 1965; Meritt, 1972) to $W \sim x^{0.33}$ (Schooley and Stewart, 1963). Merritt (1972) studied the effect of stratification on wake growth in the laboratory and found that during the period when the wake is collapsing vertically, horizontal wake growth is enhanced with $W \sim x^{0.5}$. While the present experiments were performed with a mixed-layer depth of 25 m, well beyond the wake depth, inhibited vertical motion at the air-sea interface is expected to similarly increase the horizontal growth rate of a surface wake. The excellent agreement between measured wake growth in the field and that measured in laboratory studies lends a high degree of confidence that the dye plume was well characterized and follows physical relationships determined under controlled conditions in the laboratory.

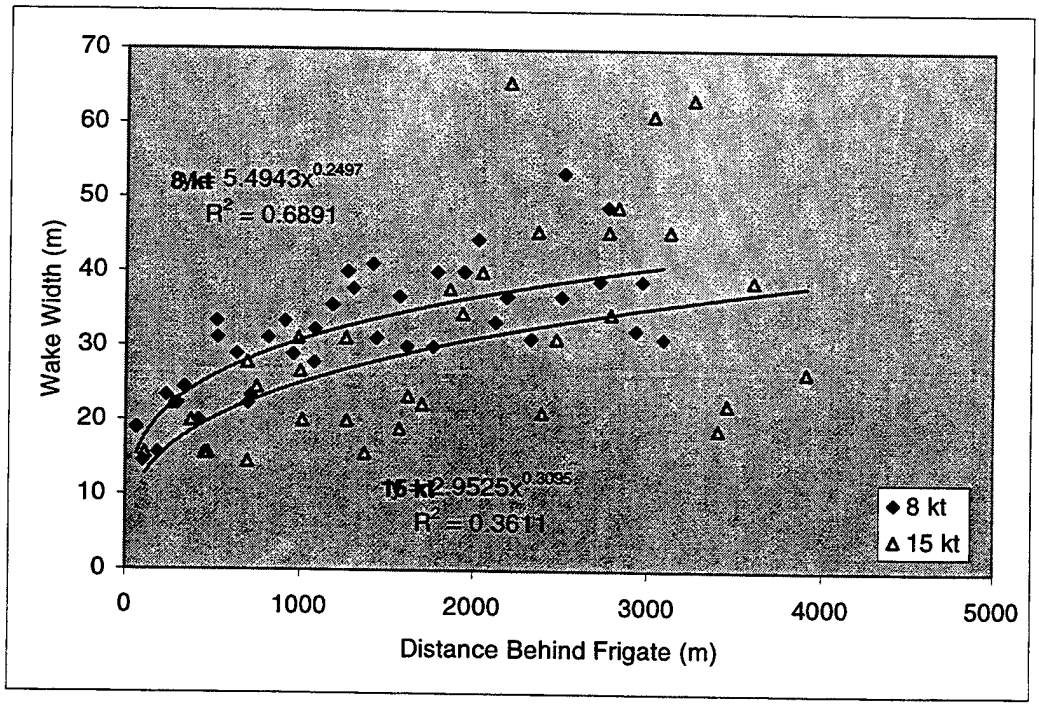

Figure 5.1-24. Wake width as a function of distance behind the frigate for both 8-kt and 15-kt data.

Mass Balance. Okubo (1971) and Csanady (1981) have suggested that at least half the mass discharged into the wake should be accounted for by measurements to have confidence that the most concentrated part of a discharge plume was sampled sufficiently. Therefore, a mass balance for the discharged pulp and dye was performed to determine if the measurements reliably mapped the discharge field. Because the dye field was sampled at a higher spatial density, mass balance for these data were considered first.

The dye discharge rate for both frigate speeds was 6.7 $g \cdot s^{-1}$. At 8 kts, the mass discharged per meter length is, therefore, 1.67 g, while at 15 kts, the mass discharge was 0.89 $g \cdot m^{-1}$. The mass of dye at each crossing was calculated by integrating the data (interpolated grid file) over the whole cross-section using a 1-m thickness. The results of these calculations are plotted for the 8-kt case in Figure 5.1-25a and for the 15-kt case in Figure 5.1-25b. In both cases, the calculated mass values randomly bounce around the expected mass discharge value showed as a line in the plot. The mass values measured at individual cross-sections for all data ranged between a factor of 3 too high to a factor of 6 too low. Much of this variation comes from data collected from less than 500 m behind since dropping these data out reduces the range from a factor of almost 3 too high to a factor of 2 too low. However, the average value for the 8-kt case (all data) was 1.89 ±0.91 $g \cdot m^{-1}$, approximately 13% higher than expected. For the 15-kt case, the average mass calculated (all data) was 0.90 ±0.37 $g \cdot m^{-1}$, or roughly 1% higher than expected. The good agreement between average measured and predicted amounts suggests that the dye discharge was sampled effectively.

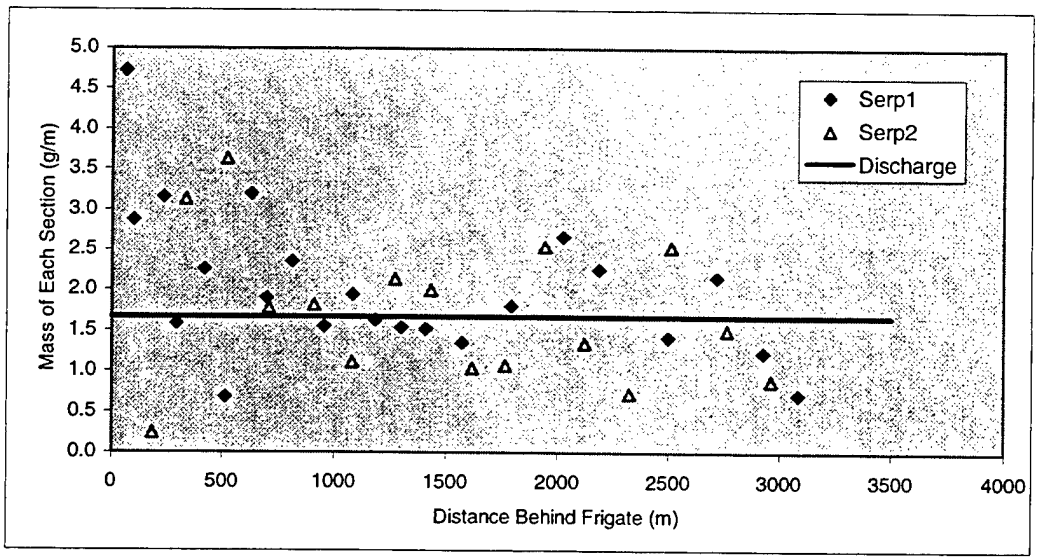

Figure 5.1-25a. Mass balance of dye as a function of distance behind the frigate for the 8-kt case. The discharge rate was 1.67 $g \cdot m^{-1}$.

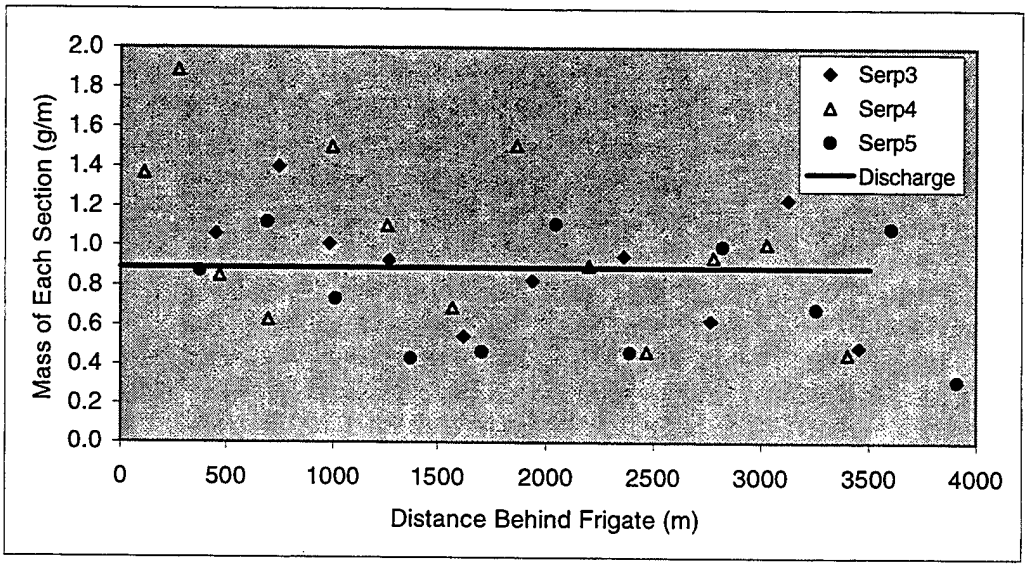

Figure 5.1-25b. Mass balance of dye as a function of distance behind the frigate for the 15-kt case. The discharge rate was 0.89 $g \cdot m^{-1}$.

The discharge rates of pulped paper and dye were held constant throughout the surveys. Thus, the mass ratio of pulped paper to dye measured in the wake should remain constant, assuming particles did not settle out of below the sample intakes, and that the wake was sampled effectively. The ratio of pulped paper to dye mass in the discharge was 30.5 $g \cdot s^{-1}$ to 6.7 $g \cdot s^{-1}$, or a value of 4.6. The average pulped paper and dye concentrations measured for the FTL runs (Tables 5.1-7, 5.1-8 and 5.1-11) were then used to calculate the measured ratio of pulped paper to dye. These calculated ratios are shown in Table 5.1-12.

While the overall measured mass ratio calculated was 3.6, a value that is within 25% of expected, the data averaged at each individual section, or with depth, vary considerably. The mass ratio when averaged for each cross-section, was underestimated at 1 and 15 ship-lengths, overestimated at 5 ship-lengths, and either over or underestimated at 10 ship-lengths, depending on the measurement technique considered. When averaged by depth, the ratios were underestimated at the surface and middle depths, and overestimated at the bottom, an effect of particle settling. The calculated ratios were all within a factor of two of predicted, except for those at 1 ship-length. At this separation distance, the likelihood was that the pulp was not fully entrained in the wake, and virtually all the material was still present at the surface. By 5 ship-lengths, the pulp and dye were entrained into the wake and mass was conserved within a factor of two or better. If only data in the range of 5 to 15 ship-lengths are considered, the average calculated ratio of 4.5 matches well to the predicted ratio of 4.6 quite well. From a distance back of 5 ship-lengths or more, mass was sufficiently conserved during the FTL runs and, thus, the measurements provide a reasonable characterization of the wake.

Table 5.1-12. Mass ratio of pulped paper to dye measured during FTL runs at 8 kts. The ratios were calculated from data in Tables 5.1-7, 5.1-8, and 5.1-11. A ratio of 4.6 is expected.

	Distance Back (Ship lengths)	Distance Back (m)	1.3 m	4.6 m	8.8 m	Average by Cross Section (geometric mean)
Fluorometric	1	126	3.63	0.19	-	0.84
	5	630	2.51	2.51	29.06	5.68
	10	1260	2.39	2.95	5.09	3.30
	15	1890	2.98	2.54	5.06	3.37
Gravimetric	1	126	1.57	-	-	1.57
	5	630	2.01	4.37	69.05	8.46
	10	1260	2.97	3.37	19.33	5.79
	15	1890	2.54	1.80	3.99	2.63
Average By Depth			2.573	2.533	21.93	**Overall Mean: 3.6** **Mean 630-1890 m: 4.5**

CONCLUSIONS

Full-scale field tests successfully characterized wake dilution of solid wastes discharged from the frigate, USS *Vandergrift*. Independent measurements of pulped paper and of dye made simultaneously at multiple depths and at variable distances behind the frigate were sufficient to define the average and minimum dilution levels throughout the wake. By the end of wake mixing for the 8-kt case, or at about 15 ship-lengths, measured pulp dilution values reached $3.6 \cdot 10^5$ while comparable model dilution values were $4.4 \cdot 10^5$, a difference of about 20%. These values represent average dilution levels in the wake that would be present within 8 mins after discharge. The comparable average dilution measured and modeled for the liquid phase of the discharge is $3.9 \cdot 10^5$ and $3.4 \cdot 10^5$, respectively, a difference of about 15%. Measured and modeled minimum dilution levels for these same conditions would be $7.3 \cdot 10^4$ and $8.7 \cdot 10^4$, respectively. These dilution levels would double for a frigate traveling at 15 kts.

The full-scale field tests were also successful in validating TBWAKE model predictions. Though differences of nearly a factor of 2 were found between model predictions and pulp concentrations measured within 5 ship-lengths of the frigate, the differences were typically less than 20 % at the end of wake mixing, about 15 ship-lengths. The excellent agreement between model and field results suggests that TBWAKE can be used successfully to predict the short-term fate of solid wastes discharged from ships under a variety of conditions. The concentration estimates provided by the model are critical to determine the potential ecological impacts of solid waste discharges to organisms in the water column. Given a ship speed of 8 kts and a standard operational discharge rate of 45 $kg \cdot hr^{-1}$, which represents a starting pulp concentration of 3.9 $g \cdot L^{-1}$, the model predicts an average concentration of pulped material of 0.009 $mg \cdot L^{-1}$. The maximum model concentration estimate for these conditions is 0.048 $mg \cdot L^{-1}$.

REFERENCES

Csanady, G.T. 1981. *An Analysis of Dumpsite Diffusion Experiments*: In Ocean Dumping of Industrial Wastes. Eds. B.H. Ketchum, D.R. Kester, Plenum Press, New York and London, pp. 129.

Hyman, M., Kamman, J., Smith, R. and Nguyen, T.C. (1987) *Bubble Transport In Ship Wakes With Application To Wake Modification*. Naval Coastal System Center Technical Memorandum, June.

Hyman, M.C. (1990) *Numerical Simulation Of The Hydrodynamic Wake Of A Surface Ship*. Naval Coastal System Center Technical Note 544-90, Apr.

Hyman, M.C. (1994) *Modeling Ship Microbubble Wakes*. Coastal Systems Station Technical Report, CSS/TR-94/39, Aug.

Okubo, A. 1971. *Oceanic Diffusion Diagrams*. Deep-Sea Research, V18, pp. 789.

Nguyen, T.C. and Hyman M.C. (1988) *Simulation Of Surface Ship Wakes Using A K-Epsilon Turbulence Model*. Naval Coastal System Center Technical Note 940-88, Nov.

Nguyen, T.C. and Hyman M.C. (1988) *Free Shear Flow Simulations With An Algebraic Stress Model*. Naval Coastal System Center Technical Note 928-88, July.

Smith, R.W. and Hyman, M.C. (1987) *Convective-Diffusive Bubble Transport In Ship Wakes*. Naval Coastal System Center Technical Note 857-87, Feb.

5.2 FAR FIELD DISPERSION OF PAPER PARTICULATES FROM SURFACE VESSEL DISCHARGES IN MARGINAL SEAS, PART II

by Scott A. Jenkins, Ph.D. and Joseph Wasyl

INTRODUCTION

This study effort performs numerical dilution modeling of paper particulate discharges in the far field of an aircraft carrier wake. These dilution simulations account for ambient advection and mixing effects at a sufficiently large distance downstream from the vessel that residual mixing from the wake turbulence was assumed to be negligible. The ambient advection and mixing effects are associated with: 1) the action of wind stress throughout the depths of the mixed layer; 2) surface wave boundary layers due to sea and swell conditions; 3) interfacial shear from current variations across the pycnocline; 4) hindered settling from density variations across the pycnocline; and 5) bottom current boundary layers associated with sea floor roughness. The far field advection-mixing boundary value problem is specified for characteristic ambient conditions for: 1) the central Baltic Sea in winter; 2) the south central Black Sea; 3) the Caribbean Sea in winter between Barbados and Topango; 4) the western Mediterranean Sea in fall; 5) the southern portions of the North Sea in summer; 6) the northern Persian Gulf; 7) the northern Red Sea-, and 8) the southern Red Sea. The particle distributions used to initialize the ambient advection-mixing code (SEDXPORT) were provided by the far field cross-wake data plane from the wake code, TBWAKE, at a distance of 3061 m behind the aircraft carrier.

The SEDXPORT code used to calculate the far field particle dilution has evolved from a sediment transport model originally developed for non-interacting spherical particles in a field of gravity waves (Jenkins and Inman, 1985). It was subsequently expanded to include dispersion by both currents and waves, and was adapted to solve problems of sewage dispersion for the State of California Water Resources Control Board (Jenkins et al., 1989). The model was further refined to include cohesive particle dynamics in problems of scour and erosion of muddy seabeds with bedforms (Jenkins and Wasyl, 1990), and hindered settling dynamics due to particle to-particle stress transfer in high concentration suspensions (Aijaz and Jenkins, 1994). Recently, the model has been expanded to include vertical stratification of water column due to river plumes and mixed layer dynamics, calculating features of hindered settling layers at the pycnocline interface and bottom turbid layers. In this most recent version, the model has been integrated into the Navy's Coastal Water Clarity Model (CWC) and the Littoral Remote Sensing Simulator (LRSS) (see Hammond et al., 1995). The SEDXPORT code has been validated for relatively small (less than 30 microns) optically active particles in mid-to-inner shelf waters (see Hammond et al., 1995, and Schoonmaker et al., 1994). Validation of the SEDXPORT code was shown by three independent methods: 1) direct measurement of particle numbers and particle size distributions by means of a laser particle sizer, 2) measurements of water column optical properties, and 3) comparison of computed particle dispersion patterns with LANDSAT imagery. The integrated tandem of TBWAKE (near field) and SEDXPORT (far field) has been partially validated in tow tank studies and in San Diego Bay on prototype scales (see Hyman et al., 1995).

The SEDXPORT code is a time-stepped finite element model that solves the advection diffusion equations over a fully configurable three-dimensional grid. The vertical dimension is treated as a two-layer ocean, with a homogeneous surface mixed layer and a homogeneous bottom layer separated by a pycnocline interface. The code accepts any arbitrary density and velocity contrast between the mixed layer and bottom layer that satisfies the Richardson number stability criteria and composite Froude

number condition of hydraulic state. The code does not time split advection and diffusion calculations, and will compute additional advective field effects arising from spatial gradients in eddy diffusivity, i.e., the so-called "gradient eddy diffusivity velocities" after Armi, 1979. Eddy mass diffusivities are calculated from momentum diffusivities by means of a series of Peclet number corrections based upon particle size and mass and upon the mixing source. Peclet number corrections for the surface and bottom boundary layers are derived from the work of Nielsen, 1979; Jensen and Carlson, 1976; and Jenkins and Wasyl, 1990. Peclet number correction for the wind-induced mixed layer diffusivities are calculated from algorithms developed by Martin and Meiburg, 1994, while Peclet number corrections to the interfacial shear at the pycnocline are derived from Lazaro and Lasheras,1992a and 1992b. The momentum diffusivities to which these Peclet number corrections are applied are due to Thorade (1914), Schmidt (1917), Durst (1924), and Newman (1952) for the wind-induced mixed layer turbulence and to List et al. (1990) for the current-induced turbulence.

GRIDDING

In the far field, the ship wake is treated as an infinite line source of particles. Therefore, the ambient advection-mixing problem was treated as two-dimensional in the cross-wake plane. The cross wake data plane was located 3061 m downstream from the vessel at time, t=0, in the far field advection-mixing problem.

Shallow Seas. For the shallow seas (Baltic, northern Persian Gulf, southern Red Sea, and North Sea), SEDXPORT was gridded in a YZ-computational domain with 1.0 meter depth increments (Zdimension) and 1.53061 meter horizontal increments in the cross-wake dimension, (Ydimension). This allowed the cross-wake data plane of the initial particle distribution from the TBWAKE code to be nested inside the far field grid using compatible grid cell dimensions. The TBWAKE YZ-data plane at 3061 m downstream from the vessel consisted of 99 grid cells in the cross-wake dimension and 41 grid cells in the in the vertical dimension. It was centered inside the SEDXPORT grid with the sea surface at Z=0. The remaining portions of the SEDXPORT grid not occupied by the TBWAKE grid were initialized with zero particles at time. t=0. The SEDXPORT YZ-computational grid plane consisted of the following array sizes for these shallow sea cases:

- 200 x 200 central Baltic Sea
- 200 x 50 northern Persian Gulf
- 200 x 180 northern Red Sea
- 200 x 50 southern North Sea

The thickness of the YZ grid plane in the along-wake dimension is Δ=1.0 m.

Deep Seas. For the deep water marginal seas (Black Sea, Caribbean, Mediterranean, and northern Red Sea), the original grid cell dimension from TBWAKE could not be retained. The computations with the large arrays resulting from these small grid cells could not be accommodated by the available RAM and CPU time on the SUN SPARK-IO used for this work. Consequently, the cross-wake data plane input to SEDXPORT from TBWAKE was modified by merging grid cells in ensembles of 5 x 5 to create aggregate grid cells with dimensions in the far field plane of A Z = 5 m along the depth axis and AY = 7.65305 m along the cross-wake axis. The far field YZ-computational grid plane using these coarse grid cell dimensions consisted of the following array sizes for these deep sea cases:

- 440 x 400 south central Black Sea
- 440 x 440 Caribbean Sea
- 300 x 300 western Mediterranean Sea
- 300 x 200 northern Red Sea

The thickness of the YZ grid plane in the along-wake dimension is Δ=1.0 m.

PARTICULATE PROPERTIES AND INITIALIZATION

The particulate discharge into the wake of the aircraft carrier results from the activity of three large pulpers and one small pulper, each discharging a slurry of sea water and paper. Each large pulper discharges 500 lbs of paper particulate per hour and 180 gallons of seawater per minute. The small pulper discharges 100 lbs of paper particulate per hour and 50 gallons of seawater per minute. The combined action of these pulpers produces a discharge concentration ("end of the pipe") of 5420 grams of paper particulate per cubic meter of seawater. The specific gravity of the individual paper particles within this slurry is 1.54.

The pulping action produces a mixture of paper particles of varying size. For the purposes of these calculations, the particle size distribution was partitioned into nine particle size bins ranging in diameter from 0-6000 microns. The relative abundance of number of particles in each of these size bins throughout the far field initial data plane is plotted in Figure 5.2-1 and tabulated in Table 5.2-1. The distribution of particle mass among the nine size bins is plotted in Figure 5.5-2 and tabulated in Table 5.2-1. These particle numbers and mass that have accumulated in the far field initial data plane are based upon a vessel speed of 20 knots.

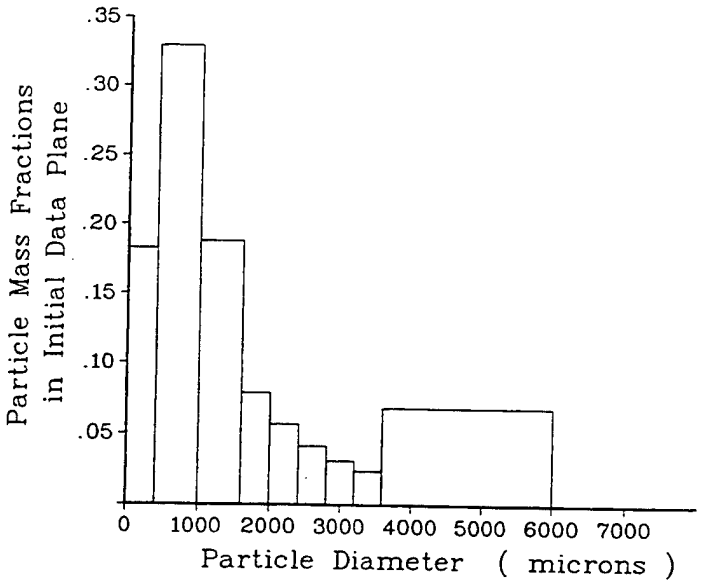

Figure 5.2-1. Size distribution of paper particulate discharge based upon fraction of the total mass distributed among 9 size bins.

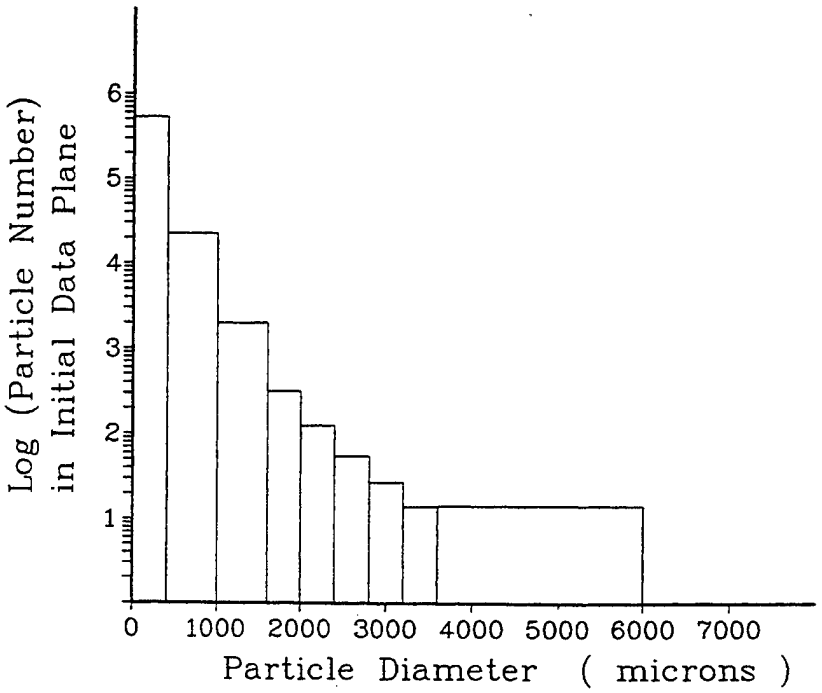

Figure 5.2-2. Size distribution of paper particulate discharge based upon particle numbers in each of 9 size bins.

Table 5.2-1. Particle size in the far field initial data plane at 20 knots.

Bin #	Bin Radius Interval (μ)	Bin Mean Diameter (μ)	# of Particles	Mass (grams)	Mass Fraction
1	0 - 200	200	533,029.312	3.436688	0.182797
2	201-500	700	22,401.914	6.192676	0.329388
3	501-800	1300	1,997.856	3.537475	0.188158
4	801-1000	1800	315.015	1.4806345	0.0787549
5	1001-1200	2200	123.702	1.0615584	0.056464
6	1201-1400	2600	54.883	0.7774223	0.041351
7	1401-1600	3000	26.848	0.5842178	0.0310745
8	1601-1800	3400	14.112	0.447017	0.023776
9	1801-3000	4800	14.393	1.282845	0.0682344

TOTAL MASS = 18.8005339 grams

Inspection of Table 5.2-1 reveals that the smallest size bin having a mean diameter of 200 microns contains the predominant number of particles but only makes up 18.27% of the mass. The second size bin having a mean diameter of 700 microns contains the most mass; and, the first three size bins, spanning a range of mean diameter from 200 microns to 1300 microns, account for 70% of the total mass of the discharged slurry. The total mass of particles of all sizes in the far field initial data plane (3,061 m

downstream from the vessel) is 18.8 grams. There are a relatively small number of large particles that account for less than 10% of the total mass.

Time step lengths used in the mixing-advection computations varied depending upon the size of particulates and the grid cell dimensions. SEDXPORT computes advection-mixing dynamics independently for each of the size fractions, which make up the particulate distribution, because each size fraction has a different Peclet number and corresponding diffusivity. Typically, time-step lengths would also be controlled by the mean currents; but because no information is available on the spatial structure of the current field for the particular sites nor the orientation of the ship track relative to the currents, the currents are assumed to be normal to the computational plane, i.e., parallel to the axis of the wake. Similarly, the wave propagation is also assumed to be parallel to the ship track. Consequently, particle advection in the solution plane is exclusively due to settling and the only dynamic influence of the currents is to enhance diffusivities by interfacial shear at the pycnocline or by current boundary layer turbulence at the bottom. This assumption gives a worst-case scenario with respect to particle dilution, dispersion, and residence time.

The particle size-dependent settling velocities are plotted in Figure 5.2-3 and tabulated together with time-step lengths in Table 5.2-2.

Table 5.2-2. Particle size dependent dynamic parameters.

Mean Particle Diameter (microns)	Settling Velocity (cm/sec)	Shallow Sea Time Step Length (sec)	Deep Sea Time Step Length (sec)
200	0.07765961	4,108	20,538
700	0.61752760	517	2,583
1,300	1.3893090	230	1,148
1,800	1.8788190	170	850
2,200	2.1628680	147	737
2,600	2.3795130	134	670
3,000	2.5517610	125	625
3,400	2.6914170	119	593
4,800	2.9686930	107	537

The settling velocity curve plotted in Figure 5.2-3 exhibits features similar to that for natural sediment, with a viscous regime at small particle diameters where the settling velocity increases as the square of the particle diameter, transitioning to an inertial regime at large particle diameters where the settling velocity grows as the 1/2 power of the particle diameter. The time step lengths indicated by Table 5.2-2 ensure that the particles move only a few grid cells (less than four) in a time-step to maintain numerical stability of the resulting solutions. Because the larger particles advect vertically faster due to gravity, they require shorter time-step intervals.

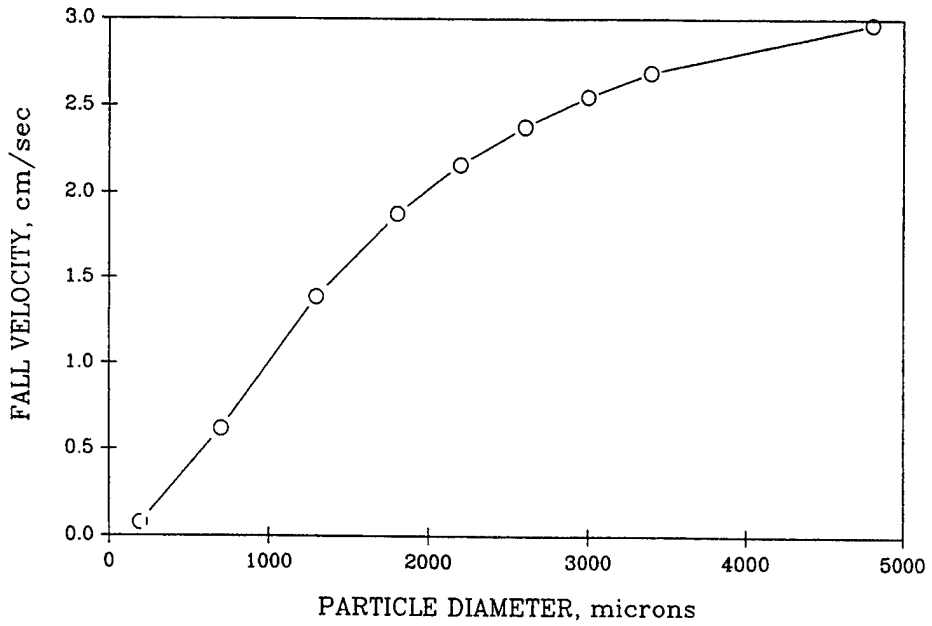

Figure 5.2-3. Settling velocity of paper particulate based upon laboratory observations (NRaD).

ENVIRONMENTAL PROPERTIES AND INITIALIZATION

The environmental conditions and forcing functions appropriate for the Baltic, Black, Caribbean, North, Mediterranean, and Red Sea as well as for the Persian Gulf were specified from characteristic "climate atlas" statistics as provided by SSC San Diego. SEDXPORT boundary conditions and forcing function inputs for the shallow sea cases (depth less than 1000 m) as derived from these climate atlas statistics are shown in Table 5.2-3 below.

Table 5.2-3. Boundary conditions and input forcing for shallow sea cases.

	Central Baltic (WINTER)	Northern Persian Gulf	Southern Red Sea	Southern North Sea
Depth	200 m	50 m	180 m	50 m
Swell Height	0 m	0.6 m	0.6 m	0 m
Swell Period	0 sec	6.0 sec	6.0 sec	0 sec
Wind Wave Height	2.0 m	0.6 m	1.0 m	0.5 m
Wind Wave Period	6.0 sec	6.0 sec	6.0 sec	6.0 sec
Winds	9.0 m/sec	3.0 m/sec	5.0 m/sec	5.0 m/sec
Mixed Layer Depth	50 m	50 m	180 m	50 m
Mixed Layer Density	6.0 sigma t	29.35 sigma t	27.1 sigma t	24.6 sigma t
Bottom Layer Density	12.0 sigma t	N/A	N/A	24.6 sigma t
Mixed Layer Current	0 cm/sec	30 cm/sec	24.5 cm/sec	10 cm/sec
Bottom Layer Current	0 cm/sec	N/A	N/A	0 cm/sec
Bottom Roughness	2.0 cm	16.0 cm	14.0 cm	10.0 cm

The corresponding boundary conditions and forcing function inputs for the deep sea cases (depth 1000 m or greater) are given in Table 5.2-4.

Table 5.2-4. Boundary conditions and input forcing for deep sea cases.

	South Central Black Sea	Caribbean (WINTER)	Western Mediterranean (FALL)	Northern Red Sea
Depth	2000 m	2200 m	1500 m	1000 m
Swell Height	0.3 m	0 m	1.5 m	0.6 m
Swell Period	6.0 sec	0 sec	8.0 sec	6.0 sec
Wind Wave Height	0.6 m	1.5 m	2.0 m	1.0 m
Wind Wave Period	6.0 sec	6.0 sec	6.0 sec	6.0 sec
Winds	5.0 m/sec	10 m/sec	7.0 m/sec	5.0 m/sec
Mixed Layer Depth	100 m	200 m	50 m	180 m
Mixed Layer Density	15.0 sigma t	24.0 sigma t	27.0 sigma t	27.1 sigma t
Bottom Layer Density	17.0 sigma t	27.5 sigma t	28.8 sigma t	27.3 sigma t
Mixed Layer Current	29 cm/sec	50 cm/sec	25 cm/sec	8.0 cm/sec
Bottom Layer Current	14.5 cm/sec	10 cm/sec	10 cm/sec	48.5 cm/sec
Bottom Roughness	12.5 cm	11.0 m	12.0 cm	16.5 cm

For all cases shown in Table 5.2-3 and 5.2-4, no specific bathymetry was evaluated for effects on mean advection or current boundary layers. Thus, it was not possible to resolve horizontal gradients in eddy diffusivity. The absence of such gradients ensures that the two-dimensional YZ computational plane remains adequate for representation of the problem. The bottom was treated in the following dispersion and dilution simulations as a flat-plane boundary with hydraulic roughness according to the characteristic bed form elevations given by the last row in Table 5.2-3 and 5.2-4.

RESULTS

The water column dispersion, dilution and bottom accumulation computations preformed on the eight marginal sea cases listed in the previous section resulted in approximately 250 separate graphics that are contained in the appendices of this report (not included in this Addendum). The appendices are arranged according to:

APPENDIX I - Central Baltic (Winter)
APPENDIX 2 - Southern Central Black Sea
APPENDIX 3 - Caribbean (Winter)
APPENDIX 4 - Western Mediterranean (Fall)
APPENDIX 5 - Southern North Sea
APPENDIX 6 - Northern Persian Gulf
APPENDIX 7 - Northern Red Sea
APPENDIX 8 - Southern Red Sea

These appendices contain at least six water column dispersion plots showing contours of particle number concentrations in the cross-wake solution plane for each of three separate particle size bins spanning the particles size distribution. The three size bins represented in these dispersion plots are 200, 1300, and 4800 microns. Appendix 4 for the Western Mediterranean gives dispersion plots for all nine-size bins. For any given size bin, the six dispersion plots include the t = 0 distribution in the wake at the surface, and five other cases which sequentially track the progress of that size bin as it mixes and settles to the seabed. In addition, the appendices contain: 1) a vertical profile of the maximum and mean particle number concentrations of each size bin remaining in the water column at the end of the simulation series; 2) plots of the particle accumulations on the seabed per square meter for each size bin along a cross-wake transect; and 3) plots of the time histories of minimum and average dilutions throughout the dispersion simulation of each size bin. These results have been summarized in Table 5.2-5 for the northern Persian Gulf and southern North Sea; in Table 5.2-6 for the central Baltic and southern Red Seas; in Table 5.2-7 for the south central Black Sea and the Caribbean Sea; in Table 5.2-8 for the northern Red Sea and three characteristic size bins of the western Mediterranean; and in Table 5.2-9 for the remaining six size bins of the western Mediterranean Sea. In these tables the residence time refers to the time required for the center of mass of the dispersion pattern of a particular size bin to reach the sea bed and for the residual mean particle concentration in the water column to vary by less than 1% from the preceding time step. Because of bottom resuspension arising form the threshold of motion algorithms in SEDXPORT, there is typically a small residual suspension of particles remaining near the seabed at the end of each simulation sequence. The end time of the dispersion sequences in the appendices and the residence times in Tables 5.2-5 to 5.2-9 are generally the same.

Because all nine size bins were studied in the case of the western Mediterranean in fall, it was possible to compute a dilution time history of the total particulate discharge. These time histories for both minimum and average dilution are shown in Figure 5.2-4 during the first 200 hours and in Figure 5.2-5 for the full residence time. Comparison of these time histories for the dilution of total discharge with the dilution

time histories for the individual size bins in APPENDIX 4 reveals a number of qualitatively similar features. Minimum dilution at 3,061 m downstream from the vessel begins on the surface in the far field wake at 98,899 to one. There is subsequently a rapid increase in minimum dilution as particles settle through the mixed layer. This rapid initial dilution is aided by both wind-induced mixing and initially large concentration gradients. As the particulate plume "pancakes" on the pycnocline due to hindered settling (about 8 to 12 hours into the simulation) there is a marked slowing in the initial dilution rates. Once the gravity forces on the plume manage to push it through the hindered settling region in the neighborhood of the pycnocline, the dilution rate again increases until the concentration gradients are sufficiently diminished by mixing in the bottom layer. There after, the dilution rate remains relatively slow for the remainder of the residence time. The final minimum dilution achieved at the end of the residence time in the water column is found to be 421,113,358 to one. The average dilution of the total discharge varies from 882,735 to one in the far field wake at the surface to 1,206,493,054 to one at the end of the water column residence time near the seabed. The greatest amount of particle dilution was found in the Caribbean (see APPENDIX 3). Here the minimum dilution near the seabed reached 7,218,795,969 to one while the average dilution was as high as 12,367,620,000 to one. The worst-case scenario was the northern Persian Gulf where the minimum dilution reached only 1,251,968 to one and the average dilution was only 9,851,617 to one near the seabed.

Inspection of the dispersion plots in Appendices 1 or 5 reveals certain features in the initial far field particle distributions that are due to the nature of the ship discharges. All particle size fractions are released from separate port and starboard discharges which appear in the initial distributions as four distinct "blobs" two on the port side and two on the starboard side of the wake centerline. In all initial far field distributions, the port side blobs have greater particle abundance than the starboard side blobs. It is interesting how the 200 microns size particles begin merging of the port and starboard blobs as they pass through the hindered settling regime at the pycnocline depths. Below the pycnocline, the port and starboard blobs tend to become fully merged, with an asymmetric center of mass displaced to the port side of the wake. The degree of merging is greater for the deeper seas. The larger size particles, which fall faster also, have smaller diffusivities. Consequently, they are less well-mixed after crossing the pycnocline and the dispersion patterns continue to show distinct port and starboard blobs throughout the residence time in the water column, particularly for the shallow seas.

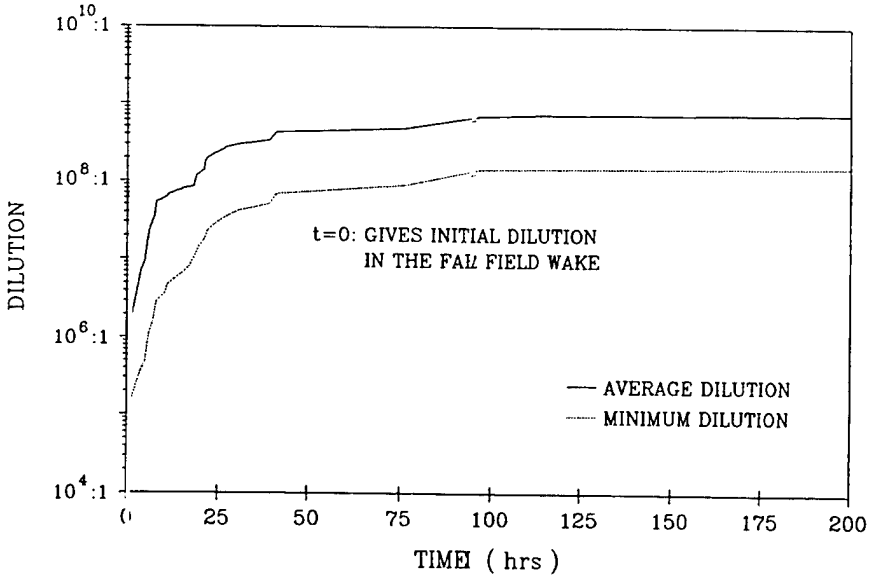

Figure 5.2-4. Dilution history of total discharge during the first 200 hours, western Mediterranean Sea (fall).

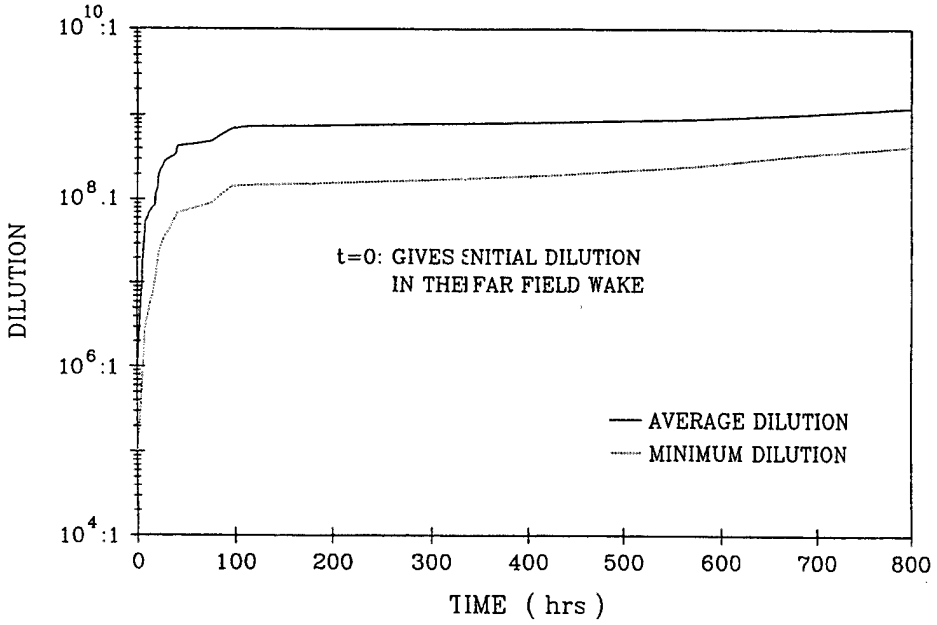

Figure 5.2-5. Dilution history of total discharge over complete residence time, western Mediterranean Sea (fall).

Table 5.2-5. Summary of residence time, dilution and seabed particle accumulation, northern Persian Gulf and southern North Sea.

	Northern Persian Gulf			Southern North Sea		
Particle size (Microns)	200	1300	4800	200	1300	4800
Residence Time	34.2 hr	91.8 min	44.8 min	34.2 hr	95.6 min	44.8 min
Minimum Dilution (Water Column)	$1.25x10^{6}$	$1.12x10^{7}$	$6.67x10^{5}$	$2.00x10^{6}$	$1.05x10^{7}$	$9.31x10^{5}$
Average Dilution (Water Column)	$9.85x10^{6}$	$9.70x10^{7}$	$5.38x10^{6}$	$1.79x10^{7}$	$7.23x10^{7}$	$8.61x10^{6}$
Maximum Seabed # Density (#'s/m ^{2})	12,871	69.18	0.50	9,951	58.42	0.51

Table 5.2-6. Summary of residence time, dilution and seabed particle accumulation, northern central Baltic Sea and southern Red Sea.

	Central Baltic Sea			Southern Red Sea		
Particle size (Microns)	200	1300	4800	200	1300	4800
Residence Time	128.9 hr	6.38 hr	2.69 hr	108.4 hr	4.97 hr	2.18 hr
Minimum Dilution (Water Column)	$1.71x10^{7}$	$3.86x10^{6}$	$1.66x10^{7}$	$9.50x10^{6}$	$3.25x10^{6}$	$1.83x10^{6}$
Average Dilution (Water Column)	$4.42x10^{7}$	$1.91x10^{7}$	$7.49x10^{7}$	$3.53x10^{7}$	$1.76x10^{7}$	$1.11x10^{7}$
Maximum Seabed # Density (#'s/m^{2})	1,970	29.60	0.24	3,902	36.78	0.28

Table 5.2-7. Summary of residence time, dilution and seabed particle accumulation, northern south central Black Sea and Caribbean Sea.

	S. Central Black Sea			Caribbean Sea		
Particle size (Microns)	200	1300	4800	200	1300	4800
Residence Time	912.8 hr	49.42 hr	23.13 hr	1,027 hr	55.80 hr	25.37 hr
Minimum Dilution (Water Column)	$9.98x10^8$	$8.05x10^7$	$5.05x10^7$	$7.22x10^9$	$2.58x10^8$	$1.23x10^8$
Average Dilution (Water Column)	$2.27x10^9$	$6.15x10^8$	$4.98x10^8$	$1.23x10^{10}$	$1.12x10^9$	$7.38x10^8$
Maximum Seabed # Density (#'s/m^2)	20.50	0.49	0.0053	4.57	0.23	0.0025

Table 5.2-8. Summary of residence time, dilution and seabed particle accumulation, northern Red Sea and western Mediterranean Sea.

	Northern Red Sea			Western Mediterranean		
Particle size (Microns)	200	1300	4800	200	1300	4800
Residence Time	570.5 hr	29.65 hr	13.43 hr	799 hr	41.45 hr	18.66 hr
Minimum Dilution (Water Column)	$4.66x10^8$	$7.15x10^7$	$9.07x10^7$	$1.52x10^9$	$1.45x10^8$	$6.87x10^7$
Average Dilution (Water Column)	$1.39x10^9$	$6.47x10^8$	$9.82x10^8$	$2.85x10^9$	$7.71x10^8$	$4.97x10^8$
Maximum Seabed # Density (#'s/m^2)	51.16	1.29	0.012	19.33	0.62	0.007

Table 5.2-9. Summary of residence time, dilution and seabed particle accumulation, western Mediterranean Sea.

	Western Mediterranean Sea					
Particle size (Microns)	700	1800	2200	2600	3000	3400
Residence Time	96.85 hr	30.65 hr	26.63 hr	24.21 hr	22.22 hr	20.58 hr
Minimum Dilution (Water Column)	$2.56x10^8$	$9.85x10^7$	$1.26x10^8$	$1.52x10^8$	$1.28x10^8$	$8.63x10^7$
Average Dilution (Water Column)	$1.02x10^9$	$6.02x10^8$	$7.73x10^8$	$9.52x10^8$	$7.83x10^8$	$5.87x10^8$
Maximum Seabed # Density (#'s/m^2)	4.32	0.121	0.049	0.023	0.011	0.0062

CONCLUSIONS

1) Dilution and residence time decrease with increasing particle size for any marginal sea which is vertically stratified. The particle blobs are spread laterally across the wake as they pass through the pycnocline, thereby promoting their subsequent dilution below the pycnocline. Only the North Sea and Persian Gulf which are essentially homogenous and well-mixed showed slightly higher dilutions for the 1300 micron particles than for the 200 micron sized particles. This was an artifact of the threshold of motion criteria adapted to the paper particulate from natural sediment, which made the 1300 micron sized particles slightly more susceptible to the bottom resuspension and secondary dilution. The true threshold Shield's number of the paper particulate on the seabed is not known, and the curiously large dilution found for the 1300 micron particles in the shallow well-mixed seas may not be real.

2) Larger particles showed more rapid initial dilution because their higher fall velocities spread them vertically across the water column more rapidly than the slower settling small particles.

3) Maximizing depth of water is the leading order factor in promoting maximum dilution of particles in the water column and minimum number densities of particles accumulated on the sea floor. However, deeper water also promotes longer particle residence times in the water column.

4) In shallow seas (North Sea, Persian Gulf, southern Red Sea, and Baltic), wind induced mixing is the next most important factor for promoting dilution and minimizing particle number densities on the seabed.

5) In deep seas (Caribbean , Black Sea, northern Red Sea, and Mediterranean), current-induced mixing exerts a greater effect than wind in promoting dilution and minimizing particle number densities on the seabed. This is due to the fact that in deep seas, a greater fraction of the particle's residence time is spent below the mixed layer, beyond the reach of wind mixing effects.

REFERENCES

Armi, L.A., 1979, *Effects Of Variations In Eddy Diffusivity On Property Distributions In The Oceans, Journal of Marine Res., v. 37, n. 3, pp. 515-530.*

Durst, C.S., *The Relationship Between Current And Wind,* Quart. J. R. Met. Soc., v 50, p.113 (London), 1924.

Jenkins, S.A., and D.L. Inman, *On A Submerged Sphere In A Viscous Fluid Excited By Small Amplitude Motions,* Jour. Fluid Mech., v. 157, pp. 199-224.

Jenkins, S.A., J. A. Nicholas and D.W. Skelly, 1989,*Coupled Physical-Biological Dispersion Model For The Fate Of Suspended Solids In Sewage Discharges Into The Ocean,* SIO Reference Seri s 89-3, 53 pp.

Jenkins, S.A., and J. Wasyl, 1990,*Resuspension Of Estuarial Sediments By Tethered Wings*, Jour. of Coastal Res., v. 6, n. 4, pp. 961-980.

Jenkins, S.A., and S.Aijaz, 1994, *On The Electrokinetics Of The Dynamic Shear Stress In Fluid Mud Suspensions*, Jour. Geophysical Res., v. 99, n. C6, pp. 12,697-12-706.

Jenkins, S.A., and 1. Wasyl, 1994 *Time Stepped Suspended Transport Model For The Dispersion Of Optical Particles In Coastal Waters,* submitted to Office of Naval Research, Code 1153, 84 pp.

Hammond, R.R., Jenkins, S.A., Cleveland, J.S., Talcott, J.C., Heath, A.L., Wasyl, J.,Goosby, S.G., Schmitt, K.F., and Levin, L,A., 1995, *Coastal Water Clarity Modeling* SAIC, Technical Report 01-1349-03-4841-000, 491 pp.

Hyman, M., Rohr, J., Schoonmaker, J., Ratcliffe, T., Chadwick, B., Richter, K., Jenkins, S., and J. Wasyl, 1995, *Mixing In The Wake Of An Aircraft Carrier,* Proc. Oceans 95, p. 1- 15.

Lazaro, B.J., and Lasheras, J.C., 1992a, *Particle Dispersion In A Developing Free Shear Layer, Part 1, Unforced Flow,* J. Fluid Mech. 235, pp. 143-178.

Lazaro, B.J. and Lasheras, J.C., 1992b, *Particle Dispersion In A Developing Free Shear Layer, Part 2, Forced Flow,* J. Fluid Mech. 235, pp. 179-221.

List, E.J., Gartrell, G., and C.D. Winant, 1990, *Diffusion And Dispersion In Coastal Waters, Jour. Hydraulic Eng.,* v. 116, n. 10, pp. 1158-1179.

Martin, J.E., and Meiberg, E., 1994, *The Accumulation And Dispersion Of Heavy Particles In Forced Two-Dimensional Mixing Layers*, 1: *The Fundamental And Subharmonic Cases*, Phys. Fluids, A-6, pp. 1116-1132.

Neumann, G., *Ober Die Kompl E Natur Des Seeganges, Teil 1 And 2*, Deut. Hydrogr. Zeit., v. 5, n. 2/3, pp. 95-110,, n. 5/6, pp. 252-277, 1952.

Nielsen, P., I.A. Svendsen, and C. Staub, *Onshore -Offshore Sediment Movement On A Beach*, In Proceedings Off 16tb International Conference Of Coastal Engirleering, pp. 1475-1492, ASCE, New York, 1978.

Schoonmaker, J.S., R.R. Hammond, A.L. Heath and J.S. Cleveland, 1994, *A Numerical Model For Prediction Of Sub-Littorial* Optical Visibility, SPIE Ocean Optics Xfl, pp. 18.

Thorade, H., *Die Geschwindigkeit Von Triftstromungen And Die Ekman sche Theorie*, 1914, Ann. d. Hydr. u. Mayit. Meteorol., v. 42, p. 379.

6. ANALYSIS: A PERSPECTIVE OF THE FINAL STUDY RESULTS

The analysis presented in TR 1716 was organized into three areas for both the pulped and shredded waste streams: 1) a general discussion of the fate and effects from a typical ship discharge operation; 2) an analysis of the potential effects of hypothetical multiship operational scenarios in each of the Special Areas; and 3) an analysis of basin scale mass loading issues based on historical operational data from specific MARPOL Special Areas. This section reviews the previous analysis, taking into account the final information from the ongoing studies and noting any resulting changes. Much of the previous analysis remains unchanged will not be the focus of this discussion. The new information will include: 1) an update of the fate and effects of the pulped material with regard to degradability, sardine filter-feeding, water column processes (dilution, exposure and effects), and sea floor processes (degradation and sensitive species/habitats); 2) additional data on the transport of shredder bags on the sea floor; 3) an analysis of the remaining Special Areas with regard to operational and basin-wide effects; and 4) an analysis of potential impacts to coral reef systems and threatened and endangered species.

The discharge conditions remain the same in terms of rate, duration, discharge location, area of impact or discharge density (depending on the specific waste stream), and operational and basin-wide scenarios (although three new Special Areas are included). With the exception of microbial degradation and the composition of inorganic components of the pulped material, the waste stream characterization also remains the same. And, other than the long-term (30-day) sardine filter-feeding results, the biological effects analyses also remain the same. The topics discussed below represent the body of new information acquired since the publication of TR 1716, "Environmental Analysis of U.S. Navy Shipboard Solid Waste Discharges: Report of Findings," dated January 1996.

6.1 FATE AND EFFECTS OF THE PULPED WASTE STREAM

Several aspects of the pulped waste stream analysis had follow-on efforts after the original report of findings was published. Although none of the results significantly alter the overall findings, they are discussed below in the interested of completion and thoroughness.

WASTE STREAM CHARACTERISTICS

Chemical Composition of the Inorganic Portion of Paper and Cardboard. In the original report, the discussion on chemical characteristics of the pulped waste stream consisted primarily of the organic components. Subsequently, the inorganic components were analyzed. A qualitative analysis of the inorganic components of the pulped waste stream using a Scanning Electron Microscope (SEM) yielded the following major elements: calcium, chlorine, titanium, silicon, and aluminum. Somewhat smaller amounts of sodium, magnesium, potassium and iron were present, with a trace of sulfur. A quantitative estimate using Inductively Coupled Plasma atomic emission spectroscopy (ICP) showed good agreement with the qualitative results, yielding the following estimates for the major inorganic components as measured in weight percent: calcium; 0.96; titanium, 0.89; aluminum, 0.57; and silicon - 0.34. Calcium would most likely be in the form of calcium carbonate, and non-toxic. Titanium and silicon would probably be in the form of oxides. These percentages are comparable to those found in typical marine sediments (Chester, 1990) and therefore the pulp should pose no ecological risk to benthic organisms. The results here corroborate the original findings that the pulped material is primarily (>95%) composed of organic cellulose.

Degradability. The ongoing microbial degradation work included completing the matrix of degradation rates for a full range of temperature and nutrient regimes; obtaining and analyzing degradation in water from the Arctic, the Sargasso Sea, the Northern Pacific Ocean, the U.S. Shelf, and coastal Georgia; adding the bacterial respiration method for analysis; and conducting longer term (30-day) tests. Q_{10} values for cellulose decomposition were found to be slightly different than previously determined, with an average 1.85 for temperatures between 8°C and 28°C and a higher increase in decomposition rate per given temperature rise between 4°C and 8°C. Taking into account all of the methods used, degradation rates varied from $0.4\%\cdot d^{-1}$ at 28°C to $0.04\%\cdot d^{-1}$ at 4°C (Figure 6.1-1). This corresponds to half-lives of 173 to 1773 days, respectively. Because most of the material will sink to the sea floor in open ocean areas where the temperatures are generally colder and the bacterial communities are less developed, one would expect the degradation rates to be on the longer end of the range.

Additionally, the new results from the sugar analysis indicated that sugars accounted for 98 $\pm$4% of the total dry weight of the organic fraction of the pulp. Thus, with the organic and inorganic analysis, essentially all of the components of the pulped waste stream have been identified.

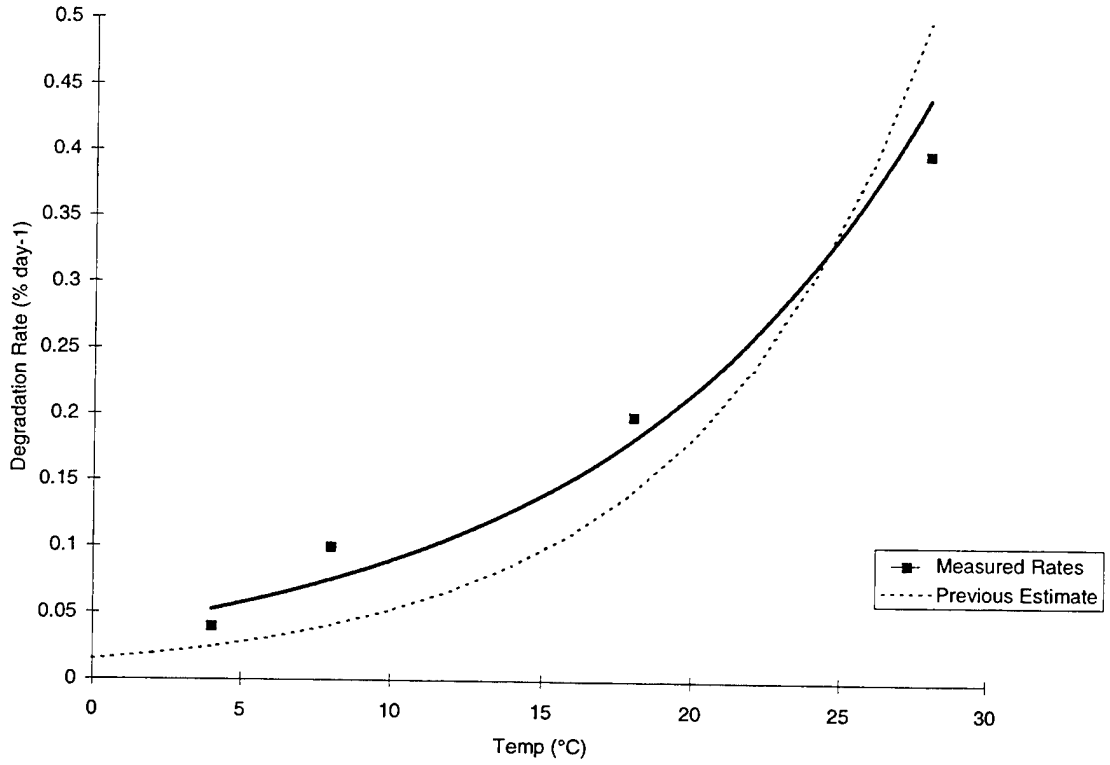

Figure 6.1-1. Degradation rate of pulped paper waste as a function of water temperature. Degradation rates at 4°C, 8°C, 18°C, and 28°C are laboratory measurements on pulped paper. The bold line is an exponential curve fit based on the measured points. The dashed line uses a previously measured point at 28°C and is extrapolated to other temperatures based on an average Q_{10} value reported by Benner et al., 1986.

Biological Effects. The follow-on biological interaction work consisted of a long-term feeding interference study (30 days) using sardines. As in the short-term (8-hour) tests previously done, there were apparent effects, in this case on weight gain and stomach contents. The sardines experienced a weight loss at each of the concentrations (0.01, 0.1 and 1.0 $mg\cdot L^{-1}$) over the 30-day period; experimental constraints prohibited testing at lower concentrations. To assess the impact to sardines in the real world,

the dilution of the pulped material and the exposure duration that sardines may encounter should be taken into account. In the short term, the sardines could experience concentrations in the wake of approximately 0.17 $mg \cdot L^{-1}$. Relative to the 8-hour tests conducted on a range of concentrations from 30 $mg \cdot L^{-1}$ down to 0.01 $mg \cdot L^{-1}$ and the recovery tests, potential feeding interference effects are considered to be sublethal and transient at concentrations of approximately 1 $mg \cdot L^{-1}$ and above. Although during the 30-day test, sardines showed weight loss and stomach clogging at all concentrations tested, the potential effect would most likely be only transient, if experienced at all, due to the rapid dispersion of the pulped material in the wake, the continual dispersion in ambient conditions, and settling of the material to the sea floor. The concentrations the sardines may experience for a significant duration will be below those showing effects in the laboratory experiments (see Water Column Exposure and Effects section).

WATER COLUMN PROCESSES

Initial Dilution. Initial dilution in the wake of a moving ship was considered to be critical to quickly reducing the concentration of the pulp discharge in the receiving environment below levels that have an ecological consequence. Field tests conducted after the original report was produced, successfully characterized wake dilution of solid wastes discharged from a frigate at 8 and 15 kts. The field test results were also successful in validating computer model (TBWAKE) predictions suggesting that the model can be used successfully to predict the short-term fate of solid wastes discharged from a variety of ships under a variety of conditions.

Model predictions, validated with field results, indicated that minimum dilution for a frigate at 8 kts is defined by a dilution/time equation of $D = 346 \cdot x^{0.732}$, where time, (x), is in meters behind the frigate. This corresponds to a minimum dilution of $8.7 \cdot 10^4$ out at 1890 m, or about 8 min after discharge. Given a standard discharge rate of 45 $kg \cdot hr^{-1}$ for a small pulper used aboard frigates, the maximum concentration of pulp expected in the water column at that time would be 0.048 $mg \cdot L^{-1}$. Comparable model simulations for an aircraft carrier moving at 10 kts and discharging at a maximum rate of 678 $kg \cdot hr^{-1}$, considered to be a worst-case scenario with regards to wake loading, predict a maximum concentration of pulp in the water column, 10 min after discharge, of about 0.17 $mg \cdot L^{-1}$.

Ambient Dilution and Transport. Dilution of the pulped material continues after wake mixing has dissipated because of gravitational settling, lateral transport, and ambient mixing. The model SEDXPORT was used to estimate ambient dilution, under conditions commonly found in each Special Area.. SEDXPORT modeling began at roughly 10 min after discharge, using the initial concentration conditions generated by TBWAKE, along with inputs of settling rates (Figure 6.1-2), and common oceanographic conditions found in the literature. The simulations were run out as long as 1000 hours to characterize both pulped waste concentrations in the water column and to estimate the resulting particle density on the sea floor after deposition.

The original report included modeling results only for the Baltic and North Seas. Model simulations for all Special Areas (excluding the Antarctic) for an aircraft carrier discharge, predict ambient dilutions ranging from a minimum of $1.8 \cdot 10^5$ in the shallow Persian Gulf to $1.2 \cdot 10^8$ in the deep Caribbean Sea. These worst-case dilution values correspond to water column residence times for large particles (4800 um) of 25 min to 25 hours (without degradation). Assuming a strarting concentration of 1%, particle concentrations just above the seafloor would range from 0.056 $mg \cdot L^{-1}$ to 0.000081 $mg \cdot L^{-1}$. These results indicate that exposure levels at the seafloor would be reduced below those found in the wake by factors of about 3 to 1000.

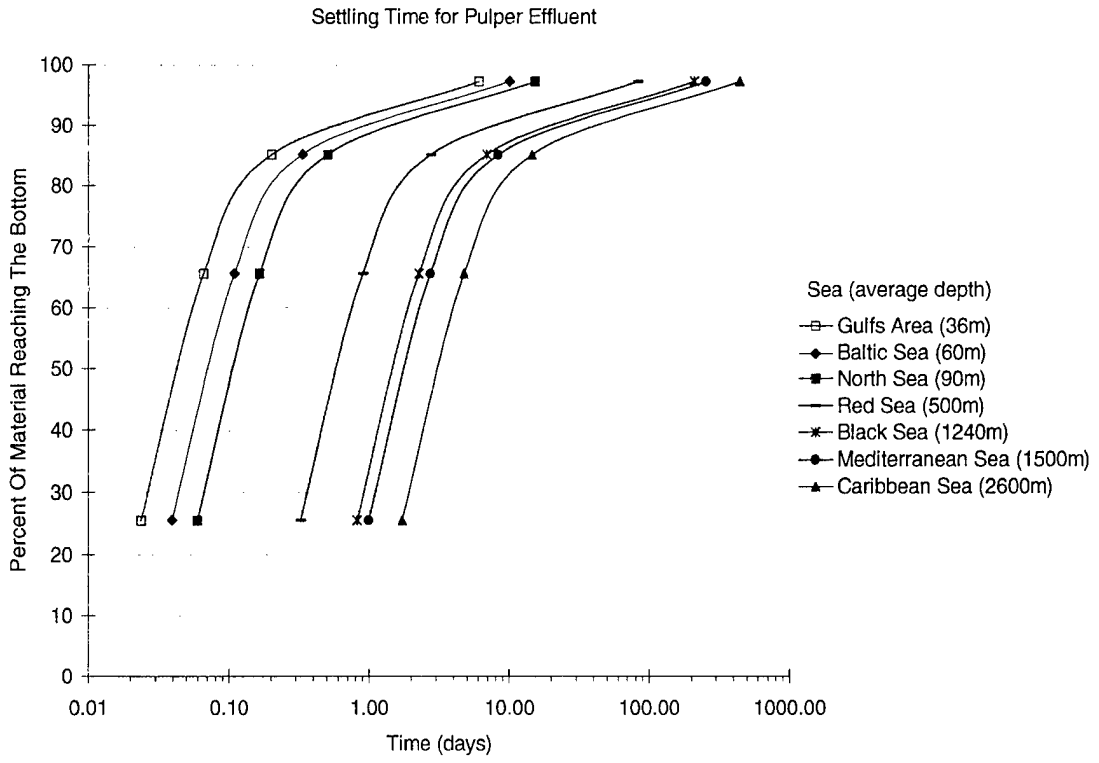

Figure 6.1-2. Settling time of pulper effluent for each of the Special Areas assuming no degradation. Settling times are based on the average depths for the Special Areas. Approximately 85% of the material (by weight) settles rapidly within a time range of less than a day to 10 days. A slower settling fraction, representing about 12% of the material, settles in about 10 to 300 days. The remaining ~3 percent degrades in suspension.

Water Column Fate. Using the current degradation rates estimated in the microbial degradation study, and the first-order kinetics equation discussed in the original report, a new table has been developed showing the estimated fate of a typical 1-day discharge of pulped paper from a CVN class ship in each of the Special Areas (see Table 6.1-1). This table indicates the predictions for pulp remaining in the microlayer, degrading in the water column and settling to the sea floor. As previously done, the temperature regime was simplified to a two or one-layer profile, however, the new Q_{10} value of 1.85 which was derived from measurements for temperatures between 8°C and 28°C was used instead of the previous average of 3.5. The new results indicate no change from the previous results, showing that the rapid settling of the pulped material will limit the exposure and degradation processes in the water column.

Table 6.1-1. Estimated fate of a typical one day discharge of pulped paper from a CVN 68 class ship under a range of conditions representing all MARPOL Special Areas.

Special Area		Caribbean	Mediterranean	North Sea	Baltic Sea	Black Sea	Red Sea	Persian Gulf	Antarctic	Average %
Surface Layer	Depth (m)	100	75	50	40	200	200	20	100	
	Temp (deg C)	28	26	10	10	16	26	20	2	
	Deg Rate %·d^{-1}	0.40	0.37	0.09	0.09	0.15	0.27	0.22	0.04	
Bottom Layer	Depth (m)	2500	1500	n/a	150	1300	500	40	5000	
	Temp (deg C)	4	14	n/a	5	9	22	18	-1.5	
	Deg Rate %·d^{-1}	0.040	0.130	n/a	0.060	0.080	0.260	0.180	0.030	
Mass Fraction	Small (kg)	95	95	95	95	95	95	95	95	
	Med (kg)	381	381	381	381	381	381	381	381	
	Large (kg)	2700	2700	2700	2700	2700	2700	2700	2700	
Settling Rate	Small (m·d^{-1})	0	0	0	0	0	0	0	0	
	Med (m·d^{-1})	6	6	6	6	6	6	6	6	
	Large (m·d^{-1})	864	864	864	864	864	864	864	864	
Wake	Width (m)	90	90	90	90	90	90	90	90	
	Length (km)	130	130	130	130	130	130	130	130	
Microlayer	Thickness (um)	10	10	10	10	10	10	10	10	
	Concentration (mg·L^{-1})	0.50	0.50	0.50	0.50	0.50	0.50	0.50	0.50	
Total Mass		3176	3176	3176	3176	3176	3176	3176	3176	
Microlayer (kg)		0.06	0.06	0.06	0.06	0.06	0.06	0.06	0.06	0.002
Degradation	Surface Layer (kg)	121	113	98	98	115	142	98	98	3.5
	Bottom Layer (kg)	58	107	n/a	6	61	70	5	88	1.8
	Total (kg)	179	220	98	104	176	211	103	186	5.0
Deposition (kg)		2997	2956	3078	3072	3000	2965	3073	2990	95.0

Water Column Exposure and Effects. The water column exposure and effects analysis is basically the same as found in the original report. However, two important additions include the results of the long-term sardine exposure study and the results of the integrated wake and ambient model predictions. The 30-day sardine test showed effects on weight gain for all concentrations tested (1.0, 0.1, and 0.01 $mg \cdot L^{-1}$). However, the potential for impact is dependent upon the exposure levels, concentration and duration, that the sardines may experience. Because of the high dilution in the wake, and subsequent dilution in the ambient environment, a sardine would experience the concentrations found to have an effect only within the first hour after discharge. According to the models which have been validated by field tests, the concentration remaining in the water column 30 days after discharge would be approximately 3 orders of magnitude less than the lowest concentration exhibiting the effect of weight loss on the sardines (approximately 0.000033 $mg \cdot L^{-1}$). A no-effects level was not determined because the experimental limitations did not allow for testing low-enough concentrations. However, in comparing the estimated water column exposure limits with the biological response levels for the pulped paper particles, the low-effects level falls well outside the area of potential exposure (see Figure 6.1-3).

The version of Figure 6.1-3 in the original report was based on initial estimates of exposure and on the response data available at that time. The current graph uses exposure data based on model results for minimum wake dilution of an aircraft carrier at 10 kts and minimum ambient dilution in a moderately deep water scenario as would be found in the western Mediterranean. This dilution line indicates a slowdown occurring near the thermocline at time equal to approximately 0.1 to 1 hour after discharge. The current graph also incorporates the long-term sardine feeding test results. The resultant concentration-time plot is therefore a best estimate of the maximum exposure regime expected in the water column over approximately 40 days. All biological responses measured over that time period fall above the exposure line indicating that the exposure is sufficiently low as to not cause an effect.

The overall analysis of the water column processes are generally unaffected by the new data, with settling, degradation, transport, and biological effects remaining essentially the same as concluded in the original analysis. Approximately 95% of the pulped material is expected to reach the sea floor, with most of the remaining fraction being degraded in the water column (~5%) and only a very small fraction (<0.002%) possibly partitioning to the microlayer. Lateral transport of the material is minimized by its rapid settling. The worst-case peak concentration after discharge into the wake of a moving vessel would be approximately 0.17 $mg \cdot L^{-1}$ which would further disperse in the ambient condition to 0.001 $mg \cdot L^{-1}$ within about 10 hours and 0.0001 $mg \cdot L^{-1}$ within about 4 days. Given the rapid dilution of the material and the expected exposures, no biological effects are expected from the pulped discharge.

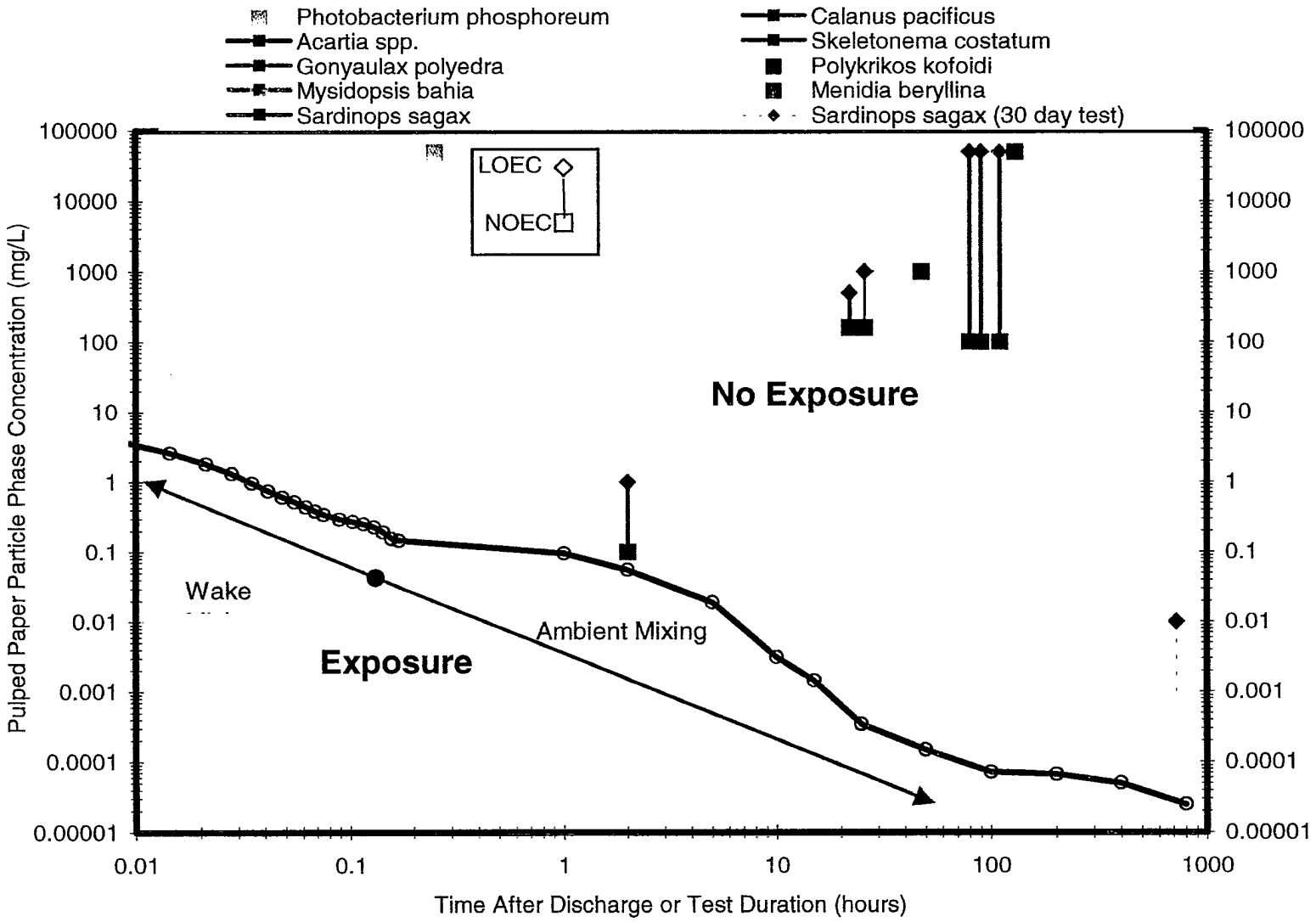

Figure 6.1-3. Estimated water column exposure limits based on model results compared to measured biological response levels for the pulped paper particle phase. A no observable effects level (NOEL) was not determined for the *Sardinops sagax* 30-day test.

SEA FLOOR PROCESSES

Degradation. Although no additional tests were performed on sediment degradation, the rates can be assumed to be controlled by the same factors as for the water column, primarily temperature, along with nutrient and oxygen levels, and bacterial community structure. Taking into account the bottom temperatures of all of the Special Areas, the half-life for the pulped material would be toward the upper values in the range of 173 to 1773 days.

Fate on the Sea Floor. The effects of bioturbation versus degradation or consumption by particle feeders were discussed for the first four Special Areas studied in the original report. Using the same methodology based on the conditions in each Special Area, Figures 6.1-4 and 6.1-5 depict the results for all of the Special Areas. The first figure shows the predicted concentration of pulped material in sediment as a function of time based on estimated rates of vertical mixing, burial, and degradation (Figure 6.1-4), while the second figure presents the fraction of the pulped material remaining in the sediment over time based on estimated removal rates due to biodegradation alone. As in the original analysis, these results suggest that the concentration of the pulp in the sediment for a typical discharge will be controlled initially by bioturbation, with concentrations at day 10 ranging from 20 to 100 $mg \cdot kg^{-1}$. The effects of degradation are not apparent until after approximately 100 to 1000 days, with concentrations reducing to approximately 0.0001 $mg \cdot kg^{-1}$ within a 1000 days or more with the continued action of degradation and bioturbation, as well as some sedimentation. The effect of sedimentation appears to be small since the time scale for sedimentation to cause the same dilution as bioturbation is approximately 30 years as compared to a number of days.

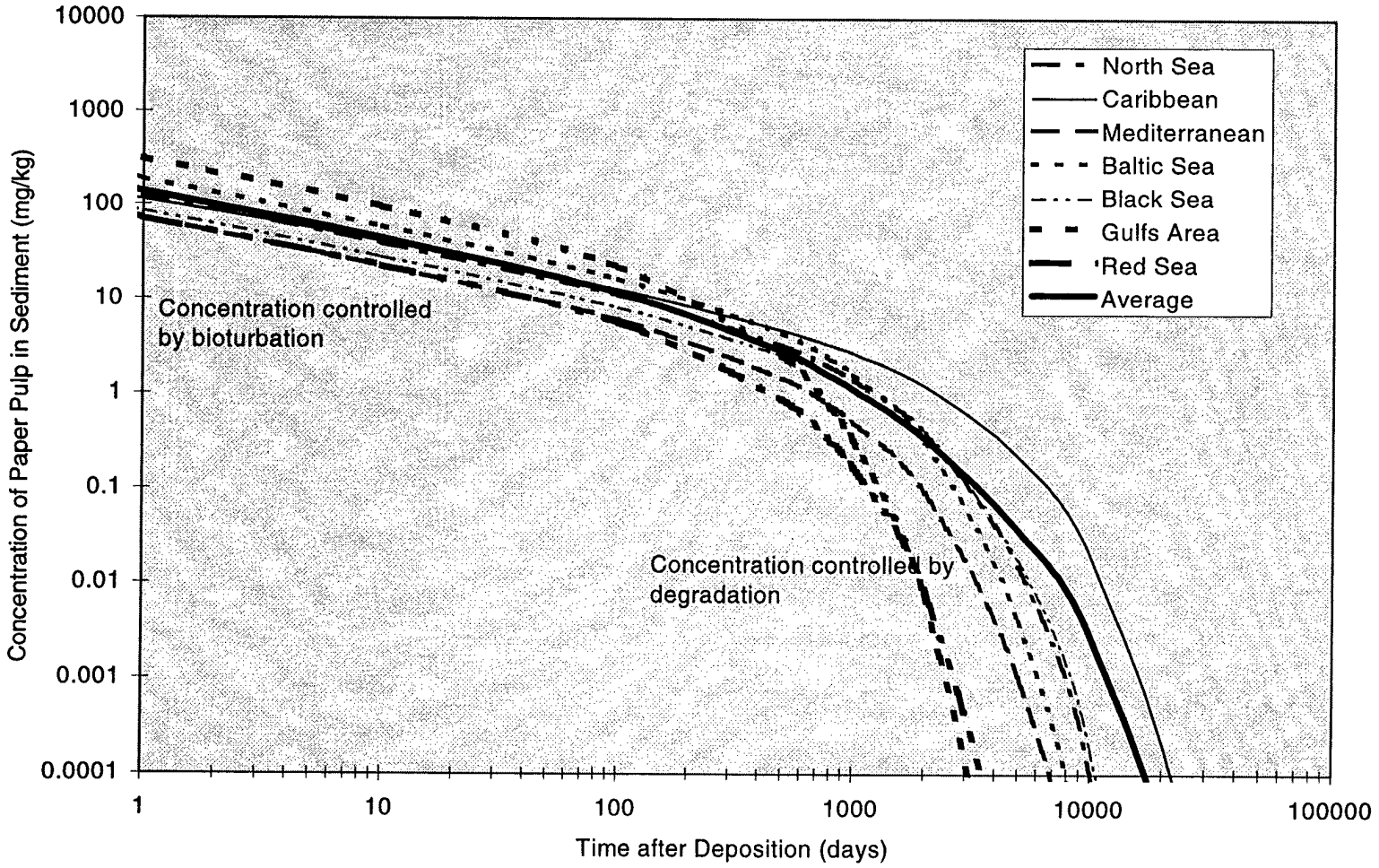

Figure 6.1-4. Predicted concentration of paper pulp in sediment as a function of time based on estimated rates of vertical mixing, burial, and degradation. Resuspension and consumption by particle feeders are neglected.

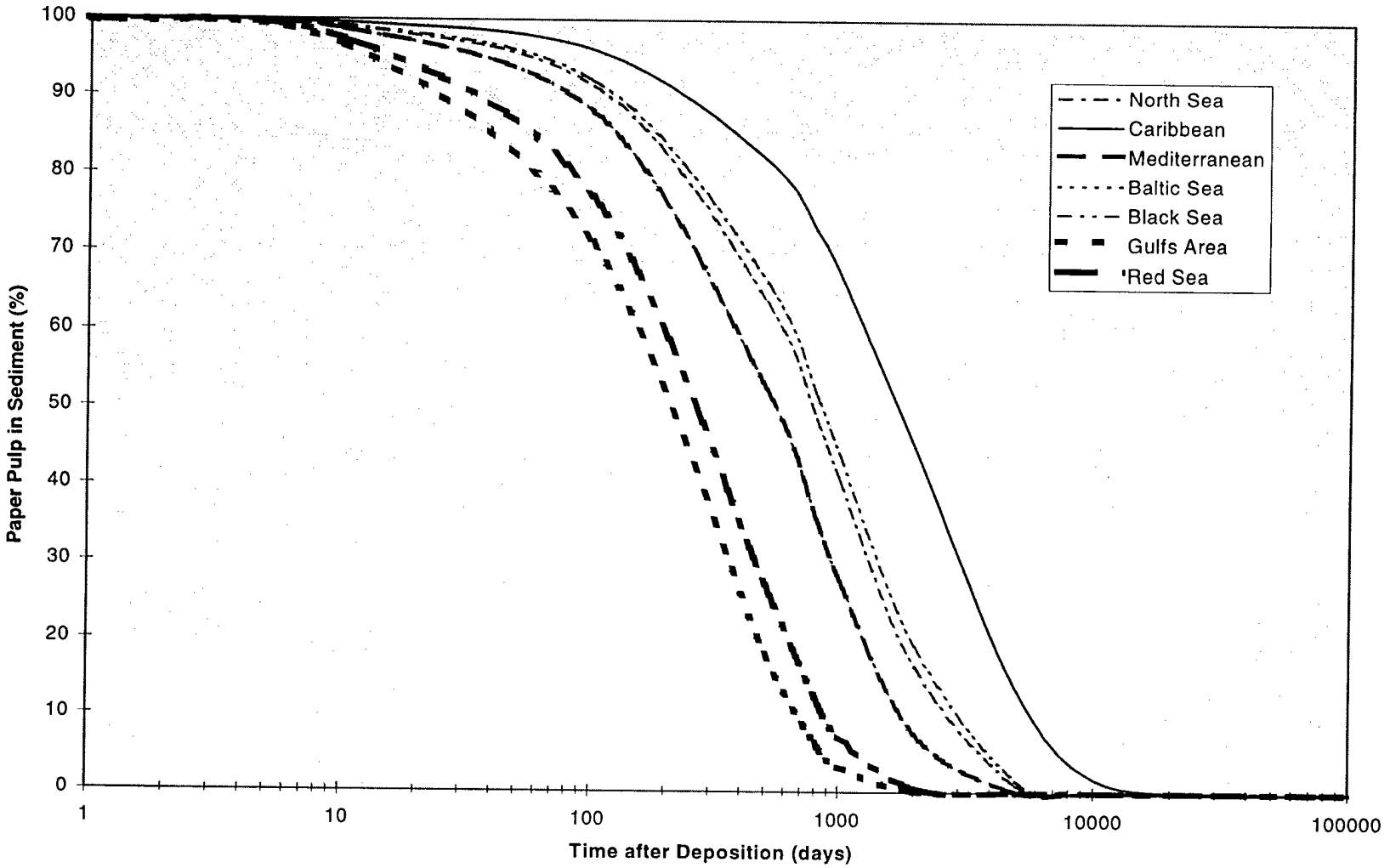

Figure 6.1-5. Fraction of pulped paper remaining in sediment over time based on estimated removal rates due to biodegradation.

Exposure and Effects on the Sea Floor. An analysis of potential impacts to coral reef systems was completed after the original report was published. The analysis included identifying the locations of coral reef systems within Special Areas, determining the extent of Navy operations, and assessing the potential impact to coral reefs from the solid waste discharges. The motivating concern was relative to the pulped material, however, potential impacts from both the pulped and shredded material were addressed. The analysis indicates that the potential effects of pulped paper are minimized by several factors including the high initial dilution of the waste stream, the non-toxic nature of the waste material, and the limited overlap between ship operations and coral reef locations. Estimated maximum suspended particle loads following discharge and long-term sedimentation rates were found to be well below reported background and effects levels for a number of coral reef studies. Similarly, because the majority of the material settles rapidly, estimated reductions in light levels due to localized increases in suspended particle loads were shown to have negligible effects on the light penetration depths. Together, these results indicate the likelihood of significant effects on coral reefs in MARPOL Special Areas from pulper discharges is highly unlikely.

Likewise, potential effects of physical impacts to coral reefs from shredder bags are limited by the rapid settling of shredder bags, the non-toxic nature of the material , and the limited overlap between ship operations and coral reef locations. Maximum lateral transport of shredder bags from the discharge location was shown to be about 350 m, indicating that bags will only be likely to land on coral reefs if the ships are transiting directly above them. As with the pulped waste stream, these results suggest that the likelihood of significant effects on coral reefs in MARPOL Special Areas from shredder discharges is very low.

OPERATIONAL SCENARIOS

Although it has been shown that the single CVN class is the worst-case loading, an operational scenario was developed in order to analyze a potential areal effect. This was done for the Caribbean Region, the Mediterranean Sea, the North Sea, and the Baltic Sea in the original report. Below is a table which presents the results of estimated steady-state exposure levels and fate for all Special Areas, including the remaining Black Sea, the Red Sea, and the Gulfs Area but not the Antarctic Area because of the lack of naval ship traffic (see Table 6.1-2). These steady-state concentrations indicate, for a Battle Group (BG) and an Amphibious Ready Group (ARG), what the range of concentrations in the surface layer and the bottom layer would be within a 10000 nmi^2. The results from using the final decomposition rate constants showed little variation from the previous results. Using a simple steady-state model, the overall partitioning of the material was still controlled primarily by settling and advection. Of the total material, approximately 66% could be expected to settle to the sea floor within the same area, with the remaining 44% being advected out of the operational area. The results continue to suggest that the operation of multiple ships within a limited area should not produce concentrations of pulped paper in the water column or the sea floor which are greater than local exposures due to a single ship, which are not expected to cause adverse environmental impacts. Thus, significant biological effects would not be expected to occur under these conditions.

Table 6.1-2. Estimated steady-state exposure levels and fate in four MARPOL Special Areas from the combined pulped paper discharge of one BG and one ARG within 10000 nmi^2 (32400 km^2) operational area.

Special Area		Caribbean	Mediterranean	North Sea	Baltic Sea	Persian Gulf	Red Sea	Black Sea	Antarctica	Average %
Operational	# of Battle Groups	1	1	1	1	1	1	1	1	
	# of Amphib. Ready Groups	1	1	1	1	1	1	1	1	
	Area (km^2)	32400	32400	32400	32400	32400	32400	32400	32400	
	Duration (months)	6	6	6	6	6	6	6	6	
	Total Input Rate (kg/day)	7443	7443	7443	7443	7443	7443	7443	7443	
Surface Layer	Depth (m)	100	75	50	40	20	200	200	100	
	Temp (deg C)	28	26	10	10	20	26	16	2	
	Deg Rate %/day	0.400	0.370	0.090	0.090	0.220	0.370	0.150	0.040	
	Velocity (m/s)	0.75	1.5	0.5	0.05	50	50	0.2	0.5	
Bottom Layer	Depth (m)	2500	1500	n/a	150	40	500	1300	5000	
	Temp (deg C)	4	14	n/a	5	18	22	9	-1.5	
	Deg Rate %/day	0.040	0.130	n/a	0.060	0.180	0.260	0.080	0.0300	
	Velocity (m/s)	0.5	0.5	n/a	0.02	0.1	0.05	0.1	0.5	
Mass Fraction	Small (kg/day)	223	223	223	223	223	223	223	223	
	Med (kg/day)	893	893	893	893	893	893	893	893	
	Large (kgday)	6327	6327	6327	6327	6327	6327	6327	6327	
Settling Rate	Small (m/day)	0	0	0	0	0	0	0	0	
	Med (m/day)	6	6	6	6	6	6	6	6	
	Large (m/day)	864	864	864	864	864	864	864	864	
Surface Layer	Concentration (mg/L)	**1.06E-06**	**7.97E-07**	**2.32E-06**	**1.11E-05**	**2.16E-07**	**4.16E-08**	**1.66E-06**	**1.42E-06**	
	Mass in Layer (kg)	3423	1937	3763	14367	140	270	10727	4614	
	Advection (kg/day)	1232	1394	903	345	3365	6476	1030	1107	26.6
	Degradation (kg/day)	14	7	3	13	0	1	16	2	0.09
	Settling (kg/day)	6197	6042	6537	7085	4078	966	6397	6334	73.3
Bottom Layer	Concentration (mg/L)	**1.34E-07**	**1.57E-07**	**n/a**	**3.37E-06**	**1.88E-07**	**3.57E-08**	**2.99E-07**	**9.65E-08**	
	Mass in Layer (kg)	10880	7646	n/a	16354	243	579	12607	15639	
	Advection (kg/day)	2611	1835	n/a	157	12	14	605	3753	17.2
	Degradation (kg/day)	4	10	n/a	10	0	2	10	5	0.1
	Sedimentation (kg/day)	3582	4197	6537	6918	4066	951	5782	2576	66.4
	Amount deposited over 6 mos (mt)	644.7	755.4	1176.6	1245.3	731.9	171.1	1040.7	463.6	
	Layer thickness deposited over 6 mos um	0.080	0.093	0.145	0.154	0.090	0.021	0.128	0.057	

BASIN-SCALE SCENARIOS

In the original report, the basin-wide analysis showed that the inputs of the pulped and shredded waste streams were insignificant with respect to the overall constituent budgets within the four MARPOL Special Areas addressed (Wider Caribbean Basin, Mediterranean Sea, North Sea, and Baltic Sea). The solid waste discharges are delivered randomly over a wide spatial area, and constitute a distributed input which is not large enough to cause significant basin-wide effects. Subsequent analysis on the remaining Special Areas show a similar result. Water quality parameters including suspended solids (TSS), 5-day biochemical oxygen demand, (BOD_5), phosphorus, (P), chemical oxygen demand, (COD), nitrogen, (N), total organic carbon, (TOC), and zinc, (Zn), which were measured in the original analysis, were used in the same manner with overall loading data to calculate annual basin-wide constituent loading from each of the remaining MARPOL Special Areas. These results of all Special Areas are shown in table 6.1-3. During the original study, data on regional inputs were obtained from various sources including literature reviews and direct contact with environmental managers and municipal treatment plants surrounding the four Special Areas. A comparison was made for each of the constituent loadings. Unfortunately, detailed regional data was not obtainable for the remaining Special Areas (Persian Gulf, Red Sea, and Black Sea) in order to do a similar comparison, however, overall figures were estimated using literature values and are shown in comparison to naval vessels in Table 6.1-4.

Table 6.1-3. Annual basin-wide constituent loading from U.S. Navy ships into eight MARPOL Special Areas ($kg \cdot yr^{-1}$) based on estimated pulped paper discharges and results from chemical analysis.

Special Area	Caribbean Sea	Mediterranean	North Sea	Baltic Sea
TSS	1,284,068	1,730,681	16,264	11,568
BOD_5	87,365	117,752	1,107	787
P	61.6	83.1	0.8	0.6
COD	156,445	210,858	1,981	1,409
N	508	685	6	5
TOC	812,701	1,095,368	10,293	7,321
Zn	8	10	0.10	0.07
Special Area	**Persian Gulf**	**Red Sea**	**Black Sea**	**Antarctica**
TSS	715,950	234,900	4,140	0
BOD_5	48,680	15,900	280	0
P	34.4	11.3	0.20	0
COD	93,070	30,540	540	0
N	294	96	2	0
TOC	448,900	147,300	2600	0
Zn	4.3	1.4	0.02	0

Table 6.1-4. Comparison of basin-wide constituent loading from Navy ships

Constituent	Est. Loading from Navy Ships ($mt \cdot yr^{-1}$)	Loading from Manmade Sources ($mt \cdot yr^{-1}$)	% Contribution of Navy Ships
TSS	4.1 - 1730.7	$5.0 \cdot 10^6 \cdot 320.0 \cdot 10^6$	0.00008 - 0.0005
BOD_5	0.3 - 117.8	$1.7 \cdot 10^6 \cdot 3.3 \cdot 10^6$	0.00002 - 0.003
N	0.002 - 0.7	N/A	N/A
TOC	2.6 - 1095.4	$1.5 \cdot 10^5 \cdot 3.7 \cdot 10^6$	0.002 - 0.03
Zn	0.00002 - 0.01	$1.0 \cdot 10^4 \cdot 2.5 \cdot 10^4$	0.0000002 - 0.00004

Taking into account the new analysis for the additional Special Areas, Navy vessels continue to represent a very small fraction of the total regional input in all of the Special Areas. The analysis of the basin-wide inputs of pulped paper from the vessels suggests that this source is insignificant in the overall constituent budgets of the Special Areas. Thus, potential broad-scale effects such as eutrophication due to the nutrient inputs or oxygen depletion due to organic loading do not appear to be an issue on the basis of this source alone. In areas where these problems already exist, these inputs will probably not contribute to the existing imbalance to any measurable extent.

6.2 FATE AND EFFECTS OF THE SHREDDED WASTE STREAM

Only a few areas of the shredded waste stream analysis were updated. The first was a follow-on study to estimate the flow speeds necessary to initiate transport of shredded cans lying on the sea floor. The second was a study to analyze potential impacts to threatened and endangered species with regard primarily to the shredded waste stream. In addition, several tables were updated to include the three remaining Special Area data. The updated information is discussed below.

SEA FLOOR PROCESSES

Redistribution on the Sea Floor. Five water tunnel tests were performed to estimate the hydrodynamic force initiating movement of shredded can samples over a range of bottom roughness and various turbulent profiles selected from the literature (see section 3.3). The analysis did not take into account lift, torque, bottom friction, sediment suspension, or scouring effects. Scouring is thought to be the most important effect as it would tend to bury the metal can samples. The mean velocity of the flow 100 cm above the ocean bottom was calculated for each case once motion was observed. The estimates of laminar flow needed to cause movement ranged from 0.5 to 2.3 $m \cdot s^{-1}$. Typical ocean bottom values range from 0.1 to 1.0 $m \cdot s^{-1}$, with lower values reported to occur most frequently. Geological evidence and scattered observations do indicate that flows exceeding the critical transport speed occur intermittently in nature. Thus, there is the potential for an occasional disruption of the sea floor by metal can redistribution once the bags have degraded, but this will most likely be a localized, intermittent event which creates no significant environmental impact on the sea floor.

Potential Effects on Threatened and Endangered Species. Of the range of listed threatened and endangered species, only gray whales and five species of turtles were found to have feeding habits which may put them at risk for ingestion of shredded metal and glass disposed in burlap bags. For these species, restrictions from discharging less than 12 nmi from shore significantly limit the chances of any of the species encountering bagged waste. In addition, low spatial distribution of the bags and specific behaviors of the animals further serve to decrease the risk. Most of the turtles tend to feed in nearshore areas and do not dive deeply for their food. The gray whales are able to dive deeply but have feeding mechanisms which help preclude the ingestion of large and/or heavy materials. In general, the extremely low chance of exposure to the shredded material indicates that the likelihood of impact to threatened or endangered species is very low.

BASIN-SCALE SCENARIOS

The total yearly input of metal and glass from all Navy shipboard operations was considered in the original report of findings. At that time only four of the Special Areas were included in the mass loading, oxygen utilization, and steady-state estimates. The tables shown below (tables 6.2-1, 6.2-2, and 6.2-3) include the updated data for the remaining Special Areas. The purpose of the analysis was to determine the contribution of the shredded waste stream relative to other sources in each of the Special Areas and to look at how they might impact each region as a whole. The methods used in determining values for the remaining Special Areas were the same as in the original report which used the estimated generation rate for shredded material of 0.25 $kg \cdot d^{-1} \cdot person^{-1}$. As shown in Table 6.2-1 (not including Antarctica which has no naval vessel traffic), the mass loading of shredded metal and glass ranged from 2 $mt \cdot yr^{-1}$ in the Red Sea to 859 $mt \cdot yr^{-1}$ in the Mediterranean Sea.

Table 6.2-1. Annual mass loading estimates of the shredded metal/glass waste stream and Fe and Sn components into Special Areas by U.S. Navy ships. The inputs of the Fe and Sn are compared to river inputs to Special Areas using particulate loadings (tables 6.1, 6.2, 6.3 and 6.4 of the original report and tables 2.1-1, 2.2-1, 2.3-1, 2.3-2, and 2.4-1 in this Addendum) and concentration estimates of Chester, 1990.

	Baltic Sea	North Sea	Caribbean Basin	Mediterranean	Persian Gulf	Red Sea	Black Sea
Total Waste Stream Loading ($mt \cdot yr^{-1}$)	5.8	8.1	638	859	114	2	348
Total Waste Stream Loading ($bags \cdot yr^{-1}$)	1200	1700	$1.3 \cdot 10^5$	$1.8 \cdot 10^5$	$2.4 \cdot 10^4$	420	$7.3 \cdot 10^4$
Waste Stream Fe Loading ($mt \cdot yr^{-1}$)	4.1	5.7	446	601	244	80	1.4
Waste Stream Sn Loading ($mt \cdot yr^{-1}$)	0.04	0.06	4.5	6.0	2.4	0.8	0.014
Riverine Fe Loading ($mt \cdot yr^{-1}$)	$2.4 \cdot 10^5$	$9.6 \cdot 10^5$	$1.5 \cdot 10^7$	$1.7 \cdot 10^7$	---	0	717
Riverine Sn Loading ($mt \cdot yr^{-1}$)	10	40	625	708	---	0	0.03
U.S. Navy/Riverine Ratio (ppm) for Fe	17	6	30	35	N/A	N/A	1950
U.S. Navy/Riverine Ratio (%) for Sn	0.4	0.2	0.7	0.8	N/A	N/A	47

The number of bags dropped annually in each area would, thus, range from 420 in the Red Sea to $1.8 \cdot 10^5$ in the Mediterranean Sea. Based on the waste stream composition of Fe that is 70% of the total shredder waste stream and Sn which is 0.7%, the annual loading of these components ranges from 1.4 to 601 $mt \cdot yr^{-1}$ for Fe and 0.014 to 6.0 $mt \cdot yr^{-1}$ for Sn in the Black Sea and the Mediterranean Sea, respectively. In comparison, the riverine loading for the areas that information was obtained ranged from 717 $mt \cdot yr^{-1}$ in the Black Sea to $1.7 \cdot 10^7$ $mt \cdot yr^{-1}$ in the Mediterranean Sea for Fe, and 0.03 $mt \cdot yr^{-1}$ to 708 $mt \cdot yr^{-1}$ for Sn in the same seas, respectively. The Red Sea does not have freshwater inflow and the Persian Gulf and Antarctica inflows were not defined. Therefore, the ratios of the ships inputs versus the riverine inputs range from 6 parts per million (ppm) in the North Sea to 1,950 ppm in the Black Sea for Fe, and from 0.2 % to 47 % for Sn in the same seas, respectively. Previously, the time it took for the shredder bag inputs to match the annual discharge of Fe and Sn from natural sources into the Special Areas was 30,000 years and 100 years, respectively. However, the Black Sea has unique characteristics which bring those number to 500 years for Fe and 2 years for Sn.

As discussed in the original report, corrosion of metal material will result in oxygen utilization in a stoichiometry that will be roughly 45 moles $O_2 \cdot bag^{-1}$. The total oxygen utilization that can be expected to occur on a basin-wide scale would therefore range between 1.7 $mt \cdot yr^{-1}$ and 255 $mt \cdot yr^{-1}$ (see Table 6.2-2), which are the same as in the original report. The standing stock of oxygen in each of the Special Areas, estimated using a typical oxygen value of 5 $mL \cdot L^{-1}$, ranges from $1.8 \cdot 10^6$ $mt \cdot yr^{-1}$ in the Red Sea to $2.6 \cdot 10^{10}$ $mt \cdot yr^{-1}$ in the Mediterranean Sea. Therefore, there is at least a million to several billion times more oxygen available in the Special Areas than would be required to completely oxidize all the metal discharged annually. It remains highly unlikely that the discharge of shredded metals by U.S. naval

vessels will have any impact on the oxygen budget within the Special Areas, however, minor local effects may occur.

Table 6.2-2. Estimate of oxygen utilization for the complete corrosion of the annual shredded metal waste stream into each Special Area. The estimates are based on annual inputs and general stoichiometry for oxidation. The standing stock of oxygen in each area is based on a seawater oxygen concentration of 5 $mL \cdot L^{-1}$.

	Baltic Sea	North Sea	Caribbean Basin	Mediterranean	Persian Gulf	Red Sea	Black Sea
Total Oxygen Utilization ($mt \cdot yr^{-1}$)	1.7	2.4	189	255	105	34.5	6.0
Oxygen Standing Stock ($mt \cdot yr^{-1}$)	$1.6 \cdot 10^{8}$	$3.9 \cdot 10^{8}$	$4.7 \cdot 10^{10}$	$2.6 \cdot 10^{10}$	$6.2 \cdot 10^{7}$	$1.8 \cdot 10^{6}$	$3.8 \cdot 10^{9}$

Another question to consider for basin-wide effects is how much of the shredded material in the naval vessel waste stream will accumulate over time. This was estimated using the concept of steady-state in which the inputs will be balanced by removal processes. As such, this will be an appraisal of how much of the material is ostensibly altered from being a component of litter to being integrated into the sea floor similarly to other sedimentary material. Under steady-state conditions, the removal process balances the inputs according to:

$$M = \frac{I}{D}(1 - e^{-Dt})$$

where: M = accumulated mass on the sea floor
I = mass input rate
D = corrosion rate (removal rate)
t = time

This condition cannot truly be reached because the amount corroded is a fixed fraction of the amount available and as inputs increase, so do the losses. Thus, steady-state can be estimated as it is approached over time, in this case, using 95% of steady-state.

Table 6.2-3. Steady-state loading estimates of Fe and Sn in Special Areas. Estimates are made using the same equation as in the original report, (shown above). The calculation used the amount of time to reach 95% of steady-state, which for Fe, is 7.5 years and for Sn, is 0.18 years. All values are in metric tons.

	Baltic Sea	North Sea	Caribbean Basin	Mediterranean	Persian Gulf	Red Sea	Black Sea
Fe							
U.S. Navy Annual Input ($mt \cdot yr^{-1}$)	4.1	5.7	446	601	244	80	1.4
Steady-state Accumulation (mt)	9.7	13.5	1060	1427	580	190	3.3
Sn							
U.S. Navy Annual Input ($mt \cdot yr^{-1}$)	0.04	0.06	4.5	6.0	2.4	0.8	0.014
Steady-state Accumulation (mt)	0.002	0.003	0.26	0.34	0.14	0.046	0.001

Considering the equation for Fe and Sn for typical conditions of inputs and corrosion rates for each area (Table 6.2-3), the amount accumulated in each area for a time equivalent to 95% of steady-state will range from 3.3 mt of Fe in the Black Sea to 1427 mt in the Mediterranean Sea. For Sn, the amount accumulated will range from 0.001 mt tons in the Black Sea to 0.34 mt in the Mediterranean Sea. These results suggest that the accumulation of metal materials, as litter, will be between two and three times the annual rate and still a very small fraction of the total inputs of these components from natural sources.

The annual input of the shredded metal/glass waste stream from U.S. Navy ships operating in Special Areas constitutes a tiny fraction of basin-wide inputs. The estimates made in the original report remain valid with the exception of Fe and Sn inputs into the Black Sea. In general, it is estimated that it would take hundreds to thousands of years of Navy shipboard shredded discharges to match a single year of other basin-wide discharges. The Fe and Sn loading from naval vessels in the Black Sea is greater proportionally because of the relatively small loading of these constituents from riverine sources. Other analysis results from the original report remain the same in that it the amount of shredded material discharged annually would cover only a tiny fraction of the sea floor. According to the steady-state estimates, the amount accumulated on the sea floor as a litter component would be roughly equivalent to about 2 to 3 years of discharge, ensuring that the amount covering the sea floor would remain a tiny fraction. And there is at least a million times more oxygen available to completely oxidize the material than is needed.

REFERENCES

Benner, R, A. E. Maccubbin, and R. E. Hodson. 1986. *Temporal Relationship Between The Deposition And Microbial Degradation Of Lignocellulosic Detritus In A Georgia Salt Marsh And The Okefenokee Swamp.* Microb. Ecol. 12:291-298.

Chester, R.C. 1989. *Marine Geochemistry.* Unwin Hyman, publisher, London. 698 pp.

7. CONCLUSION

The conclusions for this updated analysis are essentially the same as those for the original pulped and shredded waste stream fate and effects analysis. As discussed in the Analysis section, the overall environmental impact of the pulped and shredded waste streams appears to be benign to minimal. Input levels are at or below background levels and expected exposure levels after dispersion are also below those found to cause effects in the laboratory. The techniques of pulping and shredding are an improvement over previous methods. The size fractions inherent in the pulping process are beneficial for rapid descent of the material to the benthos. Likewise, the shredded material packaged in burlap bags is optimized for rapid descent. In each case, the sea floor processes are the dominant ones, and there is no evidence that exposure levels of either waste stream in the benthos will cause a negative environmental effect to the benthos. The updated information and the results from the continued studies do not alter the previous findings that suggest that there will be no significant adverse environmental impact from the discharges studied.

REPORT DOCUMENTATION PAGE

Form Approved
OMB No. 0704-0188

Public reporting burden for this collection of information is estimated to average 1 hour per response, including the time for reviewing instructions, searching existing data sources, gathering and maintaining the data needed, and completing and reviewing the collection of information. Send comments regarding this burden estimate or any other aspect of this collection of information, including suggestions for reducing this burden, to Washington Headquarters Services, Directorate for Information Operations and Reports, 1215 Jefferson Davis Highway, Suite 1204, Arlington, VA 22202-4302, and to the Office of Management and Budget, Paperwork Reduction Project (0704-0188), Washington, DC 20503.

1. AGENCY USE ONLY *(Leave blank)*	2. REPORT DATE	3. REPORT TYPE AND DATES COVERED
	February 1999	Final

4. TITLE AND SUBTITLE
ENVIRONMENTAL ANALYSIS OF U.S. NAVY SHIPBOARD SOLID WASTE DISCHARGES: ADDENDUM TO THE REPORT OF FINDINGS

5. FUNDING NUMBERS
PE: 0603721N
AN: DN309084
WU: ME40

6. AUTHOR(S)
S. L. Curtis, C. N. Katz, D. B. Chadwick

7. PERFORMING ORGANIZATION NAME(S) AND ADDRESS(ES)
SSC San Diego
San Diego, CA 92152–5001

8. PERFORMING ORGANIZATION REPORT NUMBER
TR 1716 ADDENDUM

9. SPONSORING/MONITORING AGENCY NAME(S) AND ADDRESS(ES)
Naval Sea Systems Command
2531 Jefferon Davis Highway
Arlington, VA 22217-5160

10. SPONSORING/MONITORING AGENCY REPORT NUMBER

11. SUPPLEMENTARY NOTES

12a. DISTRIBUTION/AVAILABILITY STATEMENT
Approved for public release; distribution is unlimited.

12b. DISTRIBUTION CODE

13. ABSTRACT *(Maximum 200 words)*

This Addendum provides follow-on findings to a report published by SSC San Diego (TR 1716) in January 1996 detailing a study of the fate and effects of U.S. Navy shipboard solid waste discharges. The study was requested as part of the Navy's effort to evaluate solid waste discharge compliance alternatives. The objective of the study was to determine to what extent, if any, Navy solid waste discharges lead to adverse marine environmental effects. Along with the original findings, the final results presented in this Adendum suggest that there will be no significant adverse environmental impact from the discharges studied.

14. SUBJECT TERMS
Mission Area: Environmental Quality
ecology — environmental assessment
toxicology — biochemistry

15. NUMBER OF PAGES
370

16. PRICE CODE

17. SECURITY CLASSIFICATION OF REPORT	18. SECURITY CLASSIFICATION OF THIS PAGE	19. SECURITY CLASSIFICATION OF ABSTRACT	20. LIMITATION OF ABSTRACT
UNCLASSIFIED	UNCLASSIFIED	UNCLASSIFIED	SAME AS REPORT

21a. NAME OF RESPONSIBLE INDIVIDUAL	21b. TELEPHONE *(include Area Code)*	21c. OFFICE SYMBOL
S. L. Curtis	(619) 553–5255 e-mail: stacey@spawar.navy.mil	Code D362

INITIAL DISTRIBUTION

D0012	Patent Counsel	(1)
D0271	Archive/Stock	(6)
D0274	Library	(2)
D027	M. E. Cathcart	(1)
D0271	D. Richter	(1)
D362	S. L. Curtis	(10)

Defense Technical Information Center
Fort Belvoir, VA 22060–6218 (4)

SSC San Diego Liaison Office
c/o PEO–SCS
Arlington, VA 22202–4804

Center for Naval Analyses
Alexandria, VA 22302–0268

Navy Acquisition, Research and Development
Information Center (NARDIC)
Arlington, VA 22244–5114

GIDEP Operations Center
Corona, CA 91718–8000